Freeze-Thaw Resistance of Concrete
Effect of :
Curing Conditions, Moisture Exchange and Materials

by

Terje Finnerup Rønning

Thesis submitted for the degree of
Dr.Ing.
at
The Norwegian Institute of Technology,
Division of Structural Engineering,
Concrete Section

Trondheim

Anno 2001

URN:NBN:no-6354

With special thanks
to
Birger Søpler

URN:NBN:no-6354

Summary

General

Research on freeze-thaw resistance of concrete in general and on curing and moisture conditions in particular is motivated from an economic and product sustainability point of view. Specifically, it is argued for the importance of considering the effect of curing and test exposure conditions on the moisture uptake and performance during freeze-thaw. Due to the demonstrated importance of moisture conditions on performance, they should be related to those of field service conditions when choosing a test procedure in a particular case. This is vital for adequate testing of new and more sustainable concrete materials.

General on freeze-thaw mechanisms / Literature review

A number of mechanisms affecting the material performance during freeze-thaw are reviewed (Section 2) to put the present work into perspective, without intending to completely cover the subject. Evidently, no single mechanism can explain fully freeze-thaw damage of concrete. Several mechanisms occur simultaneously, and it appears impossible today to "calculate" the performance based on mechanisms, concrete material characteristics and exposure data. As a consequence, current practice is to apply concrete design specifications, based on "local" experience like the national application documents of [EN 206]. These specifications normally include requirements to w/c-ratio and air characteristics, as well as curing. Laboratory testing is mainly used for ranking. However, such a "current practice-concept" is a restraint for applying new materials. This strongly motivates a stronger focus on field versus laboratory correlation. For freeze-thaw deterioration, the material-environmental interaction is decisive for this correlation.

Curing of concrete / Freeze-thaw resistance

The curing regime strongly affects the results of the freeze-thaw testing :

Dry curing, i.e. storage with no or little water supply prior to freeze-thaw testing resulted in relatively good performance - and better than the standard curing according to [prEN xxx]. It also appears that postponing the water storage period in time (closer to the actual freeze-thaw exposure !) results in improved freeze-thaw performance – probably because of smaller water suction in this period.

It is suggested that initial water curing – right after de-moulding - for longer than a very short period of time (24 hours ?) will not promote the curing significantly, but only increase the initial degree of saturation. Water curing of a w/c = 0.48 mortar leads to a capillary degree of saturation in the range of 100 %, it even leads to some water in the air voids. This early age water exposure and increased degree of saturation does not comply with modern construction practice, where the early age concrete generally is protected against moisture loss by the formwork or application of curing compounds.

Sawing the test surface right after water storage (at 7 days in stead of 21 days), and then subjected to drying at the prescribed laboratory climate, lead to increased freeze-thaw scaling as expected. Drying at elevated temperature (3 days at 40 ^{o}C) confirmed previous studies reporting substantial increase in freeze-thaw scaling, but less so for silica fume concrete.

Moisture exchange versus freeze-thaw resistance

The investigations on effect of curing were used to consider moisture exchange phenomenon specifically. Plastic curing lead to very low moisture loss that was easily regained during the re-saturation procedure prior to freeze-thaw testing. Very low freeze-thaw damage occurred. Sawing the test surface at 7 days in stead of 21 (“standard”) days - allowing for drying in laboratory climate until freeze-thaw test initiation at 31 days – lead to substantial moisture loss. The freeze-thaw scaling was increased. Drying at 40 ^{o}C for three days similarly lead to substantial weight loss that was not recovered during re-saturation, and the scaling was severe.

No direct relation between moisture loss during curing – for different curing regimes – and water uptake during the re-saturation procedure was found. Nor did the moisture loss relate to water uptake during freeze-thaw. Though, a correlation between freeze-thaw scaling and water uptake during freeze-thaw was confirmed. The scaling also correlated to the accumulated water uptake during re-saturation *and* freeze-thaw. For internal damage, no such correlation was demonstrated.

Moisture exchange during freeze-thaw

Several mechanisms leading to water uptake during freeze-thaw were theoretically considered (Section 7). Examining the weight changes during freeze-thaw testing (tested w/c-ratio of 0.48 only) revealed a weight loss on thawing under water, even if there was a net water uptake increasing with the number of freeze-thaw cycles. This net water uptake constitutes the normally denoted “pumping effect”.

Attempts to determine internal re-distribution of moisture due to other thermally induced effects did not document such effects. However, such effects may still exist. Using different duration of freezing and measuring weight changes for several hours after thawing did not show any time-dependent water uptake (from the external) caused by such internal re-distribution. The extent of weight loss during thawing suggests that thermally induced pressure changes in the air voids are the dominant factors in the external moisture exchange. However, this should be verified as proposed (Section 9).

During isothermal frost, a certain freeze-drying (loss of moisture from the samples) appears to exist after the initial absorption during freezing. The pre-testing curing regime seemed to have little influence on the effects above.

Laboratory test results versus field performance / Material

The data from the laboratory testing provide a good basis for the field versus laboratory comparison (Section 5) : Only air-entrained concrete performed well in the laboratory test, even with w/c-ratio of 0.35 ; a spacing factor in the range of 0.4 or less appeared vital to ensure good performance.

The implication of the curing/moisture condition/deterioration-relations above is to emphasise the importance of applying a testing regime with field relevant moisture conditions. A field versus laboratory study (Section 5) addresses the issue of correlation between laboratory freeze-thaw testing and field performance. After two winter seasons at a highway with frequent use of de-icing salt, all the mixes investigated had none or very small visible surface damages and no visible cracking. This applied to all mixes, whether the performance in the initial laboratory testing was good or not. Limited data on the capillary degree of saturation in the field indicate that this parameter is lower than during laboratory testing – and that it depends on the w/c-ratio. However, two years of field exposure is too short to conclude on field performance - and thus on the relation to laboratory testing.

Materials

As mentioned, only air entrained concrete performed well in laboratory freeze-thaw testing, even with a w/c-ratio of 0.35. With the w/c-ratios investigated, i.e. 0.45 and below, spacing factor in the range of 0.4 or less appears vital to ensure good performance in the laboratory freeze-thaw test procedure. Studies to verify the field performance is still on-going and will be reported later. After two years of exposure in highway climate with frequent use of de-icing salt, damages are almost non-existent for all the concrete qualities included in the present report (Section 5).

The positive effect of silica fume on freeze-thaw resistance from earlier reports was confirmed. This concerns both effect of early age drying on scaling and generally less moisture exchange prior to and during freeze-thaw. The effect somewhat depended on cement type. The effect of silica fume on (indoor) ageing was positive in the majority of cases. However, it was demonstrated that the effect of silica fume depended on the type of curing and on the cement type. Larger positive effect was found with a “standard” CEM I 42.5 cement and cyclic dry and wet curing than with a low alkali, high strength cement.

The study confirmed earlier reported evidence on especially good freeze-thaw resistance with a particular SR-LA cement (Section 3). The effect of the cement was pronounced at low air void levels. There are clear indications of favourable air void characteristics with this cement or cement-admixture combination compared to that of the CEM I 42.5 R cement. Still, the differences observed, e.g. from ageing, suggests that the difference in performance can not be attributed to air void characteristics only. With a proper air void system, also the standard cement performed well. Similarly, another CEM I SR-LA and a CEM I LA 52.5 R cement appeared somewhat superior to a CEM II/A-V 42.5 R cement, but all cements performed well with a given air void system (Section 5). It should be pointed out that the somewhat poorer performance by the laboratory test of the fly ash cement may be due to the slower reactivity of the fly ash, and thus probably is time dependent. This addresses the curing procedure.

Addition of high amounts of superplasticizer to mixes of high water demand did to some extent affect the air void characteristics or paste homogeneity negatively. This occurred both with (Section 3) or without (Section 5) silica fume and indicates an influence of fresh concrete properties on the microstructure, and hence on durability properties.

Testing of frost or freeze-thaw resistance

Different salinity inside and outside the sample (Section 4) seemed to promote the deterioration process during the first 10 – 15 freeze-thaw cycles. This may be due to an osmotic effect, at least temporarily increasing the degree of saturation close to the surface. It is not in contrast to the general finding that salt solution at the exterior causes by far the more severe attack than pure water.

Internal cracking was found to be detectable by ultrasonic pulse velocity technique. The latter was an issue within the framework of the main project of which the present study was a part.

Chemical shrinkage

Supplementary to the study of moisture exchange during freeze-thaw (Section 7), chemical shrinkage tests on cement paste and mortars were performed (Section 6). The objective was to determine capillary degree of saturation and if filling of macro pores took place during water storage - prior to freeze-thaw exposure.

However, a difference in chemical shrinkage between cement paste and mortar of “identical composition” was also demonstrated.

A study on potential errors during tests of chemical shrinkage using the Erlenmeyer Flask principle was carried out, and Section 6 contains general advice on the procedure.

List of Contents

3 Curing and ageing with and without silica fume

4 Damage versus moisture loss and absorption

5 Field performance versus laboratory testing of freeze-thaw

8 Common trends on effect of curing conditions, moisture exchange and materials

9 Suggestions for Further Research

10 Conclusions

11 References

Appendices

A Description of test method : Reference Method in [prEN xxx].
B Section 4 : Damage versus curing, moisture loss and absorption. Additional data.
C Section 6.3.4 : Chemical shrinkage data.
D Section 6.3.5.2 : Moisture content and porosity. Detailed data.
E Section 5 : Additional data.
F Section 3 : Additional data and plots.
G Section 7 : Additional data.
H Fresh concrete air void characteristics. Brief description of the test method.
I Chemical shrinkage test method : Pilot study on the effect of sample thickness and some potential errors.

Acknowledgement

I want to express my sincere gratitude to Birger Søpler, the R&D manager of Norcem A.S. He enabled and inspired the initiative of this work, supported me in several practical and financial matters and preliminarily re-organised the laboratory department to enable me to concentrate on the programme. My gratitude also comprises the commercial director of Norcem, Kjell Skjeggerud, and the former R&D Director Øivind Høidalen, for allowing this work. Mr. Skjeggerud was also the project manager of one of the early project tasks.

I also express my sincere gratitude to my adviser, Professor Erik J. Sellevold for his personal commitment, accommodating and supportive attitude, open discussions and fruitful criticism.

I am grateful to my colleagues at the Norcem R&D section, especially to Per Kjetil Zachariassen, who performed or assisted in much of the frost scaling assessment. Valuable laboratory assistance was also given by Per Omenås, Tormod Busk, Torbjørn Sandersen, Knut Wingereid, Thore Tinderholt, Leif Johnsen and other co-workers. Sigrun Kjær Bremseth assisted on structural analyses, and Knut Kjellsen in various discussions. My co-workers Finn Coch and Liv-Margrethe H. Friberg did their best to enable me to concentrate on the project. Berit Hansen assisted in the editorial work.

I wish to express my thanks to the many external contacts on the different tasks : Scancem Chemicals A.S enabled the study of Section 3 of this publication. The European Research Project “Standard Methods for Testing the Resistance of Concrete to Freezing and Thawing”, chaired by Dr. Siebel at VDZ, financed parts of the study in Section 4. The Swedish National Testing and Research Institute in Borås, Sweden, organised the framework of the field versus laboratory study in Section 5, my special thanks to Peter Utgenannt for various assistance. I also want to thank Dr. Per-Erik Petersson, Dr. Dirch Bager, Professor Göran Fagerlund, Monica Lundgren, Dr. Stefan Jacobsen, Professor Max J. Setzer and Professor Jochen Stark for fruitful discussions.

I am grateful to the Norwegian Research Council for funding parts of this work, especially the scholarship in 1999.

Last, but not the least my special thanks to Vera, who supported in maintaining a certain disciplinary pressure and taking care of responsibilities as well as social life.

URN:NBN:no-6354

1 Introduction ; Aim of the Project

1.1 Why research on frost and freeze-thaw resistance ?

The serviceability of construction materials in general is of significant economic importance. This is especially so with structures and materials which are part of the infrastructure of a modern society. Concrete is a material heavily used in urban development, meeting the modern needs of transport with high density traffic by means of aesthetic and durable structures.

The continuous development of knowledge, concrete products and attempts in improving the durability and increasing the service life of such structures provide important contribution to public and private economy – and towards a sustainable development.

Reduced service life in the sense of lack of durability may be due to a number of different reasons, e.g. planning/capacity (over-loading), improper structural or material design, construction practice or inadequate maintenance – or lack of knowledge. The accumulated rehabilitation needs of the American bridges and roadways by the early nineties were estimated to range from US$90 to US$150 billion [M 1994]. A large portion of this is due to inadequate design or maintenance and can be linked to the use of de-icing salt.

In middle and northern Europe, as well as in North America and Japan, the widespread use of de-icing salts is considered a major cause of rapid degradation of concrete structures. The de-icing salt leads to attack on the concrete reinforcement, disturbing the electrochemical immunity of the steel. The corrosion process depends on the diffusion of chloride ions through the concrete cover. Further, the de-icing salt together with repeated freezing and thawing may cause failure of the concrete cover by surface scaling, which combined with steel corrosion may critically reduce the structure's service life.

It is very difficult to estimate the direct repair and maintenance costs caused by freeze-thaw damages of concrete structures. However, due to its still non-revealed secrets concerning deterioration mechanisms, freeze-thaw resistance has received significant attention in Middle and Northern Europe, as well as in

North America, Canada, Japan and Russia for several decades. However, even within these specific regions, experience varies considerably, partly due to different construction practice and/or applied concrete materials and – constituents.

In Norway, freeze-thaw damages have not been considered a very severe problem, which is believed to relate to adequate concrete design. Still, even here concrete surface spalling, e.g. on concrete road safety barriers, is commonly observed [F 1992], and damages on pre-cast paving blocks are frequent. The latter is a relatively new established concrete market in the Nordic countries and can be expected to attract increased attention in the future, based on field observations and experience from laboratory performance testing [R 1995].

Further, frost damages may result in cracking in stead of spalling. Surface cracking is often observed. Cracking caused by freeze-thaw damages requires detailed investigations and is normally not classified as such. A particular deterioration mechanism may not produce damage that is exclusive for that specific mechanism. This fact impedes clear diagnosis, which may lead to ignorance of the real cause of damages, as well as corrective and preventive actions on design, manufacturing or maintenance.

Even if present practice in certain markets might be considered adequate to meet the field service requirements, on-going and future concrete material development towards an improved, sustainable construction practice will introduce new challenges. Future development of concrete will increase the focus on application of supplementary cementing materials and filler materials, also for structures subjected to high performance requirements, like in infrastructure projects. In this context, increased knowledge about the detrimental mechanisms may provide essential information of significance to the product development.

1.2 Significance of research on moisture conditions

Frost and freeze-thaw resistance of concrete has been a challenge to researchers for the major part of the last century. Even if modern equipment provides new and more precise information, scientists working e.g. in the US performed quite advanced studies on the issue during the 1940s and 50s. As will be outlined in subsequent sections, several mechanisms detrimental to the concrete material have been identified through these studies.

With several, simultaneously acting mechanisms, it has not been possible to identify the critical one(s) for a specific material design and environment. The scatter in material characteristics and properties is pronounced, as is the variety of environmental conditions. Under frost and freeze-thaw conditions, the boundary conditions with respect to moisture “loading” of the concrete material is essential to the potential degradation – and to whether a detrimental mechanism will act or not.

It is no secret that freeze-thaw testing in accordance with various standardised or non-standardised test methods may destroy any concrete material. The phrase “in the lab, we can destroy anything” is evident in this field, while there is a severe lack of correlation between laboratory and field performance. Hence, as for any accelerated (laboratory) testing, it is essential to a) create artificially conditions simulating field conditions, or b) in other ways calibrate the test results against field experience. For freeze-thaw testing, the most crucial boundary conditions relate to the temperature and moisture vs. time testing regime.

The use of existing materials or construction practice may of course rely more or less entirely on long term field experience. However, the introduction of new materials or concepts – or new fields of application for existing materials – requires some system of evaluation and documentation prior to application. During the last decade, the reliability of certain testing methods has been questioned [M 1994]. One issue is of course the “ever-arising” question related to reproducibility. Even more important to the present author’s opinion is the question of the severity of the testing methods. Too “liberal” tests and evaluation criteria may cause the use of inadequate materials. On the other hand – and maybe more likely in this particular case – too conservative criteria may unjustly exclude excellent materials with adequate properties. This includes the introduction of composite binders for concrete, improving the sustainability of concrete in general - and possibly also other durability properties.

Even the commercial interests of the European cement and concrete industry cover a wide range of binder types and properties. Within the framework of the European standardisation activities, a task group (CEN TC 51 / WG 12 / TG 4) is currently concerned with the selection of a representative reference method and testing conditions for cementing materials.

When considering the moisture conditions of concrete for freeze-thaw testing, it becomes obvious that not only the boundary conditions during testing are vital but also the pre-testing curing conditions. Secondly, the field and laboratory conditions must be compared. Thirdly, the physical nature and thermodynamic laws during freeze-thaw exposure result in changes and for redistribution of the moisture within the porous concrete material. Decisive for the moisture conditions of the concrete material are not only the outer boundary conditions but also the porosity characteristics of the material itself.

1.3 Aim of the project

Following the arguments above, the aim of the research work has been to establish qualitatively and, if possible, quantitative information on :

- Effect of curing conditions on performance during freeze-thaw exposure.
- The moisture uptake during freeze-thaw testing.
- Moisture re-distribution within the material subjected to freeze-thaw exposure.
- Correlation between field exposure and laboratory testing.

The work covers several separate studies over a number of years. It includes various material combinations / concrete mix designs, depending on the particular issue dealt with. However, some restrictions apply due to practical and financial boundary conditions. Hence, the separate studies do not comprise identical materials, which is believed not to influence the intention of the work negatively.

The basic work will furthermore concentrate on only one specific, fundamental testing procedure, mainly due to the limitations mentioned above.

2 Freeze-Thaw Resistance of Concrete

2.1 Objective

The objective of this section is to give an outline of phenomena and mechanisms dealt with in the literature, in order to provide an understanding for the discussions to follow – and to place the present work within a framework. References will be made to studies examining these phenomena in detail.

It is not the aim to provide a (another) full literature review with a comprehensive discussion, confronting ideas and studies generally outside the scope as presented in the preceding section.

Discussions of the topics investigated in this study will also follow in the appropriate sections.

2.2 Freeze-thaw damages

Freeze-thaw damages may appear as surface scaling or internal cracking. The former may occur on both horizontal and vertical surfaces, but mainly where water or snow can naturally deposit and the surface remain wet for periods. The susceptibility to surface scaling will increase significantly in the presence of de-icing chemicals, normally NaCl-solutions. The phenomenon is commonly observed to larger or lesser extent on concrete paving blocks and road structures, like concrete safety barriers.

Internal cracking under field conditions is less commonly observed or recognised. Sampling for structural analyses by plane sections or thin sections will provide valuable information for the identification and elimination of other causes. The phenomenon may be observed on parts of structures in direct contact with free water and subjected to capillary suction, such as the lower parts of supporting walls and dam structures above the water surface. It is also believed that freeze-thaw cracking may combine with or start after deterioration initiated by other detrimental mechanisms, such as alkali aggregate reactions. However, in contrast to surface scaling, the cracking may start at the interior and initially not be visible at the outside. A consequence is an increase in volume.

Figure 2.2.1 : Surface damage on a concrete pavement [P 1985].

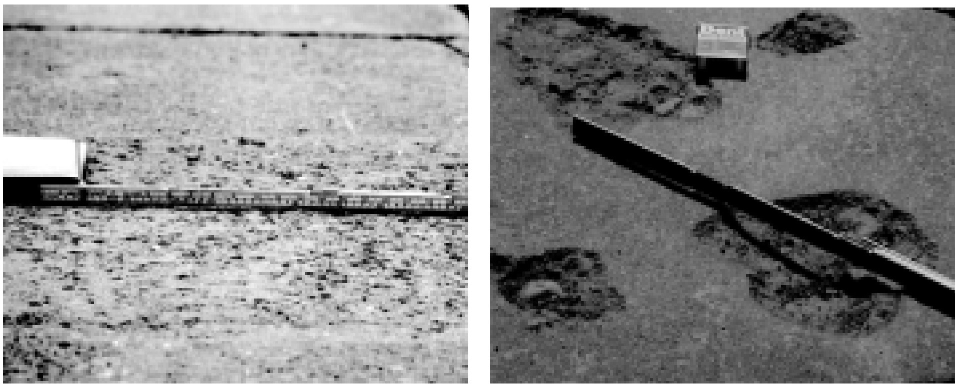

Figure 2.2.2 a & b : Surface damage on a concrete bridge pavement, displaying two various kinds of deterioration patterns ; a) even surface scaling on individual sections and b) local damage reducing the reinforcement cover significantly. Near the premises of Norcem, Brevik, Norway.

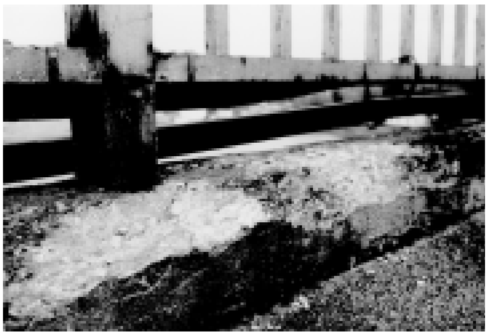

Figure 2.2.3 : Concrete damage at a vulnerable part of a bridge section, exposing the reinforcement to corrosion conditions. Near Vordingborg, Denmark.

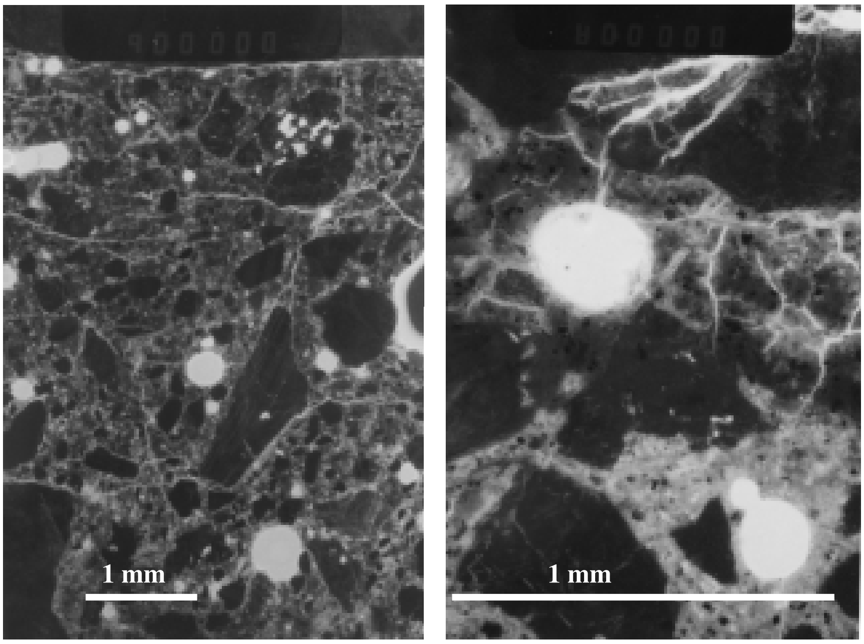

Figure 2.2.4 a & b : Internal crack pattern of concrete pavement sections from an air field, after several years of outdoor storage (but not in service) and 56 freeze-thaw cycles in the laboratory. (Picture 3 mm across) The upper surface is the external one. Previously non-published material by the present author and co-worker.

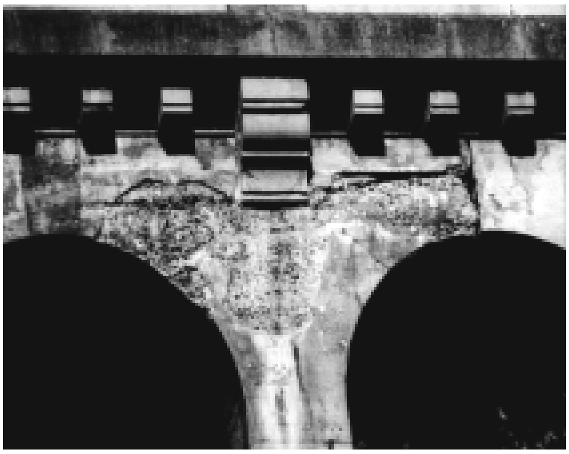

Figure 2.2.5 : Frost damage on the side of a bridge, near Washington D.C.

Figure 2.2.6 : Freeze-thaw damages of concrete flags at an outdoor testing facility.

Figure 2.2.7 : Damages at a minor road safety barrier. The damage is not proven to be frost damage, but exhibits 10 cm deep cracks without alkali-aggregate reaction being identified.

Both surface scaling and internal cracking are progressive phenomena; i.e. the deterioration is gradual. Sudden failures have not been reported to the knowledge of the present author.

The damage is connected to the porous part of the concrete material. In the case of "porous" aggregate materials, this constituent is likely to initially be susceptible to damage. In the case of dense and sound aggregate materials, the damage will be located in the cement paste.

Coarse, non frost resistant aggregates, possessing a pore size distribution causing suction of water, may expand during freezing and stress the layer on the outside, causing damages named as pop-outs. It should be emphasised that the total porosity of the aggregate is no good indicator on the susceptibility to such damage, since even low total porosity aggregates may exhibit such properties.

As pointed out by Jacobsen [J 1999c], this issue (among others) is also relevant when using recycled concrete as coarse aggregate in new concrete and should be considered in such a case. Otherwise, it is not considered a serious problem in the Nordic countries.

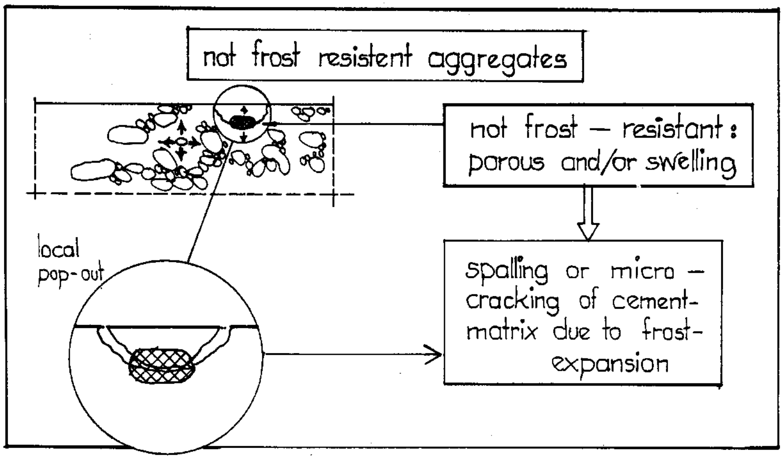

Figure 2.2.8 : Damages caused by coarse aggregates susceptible to frost deterioration [R 1989].

There is no doubt that concrete of adequate quality to resist field requirements of freezing and thawing may be designed and manufactured according to present technology and practice. A concrete pavement on the Norwegian highway E18, subjected to combined freeze-thaw at the presence of de-icing salt and the wear of studded winter tyres was replaced after 15 years of service. At that time, the adjacent asphalt pavement had been replaced six times.

Surface scaling on a 70-year-old dam structure, subjected to approximately 60 freeze-thaw cycles (with freshwater) per year, deteriorated 10 mm, or 5 g per m^2 and cycle [J 1999b]. The same reference displays a road safety barrier with 15 years of service at estimated 120 freeze-thaw cycles (and de-icing salt) per year that deteriorated 5 mm, or 12 g per m^2 and cycle. In the latter case, however, the deterioration tended not to be evenly distributed.

Evenly distributed deterioration may be compensated by adequate thickness of the reinforcement cover - thereby maintaining the service life. The surface scaling may negatively influence aesthetics. Damages occurring as “pitting” and larger cavities are more difficult to cope with, and road safety barriers often have to be replaced.

2.3 Concrete material characteristics

2.3.1 General

This section summarises some general material characteristics central to the phenomena and theories discussed later. Properties relevant to specific mechanisms are left for the appropriate sections – or given by reference to be found elsewhere.

2.3.2 Concrete material

It is very difficult to distinguish the actual process of the mechanisms within concrete subjected to freeze and thaw. One reason is that the concrete constitutes a microclimate of its own, and it is difficult to detect changes in the latter as responds to the macro (outside) climate. Some of the material characteristics are displayed in figure 2.3.1-2.

Some of the key properties of concrete with respect to durability relate to the porosity, which in turn mainly is a property of the hydrated cement paste. Non-reacted cement is a very dense material, and the reacted cement, the gel, as well. The gel water is physically absorbed to the internal surfaces and practically removable by drying at very low relative humidity levels only. It will be argued later on that the transport properties are of particular interest. The gel pores are considered inactive in the context of contribution to permeability to external substance [N 1995]. In fact, it is the upper pore size range of more or less continuous capillary pores and air voids that allow the ingress of external substance, among which water. Hence, doubling the total amount of capillary pore volume may not only increase the permeability by the same percentage, but with an order of magnitude. Properly entrained air voids may reduce capillary suction.

When cooling a cement paste sample, measuring the apparent heat capacity reveals ice formation at certain temperature intervals. This effect has been attributed to the freezing of pore water of specific pore sizes [B 1987], i.e. freezing of gradually smaller pores and thus describing the pore size distribution (See figure 2.3.3). However, this has been questioned by others [L 1998]. Still, it remains a fact that freezing at normal outdoor conditions will lead to freezing of a part of the pore water only (See subsequent section).

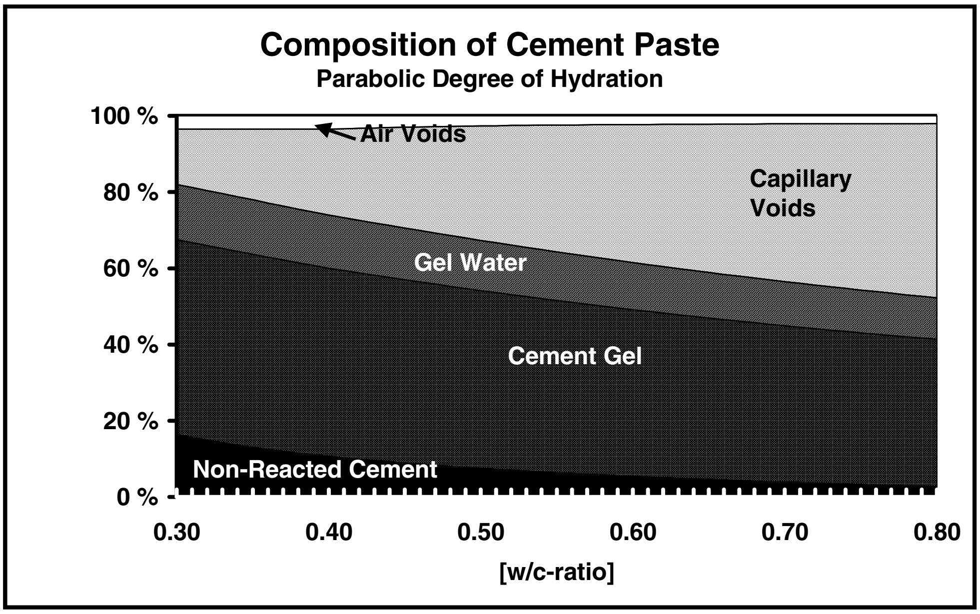

Figure 2.3.1 : The structural components of cement paste in concrete. The design is based on the original provided by [H 1979] but has been recalculated. The basic changes relate to the degree of hydration : In the present version, the degree of hydration varies by a parabolic function from 50% at w/c = 0.25, via 75% at w/c = 0.40 to 90% at w/c = 0.80. (Further, the calculations are based on results presented by Sellevold [S 1993]: Chemically bound water W_n *= 0.23 x hydrated cement [g], Gel water* W_e *= 0.15 x hydrated cement [g]. Contraction pores are calculated as* ε_c *= 0.254 x* W_n *and defined as part of the capillary pores.)*

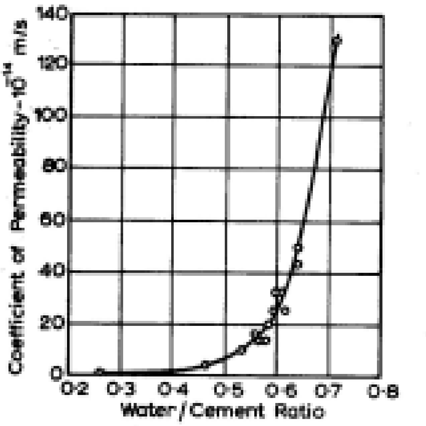

Figure 2.3.2 : Relation between permeability and w/c-ratio for mature (α = *0.93) cement paste (pure paste ; not paste fraction in concrete), referred to by [N 1995].*

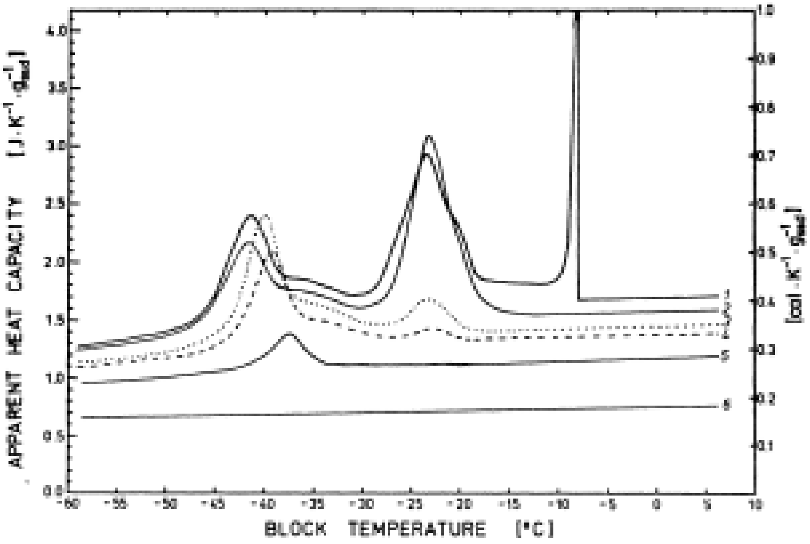

Figure 2.3.3 : Apparent heat capacity curves for partly dried specimens with w/c-ratio of 0.50. Curve 1 : Saturated, C2 : Degree of saturation p/p$_s$ = 0.92, C3 : p/p$_s$ = 0.83, C4 : p/p$_s$ = 0.75, C5 : p/p$_s$ = 0.58, C6 : Dry. From [B 1987].

The freezing of water is accompanied by a volumetric expansion of 9 %. Hence, it is commonly accepted that the degree of saturation of the pore system of the concrete is a critical factor. The compressive strength of concrete for normal, structural purposes ranges from approximately 30 to 80 MPa, while the tensile strength – challenged by the expansion of internal ice – attains only one tenth of these values or less. Several other effects or mechanisms are proven or substantiated, but so far lack clarification concerning their relative importance.

From the 9 % volume increase of water upon freezing, the theory of 91.7 % as the critical degree of saturation arises (more accurate considerations are provided by [D 1960]). However, as will be shown in the subsequent section, not all the pore water will freeze, and higher saturation levels may occur without being critical. Nevertheless, the principle together with experience lead to the commonly accepted and standardised measure to introduce air voids to accommodate for the expansion of the water. These air voids, typically 4-6 % by volume of the concrete, require a certain size- and homogeneous distribution to perform satisfactory. Normally, the air voids are not water filled under ambient conditions.

The total air content of concrete may be determined on fresh or hardened concrete. The former procedure is based on the pressure principle (pV/T = const.), at constant temperature. The latter is based on microscopic examination on cross-sections of samples according to point count or air void chord length measurements like ASTM C 457-90 [A 1990].

The latter procedure also contains procedures to determine the air void size distribution. Formulas are derived for calculation of :

- The specific air void surface area, designated α. It describes the total volume of air voids related to their volume, expressed as [mm^{-1}] (or $\mathrm{mm}^2/\mathrm{mm}^3$).
- The spacing factor, designated $\overline{L}$, describing the half, mean distance between (the periphery of) adjacent air voids, expressed in [mm]. It thus describes "the maximum, mean distance" to an air void from an arbitrary position in the cement paste.

- - -

It is a general requirement for good durability performance that the concrete is properly designed, mixed, placed and cured to secure a homogeneous structure without flaws enhancing permeability or the accumulation of harmful substances.

2.4 Introduction to thermodynamic properties of water

In the present context, the most significant property of water is the 9 % volume increase by freezing, challenging any constraints.

Further, as reviewed by Lindmark [L 1998], the entropy of adsorbed water is lower than that of bulk water. Thermodynamic considerations imply that the finer part of the pore system is the first to become saturated and the last to be dried out. This is one of the main features of water contained in a porous media at the temperature range in question and will be explained below :

The balance between the chemical potential of water and ice should be given some consideration. The deduction below is based on Sellevold's review [S 1993b&c], starting with the chemical potential :

$$d\mu^g = -s^g dT + v^g dP^g \qquad \text{(Eq. 2.4.1)}$$

where g denotes the gas phase, T is the absolute temperature, P is the pressure, and μ and s denote the molar chemical potential and entropy of water in the gas state (vapour), respectively. Keeping in mind that $v^g = RT/P^g$ for an ideal gas (the gas equation (pV = nRT) for one mole (n = 1)) ;

$$\begin{aligned} & v^g dP^g = RT\frac{dP^g}{P^g} = RTd\ln P^g \\ & hence, \qquad\qquad \text{(Eq. 2.4.2)} \\ & d\mu^g = -s^g dT + RTd\ln P^g \end{aligned}$$

For bulk water and adsorbate, denoted "l" and "σ", respectively, the corresponding equations are :

$$\begin{aligned} & d\mu^l = -s^l dT + v^l dP^l \\ & and \qquad\qquad \text{(Eq. 2.4.3)} \\ & d\mu^\sigma = -s^\sigma dT + v^\sigma dP^\sigma + \left.\frac{\partial \mu^\sigma}{\partial \Gamma}\right|_{T,P^\sigma} \cdot d\Gamma \end{aligned}$$

where Γ is the surface concentration of adsorbed water in [mole/m^2]. The first part of equation 2.4.3 relates to the properties of bulk water. Pore water at a relative humidity (RH = P^g/P_0^g) exhibits a chemical potential compared to bulk water (i.e. saturated vapour P_0^g) given by the integral of the second part of equation 2.4.2, hence :

$$\Delta\mu = RT\int_{P_0^g}^{P^g} d\ln P^g = RT\ln RH \qquad \text{(Eq. 2.4.4)}$$

Drawing the curves for the chemical potential of bulk water – and the corresponding curve for ice, the two of them cross at 0 °C, see figure 2.4.1.

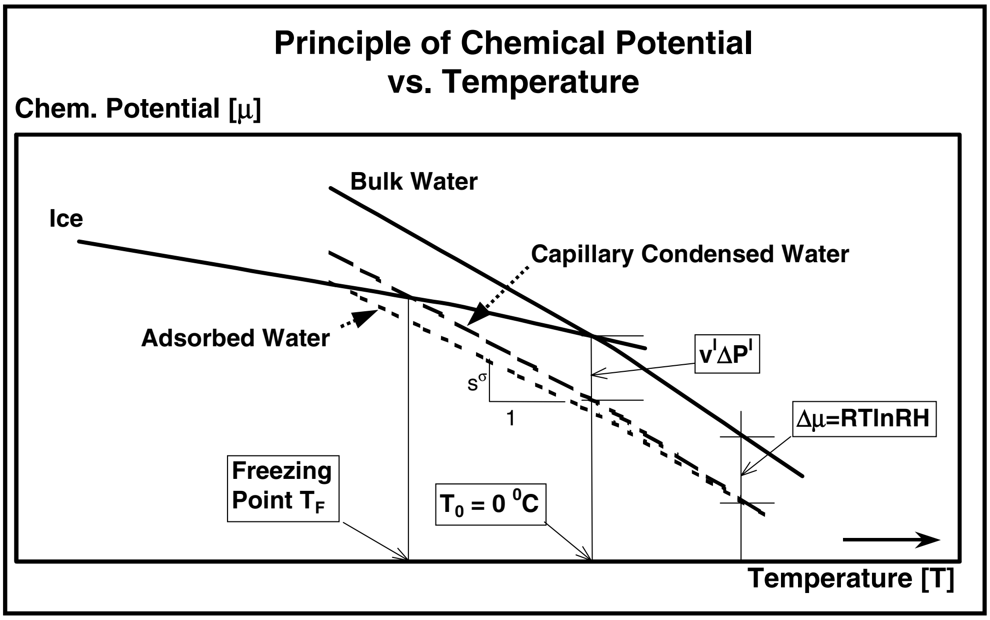

Figure 2.4.1: The principle of chemical potential of water and ice. See text for explanation. From [S 1993 b&c].

The fact that these two curves cross at 0 °C simply represents the natural phase transition between ice and (bulk) water at atmospheric pressure : There must be a potential difference in order to create a process, and the process will go from a higher to a lower potential (2nd law of Thermodynamics). The main implication of these relations for a porous material containing two or more of these phases, is the continuous redistribution until equilibrium is re-established. A decreased temperature will cause a water transport potential from the larger capillary pores to the adsorbed phase.

Furthermore, parts of the pore water is capillary condensed (i.e. not adsorbed on the pore wall surfaces) with thermodynamic properties as for bulk water. The slopes (the derivative with respect to T) of both are identical with the entropy s^g and s^l, respectively (see the equations). The difference between the absolute levels of the two diminishes as the relative humidity gets close to 1.0 (100 %).

The practical implication of the effect of the relative humidity is the drastic reduction in ice formation with reduced moisture content, figure 2.3.3. The effect is particularly evident at (negative) temperatures close to 0 °C. Already at a relative vapour pressure of $P/P_0 = 0.9$, any hydrated cement paste can be expected to be frost resistant [M 1994], if equilibrium with the moisture content has been established.

- - -

Now, to establish the freezing point depression of capillary condensed water depending on the pore size, we start with the general expression for the chemical potential. However, first a short exercise on the (under-)pressure balance of capillary condensed water :

Let us assume a cylindrical pore with pore radius r and full wetting (i.e. zero contact angle between water and pore wall and meniscus radius = pore radius) : The capillary force will amount to $2\pi r\sigma^{lg}$, where σ^{lg} denotes the capillary tension force at the liquid-gas interface along the cylindrical pore wall. The internal pressure induced in the capillary condensed water to balance it, is $2\pi r^2 P^l$. Balancing the two equations provides an expression for P^l depending on the pore radius :

$$2\pi r\sigma^{lg} = 2\pi r^2 P^l$$
$$P^l = \frac{2\sigma^{lg}}{r} \qquad \text{(Eq. 2.4.5)}$$

Hence, the expression $v^l \Delta P^l$ in figure 2.1.11 can be written $2\sigma^{lg} v^l / r$ and be inserted in equation 2.4.6 below when integrating for the liquid phase :

The chemical potential, and integrating for ice (s = solid) and capillary condensed water :

$$d\mu = -sdT + vdP \qquad \text{(Eq. 2.4.6)}$$
$$\mu^s(T) = \mu_0 - \int_{T_0}^{T_F} s^s dT \qquad \text{(Eq. 2.4.7)}$$
$$\mu^l(T) = \mu_0 - \frac{2\sigma^{lg} v^l}{r} - \int_{T_0}^{T_F} s^l dT \qquad \text{(Eq. 2.4.8)}$$

At thermodynamic balance between ice (Eq. 2.4.7) and capillary water (Eq. 2.4.8), assuming σ^{lg}, v^l, s^s and s^l not to vary (much) with the temperature range in question, an expression for the freezing point depression of the capillary water is derived :

$$\Lambda T = T_0 - T_F = \frac{2v^l\sigma^{lg}}{(s^l - s^g)} \cdot \frac{1}{r} \qquad \text{(Eq. 2.4.9)}$$

Equation 2.4.9 clearly states that the freezing point depression is in inverse ratio of the pore radius. Adsorbed water has an even lower entropy and even larger freezing point depression. Figure 2.4.2 illustrates this phenomenon by results referred to by Marchand et al [M 1994]. As previously mentioned, a large portion of the pore water will remain unfrozen, even at very low temperatures.

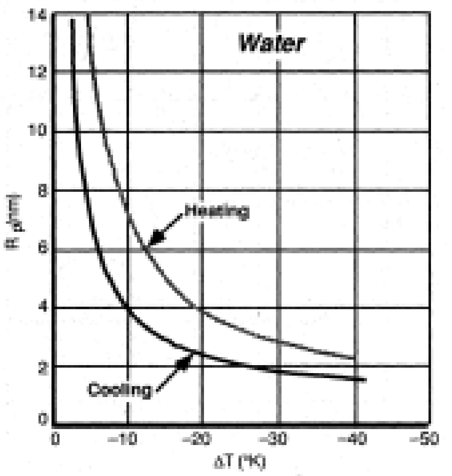

Figure 2.4.2 : Freezing point depression caused by the differences of the chemical potential of pore water and ice as described in the text. Reviewed by [M 1994].

The phenomena explained above should not be confused with the phenomenon of super-cooling, which is due to lack of available, adequate particles for nucleation :

Ice may theoretically start to form at 0 ^{o}C when lowering the temperature at normal atmospheric pressure. However, ice formation depends on nucleation ; the growth of an ice crystal requires a stable nucleus in the liquid or at the solid-liquid interface. In the liquid, this may happen on a foreign body, a dispersed particle. Helmuth [H 1960] states that the structure of cement paste does not facilitate ice nucleation on its pore walls, an effect being responsible for the often observed super-cooling of water in the pore system.

Water is an ideal solvent for NaCl, which is widely utilised as a de-icer. NaCl-solutions are effective in depressing the freezing point of (concrete pore-) water.

These – and related issues, like the viscosity of water and its relevance - are further elucidated in the review by Lindmark [L 1998].

2.5 Freeze-thaw damage theories

2.5.1 General

In the preceding, examples and general information on freeze-thaw damages is included, as well as a short review on certain concrete material characteristics and properties of water. In the present section, different theories trying to explain the damage in the sense of mechanisms are given a brief introduction :

2.5.2 Hydraulic pressure

When ice forms in the capillaries, the boundaries – the pore walls – seek to resist the expansion. According to the classic hydraulic pressure theory [P 1985], a hydraulic pressure is created within the unfrozen water of the continuos capillary and gel system, i.e. in front of the freezing front.

The pressure may be relieved if water is allowed to escape through this system to non-saturated (air) voids. If the degree of saturation is too high and the material structure unable to resist the pressure, cracking of the material will occur.

The hydraulic pressure theory is probably the most widespread explanation for frost deterioration and the protective effect of entrained air voids. It also accounts for the importance of a well-distributed air void system, reducing the maximum distance of water transport from an arbitrary location to relieve the pressure.

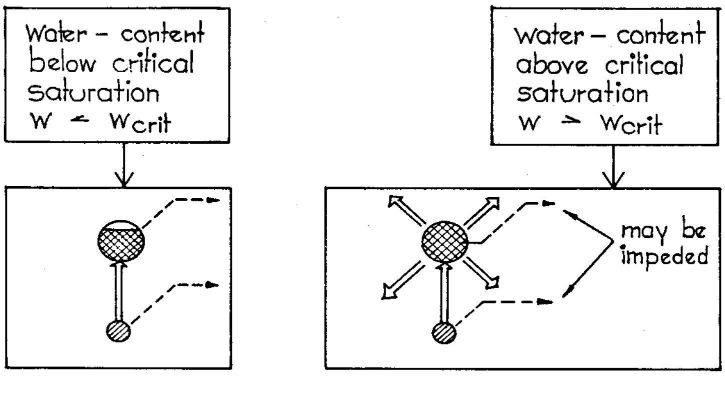

Figure 2.5.1 : The principle of hydraulic pressure, part a), from Rostam [R 1989].

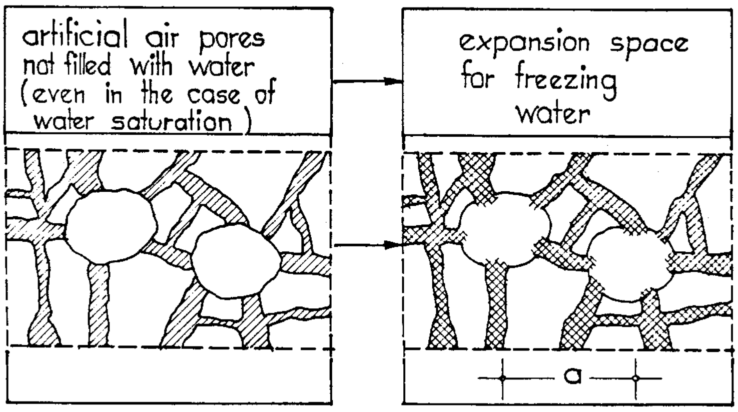

Figure 2.5.2 : The principle of hydraulic pressure, part b) from Rostam [R 1989].

However, Powers concluded that his theory did not work for higher quality concrete. As pointed out by Jacobsen [J 1999b], reduced permeability by reducing the w/c-ratio would be expected to increasingly demand the air void system, while the opposite is the case. This may be due to reduced degree of saturation, but direct relation between pressure and degree of saturation - or permeability - has not been verified to the knowledge of the present author. The main point however, is that there is much less ice present in low w/c-ratio concrete.

Still, reduced w/c-ratio will also increase the compressive and – to some extent – the tensile strength, improving the material structure's ability to resist the pressure. The swelling pressure of the water film at the pore walls, i.e. between the ice and the pore walls, is reported to amount to 8-10 MPa [C 1966, L 1998]. This is above the macro tensile strength of concrete but should be treated from a fracture mechanics point of view, an approach that has not yet been fully explored. Hence, this theory will not be discussed further.

2.5.3 Osmotic pressure

The thermodynamic basis of osmotic pressure is briefly reviewed in section 7 : The free energy of the solvent in a solution is less than the free energy of the solvent in pure solvent. There results, therefore, a spontaneous tendency for the solvent to move from the relatively high free-energy state of the pure solvent to the relatively low free-energy state of the solution.

The osmotic pressure theory as a concrete deterioration mechanism was suggested and discussed by Powers [P 1975, P 1976] as an explanation for the observed, continuous ice growth at constant temperature below 0 °C. When ice starts forming in the coarse (capillary or cavity) pores, it was assumed that different salts would concentrate in the non-frozen water close to the pore walls. This increasing salt concentration would cause an osmotic pressure, i.e. a potential trying to re-establish the equilibrium with the surroundings by migrating water from the non-frozen parts towards the ice-containing pores. The osmotic pressure would superpose that of the hydraulic pressure. The process has also been described by Schäfer [S 1964].

The formation of osmotic pressure does not only depend on differences in salt concentration, but also on the existence of a semi-permeable membrane, allowing the solvent to pass but not the salt molecules (in the opposite direction). Though contradicted by Litvan [L 1976] as a possible effect, Powers [P 1976] referred to studies by Verbeck, demonstrating the membrane effects of cement paste : The membrane resists the movement of alkali ions more than it does water molecules, and an osmotic pressure will develop and be manifested throughout the period of diffusion (of ions) and counter-diffusion (of water). Consequently, the cement paste seems able to function as a semi-permeable membrane, even though it is not semi-permeable in the conventional sense.

Even though he contradicts the possibility of osmotic effects within the concrete, Litvan [L 1976b] claims that the first freezing and forming of ice bodies comprises the freezing of pure water only. The “second” freezing, taking place at approximately –22 °C, he claims, is attributed to the freezing of the remaining eutectic solution. This statement supports that during a period of cooling, pores or parts of pores may contain solution with high (and increased) salt concentration, causing salt gradients.

The discussion above however, relates to the creation of osmotic pressure randomly in the structure, depending on the equivalent randomly forming ice bodies – and a freezing process slow enough to enable increased concentration in the remaining pore water. This is in contradiction to the studies of Gran [G 1995], who stated that the rapid growth of ice crystals would by far exceed the possible salt ion diffusion within the pore liquid. Hence, according to his conclusions, ions of any kind are likely to be entrapped by the ice. This supports the idea of the thermodynamic in-equilibrium between non-frozen pore water and ice (section 2.4) being responsible for internal re-distribution of water during cooling – and the continuous ice growth at constant temperature (below 0 °C).

However, osmotic pressure may still apply to salt gradients close to the surface : Exposed to a salt solution at the surface, salt ions will slowly start to penetrate into the concrete. If, initially, this creates a salt gradient, the gradient will generate an osmotic pressure, which in turn may cause water migration from the interior towards the surface. In this case, an increased saturation close (< 1 mm ?) to the surface would theoretically be possible.

Petersson [P 1985b] made an attempt to investigate this by pre-storing concrete samples in different salt concentrations prior to freeze-thaw testing. Based on the results, Figure 2.5.4, it was concluded that the damage is controlled by the outside salt concentration, but "existence of chlorides in the pore water seems to reduce the damage when (freeze-thaw) tested in 3 % salt. Further, it was claimed that damage is not related to osmotic pressure, whether internally or close to the surface.

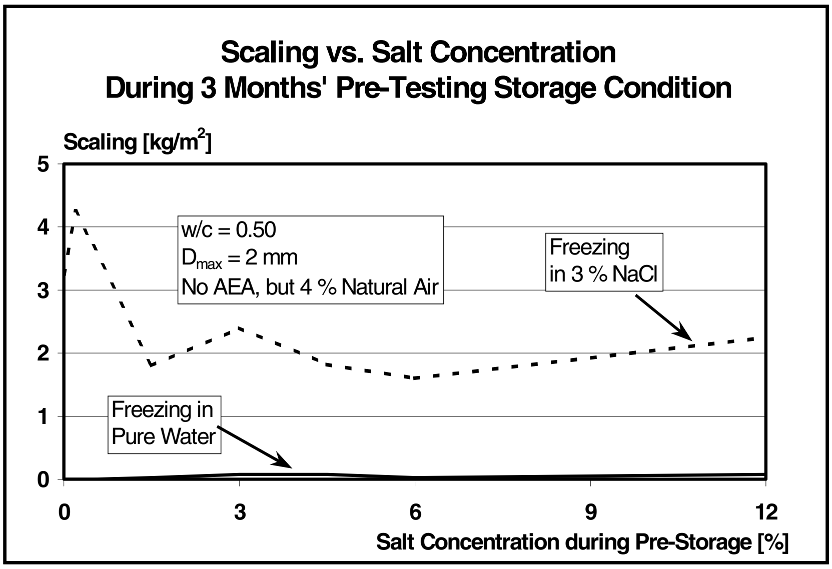

Figure 2.5.4 : Investigation osmotic effects on samples pre-stored in different salt (NaCl-) concentrations prior to a scaling test, the main principles of which in accordance with S 2000. The scaling values are obtained after 5 (!) freeze-thaw cycles only. Reprint of results reported in [P 1985b].

Sellevold and the present author made a similar attempt on dried, re-saturated samples [S 1988b], the results of which are presented in figure 2.5.5. The freeze-thaw testing comprised 3 % NaCl only but two concrete qualities. As expected from the amount of freezeable water within the temperature range in question, the scaling is reduced when the salt concentration of the pore water increases (figure 2.5.5). If – by any chance – there is an osmotic effect when increasing the pore water concentration from zero to 6 %, it will be counteracted by the reduced amount of freezeable water.

However, in this context, the attention should be focused on the last part of the curves, displaying increased scaling when increasing the internal salt concentration from 9 to 12 %. The same tendency is evident in the results by Petersson (figure 2.5.4), although probably not taken as statistically significant by him. Hence, increasing difference in salt concentration between internal and external salt solution seems to increase the damage, even if the internal, freezeable water amount is likely to decline. This could be due to increased suction from the external, caused by an osmotic pressure.

An even stronger argument for this mechanism would be if the effect diminished with time, as a function of proven changes in the salt gradient. Such studies, however, were not included in the work performed at that time.

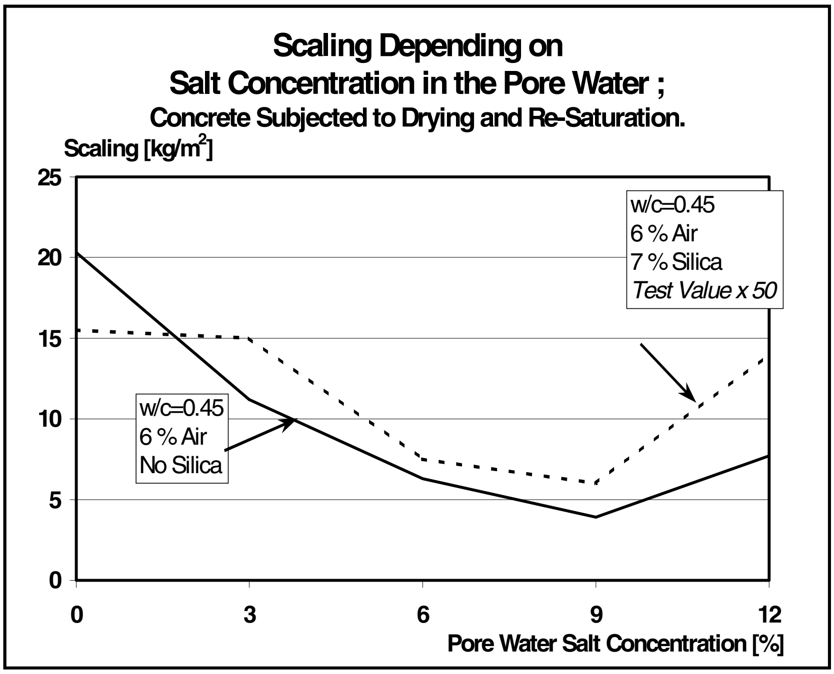

Figure 2.5.5 : Scaling test with 3 % salt solution on the top surface according to S 2000 on two concrete qualities subjected to a) drying at 50 °C for two weeks, then b) immersed in salt solutions of nominal salt concentration as indicated, values attained after 42 freeze-thaw cycles. Previous works had demonstrated that the salt concentration of the pore water was very close to that of the respective immersion salt solutions. Previously non-published data by Sellevold and the present author reported in [S 1988b].

Summarising the issue of osmotic pressure, there is no evidence that osmotic pressure arises in the "bulk" structure of the concrete. The continuous ice growth at constant temperatures below 0 °C is most probably caused by non-frozen pore water moving towards the ice surfaces in the coarser part of the pore system, thereby reducing the free energy of the water. Osmotic effects may however, still occur at the concrete surface, see section 7 for further discussion and references.

2.5.4 Crystallisation pressure

The growth of salt crystals in larger pores of the cement paste could also lead to pressure generation in the solid (salt) phase [H 1978]. A prerequisite would be the presence of a supersaturated salt solution, produced either by the evaporation (warming) of water or by freezing a part of the pore water (cooling). In the latter case, freeze-drying of parts of the pore system due to the thermodynamic in-equilibrium previously discussed might be the triggering factor.

Harnik et al [H 1978] anticipates that the formation of salt crystals would start in the largest pores when the solution reaches its super-saturation. Analogous to the water transport, a transport of salt ions might take place, from the smaller pores (which hinder crystallisation) toward the salt crystals. If it is possible for the solution to penetrate between the salt crystals and the surrounding boundaries, the crystals may be able to grow and to exert an increasing pressure on the cement gel.

Publication on the issue has been relatively rare, and it has received little attention during the last two decades. Thus, the theory is presently not considered as an important contribution in explaining deterioration during freeze-thaw.

2.5.5 Temperature shock

The application of de-icing agents to a frozen concrete surface, covered by ice, will lead to a temperature shock and stresses in the surface : The ice will not be stable in the presence of (an appropriate amount of) salt. The thawing of the ice will cause a significant heat loss from the concrete surface. This heat loss will be limited to the very outer layer, causing a substantial temperature drop within it. Thus, there is a risk of introducing temperature stresses exceeding the tensile strength of the concrete cement paste. The principle is illustrated in figure 2.5.6.

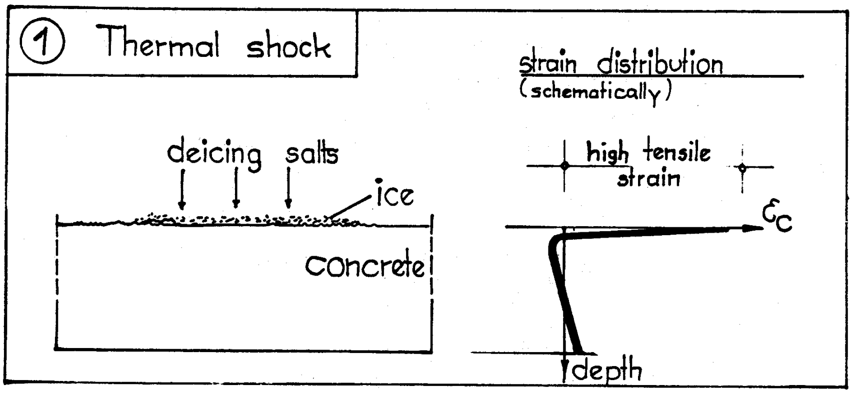

Figure 2.5.6 : Thermal shock to a concrete surface layer, caused by application of a de-icer to a frozen surface covered by ice. From [R 1989]. The phenomena are outlined more in detail by Rösli & Harnik [R 1980].

2.5.6 Displacement of the freezing front

A damage sometimes observed in the field is that spalling of a 10 – 20 mm thick layer in one freezing cycle occurs “suddenly”. Rostam [R 1989] explains this special scaling feature as a displacement of the freezing front due to salt in the pore water, see figure 2.5.7. He considers the phenomenon to be caused by simultaneous salt- and temperature-gradients, leading to initial freezing of the surface and a separate layer somewhat further down. This is supposed to entrap water, seeking to escape, when the middle layer finally freezes.

However, considering the normal air void requirements, water is not expected to be expelled more than one mm at the maximum. Hence, it is probable that the expelled water must be accommodated locally, i.e. within each of the indicated layers, whether neighbouring layers are already frozen or not.

An alternative explanation is that the salt concentration in the outer layer depresses the freezing point in the outer layer, but not further down. Hence, temperature drop from the outside under such conditions may cause the deeper level to freeze first. In either case, the damage may occur as the spalling-off of a layer as described above.

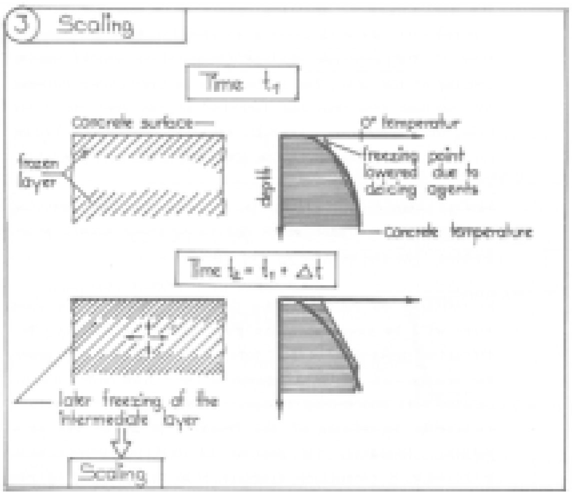

Figure 2.5.7 : Displacement of the freezing layer caused by salt gradients within the concrete close to the surface, from [R 1989]. See text.

2.5.7 Further effects of de-icing chemicals

The use of de-icing chemicals will increase the content of such chemicals in the pore water of the concrete, at least in the surface layer. The result will be a depression of the freezing temperature, having several consequences.

Depending on the environmental conditions (temperature cycle), this may increase the number of freeze-thaw cycles – or it may reduce it. Further, the pore water remains liquid for a longer period. This will reduce the amount of ice present at temperatures a few degrees below zero. The reduced amount of ice formation should be positive, but there might be negative effects in contributing to unfavourable (prolonged in time) re-distribution of water. Also, when the pore water finally freezes, this happens faster than freezing without depression of the freezing temperature. This may increase the effect of the hydraulic pressure, since the time frame available for the pressure relief is reduced.

Salt is a hygroscopic material and exposed on a surface, it will contribute in keeping the surface wet. Applied to an ice or snow covered surface, it will provide additional water, causing increased degree of saturation.

There is clear evidence that there is a certain pessimum (“negatively optimum”) concentration of the external de-icing chemical, by which the damage is maximised. Both lower and higher concentration will reduce the deterioration.

Figure 2.5.8 by Verbeck & Klieger [V 1956] is classical, in fact, they refer to studies performed already in 1943 by the Swedish road administration.

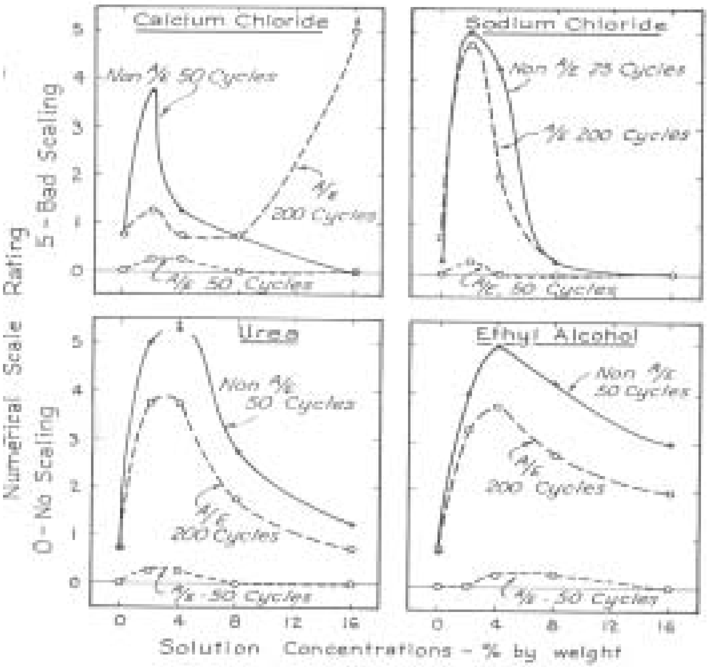

Figure 2.5.8 : Effect of de-icer concentration on concrete surface scaling [V 1956].

The reason for this pattern has never been fully explained, but several of the previously (combined) explanations are possible. At the time of the study, there was a discussion whether frost damage was a partly chemical or purely physical effect. The test results were taken on the account of the latter.

The very important fact remains however, that the damage to concrete is greatly increased in the presence of de-icing salts.

2.5.8 Miscellaneous

It follows from this section that re-distribution of moisture is a factor contributing to the complexity of freeze-thaw damage. Since it will be further dealt with in subsequent sections, it will not be discussed at the present. However, it should be mentioned that Sellevold [S 1988b] included studies confirming that the damage depended on the exposure time at the minimum temperature level of the freeze-thaw test, confirming ice growth at constant temperature.

From the same and many other works, it was evident that minor structural changes of the concrete - in the sense of minor changes in design or workmanship/manufacture - may significantly change the performance of concrete subjected to freeze-thaw. This also addresses an experience of the present author : Numerous investigations (e.g. [R 1995, B 1997]) performed on field or laboratory manufactured samples exhibited various degrees of bleeding and disadvantageous void structure due to improper use of chemical admixtures (additives) in concrete design or placing technique. This improper structure seemed closely related to the outcome of consecutively performed freeze-thaw tests, see subsequent sections.

Stark [S 1996, S 1993d] proposed chemical instability of mono-sulphate - being transformed to ettringite - as a potential degradation process in combination with freeze-thaw. For portland cement binders, they demonstrated a correlation between the C_3A content of the cement and deleterious amounts of freeze-thaw induced formation of ettringite.

Also, binders containing ground granulated blast furnace slag may form unstable forms of $CaCO_3$ when subjected to carbonation. Combined with leaching, this may increase the surface porosity. In contrast, the carbonation of portland cement binders is considered to improve the freeze-thaw properties.

Bager and Jacobsen [B 1999] presented what they called “a conceptual model”, for the frost deterioration, based on different simultaneous or alternating mechanisms. They considered three different (ambient) conditions, described in short below :

1. Freezing in air, ice formation will take place randomly at different temperature levels. The individual, micro ice bodies forming will attract water from the surroundings due to the lack of thermodynamic equilibrium, with local swelling as a result. The gel, on the other hand, will shrink. The authors believe the net effect to be expansion for highly saturated concrete of high w/c-ratio, shrinkage at low w/c-ratio as long as the capillary suction is insufficient. Concrete subjected to expansion in this way will develop cracks around the coarse aggregate particles.

2. Freezing with water at the outer surface, ice formation will start at this surface, due to the temperature gradient, and penetrate into the material as an ice front via the continuous capillary system. Water will migrate as in the former case. Additionally, water from the outside will be taken up by :

- the ice in the interior, from the surface water during melting (when melting first occurs at the surface).
- suction arising when the internal ice melts with a 9 % volume reduction.

The water uptake will result in an even distribution of the degree of saturation and, therefore when critically saturated, internal cracking.

3. Cooling with salt solution at the external surface, a depression of the freezing temperature will occur externally. Hence, ice nucleation may appear randomly in the pore system saturated by water and progress as previously described. As long as there is still liquid at the exterior, the saturation may continue to increase by migration of water towards the internal ice bodies. Supposing the main ice formation initially to take place close to the external surface, the thermodynamic potential may draw water from the interior towards the surface and “artificially” increasing the saturation at this point. Any osmotic pressure – caused by the externally, higher salt concentration - would have effect in the same direction. The result might very likely be surface scaling, in contrast to the internal cracking described in the two other cases.

Some of these hypotheses remain to be verified. For instance, when freezing with external salt solution, the freezing point depression of the external salt solution would have to exceed the super-cooling of the pore water close to the surface. Practically, there would have to be almost no temperature gradient.

However, the objective of this section is to provide an outline of the phenomena related to freeze-thaw mechanisms and to motivate the subsequent studies, not to discuss every aspect. Hence, the discussion of the general points will be closed at this stage.

2.5.9 Synopsis

There is evidently no single deterioration mechanism that can account for the damage - or resistance to such – by concrete subjected to freeze-thaw, with or without the presence of de-icing salt. Nor have any of the single mechanisms described above been rejected by convincing arguments, nor established clearly.

Obviously depending on the actual, environmental - as well as material – parameter in the specific case and exposure, several of these simultaneously and partly counteracting mechanisms will play a role.

The key action in material testing, material design and future product development under such circumstances must be to conduct studies, enabling the (potential) mechanisms to act as closely related to those of field exposure as possible. In particular, this seems to apply regarding the moisture mechanics resulting from the interaction between the external and the internal environments. The investigation of such relations became one of the objectives of the present work.

2.6 Testing of Frost and Freeze-Thaw Resistance

2.6.1 Introduction

Concrete strength can be fairly well predicted when the concrete constituents and their characteristics are known. Concrete strength within common strength classes and normal manufacturing processes is normally predictable within some MPa, i.e. 10-20 % of the target strength. Concerning durability properties, the relative uncertainties often are 10 times higher or more. This is especially so if the materials parameters (e.g. w/c-ratio, air content, type of binder) are close to "threshold values". This is the reason for specifying concrete composition parameters, rather than specifying performance requirements in a given test method. The specifications have to take into account the environmental conditions of the structure's service life – the field conditions – like it has been done in the standard EN 206 "Concrete performance, production, placing and compliance criteria". Specifications normally include requirements with respect to the w/c-ratio. For particular projects, they may also include air void structure requirements, obtained from trial mixes and/or throughout the execution of the work. The principle of specifications, of course, relies on certain established relations.

Of course, such materials specifications do not very accurately predict the performance. Also, new materials or combinations may not have adequate field records of proven properties. Last, but not the least, the durability properties of a concrete structure are a combination of the potential material properties – and the casting, placing or finishing technique and the curing applied. All this makes it desirable to perform testing of durability properties, as is the case with respect to frost and freeze-thaw resistance. The testing principles commonly used with respect to frost deterioration comprise different approaches :

- A performance test is the critical degree of saturation method, as described in principle in the following section. This is a combined test of the degree of saturation likely to occur in the specific material – compared to the degree of saturation the concrete can have and still remain undamaged by freeze-thaw treatment.

- For scientific approaches aimed at understanding mechanisms, special methods may be used, e.g. low temperature calorimetry measurements (previously mentioned). To diagnose after freeze-thaw, the dilation during cooling – and the residual length change after a number of freeze-thaw cycles have been studied. However, these are rather delicate, time consuming or costly methods, used for fundamental research.

The principles mentioned above do not take into account the interaction between the environmental conditions and the moisture content changes or re-distribution within the concrete material. This consideration motivates :

- More direct performance tests comprise a variety of different procedures, believed to represent at least some field conditions in principle. The methods include surface scaling and some way of determining internal cracking. The common feature of the methods is that samples are subjected to a higher number of freeze-thaw cycles, where moisture interaction with water or salt solution external to the sample is allowed. Further, the test methods are easy and practical – although they may last a few months – and several are not very costly. In sections 2.6.3 - 5, such performance test methods will be discussed.

2.6.2 Degree of saturation

As already argued, the degree of saturation is essential in that it determines the amount of ice forming during freezing. The maximum level of saturation not causing any damage is defined as the critical degree of saturation [F 1976, F 1976b]. The value is assessed by exposing samples, pre-wetted to different levels of saturation, to freezing and thawing. Subsequently, the samples are tested to a performance criterion, e.g. the dynamic modulus of elasticity, see figure 2.6.1.

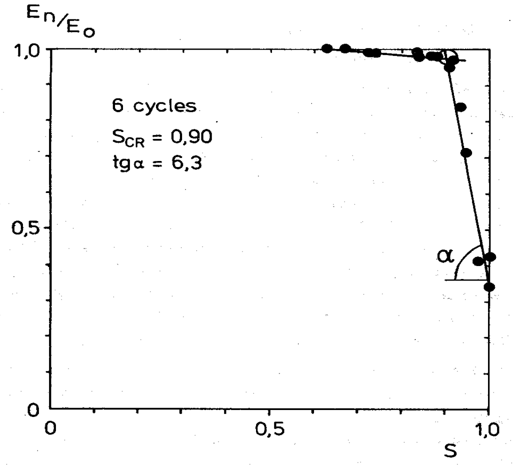

Figure 2.6.1 : Example of the determination of critical degree of saturation, determining the elastic modulus of elasticity on samples pre-saturated to various levels and subjected to a number of freeze-thaw cycles. From [F 1976b].

The derived, critical degree of saturation, S_{cr}, is then compared to the potential, in-service degree of saturation, called "actual degree of saturation", S_{act}. In many cases, S_{act} may be replaced by the degree of saturation caused by capillary suction, S_{cap}. If the actual degree of saturation is lower than the critical degree of saturation, the concrete is considered to be frost resistant. Fagerlund [F 1976b] discusses the theory in detail and provides a formulae, yielding a sort of potential freeze-thaw resistance :

$$F = S_{cr} - S_{act} \qquad \text{(Eq. 2.6.1)}$$

Fagerlund [F 1981] also suggests a principle for estimating the service life based on the same theory, using the modelling (extrapolation) of capillary suction – and indirectly – the "initiation period" – as qualifications for the service life limitation. In the resulting Rilem recommendation, the principle is used for estimating the risk of frost damage [F 1977].

The principle of this test procedure is clear. However, the practical assessment of these values becomes very difficult for dense concrete qualities. Water penetration will be limited or take very long time, complicating correct and even distribution of the pore water. Also, it does not necessarily take into account whether the effect of the freezing and thawing action on the internal microclimate is representative for the field conditions. The latter means that there should still be applied a freeze-thaw test providing certain boundary conditions relevant for service life, reproducing the relevant thermodynamic conditions.

Though, the externally related moisture conditions are considered fixed prior to the freeze-thaw test, and experimental evidence shows that only a few cycles are necessary to force the damage. Also, some of the obstacles for more widespread use of the method may have been removed by the suggested use of thin plates for assessing the critical degree of saturation. Fagerlund [F 1999] described a refined version of the original method, solving some of the problems.

2.6.3 Beam tests : Internal damage

ASTM C 666. The two principles of this test procedure are a) freezing and thawing in water or b) freezing in air and thawing in water. The beam samples are of typically 3-4 x 16 inches. The number of freezing and thawing cycles may be 6 per 24 hours. Instead of water, submerging in salt solution has been frequently applied during the last 25-30 years [J 1997]. The basic principle – submerged beams – is also used in the Austrian standard ÖNORM B 3303.

The principle of these test methods is the more or less complete immersion of samples subjected to a high number of freezing and thawing cycles. At certain intervals, the dynamic E-modulus of the samples is determined, as a way to detect deterioration.

The testing principle is used to evaluate damage caused by internal cracking. No clear relationship exists between the “degree of durability” for internal deterioration and mass loss, i.e. surface scaling [J 1997]. Nor does the application of a salt solution necessarily produce results different from those obtained with pure water. This is in clear contrast to field conditions and scaling tests where salt solutions always leads to increased damage.

2.6.4 Scaling tests

A variety of national and international test methods [prEN xxx, SS 13 72 44, ASTM C 672, CDF/CF-Test (See [S 2000] and [S 1995])] employ this principle : Concrete samples are exposed to water or salt solution on one side and a more or less one-dimensional heat flow during a number of freeze-thaw cycles. One or two temperature cycles per 24 hours (within certain limits) are prescribed. At certain intervals, the scaled off material is collected, dried and weighed. The samples may also be weighed or rated in other ways.

A special feature of the CDF/CF test is that the samples are exposed to the freezing medium (water or salt solution) upside-down. Also the temperature regime of this test is very strictly defined.

The reference method of prEN xxx is a modified version of SS 13 72 44 and is often referred to as the (Scandinavian) slab test. Horizontal slabs are insulated on the lateral sides and the bottom, and the top surface is covered with a 3 % sodium chloride solution – or de-ionised water. This freezing medium is protected against evaporation to avoid changes in the salt concentration throughout the test. The samples are then subjected to specified freeze-thaw cycles – one per 24 hours. Standard test duration of this procedure is 56 cycles (8 weeks). However, the test procedure also comprises a closely specified pre-curing and preparation procedure, completed by three days of re-saturation of the test surface by water, prior to the freeze-thaw test. Since this procedure has been used extensively in this work, a more detailed description is included in appendix A.

2.6.5 Miscellaneous

Some of the methods above have been further modified to more specific – and partly simplified - versions for product performance testing. Examples of such are prEN 1338 and 1339 for concrete paving blocks and pre-cast concrete flags.

Lately, i.e. after completion of most of the present studies, attempts have been made trying to combine scaling and internal cracking in a single test. Examples of such work are given in the studies of CEN TC 51 / WG 12 / Task Group 4 and the Rilem committee TC IDC. Some early studies were carried out by Jacobsen [J 1995], Studer [S 1993f] and the present author.

Attempts have been made to compare or correlate different test methods to each other : Pigeon et al obtained lower values for the critical spacing factor when introducing silica fume and testing according to the ASTM C 666 test [P 1987], i.e. silica fume enhanced the requirements. In a previous study [P 1986], the scaling was found to decrease when adding silica fume, i.e. silica fume improved the scaling resistance. In the same report, silica fume was found to increase the internal cracking (ASTM C 666) of air entrained concrete, but not that of non-air-entrained concrete. The whole phenomenon was attributed to the different nature of scaling and internal cracking. The important question should be which of the methods correlated better to the field conditions.

Another comparison of scaling and internal damage was made by Sellevold and Jacobsen [S 1993e]. The investigation showed much poorer performance in the ASTM C 666 test compared to scaling tests.

\- - -

Furthermore, precision data of the specific test procedures is an important issue [S 1990]. Poor reproducibility of a freeze-thaw test procedure and material scatter may influence the conclusions negatively. However, test procedures with enhanced precision are not necessarily more relevant to field exposure than those with poorer precision. Since field exposure and its correlation to testing has not received very much attention, there is a risk that laboratory tests may be adopted on the basis of precision alone. Therefore, field exposure should receive more attention :

2.7 Field exposure

Field exposure tests deviate significantly from that of the exposure in a laboratory test. The deviations include environmental conditions like the temperature and moisture regime, as well as the properties of the exposed material :

The laboratory curing procedures normally lead to higher degree of saturation than field exposure at the initiation of freeze-thaw. Both the moisture and the temperature conditions in the field varies considerably, see section 5. In contrast to the laboratory tests, the temperature cycles in the field will vary significantly over time. There will be long periods of temperatures above zero and/or with low external relative humidity, allowing the concrete to "breathe".

While laboratory tests are mainly performed on young concrete, the maturity of the field concrete normally is much higher at the point of the first freeze-thaw attack. This implies a more developed microstructure and higher degree of hydration of the cement or other binders. Further, there normally has been an interaction between the concrete surface and the external environment in the sense of drying and re-wetting of the outer surface. This is one of the major processes involved in the ageing of concrete. It is demonstrated by Bager and Sellevold [B 1986b] that the drying and re-wetting of cement paste increases the volume of the large pores and the continuity of the pore system. It is also well known [L 1997] that substances over long term will deposit in parts of the pore system, depending on the environmental conditions. Possibly, this reduces the "relieving" function of the air voids in connection with freeze-thaw. As reviewed by Marchand et al [M 1994], the carbonation of the surface layer will change the porosity properties of that layer as well : Portland cement paste will be denser as a result of the carbonation, while the opposite seems to occur with slag containing binders. This may influence the water uptake. Although such changes may be "reproduced" under laboratory conditions [K 1992], it is uncertain to what extent these changes equal those under field conditions.

Not many studies actually report field observations on freeze-thaw resistance. Farstad [F 1992] investigated the field and laboratory performance of New Jersey road safety barriers along roads of the Oslo region. The roads had heavy traffic flow and frequent application of de-icing salt. Barriers with a southern exposure direction had significantly larger damages – compared to others of equal traffic flow. Hudec et al [H 1986] also investigated concrete barrier walls in the field. They reported a more severe microclimate on south facing walls ; a greater number of freeze-thaw cycles, higher freezing and thawing rates, more severe temperature gradients in the surface layer and more wetting and drying. Also, the number of times above “critical” saturation was reported as more frequent.

- - -

The main characteristic of field exposure is climatic variations, resulting in variable moisture history in the concrete (at least the surface). There is also an interaction between the environment and the long-term changes naturally occurring in the concrete, like chemical modification and pore changes mentioned. All the deviations between laboratory and field conditions strongly motivates studies on the correlation between them :

2.8 Correlation between laboratory testing and service life

Because of the differences between field and laboratory conditions mentioned above, there has been an increasing need for correlating the two types of exposure. Laboratory testing should provide an accelerated way to predict the performance of the material during its field service life. Still, laboratory testing must activate the mechanisms occurring in the field. This is utterly important, since the decisive mechanisms are not yet fully understood : Even if single mechanisms are identified from a theoretical point of view, it has not been determined which ones become critical under which circumstances.

The study by Farstad [F 1992] mentioned above showed little correlation between the field performance and subsequent laboratory testing on samples obtained from the field elements. Nearly all the samples failed severely in the laboratory, independent of the preceding field performance. In connection with several concrete pavement investigation for Norwegian highways in the late 1980’s, even non-air-entrained concrete of w/c-ratios up to 0.40 exhibited acceptable performance in the laboratory [R 1989b] according to the scaling test SS 13 72 44. It also performed well in the field, exposed to freezing and de-icing salts, for at least a decade. However, from the previously mentioned [S 1993e] and many other works, it is reasonable to raise the question concerning similar experience based on ASTM C 666 testing.

Petersson [P 1995] reported field exposure both in marine and highway environment, stating that the latter was by far more aggressive. Contrary to laboratory test results, there are indications that non-air entrained concrete seems to perform well in both types of field exposure, provided that they satisfy certain maximum w/b-ratios. However, the field samples are subject to prolonged exposure ; this will be reported later.

A major new Swedish study reported by Utgenannt [U 1999] - after the completion of most of the work of the present author - compares the field performance of concrete in a highway environment to that of the initial laboratory testing on parallel samples. He concludes after three years of field exposure that the slab test (SS 13 72 44) seems to estimate the field performance reasonably well for portland cement concrete. The correlation with slag cements in particular – and partly silica fume concrete is less evident. The complete study is expected to appear as a dissertation in a couple of years from the present date. However, the results should be regarded as preliminary and subject to further study.

- - -

The applicability of test procedures, based on their relevance for field conditions should be given high priority for further investigation [S 1999]. For the internal cracking test principle, it has been argued that “such a correlation is totally absent” (quote [V 1999]). This is a very categorical statement, but at least it is important to raise the issue, both on surface scaling and internal damage.

2.9 Synopsis

It seems evident that the present lack of correlation between field and laboratory data should make this an important topic of technical and commercial interest. Geiker et al [G 1999] stresses the need of verifying the service life of concrete with respect to freeze-thaw resistance.

Several countries specify concrete composition for the environmental conditions in question. However, there is a unanimous opinion that this concept is not sufficient [S 1999] : New concrete constituents and modified concrete composition without field records or known properties are being used. Also, the committee preparing the new concrete standard EN 206 encourages development on performance test methods. Both CEN and Rilem task groups have accepted the challenge.

In the present work, it was decided to proceed on issues related to the interaction between age, curing, moisture changes and materials of concrete subjected to freeze-thaw. It was decided to base the testing on SS 13 72 44 (See description elsewhere).

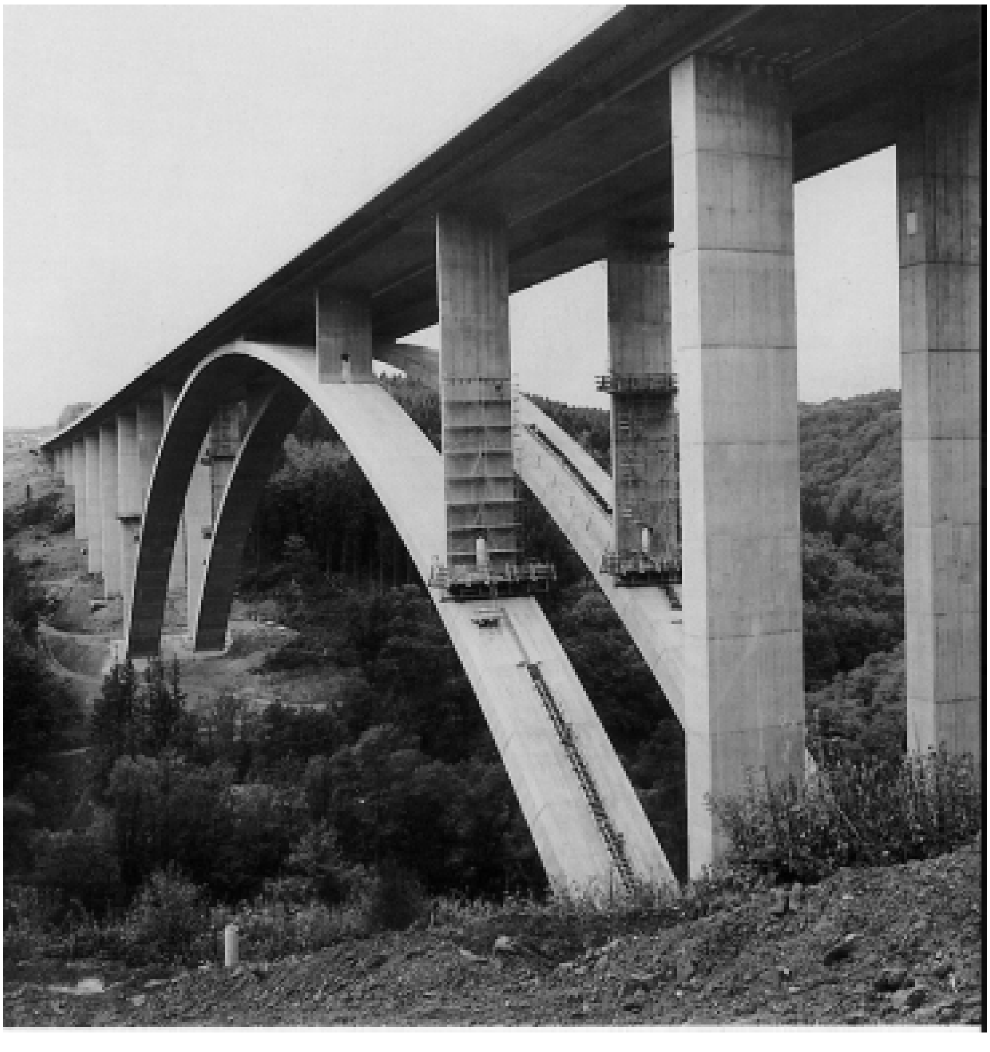

Figure 2.9.1 : The longest arch bridge of Europe, the Kyll valley highway bridge on the A 60 near Bitburg (also known for another type of prosperous substance …), Germany, constructed with a CEM II/B-S 42.5 (slag) cement. Blended cements are increasingly used for such structures. From [V 1999c].

3 Curing and ageing of concrete with and without silica fume

3.1 Objective

From the preceding section, it becomes evident that freeze-thaw resistance testing of four weeks old, laboratory cured concrete samples not necessarily represent the scaling resistance under field conditions. The deviation from field performance would expectedly increase if the concrete mix design requires extra curing time compared to “ordinary portland cement” concrete. The same is probably true for the degree of saturation if it is disfavoured by a non-representative extent of water exposure prior to testing. Early water curing of slowly reacting/”maturing” concrete may allow for higher water intrusion at this stage compared to that of concrete containing pure portland binder. If the water exposure is unrealistic for such young concrete under field curing conditions, this may particularly disfavour slowly reacting binders. Hence, especially the test results from standard laboratory curing and freeze-thaw testing of concrete containing pozzolanic materials should be treated with care.

The objective of the present study was to investigate the performance of concrete with silica fume under different curing conditions. At the time of the initiation of the present study, several researchers had investigated the influence of pozzolanic materials on a variety of properties without considering such a parameter [C 1992]. In order to demonstrate the importance of the issue, it was decided to let the study include concrete with and without silica fume with respect to freeze-thaw scaling resistance. The main variables were the influence of different moisture conditions and the effect of ageing prior to the scaling test.

The study included three levels of nominal air content; 1, 3 and 6 %, slump levels 50 mm and 150 mm, two cement types ; C_3A - contents of 8 % and 1.5 %, alkali contents of 1.15 % and 0.45 %, respectively. Dosages of silica fume were 0 % and 10 % of the cement content, w/(c+s)-ratio was kept constant at 0.45. It was expected that this range of concrete design would provide a range of results, creating a pattern to clarify the effects of silica fume.

This section is based on a paper presented by Rønning et al [R 1995b] but has been completely re-written and extended with respect to the discussion of the test results.

3.2 Introduction

3.2.1 General

A state-of-the-art report concerning silica fume concrete had been provided by FIP [S 1988c]. Numerous questions remained unsolved. Silica fume concrete (containing 19 % silica fume) had also been reported to behave quite differently (negatively) to that of pure portland cement concrete when subjected to freezing in a saline environment [P 1986b] : Petersson described two principal stages in salt-frost attack : 1) The first exhibits initial scaling during the first freeze-thaw cycles and then levelling off for good quality concrete. 2) A second stage starting later, possibly caused by an over-critical degree of saturation. This second stage was reported to be more pronounced and typical for silica fume concrete, leading to much more severe deterioration.

3.2.2 Air entrainment

When using silica fume, a water reducer or a superplasticizer would normally also be used to compensate for the increased water demand. Combining this with air entraining agents will give rise to additional complexity in mix design and air void stability. Still, proper air entrainment in silica fume concrete can easily be obtained.

Sellevold [S 1988c] also refers to Petersson, comparing the effect of air-entraining agents alone and combined with water-reducing agents. For equal, total air content the salt scaling was much higher for the admixture combination. This was clearly explained by a coarser air void system. (These mixes did not contain silica fume.)

Introducing water-reducing admixtures without changing any other parameter will change the viscous properties of the concrete. In the study above, water-reducing admixtures seem to have been added *without a corresponding change in water requirement* of the fresh concrete. The implication is that the yield value of the fresh concrete is likely to change drastically [W 1990]. The coarsening of the air void system is likely to be due to this change. Whether the change was “provoked” by the water-reducing agent or could have happened by an alternative increase in water content (to achieve same slump level) is another matter. Also, the change in apparent air void characteristics under such conditions are not necessarily representative to that of simultaneous use of water reducing agents and silica fume, the latter increasing the water requirement.

3.2.3 Freeze-thaw testing

Opsahl [O 1990] found that silica fume in combination with water reducing agent improved the performance (ASTM C666 / Procedure A; 25 mixes of different composition). This was attributed to changes in the capillary pore system. The efficiency factor of silica fume with respect to durability was found to exceed that of compressive strength for these mixes [S 1988c]. Hooton [H 1993] similarly experienced that while the control portland cement concrete failed in ASTM C666 Procedure A, silica fume concrete survived 900 cycles (high strength, non-air entrained concrete mixes). This was contradictory to studies reported by Malhotra, who found that all mixes without air entrainment, but with silica fume and water/binder-ratios from 0.25 to 0.36 mm, failed [S 1988c].

Hammer et al [H 1990] also found a negative effect of silica fume. However, they tested a moulded surface. Such a surface may have properties deviating from the bulk properties. Between mixes of a series, the deviations may be different with different fresh concrete properties. Although the authors pointed out no reason for the behaviour, they characterised the results as unexpected, based on supplementary data.

Malhotra et al [M 1987] tested numerous mix designs for high strength concrete, with w/(c+s) ranging from 0.25-0.36 according to ASTM C666 Procedure A. They found poor performance, even with 4 % air entrainment or more. They pointed out that this might be attributed to unsatisfactory air void spacing factor, even with entrained air. This is consistent with Aitcin [A 1986] : The spacing factor had a tendency to increase with the amount of silica fume present. Though, this again may be attributable to the simultaneous increase in superplasticizer dosage, which will provide a poorer air void system unless measures are taken.

Nevertheless - as previously mentioned - Pigeon et al [P 1986] found evidence for a significantly lower critical spacing factor for silica fume concrete when exposed to ASTM C666. This was true even if the surface scaling of the same concrete was reduced – without reducing the spacing factor. In a further experiment, Pigeon et al [P 1987] even found a higher susceptibility to scaling, when tested according to ASTM C672. Still, they found that silica fume concrete performed just as well in the field as reference concrete. This was in spite of slightly higher w/c-ratio of the former, but with air void spacing factors in the range below 0.20 – 0.25 mm [S 1988c]. Virtanen [V 1990] also argues that ageing outdoor, at least in ambient conditions in Finland, is not so harmful to concrete containing additions as has been claimed by testing of artificially aged concrete. Correspondingly, his results indicate improved salt scaling resistance when silica fume is applied.

Summarising, this leaves us with confusion both for scaling and ASTM C666 testing of silica fume concrete. Both direct parameter changes like capillary pore system refinement as well as indirect changes (change in dosage or interaction of admixtures) are used to "explain" the observations.

3.2.4 Moisture content

The "critical degree of saturation"-concept presented by Fagerlund [F 1977, F 1999] (see section 2) is considered to be a material property. The method allows for the prediction of the service life, equivalent to the time needed to reach the critical degree of saturation. However, with dense concrete – like very often with silica fume concrete – the procedure becomes very time consuming and difficult to perform.

Substitution of cement by 8 % silica fume has been shown to reduce salt frost scaling both after drying/re-wetting treatment and curing at high temperatures [J 1992]. This finding is supported by Sellevold [S 1988b], who compared such experiments to results from low temperature calorimetry : Performance testing (scaling) showed improved behaviour of silica fume concrete. Also when subjected to increased curing temperature or drying/re-wetting prior to the scaling test, the silica fume improved the properties. This was consistent with reduced (increase of ;) freezeable water - compared to ordinary portland cement concrete subjected to the same pre-treatment.

Calorimetric determination of ice formation in hardened cement paste with various amounts of silica fume exhibited a change in the primary freezing peak. With w/c-ratio of 0.60 and 8 % silica fume, it disappeared [S 1988c]. Drying a parallel sample "gently" at 58 % relative humidity and re-saturated, a distinct primary peak re-appeared. With very low w/c-ratios and high silica fume contents, the primary peak has been found to remain absent even after such treatment. Values of 0.30 and 10 %, respectively, have been indicated.

Implicitly in the calorimetric studies, the moisture content is (re-)established artificially without considering the importance of the field conditions and the internal material moisture response. The calorimetric test on saturated samples describes the properties of the pore water – and the pore structure – *if* the concrete/paste is saturated. Even if it is not a direct performance test, it may overestimate the stress/load, to which the material is subjected to during its service life.

Though, as pointed out by Sellevold [S 1988c], the calorimetric studies indicate major differences between silica fume concrete and reference concrete in their drying and re-wetting behaviour. The difference in behaviour is probably important for practical conditions, but are normally not taken into account in the standard tests described above.

3.2.5 Synopsis

Evidently, the present situation is unclear. The various reports on testing give different and confusing results. At least partly, this may be attributed to lack of considerations with respect to the moisture conditions. The moisture response of the different material qualities will depend on the pre-curing and testing regime. The response is also subject to change with the material's own structural properties. Hence, there is a need to use procedures that take into account the field moisture conditions and create realistic moisture response in the material to be tested.

Whether air entrainment is applied or not, the fresh concrete properties should be considered as an inevitable factor of influence when testing for freeze-thaw resistance : This is probably a key factor determining the homogeneity of the binder phase, dispersion of the silica fume, the properties of the paste-aggregate interface and stability of the air void structure. These factors are probably also important for the capillary pore size distribution and hence, for the internal moisture response of the material under external (moisture) boundary conditions.

3.2.6 Subject to study

It was decided to initiate a task assessing durability and strength development of silica fume concrete on longer terms than the "usual 28 days horizon", depending on curing conditions and ageing. The present publication comprises the following activities on freeze-thaw resistance :

3.2.6.1 Materials

The main idea was to investigate the effect of silica fume under the conditions described. In order to maximise any effects within a realistic range, 0 and 9 % silica fume of total binder was chosen.

Two different portland cement types were chosen, for a couple of reasons : It is known that the cement type may play an important role for the reactivity and strength “gain” with a specific pozzolanic material [S 2000b]. The alkali content of the cement has been stressed as important for the reactivity, but the relation is not coherent. Secondly, silica fume has proven useful in many studies together with the CEM I / ASTM type I cement chosen in the present work. Swedish studies of silica fume together with the CEM I / ASTM type V cement has often proven less successful, see subsequent discussion. Finally, the two cement types are important within the same market segments for the sponsors of this programme.

Chemical admixtures and ~combinations commonly used together with the two cement types were chosen, in order to address concrete mix design as close to practical interest as possible.

Also commercially available aggregate of normal water requirement for these types of concrete quality was chosen.

3.2.6.2 Mix design

With reference to normal concrete mix design for the external environment in question, the w/(c+s)-ratio was fixed to 0.45. This is close to practice for such structures in the Nordic countries.

Freeze-thaw scaling resistance may be sensitive to minor changes in air void characteristics. Identical air void characteristics for a series of mixes are almost impossible to achieve. These are sensitive to total air void content, dosage of air entrainer and the binder-fine aggregate particle system. There also is a dependence of air entrainer dosage / air void content on the amount and consistency of the cement/binder paste. Therefore, “natural”, medium/sensitive and “high” air content was chosen.

From the discussions above, air voids characteristics may be influenced by the viscous properties of the concrete. Additionally, the (rate of) moisture exchange with the external environment may be influenced by changes in the capillary pore size distribution. Such “properties” may also be influenced by the viscous properties of the fresh concrete. Even with the same slump level, the viscous properties are likely to change with the cement characteristics. The latter lead to different admixture dosage requirement for the two different cement series. All these direct and indirect influences lead to the conclusion of including two different slump levels.

3.2.6.3 Curing regimes

Looking for potential effects of different curing conditions, it was decided to choose three principally different curing regimes within a probable range of field service conditions, prior to freeze-thaw. This was believed to provide a range of realistic moisture exposure and relatively well cured concrete prior to testing :

A supposedly “optimum” (for hydration ;) curing condition was believed to comprise water curing for four weeks, then air storage for another four weeks prior to testing. The last four weeks of air storage was believed to imply a more realistic water exposure than prolonged water curing. An alternative curing condition providing reasonable maturity prior to testing but very limited water exposure was also chosen. This procedure comprised eight weeks of air storage only. The third procedure, believed to be the most realistic one, comprised cyclic dry and wet curing over a period of four months prior to testing.

Finally, to gain some experience on the effect of ageing, samples exposed to the three curing conditions described above were stored for one year (appr. +20 ^{o}C, 50 % RH) and then tested. These samples were “fresh” samples, subjected to standard pre-testing procedure the last ten days prior to testing. See details in subsequent section.

Very important to the main issue : Cylinders were cured whole as described, and sawn ten days before test start. The sawn surface was the test surface in all cases. This choice of testing procedure implies that any tested surface was not the one exposed directly to the external, varying curing and ageing (like carbonation) – until the last ten days prior to test initiation. The primary idea of this (normal) approach is to eliminate potential effects of varying surface finishing technique. The tested surface represented the “internal material and moisture response to the external boundary conditions”, the potential properties. It means that even in this study, the effect of curing etc. investigated only comprises that of the internal concrete’s response to the boundary conditions.

3.3 Experimental procedure

3.3.1 Materials

Portland cement: CEM I 42.5-R according to NS-ENV 197-1 (ASTM type I), manufactured by Norcem A.S, Dalen plant. CEM I 42.5-BV-SR-LA according to SS 13 42 01 (ASTM type V, high sulphate resistance) manufactured by Cementa AB, Degerhamn plant. “SR” designates sulphate resistance, “LA” low alkali and “BV” limited heat development. Information on physical and chemical properties is provided in appendix F.

Silica fume: Condensed silica fume, supplied by Scancem Chemical A/S, properties are included in appendix F.

Chemical admixtures : Three commercially available and commonly used chemical admixtures were applied. A lignosulphonate based water reducer (WRA) was added by a constant 5 % by weight of silica fume dosage. Secondly, a melamine formaldehyde based superplasticizer (HRWRA) was used to adjust the slump value to the specified level. The water content of both of these admixtures was 60 %. The air-entraining agent (AEA) was based on tall oil/fatty acid.

Aggregates: A natural sand 0-8 mm and crushed 8-11 & 11-16 mm coarse aggregates were graded according to the Norwegian Standard NS 3099, Reference Concrete. The grading curve is shown in appendix F. Accurate absorption values are not available, but this is a low porosity aggregate.

3.3.2 Test methods

Freeze-thaw scaling test: The test was performed on sawn surfaces; slices cut from Ø100 mm cylinders, with 3 % NaCl-solution according to the Swedish Standard SS 13 72 44, also referred to as the "Boraas Method" or “Scandinavian slab test”. The procedure deviates from the one in [S 2000] / [prEN xxx] - and provided in the appendix - on only two points :

- The minimum temperature of the freeze-thaw cycle is –18 +/- 2 ^{o}C (instead of –20 +/- 2 ^{0}C)
- In contrast to SS 13 72 44, prEN xxx prescribes demineralised water for re-saturation and freeze-thaw testing when only water is used during the test. However, such testing was not performed in the present study.

The specimens were insulated on all sides except for one, in order to ensure a one-dimensional heat flow. A plastic cover was applied to prevent evaporation from the 3 mm deep salt solution on the test surface. The set-up can be found in the test procedure description included in the appendix. In contrast to the standard procedure, the present study included initial curing times of 56 days, 112 days or 14 months.

Air content level was determined in fresh concrete by the pressure test, and subsequently confirmed by image analyses on polished sections.

Compressive strength was determined on 10 cm concrete cubes, stored in water at 20 °C until the age of testing.

3.3.3 Concrete mix design

As outlined and motivated in section 3.2.6, the concrete mixes were proportioned with a constant water/binder ratio of 0.45, close to practice for exterior structures in aggressive environment in the Nordic countries. The content of silica fume was 0 and 9 % by weight of the binder content.

Three levels of air content were chosen:

(N) Natural air content:	0,9-1,5 %
(M) Medium level of air content:	2,8-3,5 %
(H) High level of air content:	5,5-6,6 %

Constituents	Mix no.			
	1-6	7-12	13-18	19-24
Cement CEM I 42.5-R	415	378	0	0
Cement CEM I 42.5-BV-SR-LA	0	0	404	367
Silica Fume	0	36	0	37
Aggregate 0-8	820	820	820	820
Aggregate 8-11	500	500	500	500
Aggregate 11-16	500	500	500	500
Water (total)	186	186	182	182
w/(c+s)	0.45	0.45	0.45	0.45
s/(c+s), %	0	9	0	9

Table 3.3.1 : Concrete mix proportions, part 1.

Further, as argued in section 3.2.6, the variables comprised two different levels of fresh concrete consistency ; slump levels of approximately 50 mm and 150 mm. They were designated L and H, respectively.

Designation and detailed mix proportion data are presented in the tables 3.3.1 & 3.3.2.

3.3.4 Mixing and placing

Slightly different mixing procedures were applied to secure well-dispersed and homogeneous mixes. Total mixing time amounted to 240 seconds for all mixes.

No silica fume or WRA:

1. Dry material mixed for 60 sec.
2. Water and AEA added.
3. Wet mixing for 180 sec.

No silica fume, HRWRA applied:

1. Dry material mixed for 60 sec.
2. Water and AEA added.
3. Wet mixing for 60 sec.
4. HRWRA added.
5. Wet mixing for another 120 sec.

Silica fume mixes:

1. Dry material mixed for 60 sec.
2. Water, WRA and AEA added.
3. Wet mixing for 60 sec.
4. HRWRA added.
5. Wet mixing for another 120 sec.

For freeze-thaw testing, Ø100x200 mm cylinders (Mix 1-12) and 150 mm cubes (Mix 13-24) were cast following the SS 13 72 44 procedure ; in two layers, each layer being vibrated depending on the slump level.

Mix No.	Cement Type CEM I		Silica Fume s/(c+s) [%]	Slump Level		Air Content Level [N,M,H]	Chemical Admixtures [kg/m^3]		
	42.5-R	42.5-BV-SR-LA		L	H		WRA	HRWRA	AEA
1	x		0	x		N	-	-	-
2	x		0		x	N	-	4.15	-
3	x		0	x		M	-	-	0.025
4	x		0		x	M	-	4.15	0.050
5	x		0	x		H	-	-	0.133
6	x		0		x	H	-	4.15	0.108
7	x		9	x		N	1.80	2.36	-
8	x		9		x	N	1.80	6.50	-
9	x		9	x		M	1.80	2.36	0.032
10	x		9		x	M	1.80	6.50	0.053
11	x		9	x		H	1.80	2.36	0.100
12	x		9		x	H	1.80	6.50	0.108
13		x	0	x		N	-	-	-
14		x	0		x	N	-	1.82	-
15		x	0	x		M	-	-	0.028
16		x	0		x	M	-	2.02	0.040
17		x	0	x		H	-	-	0.149
18		x	0		x	H	-	2.02	0.174
19		x	9	x		N	-	3.63	-
20		x	9		x	N	-	6.54	-
21		x	9	x		M	-	3.52	0.056
22		x	9		x	M	-	6.54	0.061
23		x	9	x		H	-	3.35	0.121
24		x	9		x	H	-	6.26	0.133

Table 3.3.2 : Concrete mix proportions, part II.

3.3.5 Curing and preparation

All specimens were left to cure in the moulds at 20°C and relative humidity (RH) above 95 % for 24 hours. Subsequently, three different curing conditions were chosen (for the complete cylinders, prior to sawing, see later) :

C1 : Water curing: In water at 20°C until 28 days of age, then in air controlled at 20°C and RH of 50 %.

C2 : Dry curing: Air storage at 20°C and RH 50 %.

C3 : Cyclic curing: Air storage at 20°C and RH 50 % until 21 days of age, then 7 days in water at 20 °C. Subsequently two more cycles of 21 days in air and 7 days in water, finally air storage at 20°C and RH 50 % until testing.

Ten days prior to freeze-thaw testing, 5 cm slices were cut from the specimens. These were prepared and "re-saturated" according to the standard procedure, for freeze-thaw exposure of the sawn surface. One series always consisted of six (Mix 1-12) or four (Mix 13-24) parallel slices from different specimens in order to secure a representative surface selection and size.

Age of specimens at start of freeze-thaw testing :

Age 1 : 56 days ; Curing C1 & C2
112 days ; Curing C3

Age 2 : 14 months; All curing variants. All the samples subjected to testing at 14 months, had been stored in air at 20 °C and 50 % RH from the initial 56 or 112 days' curing periods. From ten days prior to the testing, the procedure followed as described above. Consequently, carbonation of the test surface did not start until after the sawing at 14 months.

3.4 Test results

3.4.1 Fresh concrete properties

Fresh concrete properties are presented in table 3.4.1. All mixes lay within a proper workability range. The fresh concrete air content is plotted against AEA dosage in appendix F. The relation is reasonably linear, indicating "stable air entraining conditions". However, the AEA dosage requirement depends somewhat on the slump level and silica fume, apparently more so for the sulphate resistant cement.

Mix No.	Cement Type CEM I		Silica Fume	Slump Level		Air Content Level	Achieved values [kg/m^3]	
	42.5-R	42.5-BV-SR-LA	s/(c+s) [%]	L	H	[N,M,H]	Slump [mm]	Air Content [Vol.-%]
1	x		0	x		N	45	1.4
2	x		0		x	N	160	0.9
3	x		0	x		M	40	3.0
4	x		0		x	M	155	3.3
5	x		0	x		H	60	5.7
6	x		0		x	H	180	6.0
7	x		9	x		N	45	1.4
8	x		9		x	N	140	1.1
9	x		9	x		M	75	3.5
10	x		9		x	M	150	3.1
11	x		9	x		H	80	6.0
12	x		9		x	H	190	6.3
13		x	0	x		N	50	1.1
14		x	0		x	N	150	0.9
15		x	0	x		M	50	3.0
16		x	0		x	M	130	3.1
17		x	0	x		H	65	5.8
18		x	0		x	H	150	5.7
19		x	9	x		N	45	-
20		x	9		x	N	155	-
21		x	9	x		M	55	3.2
22		x	9		x	M	155	2.8
23		x	9	x		H	60	6.0
24		x	9		x	H	155	5.9

Table 3.4.1 : Fresh concrete properties.

3.4.2 Compressive Strength

For reference and comparison, compressive strength values at 3 months and 1 year age are included in appendix F. As expected, the strength level was closely related to the air content. Strength drop per vol-% air (for concrete of otherwise identical composition) is often estimated according to an exponential expression, see equation 3.4.1 :

$$F_C = b^{\Delta A} \times F_{C0} \qquad \text{Eq. 3.4.1}$$

where :

F_C : Strength of the concrete of higher air content
F_{C0} : Strength of the concrete of lower air content
ΔA : Difference in air content between the two mixes
b : Factor to be determined by equation 3.4.2 :

$$b = e^{\frac{\ln(\frac{F_C}{F_{C0}})}{\Delta A}} \qquad \text{Eq. 3.4.2}$$

This exercise was performed on comparable mixes, with input data from the mixes of lowest and highest air void content within each group. The intermediate levels were not used because of the higher relative importance of measuring errors. Three months compressive strength values (appendix F) were applied. The result of the calculations are included in table 3.4.2 :

Mix nos. compared	Parameter			
	F_C [MPa]	F_{C0} [MP]	ΔA [Vol-%]	b
1, 5	48	68	4.3	0.922
2, 6	54	68	5.1	0.956
7, 11	61	76	4.6	0.953
8, 12	63	81	5.2	0.953
13, 17	63	84	4.7	0.941
14, 18	65	85	4.8	0.946
19, 23 (ΔA missing)	-	-	-	-
20, 24 (ΔA missing)	-	-	-	-
Mean value for b :				0.945

Table 3.4.2 : Calculation of percentage strength loss per vol-% air content for some of the mixes, based on Eq. 3.4.2. See above for designations.

One of the values (0.922) in table 3.4.2 appears to be an outlier, the remaining values confirming the factor 0.95. The 5 % strength drop "rule" per volume-% air may be used to consider the fresh concrete air content values achieved. The strength versus air for C1 is plotted in the figures 3.4.1a&b. The plots indicate that the air content of mix 6 is slightly over-estimated but still is in the “high range level”. Correspondingly, the actual air content of the mixes 16&21 would probably be closer to 4 % than 3 %. The assumption concerning mix 21 was later confirmed by plane section analyses, mix no. 16 not. Mix no. 6 was found to have 5.6 % air. However, the plane section analyses are vulnerable to random occurrence of large voids and provide no satisfactory measure to check the total air volume.

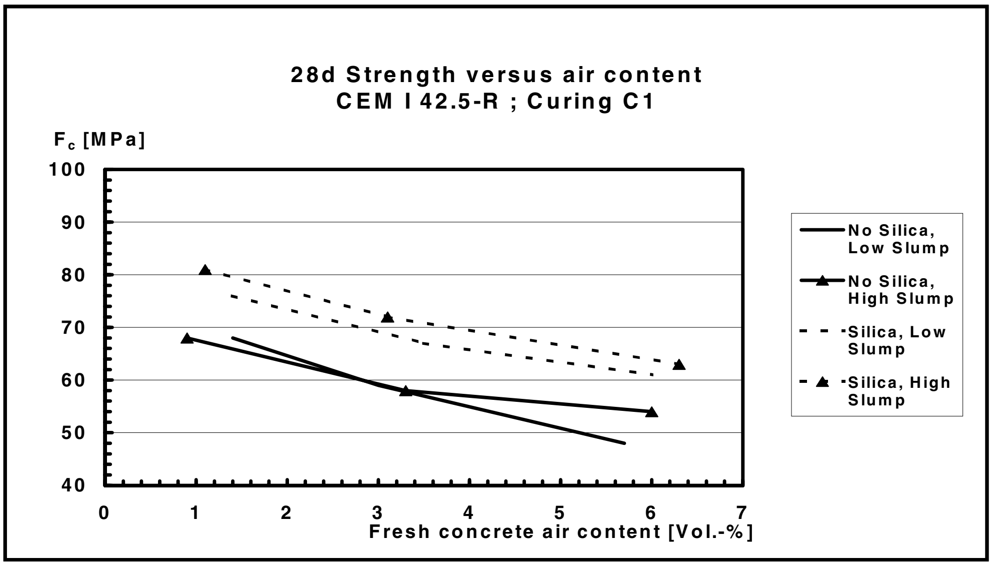

Figure 3.4.1a : Compressive strength versus fresh concrete air content, Mix 1-12.

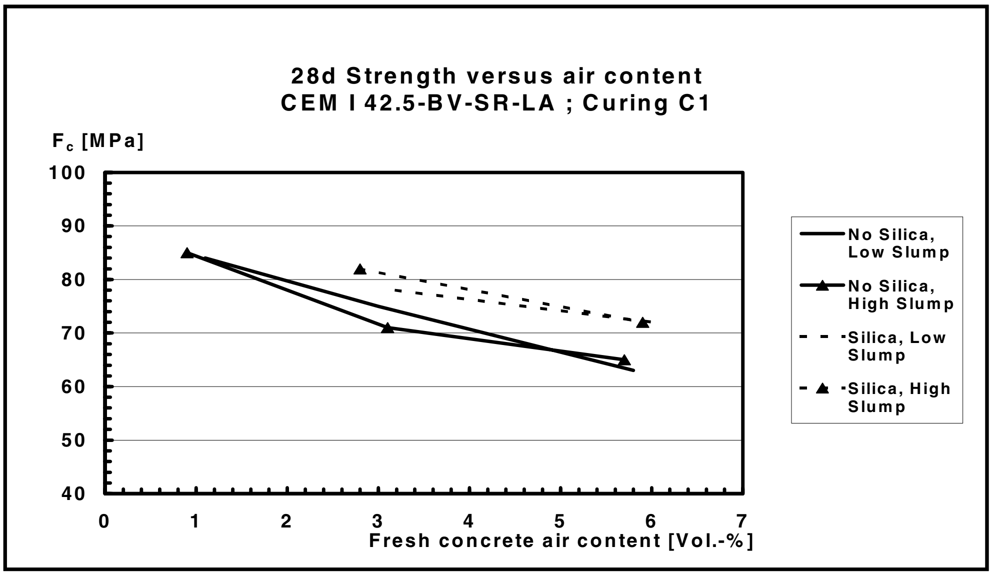

Figure 3.4.1b : Compressive strength versus fresh concrete air content, Mix 13-24 (Mix no. 14 & 20 missing ; air volume not obtained).

The strength values have previously been published by Skjeggerud [S 1992b]. The curing conditions influenced the strength considerably : 28 days of water curing exhibited 20 % higher strength after one year than for concrete cured in air. For silica fume concrete, increased slump values achieved by superplasticizer also increased the compressive strength. This was attributed to improved dispersion of the silica fume. For further discussion of strength, please see [S 1992b].

3.4.3 Air void parameters

Mix No.	Specific Surface α [mm^{-1}]	Spacing Factor $\bar{L}$ [mm]
1	12	0.59
2	22	0.37
3	14	0.54
4	19	0.35
5	36	0.26
6	24	0.29
7	13	0.70
8	17	0.57
9	21	0.35
10	15	0.47
11	20	0.31
12	16	0.30
13	15	0.60
14		
15	13	0.50
16	26	0.21
17	24	0.18
18	24	0.17
19	12	0.60
20		
21	13	0.30
22	17	0.35
23	23	0.16
24	22	0.18

Table 3.4.3 : Test results : Air void parameters. See table 3.5.1 and section 3.5.3 with respect to effect of cement type, table 3.5.3 and section 3.5.6 concerning effect of silica fume on air void structure.

Air void parameters obtained on hardened concrete are included in table 3.4.3. With the CEM I 42.5-R cement (Mix nos. 1-12), the addition of silica fume and superplasticizer resulted in poorer (increased) spacing factor in five cases and improved value in one case. With the CEM I 42.5-SR-LA cement, the spacing factor was improved in two cases and increased in two cases. In one case, no change was observed.

3.4.4 Freeze-thaw scaling

Accumulated, mean scaling level after 56 freeze-thaw cycles for all mix- and curing-combinations is included in the appendix F. Values of 18 kg and above are extrapolated (doubled) from the values at 28 cycles. This is due to the necessary interruption of the test at this high scaling level. Hence, the absolute scaling level of these mixes are not quite correct, but are still considered appropriate for ranking. Alternatively, the subsequent discussion might be based on the 28 cycles test results. The ranking of mixes would be the same, but the information about actual performance of the intermediate and good mixes from 28 to 56 cycles would be missing – or more complicated to display. The (lack of) statistical significance will be considered in the following discussion, based on recent mapping of precision data and practical experience.

3.5 Discussion of freeze-thaw test results

3.5.1 General

This study provided a lot of data that may be treated in many different ways. According to the objective of this publication, the following discussion will concentrate on the effects of curing, ageing and silica fume addition.

To the issue of statistical significance of the test results : Efforts to provide for the reader single test results in tabular form - of the more than 700 samples – has not been made. Based on reviewing of the test results, however, differences in mean values exceeding 10 % of the absolute level can be considered significant. An equally important qualification is the even distribution of the damage on the test surface, which was acceptable. An exception to the 10 % rule is when the absolute level of scaling amounts to 0.030 kg/m^2 or less. In the latter case, it is the author’s opinion that the random distribution of damage increases the relative, natural scatter in results. However, variations at such a low scaling level should in any case be considered irrelevant.

There was no systematic effect of slump level on scaling. Nor was this to be expected from the examination of the air void spacing factor, which exhibited no systematic pattern. However, the systematic addition of (increased amount of ;) WRA/HRWRA might have caused a poorer air void system or a less homogenous paste with varying capillary porosity (section 3.2). Attempts to obtain MIP data (Mercury Intrusion Porosimetry) partly failed, due to technical obstacles. Still, slightly lower porosity in the 10-30 nm range for the lowest slump level was indicated for one mix (nos. 11 vs. 12 ; 6 % air and silica fume). However, in this case the spacing factor was also very slightly improved and no direct relation found.

3.5.2 Scaling versus spacing factor

Scaling versus air void spacing factor for curing condition C1 is plotted in figure 3.5.1. Curing condition C2 exhibits a similar picture. The latter and other curing combinations are included in appendix F. (The air void characteristics were determined once for each mix only. The values used in the plots in the appendix are identical to those of the samples in figure 3.5.1.) Below 0.25 mm, all mixes exhibited a low damage. Above this value, the picture is mixed, with some mixes performing well in the test, others poorly.

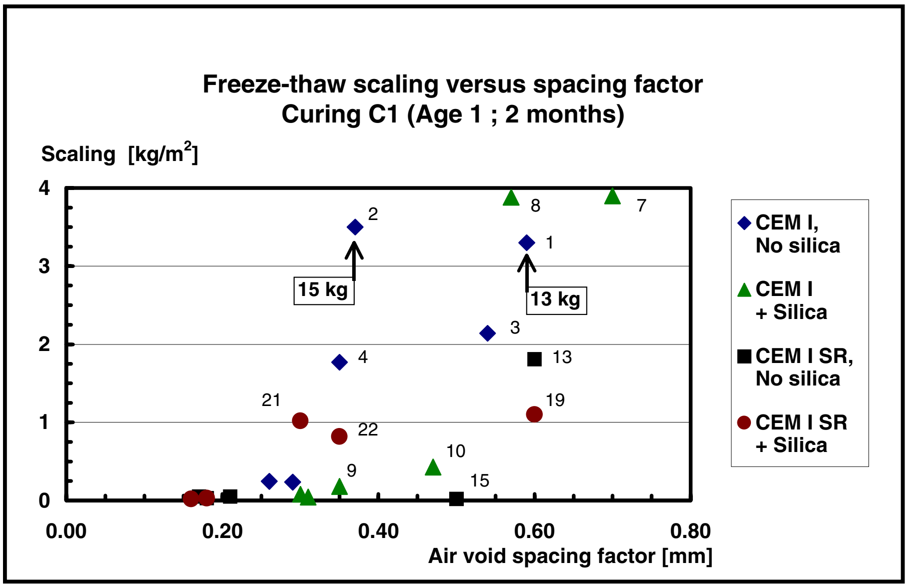

Figure 3.5.1 : Freeze-thaw scaling versus air void spacing factor for curing condition C1 and all mixes, except for mix nos. 14 & 20. Mix nos. are indicated for some of the mixes.

Hence, the test results confirm a critical spacing factor in the range of 0.25 mm. There is no indication that the critical spacing factor depends on the silica fume content. If existing at all, the indication of lower critical spacing value for the highest slump range is very vague. Without silica fume, there is an indication that the CEM I – SR cement has a higher critical spacing factor compared to the "standard" cement :

3.5.3 Effect of cement type

There is a significant difference between the results obtained with the two different cements. The overall level of scaling is lower with the sulphate resistant cement. Though, with 6 % air content – or spacing factor below 0.30 - all mixes perform excellent. The total air void level requirement with this specific sulphate resistant cement appears to be very low. This is in accordance with Malmström [M 1990].

In the present study, mix nos. 1-12 were tested by the present author, while the testing of the remaining 12 series had to be tested at a commercial laboratory. In order to try to eliminate the potential influence of between-laboratory variation, two mixes from the latter series were repeated by the present author. The results, although not included in the present publication, were fully in line with the original ones. The lack of general awareness of the important influence of the cement type is probably due to a combination of the following points :

- The use of SR-LA cement for general, outdoor construction and ready-mix concrete is not a standard line of action. In Sweden, however, this cement is normally prescribed for all road construction.
- When air-entrained, more "normal" portland cement concrete exhibit acceptable freeze-thaw resistance. Any differentiating therefore becomes of less practical significance.
- Even if recognised as more frost resistant than alternative cements in Sweden, this experience is probably mainly based on laboratory testing [M 1990] – as is most of the freeze-thaw experience, including the present work.

Apart from the study cited above, few other researchers have looked into the effects of the type of portland cement on freeze-thaw resistance. To the knowledge of the present author, no explanation has been given for different behaviour. Possible interaction between cement characteristics and admixtures in creating an adequate air void system has been mentioned, but has not been systematically investigated.

Table 3.5.1 displays a comparison of the air void structure between the mixes with the two different cement types. There is a significant difference in air void spacing factor between the two series : Not considering the non-air entrained mixes, the standard cement mixes (medium or high air level) had a mean spacing factor value of 0.36 mm, with a standard deviation (8 mixes) of 0.10. The corresponding values with the SR-LA cement were 0.26 mm and 0.12, respectively. These differences may be directly attributed to the higher dosages of superplasticizer required with the standard cement (table 3.3.2). Still, partial replacement of superplasticizer by lignosulphonate (series 7, 9 and 11 vs. 19, 21 and 23) would normally be considered positive with respect to air void structure.

Mix No.	Specific Surface α [mm^{-1}]	Spacing Factor	
		$\bar{L}$ [mm]	Change
1	12	0.59	
2	22	0.37	
3	14	0.54	
4	19	0.35	
5	36	0.26	
6	24	0.29	
7	13	0.70	
8	17	0.57	
9	21	0.35	
10	15	0.47	
11	20	0.31	
12	16	0.30	
13	15	0.60	+ 0.01
14			
15	13	0.50	- 0.04
16	26	0.21	- 0.14
17	24	0.18	- 0.08
18	24	0.17	- 0.12
19	12	0.60	- 0.10
20			
21	13	0.30	- 0.05
22	17	0.35	- 0.12
23	23	0.16	- 0.15
24	22	0.18	- 0.12

Table 3.5.1 : Changes in scaling when applying the SR-LA cement in stead of the standard cement, with or without silica fume, (no. 13 vs. 1, no. 15 vs. 3, no. 16 vs. 4, etc.).

The phenomenon has not received much attention in general. Of course, the present study is much too limited to draw general conclusions on the influence of cement type in (pure) portland cement concrete. (Neither was it intended – these mixes were meant as reference for the silica fume mixes ; see section 3.2.6). However, the results above strongly indicate the importance of using "compatible" cement-admixture and admixture-admixture combinations.

It would also be appropriate at this stage to mention that the SR-LA cement according to the Swedish experience is considered exceptional with respect to frost resistance. This property is not attributed to improved air void structure (in Sweden), but was not yet explained [M 1990]. The other CEM I cement is considered "normal" with respect to freeze-thaw resistance.

It appears from figure 3.5.1 that with curing C1 and initial testing, the 42.5-R cement with 9 % silica fume had a larger, critical spacing factor than the SR-LA cement with silica fume. The same appears from curing C3 (appendix F), but not with the dry condition C2. The same picture is found at testing after one year. However, the observation depends on one or two determinations of the air voids characteristics, and the conclusion should not be stretched too far.

As mentioned above, the reason for the different scaling behaviour with the two different cements may not entirely be one of different air voids characteristics. The subsequent sections comment on parameters that may make the cements liable to different performance.

3.5.4 Scaling versus curing condition

Freeze-thaw scaling versus curing condition and ageing is plotted in the figures 3.5.2-5. The first two figures (mix nos. 1-6 & 7-12) are plotted with two different scales to enable a better distinction between the series. For the remaining series, additional plots will not provide further information. Still, note that the scale differs between the figures.

Some of the displayed differences may be due to scatter of test results, especially at low levels of damage. However, there is clear evidence that the scaling depended on the curing regime applied. This must be due to differences in curing (maturity, strength) of the material or internal moisture response to the external boundary conditions.

Initial testing

Considering the initial testing age, i.e. at the age of 2(3) months, the dry curing (C2) appears advantageous compared to wet curing (C1). The cyclic curing (C3) resulted in a scaling level very close to that of the dry one. With the CEM I 42.5-R cement without silica fume, this was the tendency in almost all the cases. With the CEM I 42.5-SR-LA cement, the same comment appears evident for the dry curing, unless at very low damage, where the changes are insignificant. With this cement, the cyclic curing may increase the scaling again. It is probable that a coarser capillary structure of the latter mixes enables increased water ingress during the cyclic curing, i.e. increasing the degree of saturation. This is the only possible “negative” effect of water curing and may have enhanced the subsequent scaling.

When using silica fume and tested at the age of 2(3) months, there is no significant change from curing condition C1 to C2 with the CEM I 42.5-R cement. The cyclic wet and dry curing (C3) appeared slightly more deleterious with this material combination. With silica fume and the CEM I 42.5-SR-LA cement, the dry curing (C2) clearly appeared to be favourable. The cyclic curing (C3) increased the damage if low or medium air content. Again, the different behaviour might be due to difference in water ingress. With the slower reacting SR-LA cement, the $Ca(OH)_2$-depending silica fume reaction may have been retarded, compared to the high alkali, standard cement. Coinciding, and possibly even more important, the capillary structure may still be coarser (than with the CEM I 42.5 R), enabling a higher initial degree of saturation when cured wet or cyclic. Still, with no measurements of these properties available, these ideas remain speculation.

One year later

Testing after one year with the CEM I 42.5-R cement, there are no clear differences between C1 and C2. Cyclic, dry and wet curing appears somewhat more susceptible to damage with the superplasticized concrete. A possible explanation is a less homogeneous paste (low yield value [W 1990]) of these kinds of concrete, resulting in higher susceptibility to pore structure changes upon drying and re-wetting. Such a phenomenon may increase the suction upon freeze-thaw testing, as well as increase the initial degree of saturation. Again with the SR-LA cement, the picture is modified : For the non-air entrained concrete, initial water storage (C1) appears more harmful than both dry (C2) and cyclic (C3) curing. If a high degree of saturation were the reason for the C1 versus C2 behaviour, the same should apply to C3. If alteration of the pore structure is the reason, the implication appears that drying after initial, extra suction is more destructive than immediate (light) drying, C2. Without data on moisture content/changes or capillary pore structure, further theories remain speculations.

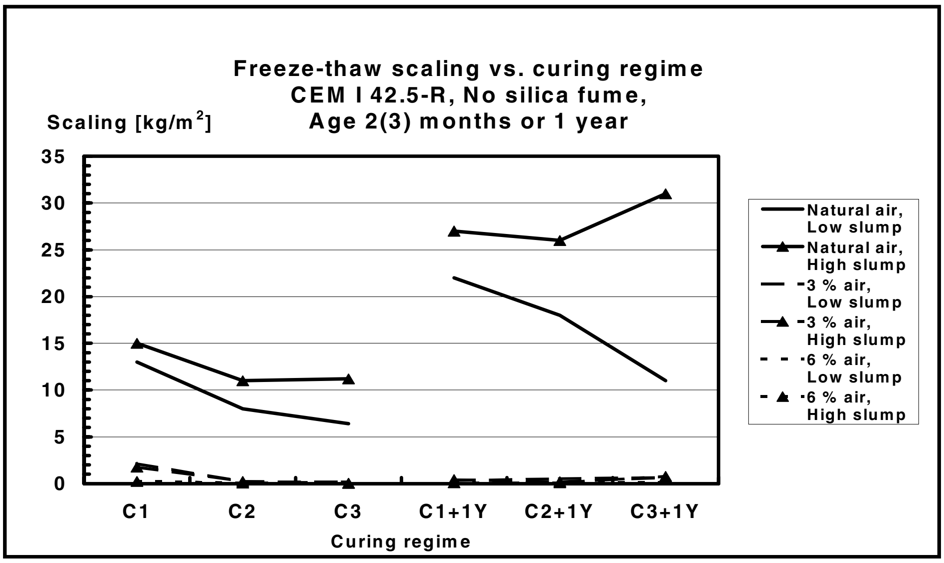

Figure 3.5.2a : Effect of curing condition, mix nos. 1-6, CEM I 42.5-R, no silica fume.

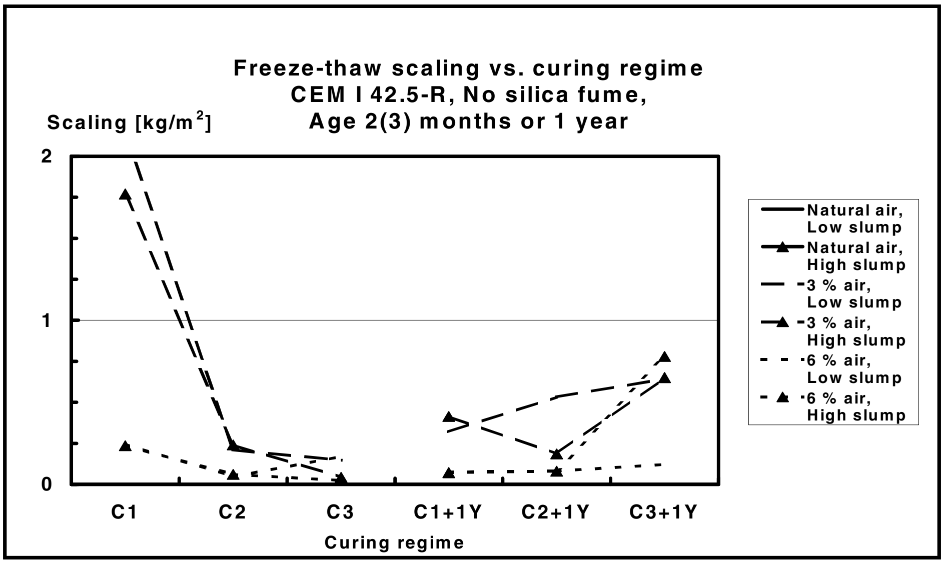

Figure 3.5.2b (as 3.5.2a, but increased scale) : Effect of curing condition, mix nos. 1-6, CEM I 42.5-R, no silica fume.

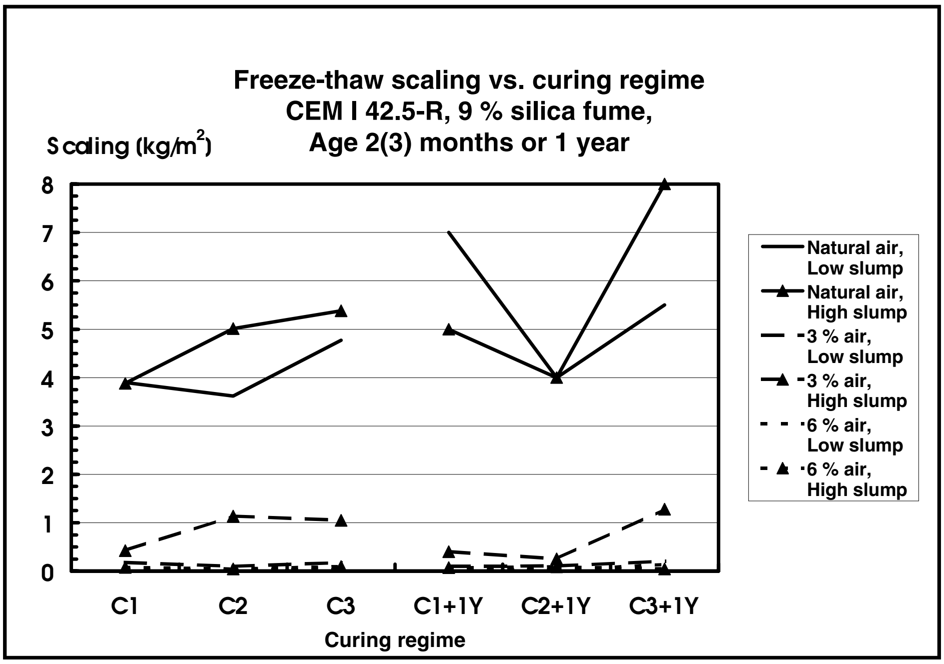

Figure 3.5.3a : Effect of curing condition, mix nos.7-12, CEM I 42.5-R and silica fume.

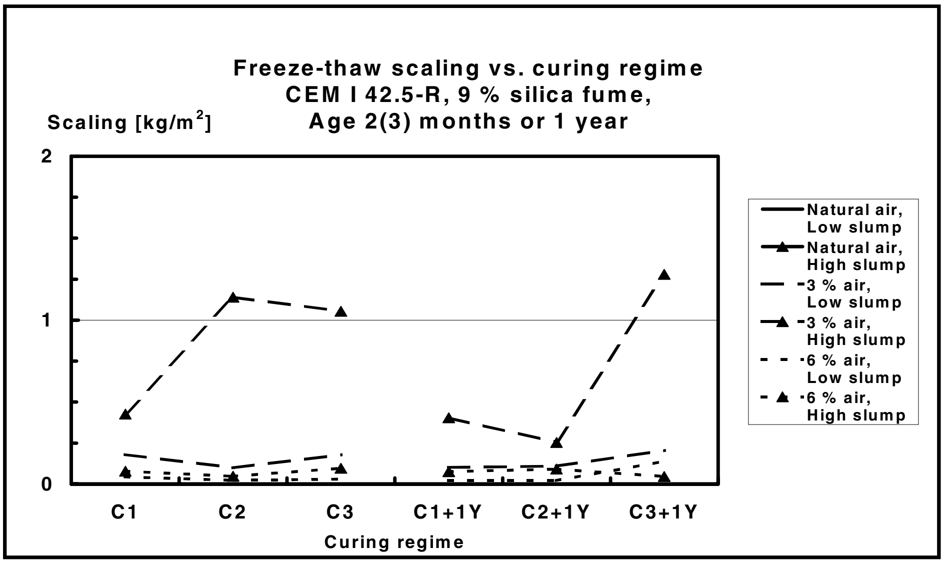

Figure 3.5.3b (as 3.5.3a, but increased scale) : Effect of curing condition, mix nos.7-12, CEM I 42.5-R and silica fume.

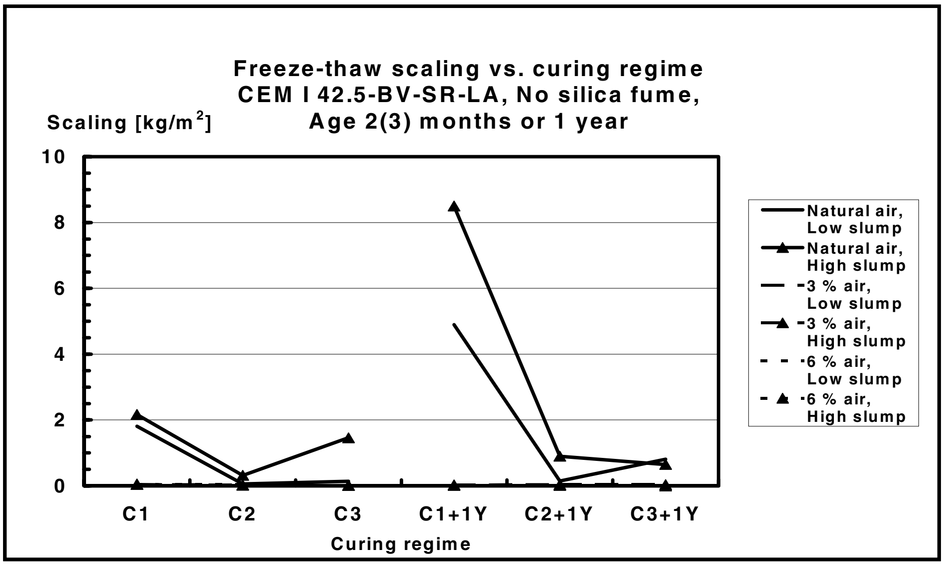

Figure 3.5.4 : Effect of curing condition, mix nos. 13-18, CEM I 42.5-SR-LA, no silica fume.

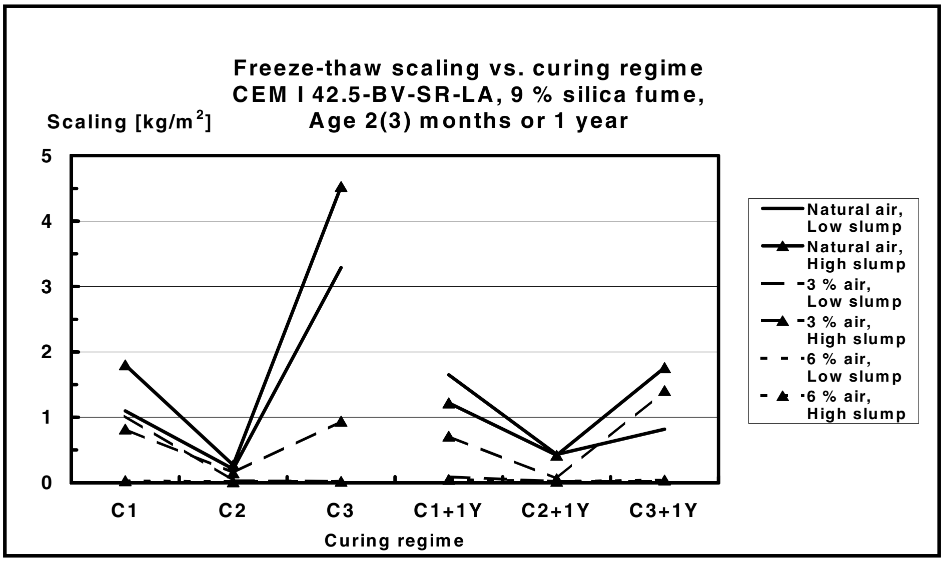

Figure 3.5.5 : Effect of curing condition, mix nos. 19-24, CEM I 42.5-SR-LA and silica fume.

Tested after one year, with silica fume and whenever significant, dry curing (C2) exhibits the lowest scaling. This may indicate that the silica fume reaction at this stage has reached an acceptable level. In any case, the degree of saturation must be expected to be the lowest in this case, overshadowing any negative restraints on reaction kinetics.

In the context of reaction kinetics and “curing”, it should be reminded that the test surface was not directly subjected to drying. It is probable that all test surfaces of the (w/(c+s) = 0.45) concrete were appropriately cured. The implication is that the curing of concrete at such water-binder-ratios are rather insensitive to drying a short distance from the surface. After all, hydration may continue down to or below humidity values of 80 % RH. This, of course, does not prevent the water curing from influencing the degree of saturation .....

3.5.5 Scaling versus ageing

Some mixes improved their performance after one year, compared to the initial testing, some not. Table 3.5.2 presents an overview of the change in scaling. The following observations may be made :

It appears that with the CEM I 42.5-R cement and natural air content, the influence of ageing is without doubt negative, i.e. increased scaling. With increased air content (and freeze-thaw resistance), the influence of ageing becomes less evident. In all these cases, the capillary degree of saturation would be expected to be the same. Correspondingly, the changing ageing properties from natural air content to air-entrained concrete is hardly an effect of changes in pore water mentioned above. With the still significant values of the “M”-column, it is not believed that the change from “left to right” is merely an effect of less damage and statistical significance.

The “ageing effect” (storing at 50 % RH), defined as change in behaviour from initial testing (56/112 days) to that at 24 months, may be due to :

- Changes in pore water content (50 % RH leads to drying)
- Changes in physical pore structure
- Changes in chemical properties (further hydration, internal re-distribution and re-arrangement of the hydrates)
- Changes in moisture response to the external boundary conditions
- (In the present case, carbonation as an ageing effect is no issue.)

Without specific data on these properties, theories explaining the behaviour of aged concrete - compared to that of initial conditions – remain speculations, even more than in the preceding section.

Silica fume	Slump level	Change in scaling (kg/m^2) after 56 cycles. Prolonged air storage until the age of 14 months.					
Curing C1		CEM I 42.5-R Air void level :			CEM I 42.5-BV-SR-LA Air void level :		
		N	M	H	N	M	H
-	Low	+9	-1.82	-0.17	+3.1	0	-0.02
-	High	+12	-1.36	-0.16	+6.3	-0.02	-0.04
+	Low	+4	-0.72	-0.021	-0.55	-0.93	0
+	High	+1,2	-0.02	0	-0.58	-0.11	+0.02
Curing C2							
-	Low	+10	+0.32	+0.044	-0.47	-0.03	-0.03
-	High	+15	-0.055	+0.02	+0.55	+0.02	-0.01
+	Low	+0,4	+0.10	0	+0.22	-0.01	-0.01
+	High	-1,0	-0.89	+0.044	+0.15	-0.09	+0.01
Curing C3							
-	Low	+4,5	+0.5	+0.10	+0.67	+0.01	-0.01
-	High	+20	+0.61	+0.76	-0.81	+0.03	-0.01
+	Low	+0,8	+0.03	-0.016	-2.47	0	-0.01
+	High	+2,6	+0.23	-0.05	-2.77	+0.47	+0.02
Σ							
Increase		11	5	4	6	1	0
Decrease		1	5	3	6	3	1
No change		0	2	5	0	8	11

Table 3.5.2 : The table displays the change in scaling [kg/m^2] when tested at "Age 2" (14 months), compared to that of the initial testing at "Age 1" (56/112 days). Remark : By comparison silica versus non-silica, "ageing effects" with absolute values below 0,03 or changes in absolute values below 10 % should be considered insignificant (see text).

The observations on the 42.5 R cement should also be valid for the right part of table 3.5.2, i.e. with the SR-LA cement : There is a change in pattern from the "natural air" to "high air" in this case as well. The "N" comprises both negative and positive influence that is significant. As for the standard cement, the extent partly depends on whether silica fume is applied. With SR-LA cement and high air content, the evidence of any ageing effect vanishes.

At an earlier presentation of the results [R 1995b], it was argued that carbonation might have caused the change in properties from Age 1 to Age 2. Carbonation of portland cement concrete is normally considered to improve the freeze-thaw resistance [U 1999b]. This is due to the increased density of the pore system in the carbonated layer. However, it should be reminded that atmospheric exposure period of the surface subjected to freeze-thaw was the same in both cases, since sawing of the samples took place after the pre-curing procedure, see section 3.3.5. Thus, none of the test surfaces were carbonated ten days prior to freeze-thaw testing.

Summarising, with the 42.5 R cement and N(atural air), there was a distinct negative effect of ageing, less so with M and no effect with H(igh) air content. The corresponding picture of concrete with the SR-LA cement is mixed. A proper air void system seems to offset any ageing effects due to this kind of storage.

3.5.6 Effect of silica fume

The effect of silica fume is not due to a systematic change of the air void spacing factor (figure 3.5.1 and table 3.5.3). Scaling is plotted versus total, fresh concrete air content in the figures 3.5.6-7 (Age 1, curing condition C1) and 3.5.8-9 (Age 2, C1). Additional plots for C2 and C3 are included in appendix F.

An overview of silica versus non-silica is provided in table 3.5.3, which also includes the air void characteristics. With the CEM I 42.5-R cement and initial testing, only very few cases disturbs the positive influence of silica fume. Even with 6 % air there is a difference in favour of silica fume. MIP investigation indicated reduced pore volume in the 10-30 nm range for these mixes when adding silica fume. The “disturbance” is mainly caused by mix no. 10, where the spacing factor increased from 0.35 mm for the companion mix to 0.47 mm. The same very much applies for testing after one year. The implication is that there was a clearly positive effect of silica fume in spite of slightly poorer air void characteristics, particularly with the standard cement.

Although not included in the figures, the progressive deterioration development (accelerating scaling) for "low quality concrete" (section 3.2.1) was less marked with silica fume.

With the SR-LA cement, the picture is less distinct. MIP results for the mixes with high air level, low slump and silica addition (C1; Mix nos. 11/23) exhibited higher porosity over the entire range with this cement compared to the other. The number of cases where silica fume improved the performance with respect to scaling is lower with the SR-LA. However, this may be attributable to the general lower deterioration. Still, mix no. 19 versus mix no. 13 has identical spacing factor but poorer scaling results in three of six curing/age-combinations. On the other hand, mix no. 22 exhibited higher scaling than mix no. 16, but also had poorer air void characteristics, which fits the traditional picture.

Since the present study was carried out, Meng et al [M 1998] reported that "a high level of alkali content in cement does ….. accelerate the reaction rate of silica fume". This fits with the higher relative effect of silica fume with the CEM I 42.5-R cement.

Although not of direct relevance to the present issue, it may be noted that some of the silica fume mixes were subjected to prolonged testing. None of these displayed sudden disrupter or accelerated deterioration even after more than 300 freeze-thaw cycles.

3.5.7 The effect of silica fume on ageing

An overview of the apparent effect of silica fume on ageing is presented in table 3.5.4. Note the definitions of "positive" etc. in the table subtext.

Only in three cases, a negative ageing effect with the utilised curing conditions was found. Two of these incidents were with the dry curing condition C2. The third one was with the SR-LA cement, with a scaling increase below 0.5 kg/m^2. In the majority of the cases, there was a positive "protection effect" through the addition of silica fume.

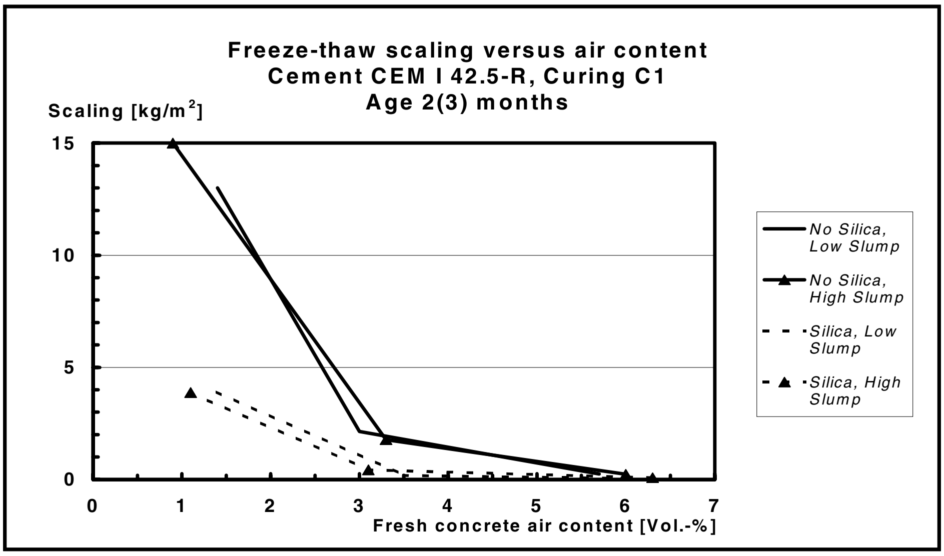

Figure 3.5.6 : Scaling after 56 freeze-thaw cycles, curing condition C1 (wet), sample age 1 (56 days) at test initiation. CEM I 42.5-R.

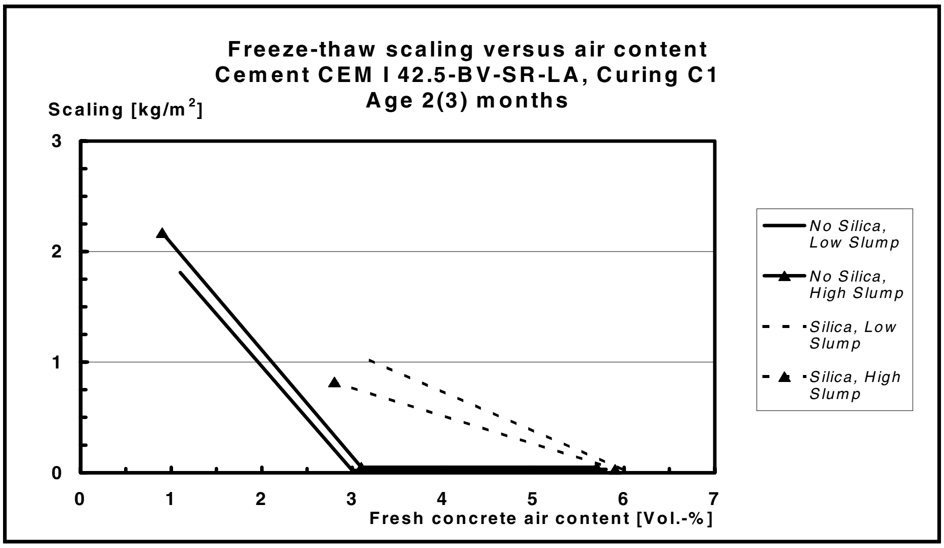

Figure 3.5.7 : Scaling after 56 freeze-thaw cycles, curing condition C1 (wet), sample age 1 (56 days) at test initiation. CEM I 42.5-BV-SR-LA.

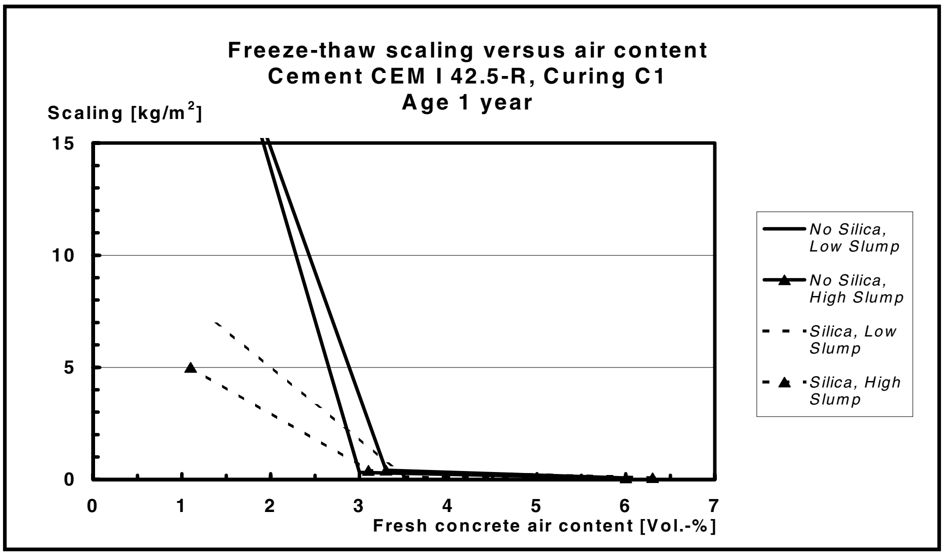

Figure 3.5.8 : Scaling after 56 freeze-thaw cycles, curing condition C1 (wet), sample age 2 (14 months) at test initiation. CEM I 42.5-R.

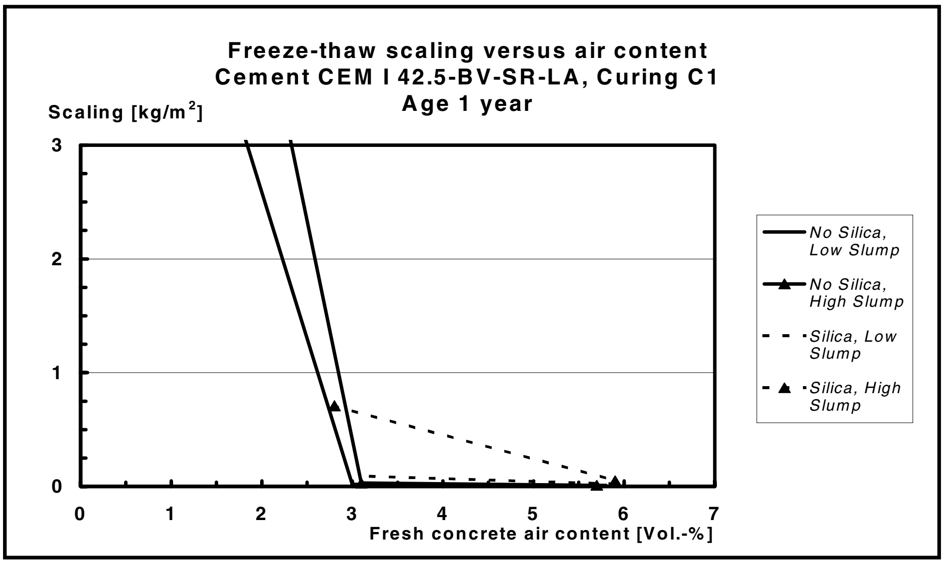

Figure 3.5.9 : Scaling after 56 freeze-thaw cycles, curing condition C1 (wet), sample age 2 (14 months) at test initiation. CEM I 42.5-BV-SR-LA.

Mix No.	Specific Surface α [mm^{-1}]	Spacing Factor		Change in scaling					
		$\bar{L}$ [mm]	Change	Age 1 / Curing :			Age 2 / Curing :		
				C1	C2	C3	C1	C2	C3
1	12	0.59							
2	22	0.37							
3	14	0.54							
4	19	0.35							
5	36	0.26							
6	24	0.29							
7	13	0.70	+	-	-	-	-	-	-
8	17	0.57	+	-	-	-	-	-	-
9	21	0.35	-	-	-	=	-	-	-
10	15	0.47	+	-	+	+	=	+	+
11	20	0.31	+	-	-	-	-	-	+
12	16	0.30	“+”	-	-	+	=	=	-
13	15	0.60							
14									
15	13	0.50							
16	26	0.21							
17	24	0.18							
18	24	0.17							
19	12	0.60	=	-	+	+	-	+	=
20				-	-	+	-	-	+
21	13	0.30	-	+	=	=	+	=	=
22	17	0.35	+	+	+	+	+	=	+
23	23	0.16	“-“	=	=	=	=	=	=
24	22	0.18	“+”	=	=	=	+	=	=

Table 3.5.3 : Changes in scaling when applying silica fume, compared to companion mix without silica fume (no. 7 vs. 1, no. 8 vs. 2, etc.). Minus sign designates reduced value (spacing factor or scaling level), plus designates increase, and "=" designates no significant difference. Based on scaling values included in the appendix F. The mix nos. 1-6 & 13-18 are included for easy comparison of the air void parameters.

Influence of silica on ageing	CEM I 42.5-R	CEM I 42.5 BV-SR-LA
Curing C1		
Positive	2	5
Not negative	4	1
Negative	0	0
Curing C2		
Positive	5	2
Not negative	0	3
Negative	1	1
Curing C3		
Positive	6	2
Not negative	0	3
Negative	0	1
Σ		
Positive	13	9
Not negative	4	7
Negative	1	2

Table 3.5.4 : Ageing effect with silica fume versus non-silica fume mixes, based on scaling values included in appendix F. Note the definitions : Positive classification if Silica Fume provides :

- *Less increase in scaling compared with non-silica*
- *Reduced scaling, while ageing without silica leads to increase.*

Not negative if :

- *Differences are below significance level, ~ 0,03 kg/m^2*
- *Both silica and non-silica are improved by ageing, independent of relative difference.*

Negative if :

- *Ageing with silica fume leads to higher scaling than ageing with non-silica fume mixes.*

3.6 Conclusions and synopsis

The present work is an extensive study with respect to amount of data and labour. Still, with hindsight supplementary studies on fundamental issues would have been useful. Such studies should include measurements of the moisture exchange with the environment and chemical and structural properties. These parameters might have enabled more decisive conclusions concerning the phenomena observed. However, keeping the original objective in mind, the present study may be regarded a valuable screening on the issue “effect of curing, ageing and silica fume”, taking into account that the test surfaces were not directly exposed to the external conditions during storing. The study also represents a solid statement on the issue of the importance of the curing conditions when testing the effect of pozzolanic materials.

The main findings of this study include :

- The study confirmed earlier reported evidence on very good freeze-thaw resistance with the particular SR-LA cement used. The effect of the cement is pronounced at low air void levels. There are clear indications of favourable air void characteristics with this cement or cement-admixture combination, compared to that of the CEM I 42.5-R cement. Still, the differences observed, e.g. from ageing – and from other researchers [M 1990] – suggests that the properties can not be attributed to air void characteristics only. With a proper air void system however, both cements perform well.

- Silica fume had a significantly positive effect on the freeze-thaw resistance with the CEM I 42.5-R cement. This was true in spite of somewhat poorer air void characteristics with the silica fume.

- The effect of silica fume with the CEM I 42.5 BV-SR-LA cement on scaling resistance was less distinct. Note the generally lower deterioration with this cement.

- The ageing effect was clearly negative for the non-air-entrained concrete and less so for medium air void level. It vanished for concrete with a proper air void system.

- The influence of silica fume on the ageing effect was found to be positive in the majority of cases for all curing conditions.

- No clear influence of slump level on scaling was found.
- No clear systematic effects of curing conditions and ageing were found. The reasons for the observed, very mixed behaviour between different curing regimes and ageing remain to a large extent unexplained.

Additional observations :

- The effect of silica fume depends on the curing condition, being very good with the CEM I 42.5-R cement and cyclic dry and wet curing.
- Generally, dry curing resulted in relatively good performance. It is important to keep in mind that the test surface was not directly exposed to the external drying. Traditionally, the test method is used to investigate the “internal potential” of the concrete, avoiding the sensitivity of surface finishing technique on the test results. “Dry curing” ($w/(c+s) = 0.45$) may still exhibit proper curing for the hydration process, which takes place for humidity levels down to or below 80 % RH. Consequently, in this respect all curing regimes may have provided appropriate curing. The remaining effect of various water curing procedures may thus mainly have been that of (increasing) the capillary degree of saturation prior to testing.
- In the same context, it is worth noting that no particular gradients in deterioration were observed : The layer close to the externally exposed surface did not deteriorate differently from the centre of the test surface. If water curing or drying changed the capillary degree of saturation, this must have happened a) for a major part of the test surface or b) on a level not sensitive for the testing conditions.
- Addition of silica fume together with appropriate amounts of HRWRA and AEA did to some extent affect the air void characteristics negatively. This effect was significant only in the case of the CEM I 42.5-R cement, requiring the highest dosage of WRA/HRWRA due to its higher water demand in fresh concrete.
- Supplementary investigations on moisture content at the initiation of the freeze-thaw test, as well as water ingress during testing, might explain some of the observations related to curing and type of binder. Characterising the capillary pore system might also enlighten the moisture exchange differences that probably would be observed.

URN:NBN:no-6354

4 Damage versus curing, moisture loss and absorption.

4.1 Introduction and objective

4.1.1 Background

The previous chapter discussed the effect of ageing (1 year) and curing on the results of laboratory testing. In particular, the moisture content at the start of freeze-thaw and water uptake during freeze-thaw were considered significant issues for further work. When applying laboratory testing, reproducibility/ repeatability and practical considerations are also very important. The testing conditions should be fixed in such a way that the testing results are not too sensitive to minor deviations in the testing procedure.

Sellevold [S 1988b] reported various investigations on the testing procedure of the slab scaling test (SS 13 72 44). Several authors looked into the effect of different cooling rates in freeze-thaw testing. Parallel to the performing of the present work, a study on the effect of various pre-drying conditions was published by Jacobsen [J 1995]. The pre-drying conditions were characterised by evaporation rate from a free water surface at the location of the storage/ curing of the concrete samples. Petersson [P 1995b] had reported studies on the relationship between the evaporation rate and scaling. It has been known that the different pre-drying conditions influence the carbonation of the concrete surface. In the meantime it has become evident that this influences the freeze-thaw scaling resistance significantly [U 1999b].

The present chapter comprises studies by the present author within the framework of a European research programme. The programme aimed at providing data for standardisation purposes. Test parameters and procedures were investigated in detail, comprising preliminary storage / curing conditions, preparation techniques and the temperature cycle during freeze-thaw. One of the objectives was to investigate the sensitivity of the testing method to marginal parameter changes. The present author took part in the parameter study of the "Borås test", also known as "The Scandinavian Slab Test" and the reference method of the future prEN xxx.

4.1.2 Objective

The programme originally investigated the effect of three different curing conditions on freeze-thaw damage. Additionally, a forth one designated “modified standard” (see later) was considered relevant for practical testing and included.

The main programme comprised freeze-thaw scaling – and internal cracking, if relevant. Additionally, the present study included weight changes throughout the curing process and before/after freeze-thaw. The main focus has been on relating the damage to the curing condition. Secondly, the weight changes were related to the curing conditions and to the freeze-thaw damage.

4.2 Experimental

4.2.1 Test method

As already mentioned, the present work was part of an evaluation of the slab test as proposed reference method within [prEN xxx]. The pre-testing conditions investigated partly coincided with other studies within the program. However, the present work was more comprehensive in the choice of curing conditions and combinations. It also had a different analytical approach to the test results.

The curing conditions comprised :

- The age of the concrete at the time of sawing, i.e. the formation of the surface subjected to curing and subsequent freeze-thaw testing.

- Storage and curing of the sawn test surface in air at 20 °C and relative humidity (RH) of 65 %, giving an evaporation rate from a free water surface of 45 g/m^2h - versus curing in plastic or drying at 40 °C.

- Type of re-saturation (water or 3 % NaCl-solution) during the three days period just prior to freeze-thaw testing. (Not all the mixes were subjected to different type of re-saturation.)

At the normal intervals, the amount of scaled-off material was determined. Further, the change in ultrasonic pulse velocity was measured on the same samples in order to detect any internal cracking. The sample weights were also recorded at each different step of the pre-testing period and upon the termination of the freeze-thaw testing. This was done to detect water loss/uptake during the different curing steps and during freeze-thaw.

4.2.2 Materials

The programme included eight different concrete compositions. The range in composition was designed to cover :

- A practical range of concrete binder/cement-types and concrete proportions used in the Nordic countries.
- A range large enough to provide a wide range with respect to damage. This meant concrete of good, intermediate and low freeze-thaw resistance.

An overview of the different concrete mix designs is provided in table 4.2.1, while details follow in the subsequent section.

w/b-ratio	**Nominal air content**	**Cement CEM I 42.5 R [1)]**	**Cement CEM II/A-V 42.5 R [2)]**	**Cement CEM I 42.5 R[1)] + silica fume**
0.45	5 %	1 : 45-I-AE	6 : 45-II-AE	8 : 45-IS-AE
0.45	Natural	2 : 45-I	-	-
0.55	4 %	3 : 55-I-AE	-	-
0.55	Natural	4 : 55-I	7 : 55-II	-
0.70	Natural	5 : 70-I	-	-

Table 4.2.1 : Mix design overview and mix number designation. [1)]*CEM I cement (Brand : Norcem Standard) with typical properties : Blaine 345* m^2/kg*, 6.5%* C_3A*,* Na_2O*-eqv. 0.95%,* F_{c1} *and* F_{c28} *of 21 and 52 MPa, respectively.* [2)]*CEM II cement (Brand : Norcem Standard FA) with 20% fly ash and typical properties : Blaine 400* m^2/kg*,* Na_2O*-eqv. 0.85% (contribution from fly ash not considered),* F_{c1} *and* F_{c28} *of 23 and 54 MPa, respectively.*

4.2.3 Curing

The general curing regime is illustrated in figure 4.2.1. Details are listed below :

Standard :

Age (Days)	0 - 1	In the mould
"	1 - 7	Water curing
"	7 - 28	Climate 20 °C/65% RH (with wind speed <0,5 m/s and evaporation rate from free water surface of 60 g/m^{2}h),
incl.:		- Sawing at 21 Days age - Preparation at 25-27 Days
"	28-31	Exposed to (depends on mix no.) : - Water : 4 specimen - 3 % NaCl : 4 specimen
"	31	Start of freezing (water or 3 % NaCl)

Modified Standard :

Age	0 - 1	In the mould
"	1 - 7	Water curing
"	7	Sawing
"	7 - 28	Climate 20 °C/65% RH, incl.: - Preparation at 25-27 Days
"	28-31	Exposed to (depends on mix no.) : - Water : 4 specimen - 3 % NaCl : 4 specimen
"	31	Start of freezing (water or 3 % NaCl)

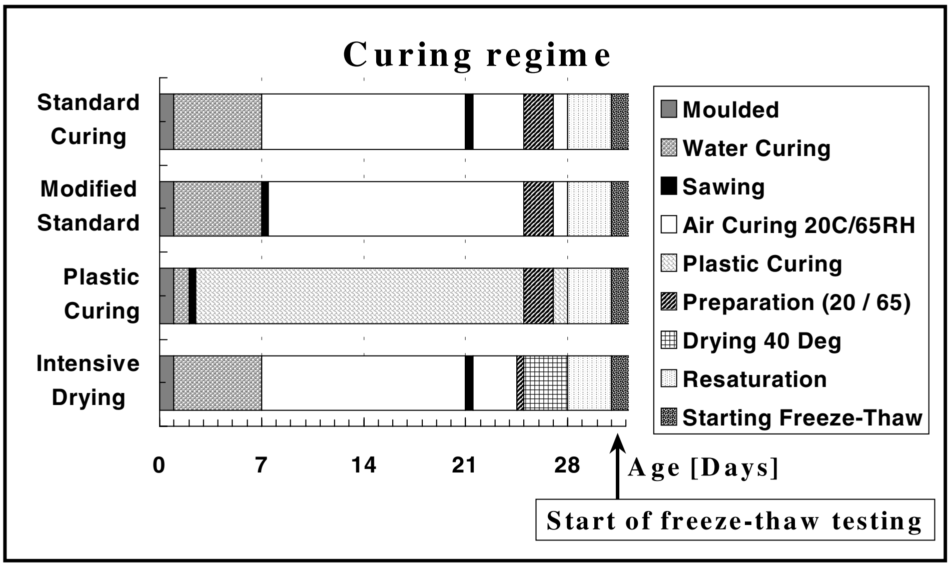

Figure 4.2.1 : Schematic presentation of the different curing regimes prior to freeze-thaw testing.

Plastic :

Age	0 - 1	In the mould
"	1 - 2	Water curing
"	2	Sawing
"	2 - 28	Stored in solid plastic bag at 20 °C, incl.: - Preparation at 25-27 Days
"	28-31	Exposed to (depends on mix no.) : - Water : 4 specimen - 3 % NaCl : 4 specimen
"	31	Start of freezing (water or 3 % NaCl)

Intensive drying :

Age	0 - 1	In the mould
"	1 - 7	Water curing
"	7 - 25	Climate 20 °C/65% RH, incl.:
"	21	Sawing
"	25	Preparation (morning)
"	25-28	Drying in climate chamber at approximately 40 °C, simultaneous measurements of evaporation rate from free water surface at different locations.
"	28-31	Exposed to (depends on mix no.) : - Water : 6 specimen - 3 % NaCl : 6 specimen
"	31	Start of freezing (water or 3 % NaCl)

Remark : It may be relevant to some readers (co-workers of the present author in the task group TC 51 / WG 12 / TG 4) that the preliminary and restricted reports on the issue did not quote all details correctly.

4.2.4 Details on concrete mix design

Concrete mix design and main properties are provided in the tables 4.2.2-9. Values in brackets are not meaningful in that they are outside the normal range of the method, see appendix H.

Constituents :	Properties
Cement CEM I – 42.5 R	400 kg
Water (No plasticizer ...)	180 kg
Air entrainer 1:9	0.93 kg
w/c-ratio	0.45
Sand 0 - 8 mm (NS)	752 kg
Crushed 8 – 11.2 mm (NS)	639 kg
Crushed 11.2 – 16 mm (NS)	326 kg
Slump	75 mm
Air content	4.5 %
Fresh concrete specific surface (DBT)	25 mm^{-1}
Fresh concrete spacing factor (DBT)	0.24 mm
28 Days Strength	46 MPa

Table 4.2.2 : Concrete mix design. Mix no. 1 : 45-I-AE

Constituents :	Properties
Cement CEM I – 42.5 R	415 kg
Water	187 kg
w/c-ratio	0.45
Sand 0 - 8 mm (NS)	780 kg
Crushed 8 – 11.2 mm (NS)	663 kg
Crushed 11.2 - 16 mm (NS)	338 kg
Slump	55 mm
Air content	1.6 %
Fresh concrete specific surface (DBT)	(8 mm^{-1})
Fresh concrete spacing factor (DBT)	(1.2 mm)
28 Days Strength (150 mm Cube)	54 MPa

Table 4.2.3 : Concrete mix design. Mix no. 2 : 45-I

Constituents :	Properties
Cement CEM I – 42.5 R	345 kg
Water	190 kg
Air entrainer 1:9	1.1 kg
w/c-ratio	0.55
Sand 0 - 8 mm (NS)	812 kg
Crushed 8 – 11.2 mm (NS)	691 kg
Crushed 11.2 - 16 mm (NS)	352 kg
Slump	70 mm
Air content	4.0 %
Fresh concrete specific surface (DBT)	44 mm^{-1}
Fresh concrete spacing factor (DBT)	0.11 mm
28 Days Strength (150 mm Cube)	35 MPa

Table 4.2.4 : Concrete mix design. Mix no. 3 : 55-I-AE

Constituents :	Properties
Cement CEM I – 42.5 R	345 kg
Water	190 kg
w/c-ratio	0.55
Sand 0 - 8 mm (NS)	803 kg
Crushed 8 – 11.2 mm (NS)	683 kg
Crushed 11.2 – 16 mm (NS)	348 kg
Slump	125 mm
Air content	1.2 %
Fresh concrete specific surface (DBT)	(7 mm^{-1})
Fresh concrete spacing factor (DBT)	(1.45 mm)
28 Days Strength (150 mm Cube)	46 MPa

Table 4.2.5 : Concrete mix design. Mix no. 4 : 55-I

Constituents :	Properties
Cement CEM I – 42.5 R	280 kg
Water	196 kg
w/c-ratio	0.70
Sand 0 - 8 mm (NS)	1 092 kg
Crushed 8 – 11.2 mm (NS)	521 kg
Crushed 11.2 – 16 mm (NS)	244 kg
Slump	75 mm
Air content	1.6 %
Fresh concrete specific surface (DBT)	(9 mm^{-1})
Fresh concrete spacing factor (DBT)	(0.9 mm)
28 Days Strength (150 mm Cube)	33 MPa

Table 4.2.6 : Concrete mix design. Mix no. 5 : 70-I

Constituents :	Properties
Cement CEM I – 42.5 R	410 kg
Fly ash content in the cement ; 20 %	
Plasticizer	0.47 kg
Air entrainer 1:9	5.5 kg
Water	187 kg
w/c-ratio	0.47
Sand 0 - 8 mm (NS)	767 kg
Crushed 8 – 11.2 mm (NS)	652 kg
Crushed 11.2 – 16 mm (NS)	332 kg
Slump	75 mm
Air content	4.9 %
Fresh concrete specific surface (DBT)	28 mm^{-1}
Fresh concrete spacing factor (DBT)	0.21 mm
28 Days Strength (150 mm Cube)	42 MPa

Table 4.2.7 : Concrete mix design. Mix no. 6 : 45-II-AE

Constituents :	Properties
Cement CEM I – 42.5 R	345 kg
Fly ash content in the cement ; 20 %	
Water	190 kg
w/c-ratio	0.45
Sand 0 - 8 mm (NS)	795 kg
Crushed 8 – 11.2 mm (NS)	676 kg
Crushed 11.2 - 16 mm (NS)	344 kg
Slump	60 mm
Air content	0.9 %
Fresh concrete specific surface (DBT)	(4 mm^{-1})
Fresh concrete spacing factor (DBT)	(3 mm)
28 Days Strength (150 mm Cube)	46 MPa

Table 4.2.8 : Concrete mix design. Mix no. 7 : 55-II

Constituents :	Properties
Cement CEM I – 42.5 R	410 kg
Silica fume	21 kg
Plasticizer	2.0 kg
Air entrainer 1:9	1.0 kg
Water	187 kg
w/c-ratio	0.46
w/(c+s)-ratio	0.44
Sand 0 - 8 mm (NS)	767 kg
Crushed 8 – 11.2 mm (NS)	652 kg
Crushed 11.2 - 16 mm (NS)	332 kg
Slump	70 mm
Air content	4.6 %
Fresh concrete specific surface (DBT)	25 mm^{-1}
Fresh concrete spacing factor (DBT)	0.22 mm
28 Days Strength (150 mm Cube)	54 MPa

Table 4.2.9 : Concrete mix design. Mix no. 8 : 45-IS-AE

As far as the concrete constituents concerns, the following characteristics may be noted (cement properties in accordance with prEN 196) :

The properties of the CEM I 42.5-R cement : F_{c2} = 32 MPa, F_{c28} = 52 MPa, Blaine 345 m^2/kg, water requirement 27.3 %, beginning of setting 130 min., alkali content 1.0 %, limestone filler content 4 %.

The properties of the CEM II 42.5-R cement : F_{c2} = 32 MPa, F_{c28} = 54 MPa, Blaine 400 m^2/kg, water requirement, water requirement 29.1 %, beginning of setting 130 min., alkali content (except fly ash contribution) 0.85 %, fly ash content 20 %.

The silica fume had an SiO_2 content of 98 % and was added as a dry powder.

The plasticizer was based on lignosulphonate, had a density of 1200 kg/m^3 and water content of 40 %. It was provided under the brand “Scancem P”.

The air entrainer was of the type “micro air”. The composition was not known, but it was chosen due to its well proven properties together with fly ash cement. The density was 1010 kg/m^2. As indicated above, it was diluted in the ratio 1:9 prior to use.

4.3 Test results and discussion

4.3.1 General

4.3.1.1 Organising the test results

Normal procedure in scientific reports is to present the test results «in bulk» and then proceed to the discussion.

This investigation provided an extensive amount of data that can be treated in different ways. The amount of data makes the traditional way of organising the data difficult. Also, it turned out not to be necessary to present all the data of all the mixes in the main chapter to draw certain conclusions. Thirdly, some of the data presentations needed explaining to an extent that it was believed convenient to combine presentation and discussions. This would not enable the traditional organisational structure of data presentation and subsequent discussions.

An alternative approach was chosen where firstly, all the aspects obtained with mix no. 1 are presented and discussed. Secondly, the same issue with the following mix (no. 2 etc.) is considered with respect to “conformity” with the previous mix(es). Then possibly new emerging issues of that mix are presented and discussed accordingly. When some of the general patterns were found to coincide with those of previously discussed or stated ones, these are referred to in the text only. In these cases, data or plots are still presented in appendix B for reference.

This means that in the following, the test results are discussed individually for each concrete mix. The data presentation of mix no. 1 in the main chapter is more extensive, while that of the other mixes are given in the appendix. The presentation and discussion of the other mixes include results in the main section for illustrating the discussion of each section only.

Finally, a summary and synopsis of the chapter is included.

4.3.1.2 Scatter and significance

It is a requirement in the description of the test method that parallel freeze-thaw samples within the series are not to be obtained from the same, cast object (concrete cube etc.). This is in order to include the effect of material scatter, and the present study is performed in compliance with this requirement. Additionally, samples for the different treatments have been selected as broadly as possible in order to include the material scatter within each of the single series.

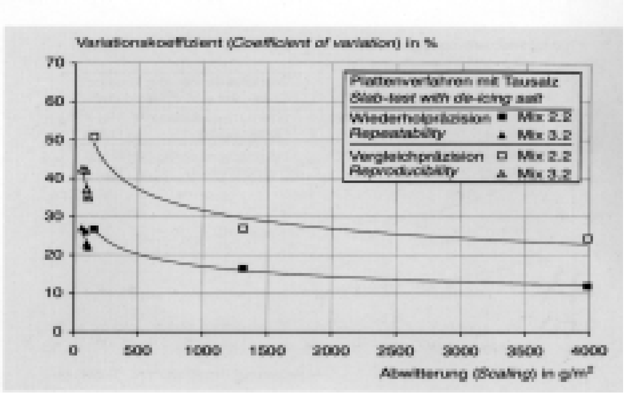

Figure 4.3.1 : Scatter of test results depending on the level of damage [S 1999]

Freeze-thaw scaling test results are subject to a natural scatter. This is partly due to variations/inhomogenity of the concrete material as mentioned above, partly to non-controlled variation in test performance : Precision data (ISO 5725) for the test procedure are provided by Siebel et al [S 1999], see figure 4.3.1. These data, based on a European Round Robin test, displayed a scatter depending on the level of damage. Hence, the coefficient of variation is a function of damage. Additionally, it is the opinion of the present author that for practical purposes, a lower limit of absolute scaling exists, under which differences are not significant. This “limit of detection” is in the range of 50 g/m^2. The present author is also of the opinion that the scatter will increase again when exceeding a scaling level of approximately 5 kg/m^2. This is due to practical limitations in providing a uniform exposure (3 mm salt solution) of the entire test surface after the formation of cavities.

In the following, only mean values of the single test series are reported in the discussions. In the appendix, mean values and standard deviation within the individual test series are provided. The scatter is treated in the following way : If the level of significance complicates the comparing of test results, it will be considered (of course). If not commented on, the differences presented are considered to be significant from a statistical-practical point of view.

Mean values and standard deviation ((3)4 to 6 samples) for the weight changes are given when relevant as follows :

- From sawing/cutting to preparation
- From preparation to the time of re-saturation
- During re-saturation
- From start of freeze-thaw to the termination of the test

in appendix B. The scatter within each series is quite low. In the following comparisons, all differences are considered significant.

4.3.1.3 Geometric effects of sample treatment

Cutting the samples at various points in time – according to the curing condition schemes – also implies that the actual size of surface exposed to drying differed between the curing regimes. This obviously has influenced the amounts of moisture loss prior to preparation and needs to be discussed separately :

The samples subjected to the various curing conditions consisted of slices of 100 mm diameter and 45 – 48 mm thickness. They were sawn from cylinders of height 200 mm, and the tested surfaces were always sawn surfaces. When subjected to storage in the 20 ^{o}C / 65 % RH, the cylinders (prior to sawing) and samples (after sawing) were placed “side by side” with the horizontal plane of the samples to be tested upwards.

This means that some of the moisture loss came from the (vertical) cylinder surface, not only the top surface. Moisture loss from the bottom is neglected in this respect due to the horizontal arrangement on a even surface.

The consequence is that all the series – except for the plastic curing one – experienced lateral evaporation in the period of 7 – 21 days. The drying effect from the cylinder surface is similar for all these three series, since both standard, modified standard and intensive drying samples were placed together. However, contrary to the other two, the modified standard series include the lateral weight loss in the subsequent "weight loss prior to preparation"-value. The surface area of this cylinder surface is relatively large (~135 cm^2) compared to the sawn surface of the samples (~78 cm^2), but the relative importance is believed to be smaller due to the sample arrangement.

However, the effect on the "weight loss prior to preparation"-values of the modified standard series is difficult to estimate. The "true" value for the loss from the test surface may be as low as 35 % of the total loss, considering the surface proportions above. Due to the sample arrangement (horizontally and next to each other), this is most probably an under-estimate. Anyway, the loss will prove to be significant. In the subsequent, it has been chosen to proceed with the total weight loss values in the data presentation but still consider (the uncertainty of) the effect in the discussions.

An alternative experimental approach would have been to seal all the cylinder surfaces in the period 7 – 21 days. However, then even the standard curing would no more fulfil that of the standard procedure. From 21 days, the surface subjected to drying/evaporation is the sawn surface only for all the series.

4.3.1.4 Nomenclature

In the presentation of the test results and the discussion, the term "re-saturation" is used frequently. The term actually is not quite correct, since it is not believed that the samples actually are "re-saturated": The use of this term assumes that 1) the samples once were saturated and 2) become saturated (again) by the second treatment. Both of these assumptions are not true. Further, the "extent of truth" varies between the different curing regimes.

A more correct description would be re-wetting. However, the term "re-saturation" is kept in the present context to conform to the nomenclature of the reference method of [PrEN xxx].

4.3.2 Mix 1 : 45-I-AE

4.3.2.1 Moisture loss prior to freeze-thaw

The weight loss of the modified standard curing (sawing at age 7 days, horizontally arranged and exposed to 20°C/65 % RH) compared to plastic curing is significant, see figure 4.3.2-3. Approx. 1.5 % of the original sample weight is lost at 20°C/65 % RH. This corresponds to 19 % of the total water, 50 % of the evaporable water content (70 % hydration assumed) !

Plastic curing produces, as expected, very low weight loss, less than 0,1 %. The parallel weight changes of specimens subjected to standard curing were not recorded. However, because these were not sawn until the age of 21 days, the diffusion-controlled process is expected to result in low water loss from the test surface prior to sawing.

After preparation, but prior to re-saturation, the weight loss of standard curing is slightly lower than the modified standard curing, already dried for two weeks. However, both these and plastic curing produce very low losses in this phase.

Intensive drying results in substantial weight loss. However, even at 40°C and an «evaporation potential» of 800 g/m^2h (mean evaporation rate from a free water surface) the weight loss is only one third of that caused at 20°C/65 % RH for two weeks (modified standard curing). A reason for such a trend could be that more mature concrete prior to drying reduces the weight loss. Correcting for the geometrical effects however, indicates that the moisture loss through the freeze-thaw test surface is at least within the same range for modified standard and intensive drying.

No correlation could be found between variation of "evaporation rate potential" due to individual placement of the single specimens (intensive drying) in the drying cabinet - and their individual weight changes during drying. The evaporation from a free water surface ranged from 600 – 950 g/m^2h, depending on the location. The relative humidity within the drying cabinet expectedly was in the range of 15 % (Laboratory air at 20 °C/50 % RH heated to 40 °C.) This means that at this evaporation rate and RH level, the moisture loss depends on the concrete material structure. Hence, marginal differences in vapour partial pressure at this level and for the relatively short period of drying can be neglected.

The difference in weight increase between water and 3 % salt is not significant.

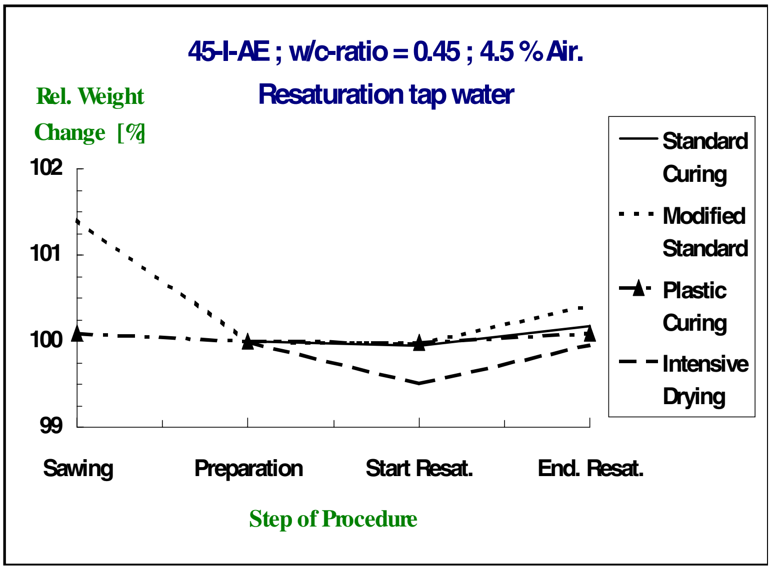

Figure 4.3.2 : Moisture loss and re-saturation (tap water) prior to freeze-thaw, mix 1 : 45-I-AE.

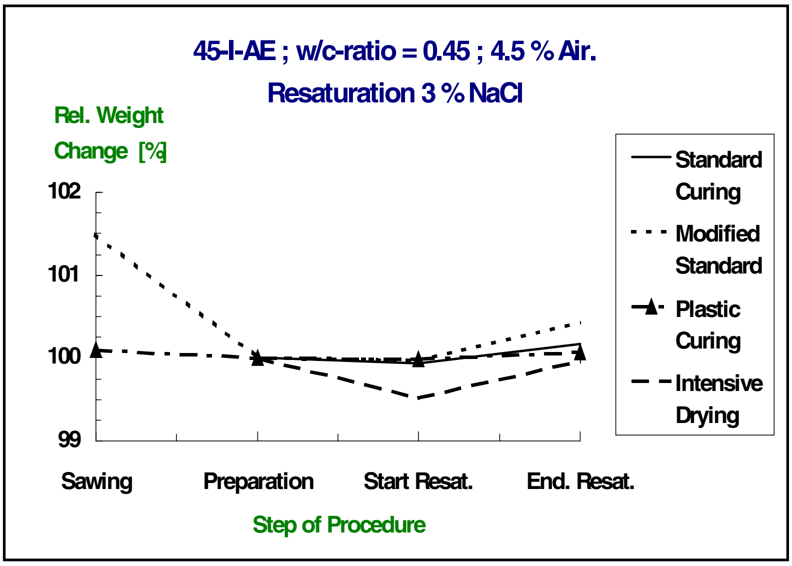

Figure 4.3.3 : Moisture loss and re-saturation (3 % salt) prior to freeze-thaw, mix 1 : 45-I-AE.

4.3.2.2 Moisture loss vs. moisture uptake prior to freeze-thaw

The different drying periods for the different curing conditions (figure 4.2.1) do not enable a simple comparison of moisture loss prior to preparation between the series : "Standard curing" and "Intensive drying" were equally treated until sawing at 21 days of age. Those are the two "most comparable" conditions. "Modified standard" was sawn at 7 days, starting the moisture loss from the test surface at this stage. "Plastic curing" was sawn already at two days of age but kept in plastic the entire period prior to freeze-thaw. Still, it is considered noteworthy to compare and discuss the weight loss during the last stages prior to freeze-thaw. This history obviously influenced the subsequent moisture uptake during the re-saturation. *Though, it is important to keep in mind that moisture uptake – in contrast to drying – took place through the test surface only.* The relation to the behaviour during freeze-thaw will be discussed in subsequent sections. First, the observed moisture loss and moisture uptake is reported and discussed. Due to the complex nature of comparing weight changes between the different curing conditions, the discussion will not be equally detailed for the concrete mix nos. 2 - 8.

During the period of re-saturation, the weight gain is lowest for plastic curing, which corresponds to the previous low moisture loss. The weight gain of standard curing is slightly higher than the former, indicating slightly larger losses or changes at previous stages.

The weight increases of modified standard and intensive drying during re-saturation are of the same order and much higher than for the others.

In accordance with the introductory remarks above, there is of course no direct correlation between weight loss subsequent to preparation and weight increase during re-saturation (figure 4.3.4 and 4.3.5b). Correcting the moisture loss of the "Modified Standard" its expectedly "true level" for the re-saturated surface (section 4.3.1.3), this statement would still be valid. The same is of course true when weight loss prior to preparation of the specimens is included in the weight loss (figure 4.3.5a).

The weight gain after intensive drying is very close to that of modified standard. Intensive drying regained 80 % of the weight loss in the drying cabinet, compared to 40 % for modified standard. Correcting for the uncertainty of the geometrical effect, the equal uptake through the test surface may actually represent an equal re-filling of the dried pore space. See next section for arguments, also.

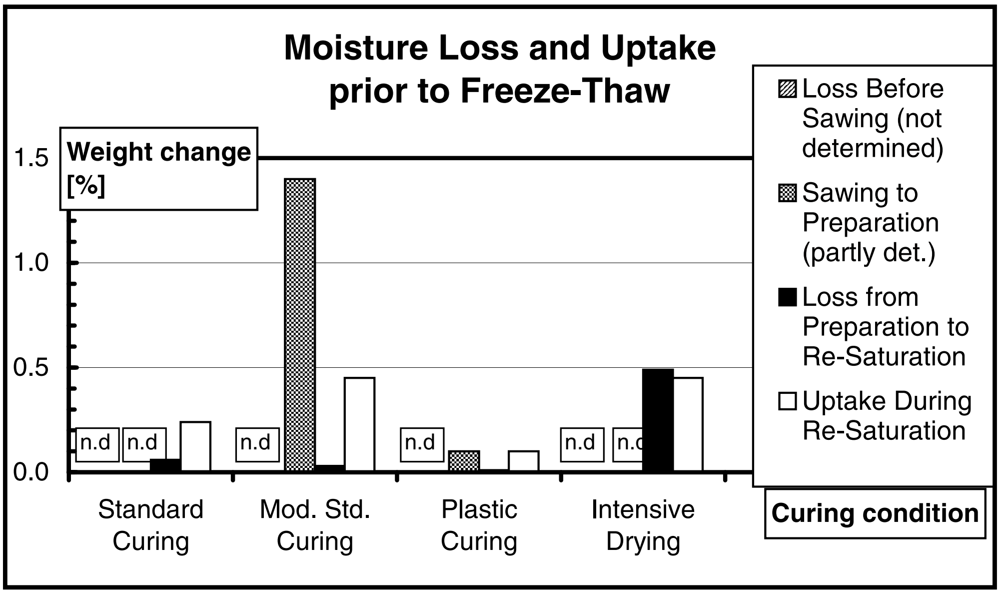

Figure 4.3.4. Bar chart diagram of the moisture loss and moisture uptake for Mix 1 subjected to the different curing conditions prior to freeze-thaw. "n.d" designates "not determined". Alternative presentation of the values given in figure 4.3.2-3. See text for "geometrical effects".

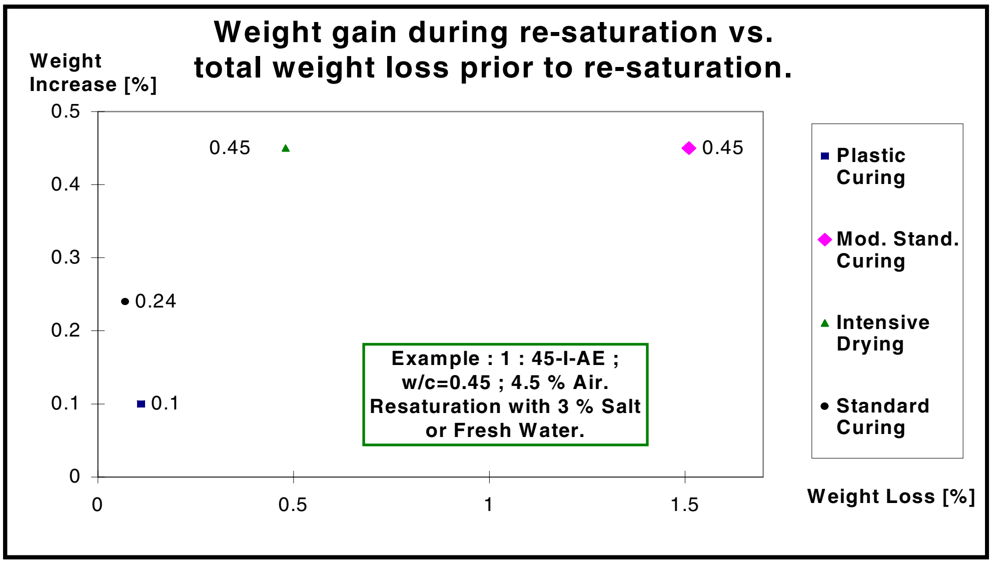

Figure 4.3.5a : Comparing weight gain during re-saturation and preceding moisture loss. Identical results achieved with re-saturation by water as with re-saturation by salt solution. See text for "geometrical effects".

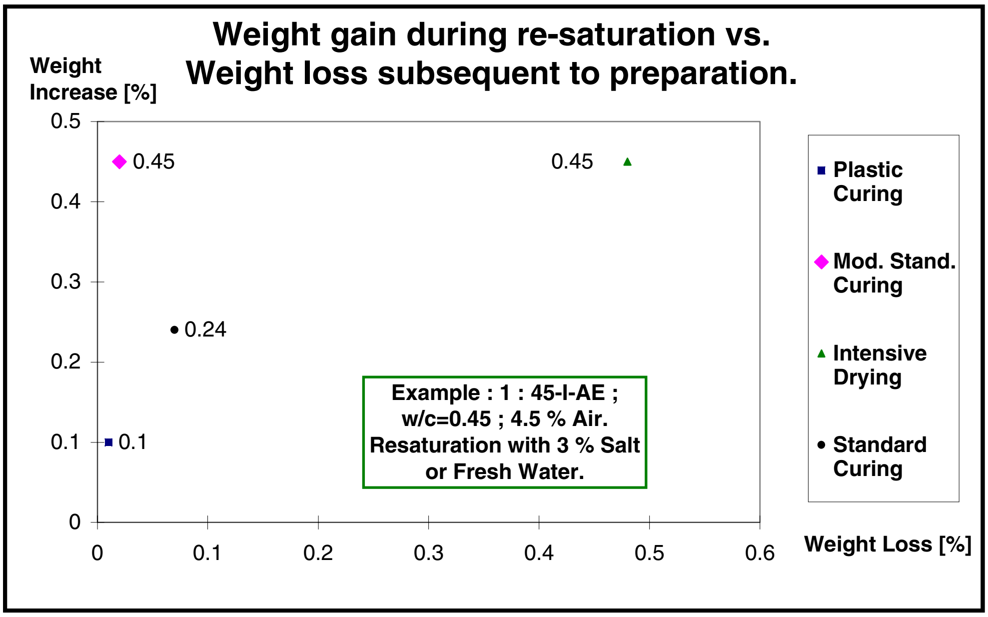

Figure 4.3.5b : Comparing weight gain during re-saturation and moisture loss subsequent to preparation. Identical results achieved with re-saturation by water as with re-saturation by salt solution. See text for "geometrical effects".

Standard curing, comparable to intensive drying prior to preparation, produced a moisture uptake only half of that of modified standard and intensive drying (figure 4.3.4).

4.3.2.3 Moisture uptake during freeze-thaw

The weight increase during freeze-thaw - corrected for weight loss due to scaling - has been measured. In doing so, a scale factor of 1.05 was applied to correct for the weight loss of the scaled material during drying. However, the intensive drying series suffered substantial weight loss due to scaling and were considered unsuitable for such weight loss correction. They are left out from the plots and discussion in this respect.

There is no apparent correlation to the weight loss prior to the freeze-thaw-testing (figure 4.3.6a/7a). More important, the moisture uptake is substantial compared to the previous weight loss and ~uptake (figure 4.3.6b/.7b). Even for plastic curing, with a re-saturation in the same range as the previous weight loss, the moisture uptake during freeze-thaw corresponds to 10 % of the evaporable water content (no air voids filled ; see section 4.3.2.1). If the entire moisture uptake is localised to the upper 10 mm, it corresponds to 50 % increase in the evaporable water content. According to figure 4.3.6b, we may assume that for plastic curing, the re-saturation just compensates for the moisture loss after preparation. Using the formula Eq. AI-7 in the appendix I, the degree of capillary saturation prior to freeze-thaw may be estimated : Assuming plastic curing as isolated curing and degree of hydration 75 %, the formula yields 86 % degree of capillary saturation. Hence, the mean value of 10 % evaporable water uptake can be accommodated in the capillary pore system.

For modified standard curing, the accumulated weight increase (in the range of 20 % of the evaporable water content) still is less than the previous weight loss after sawing. Hence, it is reasonable to believe that the capillary degree of saturation even after freeze-thaw for modified standard curing is less than that of plastic curing. This is somewhat in contrast to the subsequent observations on scaling of the two series.

For standard curing, the moisture uptake during freeze-thaw is in the same range as for that of modified standard, i.e. 20 % of the evaporable water content. Compared to standard curing, the early sawing (at 7 days) of modified standard apparently leads to higher moisture uptake during re-saturation, but not during freeze-thaw. Since the moisture loss of standard curing prior to sawing was not monitored, it is not possible to postulate the difference in capillary degree of saturation between standard and modified.

When tested with 3 % salt, an interesting phenomenon is displayed in the figures 4.3.6a/b-7a/b : There is a tendency of increased weight increase during freeze-thaw for standard and plastic curing if the samples have been re-saturated with fresh water. The difference is not statistically significant (appendix B), but the change fits with the relative change in observed scaling (see later).This may be an important observation because it opposes a theory of osmotic pressure from the interior towards the surface. According to the theory (section 2 of this publication), the osmotic effect would increase the surface degree of saturation but should simultaneously somewhat limit the (initial) ingress of the 3 % salt testing medium. The osmotic effects are also confirmed by Lindmark [L 1998].

Accumulated weight gain during re-saturation and uptake during the freeze-thaw-test provides no further information. The (lack of) correlation to the weight losses prior to testing remains the same (figures 4.3.8-9).

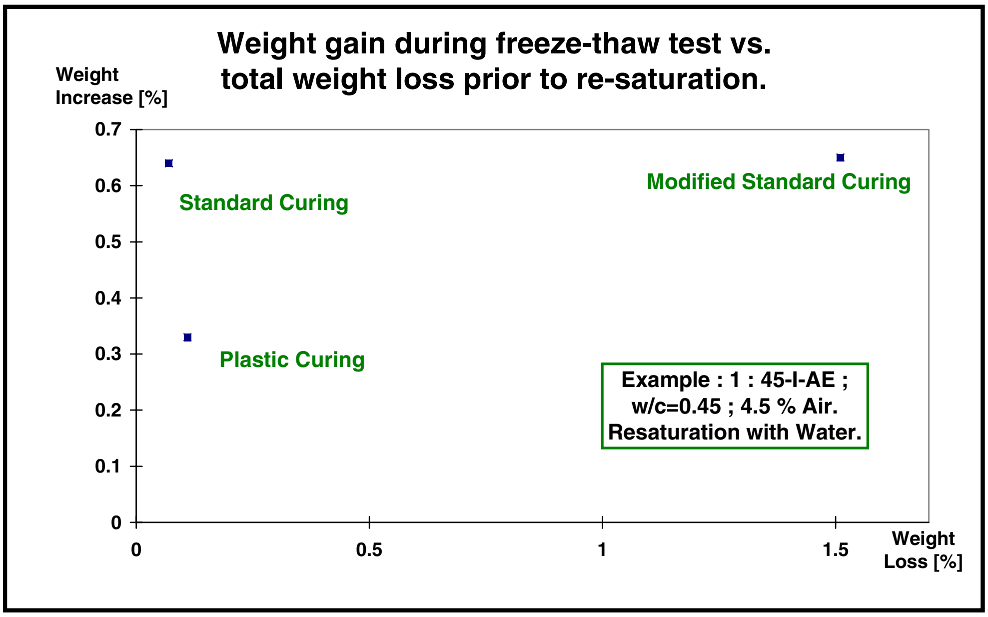

Figure 4.3.6a : Weight increase during freeze-thaw compared to weight loss prior to re-saturation (by water). See text for "geometrical effects".

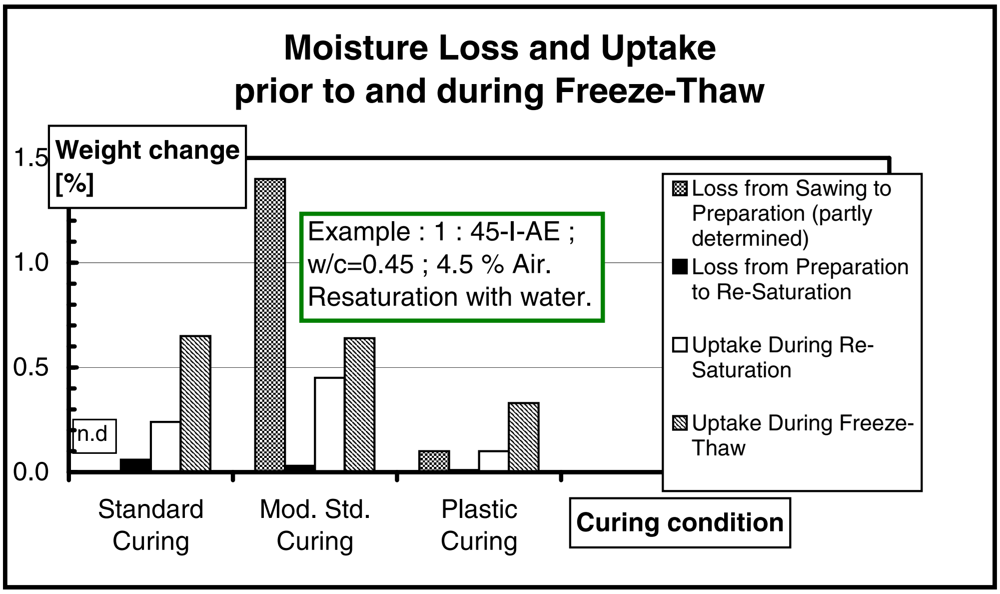

Figure 4.3.6b : Moisture loss and moisture uptake for Mix 1 subjected to the different curing conditions prior to freeze-thaw and re-saturated by pure water. "n.d" designates "not determined". Alternative presentation of the values given in figure 4.3.6a. See text for "geometrical effects".

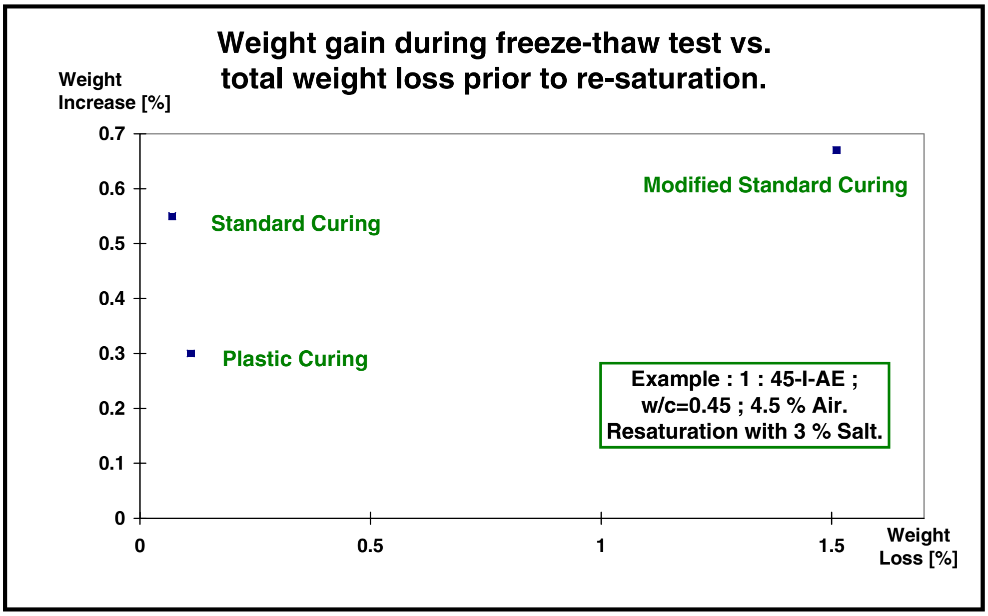

Figure 4.3.7a : Weight increase during freeze-thaw compared to weight loss prior to re-saturation (by 3 % salt). See text for "geometrical effects".

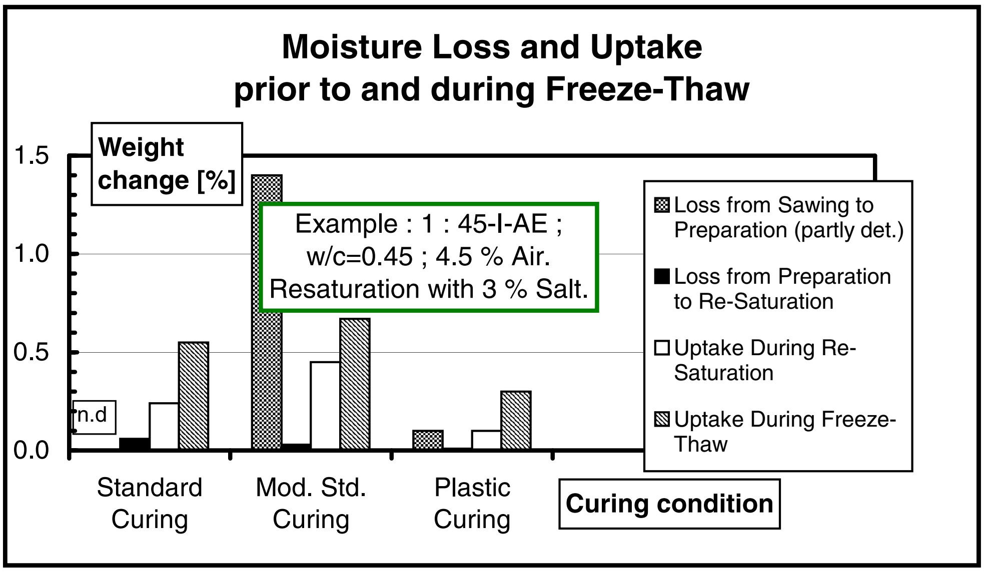

Figure 4.3.7b : Moisture loss and moisture uptake for Mix 1 subjected to the different curing conditions prior to freeze-thaw and re-saturated by 3 % NaCl. "n.d" designates "not determined". Alternative presentation of the values given in figure 4.3.7a. See text for "geometrical effects".

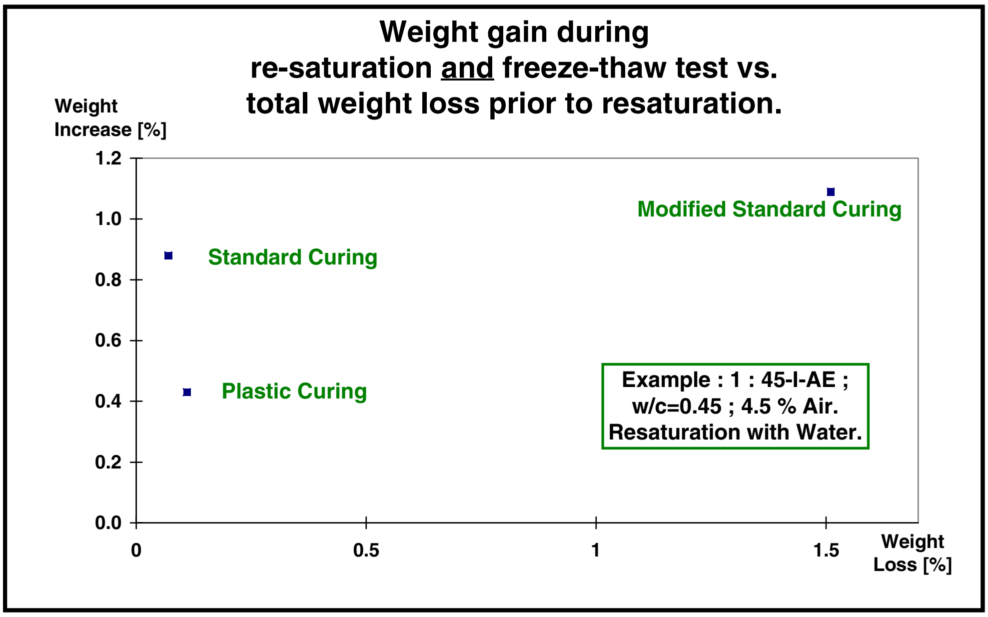

Figure 4.3.8 : Accumulated weight gain during re-saturation and freeze-thaw, compared to total weight loss prior to re-saturation (by water). See text for "geometrical effects".

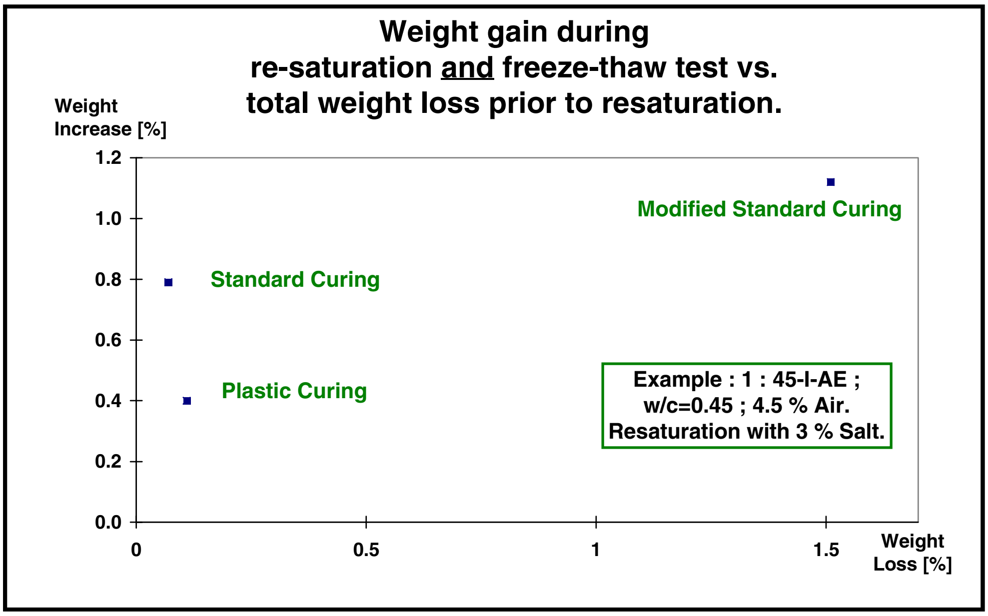

Figure 4.3.9 : Accumulated weight gain during re-saturation and freeze-thaw, compared to total weight loss prior to re-saturation (by 3 % salt). See text for "geometrical effects".

4.3.2.4 Scaling vs. curing regime and moisture movement

The mean values of scaling and corresponding standard deviations are provided in the appendix B.

Within a single series, i.e. identical curing procedure, no correlation could be found between scaling and differences in weight changes prior to preparation or during the re-saturation phase. Nor could such scatter of scaling be accounted for by the differences in evaporation rate detected (Intensive drying).

In order to explain the variations in scaling within and between the parallel specimens, a structural analysis by thin sections was performed. The standard deviation in remitted fluorescent light between different locations corresponds to equivalent, local changes in the w/c-ratio of 0.05 (spot measurements in the paste). Air void analysis was performed by point count, demonstrating a well distributed fine pore structure. However, the content of fine pores $A_{0,25}$ (<0,25 mm) could vary from 2% to 3% and the total air void level from 4.5% to 5.5 % between the samples. Such structural variations are likely to occur and may account for different behaviour. The natural scatter of scaling test results is of course partly caused by variations in the concrete material.

In all four curing regimes, re-saturation by water resulted in much higher scaling than the parallel samples re-saturated by 3 % salt (figures 4.3.10-13). This may partly be explained by the higher water uptake during freeze-thaw as commented in the previous section (figure 4.3.6 vs. 4.3.7). Why water-pre-saturation should result in larger ingress of water during freeze-thaw can not readily be explained. However, it may be a secondary effect caused by the damage itself, e.g. cracking providing water suction. For later investigations, the time- or damage-depending development in *weight increase* of the specimens during freeze-thaw should be recorded.

An alternative explanation to reduced scaling when re-saturated by 3 % salt is somewhat reduced amount of the freeze-able water due to the chloride ingress during re-saturation by 3 % salt. However, the effect seems too large to be caused by this effect, but it should be subject to closer investigations. It has been proposed by some authors to use salt solution for re-saturation prior to freeze-thaw testing. For some applications of de-icing chemicals, this might be in accordance with the field conditions.

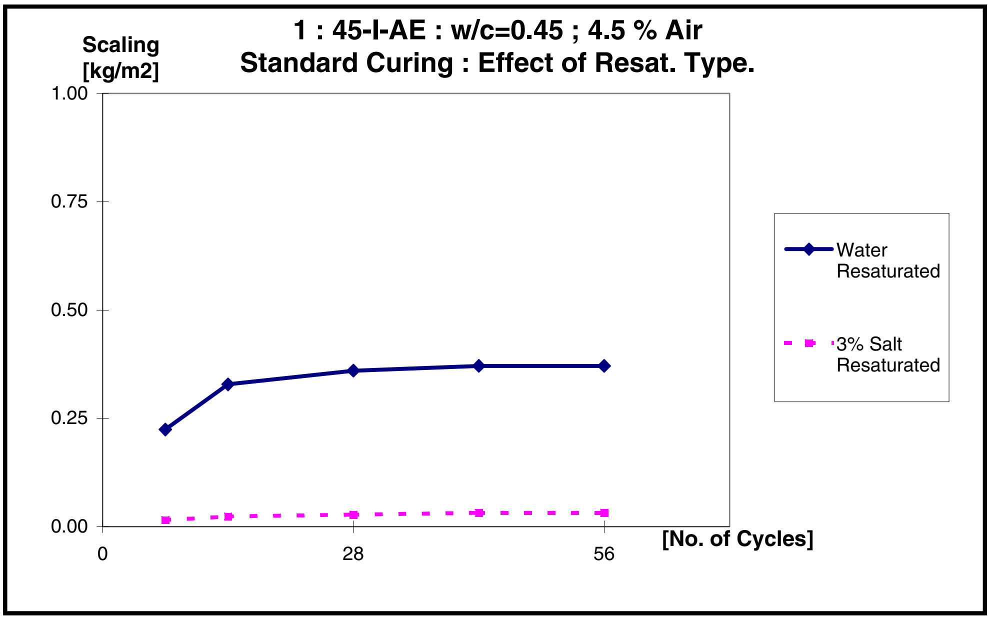

Figure 4.3.10 : The effect of the type of re-saturation. Standard curing.

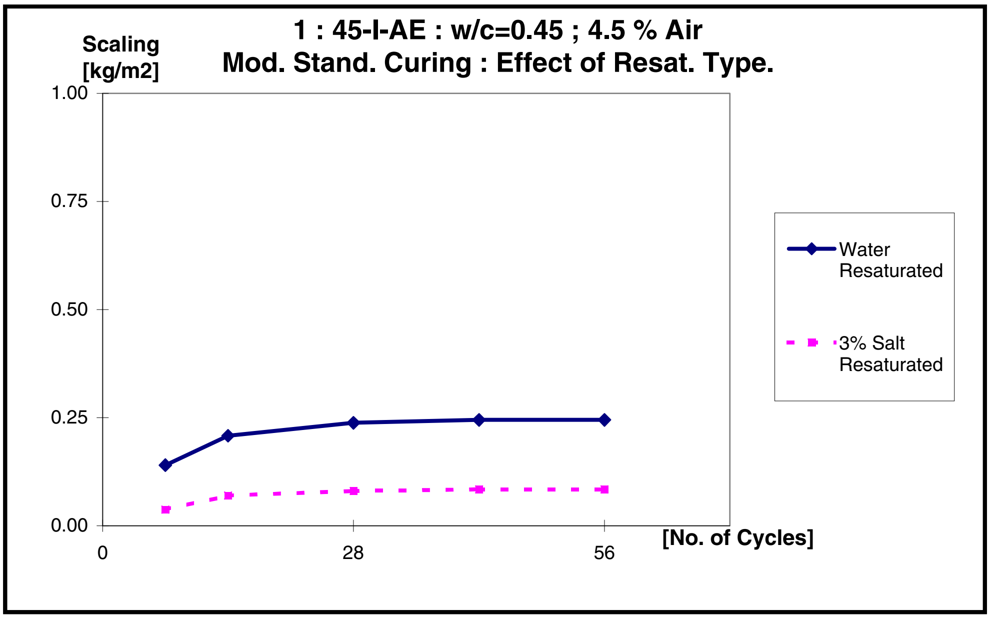

Figure 4.3.11 : The effect of the type of re-saturation. Modified standard curing.

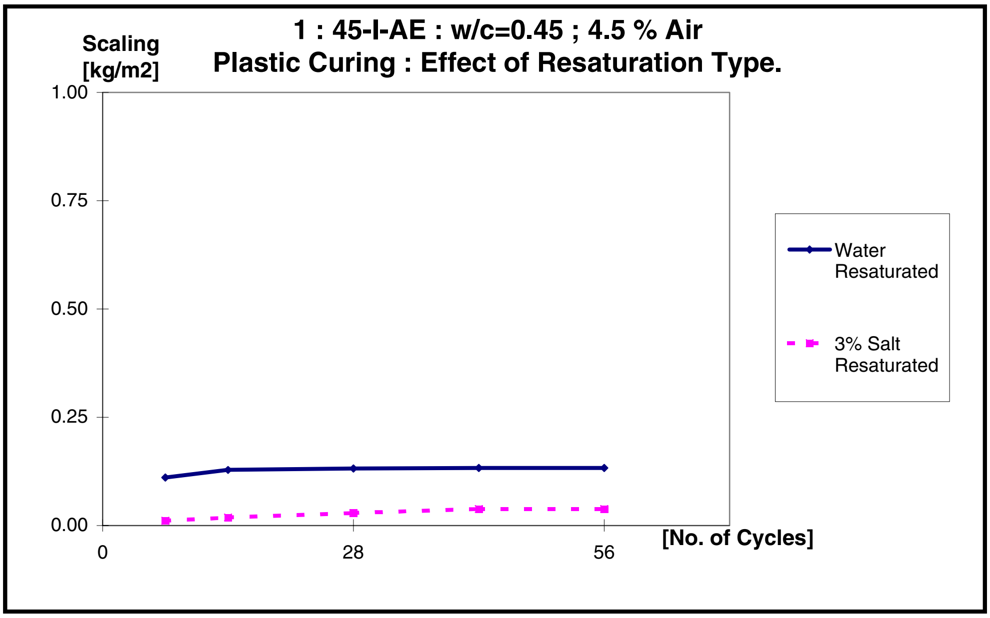

Figure 4.3.12 : The effect of the type of re-saturation. Plastic curing.

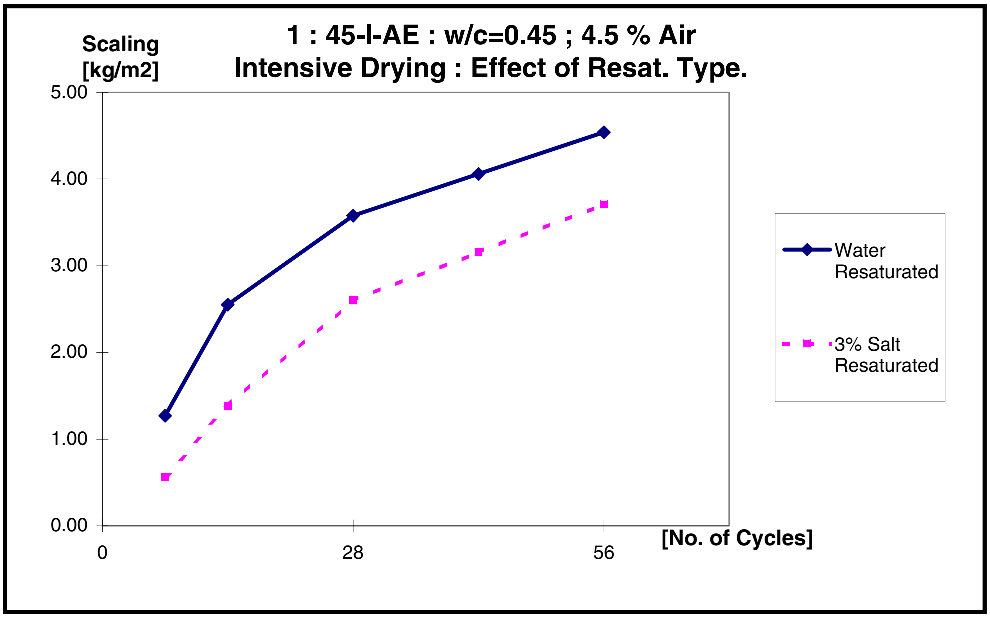

Figure 4.3.13 : The effect of the type of re-saturation. Intensive drying.

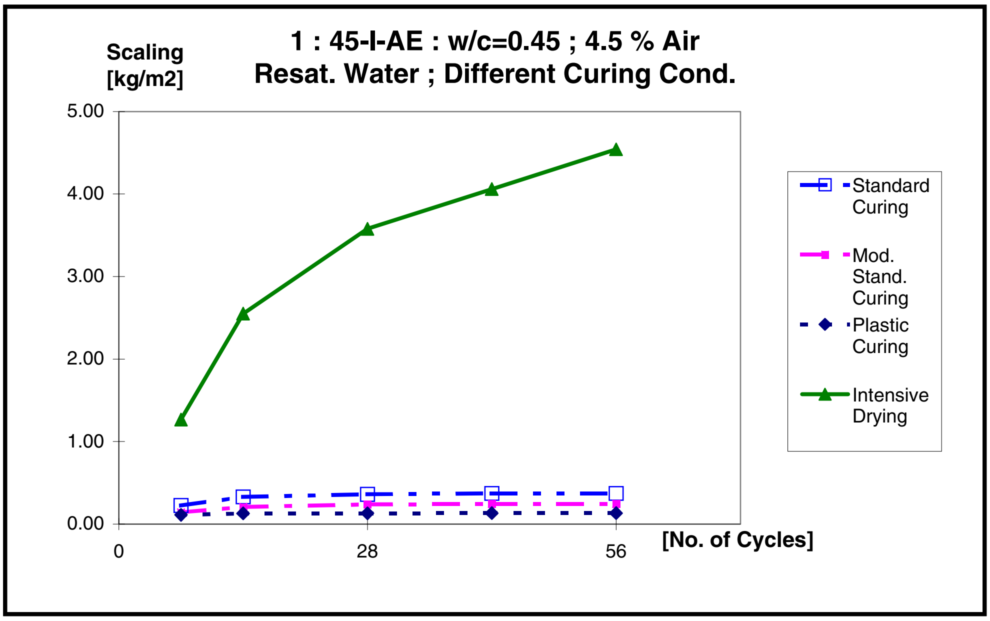

Figure 4.3.14 : The effect of the curing condition on the freeze-thaw scaling. Re-saturation by water.

Intensive drying results in substantially higher scaling than any other curing regime. The drying-re-saturation effect observed is in accordance with earlier studies [S 1988b]. However, it appears that the temperature – at least as an indirect parameter for the drying conditions – is more important than the amount of moisture loss. The direct parameter of influence may be the external, relative humidity during drying, being 50 % RH for modified standard and 15 % RH (approximately) for intensive drying. This most probably leads to more extensive changes of the pore structure prior to freeze-thaw. Unfortunately, the weight increase, i.e. absorption, during freeze-thaw was not obtained for these specimens. It would be difficult to assess accurately with the high level of scaling.

The differences between the various curing conditions – when re-saturated by water – are displayed in figure 4.3.14. Closer considerations on the scatter (appendix B) seem to allow a ranging in the order 1) Plastic curing (lowest scaling), 2) Modified standard / 3) Standard curing and 4) Intensive drying. The difference in scaling for 2) and 3) is not considered significant. There appears to be a correlation between the low scaling for plastic curing and its low weight gain during freeze-thaw – versus the intermediate values for the remaining two.

When subjected to re-saturation by 3 % salt, the differences between standard, modified standard and plastic curing are hardly significant for the present mix design (figure provided in the appendix B).

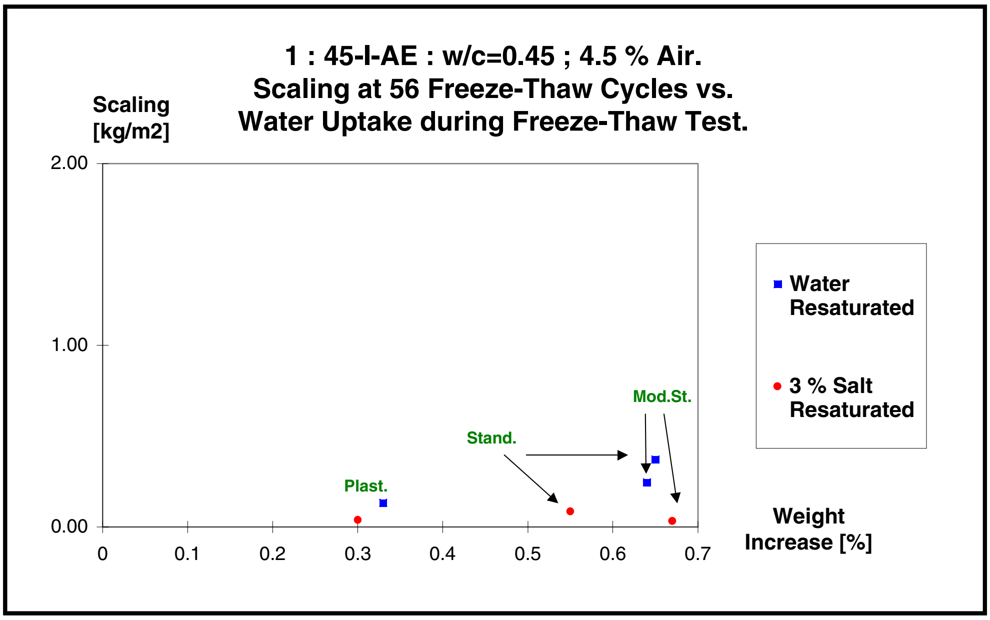

Figure 4.3.15 : Freeze-thaw scaling versus water uptake during freeze-thaw.

For re-saturation by water, there is a tendency of increased scaling with increased water absorption during freeze-thaw (figure 4.3.15). This seems even more pronounced when weight gain during re-saturation is added to the absorption (figure 4.3.16).

No direct correlation can be found between scaling at any age and weight increase during re-saturation (figure 4.3.17 and appendix B). This is possibly due to lack of significant scaling differences. However, the nature of moisture loss is probably more important than the absolute moisture loss.

When water re-saturated, there is a tendency of increased scaling with increased weight loss subsequent to preparation (figure 4.3.18-19 and appendix B). If this is a pattern, it is more pronounced at early age than later. The pattern when saturated by 3 % salt is different, except for intensive drying. Adding weight loss prior to preparation shows no relation to scaling at all (figure 4.3.20).

Hence, the best correlation shown by these plots is between scaling and total water absorption – and the early scaling versus moisture loss subsequent to preparation. In both cases, re-saturation by water (not 3 % NaCl) is assumed.

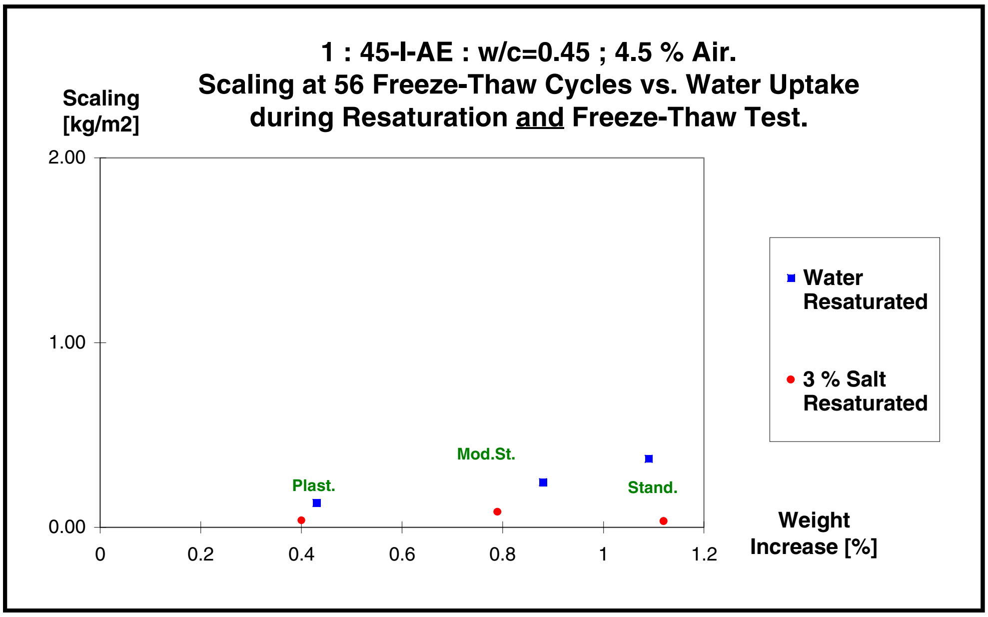

Figure 4.3.16 : Freeze-thaw scaling versus water uptake during re-saturation and freeze-thaw.

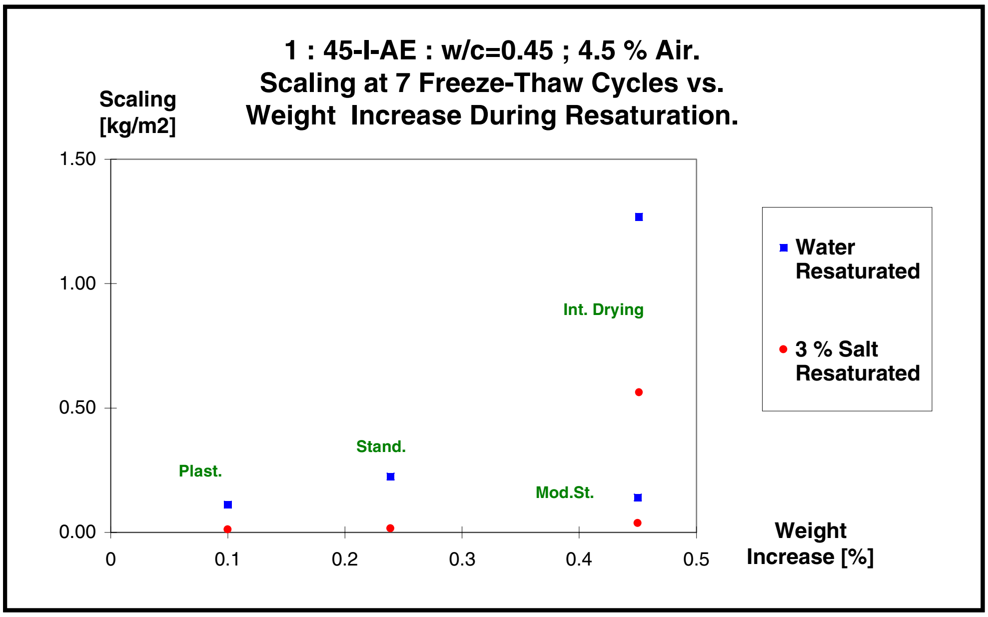

Figure 4.3.17 : Scaling after 7 cycles versus absorption during re-saturation only.

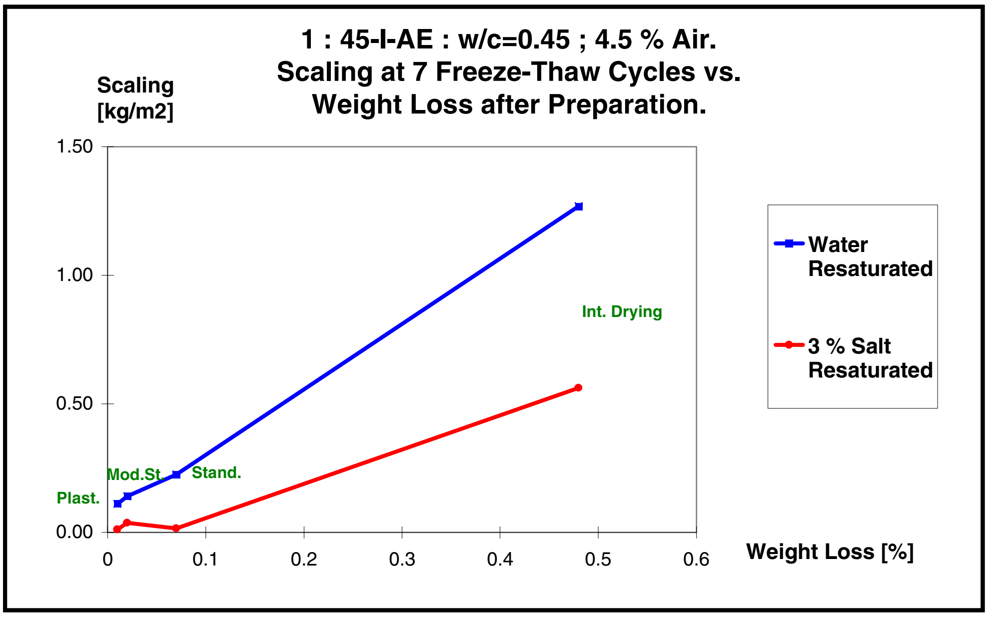

Figure 4.3.18 : Scaling after seven freeze-thaw cycles versus weight loss after preparation only.

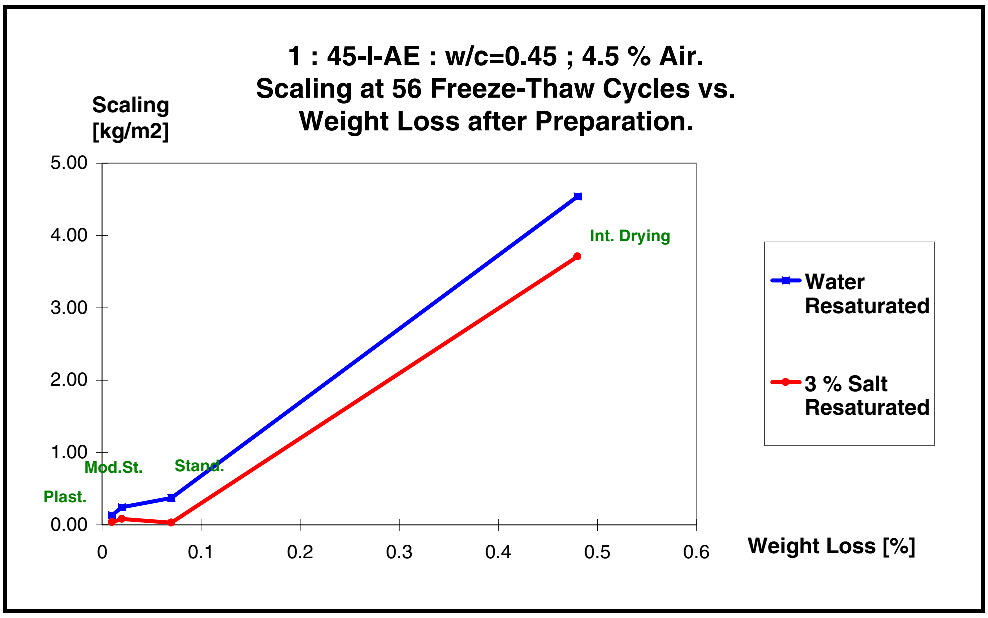

Figure 4.3.19 : Scaling after 56 freeze-thaw cycles versus weight loss after preparation only.

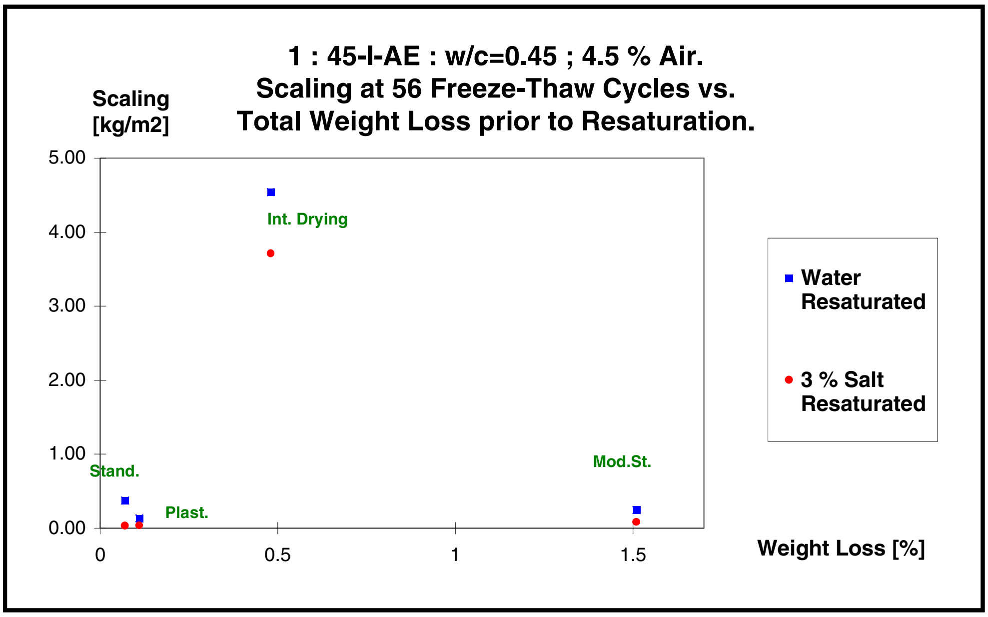

Figure 4.3.20 : Scaling after 56 freeze-thaw cycles versus total weight loss prior to re-saturation.

4.3.2.5 Conclusions

Preliminary conclusions, based on this concrete mix only may be drawn as follows (subject to comparisons for the subsequent mixes) :

- Intensive drying resulted in substantially higher scaling than any other curing regime. Indirectly, it may be attributed to the higher drying temperature, since modified standard curing suffered a moisture loss in the same range. The direct cause of the more severe damage may be attributed to the drying condition of only 15 % RH (appr.) and more severe pore structure changes. Thus it is how the moisture loss occurs, not the amount, that is important.

- In general, re-saturation by water caused higher scaling than re-saturation by 3 % NaCl. At least partly, there is a correlation between the increased scaling and the absorption during freeze-thaw (previous clause). Some of the difference may be due to reduced amount of freeze-able water.

- There was no general correlation between the moisture loss prior to freeze-thaw and absorption during freeze-thaw.

- Plastic curing produced the lowest scaling. The difference between standard and modified standard was at the limit of significance.

- The moisture uptake during freeze-thaw was substantial. Even for plastic curing, the uptake amounted to a 10 % increase in the capillary degree of saturation. It was estimated that the available capillary pore volume could accommodate this extra moisture content.

- There is indication of larger absorption during freeze-thaw when initially re-saturated by water than being re-saturated by 3 % salt (standard curing). This fits with the higher degree of scaling when re-saturated by water. It might be attributed to higher internal deterioration (cracking) causing absorption. However, such damage was not investigated for these samples (e.g. by ultrasonic pulse velocity or plane section).

- As expected, loss of moisture from the concrete depended very much on the pre-storage conditions.

- Sawing at an early age (modified standard) provided substantial loss of moisture even when stored at 20^{o}C/65 % RH, amounting to 50 % of the evaporable water. This weight loss was three times that of the one caused by drying for 72 hours at 40 ^{o}C. However, 50-65 % of the difference may be due to moisture loss from the cylinder surface (modified standard). This implies that the moisture loss from the freeze-thaw test surface may have been in the same range for these two different curing conditions.

- The weight gain during the subsequent re-saturation was of the same order for modified standard curing and intensive drying. Corrected for “geometrical effects”, it appears that the weight gain (re-saturation) per (previous) weight loss from the test surface is of the same order for modified standard curing and intensive drying.

- Different “evaporation potential” (vapour pressure differences during intensive drying) in the sense of different evaporation from a free water surface ranging from 600 – 950 g/m^2h did not produce corresponding differences in weight loss from the samples. The relative humidity in this case was in the range of 15 % RH. This implies that the relative difference in vapour pressure probably was low, and that variation in evaporation rate was due to local air speed variations.

4.3.3 Mix 2 : 45-I

4.3.3.1 Moisture changes prior to freeze-thaw

Mix 2 had mix proportions identical to those of mix 1, but was not air entrained and scaled severely. As for mix 1, the modified standard curing produced a substantial weight loss prior to preparation (appendix B). Approximately 1.3 % of the original sample weight is lost during this storage period. This corresponds to 17 % of the total, initial water content, 44 % of the evaporable water (70 % hydration assumed). These values are slightly lower than those for the corresponding concrete mix design with entrained air. A possible explanation is a higher initial water content for standard curing when air entrained, due to the one week water storage. A prerequisite for this would be partial water absorption of the air voids, which is likely ; see other parts of this publication.

As for mix 1, plastic curing produces very low weight loss, less than 0,1 %. Again after preparation, but prior to re-saturation, the weight loss of standard curing is slightly higher than that of modified standard curing, already exposed for two weeks. However, both these and plastic curing produce very low losses in this phase.

Intensive drying results in substantial weight loss, but again only one third of that caused at 20°C/65 % RH for two weeks (modified standard curing).

Again, no effect could be found of variation in "evaporation rate potential" due to individual placement of the single specimens (intensive drying) in the drying cabinet. Their individual weight changes during drying at this very low relative humidity (approximately 15 % RH) could not be related to such potential differences.

During the period of re-saturation, the weight gain is lowest for plastic curing, which corresponds to the previous low moisture loss and potential pore structure changes. The weight gain of standard curing is slightly higher than the former, indicating slightly larger losses or changes at previous stages.

The weight increases of modified standard and intensive drying during re-saturation are again of the same order and much higher than for the others.

4.3.3.2 Moisture loss vs. moisture uptake

As for mix 1, there is no apparent correlation between weight loss subsequent to preparation and weight increase during re-saturation (figure 4.3.21). The same is also true when weight loss prior to preparation of the specimens is included in the weight loss (figure 4.3.22).

Again, the weight gain of intensive drying is very close to that of modified standard, i.e. 80 % of the previous weight loss of the former, and only 35 % of that of the latter. Corrected for "geometrical effects" (conclusions of section 4.3.2), it appears that the moisture uptake during re-saturation depends on the previous weight loss (through the same test surface). The drying conditions appear less important for the amount of re-saturation.

Unfortunately, the weight increase during freeze-thaw was not determined for the present mix.

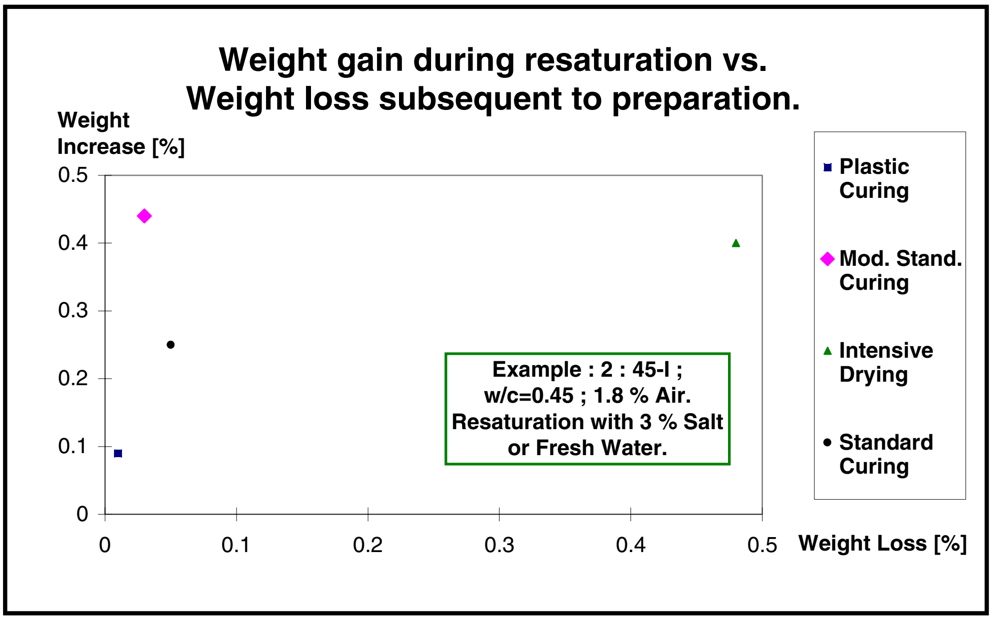

Figure 4.3.21 : Weight gain during re-saturation versus weight loss after preparation, mix 2. Identical results obtained when re-saturated by pure water as when re-saturated by 3 % NaCl.

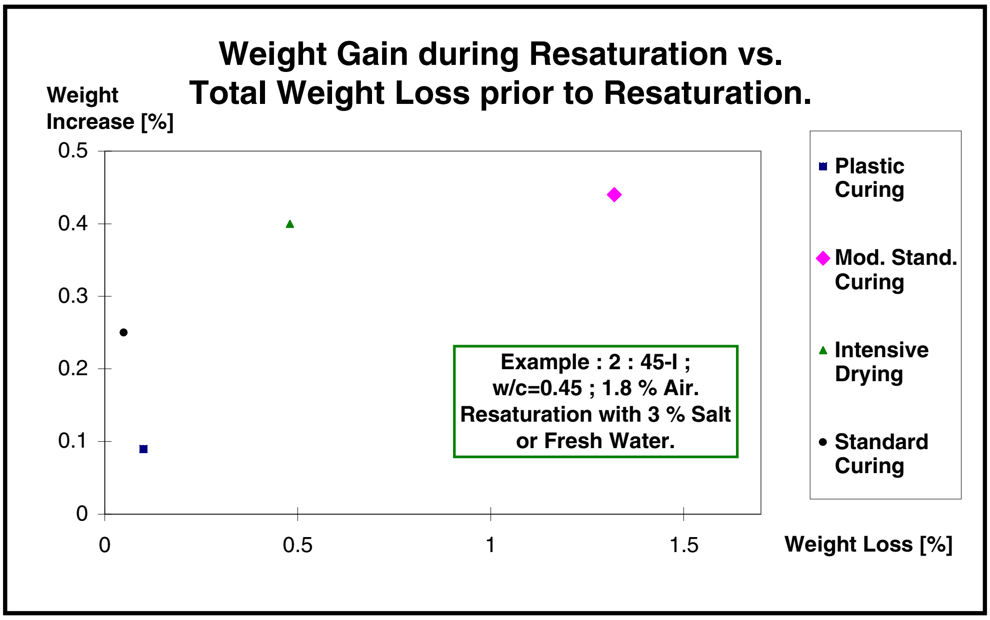

Figure 4.3.22 : Weight gain during re-saturation versus total weight loss prior to re-saturation, mix 2. Identical results obtained when re-saturated by pure water as when re-saturated by 3 % NaCl.

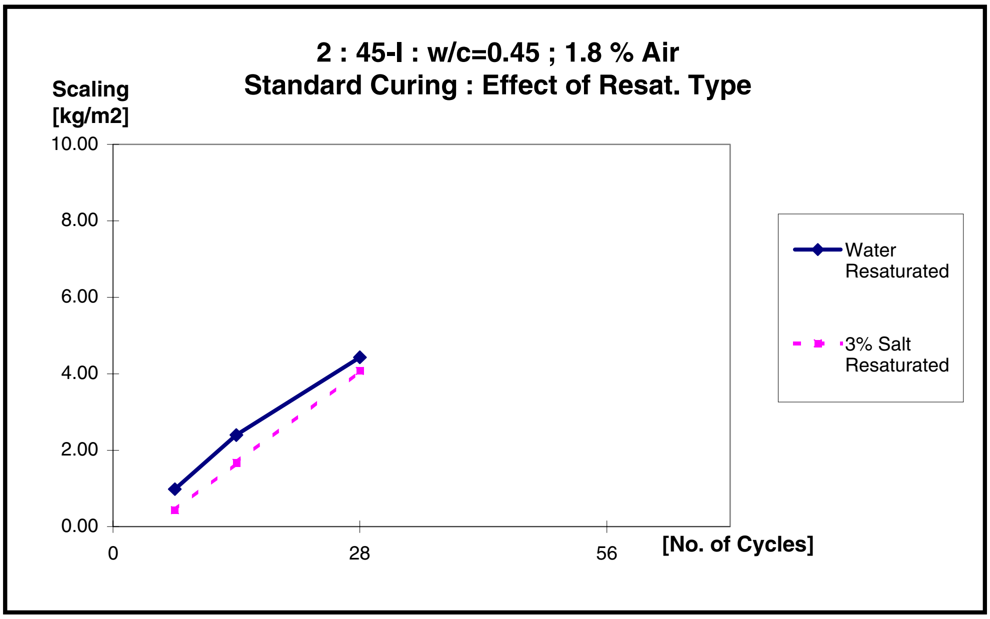

Figure 4.3.23 : Freeze-thaw scaling depending on the type of re-saturation, standard curing, mix 2.

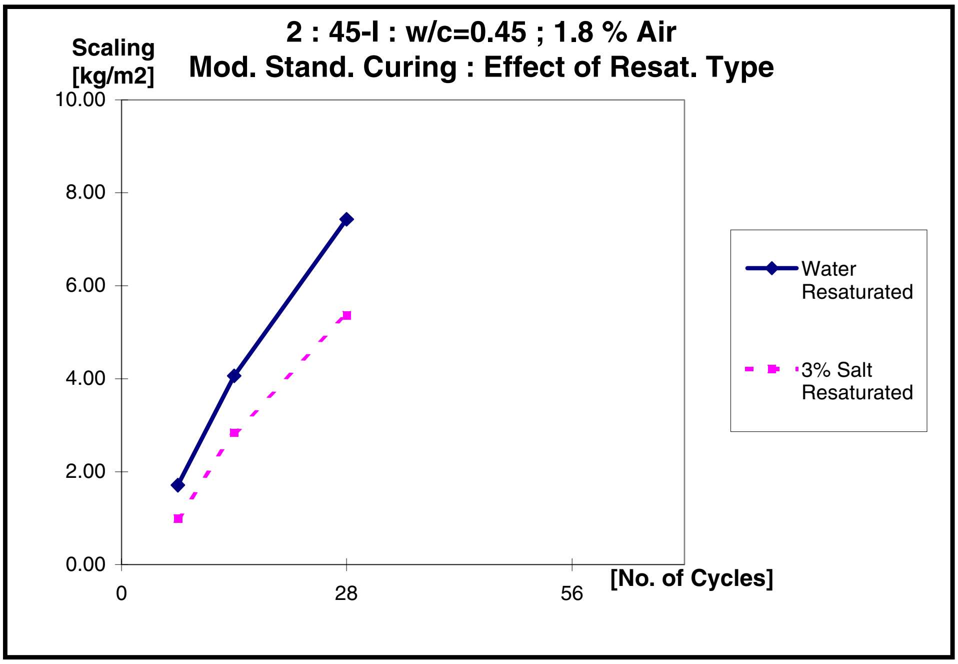

Figure 4.3.24 : Freeze-thaw scaling depending on the type of re-saturation, modified standard curing, mix 2.

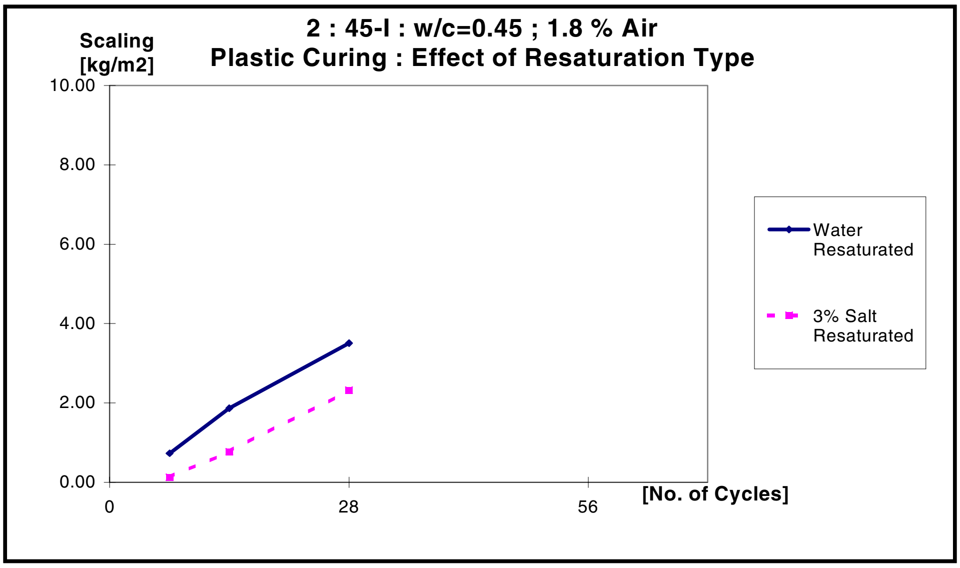

Figure 4.3.25 : Freeze-thaw scaling depending on the type of re-saturation, plastic curing, mix 2.

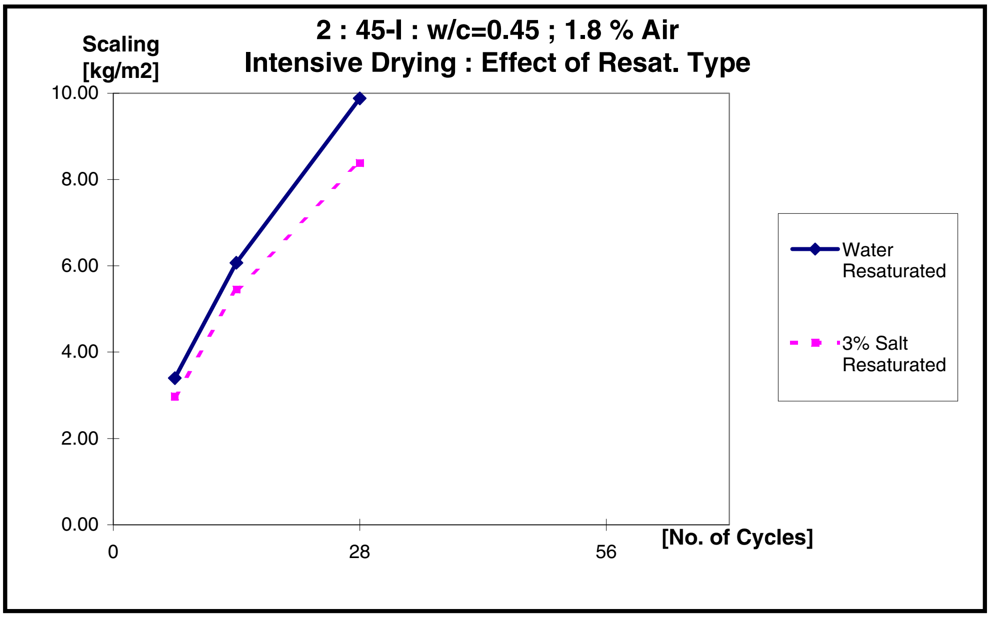

Figure 4.3.26 : Freeze-thaw scaling depending on the type of re-saturation, intensive drying, mix 2.

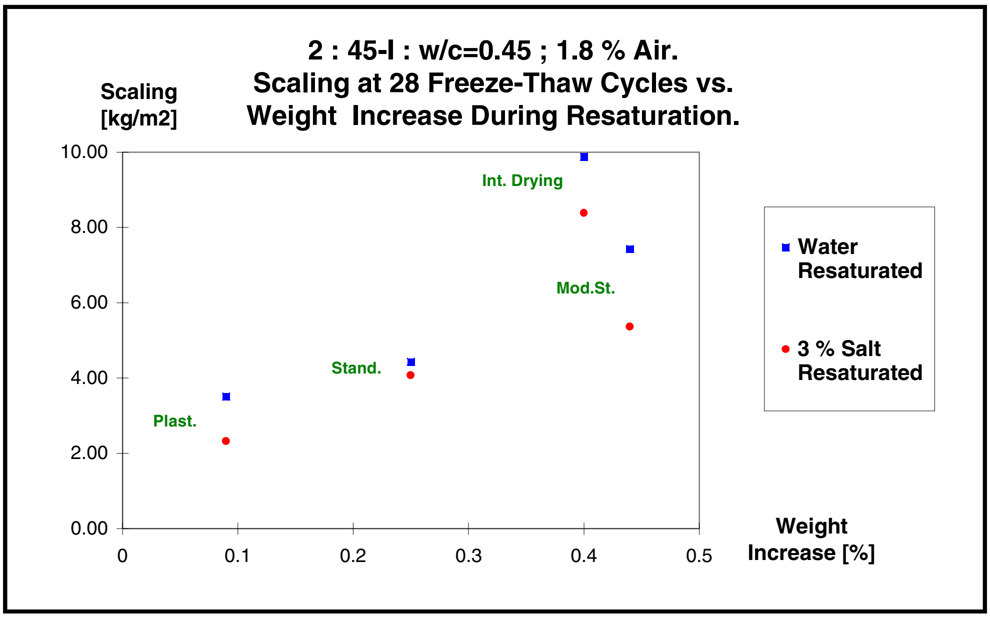

Figure 4.3.27 : Freeze-thaw scaling versus weight increase during re-saturation, mix 2.

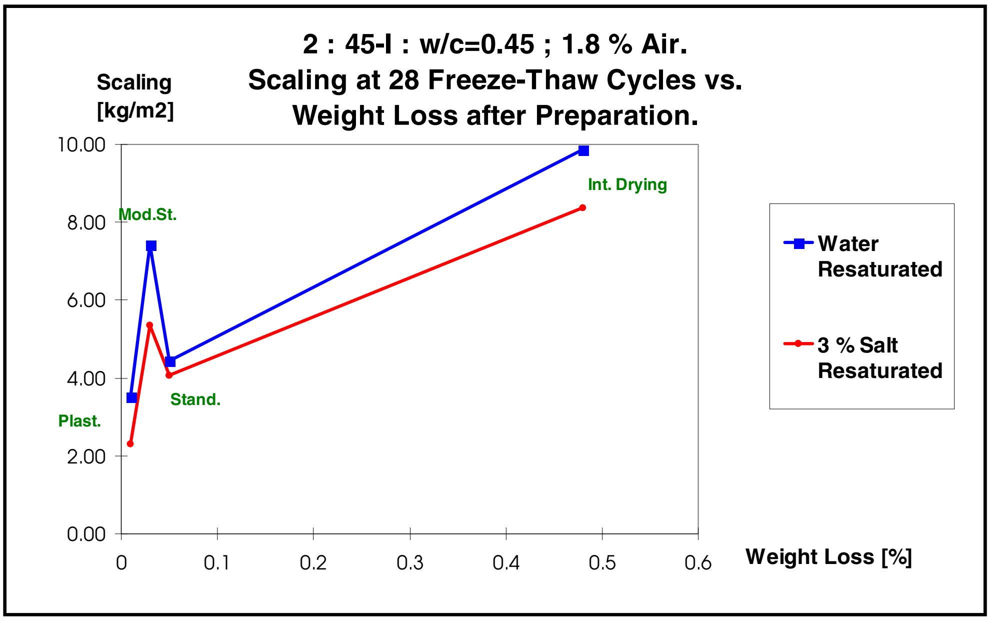

Figure 4.3.28 : Freeze-thaw scaling depending on the weight loss after preparation, mix 2.

4.3.3.3 Scaling vs. curing regime and moisture movement

Within the single series, i.e. identical curing procedure, no correlation could be found between scaling and differences in weight changes prior to preparation or during the re-saturation phase. Nor could such scatter of scaling be accounted for by the differences in evaporation rate detected (intensive drying).

The overall freeze-thaw resistance of the present mix was bad, and the test had to be terminated at 28 cycles.

Although not statistically significant in all four curing regimes, re-saturation by water provided much higher scaling than the parallel samples re-saturated by 3 % salt (figures 4.3.23-26). This correlates, and may partly be explained by the higher suction of water during freeze-thaw as commented in the previous section.

Again, intensive drying results in higher scaling than any other curing regime (appendix B). Next to intensive drying, modified standard had a high degree of deterioration, then comes standard and plastic curing : If intensive drying is left out, there seems to be a correlation between scaling and weight increase during re-saturation (figure 4.3.27 and appendix B). The deviation of the former may be linked to the much higher internal vapour pressure during drying, affecting the microstructure in a different manner.

There is no obvious tendency of increased scaling at any age with increased weight loss subsequent to preparation independent of how the weight loss was provoked (figure 4.3.28 and appendix B).

4.3.3.4 Conclusions

- As expected, the scaling of mix 2 was considerably higher than that of mix 1. Again, intensive drying produced much higher scaling than any other curing regime. Then followed modified standard, standard and plastic curing.

- In general, re-saturation by water caused higher scaling than re-saturation by 3 % salt.

- If intensive drying is not considered, there was an apparent correlation between scaling and weight gain during re-saturation.

- As for mix 1, the loss of moisture from the concrete pore system prior to freeze-thaw depends very much on the pre-storage conditions.

- Sawing at an early age (Modified Standard) provides substantial loss of moisture even when stored at 20°C/65 % RH. This weight loss is three times of that caused by drying for 72 hours at 40 °C. However corrected for geometrical effects, the loss through the test surface probably is of the same range. Corresponding to this, the weight gain during the subsequent re-saturation (trough the test surface) is in the same order for these two.

4.3.4 Mix 3 : 55-I-AE

4.3.4.1 Moisture changes prior to freeze-thaw

Modified standard curing gave a weight loss of approximately 1.9 % of the original sample weight prior to re-saturation (appendix B). This corresponds to 23 % of the total water – or 42 % of the evaporable water (70 % hydration assumed). Other relations are maintained as previously described.

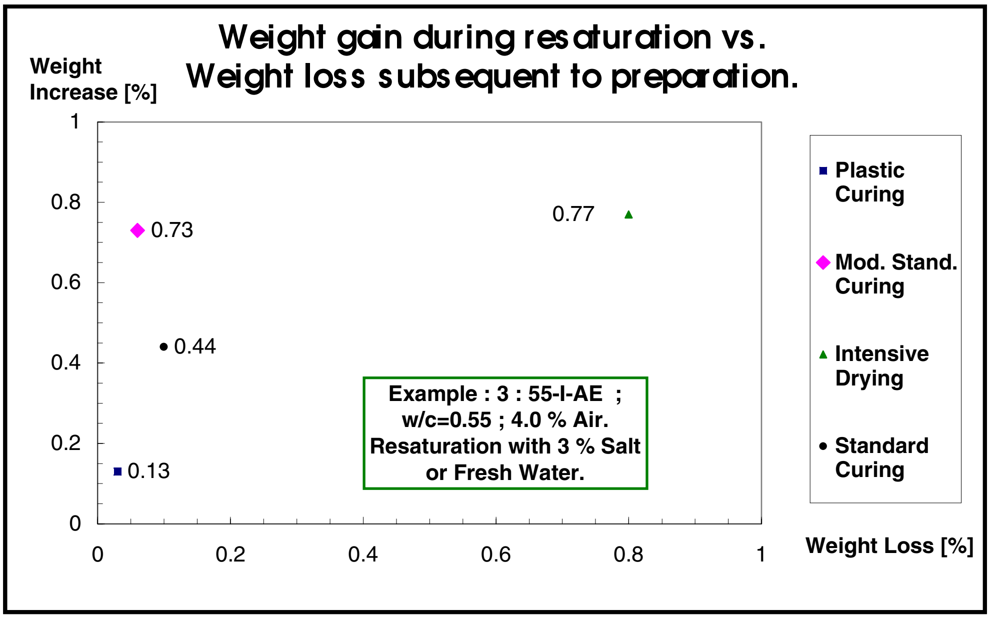

Figure 4.3.29 : Absorption during re-saturation versus moisture loss after preparation, mix 3.

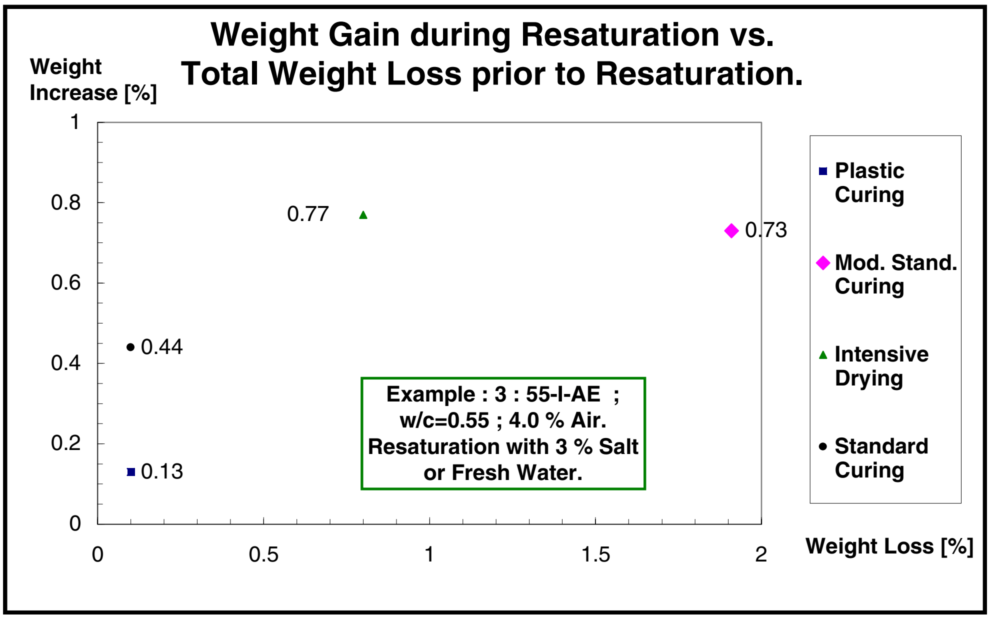

Figure 4.3.30 : Absorption during re-saturation versus total moisture loss prior to re-saturation, mix 3.

4.3.4.2 Moisture loss versus moisture uptake

Except for the higher moisture loss and –absorption values, the (lack of) correlation between these parameters (figures 4.3.29-30) mainly are as previously described. The total weight loss for intensive drying is increased to 42 % of that of modified standard.

The weight increase during freeze-thaw with 3 % NaCl, compared to the preceding weight loss, is displayed in figure 4.3.33. Again however, even when tested with pure water the weight increase during freeze-thaw is higher when re-saturated by water compared to re-saturation by 3 % NaCl (figure 4.3.31-32).

4.3.4.3 Scaling versus curing regime and moisture changes

When tested in water, the scaling is so low that any differentiation is irrelevant. This also precludes any relation between scaling in water and any moisture change data.

Tested in 3 % NaCl, the previous ranging of curing regime is confirmed, see figure 4.3.34. Again leaving out intensive drying, there is a tendency of increased scaling with increased absorption during the re-saturation (figure 4.3.35). The relation between scaling and cumulative absorption during re-saturation and freeze-thaw (figure 4.3.36) exists as well. These relations are better than that between scaling and absorption during freeze-thaw alone (appendix B).

4.3.4.4 Internal damage

For mix 3, signs of internal damage were assessed by ultrasonic pulse velocity. As expected with a w/c-ratio of 0.55 and air entraining, there was no evidence of degradation. In fact, the values are improving with time within the period of testing. General data are not included in the present publication. However, it still would be interesting to compare the development in ultrasonic pulse velocity considering the different moisture absorption during freeze-thaw : The latter depended on re-saturation by water (higher) or 3 % NaCl (lower).

Such measurements show a scatter of a few percent from the mean value. However, there is an indication that the higher water absorption during freeze-thaw have actually improved the UPV values attained (figures 4.3.37-38). For comparison, results from testing in 3 % NaCl is included in figure 4.3.39.

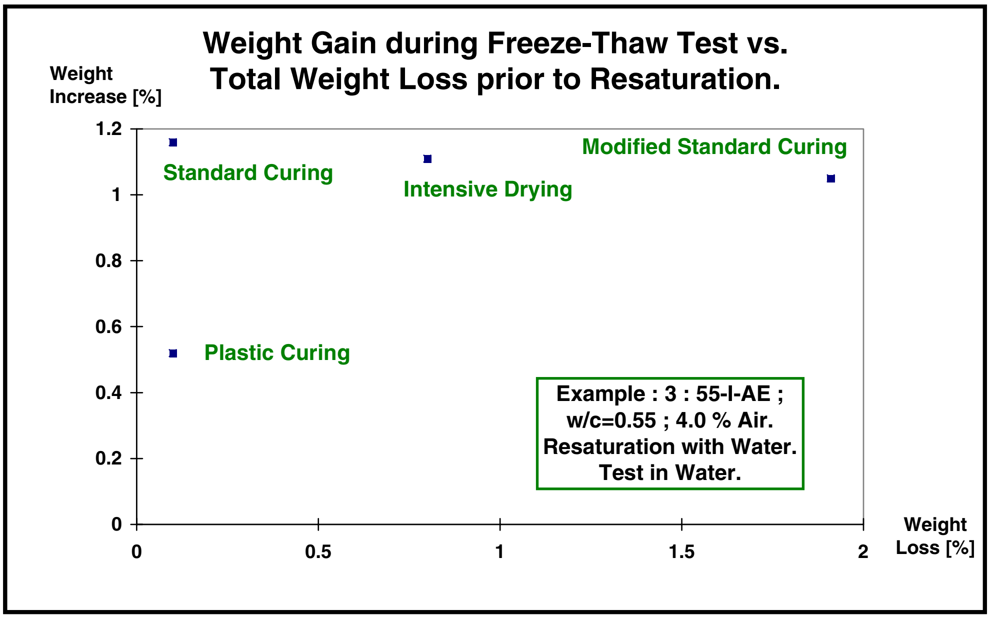

Figure 4.3.31 : Moisture absorption during freeze-thaw versus total weight loss prior to re-saturation, re-saturated by water and tested with water, mix 3.

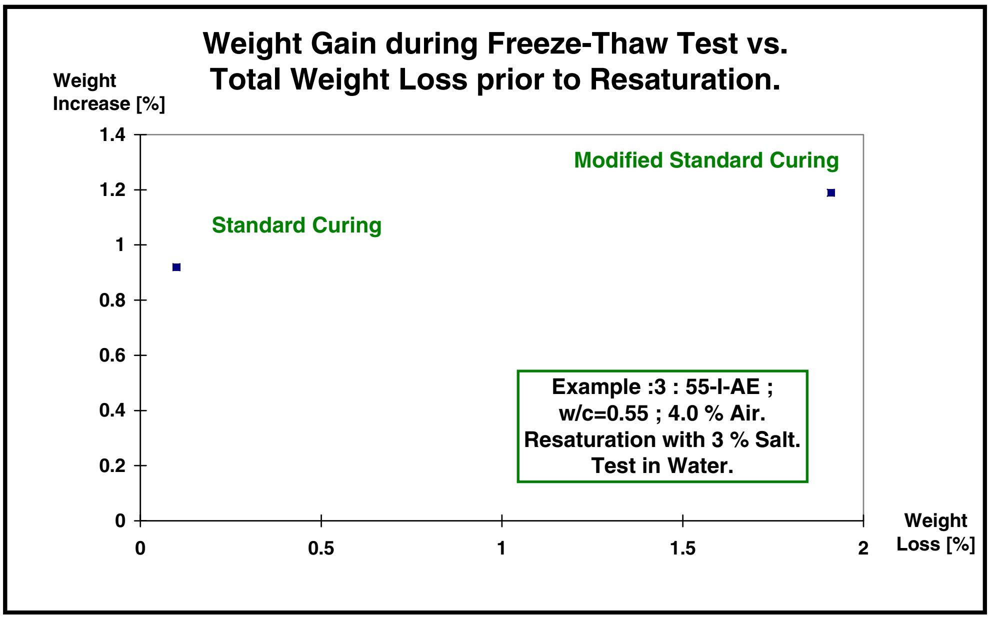

Figure 4.3.32 : Moisture absorption during freeze-thaw versus total weight loss prior to re-saturation, re-saturated by water and tested with water, mix 3.

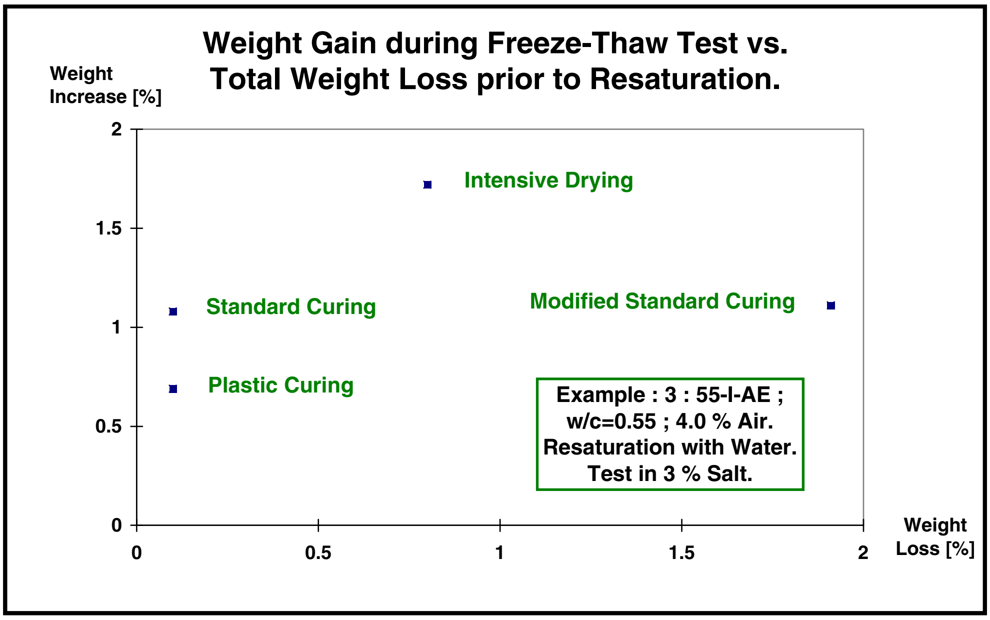

Figure 4.3.33 : Moisture absorption during freeze-thaw versus total weight loss prior to re-saturation, re-saturated by water and tested with 3 % NaCl, mix 3.

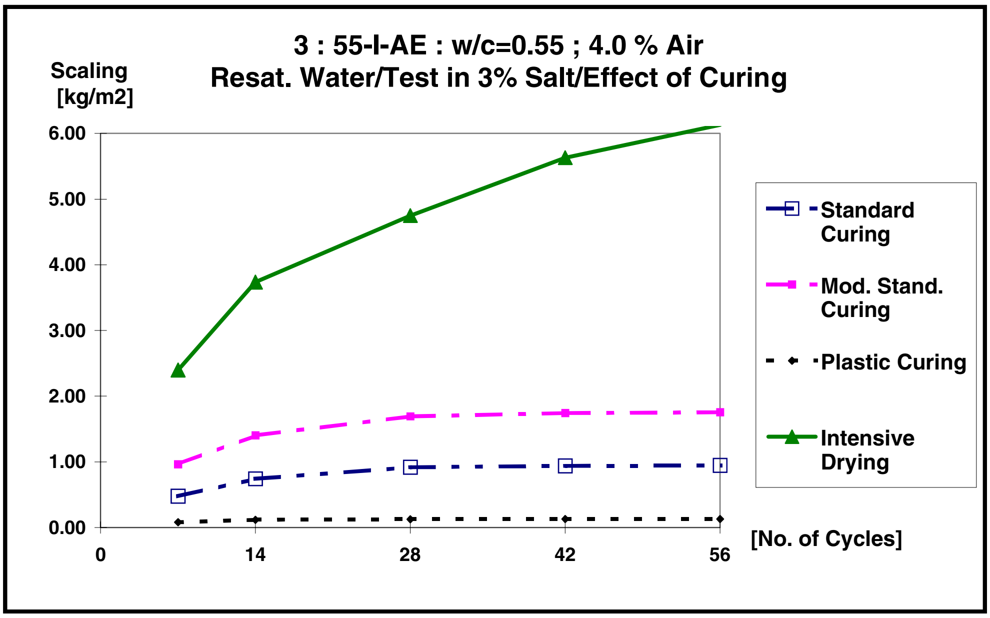

Figure 4.3.34 : Scaling depending on the curing regime, re-saturated by water and tested with 3 % NaCl, mix 3.

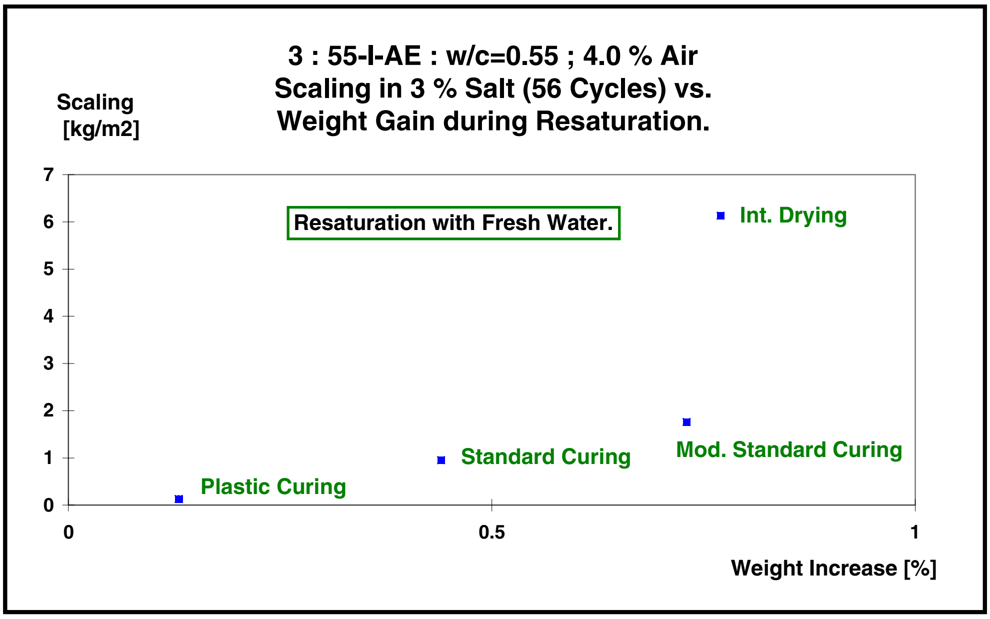

Figure 4.3.35 : Scaling in 3 % NaCl versus weight increase during re-saturation (by water), mix 3.

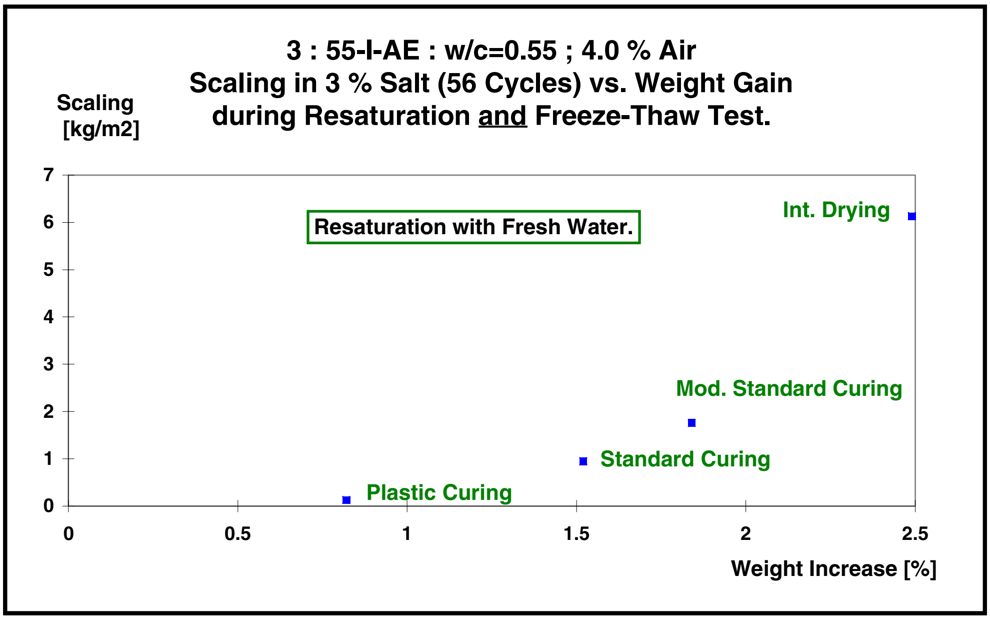

Figure 4.3.36 : Scaling in 3 % NaCl versus weight increase during re-saturation (by water) and freeze-thaw, mix 3.

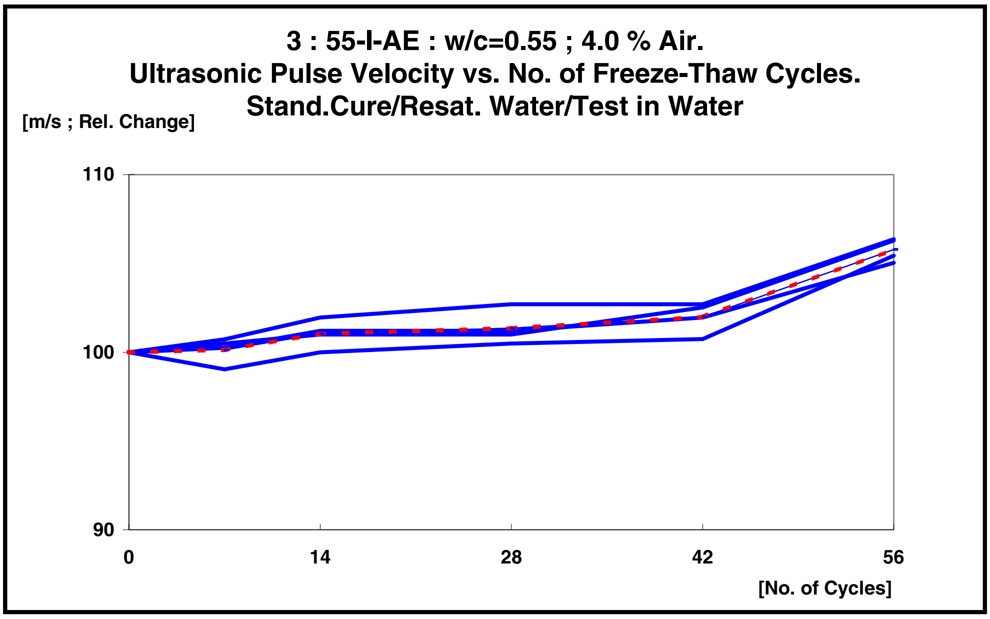

Figure 4.3.37 : UPV development for standard curing, re-saturated by water and tested in water, mix 3 (Dotted line indicates mean value).

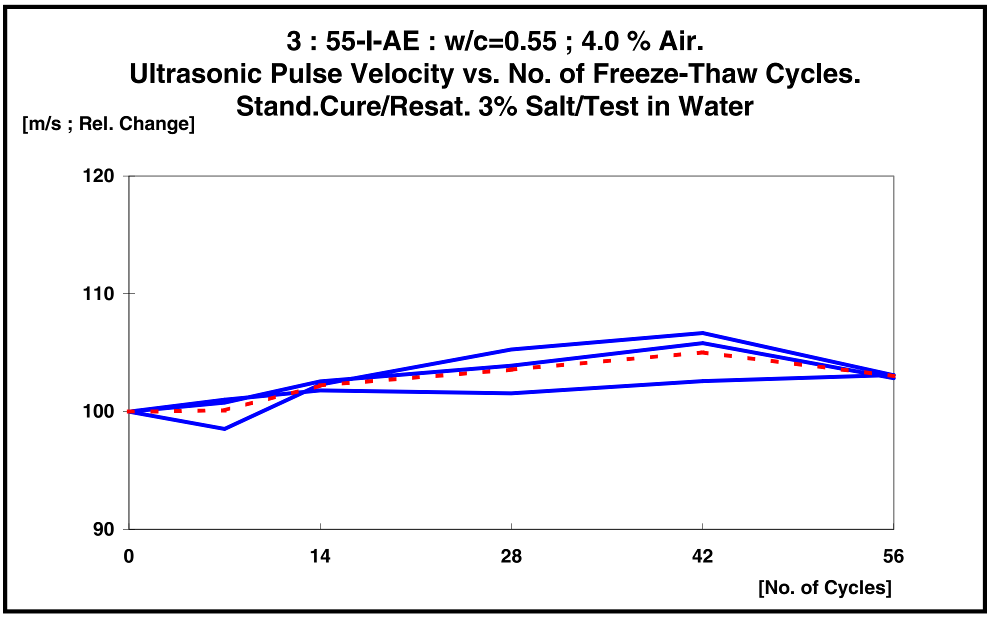

Figure 4.3.38 : UPV development for standard curing, re-saturated by 3 % NaCl and tested in water, mix 3 (Dotted line indicates mean value).

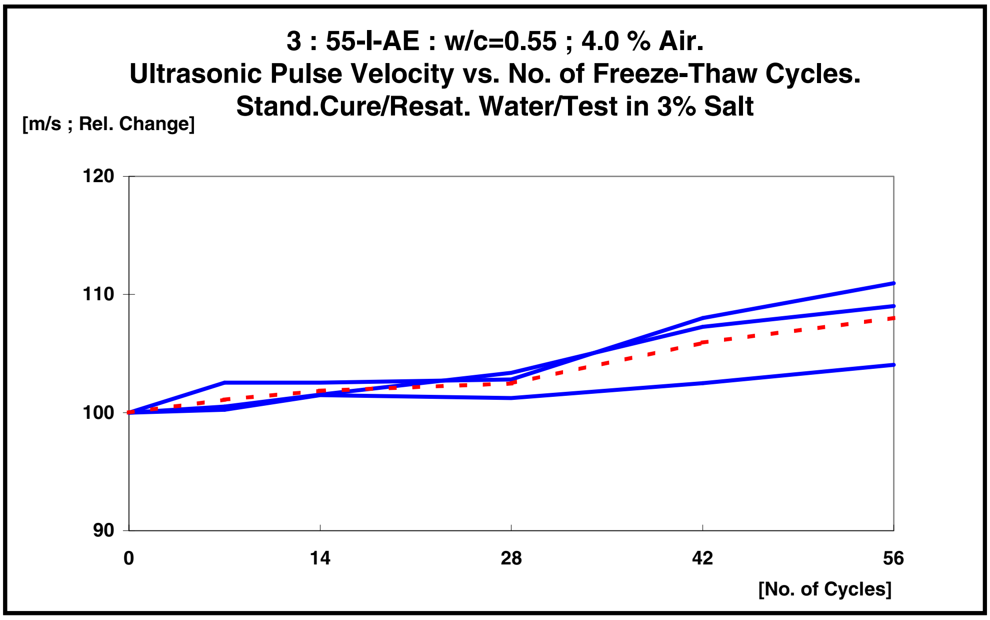

Figure 4.3.39 : UPV development for standard curing, re-saturated by water and tested in 3 % NaCl, mix 3 (Dotted line indicates mean value).

4.3.4.5 <u>Conclusions</u>

- Mix 3 had considerable and clearly curing dependent scaling (figure 4.3.34).

- With mix 3, a correlation between scaling and absorption during freeze-thaw – or total absorption - was found.

- The increased absorption during freeze-thaw when re-saturated by water – compared to that when re-saturated by 3 % NaCl – was also confirmed. The new aspect in this context appears to be the validation also when tested in pure water.

- The increased absorption (during freeze-thaw) when re-saturated by water could not be related to internal damage detected by ultrasonic pulse velocity. On the contrary, the UPV values were even improved under these conditions.

- Tested in water (re-saturated by water <u>or</u> 3 % NaCl), the scaling was so low that no differentiation with respect to curing condition was possible.

4.3.5 Mix 4 : 55-I

4.3.5.1 Test results and discussion

Mix 5 scaled severely, as expected. Even though the scaling exceeded that of the previous mixes, the curing dependence was confirmed : Intensive drying produced the largest damage, then modified standard, standard curing and finally plastic curing. The differences are not statistically significant at all the terms, but the trend remains clear.

For modified standard curing, approximately 1.8 % of the original sample weight was lost prior to preparation, corresponding to 22 % of the total water, 46 % of the evaporable water (70 % hydration assumed).

The relation between scaling (with 3 % NaCl) and moisture absorption during re-saturation was confirmed. Unfortunately, the weight increase during freeze-thaw was not attained for mix 4, since scaling was too large.

Some of the results are included in the appendix B for illustration.

4.3.5.2 Conclusions

- The ranking of the different curing regimes on scaling displayed the same tendency as previously, even if the scaling was considerably higher.
- The correlation between scaling and moisture absorption was confirmed with mix 4.

4.3.6 Mix 5 : 70-I

4.3.6.1 Test results and discussion

Mix 5 was freeze-thaw tested in water only, and it was expected to deteriorate. This mix was included in order to investigate the effect of curing on both scaling and internal damage. Mix 3 was a "parallel" test on internal damage with salt (on higher concrete quality level). As it turned out, the concrete of mix 5 disintegrated after 14 freeze-thaw cycles. After this point, the scaling values became irrelevant, and the damage is displayed only as decrease in ultrasonic pulse velocity.

Hence, the observed phenomena deviate from those of the previous mixes and will be discussed in consecutive order :

a) Moisture loss prior to freeze-thaw :

For modified standard curing, approximately 2.1 % of the original sample weight was lost prior to preparation, corresponding to 25 % of the total water, 42 % of the evaporable water content (70 % hydration assumed). Compared to mix 4, the latter value is lower due to the lower cement and higher water content of mix 5.

b) Scaling (14 cycles) depending on type of re-saturation :

As stated above, mix 5 is tested with pure water only. In contrast to the mix numbers 1 & 2 (testing with 3 % NaCl), higher scaling values (until 14 cycles) are obtained when re-saturated by 3 % NaCl, compared to that of re-saturation by water (figure 4.3.40 and appendix B). After 14 cycles, the samples cracked, and the testing medium (water on the top surface during freeze-thaw) percolated/penetrated the sample, accumulating at the bottom. Attempts were made to compensate by frequent re-filling, but (as normally) with no success in maintaining realistic scaling levels after this point.

c) Internal damage (not) depending on type of re-saturation :

From the experience of the present author with ultrasonic pulse velocity, the systematic behaviour of parallel samples is somewhat coincidental (figure 4.3.41). Though, the tendency normally is clear and provides a good picture of the progress of the internal breakdown [S 1998]. The development of the internal breakdown, depending on the type of re-saturation, is displayed in the figures 4.3.42a-b.The two types of re-saturation appear to produce an identical pattern concerning time-/cycle-dependent deterioration. The probable implication is that internal cracking and percolation is not responsible for the difference in scaling behaviour.

d) Indication of osmotic effect on local saturation (?) :

Tested in water, re-saturation by 3 % NaCl resulted in higher scaling (0 – 14 cycles) than after re-saturation by pure water. This is opposite of the scaling behaviour of the mix numbers 1 & 2, tested in 3 % salt. One possible explanation is a controversial one : In both cases, the different salinity of the internal and external environment may – at least initially – account for a higher degree of saturation in the very top layer of the sample due to osmotic potential, “drawing” water to the interphase.

In the case of applying external salt, such an effect would lead to potential water “flow” from below the top surface, trying to re-establish the equilibrium. The effect, if existing, would probably cease when free water from the interior is no longer available. It would also cease when salt migrates into the concrete, eliminating the sharp salt gradient. The latter will take several weeks according to Relling [R 1999].

In the case of external water and re-saturation by 3 % NaCl, the implication of an osmotic effect would be accelerated “suction” from the outside only, also increasing the water content in the surface-close structure. Towards the interior, the salt would probably be fairly well distributed according to the suction of solution during the re-saturation [S 1988b], i.e. with no distinct gradients. The effect, if existing, may cease after “counter-diffusion” of salt ions back into the external testing medium, reducing the salt gradient.

In both cases, a retarded development of deterioration would be expected – as observed in our cases. In practical freeze-thaw testing, this is often what happens. An exception is with very high levels of damage, where the practical, critical factor for the degree of deterioration possibly is the amount of liquid available for intrusion.

The retarding effect observed has very seldom been commented on. Personal communication between the present author and fellow researchers often attributed the phenomenon to the initial deterioration of areas of particular poor quality, i.e. local phenomena. However, such a pattern can be observed for concrete with scaling levels as high as 2 kg/m^2. This is in the range of 1 mm mean deterioration depth on the samples. Under such circumstances, more than 50 % of the entire surface would normally be affected, unless the quality is very poor and large cavities are formed.

e) Crack formation process :

The damage occurring as a crack-pattern is displayed for two samples in figure 4.3.43. The majority of the cracks surround the coarse aggregates, i.e. in what would be expected to constitute local zones with increased porosity. However, frequent cracks are evident in the mortar and paste as well.

Subsequent to the performance of the present work, Bager & Jacobsen [B 1999] introduced what they called a “conceptual model”. The model attributes the initiation of the cracks to the expansion of the paste surrounding the aggregates. After further water uptake (or internal re-distribution), the cracks are expected to become saturated, accelerating the degradation process. The study included water absorption, length change and acoustic emission.

It is the experience from non-published studies of the present author that the crack initiation will start within 10 mm of the exposed surface and then propagate. The development and extent of cracks and crack pattern may vary between various test methods [S 1993f] and might be a parameter to consider for choosing field relevant test methods. The crack development is principally easy attainable.

4.3.6.2 Conclusions

- Mix 5 was tested in water only and exhibited gradual disintegration after 14 freeze-thaw cycles, after which point obtained scaling values were no longer relevant. At this stage, internal cracking lead to increasing leakage of the testing medium (water) from the sample surface.

- Accumulated scaling after 14 cycles was considerably higher when re-saturated by 3 % NaCl, compared to re-saturation by pure water.

- Still, the type of re-saturation did not affect the rate of internal damage, measured by ultrasonic pulse - on the contrary.

- The implication is that the unfavourable effect of re-saturation by 3 % NaCl on scaling in this case (testing with water) is real. The different scaling rates (until 14 cycles) is not caused by (difference in ;) cracking and leakage from the test surface.

- A possible explanation for this phenomenon is an osmotic effect – at least temporarily – causing a higher degree of saturation in the surface layer. This may happen whenever the salt gradient at the surface is large enough (internal salt and external water – or visa versa), but is expected to cease after a while. Such retarding deterioration is often observed during freeze-thaw testing.

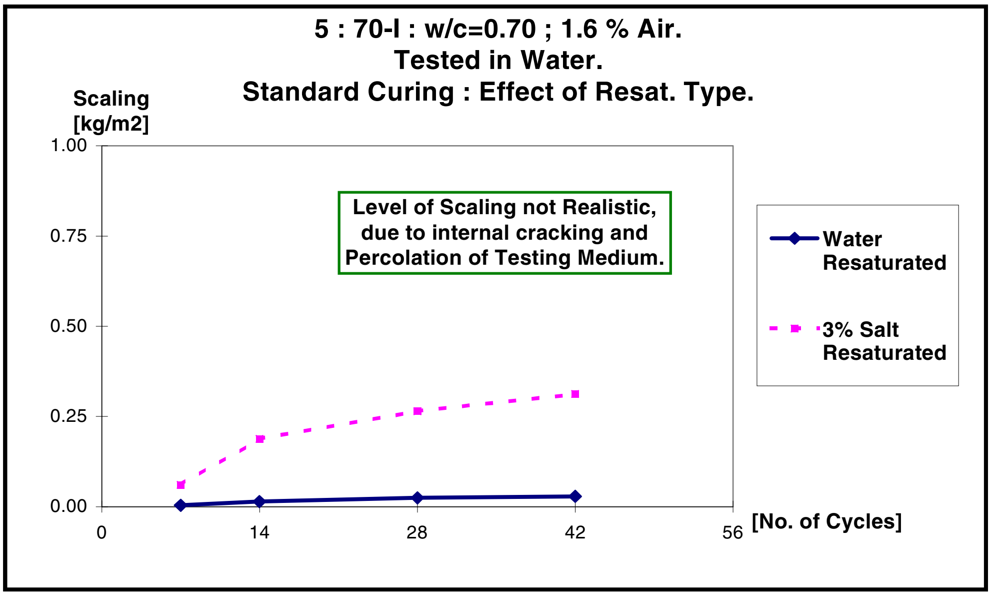

Figure 4.3.40 : Scaling in water for standard curing, depending on the type of re-saturation, mix 5. Note comment on (limit of ;) interpretation : Scaling values after 14 cycles are not considered relevant.

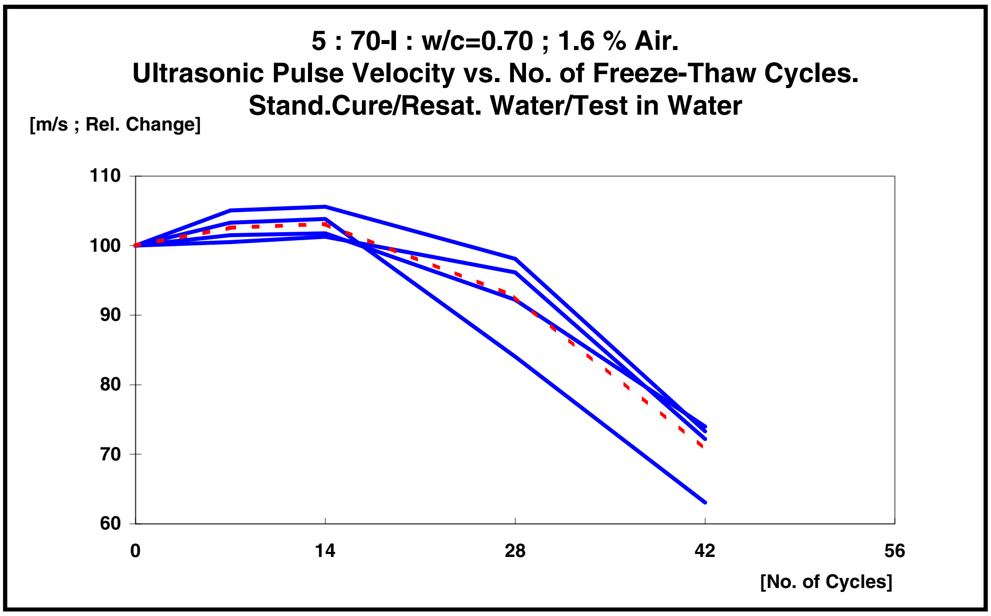

Figure 4.3.41 : Internal deterioration measured by ultrasonic pulse velocity : Typical scatter between parallel samples (dotted line = mean value), obtained from mix 5.

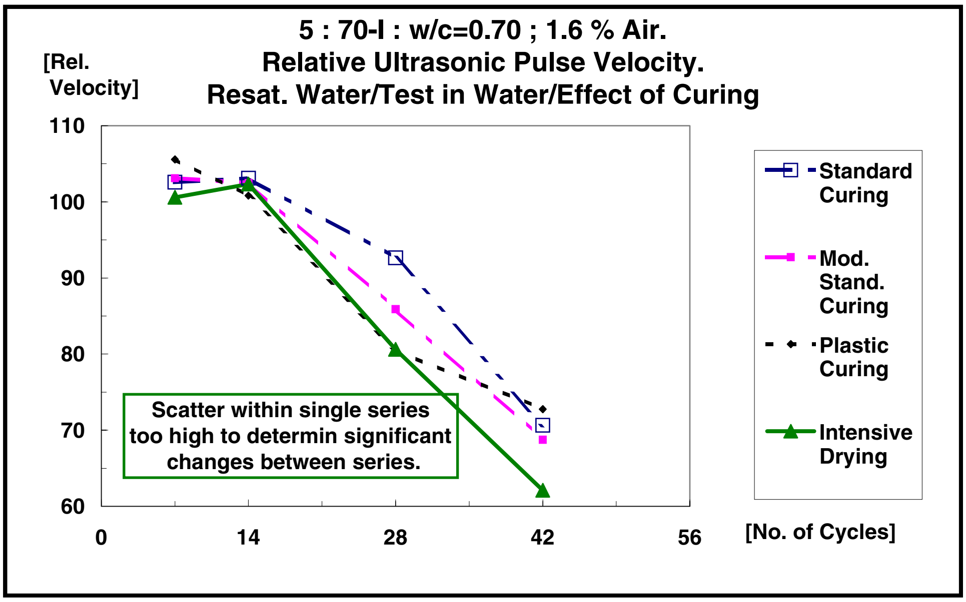

Figure 4.3.42a : UPV measurements for mix 5, re-saturated by water.

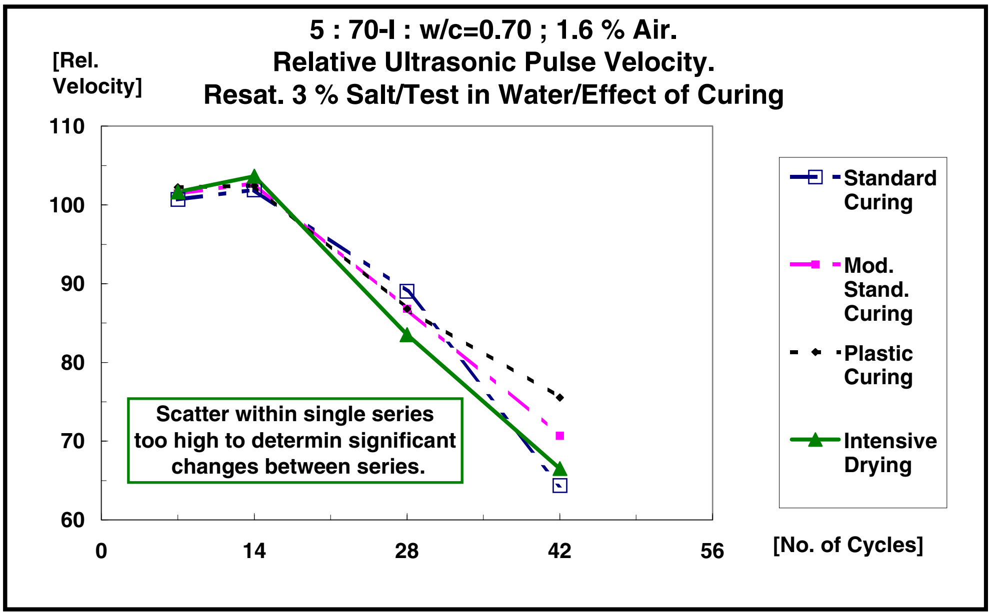

Figure 4.3.42b : UPV measurements of mix 5, re-saturated by 3 % NaCl.

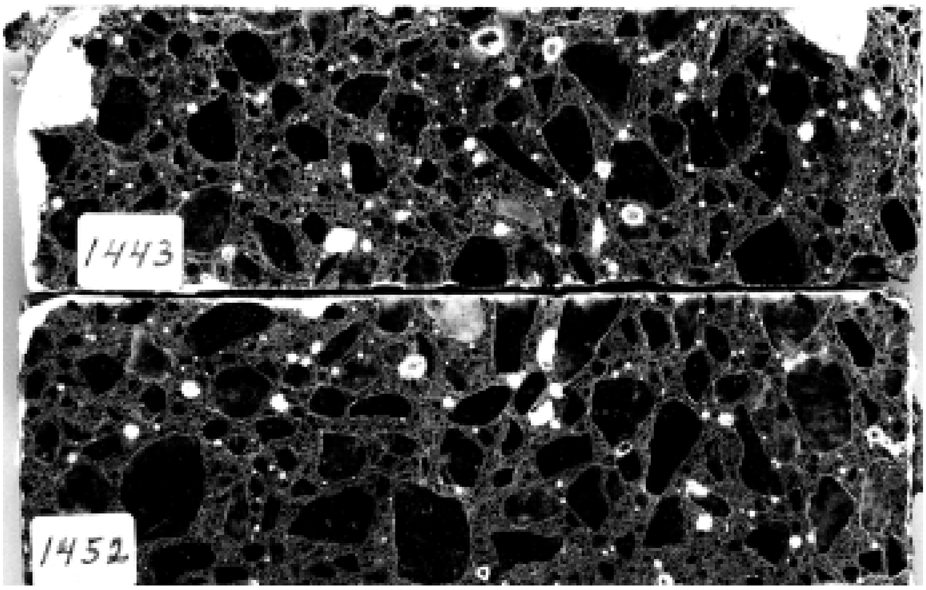

Figure 4.3.43 : Plane section obtained from mix 5 after the termination of the test, displaying crack pattern. Standard curing (sample 1443) and plastic curing (sample 1452). Sample preparation included impregnation with an epoxy containing fluorescent dye, subsequent to gently drying.

4.3.7 Mix 6 : 45-II-AE

4.3.7.1 Test results and discussion

Mix 6 (fly ash cement) exhibited somewhat higher scaling (figure 4.3.44) than the comparable mix 1. As earlier, intensive drying resulted in the by far highest scaling level. Then follows standard curing and lowest damage with plastic and/or modified standard curing. The picture (figure 4.3.44) very much resembles that of mix 1 (figure 4.3.14) with standard portland cement.

Modified standard curing of mix 6 produced a weight loss prior to preparation amounting to 1.6 % of the original sample weight, corresponding to 20 % of the total water content and 39 % of the evaporable water content (water consumption according to 70 % hydration of the clinker part only assumed). The values are slightly above those of mix 1 with CEM I cement.

The earlier correlation between scaling level and moisture absorption during re-saturation and/or freeze-thaw is not evident with mix 6.

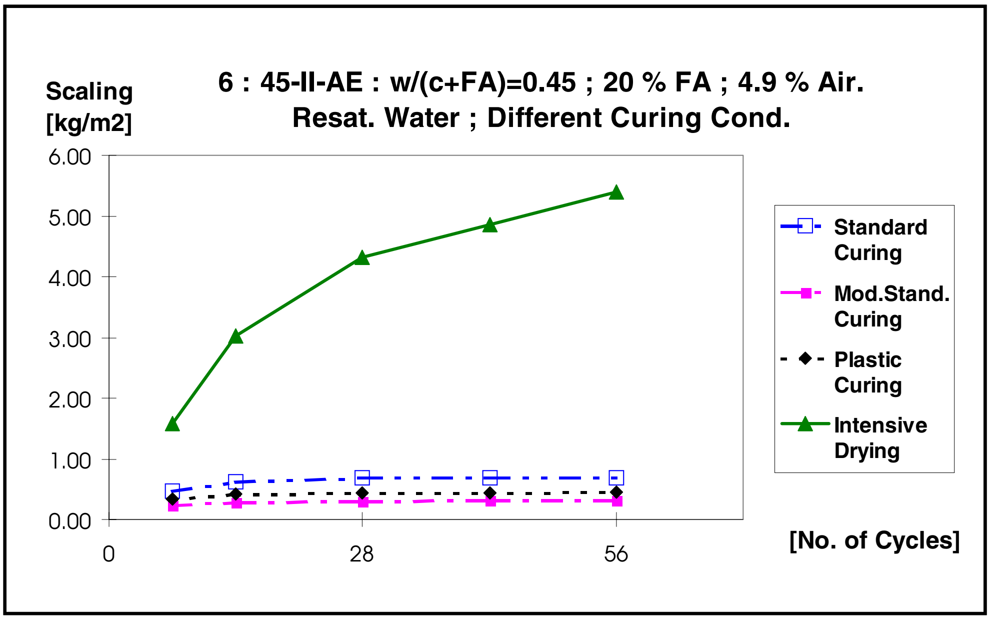

Figure 4.3.44 : Freeze-thaw scaling of mix no. 6, re-saturated by water and tested in 3 % NaCl. Different curing conditions.

4.3.7.2 Conclusions

- Mix 6 (CEM II/A-V (20 % fly ash)) had somewhat higher scaling than the comparable mix 1 (CEM I).

- The scaling dependence on curing resembles that of mix 1, with significantly higher damage after intensive drying. Then followed standard curing, while modified standard and plastic curing was close together and difficult to differentiate.

- With mix 6, the previous correlation between scaling and moisture absorption prior to or during freeze-thaw could neither be confirmed, nor rejected.

- The moisture loss produced by modified standard curing fits fairly well with that of mix 1, CEM I cement but otherwise identical mix design.

4.3.8 Mix 7 : 55-II

4.3.8.1 Test results and discussion

As should be expected, this concrete mix suffered from extensive damage, tested for scaling with 3 % NaCl. Particularly the standard curing produced a high relative scatter, though a normal behaviour at this level of damage (Section 4.3.1).

The scatter complicates an interpretation with respect to the level of scaling versus moisture absorption – as well as the ranking of the curing regimes. Still, the former tendencies are not contradicted. The lower damage level of plastic curing and the higher with intensive drying is confirmed (see appendix B).
The weight increase during freeze-thaw was not measured for mix 7 ; it would be difficult to accomplish with the high damage levels produced. (High levels of scaling make it difficult to obtain representative weight corrections for the scaled material of the sample.)

The ultrasonic pulse velocity would have been an interesting parameter to obtain for this mix design. Unfortunately, it was not.

4.3.8.2 Conclusions

- Mix 7 exhibited a high level of scaling and scatter, as expected. Still, the former tendencies of scaling versus absorption and the effect of curing regime were not counteracted : Intensive drying resulted in the highest damage, plastic curing the lowest.

- The level of scaling (CEM II/A-V (20 % fly ash) was somewhat higher than the comparable mix 4 (CEM I).

4.3.9 Mix 8 : 45-IS-AE

4.3.9.1 Test results and discussion

The modified standard curing produced a weight loss of 1.2 % prior to preparation, corresponding to 15 % of the total water and 39 % of the evaporable water content (water consumption according to 70 % hydration of the cement assumed). The values are somewhat lower than for those of the mix design without silica fume. The difference may probably be attributed to the higher diffusion resistance due to the use of silica fume.

Concerning moisture loss and absorption (prior to freeze-thaw), the relation between modified standard curing and intensive drying remains the same as previously : The weight loss of intensive drying is approximately 35 % of that of modified standard. For intensive drying, the absorption during re-saturation amounts to approximately 80 % of the preceding weight loss. Corrected for geometrical effects, the loss and uptake through the test surface remains of the same order.

The level of scaling is very low, demonstrating the positive effects of silica fume. The scaling is too low to assess the dependency on absorption prior to freeze-thaw (figure 4.3.45) (absorption during freeze-thaw was not attained). However, it remains reasonably clear that modified standard curing caused the highest damage. The first implication is that intensive drying with the silica fume concrete performed much better than intensive drying with the previous mixes. It coincides with the conclusions of Sellevold [1988b]. The idea may even be developed a bit further : With the maintained, relative moisture loss and absorption after intensive drying – compared to that of modified standard curing – the silica fume concrete seems better able to resist the structural changes caused by the intensive drying. The feature appears not that evident with modified standard curing. This phenomenon could indicate that the structural changes of silica fume concrete are more time-dependent than for concrete without silica fume.

4.3.9.2 Conclusions

- Intensive drying did no longer produce increased damage. In spite of somewhat higher scaling for modified standard curing, all mix-/curing-combinations performed very well.

- The weight loss of modified standard curing prior to preparation was lower than for that of the similar mix design without silica fume (mix 1), as would be expected.

- There are indications that the pore structure changes of the silica fume concrete, when subjected to drying, are more time-dependent than without silica fume. Additionally as demonstrated by other researchers, the negative impact of drying is smaller.

- The scaling was too low to display any significant difference depending on the water absorption. Still, the previous relations between scaling and absorption were not contradicted.

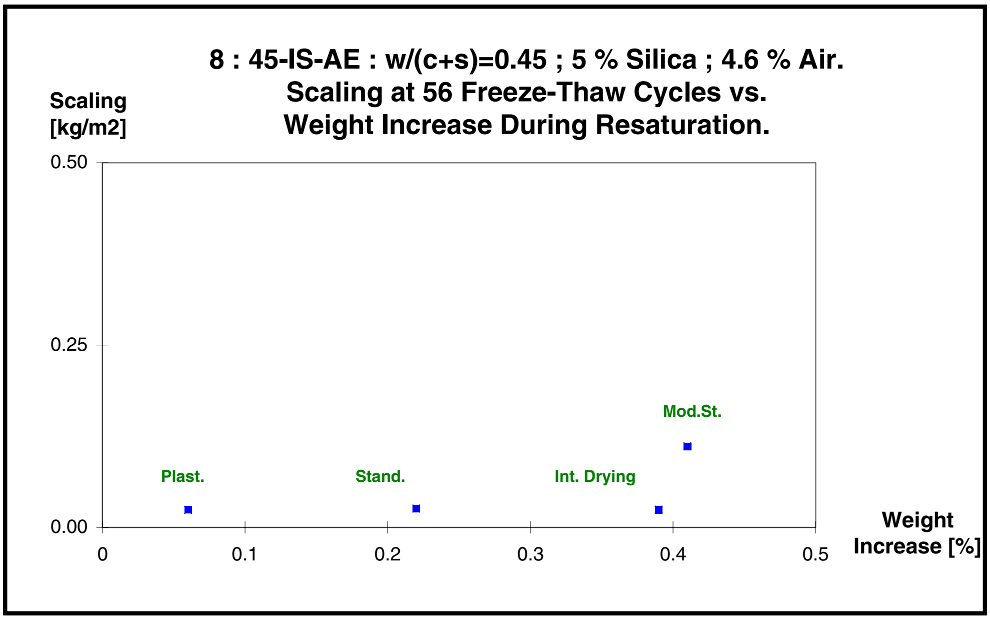

Figure 4.3.45 : Scaling versus absorption during re-saturation, mix 8.

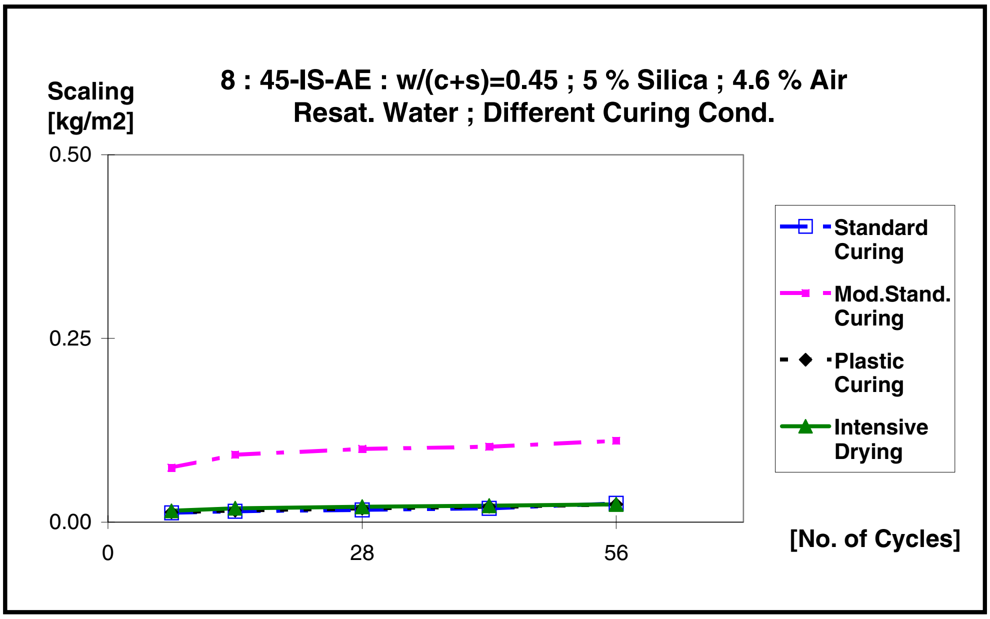

Figure 4.3.46 : Scaling versus curing regime, mix 8.

4.4 Overview

4.4.1 Freeze-thaw performance versus material design

4.4.1.1 General

In order to illustrate and discuss the performance of the different concrete mix designs, plots of scaling (figure 4.4.1-3) and moisture changes (figure 4.4.4-7) are included.

The fresh concrete air void parameters are included in the text box of figure 4.4.1-3. The values of the different mixes are within a range/level that enablies a direct comparison of their performance. This will provide input to the general discussion on material performance in section 8.

4.4.1.2 Effect of type of binder on scaling and moisture exchange

a) w/(c+s) = 0.45 :

In figure 4.4.1, the three air-entrained mixes of water/binder-ratio 0.45 are plotted together. The binders are 1) CEM I (standard portland) cement, 6) CEM II/A-V (20 % fly ash) cement and 8) CEM I cement with 5 % silica fume.
The silica fume concrete exhibited significantly lower scaling than the other mixes. During re-saturation, it took up somewhat less moisture than the others. After standard curing, but during freeze-thaw, it took up the same amount of moisture as the fly ash mix, but somewhat less than the pure portland cement concrete (figure 4.4.4). After modified standard and plastic curing, the water uptake during freeze-thaw was lowest for the silica fume concrete (figure 4.4.5-6). Hence, the lower moisture exchange with the surroundings – and especially that during freeze-thaw – coincides with the low scaling obtained after 56 cycles.

The fly ash cement concrete exhibited somewhat higher scaling than that of the portland cement concrete. The main difference appears to arise during the first 7 to 14 freeze-thaw cycles. At least after standard curing, this coincides with higher moisture uptake during re-saturation with the fly ash cement. However, the previous moisture loss was also higher with this cement. Consequently, the (surface) degree of saturation probably was not higher at the initiation of freeze-thaw, on the contrary. Also after standard curing, the water uptake during freeze-thaw was somewhat lower with the fly ash cement, despite the higher scaling.

After modified standard curing, the moisture uptake during freeze-thaw was considerably higher with the fly ash cement than with the portland cement, even though the previous moisture loss was of the same order. The scaling levels of these two mixes subjected to modified standard curing however, are very much alike. Fly ash cement concrete subjected to plastic curing had similar moisture exchange prior to and during freeze-thaw, compared to that of the portland cement concrete. The total moisture exchange was much lower than that of modified standard curing. Still, the scaling appeared to increase with the fly ash cement, but not so with the standard cement.

b) w/c = 0.55 :

Not surprisingly, the mixes 4 (CEM I) and 7 (CEM II/A-V(20 % fly ash)), both without air entrainment, exhibit scaling levels far beyond any acceptance criteria. This is valid for all curing regimes, but it is still possible to differentiate between the type of curing : Intensive drying resulted in the fastest deterioration, plastic curing the slowest, while standard and modified standard gave intermediate results.

Again, the fly ash cement concrete suffered from somewhat higher moisture loss prior to re-saturation – and took up more moisture during re-saturation. The uptake during freeze-thaw was not possible to obtain from any of these mixes, due to the high scaling level.

Finally, as normal with this rate of deterioration, no levelling off of scaling after a number of cycles is observed. On the contrary, the deterioration is almost linear, and the test had to be interrupted after 28 cycles. Nor was it possible to confirm any strengthening/”hydration” effect of the fly ash with time, as observed with the w/c-ratio of 0.45 above.

c) Summarized :

All this confirms that silica fume concrete is more resistant to scaling, at least for the number of freeze-thaw cycles tested. The increased scaling resistance coincides with the lower moisture exchange prior to and during freeze-thaw, compared to concrete of similar mix design and air void characteristics.

Secondly, it appears that fly ash concrete depends more than portland cement concrete on optimum curing conditions : The early stage moisture exchange with the surroundings is increasingly affected, partly also during freeze-thaw. Still, the increased scaling rate of the fly ash cement concrete ceased after two to four weeks, suggesting increased resistance to deterioration. This coincides with the longer “hydration” period of fly ash, compared to the portland cement.

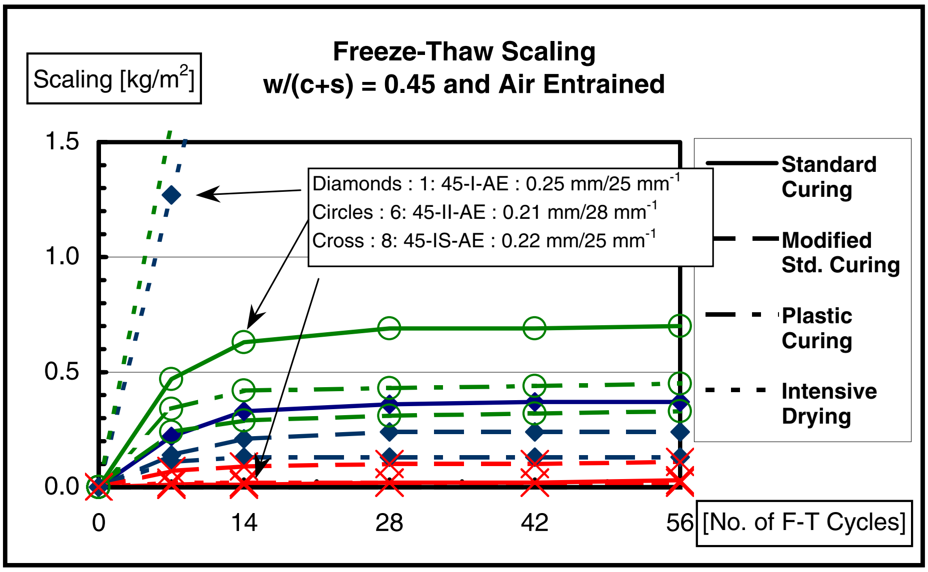

Figure 4.4.1 : Freeze-thaw scaling of the mix nos. 1 (CEM I), 6 (CEM II/A-V (Fly Ash)) and 8 (CEM I + 5% Silica Fume), four different curing conditions, all re-saturated with water prior to freeze-thaw and tested in 3 % NaCl. Fresh concrete air void parameters from section 4.2.4 are given in the text box : Spacing factor / Specific air void surface.

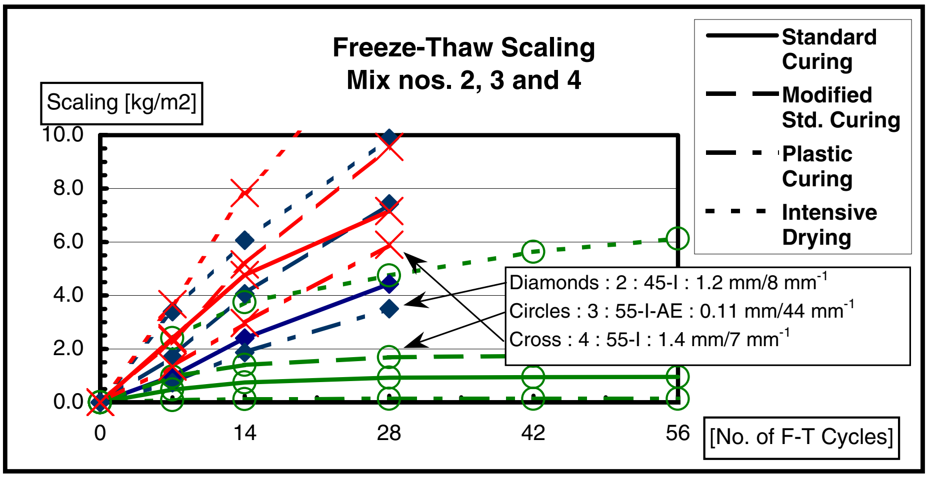

Figure 4.4.2 : Freeze-thaw scaling of the mix nos. 2 (w/c=0.45), 3 (0.55, air entrained) and 4 (0.55), all with CEM I cement, four different curing conditions, re-saturated with water prior to freeze-thaw and tested in 3 % NaCl. Fresh concrete air void parameters from section 4.2.4 are given in the text box : Spacing factor / Specific air void surface.

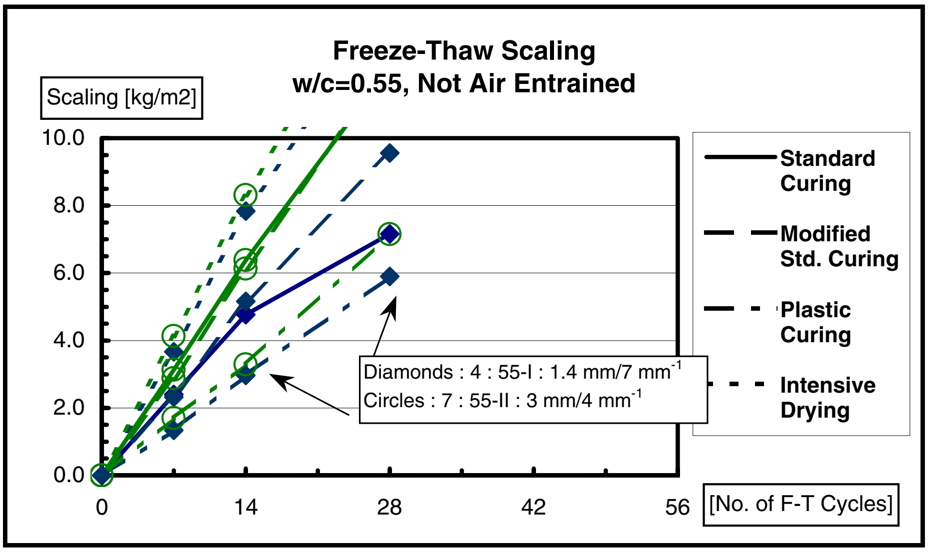

Figure 4.4.3 : Freeze-thaw scaling of the mix nos. 4 (CEM I) and 7 (CEM II/A-V), four different curing conditions, re-saturated with water prior to freeze-thaw and tested in 3 % NaCl. Fresh concrete air void parameters from section 4.2.4 are given in the text box : Spacing factor / Specific air void surface, however not to be quantitatively interpreted in the present case.

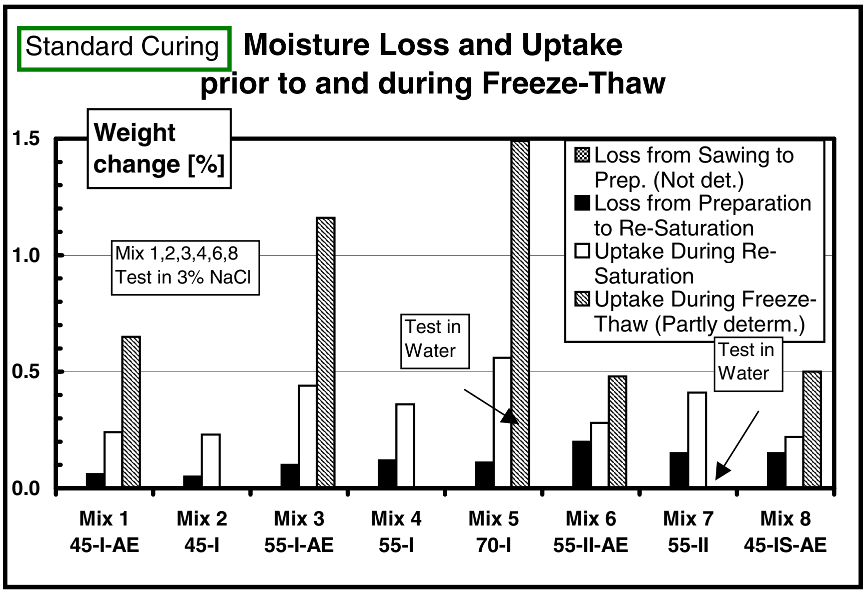

Figure 4.4.4 : Comparison of moisture loss and moisture uptake of all concrete mixes subjected to standard curing.

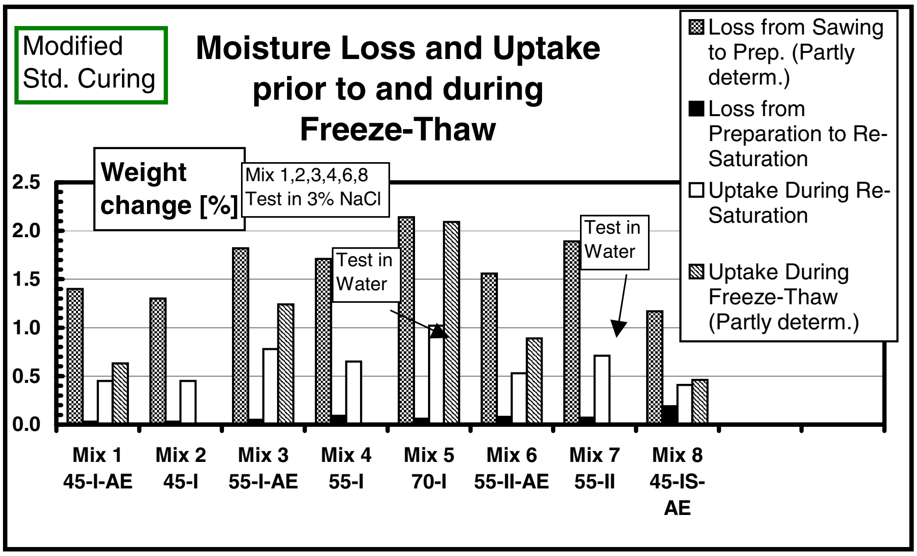

Figure 4.4.5 : Comparison of moisture loss and moisture uptake of all concrete mixes subjected to modified standard curing.

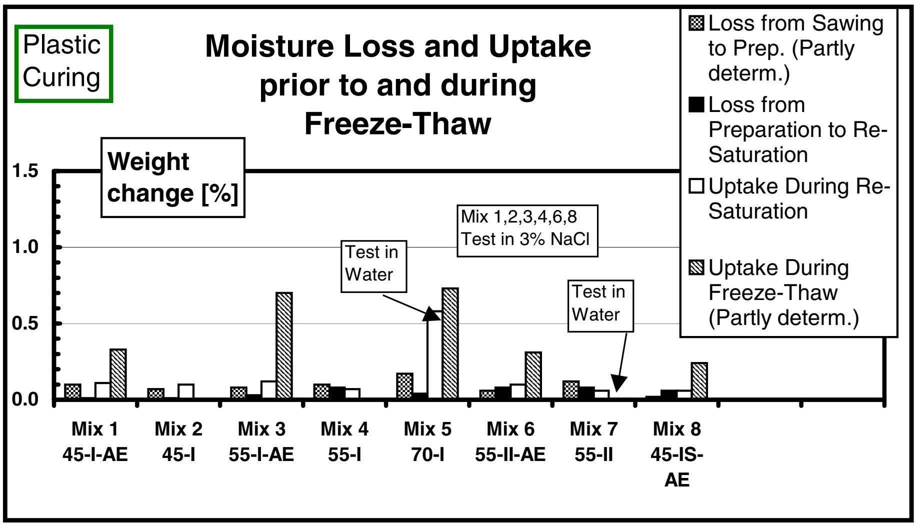

Figure 4.4.6 : Comparison of moisture loss and moisture uptake of all concrete mixes subjected to plastic curing.

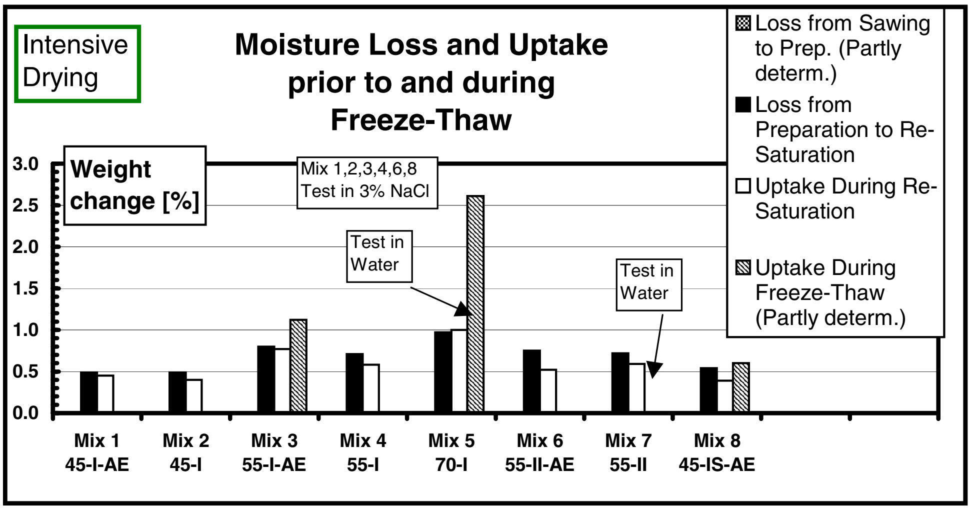

Figure 4.4.7 : Comparison of moisture loss and moisture uptake of all concrete mixes subjected to intensive drying.

4.4.1.3 Effect of air entrainment

The positive effect of air entrainment on scaling is evident in all comparable cases ; mix no. 1 versus mix no. 2, no. 3 versus no. 4 and no. 6 versus no. 7. This is not surprising within the chosen concrete quality range and will not be further discussed.

The moisture exchange prior to freeze-thaw however, appeared to depend on air entrainment – and in different ways : With CEM I and w/c-ratio 0.45 (mix 1 versus mix 2), air entrainment appears to increase the moisture loss prior to re-saturation very slightly (figures 4.4.4-5). The re-saturation was not affected.

With the CEM I cement and w/c-ratio 0.55 (mix 3 versus mix 4), the moisture loss dependence is not clear, but air entrainment seems to increase the re-saturation (figures 4.4.4-5).

With the CEM II/A-V (20 % fly ash) cement and w/c-ratio 0.55 (mix 6 versus mix 7), air entrainment increased the (prior to re-saturation ;) weight loss for standard curing, but reduced it in the modified standard curing case (the “long term drying”). In both cases, air entrainment reduced the re-saturation. The latter effect is in accordance with the perception of air voids reducing the capillary suction effect.

4.4.1.4 Summary on material

The silica fume concrete mix was more resistant to scaling than the reference mix of "identical" mix design and air void characteristics, but without silica fume. The increased resistance coincided with lower moisture loss and uptake prior to and during freeze-thaw.

Fly ash cement concrete exhibited increased moisture exchange with the surroundings and somewhat increased scaling, compared to portland cement concrete. There are indications that this is an early age phenomenon, caused by the slower reactivity of the fly ash. The phenomenon addresses the question of early age testing of "slowly developing concrete".

As expected, increasing the w/c-ratio in all cases increased moisture exchange prior to and during re-saturation. It also increased the uptake during freeze-thaw and the scaling.

The effect of air entrainment on moisture exchange is not obvious. For w/c- ratio of 0.45, the effect is marginal. Increasing the w/c-ratio to 0.55, air entrainment seemed to increase the re-saturation with CEM I cement, but reduce it with CEM II/A-V cement. The difference can not readily be explained.

4.4.2 Freeze-thaw performance versus curing regime

Except for silica fume concrete, intensive drying produces substantially higher scaling than the other curing regimes. In the case of the silica fume concrete, the intensive drying was not the most severe curing regime. Still, the relations of moisture loss and absorption between intensive drying and modified curing remained the same. This suggests that – even if the relation of moisture loss between these two curing regimes was the same as for other mixes – the structure was more resistant to alterations. This is consistent with Sellevold's report [S 1988b]. Still, the increased scaling of modified standard curing of this mix indicates that structural changes do take place with silica fume as well, but it may be a more time dependent process.

The plastic curing generally produced the lowest scaling level. This fitted with the low absorption during re-saturation with this curing regime (see previous sections). The lower scaling with this procedure is in contrast to the work by Lundgren [L 1996]. With CEM I cements, carbonation is normally considered to have a positive influence on the freeze-thaw resistance due to the increased density of the pore system. Though, Lundgren applied a completely different CEM I cement (low alkali, high sulphate resistant) than the one in the present work, and her results are not questioned. However, the more probable reason for the observed differences may be attributed to the “degree of atmospheric protection”. In the present work, it is most probable that some carbonation was allowed to happen during the stage of preparation, while great care was taken to prevent evaporation. The effect of carbonation has been known for a while, but the accurate studies performed the last couple of years has demonstrated the importance of this parameter in connection with laboratory testing of portland cements [U 1999].

Standard curing normally produces lower scaling than modified standard curing. This is in line with the lower adsorption during re-saturation and during freeze-thaw for this curing regime, sees above.

- - -

Investigating internal cracking with ultrasonic pulse velocity on concrete subjected to testing in pure water, did not indicate effects of curing on the rate of deterioration.

4.4.3 Freeze-thaw performance versus moisture changes

For some of the mixes tested with 3 % NaCl, re-saturation by water produced larger absorption during freeze-thaw than that of re-saturation by 3 % NaCl. However, the effect was not consistent. Testing with pure water, the picture was quite mixed. The former part may be attributed to higher degree of scaling when re-saturated by water, i.e. higher deterioration (cracking ?) causing absorption. Testing with water for mix 5, the cracking / disintegration made it difficult to obtain absorption values during freeze-thaw. Cracking was not investigated on a routine basis for all mixes, and the issue will be closed at this point.

There appears to be a general correlation between the scaling level and the absorption during freeze-thaw, if intensive drying is not included. The correlation also applies to the accumulated absorption prior to and during freeze-thaw.

Testing (the durable ;) mix 3 in water, did not produce more cracking when re-saturated by water, even if the absorption during freeze-thaw increased in this case. On the contrary, the ultrasonic pulse velocity showed less deterioration in this case. With the less durable mix 5, the cracking clearly progressed independently of the type of re-saturation.

Not expected, but still commented : There was no general correlation between the absorption during freeze-thaw and the preceding moisture loss. Again, this emphasises the primary importance of the whole moisture change *history* (or *procedure*), rather than the amount of moisture loss or uptake.

4.4.4 Moisture changes prior to freeze-thaw

The loss of moisture from the concrete depended very much on the pre-storage conditions. The most striking effect was the different properties of the modified curing and intensive drying. The standard and plastic curing regimes produced very low mass loss from the time of sawing until re-saturation.

The sample treatment has lead to geometric effects on the weight loss differences between the series. Except for the plastic curing, the samples have been subjected to simultaneous moisture loss from all the cylinder surfaces in the curing period from 7 to 21 days. Only for the “modified standard”, is this weight loss included in the presented weight loss values. Correcting for the geometrical effects, the moisture loss from the test surface may have been of the same order for modified standard curing and intensive drying :

Sawing at an early age and storing at 20°C and 65 % RH (modified standard curing) produced substantial moisture loss, ranging from 1.2 to 2.1 % of the initial sample weight. These figures correspond to 15 – 25 % of the initial water content, or 39 – 46 % of the evaporable water (for simplicity : water consumption corresponding to 70 % hydration of the cement/clinker, none from the pozzolanic reaction). These values are not accurate, due to some absorption taking place during the few days of water storage after de-moulding. Still, they illustrate that the moisture loss is significant. The weight loss was three times that of the one caused by drying from the test surface for 72 hours at 40 °C.

From the age of 21 days (sawing of the last samples), the weight recordings equally describe the moisture loss of all the series.

Standard curing lead to somewhat higher absorption during re-saturation than plastic curing.

No correlation could be found between variation of "evaporation rate potential" due to individual placement of the single specimens (intensive drying) in the drying cabinet - and their individual weight changes during drying. The evaporation from a free water surface ranged from 600 – 950 g/m^2h, depending on the location. The relative humidity within the drying cabinet expectedly was in the range of 15 % (Laboratory air at 20 °C/50 % RH heated to 40 °C.) This means that at this evaporation rate and RH level, the moisture loss depends on the concrete material structure. Hence, marginal differences in vapour partial pressure at this level and for the relatively short period of drying can be neglected.

Corresponding to the same range of moisture loss from the test surface for modified standard curing and intensive drying, the weight gain during the subsequent re-saturation was also of the same order for the two curing regimes.

There was no simple relation between the (one face) weight loss in the period between preparation and re-saturation – and the (one face) suction during the re-saturation. This indicates that how the concrete is subjected to moisture loss is more important for later properties than the amount of moisture loss itself.

4.4.5 Damage

Tested with 3 % NaCl, the scaling is higher when re-saturated by water compared to that when re-saturated by 3 % NaCl (mix 1 & 2). This might be attributed to a reduced amount of freeze-able water when introducing salt into the pore system. However, testing with water, re-saturation by 3 % NaCl produced higher scaling than that of re-saturation by water. A possible explanation is the existence of osmotic pressure (section 4.3.6.1), in both cases increasing the degree of saturation in the very top layer of the exposed surface, at least initially.

The effect, if existing, would cease after the fading of the salt gradient. In the external-salt-case, the gradient will take some time to fade due to the fact of the slow diffusion of salt into the structure [R 1999]. The limiting parameter may be water available from below. In the internal-salt-case, the diffusion of salt from the sample surface towards the exterior will probably be fast enough to reduce the salt gradient faster than in the former case. Water uptake from the external will not be limiting the process. In both cases and if existing, the phenomenon is likely to cause a retarded scaling propagation after a while. This in fact, is a typical pattern if the damage is not excessive (when the availability of testing medium probably becomes the critical parameter). In any case, it will not “touch” the established perception that external salt is the more severe alternative of the two cases.

The occurrence of cracks (mix 5) may make the scaling data meaningless after a certain point. The reason is that the testing medium percolates to the bottom of the sample (disappearing from the sample surface). Additionally, the internal moisture condition will be arbitrary under such conditions. The scatter between the single specimens will increase in terms of time-dependent deterioration. Monitoring cracking however, the tendency will be clear, and the low statistical significance (of the "degree" of cracking) is no practical problem for evaluating the performance. Practically, the implication for avoiding misinterpretation of scaling data is monitoring of cracking. Concrete qualities susceptible to such degradation are typically :

- those of high w/c-ratio (> 0.60) after short time of testing
- concrete blocks etc. of poor compaction, also after short time of testing
- denser concrete after very long time of water storage or freeze-thaw testing

The two latter cases are not covered by the present publication but are still according to the experience of the present author.

4.5 Conclusions

4.5.1 General

The primary objective of the present study was to investigate the effect of curing on freeze-thaw performance, i.e. scaling or internal damage. Secondly, measuring weight changes during the course of curing and freeze-thaw was used to investigate relations between moisture loss or uptake and freeze-thaw performance. Thirdly, the data have been used to consider material performance and the deterioration process. The conclusions that may be drawn from this work are grouped accordingly :

4.5.2 Main findings

- Performance is very sensitive to curing conditions : Intensive drying (40 ^{o}C, ~15 % RH) for three days prior to re-saturation and freeze-thaw testing leads to a substantial increase in scaling. One exception is silica fume concrete with a reasonable low w/(c+s)-ratio (0.45).

- Plastic curing produces the lowest scaling, in contrast to another study. Standard (according to SS 13 72 44) and modified standard curing lead to intermediate scaling levels.

- It was found a general relation between moisture uptake during freeze-thaw and scaling.

- Re-saturation by water yields higher scaling than re-saturation by 3 % NaCl, when freeze-thaw tested in 3 % NaCl. Tested in pure water, re-saturation by 3 % NaCl produced higher scaling, at least during the initial stage of testing. Thus, there are indications that different salt concentration inside/outside the concrete surface at least temporarily increase the damage. This may be attributed to osmotic effects temporarily increasing the degree of saturation close to the surface (see section 4.4.5).

- Silica fume concrete exhibited increased scaling resistance, compared to identical mix design without silica fume. Fly ash cement concrete produced somewhat increased scaling, compared to the reference mix. Both for silica fume and fly ash, the freeze-thaw properties were attributed to the moisture exchange “property”, being improved for the silica fume, but a disadvantage for the fly ash. Indications are however, that the phenomenon in the fly ash case is a time dependent one, diminishing after proper curing of the slower reacting fly ash (compared to portland cement).

4.5.3 Other findings

Effect of curing

- Intensive drying resulted in substantially higher scaling than standard curing, except for silica fume concrete. Modified standard curing was normally ranked as number two. With silica fume, modified standard curing produced the highest scaling (but still below 0.25 kg/m^2). This suggests that even if silica fume concrete possess higher resistance to structural alterations, they do take place but may require more time than for mixes without silica fume.

- Plastic (sealed) curing produced the lowest scaling. This may be due to the fact that some carbonation probably was taking place during the preparation procedure. Hence, the plastic only acted as protection against evaporation, resulting in very low moisture changes, which apparently is a very positive effect. The possible susceptibility to carbonation-induced differences makes this curing regime a vulnerable one. It should only be applied for special applications.

Freeze-thaw performance versus moisture changes

- When tested with 3 % NaCl, there were indications of larger absorption during freeze-thaw when the preceding re-saturation was with pure water – compared to that of re-saturation with 3 % NaCl. However, the pattern was not consistent.

- A correlation between scaling and absorption during freeze-thaw was indicated. The correlation also seemed to apply to absorption prior to freeze-thaw. This is consistent with other works ([J 1995]).

- No relation could be found between internal cracking (i.e. ultrasonic pulse velocity) and absorption during re-saturation. This may be due to the naturally higher scatter of the former property (mix 5) or absorption values below critical values (mix 3).

- There was no simple relation between the absorption during freeze-thaw and the preceding moisture loss. The conditions (RH, temperature, time) during moisture loss appears more important than the actual level of moisture loss.

Moisture changes prior to freeze-thaw

- As expected, the loss of moisture depended very much on the curing regime. Lowest loss and absorption was observed with plastic curing, then followed standard curing. The highest moisture loss was observed with the modified standard, i.e. higher than for the intensive drying, ranked as number two.

- The absorption during re-saturation was in the same range for modified standard curing and intensive drying. The re-filling of the latter was approximately 80 % of the loss. However corrected for geometrical effects, the absorption through the test surface may have been of the same range for these two curing conditions. On this issue, the study should be supplemented with recordings on samples with arrangement eliminating any geometric effects. Plastic curing possessed the lowest absorption at this stage.

- Still, there is no simple relation between the moisture loss prior to and absorption during re-saturation.

Internal cracking

- Internal cracking is detectable with ultrasonic pulse velocity. The deterioration rate may vary between the single specimens within a series. This causes a certain scatter between the samples, but the tendency is clear enough for assessing damage.

4.6 Synopsis

It seems evident that the absorption both during re-saturation and freeze-thaw is closely connected to scaling. They may be considered combined material-environmental parameters. The apparent correlation between these properties illustrates the importance of controlling the moisture conditions. It is necessary to secure the “potential moisture changes” to take place in a reproducible way and with a relevance to field conditions. The latter implies that it should be considered to allow the concrete to dry or “breathe“ at one or more stages during the testing procedure. This “moisture history procedure” will determine the degree of pore re-filling, initially and during the testing. For each “moisture history procedure”, there should be a close correlation between moisture loss and subsequent absorption during re-saturation. The present work illustrated a connection between the latter and freeze-thaw scaling.

In many cases, the modified standard curing might be a field relevant procedure. It certainly will be for products like concrete flags and pavement blocks. It may also be for ready mix concrete. Omitting the traditional discussion of testing the “mix design potential” or the “how to finish properly a concrete surface for the field”, the standard curing regime provides a reasonable compromise. Standard curing according to SS 13 72 44 reduces the practical obstacles in securing constant vapour pressure for a large number of testing surfaces. Still, it should be investigated more closely concerning the influence of different degree of saturation at the initiation of the main freeze-thaw testing.

In any case, the correlation to field performance must be closely considered. The absorption during “re-saturation” and degree of saturation under field conditions are vital to obtain a field relevant testing procedure. Hence, a correlation between laboratory freeze-thaw testing and field performance with respect to damage will be the focus of the following section.

5 Field performance versus laboratory testing of freeze-thaw

5.1 Introduction and objective

The previous sections demonstrate that the choice of testing regime is of vital importance for the outcome of the laboratory freeze-thaw testing procedure. Concerning the moisture state, it is in principal agreement with the degree of saturation concept by Fagerlund [F 1977]. For practical testing, it becomes of vital importance somehow to consider the moisture state in the field. Very often, the non-interrupted capillary suction approach suggested by the degree of saturation concept does not apply to the field conditions. For the field, of course, conditions vary widely with alternating wetting and drying periods of varying intensities. These changes not only affect the degree of saturation, but also modify the pore system [B 1986b, K 1999] and the suction properties of the concrete material.

Performance tests on freeze-thaw resistance like the reference method of prEN xxx expose the testing samples to a continuos wet and temperature-cyclic testing regime. The samples are not allowed to “breathe”, a fact that leads to “pumping” and accumulation of water within the material structure, as shown elsewhere in the present publication. Still, the very nature of performance testing is to accelerate the deterioration process in the field. It cannot simulate field conditions completely. Auberg [A 1998] provides a compilation of the principles concerning sample preparation, damage attack and damage assessment for a large number of testing methods. Referring to Powers questioning the ASTM C 666 procedure in this respect already 1955, he points out that the experience from testing not necessarily coincides with that of practical experience. Too often, testing methods seem to distinguish between superior and poor only, with no intermediate differentiation. The answer might be various testing methods for various applications. Auberg [A 1998] however, further refers to an ACI committee and concludes that the main question of field correlation is solved by degree of precision and “calibration”. Consequently, not only testing principles are being discussed, but also acceptance criteria concerning degree of degradation in the laboratory tests. Lack of precision concerning “field conditions” complicates the issue further.

Still, even if a 1:1 correlation between field performance and accelerated testing is not possible, the regime of moisture exposure – leading to moisture accumulation or the opposite - in the concrete material should follow the same principles in the field and in the laboratory. If not, a correlation or "calibration" between the two conditions will not be possible to obtain, at least not equally for a range of material qualities.

It is not the objective at this stage to discuss testing principles in details. Without elucidating the issue further, the reference method of prEN xxx is believed to represent relevant environmental conditions in the following aspects :

- one exposed face and one-dimensional freezing front
- application of de-icing salt
- temperature regime
- deterioration pattern
- useful both for different materials and ways of surface finishing

Previously, this testing method has been subjected to correlation tests in marine environment [P 1995, P 1996]. A few years ago, it was decided to establish another major study on field versus laboratory behaviour for a wide range of concrete mix designs [P 1995, U 1999c]. The new exposure site was on the highway RV 40 between Gothenburg and Borås in Sweden. This chapter describes the concrete mixes manufactured by the present author that are part of the field exposure – as well as initial laboratory results and some preliminary field results.

The objective of the present section is to report and discuss preliminary results of the field versus laboratory study for such an environment. The study includes a range of concrete mixes made with Norwegian cements and/or "Norwegian" mix design. Other binders and issues related to the project will be reported later [U 1999c, U 2002].

5.2 Experimental

5.2.1 General

Concrete mixes were manufactured in the laboratory (by the present author) and subjected to the normal curing procedure of SS 13 72 44 for the first month. At this stage, one series of samples from each mix design was subjected to the normal pre-qualification test of the same standard. Mix nos. 1-12 was placed at the field station at the highway at the age of four to five months, i.e. in July

1997. Prior to this, they had been water cured until the age of seven days and then stored in laboratory climate of 20 °C and 65 % RH. Mix nos. 13-18 was placed at the site in December 1997, at the age of two months after same type of curing.

5.2.2 Field exposure

The field exposure site constitutes the "saline environment" along the highway RV 40 between Gothenburg and Borås, Sweden. Application of de-icing salt follows standard procedures of that of the Swedish road authorities. The salt exposure is considered relatively severe. Amount of salt applied and salt ingress will be reported separately. The location is displayed in the figures 5.2.1 & 2. The former illustrates the exact placing of the 7 x 15 x 15 cm samples below the road safety barrier. Due to the safety of the traffic and snow clearance, the samples could not be placed closer to the traffic. The samples were tilted 1:20 compared to the horizontal plane.

Figure 5.2.1 : Location of 15 x 15 x 7 cm^3 *samples at the site. Also larger samples for other purposes like corrosion measurements etc. are located here. Front side faces traffic and is directed towards south. From [U 1999c].*

Figure 5.2.2 : The site on a winter day. From [U 1999c].

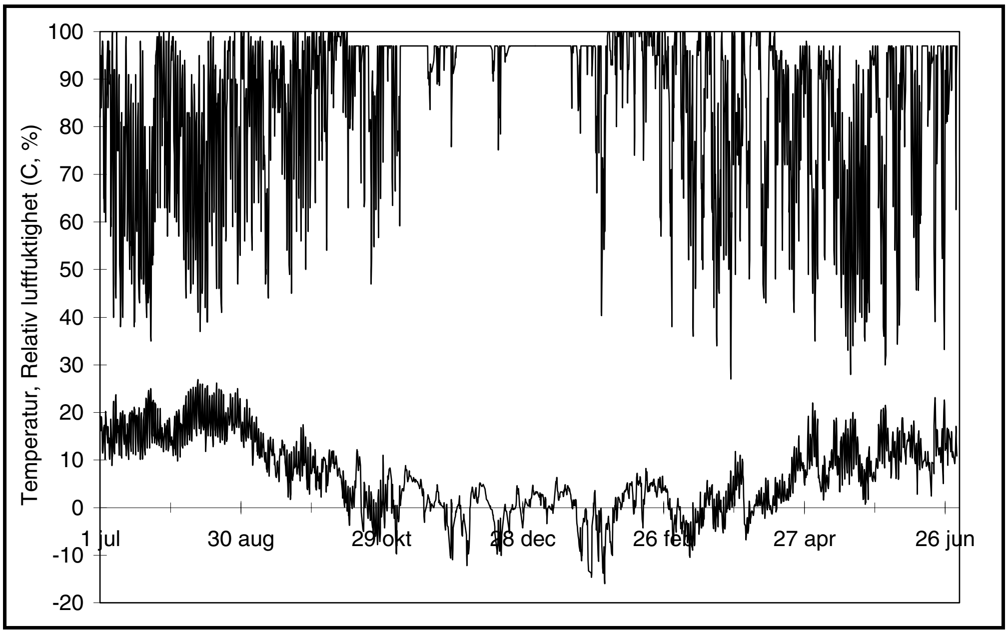

Figure 5.2.3 : Determination of temperature and relative humidity at site during the winter 1997-98. From [U 1999c].

Data on climatic characteristics are available in the project reports. Utgennant compiled and reported the temperature and relative humidity at the site, based on automatic measurements. He also reported the number of hours below 0 ^{o}C and the number of crossings of this temperature to be approximately 1750 and 70, respectively. Both values are for the winter 1997-98. It is assumed that these values are representative for many corresponding locations in Sweden, while – as mentioned – the amounts of salt applied is in the upper range.

5.2.3 Testing methods

The standard test SS 13 72 44 was performed in order to relate the results to the subsequent field performance. The detailed test is provided in appendix A, see also section 3 for minor deviations from the present prEN xxx.

Samples for the site exposure comprised four (mix no. 1-12) or two (mix no. 13-18) 15 cm cubes cut in two halves and placed with the sawn surface upwards.

Initially (just before placement at the field station) and after each winter season, the samples are subjected to the following :

- The volume is determined by weighing in air and water.
- Ultrasonic pulse velocity is measured and reported as the mean value of three measurements on each of all the samples.
- Finally, visual inspection is carried out and reported.

One of the mix designs (no. 3) was – together with some mixes from other parts of the project – subjected to periodic determinations of the capillary degree of saturation during a part of one winter season. This test was performed on samples drilled from the top and front (towards the traffic) surface of 30 x 30 x 40 cm blocks (not shown in the previous figures). These cores were first weighed, left immersed in water for a fortnight, weighed, dried at 105 ^{o}C and weighed again. The cores had been cut into sections in order to determine the gradient of the capillary degree of saturation. The concrete had been cast on September 25, 1997, and was placed in field on November 6, 1997. The measurements took place in the period mid February to the end of April, 1998.

The air void characteristics of the fresh concrete has been determined by the “DBT-method” [D 1995], a brief description of which can be found in the appendix H. Additionally, air void characteristics have been obtained on hardened concrete in accordance with ASTM C 457 with assistance from an external laboratory.

5.2.4 Mix design and materials

The objective of the mix design matrix is to answer a number of questions. A list of the Norwegian mixes is provided in table 5.2.1, and an overview is presented in table 5.2.2.

The overall objective was to investigate the laboratory behaviour vs. field performance on a set of mix design relevant to the type of field conditions in question. On doing so, the various cement types have been adopted in the design matrix only within their reasonable range of application, i.e. their "design range". This implies that the use of a fast reacting and finely ground cement at low w/c-ratios – by applying excessive amounts of superplasticizers – is not considered relevant.

The design matrix allows the comparison of two cements (of low water demand) at three different w/c-ratios ; 0.35 – 0.40 – 0.45. Both of them are low alkali and designed for this type of application.

The fly ash cement is designed to meet the properties needed for intermediate as well as low strength levels. (The intermediate level is met by the clinker composition of the cement, the lower level by its fineness and concrete surface finishing properties. The fly ash is favourable in both respects and also is a measure to deal with alkali reactive aggregates.) The fly ash cement is included at two different w/c-ratios ; 0.40-0.45, the lower one at the border of its design range.

The cement type and w/c-ratio matrix is partly designed to fit the Swedish binder matrix, reported elsewhere [U 1999c]. However, the Norwegian mixes are the only one to include the w/c-ratio of 0.45, motivated by Norwegian design codes for the environment in question.

Introducing the w/c-ratio of 0.45 also enables a comparison of all the Norwegian manufactured cement types without possible interference of water reducing admixtures interfering with the air void structure. Thus, the "Standard" and rapid hardening ("Industri") cement are added to the matrix at 0.45.

The effect of air entrainment is investigated at the w/c-ratio of 0.35, but only with the two cements considered relevant for such types of concrete.

Last but not the least, the "academic" matrix above is supplemented with two mixes in an apparently not very systematic approach. Mix no. 18 (with 4 % silica fume) meets the standard specifications of the concrete class "SV40" of the Norwegian road authorities [S 1997b]. It shall have a maximum w/(c+2s)-ratio of 0.40 and contain 3 - 5 % silica fume. Mix no. 17 (9 % silica fume) was incorrectly taken to be in accordance with the concrete class "SV30" (w/(c+2s) ≤ 0.38 and 8-10 % silica fume). However, the w/(c+2s)-ratio turned out to be 0.01 too high (...). Still, the mix properties are so close to the design code and (except for the silica fume) to that of mix no. 16 that it was considered worth while to keep it for the present study. Hence, both these mix designs are of considerable practical interest.

In order to compare binder-to-binder effects, mix nos. 1-12 was designed for aggregates received from Sweden. These aggregates were also used for a large number of other mixes. A "quality assurance test" by thin section analyses displayed a number of flaws for five of the mixes. The defects were determined to be caused by bleeding mainly, with increased porosity of the paste along the paste-aggregate interface. This phenomenon was evident for mix nos. 1, 4, 6, 7 and 8. It was attributed to the high dosages of superplasticizer that was required to maintain the fresh concrete workability with the given aggregate characteristics and aggregate-binder combinations. Such flaws of increased porosity are weak points and might locally increase the capillary degree of saturation. The possible implication is that more water can be retained in these areas or. Alternatively, they might be the first pores to become saturated when subjected to external suction. In both cases, these locations are potential sites for the initiation of structural damage.

Mix no.	Cement type according to EN 197	Trade name	w/c-ratio	w/(c+2s)	Nominal air content [%]
1	CEM I 42.5-R-SR-LA	SR	0.35	0.35	-
2	CEM I 42.5-R-SR-LA	SR	0.35	0.35	4.5
3	CEM II/A-V 42.5-R	Std.FA	0.40	0.40	4.5
4	CEM II/A-V 42.5-R	Std.FA	0.45	0.45	4.5
5	CEM I 52.5-R-LA	Anlegg	0.35	0.35	-
6	CEM I 52.5-R-LA	Anlegg	0.35	0.35	4.5
7	CEM I 52.5-R-LA	Anlegg	0.40	0.40	4.5
8	CEM I 52.5-R-LA	Anlegg	0.45	0.45	4.5
9	CEM I 42.5-R-SR-LA	SR	0.40	0.40	4.5
10	CEM I 42.5-R-SR-LA	SR	0.45	0.45	4.5
11	CEM I 42.5-R	Std.	0.45	0.45	4.5
12	CEM I 42.5-RR	Industri	0.45	0.45	4.5
- - - - -	- - - - - - - - - - - - - - -	- - - - -	- - - - -	- - - - -	- - - - - - - -
13	CEM I 42.5-R-SR-LA	SR	0.35	0.35	-
14	CEM I 52.5-R-LA	Anlegg	0.35	0.35	-
15	CEM II/A-V 42.5-R	Std.FA	0.45	0.45	4.5
16	CEM I 52.5-R-LA	Anlegg	0.40	0.40	4.5
17	CEM I 52.5-R-LA	Anlegg	0.46	0.39^1)	4.5
18	CEM II/A-V 42.5-R	Std.FA	0.42	0.39^2)	4.5

Table 5.2.1 : Mix design. More detailed information on mix design is available in appendix E. 1)9 % silica fume (s/c), 2)4 % silica fume. See text for objectives.

Cement type	w/c-ratio (air content)				
	0.35 (-)	0.35 (4.5 %)	0.40 (4.5 %)	0.45 (4.5 %)	SV [1)] (4.5 %)
CEM I 42.5-R-SR-LA (SR)	x	x,y	x	x	
CEM I 52.5-R-LA (Anlegg)	x	x,y	x,y	x	x
CEM II/A-V 42.5-R (Std.FA)			x	x,y	x
CEM I 42.5-R (Std.)				x	
CEM I 42.5-RR (Industri)				x	

Table 5.2.2 : Overview of mix design. "y" designates re-designed mix due to reasons explained in the text. [1)]Design close to that of specifications by the Norwegian road authorities, see text for explanation.

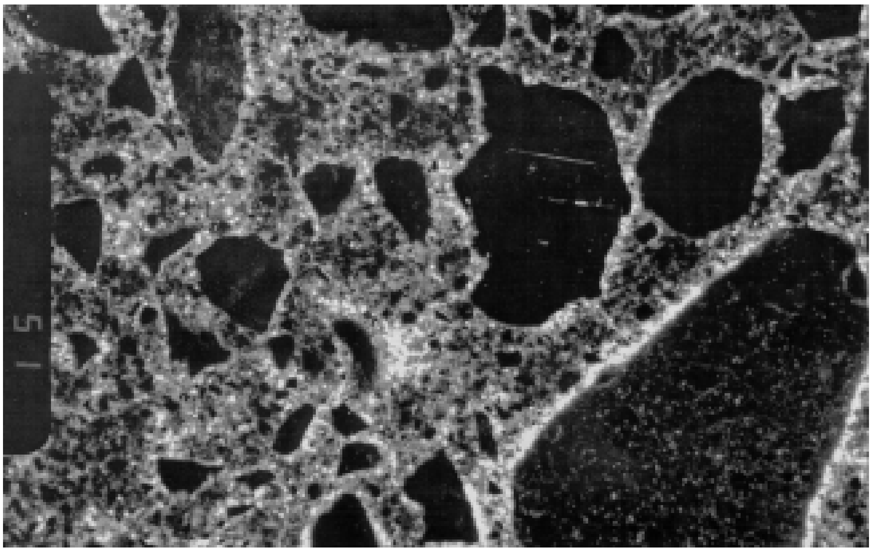

Figure 5.2.4 : Thin section analyses of mix no. 1, exhibiting bleeding around the coarse aggregate particles at numerous locations. The picture is 3 mm across. Reported in [B 1997].

Hence, it was decided to re-design some of the mixes : Less water demanding aggregate was used. Plasticizer was applied in order to reduce the amount of superplasticizer. The former contains lignosulphonate, and this admixture (combination) normally interferes less with the air void structure than the use of superplasticizer only. Both measures are in line with Norwegian domestic practice and considered improving the practice-relevance of these mixes (nos.13-16).

5.3 Laboratory test results

5.3.1 General

Compressive strength values are included in the appendix E. These data are mean values of two specimens, meant for indication only. The obtained values are in accordance with the expected strength levels of the various mix designs. However, the mix nos. 14, 15 and 16 exhibit strength values in the lower range of that to be expected based on companion mixes (nos. 5, 4 and 7, respectively). Only partly may this be explained by deviations in air void content. Some of the differences may further be due to change of cement delivery (for the mixes 13-18), but mix no. 16 still remains low compared to mix no. 17. However, with the very few samples for the strength determination, the issue will not be further discussed in the present report.

Field test values have been obtained from other project reports [U 1999, N 1999] by request of the present author for this publication.

5.3.2 Air void structure

Obtained air void characteristics are included in table 5.3.1. Total air void content, spacing factor and specific surface area are determined by two different methods. The two sets of results are compared in the figures 5.3.1-3, while specific surface area is plotted against spacing factor in the figures 5.3.4-5. Discussion of the air void parameters is left to subsequent sections.

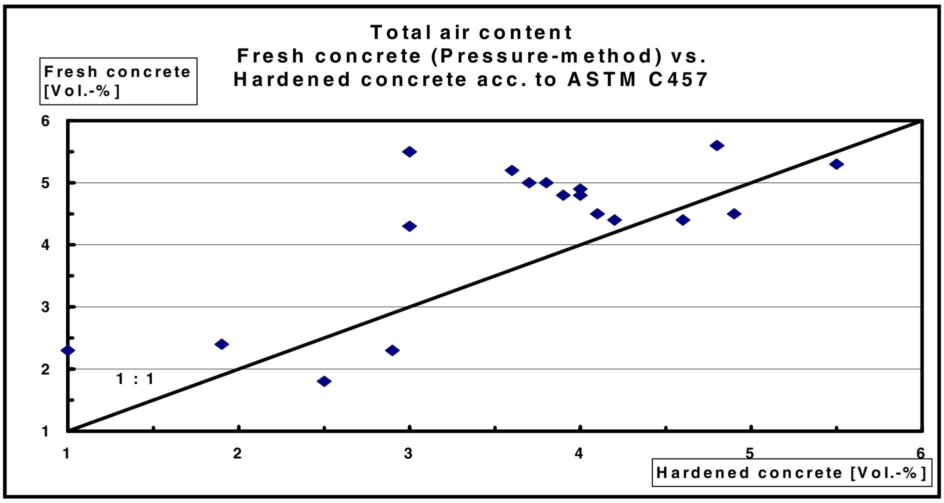

Figure 5.3.1 : Air content of fresh concrete (pressure method) versus air content determined on plane sections according to ASTM C457.

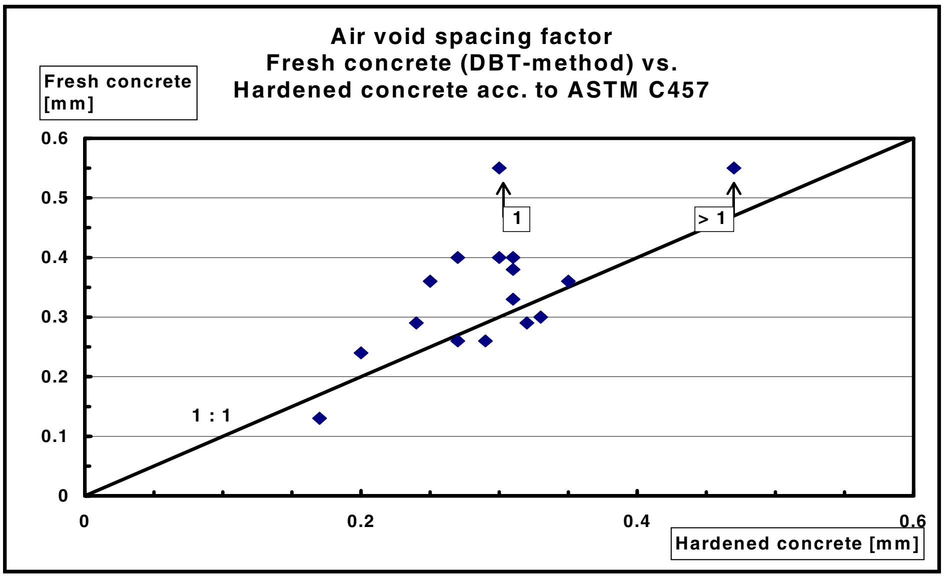

Figure 5.3.2 : Air void spacing factor determined on fresh concrete (DBT-method) versus spacing factor determined on hardened concrete in accordance with ASTM C457.

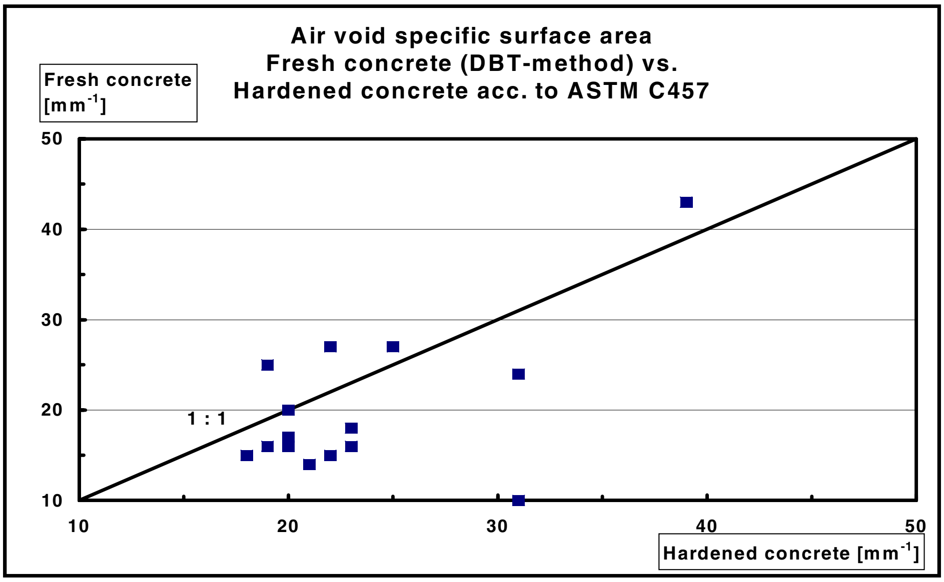

Figure 5.3.3 : Specific surface area determined on fresh concrete (DBT-method) versus specific surface area determined on hardened concrete in accordance with ASTM C457.

Mix no.	Cement type according to EN 197	w/ (c+2*s*)	Nominal air content [%]	Total air content [%]		Spacing factor $\bar{L}$ [mm]	
				Fresh	Hardened	Fresh	Hardened
1	CEM I 42.5-R-SR-LA	0.35	-	2.4	1.9	1	$0.30^{2)}$
2		0.35	4.5	5.5	3.0	0.30	0.33
9		0.40	4.5	5.0	3.8	0.40	0.31
10		0.45	4.5	4.9	4.0	0.26	0.29
13		0.35	4.5	2.3	1.0	$-^{1)}$	0.57
5	CEM I 52.5-R -LA	0.35	-	1.8	2.5	>1	$0.47^{2)}$
6		0.35	4.5	5.3	5.5	0.36	0.25
7		0.40	4.5	4.8	4.0	0.40	0.27
8		0.45	4.5	5.2	3.6	0.26	0.27
14		0.35	4.5	2.3	2.9	$-^{1)}$	0.43
16		0.40	4.5	4.8	3.9	0.13	0.17
17	(17+Silica)	*0.39*	4.5	4.5	4.9	0.36	0.35
3	CEM II/A-V 42.5-R	0.40	4.5	5.6	4.8	0.29	0.24
4		0.45	4.5	4.3	3.0	0.33	0.31
15		0.45	4.5	4.5	4.1	0.24	0.20
18	(18+Silica)	*0.39*	4.5	4.4	4.2	0.38	0.31
11	CEM I 42.5-R	0.45	4.5	4.4	4.6	0.40	0.30
12	CEM I 42.5-RR	0.45	4.5	5.0	3.9	0.29	0.32

Table 5.3.1 : Obtained air void characteristics. $^{1)}$*Expected poor value, not considered relevant to measure, see discussion or appendix H.* $^{2)}$*Not to be trusted, see discussion in text.*

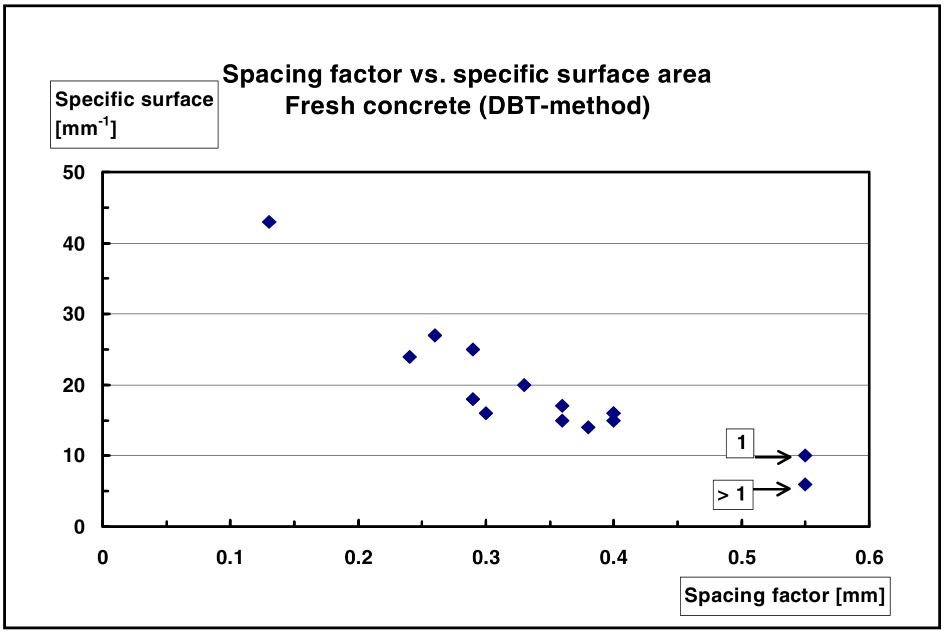

Figure 5.3.4 : Specific surface area versus spacing factor, both parameters determined on fresh concrete (DBT-method).

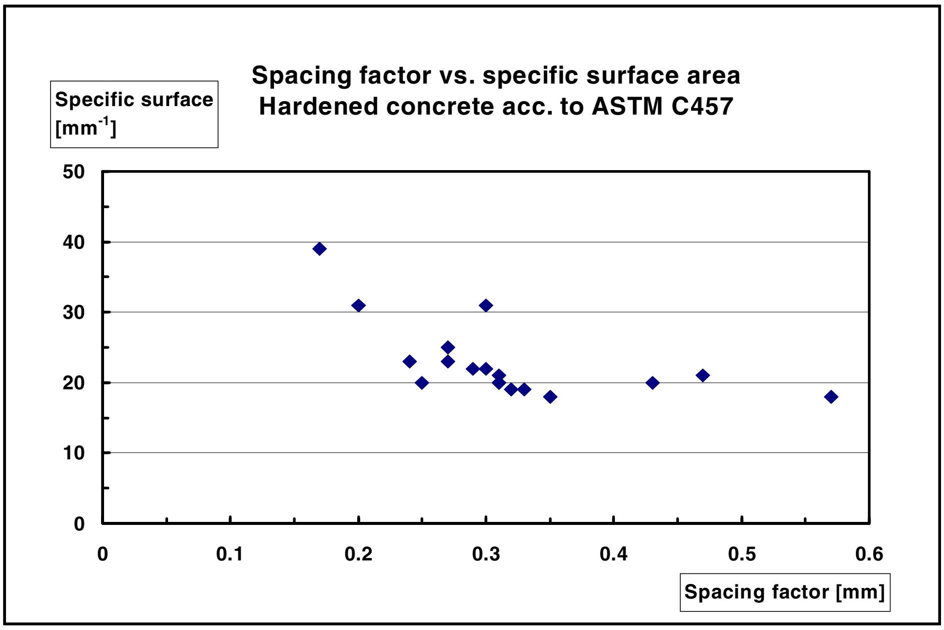

Figure 5.3.5 : Specific surface area versus spacing factor, both parameters determined on hardened concrete in accordance with ASTM C457.

5.3.3 Scaling

The scaling results of the laboratory tests are displayed in the figures 5.3.6-10, while detailed data in tabular form are available in appendix E. The first one contains all the series made with the CEM I 42.5 R-SR-LA cement, with various w/c-ratios, with and without air entrainment. Mix nos. 1 and 13 are identical except for the choice of aggregate and required admixture dosage, none of them are air entrained. Still, they behaved differently, the latter fulfilling the acceptance criteria of 1 kg/m^2, the other not. See subsequent sections for discussion and evaluation.

With the CEM I 52.5 R cement, only the air entrained mixes would fulfil any acceptance criteria in the pre-test (figure 5.3.7).

Except for mix no. 11 (CEM I 42.5 R), all air entrained mixes have scaling levels below 0.5 kg/m^2 at 56 cycles.

Several air-entrained mixes exhibit accelerating scaling between 56 and 112 freeze-thaw cycles.

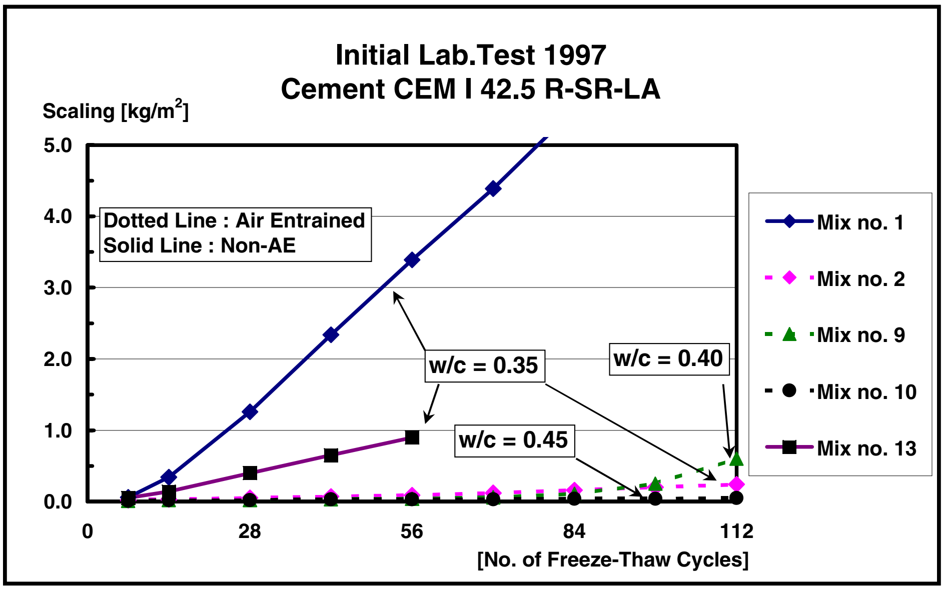

Figure 5.3.6 : Initial scaling test, part 1.

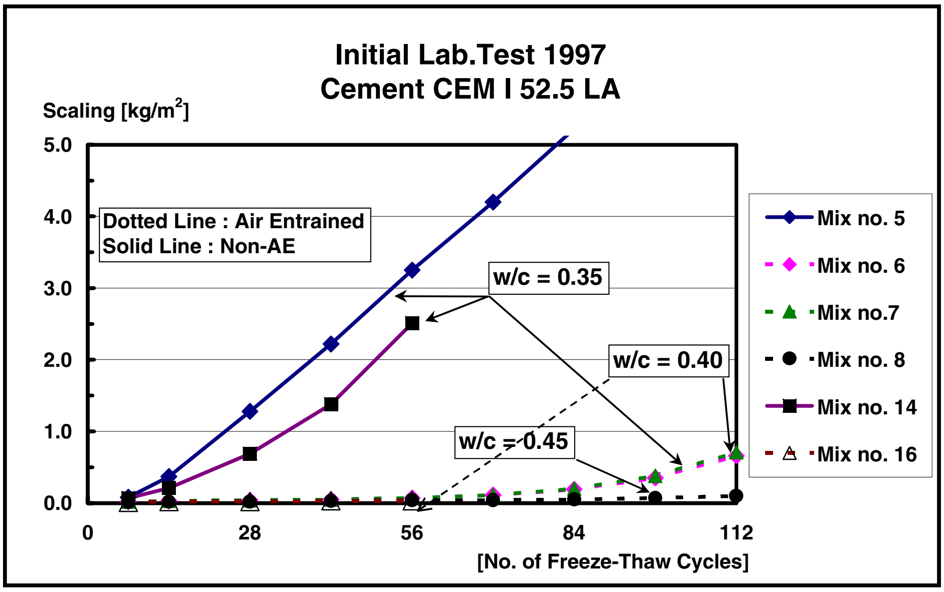

Figure 5.3.7 : Initial scaling test, part 2.

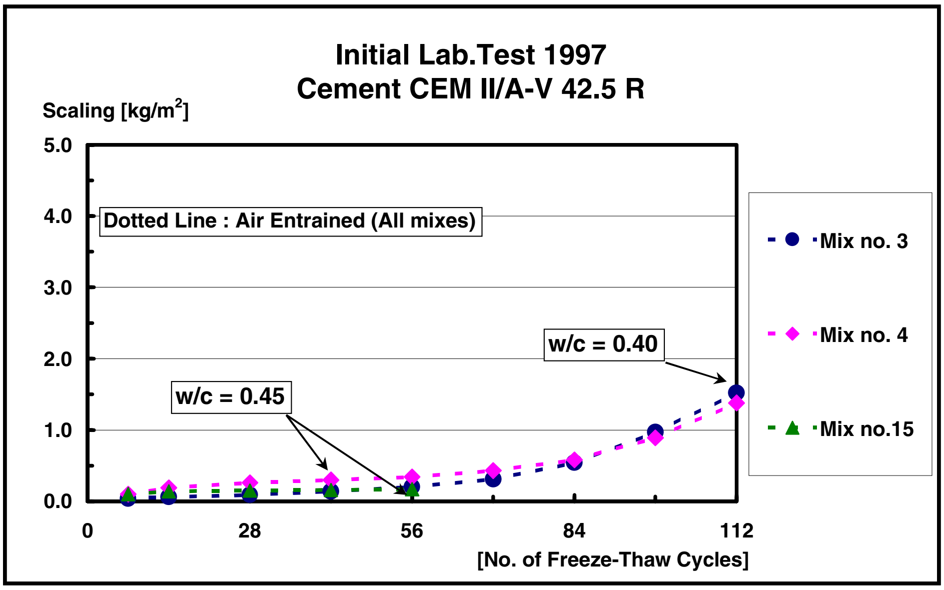

Figure 5.3.8 : Initial scaling test, part 3.

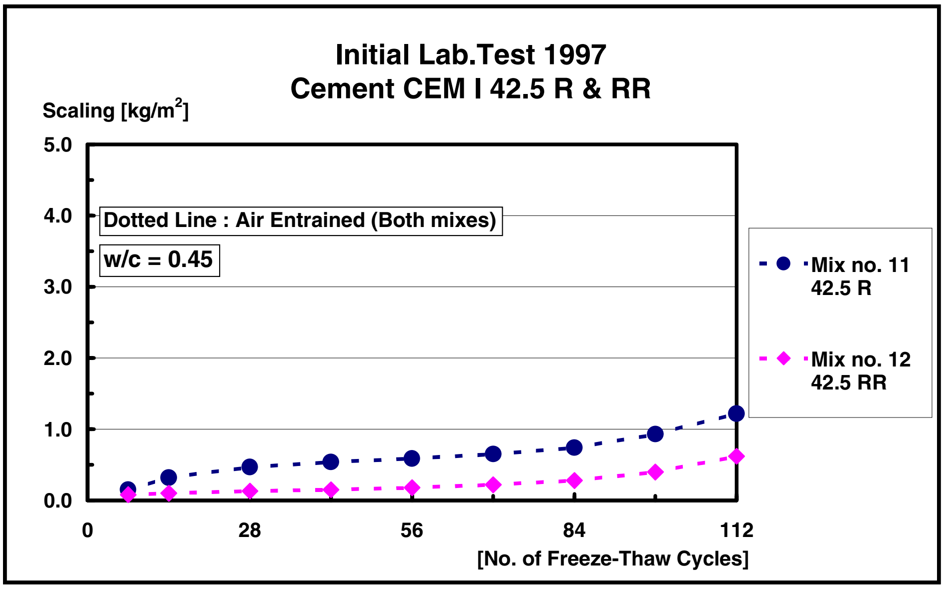

Figure 5.3.9 : Initial scaling test, part 4.

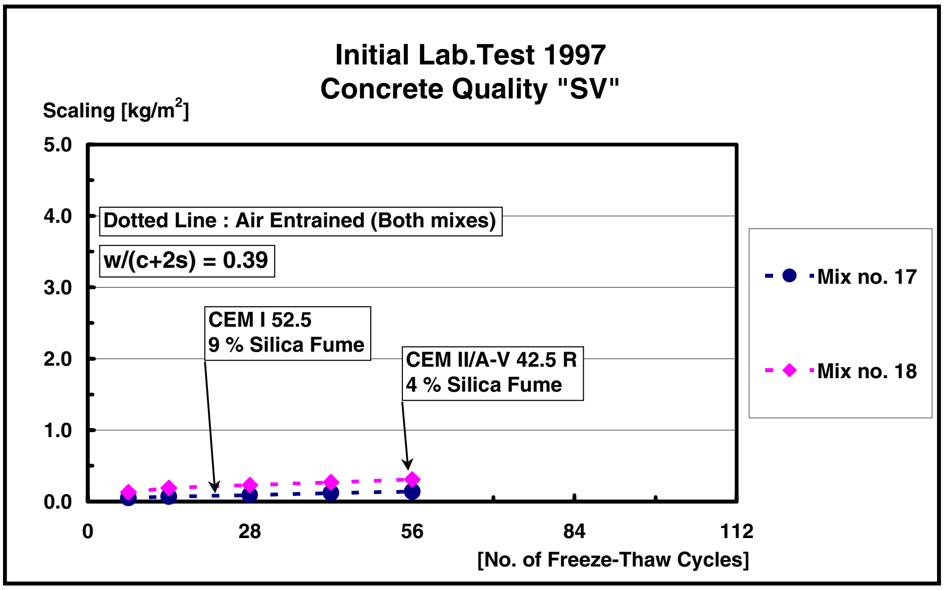

Figure 5.3.10 : Initial scaling test, part 5.

5.3.4 Scaling versus spacing factor

Freeze-thaw scaling versus air void spacing factor obtained from hardened concrete is plotted in figure 5.3.11. Equivalently, scaling versus fresh concrete spacing factor is displayed in figure 5.3.12. See subsequent discussions.

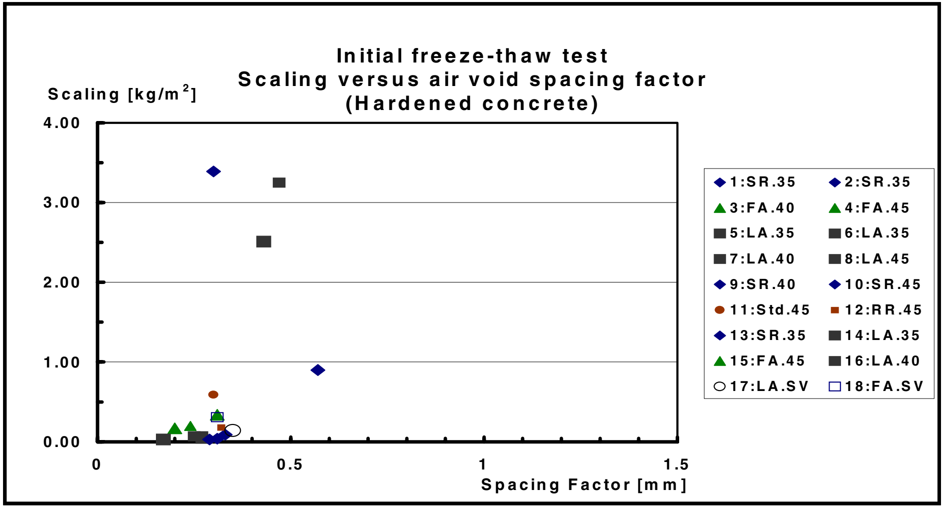

Figure 5.3.11 : Freeze-thaw scaling in initial test versus air void spacing factor determined according to ASTM C457. Note mix nos. of different w/c-ratios (but the same binder) having the same legend in the plot. For exact cement designation and properties, see table on mix design or appendix E.

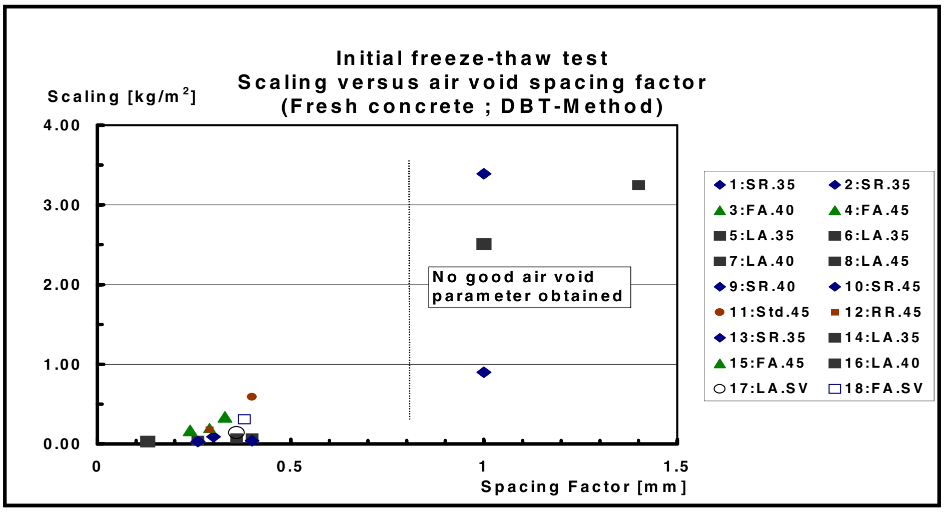

Figure 5.3.12 : Freeze-thaw scaling in initial test versus air void spacing factor determined on fresh concrete by the DBT-method [D 1995]. Note mix nos. of different w/c-ratios (but the same binder) having the same legend in the plot. For exact cement designation and properties, see table on mix design or appendix E.

5.3.5 Field test values

Plots of ultrasonic pulse velocity, weight and volume are included in the present text for the mix nos. 1 (figure 5.3.13) and 13 (figure 5.3.14) only. These exhibit the typical patterns of all the series after two winter seasons, see subsequent discussion. The remaining series are all included in the appendix E as plots. Tabular data on ultrasonic pulse velocity, weight and volume (relative values for the three latter ones) are also included in appendix E.

5.3.6 Capillary degree of saturation

The capillary degree of saturation obtained from periodic measurements on a mix identical to mix no. 3 is displayed in the figures 5.3.15-16. These values are available as plots only. See discussion.

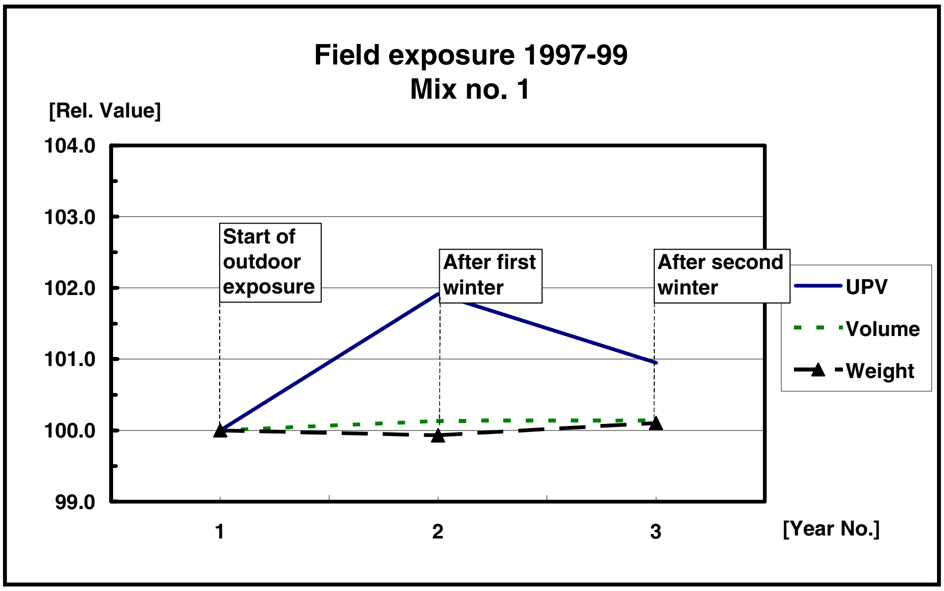

Figure 5.3.13 : Ultrasonic pulse velocity, volume and weight change on field exposed samples, Mix no. 1.

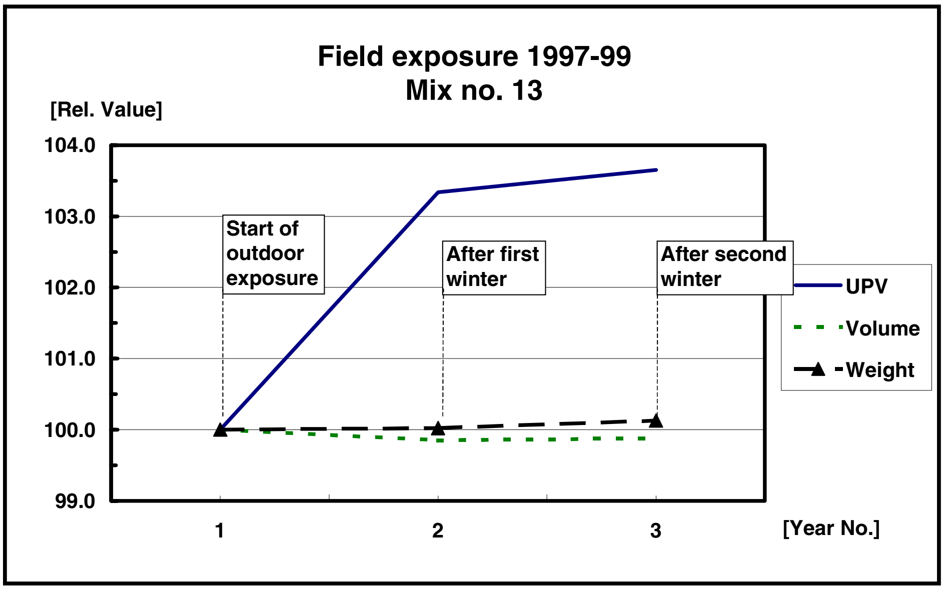

Figure 5.3.14 : Ultrasonic pulse velocity, volume and weight change on field exposed samples, Mix no. 13.

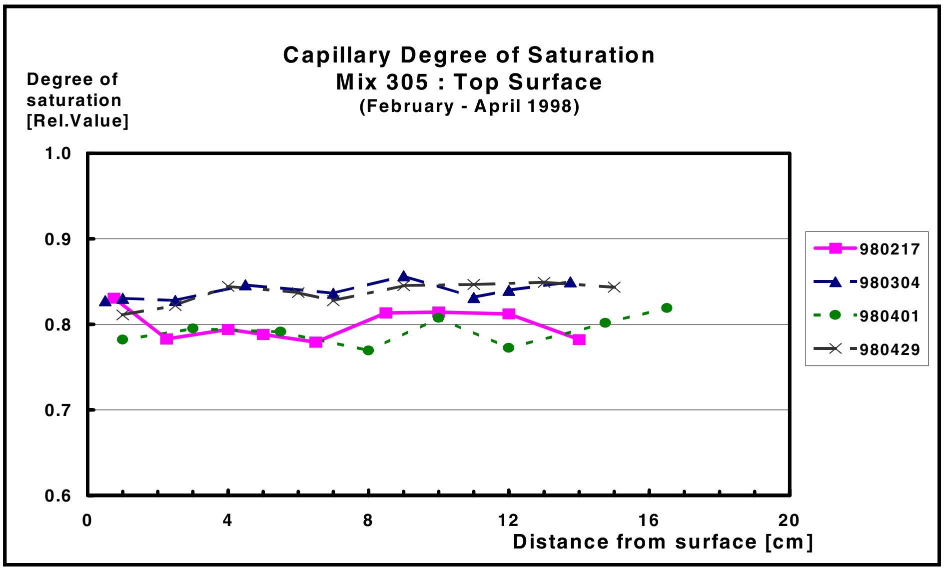

Figure 5.3.15 : Capillary degree of saturation of a mix identical to mix 3. Cast and placed during the autumn of 1997. Top surface.

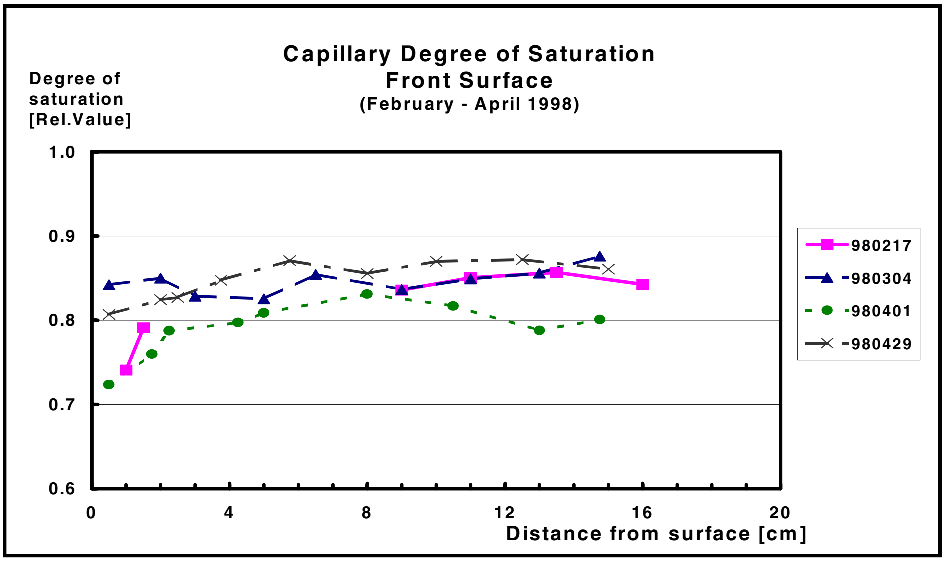

Figure 5.3.16 : Capillary degree of saturation of a mix identical to mix 3. Cast and placed during the autumn of 1997. Front surface, i.e. facing the road.

5.4 Discussion of test results

5.4.1 Air void system

a) Total air void content

The correlation between the fresh (pressure method) and hardened concrete air contents is not very good. Random distribution of larger air voids causing deviating values on the comparatively small plane sections is a possible reason. However, this can only be the case when the hardened air void content is the higher one, i.e. below the 1:1 curve.

Considering the air entrained mixes - with one exception - all mixes with 1 % drop in air content from fresh to hardened state is made with 5 kg of superplasticizer or more. These are the mix nos. 2, 4, 9 and 12. Only one of these mixes (no. 4) can also be found on the list with identified bleeding problems (previous section). The exception concerning large air content drop is mix no. 8, made with only 2 kg of superplasticizer. However, this mix had a slump value of only 30 mm, due to which the fresh air may have been overestimated by non-appropriate compaction.

Hence, there seems to have been a considerable drop in total air content in some of the mixes with high amounts of superplasticizer.

b) Spacing factor

The differences between the fresh concrete spacing factors and those of the hardened concrete also require some investigations. Since the accuracy/reliability of the former method are not widely known, some introductory comments on this method should be included. Outline of the test method as well as further comments on the documentation of the method may be found in the appendix H.

Similarly to the ASTM C457, the test procedure has some limitation in the sense of parameter or measurement range. From 2 % air void level and below, the large air voids normally dominate, the number of small air voids decreases, and the accuracy of the values is poor. The poor accuracy in such cases is of no direct relevance, since the air void characteristics are so poor that the air void system should simply be considered inappropriate. A warning is automatically given in the report.

At the opposite end, the "sampling" of air voids will automatically terminate after approximately 20 minutes, even if small air bubbles still are rising. This will artificially increase the $\overline{L}$ and decrease the α. However, the non-assessed air voids are very small (< 20-30 μ). It is argued that they will easily become filled with deposits and not act according to the intention. If the lower pore size assessed on hardened concrete is lower (e.g. 7 μ), this may cause a "deviation" between the two procedures, the DBT method producing "poorer" values. However, the latter may be more relevant.

When questioning or comparing the correlation between the DBT method and the ASTM C457 on hardened concrete, it should be kept in mind that the number of air voids recorded in the former is much higher than that of the latter. The "correlation" can never be better than the accuracy of the inferior method. Geiker et al [G 1995] refer to +/- 5-10 % on the absolute values of the spacing factor and the specific surface area as accuracy level of the DBT-method. The 95 % confidence limits between the two methods for the two parameters have been reported [D 1996]. Hence, both methods should give similar results.

Now for the present results, two of the fresh concrete values are way above those of the ASTM C457 procedure. These both belong to non-air entrained concrete with expectedly poor air void properties. Still, the ASTM C457 procedure exhibited a value of 0.30. This must be due to an error in the procedure, due to preparation or measuring failure. Both the fresh concrete values are very poor, as would be expected.

Total air void content dropped from the fresh to the hardened state when high amounts of superplasticizer were used (section 5.4.1-a). Change of spacing factor is considered correspondingly : Except for the previous cases, a ("positive") drop of 0.10 mm or more is found for the mix nos. 6, 7 and 11, all with 6.5 kg of superplasticizer or more. However in these cases, the "drop" may be due to the test procedure : The fresh concrete procedure "under-estimates" the number of very small air voids (< 20-30 µm) as described above. Hence, in these cases the ASTM C457 may give theoretically more correct values. However, there is no doubt that the DBT procedure has the ability of "producing" very good values. Also, the DBT procedure may yield more relevant values because the smallest air voids after a while may become filled with deposits.

c) Specific surface area

Even when excluding the probable erroneous reading of mix no. 1, there are several of the mixes with poorer/lower specific surface by DBT than by ASTM C457 (figure 5.3.3). If both measurements are "correct", the implication is that the air void system is improved from the fresh to the hardened state. This pattern is similar to that of the spacing factor (figure 5.3.2) as discussed above : Five mixes showed improved (lower) spacing factor in the range of 0.1 mm in the hardened state, compared to the fresh concrete values. (NB : The spacing factor and the specific surface area depend mathematically upon each other.)

Improvement of the air void system with time has only been observed – by the present author - under insufficient mixing conditions. It was never observed with simultaneous loss of total air (figure 5.3.1). Also, the mixes exhibiting this conflicting pattern include mix designs of both stable and expectedly less stable fresh concrete properties. Altogether, this suggests that the observed "improvement" is artificial and due to different testing principles.

d) Overview

Even if the DBT and the ASTM C457 test procedures are considered to give equivalent results, they differ in certain key principles. Still, it appears that the DBT fresh concrete procedure for the determination of the air void characteristics yields at least as good results as those of the ASTM C457 procedure. In fact, the plotting of the specific surface area against the spacing factor exhibits a more distinct pattern for fresh concrete. Scaling versus spacing factor should be plotted for a series with more mixes in the "intermediate" range than included in the present study.

5.4.2 Initial freeze-thaw test

5.4.2.1 General

Only air entrained concrete mixes performed well in the laboratory test, although mix no. 13 (with w/c-ratio of 0.35, the SR-LA cement and reduced amount of superplasticizer) exhibited a scaling level just below 1 kg.

The mixes re-designed with less water demanding aggregate and reduced amount of superplasticizer improved their performance in the scaling test. This appears to be evident for mix nos. 13 (vs. no. 1) and 14 (vs. no. 5), both non-air entrained. The same tendency is exhibited for the air-entrained mix nos. 15 (vs. no. 4) and 16 (vs. no. 7).

For the air-entrained mixes, this corresponds to the improved air void characteristics of these ("re-designed") mixes. For the non-air-entrained mixes, the correlation is not clear. Scaling is plotted against air void spacing factor in the figures 5.3.11&12. Figure 5.3.11, obtained on hardened concrete, does not display a clear correlation. In fact, the spacing factor value of 0.30 of mix no. 1 appears peculiar as mentioned above. Using the fresh concrete measurements, the correlation is improved, indicating that the DBT-method may be favourable.

5.4.2.2 Cement type

The system outlined in table 5.4.1 may be useful for classifying the scaling results. This system is applied below for the different mix designs, organised according to the w/c-ratio and the laboratory testing performance. Values that are questionable are marked with "(?)".

w/c-ratio = 0.45 :

The I-SR-LA and the I-LA cement appear somewhat superior to the other ones. This is not necessarily accompanied by better air void characteristics but higher strength. Still, the other combinations also performed well or fairly well.

When ranking the fly ash cement, it should be kept in mind that the fly ash component is a slower reacting or “maturing” one than the portland clinker. Hence, early age testing of this with respect to properties involving moisture transport may easily be “unfair”, compared to field service conditions. Still, the II/A-V (FA) cement improved its performance when the superplasticizer dosage was reduced.

Scaling performance	Mix characteristics	Comments
Classification of scaling results [1]	*Ref.: Mix no.* *Cement type (abbreviation)* *Mean value* $\overline{L}$ *[mm]* *Scaling 56 cycles [kg/*m^2*]* *Strength* F_{c28} *[MPa]* *Structural defects/Bleeding ?*	

Table 5.4.1 : Classification of freeze-thaw scaling. [1]*The classifications “very good”, “good” and “acceptable” are in accordance with suggested classification for testing according to SS 13 72 44. Other classification in these tables is of more qualitative (subjective) nature.*

Scaling performance	Mix characteristics		Comments
Very good	*10*	*8*	
	I-SR-LA	*I-LA*	*Both :*
	0.275	*0.265*	*Good strength*
	0.03	*0.04*	*Reasonable* $\overline{L}$
	59	*57*	
	No	*Yes*	
Good	*15*	*12*	*15 :*
	II/A-V (FA)	*I-RR (IND)*	*Medium strength,*
	0.22	*0.305*	*Good* $\overline{L}$
	0.17	*0.18*	*12:*
	44	*52*	*Good strength,*
	No	*No*	*Dubious* $\overline{L}$
Good/Fair	*4*	*11*	
	II/A-V (FA)	*I-R (Std.)*	*Both :*
	0.32	*0.35*	*Good strength,*
	0.34	*0.59*	*Dubious or poor* $\overline{L}$
	50	*50*	
	Yes	*No*	

Table 5.4.2 : Classification of scaling test results for mixes of w/c-ratio = 0.45.

w/c-ratio = 0.40 :

Most of these mixes perform very well (table 5.4.3), even if the spacing factor is poor (partly). The I-SR-LA and the I-LA cement have a very similar performance. The II/A-V (FA) cement yields slightly higher scaling, but still within what should be classified as a very satisfactory level.

Scaling performance	Mix characteristics			Comments
Very good	*9* *I-SR-LA* *0.355* *0.04* *69* *No*	*16* *I-LA* *0.15* *0.03* *57(?)* *No*	*7* *I-LA* *0.335* *0.07* *70* *Yes*	*9 & 7 :* *Good strength,* *Poor* $\bar{L}$ *16 :* *Good strength,* *Good* $\bar{L}$
Good	*3* *II/A-V (FA)* *0.265* *0.2* *53* *No*			*Good strength,* *Reasonable* $\bar{L}$

Table 5.4.3 : Classification of scaling test results for mixes of w/c-ratio = 0.40.

w/c-ratio = 0.35 :

For these w/c = 0.35 concrete mixes (table 5.4.4), the difference in laboratory test performance is considerable. All the mixes have a very good strength. The poorly performing mixes comprise both high and low levels of superplasticizer and/or structural defects. The best relation between test performance and characteristic properties is the spacing factor. Hence, these test results seem to confirm that air entrainment is necessary (for laboratory testing) even for the w/c-ratio of 0.35.

w/(c+2s)-ratio = 0.39 : w/(c+s) = 0.40 – 0.42 :

Both of these combinations give good performance (table 5.4.5). The I-LA cement plus 9 % silica fume yields somewhat better results than the II/A-V cement plus 4 % silica fume. However, both should be considered to perform at a very satisfactory level, considering the poor spacing factor. It should be considered that silica fume is a fast reacting pozzolanic material that is fully consumed at 28 days. Such early age testing may be a general disfavour of the fly ash cement, but favourable with respect to silica fume.

Scaling performance	Mix characteristics			Comments
Very good	*2 I-SR-LA 0.315 0.09 79 No*	*6 I-LA 0.305 0.07 77 Yes*		*Both : Very good strength, Dubious $\bar{L}$*
Acceptable	*13 I-SR-LA 0.57(?) 0.9 88 No*			*Very good strength, Poor $\bar{L}$*
Poor	*1 I-SR-LA 1(?) 3.4 87 Yes*	*5 I-LA 1(?) 3.3 91 No*	*14 I-LA 0.43(?) 2.5 81 No*	*All : Very good strength, Poor $\bar{L}$*

Table 5.4.4 : Classification of scaling test results for mixes of w/c-ratio = 0.35.

Scaling performance	Mix characteristics		Comments
Good	*17(0.40) I-LA + 9 % Silica 0.355 0.14 70 No*	*18 (0.42) II/A-V (FA) + 4 % Silica 0.345 0.31 55 No*	*Both : Good strength, Poor $\bar{L}$*

Table 5.4.5 : Classification of scaling test results for mixes of w/(c+2s)-ratio = 0.39.

5.4.2.3 Accelerated scaling beyond 56 cycles

Accelerated scaling from 56 to 112 freeze-thaw scaling is observed for the mix nos. 1, 2, 3, 4, 5, 6, 7, 8 (minor), 9, 11 (minor) and 12. This includes all the mixes investigated on this point, except for mix no. 10. It is difficult to attribute this to any particular property. Still, mix no. 10 (and no. 8) was made with 2 kg of superplasticizer only. If high amounts of superplasticizer are negative (see discussion in section 5.2.4) – without affecting the spacing factor – this might be attributed to changes of the capillary pore structure (not investigated).

The mix nos. 13 – 18 were not tested beyond 56 cycles. However, the mix nos. 13 & 14 exhibit acceleration from 28 to 56 cycles, mix nos. 15 – 18 not. The four latter mixes have higher water/binder-ratios. They also have less and partly other water reducing admixture combinations.

Not much is known about the reasons for such behaviour. Petersson [P 1986b] connects this "accelerating" phenomenon to dense concrete containing silica fume, which is not relevant here. However, the reasons for this behaviour in our present case remain unexplained but is clearly a negative property built into the acceptance criteria of SS 13 72 44. Fagerlund et al [F 1999b] reports breakdown of aged, self-desiccated high performance concrete subjected to long term water storage, but the time scale and exposure type is different from our case, the explanation probably also.

However, it is reasonable to believe that the moisture accumulation in the pore system with prolonged freeze-thaw "pumping" exposure is a central factor for the accelerated behaviour, see review in section 7. Considering the moisture values in section 5.4.4, the central issue for laboratory versus field performance becomes the method and extent of moisture exposure.

5.4.3 Field test

Visual inspection :

All mixes had none or only very little visible surface damages after two winters of field exposure. No cracks were reported.

UPV :

The UPV-values are not very accurate due to (lack of) resolution of the equipment and reproducibility in measuring [U 1999]. This means that values should change 2-4 % before being considered significant.

It remains somewhat suspicious that all the mix nos. 1-5 (and no. 14) have decreasing tendencies from the first to the end of the second winter (figure 5.3.13 & appendix E). Still, frost deterioration should result in much higher UPV loss, see section 4. The next couple of years will most probably settle the question, although some temporary "healing" of any possible damages may occur, as reported from laboratory tests conducted by Jacobsen [J 1995]. At present, the conclusion is that the observed UPV changes are not significant.

Volume changes

Change in sample volume may be due to swelling/shrinkage or deterioration mechanisms, e.g. internal cracking or surface scaling

Mix nos. 1-12 exhibit small volume increase during the first year (table in appendix E). This might be an indication of internal cracking. However, it does not correspond to the slightly negative UPV changes, taking place during the second winter, commented on above. During the second winter, the volume stays stable or decreases very slightly. The decrease is hardly due to surface damage. Hence, the former volume increase is most likely attributable to swelling during the first period, since the samples were rather dry at the time of placing at the field station.

Mix nos. 13-18 exhibit a slight volume decrease during the first winter, thereafter it remains stable. Since surface defects are close to zero, this indicates slight shrinkage, in spite of the weight increase mentioned below.

Weight changes

The weight changes from one winter to the next vary between the series, but are all in the range 0 – 10 % (at the very most) degree of capillary saturation.

Mix nos. 1-12 exhibit a slight weight loss during the first winter, then it increases again during the second period (appendix E). This is in contrast to swelling as an explanation of the volume increases above. It might indicate cracking as volume increase mechanism. However, low weight after the first winter might also be due to inadequate suction prior to weighing, i.e. the “saturated, surface dry”-condition (SSD) not being equally defined in the two cases. This may not necessarily be due to operator procedure, but may be caused by slower suction properties for the aged concrete.

Still, mix 13-18 exhibit slight weight increase during both periods of field exposure. This seems evident in all these cases, in spite of the slight volume decrease/shrinkage mentioned above. The values are so small that the weight increase may be less than (re-filling of) hydrated and physically bound water during the period.

- - -

In other series than mix nos. 1-18, with more or less pronounced damage [U 1999], the major part of these damages was localised at the bottom and lower parts of the samples. A possible implication is that the bottom of the samples is subjected to longer periods of suction. This results in a higher degree of saturation - and therefore scaling and cracking. The upper parts of the sample are more exposed to evaporation/drying and shrinkage.

Still, for the present mixes, it remains to be seen to what extent damages will occur. The preliminary field observations should not be over-interpreted.

5.4.4 Degree of capillary saturation

The figures 5.3.15 – 16 display the degree of capillary saturation of the top surface and the front (road facing) surface, respectively. The accuracy of the single measurements are probably in the range of 3-5 % (0.03-0.05 on the plot scale).

Compared to a few other mixes also tested [N 1999], the mix reported here (identical to mix no. 3, but one year younger) was in the lower range. However, mixes of equal w/c-ratio exhibited values at a similar level.

The most important result at this stage is probably the level of the degree of capillary saturation - and the profile of the sample : All values are at a level of 0.87 or below. Even more important may be that all the profiles appear to be at a "dry" or drying state. This is supported by Relling [R 1999] who found that the moisture condition even of bridge piers in Norwegian, coastal climate was not affected below a few cm from the surface. The "drying state" coincides with the weight loss attained for the companion mix during this (first) winter (appendix E). This leads to a concentration profile that increases from the surface inwards.

A possible implication is that a high degree of saturation in field service is not possible, unless the concrete is very permeable due to a high w/c-ratio or an open structure – or unless the surface is badly drained and covered with water for long periods. If this assumption is correct, internal cracking and/or scaling caused by high degree of saturation during long term laboratory testing is not representative for field service conditions. As mentioned earlier, there is some evidence that high strength concrete without air performs better in the field than in lab tests.

5.5 Conclusions

The initial laboratory investigation on concrete provided valuable characterisation and information on laboratory performance. This information will be central in future comparisons between laboratory and field performance.

Obviously, two years of field exposure is not enough to estimate the long term behaviour. The study is continuing long after present publication. At the present stage, the following findings and indications have been made :

Mix design / Air void system

- There seems to have been a considerable drop in total air content - from fresh to hardened state - for mixes with high amounts of superplasticizer.

- There are indications that other changes in air void characteristics from fresh to hardened state occur as well. Such changes may depend on fresh concrete properties (determined by mix design) – or be due to difference in testing principles :

Test method for air void characteristics

- The procedure of determining fresh concrete air void properties appears at least as capable of describing these properties as the ASTM C457 procedure. The specific surface relates more reasonably to the spacing factor for the fresh concrete procedure. However, certain test principles differ between the two test methods and may cause deviations in some cases :

- In some cases, the air void characteristics were improved from the fresh to the hardened state, in spite of drop in total air void content. This difference may be caused by characteristics of the test methods applied : The DBT method may underestimate the number of very small air voids. Still, the benefit of these very small voids is controversial.

Laboratory freeze-thaw testing / Mix design ranking :

- Only air-entrained concrete performed well in the laboratory test, even with w/c-ratio of 0.35. Overall, a mean (of fresh and hardened ...) spacing factor in the range of 0.4 or less appears vital to ensure good performance in the laboratory freeze-thaw scaling test procedure.

- The I-SR-LA and I-LA cements appears somewhat superior to the other cements (w/c-ratio 0.40 or 0.45). However, the others also performed well, especially with an appropriate air void structure. The fly ash cement exhibited somewhat higher scaling, probably disfavoured by the young age of testing.

- Silica fume (4 %) had no distinct effect with the II/A-V (FA) cement at w/(c+s) = 0.42, its scaling level being close to those of the 0.40 and 0.45 mixes with the same cement. This may also be a “maturity” phenomenon – not of the silica itself, but indirectly by affecting the reaction rate of fly ash.

- Silica fume (8 %) with the I-LA cement appears to be positive, but this may also be due to a simultaneous decrease of the spacing factor.

- High dosages of superplasticizer lead to structural defects in the form of bleeding pockets under aggregate particles and less homogeneous mortar/paste quality. This impaired the laboratory test results.

Field exposure :

- All mixes had none or only very small visible surface damages after two winters of field exposure. No cracks were evident. This applied whether the initial laboratory test of the specific mix design gave good results or not.

- The results of UPV, volume and weight measurements on the field samples were slightly mixed. However, this may be due to the very small magnitude of the changes. Their significance is therefore questionable, and more exposure time is needed : It still remains to be seen whether these differences represent (differences in) damage.

- The profile of the capillary degree of saturation exhibited values between 80 and 85 % and indicate a drying state for a mix identical to mix no. 3 (CEM II/A-V 42.5 R, w/c = 0.40, air-entrained). This was true at all times from the middle of February throughout April the same year – after less than one year of exposure. If higher values are not demonstrated in the future, this must be considered with respect to choice of the test conditions of the testing methods.

- Damages (of other series) were found at the bottom and lower parts of the samples. This implies that the lower parts are subjected to longer periods of suction and a higher degree of saturation. The upper parts of the sample are more exposed to evaporation/drying and shrinkage.

- In the future work, it will be valuable to include measurements of degree of saturation during late autumn and at the bottom of the samples.

URN:NBN:no-6354

6 Moisture uptake during curing : Chemical shrinkage and water absorption

6.1 Introduction

The objective of the study in this chapter is to provide information on moisture absorption during water curing, in the form of an estimate of the capillary degree of saturation near the top surface of the freeze-thaw test samples, prior to the freeze-thaw test. Such data were considered useful for the study in section 7.

The basic idea of this chapter thus becomes the monitoring of water absorption during wet curing. The wet curing ages considered are seven and 31 days. These curing ages are considered to represent the possible range in degree of saturation obtained in accordance with the curing regimes and start of testing given in the reference method of the draft freeze-thaw testing standard [S 2000].

The water absorption during curing will mainly be due to the suction provided by the water consumption of the hydration of cement. Measuring chemical shrinkage and combining it with water absorption of the mortar later subjected to freeze-thaw could be one way to try to cover the gap between “moisture mechanics” and freeze-thaw phenomena.

Geiker [G 1983] performed extensive studies on cement hydration, utilising chemical shrinkage measurements. Although linear correlation is said to exist between chemical shrinkage and degree of hydration, different specimen thickness exhibited some differences in “rate of reactivity”. The effect may be attributed to “incomplete water suction” and may be expressed as “critical thickness” [G 1983]. It was more pronounced at late ages. This “critical thickness” was found to decrease with the w/c-ratio. The latter became noticeable from about 20 hours of reaction. In both cases, the effect was confirmed by measuring non-evaporable water by ignition. (Incomplete suction resulted in reduced non-evaporable water.)

The present objective was to study a mortar of the same quality as used for later measurements during freeze-thaw testing. The material composition was chosen based on a minor study not further elucidated or referred to in this report. The aim was to design a mortar of close to optimal consistency for mixing and casting – without the use of water reducing admixtures. Such admixtures reduce the yield value of the fresh mortar [W 1990] and thereby slightly increase the risk of a less stable and homogeneous air void system. Depending on the admixture dosage, superplasticizers have been found to change the fresh "stability" properties, increasing bleeding or de-stabilising the air void structure [B 1997], a risk considered unnecessary in this study. A w/c-ratio of 0.48 was found to work well with an aggregate grading curve according to the specification in CEN 196 for standard mortar testing - and the other constituents. Further motivation for the selected properties can be found in section 7.

A study on chemical shrinkage of mortar was included by Justnes et al [J 1999]. They found somewhat higher long term water uptake by mortar, expressed as water uptake in ml per 100 g cement. However, the differences are so small that these authors do not claim that mortar behaves differently than pastes. In this context, it is important to see if the air voids take up water. Hence, in the present work both mortar (with and without air entrainment) and cement paste were included. The latter was meant as reference for the mortar test and for chemical shrinkage level data provided by literature.

Prior to the main series, it was considered appropriate to include a pilot study on sample size effects. This pilot study was performed on cement paste only, which is believed to be the critical material for such effects. At the same time, a careful examination of presumed critical factors in the experiments was carried out. The pilot study is reported in appendix I. Precautions and potential sources of error are discussed in section 6.2, the main series thereafter.

6.2 Potential errors of the chemical shrinkage test.

6.2.1 Testing method : General and objective

As stated in the introduction, it was considered important to consider certain aspects of the chemical shrinkage test prior to the execution of the main series :

For combined studies of chemical shrinkage and degree of saturation, a dilatometry technique for total chemical shrinkage was chosen. The principle of the method is to place the sample, immediately after mixing in a recipient and to fill the rest of the recipient with water. The recipient is plugged by a stopper that is penetrated by a water-filled pipette. Reading of the drop in the water level allows determination of the total (internal and external) volume change of the sample versus time. As mentioned above, the correlation between the degree of cement hydration, chemically bound water and chemical shrinkage is considered to be known for the mixes in question : Measuring the chemical shrinkage allows the calculation of the two remaining parameters. Subsequent saturation by pressure and drying at 105 °C yields the amount of evaporable water and the overall degree of saturation.

Justnes et al [J 1994] reviewed various tests for the determination of chemical shrinkage. They recommended Erlenmeyer flasks as recipient for this test method, also familiar to the present author [R 1992]. The advantage of this technique is that it provides a high surface-to-volume ratio of the cement paste. This will ease the suction of water, which again allows a higher sample mass than the “vertical cylinders” (small diameter, larger specimen height, water on the top surface) used by [G 1983]. Justnes et al [J 1994] refers to the Erlenmeyer flask principle as highly accurate, due to the very low between-sample variation. The main series to follow concerns mortar. Hence, the advantage of the larger samples possible with this recipient is believed to generally improve the accuracy. This concern was decisive for the choice of method in the following study.

6.2.2 Potential sources of error

6.2.2.1 Leaching

One objection to the Erlenmeyer flask principle could be leaching of ions into the recipient water. Dissolution of ions will increase the density of the water and influence the chemical shrinkage measurements. To avoid leaching, Geiker [G 1993] used only the water amount on top of the specimens expected to be absorbed. However, even with the Erlenmeyer flasks, the long term amount of leached ions is expected to be low, relatively to the total amount of chemical shrinkage [R 1996]. The problem is not of concern to Justnes [J 1994]. Also Boivin et al [B 1999b] used destilled water, even if (the very brief) test description in the same proceedings [T 1999] prescribes lime saturated water.

Pursuing the issue a bit further, the solubility of CaO in water under ambient conditions is about 20 mM per litre. Jennings [J 1986] reports a value of 1.17 g/l, which is of the same order. However, these figures assume saturated lime water. To estimate the actual calcium ion leaching, water samples from water storage tanks for concrete and mortar specimens was analysed. The water had remained in the tanks for two months, with frequent “addition” of fresh mortar and concrete specimens “ready for leaching”. The values obtained by atomic absorption ranged from 0.22 to 0.56 only, calculated as mg CaO per litre. The concentration was determined on the recipient water of a (spare) sample (in the present work) at the age of 24 hours. The value was obtained 2 cm above the sample surface, being 123 mg CaO per litre. The latter level is substantially higher than the values cited above, but still constitutes only 0.031 g (CaO in recipient) / 42 g (total CaO in sample), i.e. less than 0.1 % of the total CaO content. (100 g cement paste sample, 63 % CaO in the cement, 250 ml flask). Leaching will be considered insignificant in the present investigation, at least in the sense of mass loss of CaO influencing the amount of C-S-H formed.

Leaching of alkalis and sulphate might influence the amount of certain reaction products negatively – and thus the chemical shrinkage. Indirectly, it might influence the results by their effect on the rate of reaction. However with no solid argumentation on the issue available to the present author, the issue will not be further pursued in the present work.

6.2.2.2 External air

However, another factor concerning the recipient water might be of relevance. It might disturb the readings and thereby the results if air - external to the paste or mortar samples - is introduced into the system. According to handbooks [L 1961], the solubility of air at 20 °C is as much as 19 ml per 1000 ml water, i. e. almost 2 vol.-%. High amounts of dissolved air might theoretically disturb the readings of the pipette if it became unstable (due to temperature changes) and escaped from the recipient water. The use of distilled water is expected to reduce the possible influence of air [D 1995], but another measure is to boil the water.

6.2.2.3 Sample thickness

The paste thickness is not considered to influence the total shrinkage measurements in the initial phase, if kept within 1cm [J 1994]. However, the main series will contain correlation between cement paste and mortar. The latter shall have reference to specimens with a freeze-thaw testing start at the age of 31 days – to meet the pre-testing curing specification of concrete subjected to freeze-thaw according to [S 2000]. The objective is to estimate the capillary degree of saturation near the top surface of the freeze-thaw test samples, prior to the freeze-thaw test. Hence, when measuring chemical shrinkage in the main series for 31 days, it is important to consider the issue of specimen thickness carefully prior to the main study, since the literature is not very specific on the issue.

A pilot study on the possible effect of specimen thickness was chosen to clearify the issue but turned out to reveal other problems. The study is reported separately in the Appendix I. A clear thickness effect was cracking of the flasks ("aborted samples") due to swelling of the sample. Other revealed effects are included in the list of section 6.2.2, with reference to the pilot study.

6.2.2.4 Thermal effects

a) General

The previous section deals with some general measures that should be applied to ensure a smooth running of the experiment. In this section the effect of temperature variations of the water bath for sample storage is considered with respect to the reading of the pipette : The temperature of the water bath in the subsequent pilot study was controlled within 0.5 °C (20.8 – 21.3 °C). The thermal effects covered will be related to this temperature range. Temperature variation effects in this range on the reaction kinetics are neglected. The present issue will include possible temperature effects due to thermal expansion, see below. The temperature during the preceding study was checked with a digital indicator and a thermocouple, the complete system with accuracy of approximately 0.1 °C according to the certificate of calibration.

b) Volume control of the recipient water

$$\Delta V_w = \alpha_w \text{ x } \Delta T \text{ x } V_w \quad \text{(Eq. 6.2.1)}$$

where :

ΔV_w : potential thermal volume change of the recipient water
α_w : coefficient of volumetric thermal expansion of water, which at the test temperature of +20 °C is about $200 \times 10^{-6}\ C^{-1}$ [W 1973]
ΔT : potential temperature deviation from the starting point ; $< 0.5\ ^{o}C$
V_w : volume of water in the recipient ; approximately 300 ml

Using the formula with the figures given yields a potential deviation of 0.03 ml for the 0.5 °C change. This is slightly above the limit of the reading accuracy. The value may be of relevance when differentiating with respect to time [ml / 100 g cement x h] at a later stage, but not initially or with respect to the absolute level of chemical shrinkage. In the further evaluation of the test results, the effect is taken into consideration, adjusting the readings according to the recorded temperatures.

c) Volume control of cement paste

$$\Delta V_p = \alpha_p \times V_p \qquad \text{(Eq. 6.2.2)}$$

where :

ΔV_p : potential temperature induced volume change
V_p : volume of cement paste
α_p : coefficient of volumetric, thermal expansion of cement paste after setting, which may be estimated to 2×10^{-5} C^{-1} [H 1973] or 30×10^{-6} [B 1999d]

With a sample size of (at the maximum of ;) 100 ml, the potential contribution to the reading error is about 0.001 ml and may thus be neglected.

d) Volume control of air voids in the sample

$$\Delta V_a = V_a \times (T_1 - T_0) / T_0 \text{ (Pressure } p = \text{constant)} \quad \text{(Eq. 6.2.3)}$$

where:

ΔV_a : potential volume change due to temperature change
V_a : volume of air voids in the sample ; for calculation of potential effects, the value of 10 % (of sample volume) may be chosen, i.e. 10 ml of a 100 ml sample (approximately 200 g)
T_1 : end temperature [^oK]
T_0 : initial temperature [^oK]

The calculation according to the formula gives a potential error due to change of temperature of 0.01 ml, i.e. of the same magnitude as the reading accuracy of the pipette. In the subsequent work, the effect will be neglected.

e) Volume change of aggregate

This consideration is motivated by the succeeding mortar series. According to [H 1973], the coefficient of linear, thermal expansion of a granite aggregate may be estimated to 5×10^{-6} C^{-1}. The volumetric coefficient of thermal expansion may be calculated as $((1.000005)^3 – 1) = 15 \times 10^{-6}$. For a sample of 100 ml and 60 volume-% aggregate, a temperature deviation of 0.5 ^{o}C will theoretically change the reading of the pipette with less than 0.001 ml. The effect is neglected.

f) Volume control of the equipment

In order to make the estimation complete, a separate experiment was set up to check the thermal coefficient of the silicon stoppers. This was done by the buoyancy principle, compensating for the change of the density of water in the temperature range tested. The potential error is an order of magnitude less than that of the water and may be neglected. The same was evident for the Erlenmeyer flask itself.

6.2.2.5 Reading accuracy of the pipette

Pipettes of 5 ml were chosen in the preceding study for reading accuracy reasons. The nominal accuracy of the pipette was 0.1 ml, but with interpolation it was considered justified to make the reading with accuracy of +/- 0.01 ml. Hence, the error estimation (Gauss) between two readings is less than 0.02 ml.

6.2.2.6 Stopper sliding effect

Even with silicon stoppers there is a risk of sliding. Preventive measures include very basic procedure steps like proper cleaning and appropriate use of force when applying the stoppers to the flask.

The stoppers should be fixed to the Erlenmeyer flasks – or coated in such a way that sliding – and erroneous readings – can be revealed. In any case, it should be possible to reveal such failures by differentiating the shrinkage versus time curves in order to reject non-relevant test results, see Appendix I.

6.2.2.7 Settlement-temperature effects

The settlement process may involve certain shrinkage and swelling mechanisms. Also, immediate heat development during mixing may cause temperature rise of the fresh paste. It is essential to re-establish the temperature of the sample to that of the water storage tank, avoiding thermal expansion (contraction) effects during the first hours of measurements. This effect may be reduced by immediate placing of the samples in the flasks, filling (some of) the recipient water and storing it in water bath with a temperature identical to that of the storage tank. Further, it is usual to delay the initial measurement to avoid these effects.

6.2.2.8 Evaporation effect

Evaporation from the pipettes may cause serious misinterpretation. This was demonstrated in the pilot study (see Appendix I), although it was initially believed that it had been taken appropriately care of. A practical approach to control this is to record the weight of the samples at every reading of the pipettes. By weighing, erroneous readings due to evaporation can then easily be corrected for.

6.2.3 Conclusion

There are several potential errors that may lead to erroneous results of the chemical shrinkage test. However, if certain precautions are taken, it is possible to maintain test results of very high accuracy.

6.3 Chemical shrinkage and moisture condition of mortar and cement paste.

6.3.1 General and objectives

As outlined in section 6.1, it was decided to determine the degree of saturation of specimens of identical composition as in the series for determining freezing time dependent absorption. After the pilot study (Appendix I), it was decided to proceed with the chemical shrinkage test to investigate the correlation between cement paste and mortar. Precautions mentioned in section 6.2 were taken into account. Still, approximate sample sizes of 100 ml (200 g) were maintained.

With supplementary measurements on porosity and evaporable water, the following investigation was expected to provide data on the moisture conditions of the freeze-thaw specimens before starting the freezing or freeze-thaw test (subsequent section). The larger samples subjected to frost and freeze-thaw testing were not found to be suitable for estimating the moisture conditions (section 7).

The objective thus was to provide data on :

- Capillary degree of saturation,
- Degree of pore filling of macro pores,

both prior to frost or freeze-thaw testing. It included the effects of a) mortar versus cement paste and b) air entrainment.

6.3.2 Experimental outline

One cement paste, one mortar with and one mortar without entrained air were mixed and placed in Erlenmeyer flasks as described in the previous section. Four parallel 100 ml (200 g) specimens of each mix were made and subjected to chemical shrinkage measurements. Parallel samples of the same size were cast and cured for additional investigations : At the age of seven days, two specimens were removed for a) determination of chemically bound water by ignition, b) saturation under pressure, c) isolated curing until 31 days of age and d) structural analysis by thin section technique. At 31 days, non-evaporable water and water content after pressure saturation were determined.

Unfortunately, an attempt to determine non-evaporable water on samples with water curing until the age of 31 days failed. The test results were rejected due to non-consistency, probably caused by errors in the laboratory procedures.

6.3.3 Materials, mixing and casting

The materials composition is described in Table 6.3.1.

Although these are very close to the EN 196 standard mortars, the mixing procedure had to be adjusted due to the larger batches. The cement paste was initially mixed (equipment as specified by CEN 196) on the lower speed for 30 seconds. After the addition of aggregates, the mixing continued at this speed for another 90 seconds, then 60 seconds on speed level 2. The mix was then left to rest for two minutes. The AEA was added, and finally the batch was mixed at speed level 2 for 60 seconds.

The air reducing agent was added to the mix without air entrainment at the initial stage.

The pure cement paste batch was mixed for three minutes at speed level 1, interrupted twice for removing settled material at the bottom and sides. After two minutes of rest, it was finally mixed for two minutes at speed level 2.

	Mortar with air	Mortar “No air”	Cement Paste
Cement CEM I 42,5 R [g]	900	900	900
Water (distilled) [g]	432	432	432
w/c-ratio	0.48	0.48	0.48
Air content (by pressure) [%]	13	3	-
Air entraining agent [g]	3.5	-	-
Air damping/reducing agent [g]	-	0.9	-
Sand according to EN 196 [g]	2700	2700	-
Paste, exclusive air [Vol.-%]	36	40	100
Paste [Weight-%]	33	33	100

Table 6.3.1 : Mix proportions for cement paste and mortars used for determining chemical shrinkage. The cement was identical to the one used in the pilot study (See Appendix I), containing 4 % lime stone filler. The air entraining agent was a tall oil derivative from Scancem Chemicals with trademark L14 F. The air damper of same origin contained 60-100 % white spirit.

Eight samples for each of the two mortars were cast in Erlenmeyer flasks through a funnel. Sample sizes for the mortars were 200 g (+/- 5g) / 115 ml / 22 mm thickness. Four in each series were subjected to chemical shrinkage measurements. The remaining four samples (without pipettes) were stored under the same conditions.

For the cement paste, nine samples were cast, partly to repeat the study on size dependence : Six of the samples were of the size 160 g (+/- 2 g) / 86 ml / 17 mm thickness. The remaining three samples weighed 45, 112 and 239 g.

At every reading of the pipettes, simultaneous determination of the sample weight (sample + flask + recipient water +++) was performed with an electronic balance. It should be noted that the calibration of the balance with a weight equal to the samples was done at every term.

It was found that a weight loss occurred, in spite of the evaporation shield. There was no doubt that the evaporation was large enough to cause the confusion illustrated in the pilot study (Appendix I). The readings of the pipettes and the weights were logged in a spreadsheet, whereby the readings were corrected for the weight loss.

In contrast to the pilot study, the temperature of the water storage container fluctuated within 1.2 ^oC. Correction of every reading was automatically calculated in the spreadsheet, according to the thermal expansion of the recipient water.

6.3.4 Effect of composition : Test results and discussion

The chemical shrinkage of the mortars during the first 24 hours is given in figure 6.3.1, as mean values for the four specimens within each series. More detailed information can be found in appendix C.

At the age of 24 hours, the scatter within each series is small enough to assert significant differences : With 3 % air, the standard deviation at this point is 0.09 ml (4 % of the absolute level). For the 13 % mortar and the cement paste, the figures are 0.05 ml (2 %) and 0.17 ml (9 %), respectively.

The two mortars exhibited identical behaviour after the initial two hours. There appears to be a distinct difference between the mortars on one side and the cement paste on the other. The differences are easier to distinguish in the differentiated curves in figure 6.3.2. The air entrained mortar exhibited a volume increase during the first two hours, after which the activity level of the two mortars became rather equal. An immediate theory for explaining the difference between the two mortars was the thermal expansion of the extra air voids during the pre-setting period. Application of the gas equation ($pV/T = const.$) and assuming constant pressure, estimates the necessary temperature increase to be 12-13 ^oC. A specific test on this question displayed a maximum temperature difference between the middle of the sample and the surrounding water of 2 ^oC only, occurring at the age of twelve hours. Hence, the early age expansion of the air entrained mortar must be due to other reasons.

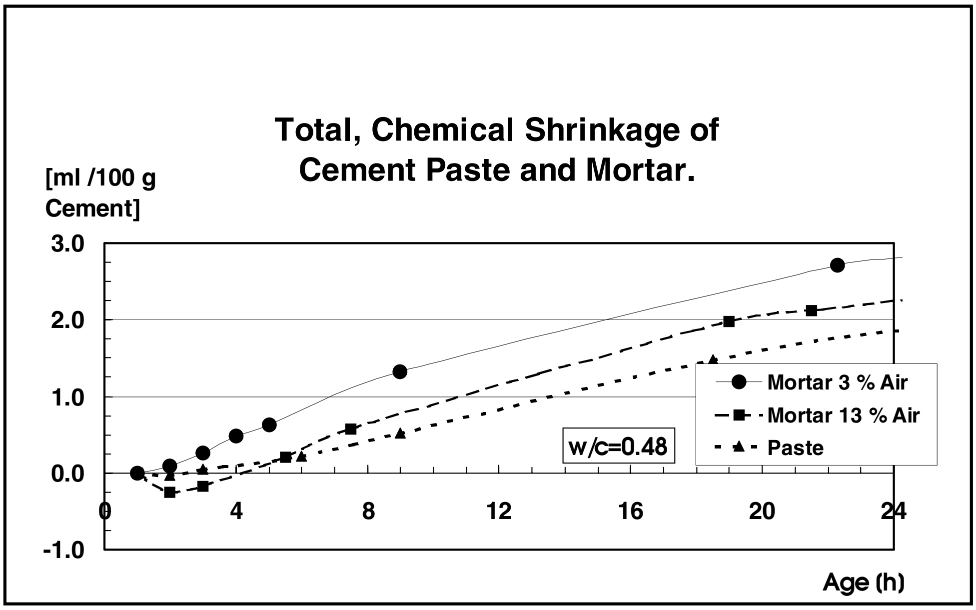

Figure 6.3.1 : Chemical shrinkage of cement paste and mortar of equal w/c-ratio 0.48 during the first 24 hours, calculated per 100 g cement.

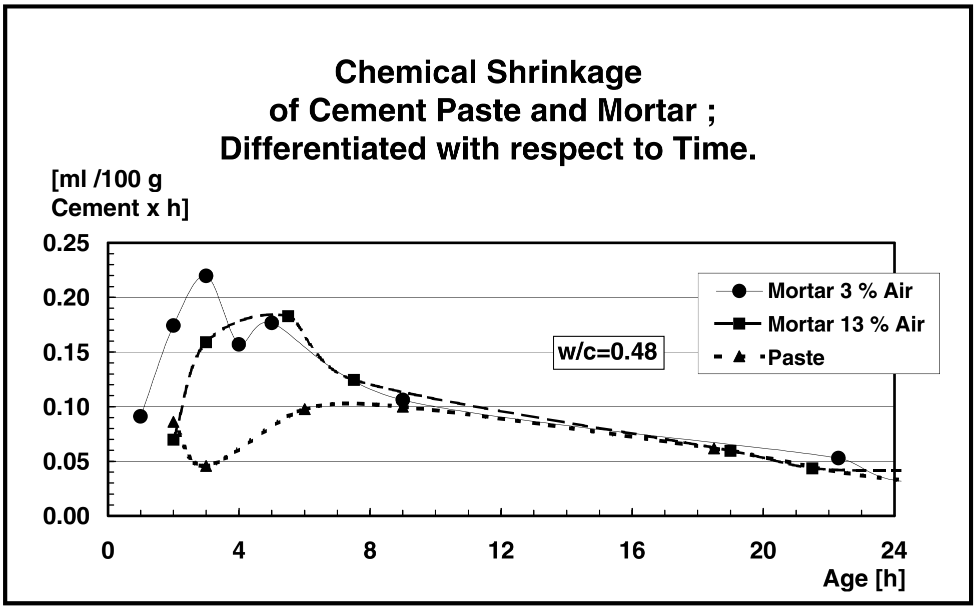

Figure 6.3.2 : Differentiation of figure 6.3.1 with respect to time.

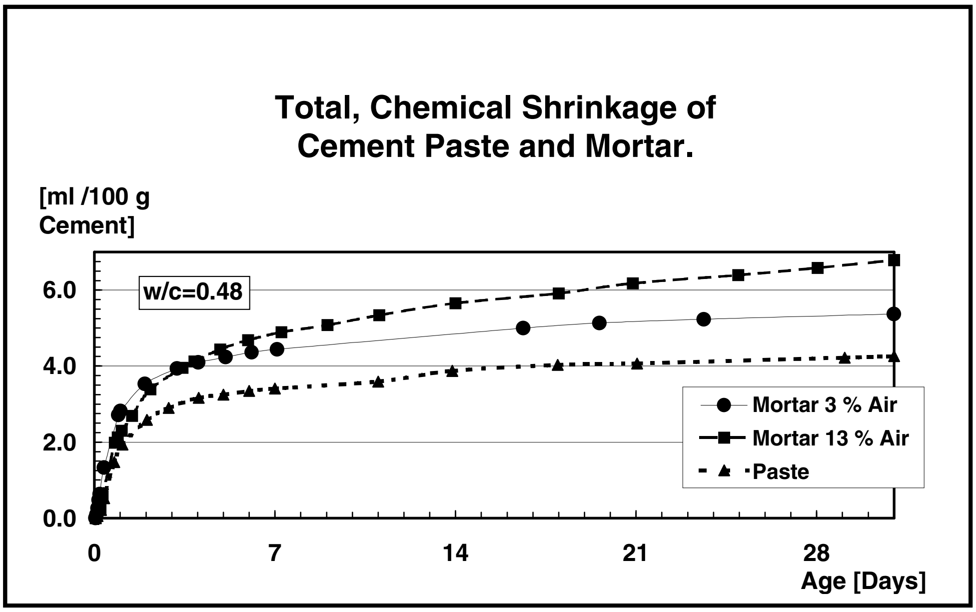

Figure 6.3.3 :Development of chemical shrinkage for the entire testing period of 31 days.

The cement paste did not catch up with the mortars in intensity (differentiated value) until 8-10 hours after water addition. Surface effects (catalyst) sand may cause the faster reaction of the mortar, but this remains speculation. The cement paste never caught up with the accumulated values of the mortars. At two days and later, there appeared to remain a more or less constant difference between the cement paste and the non-air-entrained mortar, i.e. same rate of hydration.

At three days, the air-entrained mortar takes a lead on the non-air-entrained one (figure 6.3.3). The difference increases throughout the remaining testing period ; at the end, the difference is 1.4 ml per 100 g cement between the two. The cement paste “lacks” another 1.1 ml per 100 g cement at this stage.

The difference in water consumption may be compared directly to the “unit volume” of samples containing 100 g cement. Assuming the degree of hydration to be identical for the cement paste and the mortars, the “excess water” would have to be accommodated in the air voids. This excess water amounts to 0.6 – 1.1 % of the corresponding unit sample volume, see table 6.3.2 – i.e. not unreasonable amounts.

	Mortar 13 % Air	Mortar 3 % Air	Cement Paste [1)]
Cement [g] ($\rho = 3.12$ kg/dm^3)	100	100	100
Water [g]	48	48	48
Aggregate [g] ($\rho = 2.65$ kg/dm^3)	300	300	-
Total weight [g]	448	448	148
Total "unit volume" [ml]	222	199	80
Calculations :			
• 1.1 ml related to the non-air-entrained mortar volume [Vol.-%]	-	0.6	-
• 1.4 ml related to the air-entrained mortar volume [Vol.-%]	0.6	-	-
• 2.5 ml related to the air-entrained mortar volume [Vol.-%]	1.1	-	-
• "Air volume replaced by water" for a 200 g mortar sample [ml]	1.1	0.5	-

Table 6.3.2 : Calculations on the differences in chemical shrinkage, related to the sample volume. The calculations are based on the assumption of identical degree of hydration. The latter is subject to further investigation. [1)]Air volume 0% determined by thin section analyses.

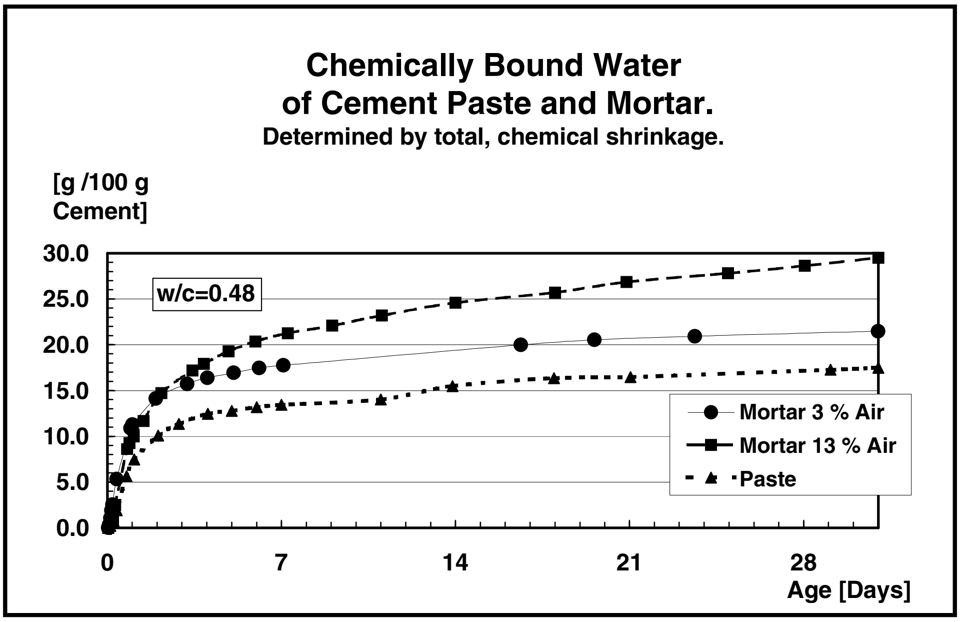

Figure 6.3.5 : Plotting of the calculated, non-evaporable water content, based on the chemical shrinkage measurements in figure 6.3.3 and according to the same principle as applied in the pilot study (Appendix I), see text.

As in Appendix I, the results of the chemical shrinkage ε_c have been re-calculated and expressed as non-evaporable water w_n. This was done according to equation AI-1 of that appendix ($w_n = \varepsilon_c/0.254$). The reason for presenting the test results as non-evaporable water, is the subsequent comparison with loss on ignition values. These data are presented in figure 6.3.5. It is obvious that at least the air entrained mortar exhibits “chemically bound water” in excess of any realistic value. The reason for the obtained values are further investigated in the following section. The cement paste exhibit reasonable results.

6.3.5 Supplementary investigations : Procedure and test results

6.3.5.1 General

The objective of these supplementary studies was to verify the former results and to draw conclusions concerning moisture content prior to freeze-thaw exposure. The investigations comprised the determination of evaporable and non-evaporable water content, initial water content versus drying and re-saturation by pressure, as well as structural analyses by thin section technique.

6.3.5.2 Structural analyses

An abstract of the investigation, reported in [B 1999c] : The samples were cut, carefully dried and impregnated with an epoxy containing a fluorescent dye prior to grinding of the surface.

The cement paste contained close to zero air. A 0.3 mm layer close to the surface had somewhat higher porosity. Some non-dispersed cement particles were identified. One crack parallel to and a few cracks perpendicular to the surface were evident. These cracks probably were introduced during the preparation procedure. Still, a “T-formed” pattern of higher porosity was identified, the “vertical leg of the T” being perpendicular to the top surface. This might be a former crack subjected to “healing” as reported by Jacobsen [J 1995], i.e. partly repaired by continued hydration.

The mortar with 3 % air (fresh air content) exhibited a mean air void content of 1.6 %, determined by point count. Different segments varied from 0.9 % (at the surface), via 1.5 % and 2.3 % to 1.5 % (at the very bottom). No signs of cracks or bleeding were visible.

The mortar with 13 % air (fresh air content) exhibited a mean air void content of 10.2 %, determined by point count. Different segments varied from 8.0 % (at the surface), via 11.8 % and 10.0 % to 11.0 % (at the very bottom). No cracks were visible within the investigated area. No signs of bleeding were found, but the capillary porosity often appeared a little higher close to the air voids.

6.3.5.3 Non-evaporable water

The Erlenmeyer flasks were carefully broken and removed from the very smooth and moist sample surface by a knife. Thereafter, the samples were cut in two halves. One of these halves from each series were dried with a towel and crushed and then further crushed in a mortar while immersed in ethanol (qualitative description : until the fineness of a filler).

The powder was left in the ethanol for half an hour, then decanted and centrifuged before new addition of ethanol and stirring. It was then left for an hour for liquid replacement of water and termination of further hydration. Finally, it was centrifuged again and placed in a desiccator at 60 ^{o}C for three days, with ascarite (suggested by Kjellsen [K 1990]). The purpose of the latter was to prevent carbonation. The drying at 60 ^{o}C was to ensure evaporation of the (flammable) ethanol prior to the heating procedure to follow.

The samples were then dried at 105 ^{o}C until constant weight and cooled again in a desiccator. After cooling to ambient temperature, samples were taken for the ignition test. The ignition procedure was performed on cement paste and mortar samples after seven and 31 days of water curing (chemical shrinkage). It was also performed on samples that had been water cured for seven days and then wrapped in separate plastic bags until the age of 31 days. Additionally, ignition measurements were performed on the mortar constituents for reference, i.e. the cement and the aggregate. Based on these data, the degree of hydration was calculated from an equation deduced by Bellander :

$$\frac{W_n}{C} = \frac{w_{105} - w_{1000} - x \cdot g(1+g)^{-1} - y \cdot w_{105}(1+g)^{-1}}{w_{1000} - w_{105} \cdot g(1+g)^{-1} + x \cdot w_{105} \cdot g(1+g)^{-1}} \qquad \text{(Eq. 6.3.1)}$$

where :

W_n : Non-evaporable water
C : Cement content
w_{105} : Sample weight after drying at 105 ^{o}C, prior to ignition
w_{1000} : Weight of ignited sample
x : Ignition loss of the aggregate (actual aggregate : 0.45 %)
y : Ignition loss of non-hydrated cement (2.51 % (4 % filler))
g : Aggregate/cement weight ratio

The degree of hydration is calculated according to (see Eq. AI-2, Appendix I) :

$$\alpha = \frac{W_n}{0.23C} \quad \text{(Eq. 6.3.2)}$$

The test results are given in table 6.3.3. These values are slightly lower than those displayed in figure 6.3.5 for the cement paste (17.5 g/100 g) and the non-air entrained mortar (21.6 g/100 g). The air-entrained mortar exhibits a 10 g higher value (29.5 g/100 g) in figure 6.3.5. The issue will be covered in the discussion in the subsequent sections.

Sample	Loss on ignition [% of weight at 105 °C]	Non-evaporable water W_n per 100 g cement [ml]	Degree of hydration [%]
Water cured 7 days :			
Cement paste	13.36	12.5	54.4
Mortar 3 % air	4.38	16.3	70.9
Mortar 13 % air	4,57	17.4	75.5
Water cured 7 days, then plastic bag until 31 days :			
Cement paste	16.23	16.4	71.2
Mortar 3 % air	4.86	19.0	82.7
Mortar 13 % air	4.87	19.1	83.0
Cement (Non-hydrated)	2.51	-	-
Sand aggregate	0.45	-	-

Table 6.3.3 : Loss on ignition, non-evaporable water and degree of hydration after 7 and 31 days according to the equations 6.3.1 - 2.

6.3.5.4 Moisture content and porosity

As already mentioned, at 7 days, 7 + 24 (= 31) days and 31 days, samples were removed from the chemical shrinkage test (or the plastic bag) and subjected to various investigations.

Procedure A (Extended “PF-procedure”) :

One sample from each series was cut vertically in two halves. One of the half-samples was subjected to porosity measurements according to the following this procedure :

After weighing, they were saturated at a pressure of 50 bar for seven days and weighed again, then subjected to drying at 105 ^{o}C for another seven days. (The seven-day saturation is relatively long. However, it had been found on mortar samples of Ø100 x 50 mm^3 that water intrusion was still taking place between 24 and 48 hours.) After 105 ^{o}C, suction in submerged condition was monitored every 30 minutes until “constant” weight for four hours, and another saturation at 50 bar for seven days followed. The suction procedure was shorter than suggested by Sellevold [S 1986] for the PF-method, which may have produced too low suction weights – see later. Finally, the specimens were weighed under water. The computed data comprised several parameters, e.g. degree of saturation, amount of “macro pores” and fraction of macro pores water filled at test termination. Detailed information on these samples is available in the appendix D, pp 2-4.

Procedure B (Pressure saturation plus drying) :

After termination of water curing at the age of 31 days, two samples from each series were subjected to seven days of saturation at the pressure of 50 bar. Subsequently, they were crushed and dried at 105 ^{o}C for 24 hours. This was done to acquire data on the moisture content after saturation by pressure – without a slow drying process enabling further hydration. Air content prior to saturation by pressure was calculated, as well as the total porosity. The suction porosity could not be attained from this procedure. Detailed information on these samples is available in the appendix D, pp 5, 7 and 9.

Procedure C (Direct drying) :

Finally, some samples were subjected directly to crushing and drying after termination of water curing at the age of 31 days. This enabled the immediate computation of moisture content without the seven days pressure period. Information on suction porosity or pore filling of macro pores could not be attained in this procedure. Detailed information on these samples is available in the appendix D, pp 6, 8 and 10.

6.3.6 Discussion of supplementary investigations

6.3.6.1 General

The discussion of the moisture data first follows, based on the direct data output values. This discussion comprises the sections 6.3.6.2-4.

Secondly, the data are re-calculated (section 6.3.6.5) on the basis of :

- an apparent irreversible porosity effect upon drying and
- adjustments because of too short suction periods prior to the second phase of saturation by pressure (procedure A).

6.3.6.2 Moisture content and porosity

Procedure A : Results and discussion :

Since some of the results may look unreasonable, some general comments on the procedure are appropriate : I) Prior to the "launching" of a sample, it was always carefully examined. To prevent potentially loose particles from disturbing the results, sharp edges were removed by a wire brush. II) Wiping off wet samples prior to weighing was always done in the same manner : With a towel (cloth, not paper), the sample surface was left moist, i.e. neither surface dry nor with any free water. III) The weighing after saturation by pressure has to proceed immediately after relieving the pressure. (Step II is not directly comparable to "SSD" – saturated, surface dry – since the surface was still moist.)

Already after 15 minutes, weight reductions due to expelled water will influence the measurements negatively. This is due to the de-compression of the remaining air in the samples. The phenomenon is clearly visible as "sweating" on the wiped-off surface.

At first sight, the moisture data presented in table 6.3.4 are quite difficult to interpret. Systematisation must include the effect of the different testing regimes for obtaining the ("same") parameters. The first approach comprises the time and curing dependency on the pore filling, i.e. the data included in appendix D, pp 2-4.

	Cement paste			Mortar 3 % air			Mortar 13 % air		
Length of curing [Days]	7	7+24	31	7	7+24	31	7	7+24	31
Macro pores [Vol.-%]	2.5	1.5	2.0	3.1	2.7	2.8	10.5	10.2	11.5
Initial moisture [Weight-%]	28.9	28.6	29.0	9.0	9.1	8.3	9.1	8.8	8.9
Init. Non-filled pores [Vol.-%]	-0.2	-0.2	-0.4	1.7	1.6	1.5	10.3	9.2	8.4
W.-filled macro pores [Vol.-%]	2.7	1.8	2.4	1.3	1.0	1.3	0.2	1.0	3.1

Table 6.3.4 : Extract of data from appendix D, pp 2-4, on moisture content. See text for description of the test procedure. Curing 7 days implies seven days of curing (chemical shrinkage) under water and then weight determination. Curing 7 + 24 implies seven days of water curing, then 24 days in plastic bag and finally weight determination. Curing 31 implies water curing for 31 days and weight determination. "Macro pores" are calculated as total porosity (by 2nd pressure saturation) minus suction porosity (after 1rst drying). They comprise air voids and other cavities. "Init. non-filled pores" means weight increase at 1rst pressure. "W.-filled macro pores" is based on initial water content and "Macro pores"(after 2nd drying), but is corrected for change in available porosity between 1rst and 2nd drying.

The cement paste values are disturbed by the fact that they actually lost a little weight on saturation by pressure. The effect was systematic and may be due to various reasons. One potential reason is the loss of minor particles, another temperature effects. (Increasing temperature will create a moisture flow from the gel to the coarser pore structure [H 1961]. However, the effect was tested by the present author on identical samples in the range of 5 – 20 °C. Within a temperature range of 5 °C, the effect may account for no more than 0.02 g per sample.) Another possible explanation is leaching from these small samples into the 50 litres of recipient water in the pressure chamber. A parallel experiment was performed by Kjellsen [K 2000], exchanging the tap water with lime "saturated" water. The results indicated the phenomenon to be a leaching effect.

These are very small values. Nevertheless, it probably implies a slight underestimate of the water uptake under pressure in the range of 0.2 – 0.4 volume-%. When considering the moisture content (in weight- or volume-%) prior to saturation, the pattern is somewhat confusing. There appears to be a lack of consistency between the individual series. This is probably due to the slight deviations in macro porosity of the individual samples within each series. The parameters "initially non-filled pores" and "water-filled, macro pores" partly neutralise these effects :

Considering the cement paste, the macro pore volume as well as the initial pore filling appears high. Thin section analyses confirmed an air pore volume close to zero. Extensive cracking due to the drying procedure may have occurred – prior to the determination of the suction porosity and finally, total porosity. However, such cracking would hardly exceed 0.5 vol.-%. A possible reason of the high amount of “macro pores” in these samples is a change of the nature of (a part of) the capillary pore system. The initial drying may have reduced the relative amount of pores able to become saturated upon repeated, capillary suction. Such effects might be due to “ink-bottle-effects” or change in amount of discontinuity of pores. This is a normal irreversibility effect after drying of “virgin samples”.

Removed from water storage at the age of seven days and then cured in plastic bag until the age of 31 days (sub-column no. 2 for each sample in table 6.3.4), the cement paste still exhibited a complete filling of the macro pores. However, the reduced pore filling value for plastic curing has to be compared to the lower macro pore volume for this particular sample.

The mortar with 3 % air exhibited some filling of the macro pores at seven days. This level was more or less maintained for the water-plus-plastic curing or 31 days water storage. The values calculated indicate a pore filling slightly less than 50 % of the macro pores, maybe a little less during the plastic bag curing. The implication is no more water uptake during the 31 days water storage than to compensate for the increase of non-evaporable water.

The mortar with 13 % air had a slightly lower moisture content when subjected to seven days water + 24 days plastic bag curing. Still, its pore filling was somewhat higher than just after seven days water curing (companion sample). Both of these samples had a low number of macro pores compared to the initial air content. If these low values were due to incomplete saturation under pressure (i.e. late weighing after start of expelling of water), more correct values of the latter would still not change the former ones. After 31 days of water curing, the pore filling of macro pores was increased to 3 %. This indicates a higher pore filling during water storage beyond seven days. This again implies higher water suction for this mortar quality than the increase in non-evaporable water.

Procedure A versus B : Results and discussion :

The seven days drying procedure produced a weight loss of 8.9 %, the intermediate water storage and crushing 7.6 % only. It is difficult to believe that the intermediate water storage for pressure relief would enable water suction - in the former case – to the extent of the difference between these two values. A possible contribution remains between-sample differences in porosity, but the issue remains unanswered.

Calculation of initially non-filled pores [Vol.-%]	Cement paste	Mortar 3 % air	Mortar 13 % air
• Subjected to seven days of drying directly after saturation by pressure ; single sample [Vol.-%]	-0.4	1.5	8.4
• Subjected to drying after saturation and intermediate water storage for pressure stabilisation. Sample crushing for fast attainment of dry weight ; two sample values [Vol.-%]	-0.2	1.5-1.6	7.4-7.5

Table 6.3.5 : Calculation of initially (i.e. after 31 days of water curing) non-filled pores according to slightly different procedures (See text).

With the mortar of 3 % air, the two different procedures provided equal results. Indirectly, this supports an assumption of between-sample variation of the other mortar quality. For the cement paste, the difference may be due to further leaching during the intermediate water storage.

Procedure A, B and C : Results and discussion :

Calculation of initial moisture content – as weight loss after drying at 105 ^{o}C	Cement paste	Mortar 3 % air	Mortar 13 % air
• Subjected to seven days of drying directly after saturation by pressure ; single sample [W-%]	29.0	8.3	8.9
• Subjected to drying after saturation and intermediate water storage for pressure stabilisation. Sample crushing for fast attainment of dry weight ; two sample values [W-%]	23.3 23.6	7.5 7.5	7.7 7.5
• Subjected to crushing and drying immediately after termination of water storage ; two (three) sample values [W-%]	23.5 24.4 24.8	7.7 8.0	8.4 8.8

Table 6.3.6 : Calculation of weight loss, based on initial (i.e. after 31 days of water curing) evaporable water content, according to the different procedures (See text).

There appears to be larger differences within the single series than between them (3 % air versus 13 % air). Especially when considering the cement paste data, the data seem meaningless as such for characterising purposes.

Summary on the issue :

There are indications that parts of the air void system is filled with water already at seven days of continuously (from before the time of setting) water curing. Only in the case of the 13 % air mortar, there is an indication of increased pore filling from seven to 31 days of continuously wet curing.

There is a slight change in available porosity after drying at 105 °C. The pore space available to saturation by pressure at 50 bar was slightly reduced in all cases but one. This is in accordance with Sellevold [S 1986], who reported both positive and negative - but in all cases – minor changes. It is believed that the drying period was sufficient to compensate for the different diffusion permeability of the series.

Concerning the procedure of attaining the moisture data, it appears preferable to include the step of determining the suction and total porosity of the individual samples. Alternatively, a higher number of parallel samples might be used enabling statistically improved data. The individual weight loss data seem to be of little direct use, since the simultaneous (macro pore) porosity has to be considered. The parameter “non-filled pores” may be useful. However, the most relevant parameter appears to be the “filled macro pores”, even if it involves more complex boundary conditions with respect to the moisture history.

6.3.6.3 Non-evaporable versus evaporable water

Before closing the issue of moisture content and porosity, an attempt should be made to compare the obtained values of non-evaporable and evaporable water content. Since data for non-evaporable water at 31 days of water storage are missing, the comparison will be limited to the a) seven days water curing and b) seven days in water + 24 days in plastic. See tables 6.3.7&8 for calculations.

For both mortar qualities, the measured evaporable water is slightly higher than the values computed as the difference between total water and loss on ignition (non-evaporable water). The difference between the two ways of calculation appears somewhat lower at seven days than at 31days (7 + 24), which remains unexplained.

The aggregate had been subjected to thermograviometric analyses (additionally to the ignition loss, section 6.3.5.3). From these measurements, it was concluded that moisture loss from the aggregate could be responsible for no more than 0.1 g weight loss (after drying at 105 °C) per 100 g cement, i.e. less than 0.05 weight-% for the unit mix above.

Calculations per 100 g cement	Cement paste	Mortar 3 % air	Mortar 13 % air
Total water content			
• Initial mixing water per 100 g Cement [g]	48.0	48.0	48.0
• Absorbed by chemical shrinkage from figure 6.3.3 and appendix C [ml]	3.4	4.4	4.9
• (1) Total water content [g]	51.4	52.4	52.9
Calculation of evaporable water			
• (2) Non-evaporable water from table 6.3.3 [g]	12.5	16.3	17.4
• (3) Evaporable water = Total water content - non-evaporable ~ (1)-(2) [g], [ml]	38.9	36.1	35.5
Calculation of dry unity weight			
• Cement [g]	100.0	100.0	100.0
• Water [g]	12.5	16.3	17.4
• Aggregate [g]	0.0	300.0	300.0
• (4) Total weight [g]	112.5	416.3	417.4
Calculation of dry unity volume (=initial)			
• Cement ($\rho = 3.12$)	32.0	32.0	32.0
• Water ($\rho = 1.0$)	48.0	48.0	48.0
• Aggregate ($\rho = 2.65$)	0.0	113.2	113.2
• Air content[1)] [Vol.-%]	0.0	3.0	13.0
• (5) Total volume [ml]	80.0	199.2	222.1
Calculated evaporable water content			
• Of dry weight (3)/(4) [W-%]	**34.6**	**8.7**	**8.5**
• Of volume (3)/(5) [Vol.-%]	**48.6**	**18.1**	**16.0**
Evaporable water from table 6.3.4 & appendix D (measured)			
• Of dry weight [W-%]	**28.9**	**9.0**	**9.1**
• Of volume [Vol.-%]	**44.5**	**19.0**	**17.4**

Table 6.3.7 : Calculation of evaporable water, based on initial composition and measured non-evaporable water at the age of seven days (water curing). Comparison with evaporable water content determined by drying. [1)]Nominal air content is used for reference ; the error is of second order.

Calculations per 100 g cement	Cement paste	Mortar 3 % air	Mortar 13 % air
Total water content			
• Initial mixing water per 100 g Cement [g]	48.0	48.0	48.0
• Absorbed by chemical shrinkage from figure 6.3.3 and appendix C (7 days) [ml]	3.4	4.4	4.9
• (1) Total water content [g]	51.4	52.4	52.9
Calculation of evaporable water			
• (2) Non-evaporable water from table 6.3.3 [g]	16.4	19.0	19.1
• (3) Evaporable water = Total water content - non-evaporable ~ (1)-(2) [g], [ml]	35.0	33.4	33.8
Calculation of dry unity weight			
• Cement [g]	100.0	100.0	100.0
• Water [g]	16.4	19.0	19.1
• Aggregate [g]	0.0	300.0	300.0
• (4) Total weight [g]	116.4	419.0	419.1
Calculation of dry unity volume (=initial)			
• Cement ($\rho = 3.12$)	32.0	32.0	32.0
• Water ($\rho = 1.0$)	48.0	48.0	48.0
• Aggregate ($\rho = 2.65$)	0.0	113.2	113.2
• Air content[1)] [Vol.-%]	0.0	3.0	13.0
• (5) Total volume [ml]	80.0	199.2	222.1
Calculated evaporable water content			
• Of dry weight (3)/(4) [W-%]	**30.1**	**8.0**	**8.1**
• Of volume (3)/(5) [Vol.-%]	**43.8**	**16.8**	**15.0**
Evaporable water from table 6.3.4 & appendix D (measured)			
• Of dry weight [W-%]	**28.6**	**9.1**	**8.8**
• Of volume [Vol.-%]	**44.1**	**19.2**	**16.9**

Table 6.3.8 : Calculation of evaporable water, based on initial composition and measured non-evaporable water at the age of 31 days (seven days water curing + 24 days in plastic bag). Comparison with evaporable water content determined by drying. 1)Nominal air content is used for reference ; the error is of second order.

For the cement paste, the different values on evaporable water obtained differ substantially, especially for the youngest samples. Additionally, the directly measuring procedure provides the lower value. This is in contrast with the mortar measurements. As an isolated effect, this could mean that the drying period at 105 ^{o}C was not sufficient for the cement paste, due to its higher diffusion resistance compared to that of the mortars. However, the seven days drying procedure (subsequent to 31 days of water storage) exhibited higher weight loss than that of crushing prior to drying (table 6.3.6). Hence, an error may have occurred in the measurements.

The figures above allow the calculation of another feature. From the determination of the non-evaporable water, the "true" chemical shrinkage can be calculated. Comparing these values with the values obtained by direct measurements provides information on "excess water absorption". This feature is displayed in the tables 6.3.9-10. For the seven days water stored samples, it seems evident that there exists such an excess absorption. This absorption was larger for the mortars than for the cement paste and increased with the air content. It confirms the pattern displayed in figure 6.3.3. It appears evident that the chemical shrinkage is larger for mortar than for cement paste. It also appears that this is due to both increased hydration and to additional absorption. Finally, the latter appears to increase with the air content.

However, such calculation on the samples subjected to plastic curing subsequent to the water storage will not make sense (table 6.3.10). The chemical shrinkage prior to the isolated storage condition will not provide data on the subsequent hydration. The following, chemical shrinkage "forces" will promote the suction of air only, the volume of which remains undetermined.

Calculations per 100 g cement	Cement paste	Mortar 3 % air	Mortar 13 % air
Absorbed by chemical shrinkage from figure 6.3.3 and appendix C (7 days) [ml]	3.4	4.4	4.9
Chemical shrinkage due to hydration			
• Non-evaporable water from table 6.3.3 [g]	12.5	16.3	17.4
• Chemical shrinkage of non-evaporable water (0.254 x W_n) [ml]	3.2	4.1	4.4
Measured shrinkage minus calculated shrinkage [ml]	0.2	0.3	0.5

Table 6.3.9 : Calculation of chemical shrinkage from the determined non-evaporable water and comparing with measured chemical shrinkage. Age seven days (water storage).

6.3.6.4 Degree of saturation

The values for the degree of saturation at the age of 31 days from appendix D are compiled in table 6.3.11. This parameter is not much influenced by the choice of procedure. As previously mentioned, the values above 100 are due to the calculation procedure and weight loss during saturation by pressure and, thus, artificial.

Calculations per 100 g cement	Cement paste	Mortar 3 % air	Mortar 13 % air
Absorbed by chemical shrinkage from figure 6.3.3 and appendix C (7 days) [ml]	3.4	4.4	4.9
Chemical shrinkage due to hydration			
• Non-evaporable water from table 6.3.3 [g]	16.4	19.0	19.1
• Chemical shrinkage of non-evaporable water (0.254 x W_n) [ml]	4.2	4.8	4.9
Measured shrinkage minus calculated shrinkage [ml]	-0.8	-0.4	0.0

Table 6.3.10 : Calculation of chemical shrinkage from the determined non-evaporable water and comparing with measured chemical shrinkage. Age 31 days (7 days in water + 24 days in plastic bag).

Curing condition All values in [%]	Cement paste	Mortar 3 % air	Mortar 13 % air
Seven days in water + 24 days in plastic bag	100.5	92.1	64.8
31 days in water :			
• Obtained by procedure a)	100.9	92.1	66.8
• Obtained by procedure b)	100.5	91.4	67.1

Table 6.3.11 : Degree of saturation at the age of 31 days for the cement paste and the two mortars, with or without air entrainment.

6.3.6.5 Re-calculation of moisture data

As already commented, there is an irreversible effect on the total porosity on drying. This means that the initial value possibly should be re-calculated before comparison with the later determined suction porosity – in order to calculate the initial degree of capillary saturation. For the cement paste, this effect is per definition the difference between the first and the second saturation.

Secondly, the suction procedure may appear very short, even if the weight appeared stable already after four hours. This means that the "suction weight" might be more correct being somewhat increased prior to comparison with the saturated weight – in order to determine the macro porosity. Assuming zero macro pores in the cement paste, the "lack of suction effect" is the difference between the saturated weight and the last, preceding suction weight.

<u>Directly from 7 days wet curing :</u>

Procedure stage	Cement paste (P)	Mortar 3 % air (M)	Mortar 13 % air (M)
1. Prior to first saturation	64.71	98.73	103.04
2. After first 50 bar saturation	64.65	99.48	108.15
3. Initially non-filled macro pores (2)-(1)	-0.06	0.75	5.11
4. Suction weight after 4 hours	63.45	97.82	102.59
5. After second 50 bar pressure	64.26	99.14	107.80
6. Sample volume [cm^3]	32.60	43.04	49.55
7. Paste volume fraction [%]	100	40	36
8. Paste : Irreversible effect (1)-(5)	0.45		
9. Paste : Adjusted initial suction (1)-(8)	64.26		
10. Paste : "Lack of suction effect" (5)-(4)	0.81		
11. Paste : Adjusted suction weight (Def.) (4)+(10)	64.26		
12 : Mortar : Irrev. effect (8)x(7)x$(6_M)/(6_P)$		0.24	0.25
13 : Mortar : Adj. initial suction (1)-(12)		98.49	102.79
14 : Mortar : "L.of suct.eff." (10)x(7)x$(6_M)/(6_P)$		0.43	0.44
15 : Mortar : Adjusted suction weight (4)+(14)		98.25	103.03
16 : Mortar : Initial DCS (13)/(15) [%]		100	100
17 : Mortar : Init. non-filled macrop. (3)/(6_M) [%]		1.7	10.3
18 : Mortar : Macro porosity ((5)-(15))/(6_M) [%]		2.1	9.6
19 : Mortar : Init. filled macrop. (18)-(17) [%]		0.4	0(-0.7)

Table 6.3.12 : Alternative approach to initial "DCS" and macro pore filling, based on re-calculation as described in the text. "DCS" designates "Degree of capillary saturation". "(6_P)" and "(6_M)"designate value in line 6 for the paste and the mortar, respectively. All values in gram unless otherwise stated. Input data from appendix D.

7 days wet curing + 24 days in plastic bag :

Procedure stage	Cement paste (P)	Mortar 3 % air (M)	Mortar 13 % air (M)
1. Prior to first saturation	84.99	112.25	118.65
2. After first 50 bar saturation	84.89	113.05	123.86
3. Initially non-filled macro pores (2)-(1)	-0.10	0.80	5.21
4. Suction weight after 4 hours	83.24	111.16	117.99
5. After second 50 bar pressure	83.89	112.46	123.75
6. Sample volume [cm^3]	42.78	48.73	56.64
7. Paste volume fraction [%]	100	40	36
8. Paste : Irreversible effect (1)-(5)	1.10		
9. Paste : Adjusted initial suction (1)-(8)	83.89		
10. Paste : "Lack of suction effect" (5)-(4)	0.65		
11. Paste : Adjusted suction weight (4)+(10)	83.89		
12 : Mortar : Irrev. effect (8)x(7)x(6_M)/(6_P)		0.50	0.52
13 : Mortar : Adj. initial suction (1)-(12)		111.75	118.13
14 : Mortar : "L.of suct.eff." (10)x(7)x(6_M)/(6_P)		0.30	0.31
15 : Mortar : Adjusted suction weight (4)+(14)		111.46	118.30
16 : Mortar : Initial DCS (13)/(15) [%]		100	100
17 : Mortar : Init. non-filled macrop. (3)/(6_M) [%]		1.6	9.2
18 : Mortar : Macro porosity ((5)-(15))/(6_M) [%]		2.1	9.6
19 : Mortar : Init. filled macrop. (18)-(17) [%]		0.5	0.4

Table 6.3.13 : Alternative approach to initial "DCS" and macro pore filling, based on re-calculation as described in the text. "DCS" designates "Degree of capillary saturation". "(6_P)" and "(6_M)"designate value in line 6 for the paste and the mortar, respectively. All values in gram unless otherwise stated. Input data from appendix D.

Adjusting the weights of the mortars proportionally to their paste content might provide improved values on suction porosity and macro porosity. Thereby, the initial degree of capillary saturation and macro pore filling would be improved accordingly. It should be kept in mind that even if this is another approach to determine the two latter values, it depends on the properties of the cement paste of the mortar being close to that of the pure cement paste. This is not necessarily true with respect to neither the irreversible effect nor to the suction porosity, since the transition zone forms the major part of the cement paste in the mortar. The re-calculations are shown in the tables 6.3.12-14.

The calculated irreversible effects of the mortars are slightly lower (7 days wet, both), in the same range (3 %, 7d+24d & 31d wet) or deviating (13 %, 7d+24d & 31d wet) from the ones actually observed (line 2 vs. 5 in the tables). For the 13 % mortar, the irreversible effect diminished (7d+24d) and turned to "negative" at 31 days wet curing. However, this has no influence on the degree of capillary suction in these cases – it remains at 100 %. Neither does it influence the degree of macro pore filling.

Directly from 31 days wet curing :

Procedure stage	Cement paste (P)	Mortar 3 % air (M)	Mortar 13 % air (M)
1. Prior to first saturation	78.37	110.20	111.76
2. After first 50 bar saturation	78.22	110.93	116.28
3. Initially non-filled macro pores (2)-(1)	-0.15	0.73	4.52
4. Suction weight after 4 hours	76.81	109.25	110.97
5. After second 50 bar pressure	77.60	110.59	117.17
6. Sample volume [cm^3]	39.66	47.48	54.10
7. Paste volume fraction [%]	100	40	36
8. Paste : Irreversible effect (1)-(5)	0.77		
9. Paste : Adjusted initial suction (1)-(8)	77.60		
10. Paste : "Lack of suction effect" (5)-(4)	0.79		
11. Paste : Adjusted suction weight (4)+(10)	77.60		
12 : Mortar : Irrev. effect (8)x(7)x(6_M)/(6_P)		0.37	0.38
13 : Mortar : Adj. initial suction (1)-(12)		109.83	111.38
14 : Mortar : "L.of suct.eff." (10)x(7)x(6_M)/(6_P)		0.34	0.39
15 : Mortar : Adjusted suction weight (4)+(14)		109.59	111.36
16 : Mortar : Initial DCS (13)/(15) [%]		100	100
17 : Mortar : Init. non-filled macrop. (3)/(6_M) [%]		1.5	8.4
18 : Mortar : Macro porosity ((5)-(15))/(6_M) [%]		2.1	10.7
19 : Mortar : Init. filled macrop. (18)-(17) [%]		0.6	2.3

Table 6.3.13 : Alternative approach to initial "DCS" and macro pore filling, based on re-calculation as described in the text. "DCS" designates "Degree of capillary saturation". "(6_P)" and "(6_M)"designate value in line 6 for the paste and the mortar, respectively. All values in gram unless otherwise stated. Input data from appendix D.

In all the cases, the initial degree of capillary saturation is 100 %. A final exercise on the subject is to compare the results above on initially filled macro pores with those of table 6.3.4, see table 6.3.14. Summarising the issue, it appears that the non-air-entrained mortar contains a low but constant amount of water in its macro pores. The air-entrained mortar increases its macro pore filling from zero to somewhere between 2 % and 3 %.

	Mortar 3 % air			Mortar 13 % air		
	Curing/Storage			Curing/Storage		
Input :	7d wet	7d+24d	31d wet	7d wet	72+24d	31d wet
Tables 6.3.11-13[%]	0.4	0.5	0.6	0	0.4	2.3
Table 6.3.4 [%]	1.3	1.0	1.3	0.2	1.0	3.1

Table 6.3.14 : Comparison of initially filled macro pores [Vol.-%] with the different curing/storage conditions, calculated in different ways.

6.3.7 Conclusions

A cement paste and two mortars, with and without air entrainment, were subjected to measurement of chemical shrinkage. Together with additional data obtained from saturation by pressure, drying at 105 °C, loss on ignition and structural analyses, the following conclusions could be drawn :

- There was a difference in chemical shrinkage between cement paste and mortar of “identical” composition (w/c-ratio = 0.48). Each of the series comprised four parallel samples of quite identical values.

- Accordingly, there was an effect of the air content of the mortar on the chemical shrinkage ; air entrainment increased the water uptake.

- The degree of hydration (w_n) was lower for cement paste than for the two mortar qualities. The two mortars exhibited quite identical degree of hydration, especially at the age of 31 days. However, strictly speaking the differences in degree of hydration have not been statistically verified, but it is unexpected due to “catalytic effect” of sand.

- The differences in water uptake were mainly, but not entirely due to the differences in degree of hydration :

- Macro pores started to take up water already at an early stage. After 31 days of curing under water, the non-air-entrained mortar had 0.6 – 1.3 volume-%, the air entrained one 2.3 – 3.1 volume-% macro pore filling. This constitutes roughly 20-30 % of the total macro pore volume.

- The degree of capillary saturation was 100 % in all the cases investigated.

7 Moisture re-distribution during freeze-thaw

7.1 Background

Concrete freezing in contact with a liquid is subject to exchange of moisture during the freezing and thawing cycle. Lindmark [L 1998] reviewed a number of mechanisms accounting for such interaction as a result of the temperature changes and differences in salt content between the interior and the exterior of the concrete material.

He also determined the actual water uptake during the first hours of “freezing”, depending on pre-storage salinity. The quotation marks are due to the fact that he actually did not let the surface freeze, but exposed the samples to salt solutions not freezing at the (negative) temperature levels investigated. Hence, there always was a more or less liquid contact between the (finer part of ;) the pore structure and the external liquid, enabling moisture exchange.

However, the internal moisture may also be re-distributed. Due to the requirement of thermodynamic equilibrium between water in liquid and solid (ice) state, the chemical potential differences will alternate with temperature changes and give rise to potential water transport : When the material is in frozen condition, i.e. coarser pores containing ice, water will move towards the ice : The low vapour pressure (chemical potential) above ice will attract non-frozen water from the surrounding gel and capillaries – since freezing cannot take place in situ.

In thawed state, the finer part of the pore structure - the gel – will attract water. Reducing the temperature (prior to freezing of the capillaries) will create a potential transport of water from the capillaries towards the gel. This effect is described by Helmuth [H 1961]. Increasing the temperature will reverse the effect.

After thawing, the water distribution may reset to “zero”, i.e. the water will return to the capillary (and larger gel ;) pores and reduce the capillary under-pressure. Water may also be sucked in from external sources.

7.2 Objective

The objective of the present section is to consider the accumulated moisture changes, depending on the time of frost - in isothermally frozen condition or in freeze-thaw cycling. Particular attention will be paid to the thawing phase, discussing possible water suction in this phase.

7.3 Introduction to moisture transport phenomena

7.3.1 General

In the following, mechanisms responsible for the water uptake as reviewed by Lindmark [L 1998] will be listed and very briefly explained. The objective is to estimate their relative influence on the total moisture changes. The thermodynamics producing internal re-distribution will also be discussed. Note that below, the thermal contraction effect for each phase is discussed separately.

The effects of the various mechanisms mentioned below will be related to the material quality and sample sizes used in the experimental work of this section, i.e. mortar with w/c-ratio of 0.48, air content of 3 % and 13 %, sample size Ø100 x 50 mm^3.

7.3.2 Mass change due to contraction of air voids

The cooling will induce under-pressure in the pore system which again will lead to suction of external moisture if available – until the under-pressure is eliminated. Applying the gas equation and assuming that the pressure will come to equilibrium (no restraints due to low of permeability) with no reduction in the air voids yields the maximum absorption caused by this effect : (See later for compensation due to overall volume reduction.)

$$\frac{pV}{T} = const.$$

$$\frac{V}{T} = \frac{V_0}{T_0}, (p = const.)$$

$$\Delta m = \Delta V = V - V_0 = V_0 \times \frac{T}{T_0} - V_0 = V_0 \times \left(\frac{T}{T_0} - 1 \right) \qquad \text{(Eq. 7.3.1)}$$

where :

Δm : mass change (ab-/desorption of water) [g]
ΔV : volume change of air [cm^3]
V_0 : initial air volume of the sample [cm^3]
T_0 : initial temperature [K]
T : actual temperature [K]

For a cylindrical sample of Ø100 mm and thickness 50 mm (sample volume approximately 400 cm^3), 3 % or 13 % air volume and a temperature change from +20 °C to –20 °C, the potential mass changes are 1.6 g and 7.0 g, respectively :

3 % air : $$\Delta m = \Delta V = 400cm^3 \times 0.03 \times \left(\frac{253K}{293K} \div 1 \right) \Rightarrow 1.6g$$

13 % air : $$\Delta m = \Delta V = 400cm^3 \times 0.13 \times \left(\frac{253K}{293K} \div 1 \right) \Rightarrow 7.0g$$

This potential is unlikely to be realized, due to the low permeability. Lindmark [L 1998] found that discs of 5 mm thickness and qualities of w/c-ratios ranging from 0.40 to 0.65 were filled in a little less than one hour. These were subjected to suction from two sides.

Assuming freezing after four hours at –3 °C of the external salt solution on top of a sample (i.e. one side suction) of w/c=0.48 tested according to [prEN xxx], 5(10) mm of the top of the sample may typically become filled by this mechanism. Below, initial temperature is still +20 °C, but the lower limit where exchange is believed to take place is –3°C. The corresponding temperature difference to cause the suction thus typically would be reduced to $\Delta T = 23$ °K. Applying these values to the formula, the volume affected is only 1/10 (or ; 1/5) of that used in the calculation above. The weight changes become :

3 % air : $$\Delta m = \Delta V = 40(80)cm^3 \times 0.03 \times \left(\frac{270K}{293K} \div 1 \right) \Rightarrow 0.1(0.2)g$$

13 % air : $$\Delta m = \Delta V = 40(80)cm^3 \times 0.13 \times \left(\frac{270K}{293K} \div 1 \right) \Rightarrow 0.4(0.8)g$$

Calculated as moisture exchange per sample surface area :

- 3 % air : 0.1 – 0.2 g / 13 – 25 g/m^2
- 13 % air : 0.4 – 0.8 g / 50 – 100 g/m^2

The effect appears to have an influence on a significant level.

On heating, the air volume will expand and expel water. Thus, if the air is not dissolved in the water, the effect is reversible. However, even if the direction of effective forces is three-dimensional both during cooling and heating, the response on water suction and expelling may be different : During cooling, suction through the upper external surface will take place, i.e. the transport is one-dimensional (vertical). During heating (even if the heat flow also is one-dimensional), the water expelling is three-dimensional. Hence, some of the water is pushed further down into the sample. One more aspect : During suction, the total air void surface area of a single pore is effective in generating the under-pressure. During heating, only the part of the air void covered by water (i.e. part of the bottom) can be effective in expelling the water from that pore. Thus, by repeatedly freezing and thawing, the thermal effect may account for accumulated water ingress and increased degree of saturation.

7.3.3 Mass change due to contraction of pore solution

The pore water will increase its density ("shrink") on cooling from +20 ^{o}C to +4 ^{o}C. If moisture were accessible at the surface during the cooling phase, this will lead to suction. By continued cooling, the density will decrease, and water may be expelled – or pressed into the air voids. The limitations concerning permeability as discussed in section 7.3.2 also apply in this case. The sample volume probably limits the effect to the upper 5-10 mm.

If freezing at the surface and in the coarse capillaries takes place at –3 ^{o}C, this will probably prohibit further expelling of non-frozen pore liquid or at least slow down the process. Using the density of water at +20 ^{o}C and –3 ^{o}C, the possible suction due to shrinkage of the pore water may be estimated.

The part of the sample volume affected (in the 5-10 mm layer) refers to the capillary and gel porosity. Using the expression for total porosity (excl. air voids) in Eq. AI-7, degree of hydration 66 % and the material composition of the mortars in section 6.3, the "suction porosity" (gel + capillaries) is 18.4 % at the maximum (less with higher amount of air voids). Assuming 100 % degree of saturation at this stage, the mass change may be calculated from the formulae :

$$\Delta m = \Delta V = -V_S \times \varepsilon_T \times DS \times \left(\rho_{T_0} - \rho_T\right) \qquad \text{(Eq. 7.3.2)}$$

where :

Δm : Mass change [g]
ΔV : Volume change of pore water [cm^3]

V_S : Volume of sample affected (5-10 mm depth) [cm^3]
ε_T : Total porosity excl. air voids [relative value]
DS : Degree of capillary saturation [relative value]
ρ_{T0} : Density of water, initial value (at 293 ^oK)
ρ_T : Density of water at actual temperature (at –3 ^oC = 270 ^oK)

The relative density of water at +20 ^oC is 0.99823 [W 1973]. Based on extrapolation, a relative density of non-frozen pore water at –3 ^oC of 0.99968 (+/- 0.00010) is assumed. Applying the values in Eq. 7.3.2 yields values of 0.01 – 0.02 g of absorbed moisture per sample, the range depending on the part of the sample being affected. The same applies even if there is no expelling below +4 ^oC.

Again for a single freezing action, the value is too low to be determined with satisfactory precision. If almost no external expelling in the course of volume increase below +4 ^oC takes place, repeated freezing and thawing may lead to accumulation of moisture in the air voids, as discussed in section 7.3.2. Hence, the degree of saturation may slowly increase due to this contraction effect. It still is an order of magnitude lower than the “air suction effect”. See below as well :

7.3.4 Mass change due to thermal contraction of the sample

The thermal effects on pore water (section 7.3.2-3) should be corrected for external volume change due to thermal contraction of the concrete (sample). If the external volumetric contraction of the sample exceeds that of the pore water contraction, water will be expelled or pressed into air voids. With a quartzite aggregate, the coefficient of longitudinal thermal expansion may be estimated to 10 x 10^{-6} K^{-1} [H 1961, H 1979]. Using a volumetric thermal expansion coefficient of 30 x 10^{-6} K^{-1}, the temperature range +20 ^oC to –3 ^oC and again the upper 5-10 mm of the sample volume being affected, the volume change calculated according to Eq. 7.3.3 yields 0.03 – 0.05 cm^3. (It is assumed that the top surface only has a degree of saturation high enough to eventually provoke water expelling due to contraction of the sample).

$$\Delta V = V_0 \times \alpha_T \times \Delta T \qquad \text{(Eq. 7.3.3)}$$

where :

ΔV : Volume change [cm^3]
V_0 : Initial volume of the sample being affected [cm^3]
α_T : Volumetric expansion of the sample

The calculated values are small but exceeding the ones in the preceding section. With another aggregate (less expanding than quartzite), the effects seem to outweigh each other. The reason may be the contraction of the pore water being mainly responsible for the overall external contraction. *Hence, the effect of volume contraction of the pore water or that of the external volume decrease does not appear to influence water suction.*

7.3.5 Re-distribution of pore water due to thermally induced flow between the gel and the capillary pores

The basic phenomena causing this effect is explained in section 2.1.3.2. On cooling, water will flow from the capillary pore system to the gel due to the entropy difference. The implication is that concrete in contact with external water may compensate the dehydration of the capillary pores by suction and increasing the overall water content.

Helmuth [H 1961] investigated the total effect of water flow caused by entropy induced temperature effects, volume contraction of the pore water (section 7.3.3) and external contraction (section 7.3.4). He found a numerical expression for the mass change by external absorption – if in contact with an external source of water during a temperature drop of 25 ^{o}C, see Eq. 7.3.4.

$$\Delta m = 0.0194 w_g + 0.0024 w_c \quad \text{(Eq. 7.3.4)}$$

where :

Δm : Mass change due to external suction [g]
w_g : Water content in gel pores = 0.74 w_n [H 1961] [g]
w_n : Chemically bound water [g]
w_c : Water content in the capillary pores [g]

As explained in appendix I, total volume may be described as (0.32 + w/c) and without pursuing the issue further, the capillary porosity (volume) of the *cement paste* is quantified by Equation 7.3.5 [L 1998].

$$w_{CV} = \frac{w/c - 0.39 \times \alpha}{0.32 + w/c} \quad \text{(Eq. 7.3.5)}$$

where :

α : Degree of hydration [rel. value]
w_{CV} : Capillary porosity [relative volume]

Using the material characteristics of the present study ; mortar with w/c-ratio 0.48 and $\alpha = 0.66$ (measured : section 6.3 (28 dg)), the w_{CV} value becomes 0.28 (of total volume). For such a cement paste containing 100 g cement, the volume is about 80 cm^3 (section 5.2 in appendix I), and w_{CV} corresponds to 0.28 x 80 cm^3 = 22.4 cm^3 capillary pore space, or holding ~22 g water when water filled.

Calculating according to Eq. 7.3.4 for the cement paste (100 g cement) above, we use w_c = 22 g (100 % degree of saturation in the affected part of sample assumed) and w_n = 19 g per 100 g cement (measured : section 6.3 (28 dg)) :

$$\Delta m = 0.0194 \text{ x } (0.74 \text{ x } 19 \text{ g}) + 0.0024 \text{ x } 22 \text{ g} = 0.33 \text{ g per } 100 \text{ g cement}$$

The material composition equals that of the mortar in section 6.3 with a cement content of 0.52 g per cm^3 of the sample (non-air entrained). Thus, the complete Ø100 x 50 mm^3 sample and a 10 mm (upper) disc yield values of Δm of 0.7 g and 0.14 g, respectively. The former value is significant, but also the lower one is well within the measurable range. If the affected sample volume becomes even less, the effect tends to be less significant. However, the figures are significantly larger than the single effects calculated in the two previous sections, confirming the statement of Lindmark [L 1998] that the entropy effect is the dominant one of the three.

The original tests of Helmuth [H 1961] were performed on 1 and 2.5 inch long cement paste samples with a hollow core cross section. The effective wall thickness could hardly have been much more than 3 mm. The cooling and heating rate of ¼ ^{o}C per minute implies that less than two hours was sufficient time for the effect to be evident throughout the sample. Faster cooling had proven not to allow for proper counterbalancing of the suction forces. Even though not explicitly stated, the w/c-ratios of the latter samples are believed to be approximately 0.45 – like for the main series. Four hour of cooling prior to freezing will affect the whole sample concerning flow from capillaries to gel. However, the external suction (i.e. the weight increase) at the top surface of a standard (SS 13 72 44) sample will hardly be effective for more than the upper 5-10 mm.

Hence, in this case weight increase due to this (combined) effect is not likely to exceed 0.10 – 0.15 g for a single freezing cycle. This corresponds to 12 – 20 g/m^2. During the heating period the effect is reversed. However, the situation resembles that of the thermal contraction/expansion effect discussed in section 7.3.2 : Due to the three-dimensional effect, some of the flow due to the suction from the exterior is not likely to be reversed. An internal accumulation in capillary pores and air voids is probable.

7.3.6 Mass change due to salt ingress

The concrete samples might show weight increase due to uptake and deposit of salt in the pore system. Lindmark [L 1998] estimated the salt ingress during 5 hours of suction (w/c=0.65) from two sides on a Ø100 mm sample to be less than 0.1 g. However, attempts to determine this experimentally partly failed. Experience from pre-dried samples subjected to suction of salt solutions of different concentration indicated that salt ingress corresponding to the concentration of the external solution might be achieved [S 1988b]. Using one side suction on a similar sample size and w/c=0.48, the process will be slower than estimated by Lindmark. The effect on weight increase can be shown to be very little and will be neglected in the present context.

7.3.7 Mass change due to osmosis

7.3.7.1 Introduction to the phenomenon

The term osmotic pressure has been used to explain water diffusion in concrete. Some authors also claimed that osmotic effects might generate stress-induced damage in the material.

The phenomenon depends on the existence of semi-permeable membranes. Such membranes are of great variety, but they are all characterised by the fact that they allow one component of a solution to pass through them and prevent the passage of another component [B 1966]. Even if concrete is not a membrane according to the normal perception of this concept, the effect on concrete was confirmed by work referred to by Powers [P 1976].

Discussing the osmotic effects from a chemical equilibrium “point of view” explains the mechanisms involved : With internal salt solution and external water (i.e. inside/outside the concrete surface “membrane”, respectively), the water will diffuse inwards faster than the salt diffuses outwards. If the (porous) material is saturated, water ingress will continue until the pressure $\Delta\Pi$ (see definition below) is so high that the water (i.e. the solvent, with relative humidity below 100 %) in the internal salt solution reaches the same chemical potential as the external water. The amount of diffused water depends on initial degree of saturation.

With external salt and internal “pure” water, the concrete pore water will diffuse out from the material until the capillary under-pressure reduces the (internal) relative humidity to the level of the relative humidity of the external salt solution. The amount of diffused water depends on the desorption isotherm, i.e.

the water loss necessary to reach a relative humidity within the concrete identical to that of the external salt solution.

In the case dealt with in section 7.4 – pre-storage in water and testing in 3 % salt – an osmotic pressure effect would cause a slight moisture loss from the samples. Lindmark [L 1998] performed a limited test on isothermally stored mortar samples of internal or external salt concentrations close to 20 (!) %. He used 5 mm thick slices of diameter 100 mm. In the case of samples pre-stored in water and subjected to two sided exposure, he determined a weight loss after 7.5 hours of approximately 0.5 g. The results did not deviate very much between the two material qualities investigated - w/c-ratio of 0.40 and 0.65 (!). The opposite effect – water ingress caused by internal salt solution of approximately 20 % - was in the same range. In the latter case, the w/c-ratio appeared to influence the rate of ingress.

7.3.7.2 Internal water, external salt

The question arising, is how much water may be lost from a sample (in a test set-up as described in section 7.4) subjected to pre-storage in water and then tested in 3 % NaCl. If the degree of capillary saturation prior to freeze-thaw is 100 % (as made probable in section 6), the task is to estimate the change in (loss of ;) water content to obtain an internal chemical potential of the water identical to that of water in the external 3 % NaCl solution. The mortar quality used in section 7.4 is within the range investigated by Lindmark. While he used two sided moisture exchange with the exterior, we have only one in our case. The time of exchange is in the range of the thawed state within a freeze-thaw cycle of the test method. Thus, using the values found by Lindmark above (internal water, external 20 % NaCl) and correcting for geometrical and concentration effects may give an idea of the magnitude of water loss in our case. The task then becomes to relate the chemical potential change of 3 % salt to that of 20 % salt. The chemical potential change in this range is nearly linear to the salt concentration, see figure 7.3.1. Thus, if the moisture loss is proportional to the change in chemical potential, it should in our case be close to 10 % of that found by Lindmark. Compensating for the one side exposure and uncertainty related to effective sample thickness loosing water, yields a value in the range of 0.025 g per sample and upwards. This corresponds to 4 g per m^2 plus. This is a very low value and may be neglected.

7.3.7.3 Internal salt, external water

Internal salt solution and external, pure water displays a somewhat different situation, as mentioned in the introduction. Looking back at the internal salt treatment of the series of mix 5 in section 4, it would be interesting to consider whether the osmotic effect on surface saturation when re-saturated with 3 % NaCl could be real : Trying to estimate the effect of 3 % internal salt solution and water at the outside, it is convenient to start with the equation for osmotic pressure. For one mole of solvent, the maximum osmotic pressure generated is [B 1966] :

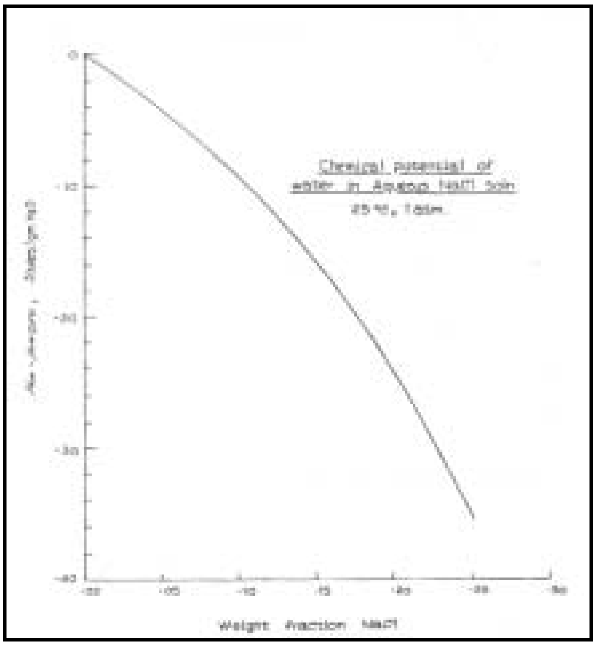

Figure 7.3.1 ; Chemical potential of water in aqueous NaCl solution at 25 ^oC, 1 atm. From [M 1983].

$$\Pi v = -RT \ln \frac{P}{P_0} \qquad \text{(Eq. 7.3.6)}$$

where :

Π : Pressure [Nm^{-2}]
v : Volume of one mole of the solvent [$m^3 \cdot mole^{-1}$]
R : Gas constant [$J \cdot mole^{-1} \cdot K^{-1}$]
T : Absolute temperature [K]
P_0 : Equilibrium vapour pressure for pure solvent [$N \cdot m^{-2}$]
P : Equilibrium vapour pressure for the (salt) solution [$N \cdot m^{-2}$]

Applying Raoult's law, the expression may be written :

$$\Pi v = -RT \ln x_A \qquad \text{(Eq. 7.3.7)}$$

where :

x_A : Mole fraction of the solvent [rel.value]

Thus, the difference in osmotic pressure generated by a *concentration gradient* between two different salt concentrations I and II of "type A" may be expressed as :

$$\Delta\Pi = -\frac{1}{v} RT\left(\ln x_{A,I} - \ln x_{A,II}\right) \qquad \text{(Eq. 7.3.8)}$$

For water diffusion into the sample in the case of internal salt, it is reasonable to assume that the ingress is proportional to the pressure difference. It will then depend linearly on the *ln* of the mole fractions of the two different solutions. Trying to quantify the effect, we will try to base the consideration on the measurements performed by Lindmark [L 1998] again, as referred above. Applying the formula above on the two different salt solutions of 3 % and 20 % by weight, respectively, the molar fractions first need to be calculated :

3 % salt

The mole weight of NaCl is 58.5 g
The mole weight of H_2O is 18 g
3 % NaCl yields 30 g ~ 0.5 mole per 1000 g solution
97 % H_2O yields 970 g ~ 54 moles per 1000 g solution
The mole fraction of the solvent thus amounts to 0.99

20 % salt

20 % NaCl yields 200 g ~ 3.4 moles per 1000 g solution
80 % H_2O yields 800 g ~ 44 moles per 1000 g solution
The mole fraction of the solvent thus amounts to 0.92

In case I (3 % salt), the $\ln x_{A,I}$ yields –0.009, while in case II (20 % salt), the $\ln x_{A,II}$ yields –0.08. The implication is that the 3 % salt yields an osmotic pressure in the range of only 1/10 of that of 20 % salt. Thus, 3 % salt solution would lead to 1/10 of the uptake found by Lindmark [L 1998], provided that the ingress is proportional to the potential difference ($\Delta\Pi$). Additionally with standard samples according to [prEN xxx], only one face is subjected to ingress, and the values applying would be 1/20 only of those obtained by him. Thus, for a single freezing cycle and the present type of samples, about 0.025 g would expectedly be taken up by osmotic pressure.

Such values immediately appear too low to be significant. Still, with a capillary degree close to or above 90 % in the very top layer, such figures may just raise the local degree of saturation above the critical value. Thus, the increased degree of saturation may be responsible for scaled material in the range of at least 10 times these values. Considering the surface area of one sample, the scaled material may amount to 30 g per m^2 *and* freeze-thaw cycle ! This is a considerable level of damage (when testing in pure water). It may explain the initial high scaling level and retarded behaviour after some cycles – when re-saturated in salt and freeze-thaw tested in water. The phenomenon at least should be subject to experimental verification.

7.3.8 Micro-ice-lens pumping

As already explained (section 2) non-frozen pore water at a certain temperature will tend to migrate towards ice already formed due to the difference in chemical potential. This is expressed by the lower vapour pressure above ice compared to that of bulk/capillary condensed/adsorbed (depends on temperature) water. At cooling or isothermal conditions, the process will continue until equilibrium is reached.

With continuous lowering of the temperature below -15 ^{o}C, the smaller pores will freeze progressively. This introduces formation of micro ice lenses and represents an “improved distribution” of the ice lens formation. During subsequent heating, the melting point of the water once contained in the smaller pores is markedly higher [S 1999b]. Upon ice melting, stress in the matrix generated by freezing is released and concrete exposed to external water may be subjected to suction. The resulting increase in saturation is called micro-ice-lens pumping. Below, these phenomena are explained more in detail, based on a review by Setzer [S 1999b, S 1999c] :

The thermodynamics of the water-ice balance as well as the pore size dependent freezing point depression is explained in section 2 of the present publication. It will not be further elucidated in the present context.

Assuming the degree of saturation is high enough, ice will start forming at a few degrees below 0 ^{o}C (Depending on the relative humidity, see section 2). The water in the coarse pores is the first to freeze, and the ice particles are “large”. Upon further temperature lowering, the chemical potential of ice is below that of the still unfrozen water in the smaller pores. Under this non-equilibrium, the potential difference is believed to cause migration of gel water to the ice surface. This continues until the vapour pressure in the gel is depressed to balance that of the ice. The vapour pressure of the gel will diminish as the gel looses water from progressively smaller pores. Frozen macroscopic (and external) water prevents suction from the exterior to balance the resulting suction forces, and the gel shrinks.

When ice formation has started, progressive freezing occurs in smaller and smaller pores as the temperature is decreased. The ice-vapour or ice-porewater interface of these pores have the same (low) vapour pressure as that of the larger ice surfaces at that point in time. However, it can be shown [S 1999b] that with decreasing pore sizes freezing, surface physics becomes increasingly important. Due to the pore ice / matrix interfaces, these small ice crystals, widely distributed, are under compression. This implies that the matrix is under tension. The theory [S 1999b] implies that at very low temperatures the gel freezes and expands.

During the subsequent heating, the “same” water melts at a higher temperature than the one at which it froze. At first, the ice-matrix interaction stress of the “ice-pores” is released. Then the remaining under-pressure in the gel will evaporate water from the larger, now thawed pores, trying to re-establish the vapour pressure equilibrium. Secondly with external water available, the capillary under-pressure of the gel may partly be balanced by external suction. The result is a higher degree of saturation after than prior to the freeze-thaw cycle.

The “water pumping effect” implied by the theory above is valid in principle. The quantitative effects of these mechanisms or their relative importance however, are hardly possible to even estimate theoretically. It also appears that the extent of the moisture loss from the gel may be sensitive to marginal changes in the lower temperature level, usually around –20 ^{o}C at standard testing. An objection to standard freeze-thaw testing at such temperature levels might be that field conditions hardly exhibit *cyclic* behaviour at this level and *at the same time* enable external suction.

7.3.9 Synopsis

The mechanisms discussed above lead to suction of water from the exterior and to internal re-distribution. An issue of practical interest is whether the normal thawing period of standard freeze-thaw testing is long enough to provide sufficient time for this suction. If not, a “suction deficit” may accumulate, and reversible mechanisms are no longer reversible.

If the suction time is not sufficient to establish equilibrium for each freeze-thaw cycle, differences within the allowable range of thawed state in freeze-thaw testing may provide for variation in increased “global” or local degree of saturation.

This will be the issue investigated in the subsequent study.

7.4 Experimental

7.4.1 General

As already mentioned, the objective of these tests was to investigate the accumulated moisture changes, depending on the time of frost - in isothermally frozen condition or in freeze-thaw cycling. Particular attention was paid to monitoring the moisture exchange during the thawing phase.

In the mechanisms reviewed above, the degree of saturation plays an important role. The materials composition (in particular w/c-ratio), the air void content and/or the environmental conditions may control the “saturation effect”.

At this stage, the study is mainly aimed at screening of such effects. Therefore, a single w/c-ratio but two different air void levels was chosen. A “normal” and a prolonged water curing were included to produce different degrees of capillary saturation. The critical factors with respect to freezing time were not known. Hence, a test set-up with differentiated time scale / number of cycles and very limited use of parallel samples was chosen.

To maximise the effects with the number of samples allowed from a practical point of view, a single standard mortar with w/c-ratio of 0.48 was chosen. The practical restraints considered important were (see programme below) :

- Parallel casting, sawing, preparation of all samples on the same day.
- Use of a single freezing cabinet for each of freeze-thaw and isothermal frost test.
- Number of samples to be weighed “simultaneously” at each term, especially after saturation by pressure.
- Physical capacity of the pressure tank.

The main idea is trying to identify the effects of the different material or environmental conditions, rather than comparing and accounting for the differences between them.

7.4.2 Materials, mixing and placing

The mortar constituents identical to those used in section 6. The mix proportions are given in table 7.4.1, the w/c-ratio and cement/sand-ratio also identical to those of section 6. The air void level (in fresh mortar) is somewhat reduced in the air-entrained mortar – and somewhat higher in the non-air entrained one, compared to earlier.

	Mortar with air	Mortar "No air"
Cement CEM I 42,5 R [g]	10 800 (24x450)	10 800 (24x450)
Water (distilled) [g]	5 184	5 184
w/c-ratio	0.48	0.48
Air entraining agent [g]	16	-
Air damping/reducing agent [g]	-	21.6
Sand according to EN 196 [g]	32 400 (24x1350)	32 400 (24x1350)
Air content (by pressure) [%]	11	4.7
Air void spacing factor (fresh) [mm]	0.24	0.6
Specific surface (fresh) [mm^{-1}]	18	11

Table 7.4.1 : Mix proportions and air void properties of the mortars.

First, small batches of 2 x 450 g cement and 2 x 1350 g sand were premixed with the appropriate amounts of water. The mixing procedure followed according to a modification of the EN 196 procedure for cement mortars in a Hobart mixer : Cement paste was mixed for 30 sec on speed 1, sand was added and mixing on speed 1 continued for another 90 sec, then 30 sec on speed 2. The mix was temporarily stored under cover while the next batch was mixed. Two mixers (and operators) operated simultaneously, and all materials for all batches were pre-weighed. This operation took about 20 min. Finally, the small batches were mixed in a flat pan concrete mixer for 30 sec. At this stage, the admixtures (air-entrainer or damping agent) were added and mixing continued for another 60 sec.

For the freeze-thaw test, cylinders of diameter 100 mm and 200 mm height were cast in two layers under appropriate vibration, 9 of each mix. Three 100 mm cubes were cast for determination of compressive strength. The samples were de-moulded after 24 hours and then water stored at 20 °C until the age of 7 or 21 days :

7.4.3 Storing, pre-curing and preparation

At seven days all cylinder samples were removed from the water bath for labelling according to the example given in table 7.4.2. The objective was to ensure an optimal distribution of samples during the succeeding test, since the lack of parallel samples might be a limiting factor in the present study.

DB142 1A ↓	DB142 2A ↓	DB142 3A ↓	DB142 4A ↓	DB142 5A ↓	DB142 6A ↓	DB142 7A ↓	DB142 8A ↓	DB142 9A ↓
1B, ↑ DB142	2B, ↑ DB142	3B, ↑ DB142	4B, ↑ DB142	5B, ↑ DB142	6B, ↑ DB142	7B, ↑ DB142	8B, ↑ DB142	9B, ↑ DB142
DB142 1C ↓	DB142 2C ↓	DB142 3C ↓	DB142 4C ↓	DB142 5C ↓	DB142 6C ↓	DB142 7C ↓	DB142 8C ↓	DB142 9C ↓
1D, ↑ DB142	2D, ↑ DB142	3D, ↑ DB142	4D, ↑ DB142	5D, ↑ DB142	6D, ↑ DB142	7D, ↑ DB142	8D, ↑ DB142	9D, ↑ DB142

Table 7.4.2 : Labelling of the samples for one of the mixes. The arrows indicate the test surface in the later frost or freeze-thaw test. Each column represents one mortar cylinder Ø100 x 200 mm.

At seven days, all cylinders were cut at the B/C intersection. The A/B-parts were all returned after sawing for continuous water storage until the age of 21 days. The C/D-parts were stored at 20 °C and 65 % RH, ensuring identical drying conditions on all surfaces. At 21 days, all the cylinder halves were cut into single samples of diameter 100 mm x 45-50 mm thickness. Then they were returned to storage at 20 °C and 65 % RH, ensuring identical drying conditions on all surfaces, until preparation.

Cylinder nos. 8 & 9 were cut into four discs already at seven days and lightly dried. An epoxy was applied on all surfaces, and the samples were stored at 20 °C and 65 % RH. The effectiveness of epoxy against weight loss was checked.

Preparation according to SS 13 72 44 was done at the age of 24 days (A/B samples) or 25 days (C/D samples). This operation also included the epoxy samples. At 28 days, a three days re-saturation period followed, except for the epoxy samples.

7.4.4 Frost and freeze-thaw test

At the age of 31 days, the re-saturation water was replaced by 3 % NaCl solution. The samples were placed in freezing cabinets according to a specific system to optimise identical treatment of samples that were to be directly compared. One cabinet was used for freeze-thaw cycles according to SS 13 72 44, another for isothermal frost at –20 °C.

After various periods (nos. of freeze-thaw cycles or hours of frost), samples were removed from the cabinets. The weight was compared to the initial weight. The times included 0, (1), 7, 14 and 28 freeze-thaw cycles and 0, 3, 6, 12, 24, 48 and 168 (= 7d) hours of isothermal frost.

Ice, including some of the scaled material, was carefully removed from the still frozen samples (an easy operation after a little softening of the ice, i.e. after five minutes storage at 20 ^{o}C). Then they were quickly wiped off and weighed, *i.e. before they were allowed to suck water through the surface.* This weight was compared to the initial weight prior to frost. They were placed horizontally with fresh water on the top surface and left to thaw. The samples were wiped off and weighed every 30 minutes, the first time also with another collection of scaled material, not contained in the already removed ice. Renewed water exposure of the top surface followed.

After reaching a stable weight, each sample was stripped and placed in a water bath, allowing suction to take place from all sides for 12 hours. Then they were subjected to saturation by 50 bar pressure for seven days, then drying at 105 ^{o}C for seven days. Another period of saturation by pressure followed, then water storage until stable weight and determination of sample volume. Weights were determined at all these terms. The epoxy covered samples were broken and not subjected to suction until after thawing.

7.4.5 Test results

7.4.5.1 General

Test results in tabular form is provided in the appendix G. Absorption during freeze-thaw calculated as gram per m^2 is displayed in the figures 7.4.1&2. Absorption during isothermal frost is displayed in the figures 7.4.3&4. All samples had increased their weight.

Weight changes during the thawing phase – with water on the surface - are displayed in the figures 7.4.5-8. All samples lost weight at this stage !

The net absorption effect, i.e. weight increase “from thawed state to thawed state”, is the one normally reported, e.g. by Bager et al [B 1999], Relling et al [R 1999] and Auberg et al [A 1997]. The net absorption values are presented in the figures 7.4.9-12. All samples exhibited a net increase.

The scaling level for all freeze-thaw samples was very low and not interesting for discussion within the present context. However for reference they may be found in the appendix G. The effect (of lower magnitude) of scaling on the sample weights has been corrected for and does not "disturb" the results of the figures 7.4.1-8.

Weight changes subsequent to thawing (submerged, under pressure or during drying) are not plotted due to reasons mentioned in the discussion below. However for reference they may be found in the appendix G.

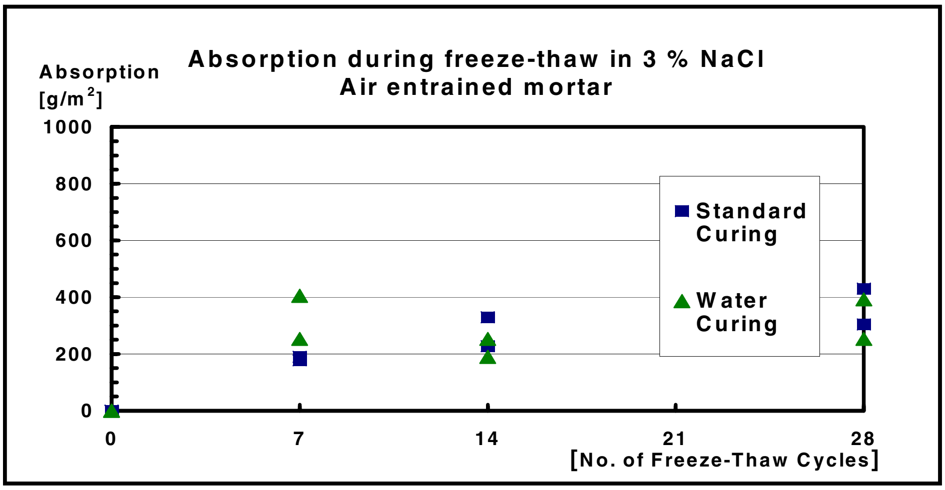

Figure 7.4.1 : Accumulated weight increase during freeze-thaw vs. nos. of freeze-thaw cycles. The values represent weight increase determined before thawing of the samples. Air entrained mortar.

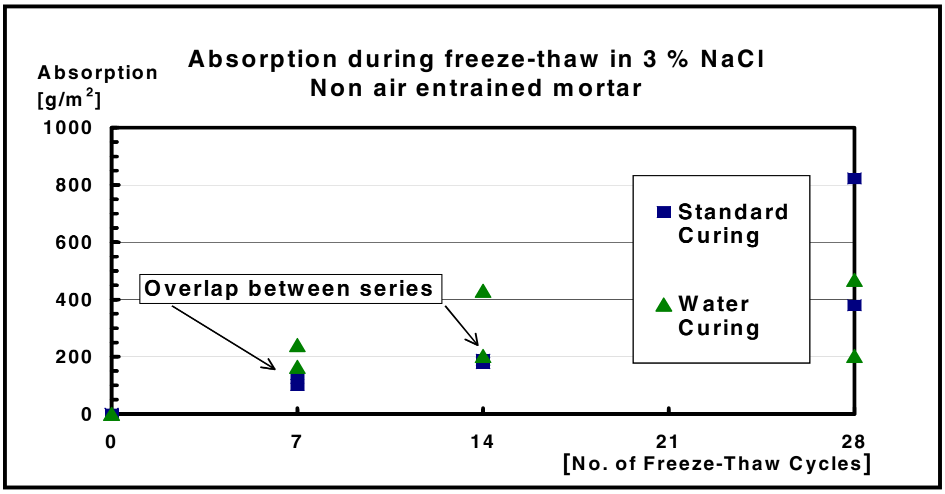

Figure 7.4.2 : Accumulated weight increase during freeze-thaw vs. nos. of freeze-thaw cycles. The values represent weight increase determined before thawing of the samples. Non-air entrained mortar.

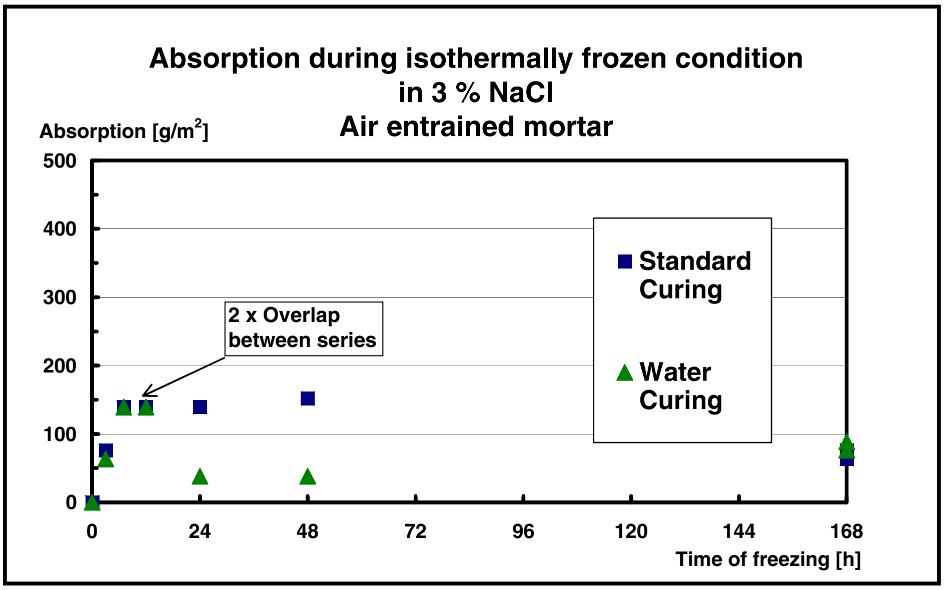

Figure 7.4.3 : Accumulated weight increase during isothermal frost vs. time of frost. The values represent weight increase determined before thawing of the samples. Air entrained mortar.

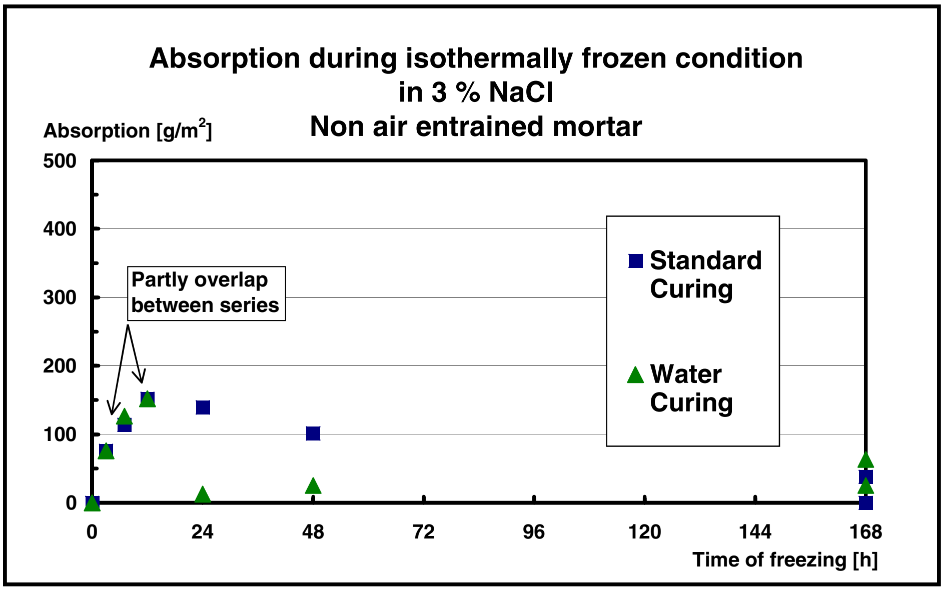

Figure 7.4.4 : Accumulated weight increase during isothermal frost vs. time of frost. The values represent weight increase determined before thawing of the samples. Non-air entrained mortar.

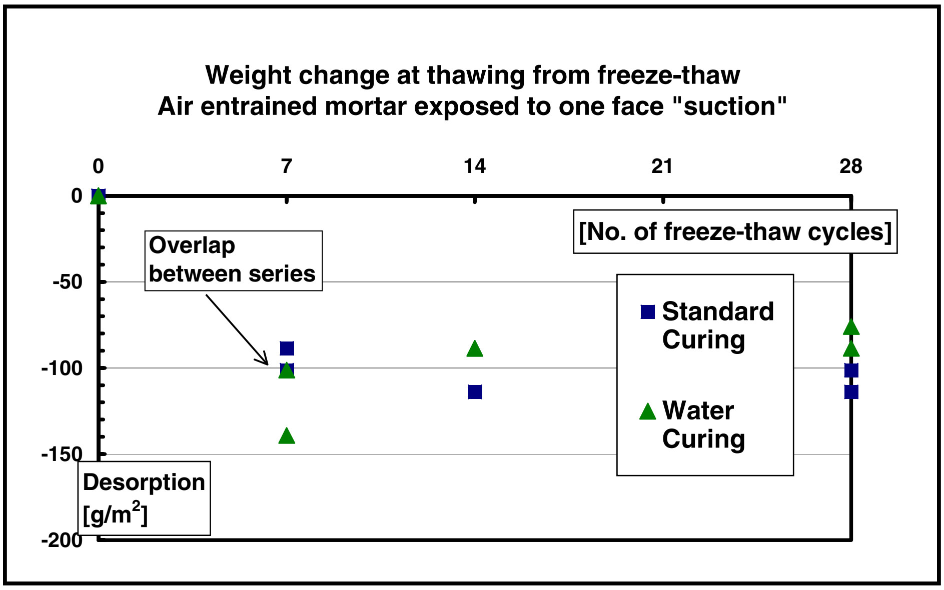

Figure 7.4.5 : Weight change during thawing under water – after freeze-thaw – vs. nos. of freeze-thaw cycles. The values represent the difference between frozen and non-frozen condition, in both cases excluding eventual scaled material. Air entrained mortar.

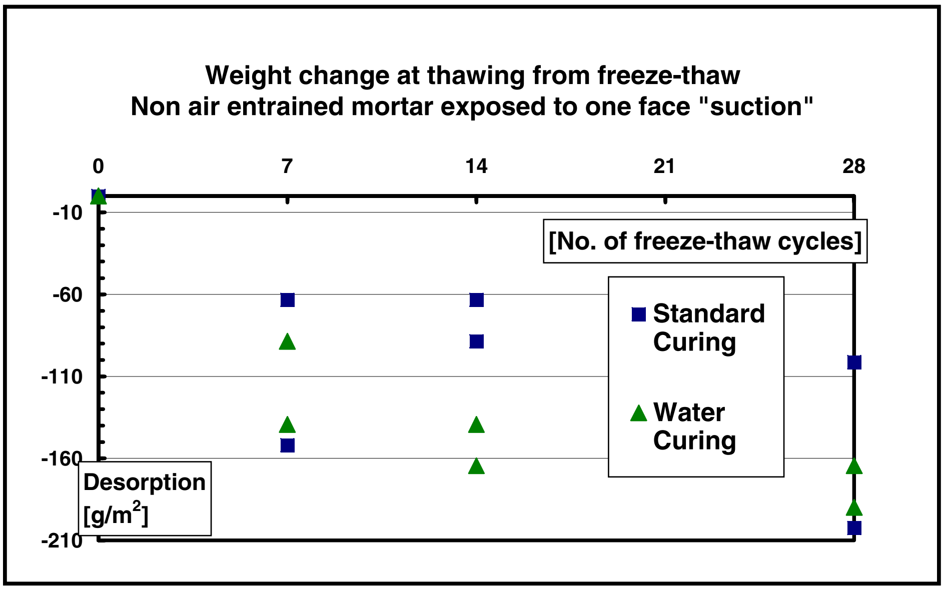

Figure 7.4.6 : Weight change during thawing under water – after freeze-thaw – vs. nos. of freeze-thaw cycles. The values represent the difference between frozen and non-frozen condition, in both cases excluding eventual scaled material. Non-air entrained mortar.

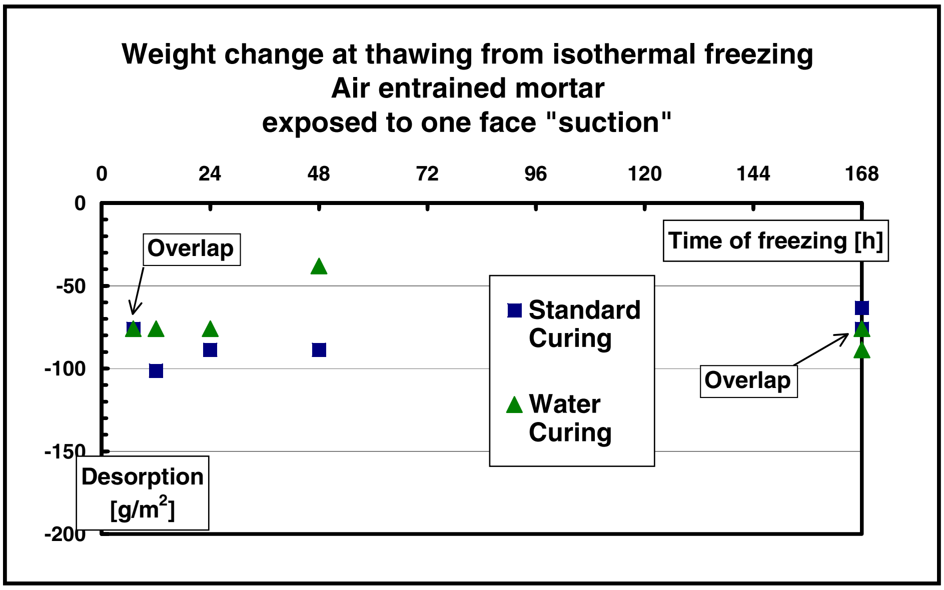

Figure 7.4.7 : Weight change during thawing under water – after isothermal frost – vs. time of frost. The values represent the difference between frozen and non-frozen condition, in both cases excluding eventual scaled material. Air entrained mortar.

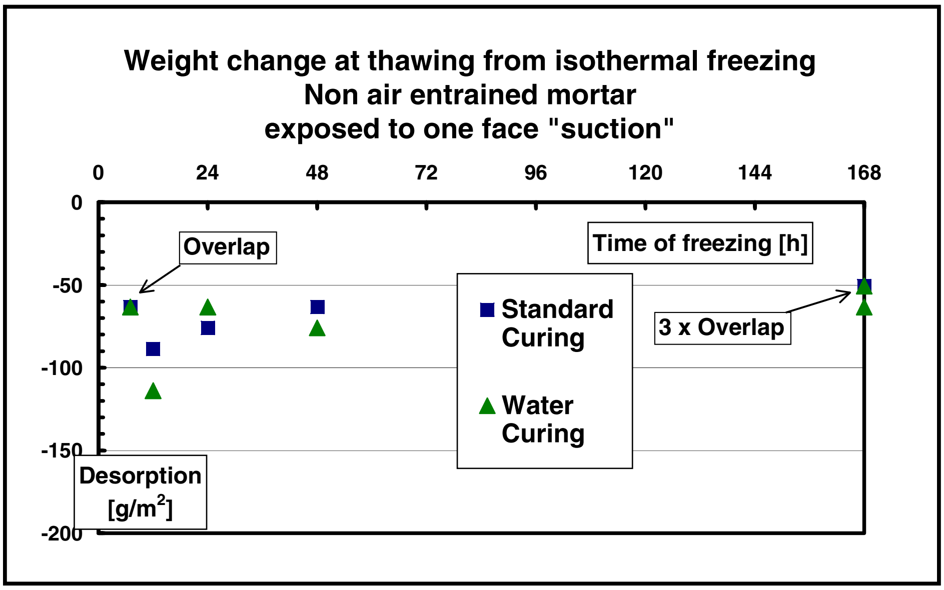

Figure 7.4.8 : Weight change during thawing under water – after isothermal frost – vs. time of frost. The values represent the difference between frozen and non-frozen condition, in both cases excluding eventual scaled material. Non-air entrained mortar.

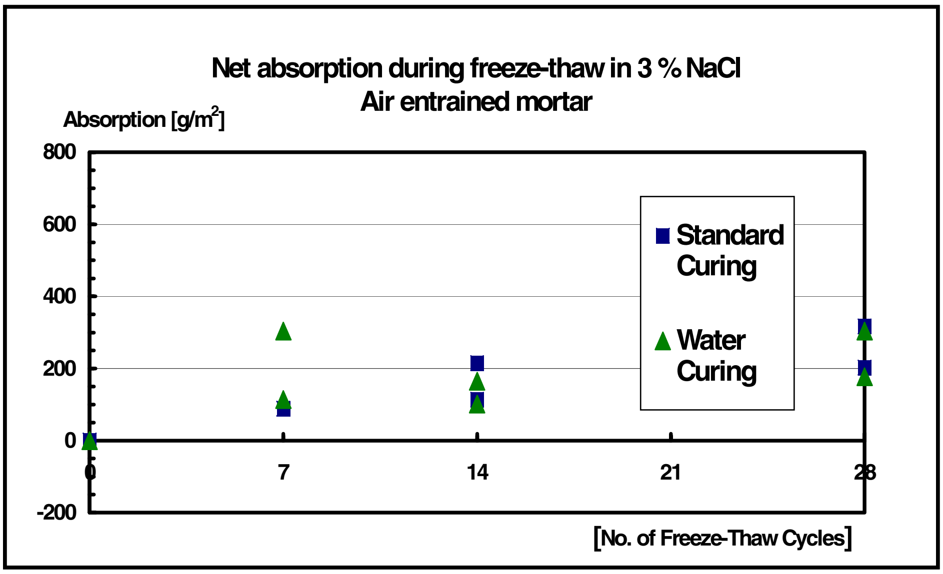

Figure 7.4.9 : The net weight change depending on the number of freeze-thaw cycles. The weight values include correction for eventual scaled material. Air entrained mortar.

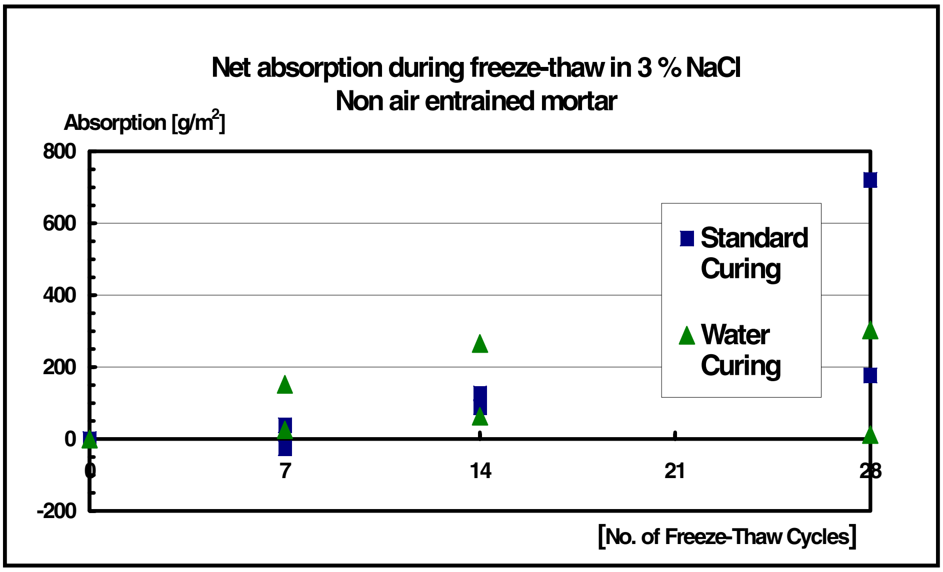

Figure 7.4.10 : The net weight change depending on the number of freeze-thaw cycles. The weight values include correction for eventual scaled material. Non-air entrained mortar.

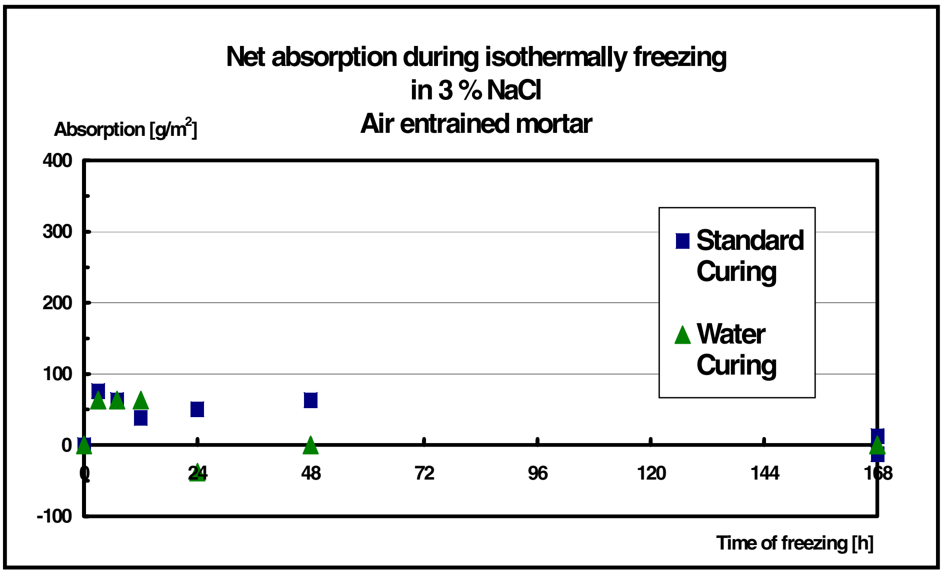

Figure 7.4.11 : The net weight change depending on the time of isothermal frost. The weight values include correction for eventual scaled material. Air entrained mortar.

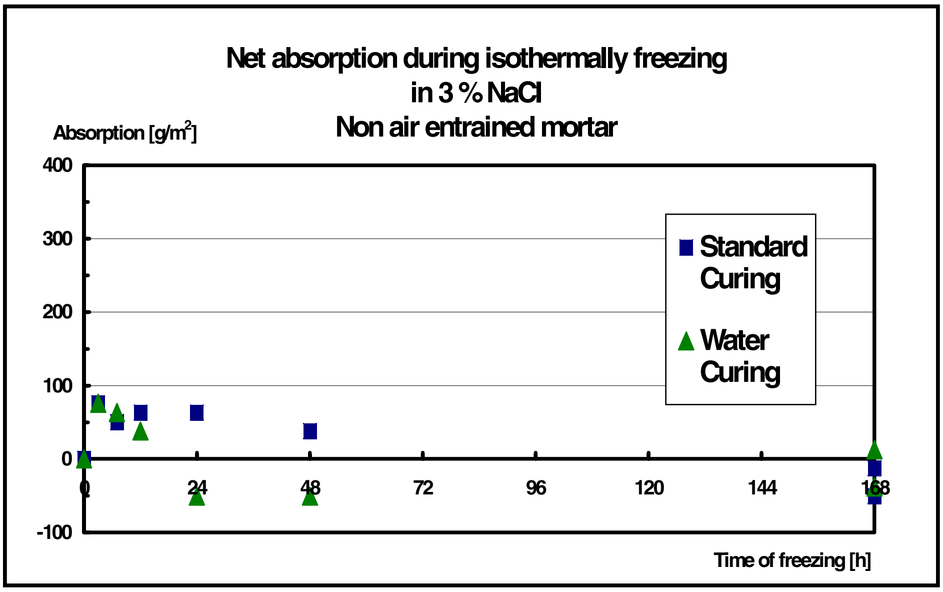

Figure 7.4.12 : The net weight change depending on the time of isothermal frost. The weight values include correction for eventual scaled material. Non-air entrained mortar.

The scatter between parallel samples was too large to allow comparison between the two different levels of air content. However, this was outside the scope, see section 7.4.1.

7.4.5.2 Initial saturation

An attempt was made to estimate the initial degree of capillary saturation as well as macro pore filling prior to frost and freeze-thaw testing. This attempt was based on the saturation and drying procedure on the samples as described in section 7.4.4 (data are included in the appendix) and investigated in section 6. As expected, the attempt of doing this on the basis of these comparatively large samples was confusing and failed.

The probable reason for this failure was the lack of ability to establish homogeneous moisture conditions throughout the samples. However, it is believed that the data range found in section 6.3 are representative for the conditions close to the upper surface of the frost and freeze-thaw samples at the age of 31 days.

These data render a probable capillary degree of saturation of 100 % in this upper region, even with some drying in connection with the preparation procedure.

With respect to macro pore filling, the values of 0.6-1,3 (non-air-entrained mortar) and 2.3-3.1 (air-entrained mortar) volume-% are probably in the upper range. A more precise or differentiated procedure in section 6.3 would have been necessary to estimate the actual level of the frost and freeze-thaw samples. With the actual procedure, it is only possible to state that some macro pore filling will have occurred for the samples water cured for 21 days, i.e. prior to their removal from the water storage.

\- - -

Separate comment on the epoxy-coated samples should be included : They had been cured moist for seven days and then coated by epoxy. Furthermore, they had not been subjected to moisture exposure during freeze-thaw. Their capillary degree of saturation was expected to be close to 100 % at the freeze-thaw start, see curing “7d wet + 24d plastic” in section 6.

The general idea then was that these might exhibit larger suction afterwards, i.e. after splitting (eliminating the epoxy “barrier”) and subjected to suction - if the internal, accumulated re-distribution was an important factor. However with the outcome described below, this was no point any more ..... No further discussion of these samples will be made in the present context.

7.4.6 Discussion of test results

7.4.6.1 Absorption during freeze-thaw

The figures 7.4.1&2 confirm the earlier results on moisture absorption during freeze-thaw, see section 4 for discussion and references. It is important to keep in mind that each point in the plots represents an individual sample. Hence, no “line” on the time/cycle axis connects them.

With the exception of one sample removed from the freeze-thaw cabinet at seven days, there is a trend of increasing absorption with the number of freeze-thaw cycles. However, the scatter between parallel samples is larger than the differences between the two types of pre-curing (standard curing or water curing until the age of 21 days).

The obtained values are based on the weight of the still frozen samples directly after removal from the freeze-thaw cabinets. They are not directly comparable with values obtained after weighing in thawed state, as reported by Bager et al [B 1999], Relling et al [R 1999] and others. Still, the trends are in line with their reports on the “pumping” effect : The moisture content increases with the numbers of freeze-thaw cycles.

The absorption after 28 freeze-thaw cycles lies in the range of 200 – 800 g/m^2. There is no significant difference between air entrained and non-air entrained mortar.

7.4.6.2 Absorption during isothermal frost

The absorption during isothermal frost is displayed in the figures 7.4.3&4. Although statistically not significant, there is a tendency of maximum absorption for the samples frozen for 24 hours. Thereafter, a very slight “freeze-drying” appears to exist. Again, there appears to be no effect of the type of pre-curing.

The absorption is in the range of 0 – 150 g/m^2, which is generally lower than that of freeze-thaw. There is no significant difference between air entrained and non-air entrained mortar.

7.4.6.3 Thawing after freeze-thaw

The most striking result is the general weight loss during thawing (figures 7.4.5-6). Initially, it was believed that this might be due to remaining ice in the surface voids. This ice would have been included in the first weighing operation but not in the second, thawed state. The idea was tested by applying a soft paste of known density on the surface of a few (thawed) samples, then determining the weight increase. The "surface pore ice" effect is difficult to estimate. Though, by this check, it could not account for more than 35g/m^2 of the weight loss *of the air-entrained mortar* at the maximum. With the appearance of the cleaned, frozen surface in mind, it is suggested that this value also is an overestimate.

With the air-entrained mortar, the "de-hydration" during thawing appears constant, and not dependent on the number of freeze-thaw cycles. The range after 28 cycles is 80 – 120 g/m^2. With the non-air-entrained mortar, the corresponding range is a little higher at 100 – 200 g/m^2. There is a very slight but not significant tendency of increase with number of cycles. The deviation between the two different air void levels could be due to the internal pressure mechanism during thawing. This would imply that the internal water would escape to the nearest available (air) void, not necessarily to the external surface. The effect would expectedly be more effective with the air-entrained mortar, since the air void spacing factor in this case is lower. However, this would imply a higher net absorption by the air-entrained mortar. This is not the case, see below. See also discussion on "ice contraction effect during thawing in 7.4.6.7.

7.4.6.4 Thawing after isothermal frost

The weight loss during thawing after isothermal frost, displayed in the figures 7.4.7-8, mainly exhibits values in the range of 50-100 g/m^2. This appears independent of type of pre-curing and frost exposure time. The values generally are somewhat lower than for those after freeze-thaw exposure.

7.4.6.5 Net absorption effect

As already mentioned, net absorption corresponds to other reported [B 1999, R 1999, A 1997] weight increase during freeze-thaw : Initial and end values are both obtained in the thawed state. The net absorption displayed in the figures 7.4.9-12 confirms the previous trends of increased absorption at increased number of freeze-thaw cycles. With the air-entrained mortar, there is a relatively narrow range for the individual absorption values after 28 freeze-thaw cycles. With the non-air-entrained one, the value ranges from (almost) zero to 700 g/m^2.

It may be noted that the type of pre-curing had no clear influence on the net absorption. As already explained in section 7.4.5.2, the initial capillary degree of saturation was believed to be close to 100 %, at least in the upper 10 – 20 mm.

After isothermal frost, the absorption is evidently lower than the former ones. The tendency of increased drying with frost time is confirmed. It also appears that the prolonged water curing, i.e. increased (surface) degree of saturation exhibits a faster relative drying of the samples.

The net absorption values displayed in the figures 7.4.9-12 exhibit very low values compared to studies by Bager [B 1999], Auberg [A 1997] and Relling [R 1999]. The reason is difficult to identify. Their studies concerned concrete of similar w/c-ratios in contrast to the present mortars. The mortar may have promoted the moisture exchange with the external environment. Water absorbed during the cooling period may have a relatively easier way of escaping from the interior during the thawing period than would be the case with concrete. Thus, the reason for the different observations probably is that the thermal pumping (and accumulation) effect is more pronounced with concrete than with mortar.

7.4.6.6 Miscellaneous

The weight loss during thawing (with water on the top surface) took place during 30 to 60 minutes. After the thawing phase, the sample weights remained stable before they were subjected to stripping and submerging for further suction.

Generally about the short time for one-face suction, it may be argued that there had not been sufficient time to generate suction after the pressure relief on thawing. To investigate this, some samples at a later stage were subjected to repeat of the freezing and thawing. They exhibited no further one-face suction for 24 hours after the thawing.

The suction during the subsequent immersion and the pressure saturation procedure provided no systematic pattern with respect to number of freeze-thaw cycles or time of frost. It appears that the individual samples deviated more in amount of air voids than in degree of pore filling. Hence, further consideration of these data is not included. For reference, these data in tabular form are included in the appendix G.

However, one idea derived from the latter procedure that may provide useful for other applications : If samples subjected to saturation by pressure are quickly removed from the pressure tank and weighed (which they should in any case), subsequent storage under water until stable weight (at least 24 – 48 hours), the weight difference indicate the remaining air content of the sample. The value may be calculated by applying the standard gas equation (pV/T = const.).

7.4.6.7 Overview

The moisture accumulation during freeze-thaw is evident, displayed by the net absorption development with increased number of freeze-thaw cycles. The results confirm earlier reported trends [B 1999, R 1999, A 1997]. Furthermore, the "pumping effect" of freeze-thaw cycles is indirectly confirmed by the drying tendency after one week at –20 ^{o}C with water on the top surface.

A consequence of the weight loss when thawing - with water on the top surface - and no further water uptake until the following cooling phase is that "suction potential" due to internal re-distribution of moisture could not be confirmed. This comprises both the "capillary to gel flow" (section 7.3.5) and the micro ice lens pumping (section 7.3.8) – for the mix designs investigated.

During freezing, the volume of water increases with 9 %. During thawing, a corresponding volume reduction of the ice takes place. If the "global volume" was kept constant during thawing (not reduced), e.g. due to internal cracking or external restraints, the volume reduction of ice might cause suction at this stage. However, if the concrete is free to contract according to the release of tension caused by the previous freezing of the capillary water, no such suction is likely to occur. This is a difference from the cooling effect of the air voids : The pressure difference of the air voids is caused by changing the temperature *but keeping the global volume (almost) constant.*

With a probable contribution by osmosis, this leaves suction on cooling due to contraction of air voids as the major moisture increasing mechanism. The other mechanisms reviewed are comparatively smaller. Any effect of air entrainment is absent but may be due to the fact that even the non-air entrained mortar ended up with almost 5 % air (table 7.4.1).

It is noteworthy that the influence of pre-curing condition is very small. However, the capillary degree of saturation is most probably 100 % at the initiation of the test, as already argued for both curing conditions. A consequence of this level of saturation is the lack of capillary suction – to provide more moisture from the outside. It also means that the air contraction mechanism may be sensitive to variation of the amounts of air void in a critical (narrow) distance from the surface. This may explain the large between-sample variations experienced in this study. Another implication is that the mechanism may be sensitive to capillary porosity differences due to their effects on permeability. This comprises resistance to suction during cooling as well as thermally generated pressure on heating.

The estimated order of magnitude for the thermal contraction effect is another indication that moisture actually moves in *and* out through the surface. The heating then leads to expelling of water, some of it ending up in other air voids or never escaping the ones it was sucked into during the cooling phase.

Even if the net absorption effect of freeze-thaw was evident, the extent of this effect in the mortar investigated was smaller than that of other studies on concrete of comparable w/c-ratio. The order of magnitude of the ab- and de-sorption indicate that as much as the upper 10 mm of the sample was involved in the process. This suggests that concrete – with larger aggregates – possess “poorer” ability for the water to be expelled in the heating phase, thus maintaining more water (in air voids) than would the mortar.

- - -

The freeze-drying effect at isothermal frost appeared to trigger a faster weight loss for water cured samples. This may indicate early evaporation of water held in macro pores close to the surface.

7.4.7 Conclusions

Various mechanisms possibly contributing to the accumulation of moisture in concrete during freeze-thaw were reviewed. Mortar with w/c-ratio of 0.48, with and without air entrainment, water stored or standard cured and prepared according to the reference method of PrEN xxx was subjected to freeze-thaw and isothermal frost. Weight changes were recorded after a number of freeze-thaw cycles and after constant freezing, both after thawing and on still frozen samples.

- Freeze-thaw lead to water uptake. No significant effect of the two air void levels was evident.

- The moisture accumulation mechanisms during frost and freeze-thaw are difficult both to identify and to quantify. Therefore, their relative importance is hardly possible to determine, based on theoretical considerations.

- Isothermal frost at –20 ^{o}C initially leads to water uptake, but after a few days, the water uptake disappears again. No significant effect of the two air void levels was evident.

- Letting a frozen specimen melt with water on the top surface lead to moisture loss. This effect was distinct. No significant effect of the two air void levels was evident.

- The net weight change (total uptake minus the loss during thawing) evidently increased with the number of freeze-thaw cycles. This is consistent with previous reports on “pumping effect” of freeze-thaw.

- The zero net (and partly negative) absorption after isothermal frost indicates a certain effect of freeze-drying after the initial absorption. This difference from freeze-thaw behaviour is another indication that the moisture accumulation happens during the cooling, not the thawing phase.

- Even if the net absorption effect of freeze-thaw was evident, the extent of this effect in the mortar investigated was smaller than those reported by other authors on concrete of comparable w/c-ratio. The order of magnitude of the ab- and de-sorption indicate that as much as the upper 10 mm of the sample was involved in the process. This suggests that concrete – with larger aggregates – possess “poorer” ability for the water to be expelled in the heating phase, thus maintaining more water (in air voids) than would the mortar. (See discussion on three-dimensional effect in section 7.3.2.)

- Correspondingly, decreasing the w/c-ratio may reduce the expelling ability during heating relatively more than it does improve the suction resistance during cooling.

- An influence of pre-curing condition was not evident, except perhaps for the freeze-drying close to the surface during isothermal frost. However, the capillary degree of saturation was most probably 100 % for both curing conditions at the initiation of the test. Such high (complete) saturation may ease the suction (and expelling) of water caused by the thermal contraction (and expansion).

- The extent of weight loss on thawing is a strong indication of the thermal contraction and expansion of the air voids being dominant in the external moisture exchange.

- For a mortar with w/c-ratio of 0.48, the relative importance of other moisture accumulation mechanisms appears to be low. This includes suction caused by internal re-distribution. It also includes mechanisms such as capillaries-gel flow and (micro) ice lens pumping. This does not imply that they do not exist, only that they do not appear to cause external suction. They may contribute to maintain water in the structure that was sucked in due to thermal contraction of air voids.

URN:NBN:no-6354

8 Common trends on effect of curing conditions, moisture exchange and materials.

8.1 Objective

The different sections of the present publication constitute separate studies with specific objectives within the main topic “Freeze-thaw resistance of concrete, effect of curing conditions, moisture exchange and materials”. The objective of the present section is to discuss and summarise common trends within these topics. Other issues are discussed in the respective sections.

8.2 Effect of curing condition

8.2.1 General

In section 3, it was observed that the effect of curing type on the freeze-thaw performance was significant. Although the curing conditions investigated in section 3 were different from those of section 4, the same statement is valid, in principle, for the results in both sections. Finally, the relation of laboratory versus field conditions is addressed in section 5.

Curing condition did not influence the degree of deterioration when investigating internal cracking. Thus, the observations below relate to concrete deteriorated by scaling.

8.2.2 Dry curing

The designation “dry curing” in the present context is used for no or little water supply during storage at 20 ^{o}C prior to freeze-thaw testing. It does not include drying at elevated temperature levels or lowering the relative humidity below normal laboratory climate :

Generally, dry curing in section 3 (storing in air after de-moulding at the age of 24 hours) resulted in relatively good performance for the w/(c+s) = 0.45

concrete. This is consistent with the very good performance after plastic curing in section 4 for a broad range of mix design. The plastic curing procedure was intended also to reduce carbonation but may have allowed this to take place for a short period of time during the preparation of the samples (Carbonation may be considered a “protective measure” for portland cement concrete subjected to freeze-thaw ; see section 4.4.2.). If carbonation actually did take place, this would expectedly improve the test performance, but not more than for standard curing. Thus, the important point remains that plastic curing must be considered a “dry” curing condition, since it included water storage between 24 and 48 hours of age only.

In section 3, standard curing according to SS 13 72 44 (or the reference method of prEN xxx) was not used. Hence, the dry curing can not be compared to standard curing in this case. However in section 4, plastic curing led to better performance than standard curing for the investigated range of mix design.

These observations strongly indicate that curing under water for several days is not necessary to develop the properties necessary to withstand freeze-thaw exposure. However, it is important to note that all these observations were made with cements/binders of relatively rapid development of strength : For plastic versus standard curing (section 4), they include cements of strength class 42.5 R. The w/c-ratio varied from 0.45 to 0.70.

The rapid binder types, in addition to the carbonation effect explained above – may be the reason for the different behaviour observed by Lundgren [L 1996] : She found improved performance with standard curing, compared to plastic curing. Her study was made on high strength, but much slower reacting cement with a 24 hours strength level in the range of 50 % of that of the cements used in section 4 of the present study (approximately 10 MPa, compared to 20 – 22 MPa). Also, the present study did not include slag containing cements (CEM II – S or CEM III) that are known to behave differently.

Effect of testing principle

Another dimension of the curing issue relates to the current practice of testing *internal* surfaces. This approach is standard procedure in order to avoid testing of surfaces subjected to (varying) finishing technique or moulded surfaces in contact with de-moulding agent. Thus, instead of obtaining test results sensitive to “minor” changes in finishing technique, the standard procedure is applied to test the “potential” of the actual mix design. Such variation due to “non-repeatable finishing” is frequently observed for concrete products [R 1995]. Still, such variation does in fact represent the scatter in performance of the product as such. On the other hand, for laboratory made samples of ready mixed concrete, this is hardly the case. However, the approach of testing internal surfaces makes the test results less sensitive to lack of curing of the outer concrete layer as well. In other words, poor curing affecting the concrete surface negatively may not be reflected in the freeze-thaw test due to the procedure : The internal surface apparently is properly cured in any case.

Alternatively, a solution for investigating the curing effect is to saw the test surfaces after a short time, and then provide different curing to the test surfaces.

Consequence of water curing

Provided that the curing conditions are sufficient for (the internal part of ;) the investigated mix design, prolonged water curing will increase the degree of saturation of the concrete. At the age of two to seven days (plastic curing versus standard curing), the water uptake of concrete within the mix design range included in this study certainly is affected by water storage. (With high strength concrete (lower w/c-ratio) on the other hand, this may not be the case – or self desiccation leads to consumption of pore water more rapidly than the water ingress.) Hence, longer water curing than to secure hydration contributes to higher overall degree of saturation. Still, this does of course not suggest that water curing should be rejected, it is a matter of optimising the positive effect of water curing and the negative effect of high saturation. See section 8.2.6 for discussion of field relevance.

8.2.3 Drying at elevated temperature

In section 4, the test surfaces were subjected to drying at 40 ^{o}C just prior to re-saturation and testing. In all cases, except for silica fume concrete, this resulted in substantially increased freeze-thaw scaling. For silica fume concrete, this was not the case, even if the moisture loss during drying compared to other types of curing was in the same range for silica fume concrete as for “pure” portland cement concrete.

The fact that the relative weight changes remained at the same level, confirms that the structure of silica fume concrete is more resistant to dry/wet-treatment, see also section 8.4. In the present section, with focus on effect of curing : The different freeze-thaw resistance (between silica and non-silica concrete) after 40 ^{o}C drying - in spite of similar behaviour with respect to weight changes – suggests that this type of drying affects the structure of concrete without silica fume much more severely.

The generally severe damage after 40 °C drying followed a pattern of high water uptake during re-saturation. It was not possible to obtain good data on water uptake during freeze-thaw on these samples, due to the severe scaling.

8.2.4 Combined wet and dry curing, including standard curing

Various curing procedures

Cyclic curing (C3) in section 3 combined three weeks of initial air storage with one week of immersion, this combination being repeated three times prior to freeze-thaw. This procedure resulted in test results very close to those of dry curing (C2), at least with the more rapid hardening cement and without silica fume.

The other wet/dry combination, four weeks of water storage followed by four weeks of air storage, tended to yield poorer scaling results than the dry or cyclic curing procedure. Following the discussion of proper curing above, it appears that water storage during the first few weeks is more negative than later, repeated water storage. It should be pointed out that the initial water storage coincides with the major chemical reactivity, when chemical shrinkage will promote water uptake. It should be investigated whether initial water storage leads to a higher overall degree of capillary saturation prior to freeze-thaw testing than water storage at a later time.

In section 3, with the slower reacting cement or with silica fume, cyclic curing (C3) yielded higher scaling than dry curing (C2). In several cases, the damage also exceeded that of four weeks water storage followed by four weeks of air storage. Attempts were made to investigate whether the observation with the slow reacting cement was accompanied by a coarser capillary structure. This might explain a higher influence on the capillary degree of saturation when exposed to late stage water storage, compared to the faster reacting cement. However, these attempts failed.

In section 4, the modified standard curing combines one week of water storage with subsequent sawing and then three weeks of air storage. This procedure lead to increase of scaling in nearly all the cases compared to standard curing, also for silica fume concrete. Even if the prolonged carbonation period prior to freeze-thaw might be expected to increase the resistance, the total effect obviously was negative : Three weeks of drying of the test surface lead to drying, increased moisture uptake during re-saturation and during freeze-thaw, and increased scaling. It is reasonable to believe that modified standard curing lead to structural changes that affected the properties negatively, including that of silica fume concrete. Low temperature calorimetry has demonstrated clearly that dry/re-wetting treatment of concrete leads to a coarser pore structure. The effect depends strongly on the drying procedure and duration.

<u>Standard curing</u>

Standard curing according to the reference method of prEN xxx combines water curing until the age of seven days with air storage until sawing at 21 days. Thus, the much later sawing and exposure of the test surface to drying in “laboratory climate” is the only difference from modified standard curing (section 4). It appears evident that the reduced drying of the test surface of standard curing leads to less water uptake during re-saturation and during freeze-thaw, as well as (somewhat) lower scaling.

Standard curing may be considered to be a practical compromise, securing proper curing of concrete with slow reacting binders (See discussion in section 8.2.2 about plastic curing). It should again be pointed out that the water uptake during the initial week of water storage depends on both chemical activity and the change in permeability in this period. Thus, the capillary degree of saturation after the one week of water storage depends strongly on the mix design. Even more important, postponing the water storage to a later stage would be expected to rate concrete of various compositions differently with respect to degree of saturation prior to freeze-thaw.

8.2.5 Ageing

One year of air storage after initial water, dry or cyclic curing was found to be negative for freeze-thaw resistance whenever differences in the scaling results were significant. The negative effect depended on mix design. Proper air void structure prevented ageing effect and silica fume also reduced the negative effect. It is important to note that the atmospheric exposure of the sample test surface was equally long in both cases, and that the ageing process most probably was due to drying and structural changes not involving carbonation.

Unfortunately, it was not investigated whether the (negative) ageing effect on scaling coincided with increased water uptake during re-saturation or during freeze-thaw.

8.2.6 Field exposure

All mixes included in the field exposure test (section 5) showed none or only very slight surface damages after two winter seasons at the exposure site. No signs of cracks or internal damages were observed. It is considered too early to conclude about the actual field performance of these mixes.

Still, the number of freeze-thaw cycles in the sense of crossing the zero on the Celsius scale amounted to 70 during the first winter (section 5.2.2), compared to the standard, initial laboratory test of 56 cycles – over a broader temperature range. Also, the limited investigation on capillary degree of saturation indicates levels below 90 %, meaning that the samples are actually in a “dry” or drying state. This was consistent with findings of Relling [R 1999] on bridge piers in western Norwegian coastal climate. The laboratory procedure on the other hand, increases the degree of capillary saturation through the pumping effect (freeze-thaw pumping of water into the concrete). This strongly points to the laboratory procedure of continuously having salt solution on the test surface as being too severe relative to field exposure.

While the initial laboratory tests resulted in very differentiated behaviour with respect to scaling, the field observations so far showed nearly identical – and excellent – performance. It is reasonable to attribute the “difference in differentiation” to the fact that the degree of saturation is quite different for the two different conditions.

Again, it is relevant to question the field relevance of initial water storage and continuous moisture exposure during freeze-thaw (no “breathing”). Even if it may be considered a relevant way of accelerating the field conditions : It becomes reasonable to question whether the laboratory testing (or curing ;) procedure accelerates the field conditions for different concrete composition in a fair way, see end of section 8.2.4. Of course that depends on the field exposure. It probably is too tough for vertical (field) exposure, possibly also for horizontal surfaces.

8.2.7 Summarising on curing

The curing regime strongly affects the results of the freeze-thaw testing :

Dry curing, i.e. storage with no or little water supply prior to freeze-thaw testing resulted in relatively good performance - and better than the standard curing according to prEN xxx. It also appears that postponing the water storage period in time (closer to the actual freeze-thaw exposure !) results in improved freeze-thaw performance – probably because of smaller water suction in this period.

It is suggested that initial water curing – right after de-moulding - for longer than a very short period of time (24 hours ?) will not promote the curing significantly, but only increase the initial degree of saturation. This early age water exposure and increased degree of saturation does not comply with modern construction practice, where the concrete generally is protected against moisture loss by the formwork or application of curing compounds.

Sawing the test surface right after water storage (at 7 days in stead of 21 days), and then subjected to drying at the prescribed laboratory climate, lead to increased freeze-thaw scaling as expected.

Drying at elevated temperature confirmed previous studies reporting substantial increase in freeze-thaw scaling, but less so for silica fume concrete.

The found effects of curing are partly a consequence of the testing principle, investigating internal surfaces. Even if this principle is applied for good reasons, it leads to smaller effects than if the various treatments were applied directly to the test surfaces. Still, this does not impair the conclusions above, but leads to a discussion of what is the most relevant way to treat laboratory tests, in terms of field relevance.

8.3 Moisture exchange

8.3.1 General

Moisture exchange related to the curing regime was obtained in section 4 only. Various kinds of water exposure were included in section 3 as well, but exact data on moisture uptake and ~loss were not obtained. Moisture exchange specifically during freeze-thaw was investigated in section 7. Section 6 provided background information on the link between curing procedures and the degree of saturation prior to freeze-thaw.

8.3.2 Moisture uptake during water curing

The water uptake during 7 or 31 days of water curing was sufficient to increase the capillary degree of saturation from approximately 90 % to 100 % for a w/c = 0.45 mortar. These test results were obtained from 2 cm thick samples subjected to chemical shrinkage measurements. Water storage also led to some water absorption in the air voids.

This confirms the suggestion in section 8.2.6 that water curing for several days after de-moulding will lead to a water uptake largely controlled by the chemical shrinkage. Large dimensions or low permeability may lead to more or less water uptake than corresponding to the chemical shrinkage.

The lack of scaling gradients across the test surfaces as a result of the different curing regimes applied in section 3 suggests that “critical” moisture gradients – from the exposed surface to the internal test surface - did not arise : The initial four weeks of water curing (C1) may have lead to an overall and high degree of saturation, water uptake being controlled by the strong suction due to chemical shrinkage. The cyclic dry and wet curing (C3) did not include water storage until the age of three weeks. At such a late stage, any water uptake may have been at such a low level - or produced gradients – so that the effect was overshadowed by the subsequent re-saturation. The effect on scaling then must have depended on material characteristics controlling the actual degree of saturation.

8.3.3 Moisture changes before freeze-thaw testing

The moisture loss very much depended on the curing regime : Plastic curing naturally produces very low moisture loss both prior to and during preparation. The moisture uptake during re-saturation was in the same range as the previous moisture loss. All comparable values were considerably lower than those of standard curing.

The sample treatment lead to geometric effects, complicating the comparison of weight losses between the series. Except for the plastic curing (see above), the samples were subjected to moisture loss from the cylinder surfaces in the curing period from 7 to 21 days. Only for the “modified standard”, was this weight loss included in the presented weight loss values.

Sawing at an early age and storing at 20°C and 65 % RH (modified standard curing) produced substantial moisture loss, ranging from 1.2 to 2.1 % of the initial sample weight. These values corresponded to 15 – 25 % of the initial water content, or 39 – 46 % of the evaporable water (for simplicity : water consumption corresponding to 70 % hydration of the cement/clinker, none from the pozzolanic reaction). These values are not corrected for absorption taking place during the few days of water storage after de-moulding. Still, they illustrate that the moisture loss is significant. The total weight loss of the samples was three times that of the one caused by drying from the test surface for 72 hours at 40 °C (i.e. at approximately 15 % RH). Correcting for the geometrical effects, the moisture loss from the test surface may have been of the same order for modified standard curing and intensive drying.

The re-saturation of modified standard and intensive drying was in the same range. It amounted to approximately 80 % of the weight loss during intensive drying, a little more for the higher w/c-ratios, a little less when air-entrained.

The weight loss of modified standard during the period of preparation was significantly lower than for that of standard curing. This fact illustrates that the previous moisture loss of modified standard curing had been considerably higher. Correspondingly, the re-saturation for modified standard generally was almost twice as high as that of standard.

Generally, there was no simple relation between the (one face) weight loss in the period between preparation and re-saturation – and the (one face) suction during the re-saturation. This indicates that how the concrete is subjected to moisture loss is more important for later water uptake (and freeze-thaw properties) than the amount of moisture loss itself.

Gradients

The various moisture exchange patterns prior to freeze-thaw testing did not lead to scaling gradients across the test surface for any of the treatments applied in this study. From the experience of the present author, gradients only arise when concrete of poor (freeze-thaw ;) quality – or (as a consequence ;) poor preparation - allows penetration of the test solution along the edges of the samples.

8.3.4 Moisture changes during freeze-thaw

Uptake in and loss from laboratory samples

The studies in sections 4 and 7 confirm water uptake during freeze-thaw. The water uptake increases with the number of freeze-thaw cycles. Even for isothermal frost, absorption during the freezing period was demonstrated, but continued frost appeared to lead to a certain (freeze-) drying.

During thawing, a moisture loss was demonstrated. This was surprising and has not yet been demonstrated by other studies to the knowledge of the present author. Still, the observations – made on a large number of samples - were clear and have to be considered. The moisture loss during thawing was less than the absorption during freeze-thaw. Considering from a theoretical point of view the different mechanisms possibly responsible for the “pumping effect” during freeze-thaw, makes this phenomenon reasonable :

The study in section 7 strongly indicates that the thermally induced pressure drop / increase in the air voids – and certain three-dimensional effects – are the main reasons responsible for the accumulation of moisture. Theoretically, the thermally induced pressure effect would depend on the air void content of the concrete. No such relation was demonstrated, but this may be due to the relatively high air void content of the non air entrained mortar investigated in section 7 : The water uptake and ~loss in both cases (both air void levels) were smaller than the calculated values based on a certain, effective sample thickness. Suction of air from the lateral or bottom surfaces may have contributed to the re-establishment of equilibrium within the samples before the “potential water suction” from the top surface could be completed.

No other mechanism responsible for water uptake, loss or internal re-distribution for the non damaged samples in section 7 could be demonstrated, see discussion in section 7.4.6.7.

For concrete suffering from a certain freeze-thaw damage, a correlation between the scaling level and the absorption during freeze-thaw was demonstrated. The correlation also included the accumulated absorption during re-saturation and freeze-thaw. The correlation was demonstrated for the various curing regimes applied in section 4, but not for intensive drying.

Weight changes in the field samples

The weight changes of the field exposed samples (section 5) were not clear. Some series gained weight, while others lost weight during the first winter of exposure. This may be due to different moisture state of the samples when subjected to field exposure : Some series may have been in a dryer state than others. Hence, the weight change versus volume change during the first winter can not be used to indicate whether a general water uptake or moisture loss took place. (Weight loss may be due to moisture loss or scaling. Volume reduction may be due to scaling or shrinkage. Volume increase may be due to swelling (moisture uptake) or internal cracking.)

Effect of type of re-saturation

For some of the mixes tested with 3 % NaCl on the surface, the preceding re-saturation by water produced larger absorption during freeze-thaw than that of re-saturation by 3 % NaCl (section 4). However, the effect was not consistent. Testing with pure water on the surface, the picture was quite mixed. The higher absorption in the first case may be attributed to higher degree of scaling when re-saturated by water, i.e. higher deterioration (cracking ?) causing absorption.

Investigating internal damage on (the durable ;) mix 3 in water, did not result in more cracking when re-saturated by water, even if the absorption during freeze-thaw increased. On the contrary, the ultrasonic pulse velocity exhibited better development in this case. With the less durable mix 5, the cracking clearly progressed independently of the type of re-saturation.

8.4 Effect of materials

8.4.1 General

The sections 3, 4 and 5 all included a range of concrete mix design, including a selection of concrete constituents such as cement types, silica fume and admixtures.

8.4.2 Effect of silica fume

The effect of silica fume on laboratory test results was generally positive. “Secondary effects” like change of air void characteristics did not disturb these observations (section 3). However, the effect seems to depend partly on the type of cement, the positive effect being pronounced with relatively rapid hardening (but still “standard” ;) cement. The improved performance seemed to be accompanied by reduced pore volume in the 10 – 30 nm range, but such pore structure investigations were too limited to draw conclusions on this point.

The effect of silica fume on the test performance after one-year indoor ageing was positive in the majority of cases. However, again it was demonstrated that the effect of silica fume depended on the type of curing and on the cement type. Larger positive effect was found with a “standard” CEM I 42.5 R cement and cyclic dry and wet curing than with the low alkali, high strength cement. However, in the cases of little positive effect of silica fume, the total scaling level was generally low.

The positive effect of silica fume demonstrated in section 3 was confirmed under different curing conditions in section 4. The increased freeze-thaw resistance coincided with lower moisture loss and uptake prior to and during freeze-thaw.

Silica fume (4 %) had no clear effect together with the CEM II/A-V (fly ash) cement at w/(c+2s) = 0.42 – compared to the positive effect of using silica fume together with pure portland cement. This was possibly due to the slower reaction of the fly ash, compared to that of the cement clinker, and possible interference in reaction rate between the two pozzolanic materials.

So far, the positive experience with silica fume from laboratory testing could not be confirmed by the field exposure, since all field exposed samples until now performed very well.

8.4.3 Effect of cement type

The study confirmed particularly good freeze-thaw performance of a specific low alkali, high strength cement (CEM I 42.5 BV-SR-LA) in laboratory testing, compared to that of a “standard” cement (CEM I 42.5 R). This was particularly true when the concrete did not have a proper air void system. The observations confirm reported work from Sweden [M 1990] but have never been explained, nor is it in the present study. The investigation (section 3) did not include comparable measurements of moisture uptake during re-saturation or freeze-thaw.

The pure portland cements included in section 5 appeared to perform well in the laboratory tests with proper air void characteristics.

Fly ash cement concrete (air entrained) exhibited increased moisture exchange with the surroundings and somewhat increased scaling compared to portland cement concrete. Still, there are indications that this is an early age phenomenon caused by the slower reactivity of the fly ash. The phenomenon addresses the question of early age testing (and curing procedure) of composite cements – or slowly developing concrete in general.

The field exposure of the concrete with different cements did not yet reveal differences in performance – such as found in the initial laboratory test. One reason probably is that the exposure period was only two years so far ; all exposed concrete performed well.

8.4.4 Air void characteristic

Air void structure still appears to be the most important parameter for freeze-thaw performance of concrete with w/c-ratio of 0.35 or above. In the mix design investigation of section 5 with no water/binder ratio above 0.45, air void spacing factor in the range of 0.4 or less appeared vital to ensure good performance in the laboratory testing. Only air-entrained concrete within this design range should be used in practice, based on general laboratory investigations.

These results were not yet confirmed in the field exposure test. Further research on the issue is still on-going.

8.4.5 Other effects of mix design

w/c – ratio

Increasing the w/c-ratio in all cases (section 4) increased the moisture exchange prior to and during re-saturation. It also increased the uptake during freeze-thaw testing as well as scaling (or internal damage, when relevant), as expected.

Use of superplasticizer

There are indications (section 5) that high superplasticizer dosage may also increase the spacing factor from the fresh to the hardened state of the concrete. This observation may also be caused by the characteristics of the applied testing methods : It is difficult to separate the influence of the testing method on the air void parameters and what is actually real change in parameter value from fresh to hardened state. Still, comparing the test methods suggests that the effect is real.

In section 3, addition of superplasticizer (together with silica fume) did to some extent affect the air void characteristics negatively (all air void parameters obtained by ASTM C 457). Comparing two different cements, the effect was observed for the one with higher water/HRWRA dosage requirement, not with the other one. Again, this suggests that excessive amounts of superplasticizer should not be used.

There also were strong indications from section 5 that high amounts of superplasticizer in some series lead to less homogeneous mortar phase or paste. Such phenomenon may cause internal bleeding and poorer aggregate-paste inter-phase, change the pore size distribution and the moisture uptake properties. Thus, it may indirectly change the freeze-thaw resistance, as observed.

8.5 Conclusions

The conclusions of this section constitute the main conclusion of the present publication. They are separated/included in section 10.

9 Suggestions for further research

9.1 Objective

The objective of this chapter is to identify some key areas of further research. However, not all the questions raised in the previous sections are addressed below. Additional ideas or points of view on the issue of further research may be indicated in the conclusions of those sections.

9.2 Moisture exchange during freeze-thaw testing

The test results on moisture exchange - especially the moisture uptake during freezing versus moisture loss during thawing - should be verified :

Supplementary temperature cycling without freezing – with similar measurements as above on saturated samples of the same quality - would be one approach. If freezing appears necessary, the observed phenomenon is not a pure thermal effect. Accumulated weight changes with or without freezing were investigated by [R 1999]. They demonstrated large water uptake during freeze-thaw – but none during cycling between +20 and +2 ^{o}C with salt solution on top. The results were not (yet) published.

The influence of material design on moisture uptake/loss-relation should be determined, including the effect of w/c-ratio and mortar versus concrete :

The major moisture loss during thawing of the mortar investigated occurred in less than one hour and thus indicates a rapid interaction with the external environment – at least close to the surface. The critical property was probably the ability of thawed water to escape from the interior (close to the surface), not the thawing process itself or the related air void pressure increase. As already argued, the kinetics of this process may be different with a larger maximum aggregate size. This may be caused by higher uptake in concrete through the porous inter-phase zone or “tortuosity effect”, the latter reducing the amount of expelled water.

With concrete (instead of mortar) or with lower w/c-ratios, the cooling and heating rate may be parameters influencing the net absorption (absorption during freezing minus de-sorption during thawing) :

The driving force of any effect of “mass change due to contraction of air voids” is the pressure difference arising from the cooling/heating process. If – during cooling – pressure relief can not take place before the surface water freezes, no more water can be absorbed. During heating, moisture exchange is possible during the entire thawing period. With permeability being a critical property, the potential “exchange layer thickness” is expected to decrease with decreasing w/c-ratio. Indirectly, this is controlled by the duration of the driving force, i.e. the freeze-thaw cycle.

For the material design matrix investigated in Section 4, a relation between (net) absorption and scaling was found. (The net effect recently was reported also by other researchers [B 1999].) This comprised w/c-ratios of a medium to high level. At least from a theoretical point of view, the absorption might be related to scaling in one material quality range and to internal damage in another range. The reason for this is that internal damage (in pure water) and surface scaling (in saline water) appear to be characteristic damages within different w/c-ratio ranges. Damage in both cases is believed to be closely related to the moisture absorption. (Note that, particularly at low w/c-ratios water absorption may enable additional cement hydration and not necessarily indicate a correspondingly increased degree of saturation.) Hence, the relation between damage and moisture uptake leading to and/or caused by damage probably differs with e.g. the w/c-ratio, depending on the actual degradation.

9.3 Laboratory versus field

Generally, it has not yet been possible to identify the mechanisms critical to degree of deterioration, and these may vary with material design and environmental conditions. It is thus important to increase the focus on laboratory versus field performance. At present, it is not even documented whether practical deterioration under field conditions is a declining, linear or progressive function of the elapsed time (environmental conditions assumed “constant”). In laboratory testing, all these patterns may be found. It would be very valuable for the assessment of field-laboratory relation to map the degradation vs. time of field exposure for a variety of material parameters. Such data are expected partly to be provided by [U 2002] :

The lab-field study reported in Section 5 – and the framework of which Section 5 is a part - will be continued. However due to the material-environmental interaction that determines the internal moisture conditions, it is crucial to consider further the access of external liquid during the exposure. The low capillary degree of saturation determined in field suggests that continuous and long-term freeze-thaw in wet state (as is done in lab testing) is not realistic. Alternative approaches are non-continuous moisture access or limitation of the number of freeze-thaw cycles. Anyway, the field vs. laboratory deterioration study should be supplemented by comparing the moisture conditions of the two expectedly, principally different exposure conditions. This should include both the surface layer (when scaling is relevant) and the internal moisture condition (for scaling and internal damage).

Further due to the material-environmental interaction, it is reasonable to believe that a specific test procedure may provide varying degrees of severity for different material qualities – compared to field exposure of the same material. An implication is that different test procedures presently being used probably favour certain material design/characteristics and may even rank them in a different way. Studies as outlined above may provide useful information in the selection and qualification of testing procedures and fair ranking of materials.

Artificially - but controlled - increasing the degree of saturation when testing freeze-thaw in the laboratory may be considered an appropriate way of accelerating the process. Accelerating is after all what laboratory testing of durability is all about. The reported lack of frost resistance when testing non-air-entrained, high strength concrete – with certain testing regimes only - has not yet been demonstrated under field conditions. An approach in the direction of controlling realistic moisture levels might explain such discrepancies, see below.

Hence, the main issue of this section is field service vs. laboratory moisture condition. Investigating this on a broad basis of material and environmental parameters as a function of time appears a feasible approach.

9.4 Initial moisture state

Concrete of different w/c-ratio submitted to standard pre-testing curing conditions will “experience” different degree of saturation at the initiation of the freeze-thaw test. The water uptake during water storage is to a large extent controlled by the chemical shrinkage in this period but also depends on the permeability (development).

An approach to securing “equal conditions” prior to freeze-thaw testing could be based on the development of formula AI-7 in appendix I : Given the w/c-ratio and (estimated) the degree of hydration, the amount of externally supplied water to bring the sample to a defined, average degree of saturation could be calculated. Bringing samples to a fixed degree of saturation (Actual degree of saturation would have to be verified.) – prior to a short procedure (1 – 3 days) of equal exposure (= “re-saturation”) could be a “fair” approach for testing and ranking of new materials. However if feasible, it would only apply to concrete of medium to high w/c-ratios due to difficulties in establishing equilibrium.

Still, even if the initial degree of saturation is important, the continuing “pumping” of water into the structure during the performance of the test appears the most critical feature. This feature of the test(s) probably remains the key property to be addressed concerning its field service relevance.

9.5 Material design development

The industry takes a major interest in developing more sustainable concrete mix design, using recycled material and reducing emissions. Such materials are likely to exhibit a slower development of durability and moisture exchange properties. Generally, the length of curing before testing should be considered accordingly. Specifically, the effect of water curing on the initial moisture state should be considered (section 9.4 and 8.3.2).

Even more important, the porosity and the moisture mechanics properties in the “mature state” are likely to deviate from those of traditional portland cement concrete. Thus, appropriate moisture conditions during testing become crucial to the application of such materials. Moisture exchange properties of such materials should be determined and compared to those of portland cement concrete.

An increased range in material properties leads to differentiating in the application of these materials, based on (the classification of ;) local environmental conditions – e.g. as described in the new EN 206. However, there is a general lack in experience, preventing differentiation of acceptance criteria to be applied for testing. Again, we are back to the missing laboratory versus field correlation. This remains the key issue to enable the development and documentation of new concrete materials.

10 Conclusions

10.1 Objective

The objective of this chapter is to point out the main findings of the present publication. However, not all the conclusions of the previous sections are addressed below. Additional points of view on the issue may thus be found in those sections. The issue of chemical shrinkage is a “secondary issue” in the main context and is not addressed in the present section – the conclusions are given in Section 6 only.

10.2 Curing and ageing

The following conclusions concerning the general influence of curing on freeze-thaw damages may be drawn :

- The effect of curing type on the freeze-thaw performance was significant.

- Dry curing, i.e. storage with no or little water supply prior to freeze-thaw testing resulted in relatively good performance : When directly compared to standard curing of the reference method of [prEN xxx], dry curing resulted in better performance together with the investigated “rapid” hardening cements.

- It appears that postponing of the water storage period in time – i.e. closer to the actual freeze-thaw exposure – results in improved freeze-thaw performance.

- It is suggested that initial water curing – right after de-moulding – for longer than a very short period of time will not promote the curing significantly – at least with respect to freeze-thaw resistance. In stead, it will increase the degree of saturation during the water storage period. It is questioned whether this procedure of increasing the degree of saturation is compatible with modern construction practice. It is also questioned whether it applies to new, composite binders with different property development.

- Sawing the test surface right after water storage (at 7 days instead of 21 days of age) and then drying at the prescribed laboratory climate, lead to increased freeze-thaw scaling.

- Drying at 40 ^{o}C (at the same time lowering the relative humidity to approximately 15 % RH and applying a high wind speed) for three days prior to freeze-thaw confirmed previous reports on substantial increase in scaling, but less so for silica fume concrete.

- The general effect of indoor ageing (testing after one year of air storage) was negative compared to initial testing, however not important enough to be significant for concrete with a proper air void system. Silica fume reduced the negative effect of ageing.

10.3 Moisture exchange ; General

The investigations on curing was used – together with specific studies on the subject – to elucidate phenomenon related to moisture exchange. The following conclusions from the moisture exchange investigation may be drawn :

- No direct relation between moisture loss during curing – for different curing regimes – and water uptake during “re-saturation” or freeze-thaw could be found.

- A correlation between scaling and water uptake during freeze-thaw was indicated. The correlation also applied to accumulated water uptake during re-saturation and freeze-thaw. This was in spite of no direct correlation between water loss prior to and uptake during re-saturation.

- No parallel relation (to the one above) between internal cracking and water uptake was found. The degree of internal cracking varies widely between parallel samples, indicating a more arbitrary deterioration process in this case.

- After 7 or 31 days of water storage, the capillary degree of saturation for a mortar of w/c = 0.48 is close to 100 %. Continuous water curing even lead to 1 – 3 % water in the air voids, depending on air void content. Comparably, isolated curing would yield values around 90 %.

- Plastic curing (sealed in plastic) lead to very low moisture loss, which was easily regained during the re-saturation. Sawing at an early age (at 7 days of age in stead of the standard 21 days) lead to loss of nearly half of the evaporable water prior to re-saturation and freeze-thaw testing. Only a fraction of this was regained during re-saturation. Due to the test set-up, it was not possible to detect the degree of re-filling in this case. Intensive drying similarly leads to substantial weight loss, and only 80 % of this loss was regained during re-saturation prior to freeze-thaw testing.

- None of the tested curing conditions leads to gradients in moisture / degree of saturation that resulted in scaling gradients across the test surface of the samples.

10.4 Moisture changes during freeze-thaw

- No single mechanism can alone account for freeze-thaw damage to concrete. Several mechanisms occur simultaneously, and it is not possible to calculate the degree of damage based on knowledge of mechanisms, material characteristics and exposure data. This statement is in line with previous findings.

- Since water uptake during freeze-thaw cycling has been demonstrated in several studies the last years, the mechanisms for such water uptake has been speculated on. The present work demonstrated that water uptake occurs during cooling and that the opposite actually happens during heating ; water is expelled from the (salt solution covered) concrete surface, provided that the moisture content is high enough. This is a new finding and has not previously been reported to the knowledge of the present author.

- The previous finding of water expulsion during heating – as well as other considerations – suggests that thermally induced pressure changes of the air voids is the mechanism mainly responsible for the water uptake during cooling. However, this should be further verified.

- While the water uptake is a uni-axial process through one surface, the water expulsion and re-distribution during heating is a three-dimensional phenomenon. This probably leads to a gradual accumulation of moisture within the concrete, causing a net weight increase for each freeze-thaw cycle.

- The net weight increase of the mortar was less than the net weight increase on concrete with similar composition reported by other researchers. Higher net uptake by concrete may be attributed to a) larger absorption via the porous inter-phase zone and/or b) reduced loss during thawing due to the larger aggregate size and increased probability of the water not being expelled from the samples during thawing.

10.5 Laboratory versus field performance

A correlation between field performance and laboratory testing is vital to rank and evaluate concrete correctly. The following conclusions may be drawn on this issue :

- All exposed concrete mixes had none or only very small visible surface damages after two winters of field exposure. No cracks or internal damage was evident. This applied whether the specific mix design performed well in the initial laboratory test or not.

- It is considered to be too early to conclude on the laboratory versus field performance. Thus, the final answer remains to be seen. The laboratory testing data will provide a solid basis for investigating such a relation.

- However, limited measurements of the capillary degree of saturation of field samples suggest that the field conditions are relatively dry compared to laboratory testing conditions.

- It is considered that concrete passing the laboratory testing will perform well under field conditions. If the laboratory testing conditions provide a significantly higher degree of saturation than may be relevant for field conditions, this may exclude good materials from practical use. The effect may at least partly be one of porosity properties : Artificially high degree of saturation when exposing high strength concrete to rapid freeing and drying may be the reason for apparent deviation between laboratory testing and experience from field service.

10.6 Material

Amongst the effects of concrete material characteristics or mix design on freeze-thaw test performance, the issues below are pointed out. However, it must be kept in mind that the laboratory results have not yet been confirmed by the field exposure :

- Only air entrained concrete performed well in laboratory freeze-thaw testing, even with a w/c-ratio of 0.35. With the w/c-ratios investigated, i.e. 0.45 and below, spacing factor in the range of 0.4 or less appears vital to ensure good performance.

- The positive effect of silica fume on freeze-thaw resistance from earlier reports was confirmed. This concerns both effect of early age drying on scaling and generally less moisture exchange prior to and during freeze-thaw. The effect depended somewhat on cement type.

- The effect of silica fume on (indoor) ageing was positive in the majority of cases. However, it was demonstrated that the effect of silica fume depended on the type of curing and on the cement type. Larger positive effect was found with a "standard" CEM I 42.5 cement and cyclic dry and wet curing than with a low alkali, high strength cement.

- The study confirmed earlier reported evidence on especially good freeze-thaw resistance with a particular SR-LA cement (Section 3). The effect of the cement was pronounced at low air void levels. There are clear indications of favourable air void characteristics with this cement or cement-admixture combination compared to that of the CEM I 42.5 R cement. Still, the differences observed, e.g. from ageing, suggests that the difference in performance can not be attributed to air void characteristics only. With a proper air void system, also the standard cement performed well. Similarly, another CEM I SR-LA and a CEM I LA 52.5 R cement appeared somewhat superior to a CEM II/A-V 42.5 R cement, but all cements performed well with a given air void system (Section 5). It should be pointed out that the somewhat poorer performance in the laboratory test by the fly ash cement may be due to the slower reactivity of the fly ash, and thus probably is time dependent. This addresses the curing procedure.

- Addition of high amounts of superplasticizer to mixes of high water demand did to some extent affect the air void characteristics or paste homogeneity negatively. This occurred both with (Section 3) or without (Section 5) silica fume and indicates a relevance of fresh concrete properties on the microstructure, and hence on durability properties.

URN:NBN:no-6354

11 REFERENCES

11.1 Literature

A 1986	Aitcin, P.-C.; Pigeon, M.: "Performance of Condensed Silica Fume Concrete used in Pavements and Sidewalks", Durability of Building Materials, No. 3, 1986, pp 353-368.
A 1997	Auberg, R.; Setzer, M.J.: "Influence of water uptake during freezing and thawing", Paper in "Frost Resistance of Concrete", pp 232-245, Rilem Proceedings No. 34, ISBN 0 419 22900 0, Chapman & Hall, London, 1997, 356 p.
A 1998	Auberg, R.: "Zuverlässige Prüfung des Frost- und Frost-Tausalz-Widerstands von Beton mit dem CDF- und CIF-Test" *("Reliable testing of frost and freeze-thaw resistance of concrete with the CDF- and CIF-test")*, Dr.-thesis at the University of Essen, 1998, ISBN 3-8265-4716-0, 248 p. (in German).
B 1966	Barrow, G.M.: "Physical Chemistry", McGraw-Hill Book Company, New York, 2nd edition, 1966, Library of Congress Catalog Card Number 65-25914, 843 p.
B 1986	Bager, D.; Sellevold, E.J.: "Ice formation in hardened cement paste, Part I – Room temperature cured paste with variable moisture contents", Cement & Concrete Research, Vol. 16 (1986), pp 709-720.
B 1986b	Bager, D.; Sellevold, E.J.: "Ice formation in hardened cement paste, Part II – Drying and re-saturation on room temperature cured pastes", Cement & Concrete Research, Vol. 16 (1986), pp 835-844.
B 1987	Bager, D.; Sellevold, E.J.: "Ice formation in hardened cement paste, Part III – Slow saturation of room temperature cured pastes", Cement & Concrete Research, Vol. 17 (1987), pp 1-11.
B 1997	Bremseth, S.K.: "Tynnslipsanalyse av betongprøver fra serie Borås" *("Thin section analyses of concrete specimens from the Borås testing series")* Project report Norcem A.S 9D4/R97030, Brevik, Norway 1997, 12 p. (in Norwegian).

B 1999 Bager, D.; Jacobsen, S.: “A conceptual model for the freeze-thaw damage in concrete”, Proceedings of the 3rd Nordic Research Seminar in Lund on Frost Resistance of Building Materials, Lund Institute of Technology, Division of Building Materials, Report TVBM-3087, Lund, 1999, pp 1-18.

B 1999b Boivin, S.; Acker, P.; Rigaud, S.; Clavaud, B.: “Experimental assessment of chemical shrinkage of hydrating cement paste”, Proceedings of the International Workshop on Autogenous Shrinkage of Concrete, Hiroshima, June 1998, Published by E & FN Spon, London/New York, 1999, ISBN 0-419-23890-5, pp 81-92.

B 1999c Bager, D.; Hansen, T.B.: “Influence of Water Binding on the Ice Formation and Freeze/Thaw Damage in Cement Paste and Concrete” (Draft version), Nordic Miniseminar on Water in Cement Paste and Concrete – Hydration and Pore Structure, Skagen, Denmark, Oct. 1999, 13 p.

B 1999c Bremseth, S.K.: “Tynnslipsundersøkelse av prøver laget i forbindelse med bestemmelse av kjemisk svinn” *(“Thin section analyses of samples manufactured for the determination of chemical shrinkage”)*, Norcem R&D Report 9D4/R99039, Brevik, 1999, 14 p. (in Norwegian).

B 1999d Bjøntegaard, Ø.: “Thermal Dilation and Autogenous Deformation as Driving Forces to Self-Induced Stresses in High Performance Concrete”, Dr.Ing. Thesis 1999:121 at the Norwegian University of Science and Technology, Trondheim, 1999, 256 p.

C 1966 Cordon, W.A.: “Freezing and Thawing in Concrete – Mechanisms and Control”, ACI Monograph Series No. 3, 1966, pp 23-41.

C 1992 Canmet/ACI 1rst – 4th International Conference on Fly Ash, Silica Fume, Slag and Natural Pozzolans in Concrete : Montebello/Québéc 1983 (ACI Special Publication SP-79) ; Madrid 1986 (SP-91) ; Trondheim 1989 (SP-114) ; Istanbul 1992 (SP-132).

C 1999 CCRL : “Rapid Method Chemical Analyses, Portland Cement Proficiency Samples Number 133 and Number 134. Final Report”, Cement and Concrete Reference Laboratory, The Nat.Inst. of Standards and Techn. (NIST), Gaitersburg, Maryland, USA, Sept. 1999, 13 p.

D 1960 Danielsson, U.: Discussion to a paper on Frost Actions in Concrete by P. Nerenst at the 4th Int. Symp. on the Chemistry of Cement, Washington D.C., 1960, Conf. Proceedings, Vol. II, pp 833-834.

D 1995 Dansk Beton Teknik : “Retningslinjer vedrørende brug av DBT friskporemåler” (“Directions for the use of DBT fresh concrete air void analyser”), Supplement to manual and training in the use of the testing equipment, Dansk Beton Teknik, Hellerup, 1995, 5 p (in Danish).

D 1996 Dansk Beton Teknik : “Air void analysis of fresh concrete”, report by Dansk Beton Teknik, Denmark, received by personal communication appr. 1996, 113 p.

F 1976 Fagerlund, G.: “Studies of the destruction mechanism at freezing of porous materials”, paper presented at Fondation Française d’Études Nordiques, the 6th international congress on problems raised by frost action, Le Havre, April 23 – 25, 1975. Reprint as CBI report 1:76, the Swedish Cement and Concrete Research Institute at the Institute of Technology, Stockholm, 28 p.

F 1976b Fagerlund, G.: “Kritisk vattenmättnadsgrads-metoden” *(“The method of critical degree of saturation”)*, presented at NBI/NORDTEST symposium “Byggetekniske prøvningsmetoder knytet til klimapåvirkninger og varmetapsforhold”, Trondheim, August 25 – 27, 1976. Reprint as CBI report 12:76, the Swedish Cement and Concrete Research Institute at the Institute of Technology, Stockholm, 43 p. (in Swedish).

F 1977 Fagerlund, G.: “The international co-operative test of the critical degree of saturation method of assessing the freeze/thaw resistance of concrete”, Materials and Structures, Vol. 10, 1977, pp 231-253.

F 1981 Fagerlund, G.: “Principer för betongs frostbeständighet” *(“Principles for the freeze-thaw durability of concrete”)*, Nordisk Betong, No. 2, 1981, pp 5-13. (in Swedish).

F 1991 Fagerlund, G.: “Scaling, absorption, and dilation of cement mortars exposed to freezing and thawing in NaCl solution”, Rilem International Workshop on Freeze-Thaw and De-icing Resistance of Concrete, Lund, Sweden, 1991. Published in “Freeze-Thaw durability of Concrete”, Rilem Proceedings no. 30, ISBN 0 419 20000 2, E & FN Spon, 1997, pp 51-66.

F 1992 Farstad, T.: Non-published material from the research project "Material Development of High Strength Concrete", Subtask 5, a joint venture with support from the Royal Norwegian Research Council and co-ordinated by Norcem A.S.

F 1999 Fagerlund, G.: "Modified procedure for determination of internal frost resistance by the critical degree of saturation method", Proceedings of the 3rd Nordic Research Seminar in Lund on Frost Resistance of Building Materials, Lund Institute of Technology, Division of Building Materials, Report TVBM-3087, Lund, 1999, pp 29-50.

F 1999b Fagerlund, G.; Nordström, K.: "Studies of the internal frost resistance of HPC", 5th International Symposium on Utilization of High Strength/ High Performance Concrete, Sandefjord, Norway, 1999, Conference Proceedings, Vol. 2, pp 1092-1103, ISBN 82-91341-25-7.

G 1983 Geiker, M.: "Measurements of Chemical Shrinkage and a Systematic Evaluation of Hydration Curves by means of the Dispersion Model", Ph.D thesis at the Technical University of Denmark, Lyngby, Denmark 1983, 258 p.

G 1995 Gran, H.C.: Personal communication with H.C.Gran at the Norwegian Building Research Institute, Oslo, in connection with his dissertation on the state of water in frozen, porous materials, studies comprising the application of nuclear magnetic resonance technique.

G 1995b Geiker, M.; Rostam, S.: "Luftinnholdsstabilitet (Prøvestøbninger Kalundborg)", *("Air void stability (Test production Kalundborg)")*, Test report "HUA-2, Opgave 7", Dansk Betoninstitue A/S, March 1995, 25 p. (in Danish).

G 1999 Geiker, M.; Engelund, S.: "On the need for data for the verification of service life models for frost damage", Proceedings of the 3rd Nordic Research Seminar in Lund on Frost Resistance of Building Materials, Lund Institute of Technology, Division of Building Materials, Report TVBM-3087, Lund, 1999, pp 57-67.

H 1960 Helmuth, R.A.: "Capillary Size Restrictions on Ice Formation in Hardened Portland Cement Pastes", 4th Int. Symp. on the Chemsitry of Cement, Washington D.C., 1960, Vol. II, pp 855-869.

H 1961 Helmuth, R.A.: “Dimensional Changes of Hardened Portland Cement Pastes Caused by Temperature Changes”, Proceedings, Highway Research Board, Vol. 40 (1961), pp 315-336.

H 1979 Herholdt, Aa., D.; Justesen, C. F. P.; Nepper-Christensen, P.; Nielsen, A.: “Beton-Bogen” *(“The Concrete Book”)*, ISBN 87-980816-0-8, Aalborg, 1979, 719 p. (in Danish).

H 1979b Harnik, A.B.; Meier, U.; Rösli, A.: “Combined Influence of Freezing and De-icing Salt on Concrete – Physical Aspects”, Proceedings of the First International Conference on Durability of Building Materials and Components, Ottawa, Canada, 1978, pp 474-484.

H 1986 Hudec, P.P.; MacInnis, C.; Moukwa, “M.: Microclimate of concrete barrier walls : Temperature, moisture and salt content”, Cement & Concrete Research, Vol. 16, 1986, pp. 615-623.

H 1990 Hammer, T.A.; Sellevold, E.J.: “Frost Resistance of High-Strength Concrete”, 2nd International Symposium on High Strength Concrete, Berkeley, 1990, ACI Special Publication SP-121, pp 457-487.

H 1993 Hooten, R.D.: “Influence of Silica Fume Replacement of Cement on Physical Properties and Resistance to Sulphate Attack, Freezing and Thawing, and Alkali-Silica Reactivity”, ACI Materials Journal, Vol. 20, No. 2, March-April 1993, pp 143-151.

H 1995 Henrichsen, A.; Vyncke, J.: “Quality assurance of air void structures in concrete”, International symposium on non-destructive testing in civil engineering, Berlin, Sept. 1995, 8p.

J 1986 Jennings, H.M.: “Aqueous Solubility Relationships for Two Types of Calcium Silicate Hydrate”, Journal of the American Ceramic Society, Vol. 69, No. 8, 1986, pp 614-618.

J 1992 Jacobsen, S.; Sellevold, E.J.: "Frost/Salt scaling of concrete: Effect of curing temperature and condensed silica fume on normal and high strength concrete". 4th CANMET/ACI International Conference on Fly Ash, Silica Fume, Slag and Natural Pozzolans in Concrete, (Supplementary Papers) Istanbul, 1992, pp 369-384.

J 1994 Justnes, H.; Reyniers, B.; Loo, D. von ; Sellevold, E. J : “An Evaluation of Methods for Measuring Chemical Shrinkage of

Cementitious Pastes", Nordic Concrete Research, Vol. 14, 1994, pp 45 – 61.

J 1995 Jacobsen, S.; "Scaling and cracking in wet freeze/thaw testing of OPC and silica fume concrete", Ph.D. Thesis 1995:101 at the Norwegian Institute of Technology, Trondheim, 1995, 286 p.

J 1997 Janssen, D.J.; Snyder, M.B.: "Mass loss experience with ASTM C 666 with and without de-icing salt", Paper in "Freeze-Thaw Durability of Concrete", pp 247-258, Rilem Proceedings No. 30, ISBN 0 419 20000 2, Chapman & Hall, London, 1997, 270 p.

J 1999 Justnes, H.; Hammer, T.A.; Ardoullie, B.; Hendrix, E.; Gemert, D. Van ; Overmeer, K.; Sellevold, E.J.: "Chemical Shrinkage of Cement Paste, Mortar and Concrete", Autogenous Shrinkage of Concrete, ISBN 0 419 23890 5, London 1999, pp 211-220.

J 1999b Jacobsen, S.; Mangor-Jensen, O.: "Frostnedbrytning av betong og andre porøse byggematerialer" *("Frost deterioration of concrete and other porous building materials")*, Byggdetaljblad 520.067, Information leaflet from The Norwegian Building Research Institute, Oslo, 1999, 8 p. (in Norwegian).

J 1999c Jacobsen, S.: "Recycled and porous aggregate in wet frost testing", Proceedings of the 3rd Nordic Research Seminar in Lund on Frost Resistance of Building Materials, Lund Institute of Technology, Division of Building Materials, Report TVBM-3087, Lund, 1999, pp 69-74.

K 1990 Kjellsen, K.O.: "Physical and mathematical modelling of hydration and hardening of portland cement concrete as a function of time and curing temperaure", Doctoral thesis 1990:76 at the Norwegian Institute of Technology, Trondheim, 1990, 222 p.

K 1992 Kukko, H.: "Frost effects on the microstructure of high strength concrete, and methods for their analyses", Dr. Dissertation at the Helsinki University of Technology, Published at the Technical Research Centre of Finland, VTT Publication 126, Espoo, Finland, 1992, 182 p.

K 1999 Kaufmann, J.: "Damage Mechanisms in Porous Materials on Phase Transition of Pore Solution under Frost De-icing Salt Attack", Dr.

thesis, in-official edition received by personal communication, Lausanne, Switzerland, 1999, 157 p.

K 2000 Kjellsen, K.O.: Personal communication.

L 1961 Lange, N.A.; Forker, G.M.: “Handbook of Chemistry”, 10th Edition, McGraw-Hill Book Company, New York / Toronto / London, 1961, 1973 p.

L 1976 Litvan, G.G.: Discussion to [Powers, T.C.: “Freezing Effects in Concrete”, Durability of concrete, SP-47, American Concrete Institute, Detroit, 1975.], ACI Journal, April 1976, pp 234-235.

L 1976b Litvan, G.G.: “Frost Action in Cement in the Presence of De-Icers”, Cement & Concrete Research, Vol. 6, 1976, pp 351-356.

L 1995 Lens, N.; Elsen, J.; Aarre, T.: “Automated air void analyses of hardened concrete”, Proceedings of the 5th Euroseminar on Microscopy Applied to Building Materials, Leuven, Belgium, Sept. 1995, pp 113-120.

L 1996 Lundgren, M.: “Milestone report WP1 & WP2”, internal project report as partial support for [S 1998b], Borås/Sweden, Oct. 1996,

L 1997 Lundevall, G.: A large number of company-internal, restricted consulting reports on concrete damages in the period 1988-1997 on behalf of customers, studies in which the present author was partly involved.

L 1998 Lindmark, S.: “Mechanisms of Salt Frost Scaling of Portland Cement-bound Materials ; Studies and Hypothesis”, Ph.D Thesis at the Lund Institute of Technology, Lund, Sweden, 1998. 266 p.

M 1987 Malhotra, V.M.; Painter, K.A.; Bilodeau, A.: "Mechanical Properties and Freezing and Thawing Resistance of High-Strength Concrete Incorporating Silica Fume". Cement, Concrete and Aggregates, Vol. 9, No. 2, 1987, pp 65-79.

M 1983 Modell & Reid : “Thermodynamics and its applications”, 2nd edition, Prentice-Hall, 1983.

M 1990 Malmström, K.: "Cementsortens inverkan på betongs frost-beständighet", *"Effect of Cement Type on the Freeze-Thaw Durability* *of Concrete"*. Technical Report 1990:07, Swedish National Testing Institute/Building Technology, Boraas, Sweden, 1990, 43 p. (in Swedish).

M 1994 Marchand, J.; Sellevold, E.J.; Pigeon, M.: "The Deicer Salt Scaling Deterioration of Concrete – An Overview", 3rd. International Conference on Durability of Concrete, Nice, France, 1994. ACI SP-145, pp 1-46.

M 1998 Meng, B.; Wiens, U.; Schieβl, P.: "Significance of the Type of Cement on the Reaction Mechanism of Pozzolans", 6th Canmet/ACI International Conference on Fly Ash, Silica Fume, Slag and Natural Pozzolans in Concrete, Bangkok, 1998, ACI Special Publication SP-178, Vol. 1, pp 109-128.

N 1995 Neville, A. M. : "Properties of Concrete", 4th Edition. ISBN 0-582-23070-5, London 1995, 844 p.

N 1999 Nilsson, L.-O.; Andersen, A.: Personal communication on moisture measurements of samples within the project named "Beständighet Tösaltad Betong" *("Durability of concrete subjected to de-icing salt"),* measurements performed by Chalmers Institute of Technology, Gothenburg, Sweden (see [U 1999c]).

O 1981 Opsahl, O.A.: "Fryse-Tine Bestandighet av Silikabetong" *("Freeze-Thaw Resistance of Silica Fume Concrete")*, Condensed Silica Fume in Concrete, Nordic Research Seminar at the Norwegian Institute of Technology, Trondheim, December 1981, Report BML 82.610, pp 203-254 (in Norwegian).

P 1975 Powers, T.C.: "Freezing Effects in Concrete", Paper from symposium sessions, held in Atlantic City, New Jersey and Ottawa, Ontario, 1973. Published in "Durability of concrete", SP-47, American Concrete Institute, Detroit, 1975.

P 1976 Powers, T.C.: Authors closure to a discussion of [L 1976] on [Powers, T.C.: "Freezing Effects in Concrete", Durability of concrete, SP-47, American Concrete Institute, Detroit, 1975.], ACI Journal, April 1976, pp 235-237.

P 1985 Poulsen, E. et al : "13 Betongsykdomme" *("13 Concrete Deseases")*, ISBN 87-563-0583-4, Statens Byggeforskningsinstitutt, Hørsholm, Denmark, 1985, 194 p. (In Danish).

P 1985b Petersson, P.-E.: “Inverkan av Salthaltiga Miljöer på Betongs Saltfrostbeständighet”, *(“Influence of Salt Containing Environment on the Salt Frost Resistance of Concrete”)*, Beton & Frost, Dansk Betonforening *(Danish Concrete Society)*, Publication No. 22, Copenhagen, 1985, pp 145-178 (in Swedish).

P 1986 Pigeon, M.; Pleau, R.; Aitcin, P.-C.: “Freeze-Thaw durability of Concrete With and Without Silica Fume in ASTM C 666 (Procedure A) Test Method : Internal Cracking Versus Scaling”, Cement, Concrete and Aggregates, Vol. 8, 1986, No. 2, pp 76-85.

P 1986b Petersson, P.-E.: "The Influence of Silica Fume on the Salt Frost Resistance of Concrete". Swedish National Testing Institute/Building Materials Technology, Technical Report 1986:32, Boraas, Sweden, 1986, 18 p.

P 1987 Pigeon, M.; Perraton, D.; Pleau, R.: “Scaling Tests of Silica Fume Concrete and the Critical Spacing Factor Concept”, Concrete Durability, Katherine and Bryant Mather International Conference, Atlanta, 1987, American Concrete Institute Special Publications SP 100, Vol. 2, pp 1155-1182.

P 1995 Petersson, P.-E.: “Betongs saltfrostbeständighet – Fältförsök” *(“The salt frost durability of concrete – field test”)*, SP Report 1995:73, Swedish National Testing and Research Institute, Borås, 1995, 64 p (in Swedish).

P 1995b Petersson, P.-E.: Personal communication within CEN TC 51 / Task Group 4, “Freeze-Thaw Resistance of Concrete”.

P 1996 Petersson, P.-E.: “Scaling Resistance of Concrete Field Exposure Tests”, Cementa Report “Durability of Concrete in Saline Environment”, pp 49-79, Published by Cementa AB, P.O.Box 144, 182 12 Danderyd, Sweden, 1996, 206 p. (in English).

P 1999 Persson, B.: “Specific volume of chemically bound water and self-desiccation in silica fume and portland cement based mortars”, Mini-seminar on water in cement paste and concrete, hydration and pore structure, arranged by Aalborg Portland, Denmark, October 1999. 19 p. To be published as part of the proceedings.

R 1980 Rösli, A.; Harnik, A.B.: "Improving the Durability of Concrete to Freezing and De-icing Salts", Durability of Building Materials and Components, ASTM STP 691, American Society for Testing and Materials, 1980, pp 464-473.

R 1989 Rostam, S.: "Durable Concrete Structures – CEB Design Guide", 2nd edition, Bulletin d'Information N° 182, Comité Euro-International du Beton (CEB), Lausanne, 1989.

R 1989b Rønning, T. F.: "Frostbestandighet veisliterelement D3" *("Frost resistance of concrete pavement section D3")*, Norcem A.S restricted R & D Report 08/89, Brevik (Norway), 1989, 7 p (in Norwegian).

R 1992 Rønning, T. F.: "Brekkasje i Taksteinproduksjon" *("Breakage in the Manufacturing of Concrete Roofing Tiles")* Restricted consultancy report ; Norcem report 9D4/R92016, 1992, 36 p. (in Norwegian).

R 1995 Rønning, T.F.: "Frostbestandighet av betongheller" *("Freeze-thaw resistance of concrete flags")* Series of restricted consultancy reports ; Norcem reports 9D4/R95019-26, 1995, 8 x 5 p. (in Norwegian).

R 1995b Rønning, T.F.; Retelius, A.; Virtanen, J.; Laaksonen, J.; Skjeggerud, K.: "Freeze-Thaw Resistance of Silica Fume Concrete – As Influenced by Curing, Cement Type, Air Content and Slump Value", 5th Canmet/ACI International Conference on Fly Ash, Silica Fume, Slag and Natural Pozzolans in Concrete", Milwaukee, USA, 1995, Supplementary Papers, pp 61-83.

R 1996 Rønning, T. F.: Non-published data from study performed by participation in [S 1998]

R 1999 Relling, R.H.; Sellevold, E.J.: Personal communication in connection with Relling : "Coastal Concrete Bridges : Moisture State, Chloride Permeability and Ageing Effects", Dr.Ing. Thesis 1999:74 at the Norwegian University of Science and Technology, Trondheim, 1999, 292 p.

S 1964 Schäfer, A.: "Frostwiderstand und Porengefüge des Betons – Beziehungen und Prüfverfahren", Der Deutsche Ausschuβ für Stahlbeton, 1964 (in German).

S 1986 Sellevold, E.J.: "Bestemmelse av luft/makro og gel/kapillær porøsitet samt relativt bindemiddelinnhold" *("The determination of air void /*

macro and gel / capillary porosity as well as relative binder content"), Project report from project O 1731 at the Norwegian Building Research Institute, Oslo, 1986, 17 p (in Norwegian).

S 1988 Sellevold, E.J.: "Bindemiddels hydratisering" *("The hydration of binders")*, Sintef Report STF70 A88093, Trondheim 1988, 35 p. (in Norwegian).

S 1988b Sellevold, E.J.: "Frostbestandighet : Salt-/frostavskalling. Effekt av prøvebetingelser og betongsammensetning" *("Frost resistance : Freeze-/Thaw scaling. Effect of testing conditions and concrete composition")*, Project Report No. 27 from "Betongens Funksjonsdyktighet", Sintef Report STF65 A88090, Trondheim, 1988, 84 p.

S 1988c Sellevold, E.J.: "Frost resistance", part of durability issue in the FIP (Fédération Internationale de la Précontrainte) state of the art report on "Condensed silica fume in concrete", London, 1988, ISBN 0 7277 1373 6, pp 20-25.

S 1990 Setzer, M.J.: "Prüfung des Frost-Tausalz-Widerstandes von Betonwaren" *("Testing of the freeze-thaw resistance of concrete products")*, Forschungsbericht aus dem Fachbereich Bauwesen Heft 49 *(Research report 49 at the Civil Engineering Department)*, Universität-Gesamthochschule (University of ;) Essen, Germany, 1990, 121 p. (in German).

S 1992 Sellevold, E.J.: "Høyfaste bindemidler : Vannbinding og porøsitet" *("High strength binders : Bound water and porosity")*, Sintef Report STF70 A92050, Trondheim 1992, 61 p. (in Norwegian).

S 1992b Skjeggerud, K.; Retelius, A.; Virtanen, J.; Laaksonen, J.: "Durability of silica fume concrete : Effect of curing conditions", 4th Canmet/ACI International Conference on Fly Ash, Silica Fume, Slag and Natural Pozzolans in Concrete", Istanbul, Turkey, 1992, Supplementary Papers, pp 513-534.

S 1993 Sellevold, E.J.: "Sementpasta & porøsitet : Powers modell & volumberegninger" *("Cement paste & porosity : Powers' model & volumetric calculations")*, Compendium at the Norwegian Institute of Technology, Trondheim, 1993, 12 p. (in Norwegian).

S 1993b Sellevold, E.J.: "Isdannelse – Frysepunktnedsettelse" ("Ice formation – freezing point depression"), Compendium at the Norwegian Institute of Technology, Trondheim, 1993, 6 p. (in Danish).

S 1993c Sellevold, E.J.: "Porevanns termodynamikk" *("The thermodynamics of pore water")*, Compendium at the Norwegian Institute of Technology, Trondheim, 1993, 7 p. (in Norwegian).

S 1993d Stark, J.; Ludwig, H.-M.: "Freeze-thaw resistance and de-icing salt resistance of concrete made with cements of different C_3A contents", Rilem international workshop on the resistance of concrete to scaling due to freezing in the presence of de-icing salts, Québec, 1993, pp 93-108.

S 1993e Sellevold, E.J.; Jacobsen, S.: "The relationship between ASTM C 666, the CDF and the Borås procedures", Discussion paper at the Rilem TC 117 internal meeting in Quebec, Sept. 1st, 1993.

S 1993f Studer, W. (EMPA, Switzerland) : Personal communication in connection with Rilem TC 117 and CEN TC 51 / WG 12 / TG 4.

S 1995 Setzer, M.J.: "Rilem TC 117 FDC : Draft Recommendation for test method for the freeze-thaw resistance of concrete – Test with water (CF) or with sodium chloride solution (CDF)" Materials and Structures, Vol. 28, 1995, pp 175-182.

S 1995b Siebel, E.: "Einflüsse auf die Luftporenkennwerte und den Frost-Tausalz-Widerstand von Beton*", ("Factors affecting the air-void parameters of concrete and its resistance to freeze-thaw with de-icing salt")*, Beton, No. 10, 1995, pp 724-730. (in German).

S 1996 Stark, J.; Knaack, U.: "Freeze and Freeze-De-icing Salt Resistance of Concrete containing Cement Rich in Granulated Blast Furnace Slag", paper presented at a Rilem TC-117 meeting in Espoo, Finland, August 1996.

S 1997 Setzer, M.J.: "Basis of testing the freeze-thaw resistance : Surface and internal deterioration", Paper in "Frost Resistance of Concrete", pp 157-173, Rilem Proceedings No. 34, ISBN 0 419 22900 0, Chapman & Hall, London, 1997, 356 p.

S 1997b Statens Vegvesen : "Prosesskode-2, Standardbeskrivelser for bruer og kaier", *("Process code 2 ; Design specifications for bridges and quay* *structures")*, The Norwegian Road Authorities, Oslo, 1997, 567 p. (in Norwegian).

S 1998 Siebel, E.; Breit, W.: "Standard Methods for Testing the Resistance of Concrete to Freezing and Thawing", Technical report from the European Research Project No. 3085 (Reference to the European Commission : MAT1-CT94-0055), VDZ Report Be-TB-1489-4/1998, Düsseldorf, Germany 1998, 155 p.

S 1998b Siebel, E.; Breit, W.: "Standard Methods for Testing the Resistance of Concrete to Freezing and Thawing", Synthesis Report from the European Research Project No. 3085 (Reference to the European Commission : MAT1-CT94-0055), VDZ Report Be-TB-1489-5/1998, Düsseldorf, Germany 1998, 42 p.

S 1999 Siebel, E.; Breit, W.: "Ergebnisse eines Europäischen Ringversuches / Results of a European Round Robin Test", Betonwerk + Fertigteil-Technik / Concrete Plant + Precast Technology, No. 11, 1999, 9 p. (in German & English).

S 1999b Setzer, M.J.: "Micro ice lens formation and frost damage", Rilem workshop on frost damage in concrete, University of Minnesota, Minneapolis, June, 1999, Edited by D.J.Janssen, M.J.Setzer and M.B.Snyder, RILEM, pp 1-15.

S 1999c Setzer, M.J.: "Mikroeislinsenbildung und Frostschaden*" ("Micro ice lens formation and frost damage")*, in "Werkstoffe im Bauwesen – Theorie und Praxis" *("Construction Materials – Theory and application")*, Published by Eiligehausen, R., Ibidem, Stuttgart, 1999, pp 397-413. (in German).

S 2000 "Test Methods for the Freeze-Thaw Resistance of Concrete – Test with Water or with Sodium Chloride Solution – Part 1 : Scaling", Draft standard by CEN TC 51, believed to be launched as an EN during the year 2000.

S 2000b Stoltenberg-Hansson, Erik : Personal communication with ~, a colleague of the present author and member of CEN 104 / WG 4 "Fly Ash for Concrete"

T 1984 Taylor, H.F.W.: "Studies on the Chemistry and Microstructure of Cement Paste", Workshop proceedings "The Chemistry and Chemically-Related Properties of Cement" at the Imperial College, London, 1994, published in Proceedings 35 by the British Ceramic Society, Shelton, Stoke-on-Trent, 1984, pp 65 – 82.

T 1999 Tazawa, E. (Editor) : “Committee report on Autogenous Shrinkage of Concrete”, Proceedings of the International Workshop on Autogenous Shrinkage of Concrete, Hiroshima, June 1998, Published by E & FN Spon, London/New York, 1999, ISBN 0-419-23890-5, 411 p.

U 1999 Utgenannt, P.: “Salt-frost resistance of concrete in highway environment”, Proceedings of the 3rd Nordic Research Seminar in Lund on Frost Resistance of Building Materials, Lund Institute of Technology, Division of Building Materials, Report TVBM-3087, Lund, 1999, pp 137-145.

U 1999b Utgenannt, P.: “Influence of carbonation on the scaling resistance of OPC concrete”, Rilem workshop on frost damage in concrete, University of Minnesota, Minneapolis, June, 1999, Draft proceedings, pp 103-114.

U 1999c Utgennant, P.: Project named “Beständighet Tösaltad Betong” *(“Durability of concrete subjected to de-icing salt”)*, extensive field and laboratory study on freeze-thaw resistance etc., related to Swedish highway environment. Various project report from the joint venture project, in which the department of the present author is one of the partners. Particular reference to project report no. 16, “Betongkvaliteter tillverkade med norska bindemedel 1997 – Resultat från uppmätning av volym och ultraljudhastighet efter twå vintersäsonger” (“Concrete qualities manufactured with Norwegian binders 1997 – Results from assessment of volume and ultrasonic pulse velocity after two winter seasons”), 1999, 55 p. (in Swedish).

U 2002 Utgennant, P.: Dr. thesis based on results from project named “Beständighet Tösaltad Betong” *(“Durability of concrete subjected to de-icing salt”),* (see [U 1999c]), probably due 2002.

V 1990 Virtanen, J.: "Field Study on the Effects of Additions on the Salt-Scaling Resistance of Concrete". Nordic Concrete Research, Publication No. 9 by The Nordic Concrete Federation ISSN 0800-6377, Oslo, 1990, pp 197-212.

V 1999 VDZ (The association of the German cement industry ; No specific author) : “Frostwiderstand hochfester Betone” *(“The frost resistance* *of high strength concrete")*, VDZ-Mitteilungen no. 111, Düsseldorf, December 1999, p 10. (in German).

V 1999b VDZ (The association of the German cement industry ; No specific author) : "Zusammenarbeit mit Flugascheerzeugern" *("Co-operation with the fly ash manufacturers")*, VDZ-Mitteilungen no. 111, Düsseldorf, December 1999, p 9. (in German).

V 1999c VDZ (The association of the German cement industry ; No specific author) : "Verwendung von CEM II Zementen im Betonbau" *("Application of CEM II cements in concrete structures")*, Offprint by VDZ, Düsseldorf, November 1999, p 10. (in German).

W 1990 Wallevik, O.: "Den ferske betongens reologi og anvendelse på betong med og uten tilsetning av silikastøv" *("The rheology of fresh concrete and application on concrete with and without silica fume")*, Dr. thesis at the Norwegian Institute of Technology, Trondheim, 1990, 185 p. (in Norwegian).

W 1973 Weast, R. C. : "Handbook of chemistry and Physics", 54th Edition. ISBN 087819-454-1, Cleveland 1973.

11.2 Standards

- ASTM C 457 : "Standard Test Method for Microscopical Determination of Parameters of the Air-Void system in Hardened Concrete". American Society for Testing and Materials.

- ASTM C 666 : "Standard Test Method for Resistance of Concrete to Rapid Freezing and Thawing". American Society for Testing and Materials.

- ASTM C 671 : "Standard Test Method for Critical Dilation of Concrete Specimens Subjected to Freezing". American Society for Testing and Materials.

- ASTM C 672 : "Standard Test Method for Scaling Resistance of Concrete Surfaces Exposed to De-icing Chemicals". American Society for Testing and Materials.

- ASTM C 682 : "Standard Practice for Evaluation of Frost Resistance of Coarse Aggregates in Air-Entrained Concrete by Critical Dilation Procedures". American Society for Testing and Materials.

- ASTM E 104 : "Standard Practice for Maintaining constant Relative Humidity by Means of Aqueous Solutions". American Society for Testing and Materials.

- ISO 5725 : "Precision of test methods – Determination of repeatability and reproducibility for a standard test method by inter-laboratory tests". International Organization for Standardization.

- SS 13 72 44 : "Betongprovning – Hårdnad betong – Avflagning vid frysning" *("Concrete testing – Hardened concrete – Scaling at freezing").* Swedish Standards Institution.

- ÖNORM B 3306 "Prüfung der Frost-Tausalz-Beständigkeit von vorgefertigten Betonerzeugnissen" *("Testing of Freeze-Thaw Resistance with De-icing Salt on Pre-Fabricated Concrete Products")* Austrian Standard.

- ÖNORM B 3303 "Betonprüfung (Abschn. 6.9, Frostbeständigkeit ; Abschn. 6.10, Frost-Tausalz-Beständigkeit*)" ("Concrete Testing (Ch. 6.9, Frost Resistance ; Ch. 6.10, Freeze-Thaw Resistance with De-icing Salt")* Austrian Standard.

- EN 206 : "Concrete : Performance, production, placing and compliance criteria", 1rst edition NS-EN 206, December 1995.

- prEN xxx : "Test Methods for the freeze-thaw resistance of concrete – Test with water or with sodium chloride solution, Part 1 : Scaling", Document prepared by CEN TC 51 / WG 12 / TG 4 as a draft standard, see also reference S 2000.

- prEN 1338 : "Concrete Paving Block"

- prEN 1339 : "Precast Concrete Flag"

- prEN 1340 : "Concrete Kerb Units"

APPENDIX A

Description of test method : Reference Method in [prEN xxx]

1. General

The formulation of this test prescription is almost identical with the description provided by [S 1998b] :

The test method described here follows the Reference Method A from the Document CEN/TC51/WG12/TG4:6/94 ("[SS 13 72 44]"), draft March 1994, with two modification, adopted by the working group of the EU-Project no. 3085 :

- The minimum temperature of the freeze-thaw cycle is -20 ± 2^{o}C, instead of -18 ± 2^{o}C.
- The test liquid for the tests without de-icing salt is de-mineralised water and not tap water, during both re-saturation and freeze-thaw test.

2 Equipment

- Equipment for making 150 mm concrete cubes according to EN ISO 2736.
- Saw with a diamond edge for concrete cutting.
- Climate chamber with a temperature of 20 ± 2^{o}C, relative humidity of 65 ± 5% and evaporation rate from a free water surface within 45 ± 15$g \cdot m^{-2} \cdot h^{-1}$. The evaporation shall be measured from a bowl with a depth of approximately 40 mm and a cross section area of 225 ± 25 cm^2. The bowl shall be filled up to 10 ± 1 mm from the brim.
- Rubber sheet, 3 ± 0,5 mm thick, which shall be resistant to the salt solution used. It also has to be sufficiently elastic down to a temperature of -22^{o}C.
- Contact adhesive, for gluing the rubber sheet to the concrete specimen. The adhesive shall be resistant to the environment in question.
- Polystyrene cellular plastic, 20 ± 1 mm thick, with a density of 18 ± 2 $kg \cdot m^{-3}$, or alternative thermal insulating material with equivalent properties.
- Polyethylene sheet, 0.1 to 0.2 mm thick.
- Freezing medium, 3 % NaCl solution consisting of 97 % by weight tap water and 3 % by weight NaCl (for tests with de-icing salt), or only de-mineralised water (for tests without de-icing salt).
- Freezing chamber, with temperature and time controlled refrigerating and heating system with a capacity such that the time-temperature curve presented in figure 2 can be followed. There shall be a good air circulation in the freezer. The shelves in the freezer shall be level, with no deviation from the horizontal plane exceeding 3 mm per meter in any direction.

- Thermocouples or an equivalent temperature measuring device for measuring the temperature in the freezing medium on the test surface, with accuracy within 0.5°C.
- Vessel for collecting scaled material. The vessel shall be suitable for use up to 120°C without weight loss and shall withstand sodium chloride attack.
- Paper filter for collecting scaled material, optional.
- Brush, with short (approx. 20 mm) and stiff bristles for brushing off material that scales.
- Spray bottle, containing tap water for washing off scaled material.
- Drying cabinet, providing a temperature of 110 ± 10°C.
- Balance, with accuracy within ± 0.05 g.
- Vernier calliper with an accuracy within ± 0.1 mm.

3 Preparation and preconditioning of the test specimens

Series of four specimens from four cubes are tested. Four 150 mm cubes are cast and compacted on a vibrating table according to the procedure described in ISO 2736. During the first day after casting the cubes are stored in the moulds at an air temperature of 20 ± 2°C, protected against drying by covering with a plastic sheet. After 24 ± 2 hours the cubes are removed from the moulds and placed in a tap water bath with a temperature of 20 ± 2°C. When the cubes are seven days old they are removed from the water bath and are placed in a climate chamber until the freeze-thaw testing starts. In the climate chamber the temperature shall be 20 ± 2°C and the relative humidity within 65 ± 5 %. Furthermore, the evaporation rate from a free water surface shall be $45 \pm 15 \mathrm{g \cdot m^{-2} \cdot h^{-1}}$. Normally, this is obtained with a wind velocity $<0.1 \mathrm{m \cdot s^{-1}}$. The evaporation rate shall be measured according to the procedure described in chapter 2 above.

At 21 days a 50 ± 2 mm thick slab is sawn from each cube perpendicular to the top surface, so that one cut surface is located in the centre of the cube and becomes the test surface. Directly after sawing the specimen is washed in tap water, the excess water is wiped off with a moist sponge and then the specimen is returned without delay to the climate chamber. The specimens shall be placed with the test surface vertically and with a space between the specimens of at least 50 mm. The side lengths of each specimen shall be measured with an accuracy of ± 0.5 mm by using vernier calliper. The variation in thickness of a specimen shall not exceed 1 mm.

When the concrete is 25 ± 1 days old, rubber sheet is glued to all surfaces of the specimen except the test surface. After gluing, an additional string of glue or silicon rubber is placed around the test surface, in the corner between the rubber sheet and the concrete. The edge of the rubber sheet has to reach 20 ± 1 mm above the test surface. (When gluing the rubber sheet the adhesive is applied evenly both to the concrete surfaces and to the rubber surfaces.)

When the concrete is 28 days old a 3 mm thick layer of water with a temperature of 20 ± 2°C is poured on the test surface. This re-saturation of the test surface shall last for 72 ± 2 hours at 20 ± 2°C. (For a specimen with the test area of 150 x 150 mm^2, 67.5 ml water gives an approximately 3 mm thick layer.)

Shortly before the freeze-thaw test, which starts when the concrete is 31 days, all surfaces of the specimen except the test surface are thermally insulated with 20 ± 1 mm thick polystyrene cellular plastic with density 18 ± 2 $kg \cdot m^{-3}$. Another material providing equivalent thermal insulation can be used as well.

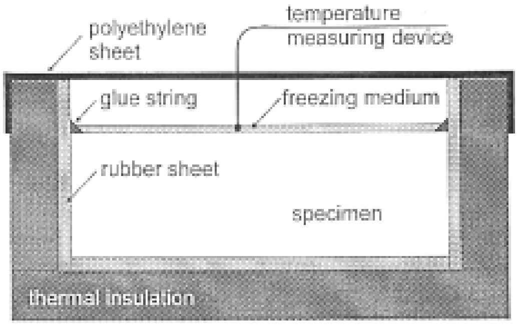

Figure 1 : Sample preparation and set-up

Not earlier than 15 minutes before the specimens are placed in the freezing chamber, the re-saturation water on the test surface shall be replaced by 67 ml freezing medium, at a temperature of 20 ± 2°C. It is important to obtain an average thickness of 3 mm.

The freezing medium is, depending on the test alternative used : 3 % NaCl solution for tests with de-icing salt, or de-mineralised water for tests without de-icing salt. The freezing medium is protected against evaporation by a flat, horizontal polyethylene sheet applied as shown in figure 1. The polyethylene sheet shall remain flat throughout the whole test.

4 Test procedure

After the specimens have been placed in the freezing chamber, they are subjected to repeated freezing and thawing. During the test, the temperature in the freezing medium for all specimens shall meet the requirements specified in figure 2. The temperature shall be continuously recorded in the freezing medium at the centre of the test surface, for at least one specimen in each freezing chamber. The air temperature in the freezer shall never fall below -27°C. When the test is begun, the specimens shall be placed in the freezing chamber at the time 0 ± 30 min. according to figure 2. The breakpoints for the upper and lower limit of the time-temperature curve according to figure 2 are listed in table 1.

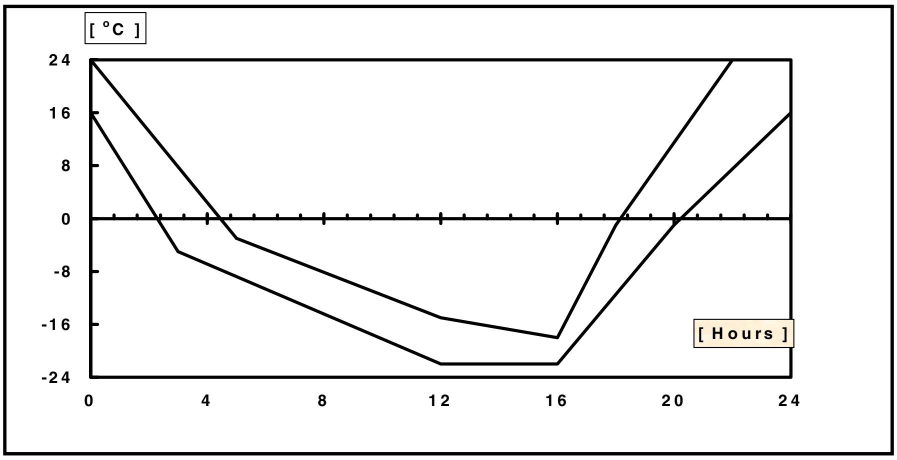

Figure 1 : Temperature cycle with upper and lower limit.

upper limit		lower limit	
Time in h	Temperature in °C	Time in h	Temperature in °C
1	2	3	4
0	+24	0	+16
5	-3	3	-5
12	-15	12	-22
16	-18	16	-22
18	-1	20	-1
22	+24	24	+16

Table 1 : Points specifying the curves in figure 2.

To obtain correct temperature cycle for all the specimens there must be a good air circulation in the freezing chamber. (The number of specimens in the freezer should always be the same. If only few specimens are tested the empty places in the freezer shall be filled with dummies, unless it has been shown that the correct temperature is achieved regardless of the number of specimens.)

After 7, 14, 28, 42 and 56 cycles the following procedures shall be carried out for each specimen, during the thawed phase between hour 20 and hour 24, according to figure 2.

a) Material that has scaled from the test surface is collected in a vessel. The surface is rinsed using the spray bottle and brushed to remove the scaled material.
b) New freezing medium is poured on the test surface in the same quantity as previously (e.g. 67 ml for 225 cm^2 test area).
c) The specimen is returned to the freezing chamber.
d) The liquid collected in the vessel is carefully poured out. It is recommended to pour the liquid through a paper filter when only small amounts of material are scaled off. The vessel (and the paper filter) is then dried out to constant weight at 110 ± 10°C. The total dry weight, corrected for the weight of the vessel (and paper filter), is noted.

5 Expression of test results

The following result shall be calculated for each measuring occasion for each specimen :

$$P = M_n/A$$

where :

P	is the amount of scaled material per unit area after n cycles in $kg \cdot m^{-2}$
M_n	is the weight of the total quantity of material scaled after n cycles in mg
A	is the area of the test surface of one specimen in mm^2.

The mean value and the individual values for each specimen after 56 cycles are used for evaluating the scaling resistance.

6 Test report

The test report shall contain at least the following information:

a) A reference to this standard
b) Origin and marking of the specimens
c) Composition of the concrete
d) Composition of the freezing medium (de-mineralised water or salt solution)
e) Amount of scaled material for each specimen, in $kg \cdot m^{-2}$, rounded to the nearest 0.02, after 7, 14, 28, 42 and 56 freeze-thaw cycles.

f) Visual assessment (cracks, scaling from aggregate particles, leakage of freezing medium, etc.) before start and after 7, 14, 28, 42 and 56 freeze-thaw cycles.
g) Any deviation from the standard test procedure.

7 Alternative applications

The description of the reference test method above is restricted to specimens with dimensions of approximately 50x150x150 mm^3, where the tests starts at an age of 31 days and the sawn surface is tested. However, the same test principle can be used for other conditions too. Most frequently it is the method of making and/or the curing of the specimens that differ from the standard test procedure. Examples of alternative applications are:

a) Other specimen geometry can be used, but the thickness must always be 50 ± 2 mm. For example, the method is suitable for testing slices from cores drilled from structures or for the testing pre-cast units;
b) Top surface and surfaces cast against formwork can bee tested instead of sawn surfaces;
c) Other curing conditions can be used and the concrete age may differ from 31 days at the start of the freeze-thaw cycling;
d) Other de-icing agents than NaCl can be used.
e) The number of freeze-thaw cycles may differ from 56.

When alternative applications are used, the specimens are sawn to a thickness of 50 ± 2 mm ten days before the start of the freeze-thaw test. During these ten days the specimens shall be stored in the climate chamber for seven days and shall then be re-saturated for three days, as described in the reference method, unless other curing conditions are of special interest. A 3 mm thick layer of freezing medium shall be poured on the test surface before the start of the freezing and thawing. The test then continues according to the reference method.

All deviations from the reference method shall be specified in the report.

URN:NBN:no-6354

APPENDIX B

Section 4 : Damage versus curing, moisture loss and absorption. Additional data.

URN:NBN:no-6354

1: 45-I-AE : Mean Values ; Accumulated Results

Curing :	Standard	Standard	Mod. Std.	Mod. Std.	Plastic	Plastic	Drying	Drying
Type of								
Resaturat.:	Water	3 % Salt	Water	3 % Salt	Water	3 % Salt	Water	3 % Salt
	Mean Values (Accumulated) [kg/m2] :							
No. of								
Cycles :								
7	0.22	0.02	0.14	0.04	0.11	0.01	1.27	0.56
14	0.33	0.02	0.21	0.07	0.13	0.02	2.55	1.38
28	0.36	0.03	0.24	0.08	0.13	0.03	3.58	2.60
42	0.37	0.03	0.24	0.08	0.13	0.04	4.06	3.16
56	0.37	0.03	0.24	0.08	0.13	0.04	4.54	3.71
	Standard Deviation at termination of test :							
[kg/m2]	0.15	0.00	0.14	0.06	0.05	0.02	0.05	0.86
% of Mid.	41	9	58	70	39	52	1	23

2 : 45-I : Mean Values ; Accumulated Results

Curing :	Standard	Standard	Mod. Std.	Mod. Std.	Plastic	Plastic	Drying	Drying
Type of								
Resaturat.:	Water	3 % Salt	Water	3 % Salt	Water	3 % Salt	Water	3 % Salt
	Mean Values (Accumulated) [kg/m2] :							
No. of								
Cycles :								
7	0.98	0.43	1.71	0.99	0.73	0.13	3.40	2.98
14	2.40	1.67	4.06	2.84	1.87	0.77	6.07	5.45
28	4.43	4.08	7.43	5.37	3.51	2.32	9.88	8.38
42		Test terminated at 28 cycles due to scaling level.						
56								
	Standard Deviation at termination of test :							
[kg/m2]	0.20	0.10	0.10	0.69	0.06	0.53	1.06	0.67
% of Mid.	5	2	1	13	2	23	11	8

3 : 55-I-AE : Mean Values ; Accumulated Results										
Curing :	Standard	Mod. Std.	Plastic	Drying	Standard	Mod. Std.	Standard	Mod. Std.	Plastic	Drying
Type of										
Resaturat.:	Water	Water	Water	Water	3 % Salt	3 % Salt	Water	Water	Water	Water
Type of										
Test :	Water	Water	Water	Water	Water	Water	3 % Salt	3 % Salt	3 % Salt	3 % Salt
	Mean Values (Accumulated) [kg/m2] :									
No. of										
Cycles :										
7	0.00	0.00	0.00	0.00	0.01	0.01	0.48	0.96	0.08	2.40
14	0.00	0.00	0.00	0.00	0.01	0.01	0.74	1.40	0.12	3.74
28	0.00	0.00	0.01	0.00	0.01	0.01	0.92	1.69	0.13	4.75
42	0.00	0.00	0.01	0.00	0.01	0.01	0.94	1.74	0.13	5.63
56	0.02	0.02	0.02	0.04	0.01	0.01	0.95	1.75	0.13	6.13
	Standard Deviation at termination of test :									
[kg/m2]	0.01	0.01	0.00	0.01	0.02	0.00	0.22	0.13	0.09	0.36
% of Mid.	67	36	24	30	116	0	23	7	72	6
	(Low scaling levels normally leads to high percentage scatter.)									

4 : 55-I : Mean Values ; Accumulated Results								
Curing :	Standard		Mod. Std.		Plastic		Drying	
Type of								
Resaturat.:	Water		Water		Water		Water	
Test in 3 % salt for all series.								
	Mean Values (Accumulated) [kg/m2] :							
No. of								
Cycles :								
7	2.40		2.32		1.34		3.67	
14	4.77		5.16		2.97		7.84	
28	7.16		9.56		5.90		14.04	
42								
56								
	Standard Deviation at termination of test :							
[kg/m2]	0.25		1.21		1.11		2.31	
% of Mid.	3		13		19		16	

5 : 70-I : Mean Values ; Accumulated Results								
	Test in Water for all series.							
Curing :	Standard	Mod. Std.	Plastic	Int.Drying	Standard	Mod. Std.	Plastic	Int.Drying
Type of								
Resaturat.:	Water	Water	Water	Water	3 % Salt	3 % Salt	3 % Salt	3 % Salt
	Mean Values (Accumulated) [kg/m2] :							
No. of								
Cycles :								
7	0.00	0.01	0.00	0.03	0.06	0.08	0.01	0.38
14	0.01	0.02	0.01	0.10	0.19	0.24	0.02	1.42
28	0.02	0.02	0.04	0.15	0.27	0.29	0.04	1.63
42	0.03	0.03	0.06	0.21	0.31	0.31	0.05	1.72
56		Test terminated at 42 cycles due to degradation of specimens.						
	Scaling levels hardly relevant due to internal cracking and loss of testing medium.							
	Standard Deviation at termination of test :							
[kg/m2]	0.00	0.01	0.08	0.09	0.05	0.13	0.01	0.25
% of Mid.	17	43	140	43	17	43	20	15

6 : 45-II-AE : Mean Values ; Accumulated Results								
Curing :	Standard		Mod. Std.		Plastic		Drying	
Type of								
Resaturat.:	Water		Water		Water		Water	
	Mean Values (Accumulated) [kg/m2] :							
No. of								
Cycles :								
7	0.47		0.24		0.34		1.57	
14	0.63		0.29		0.42		3.02	
28	0.69		0.31		0.43		4.32	
42	0.69		0.32		0.44		4.86	
56	0.70		0.33		0.45		5.40	
	Standard Deviation at termination of test :							
[kg/m2]	0.24		0.07		0.08		0.49	
% of Mid.	35		22		17		9	

7 : 55-II : Mean Values ; Accumulated Results

Curing :	Standard		Mod. Std.		Plastic		Drying	
Type of								
Resaturat..	Water		Water		Water		Water	
	Mean Values (Accumulated) [kg/m2] :							
No. of								
Cycles :								
7	3.13		2.88		1.70		4.13	
14	6.38		6.13		3.29		8.31	
28	12.11		12.27		7.15		15.65	
42								
56								
	Standard Deviation at termination of test :							
[kg/m2]	4.10		1.84		0.75		2.02	
% of Mid.	34		15		10		13	

8 : 45-IS-AE : Mean Values ; Accumulated Results

Curing :	Standard		Mod. Std.		Plastic		Drying	
Type of								
Resaturat..	Water		Water		Water		Water	
	Mean Values (Accumulated) [kg/m2] :							
No. of								
Cycles :								
7	0.01		0.07		0.01		0.02	
14	0.01		0.09		0.02		0.02	
28	0.02		0.10		0.02		0.02	
42	0.02		0.10		0.02		0.02	
56	0.03		0.11		0.02		0.02	
	Standard Deviation at termination of test :							
[kg/m2]	0.00		0.01		0.00		0.00	
% of Mid.	6		8		6		20	

Weight changes [%]	Re-saturation :	Water				3 % NaCl	
1 : 45-I-AE	Testing medium :	3 % NaCl				3 % NaCl	
Curing :	Period of change :	Mean	Std.v.	Mean	Std.v.	Mean	Std.v.
Standard	Sawing-Preparation	-	-			-	-
	Prep.-Re-saturation	-0.06	0.01			-0.07	0.01
	Re-saturation	+0.25	0.05			+0.24	0.03
	Freeze-Thaw testing	+0.66	0.14			+0.55	0.05
Mod. stand.	Sawing-Preparation	-1.40	0.10			-1.49	0.17
	Prep.-Re-saturation	-0.03	0.00			-0.02	0.00
	Re-saturation	+0.45	0.04			+0.45	0.08
	Freeze-Thaw testing	+0.63	0.16			+0.67	0.08
Plastic cur.	Sawing-Preparation	-0.10	0.02			-0.10	0.05
	Prep.-Re-saturation	-0.01	0.01			-0.01	0.01
	Re-saturation	+0.11	0.03			+0.09	0.01
	Freeze-Thaw testing	+0.33	0.03			+0.30	0.03
Int. drying	Sawing-Preparation	-	-			-	-
	Prep.-Re-saturation	-0.49	0.04			-0.48	0.06
	Re-saturation	+0.45	0.06			+0.45	0.04
	Freeze-Thaw testing	-	-			-	-

Weight changes [%]	Re-saturation :	Water				3 % NaCl	
2 : 45-I	Testing medium :	3 % NaCl				3 % NaCl	
Curing :	Period of change :	Mean	Std.v.	Mean	Std.v.	Mean	Std.v.
Standard	Sawing-Preparation	-	-			-	-
	Prep.-Re-saturation	-0.05	0.00			-0.05	0.00
	Re-saturation	+0.23	0.02			+0.26	0.07
	Freeze-Thaw testing	-	-			-	-
Mod. stand.	Sawing-Preparation	-1.30	0.12			-1.27	0.13
	Prep.-Re-saturation	-0.03	0.01			-0.03	0.01
	Re-saturation	+0.45	0.04			+0.43	0.03
	Freeze-Thaw testing	-	-			-	-
Plastic cur.	Sawing-Preparation	-0.07	0.05			-0.12	0.08
	Prep.-Re-saturation	-0.01	0.01			-0.01	0.00
	Re-saturation	+0.10	0.02			+0.08	0.03
	Freeze-Thaw testing	-	-			-	-
Int. drying	Sawing-Preparation	-	-			-	-
	Prep.-Re-saturation	-0.49	0.03			-0.48	0.06
	Re-saturation	+0.40	0.03			+0.39	0.04
	Freeze-Thaw testing	-	-			-	-

Weight changes [%]	Re-saturation :	Water		Water		3 % NaCl	
3 : 55-I-AE	Testing medium :	3 % NaCl		Water		Water	
Curing :	Period of change :	Mean	Std.v.	Mean	Std.v.	Mean	Std.v.
Standard	Sawing-Preparation	-	-	-	-	-	-
	Prep.-Re-saturation	-0.10	0.01	-0.09	0.01	-0.11	0.01
	Re-saturation	+0.44	0.04	+0.44	0.03	+0.43	0.06
	Freeze-Thaw testing	+1.16	0.06	+1.17	0.12	+0.88	0.11
Mod. stand.	Sawing-Preparation	-1.82	0.00	-1.85	0.04	-1.89	0.05
	Prep.-Re-saturation	-0.05	0.01	-0.07	0.01	-0.06	0.01
	Re-saturation	+0.78	0.02	+0.77	0.02	+0.65	0.01
	Freeze-Thaw testing	+1.24	0.03	+1.05	0.05	+1.15	0.21
Plastic cur.	Sawing-Preparation	-0.08	0.01	-0.05	0.01	-	-
	Prep.-Re-saturation	-0.03	0.00	-0.03	0.00	-	-
	Re-saturation	+0.12	0.01	+0.13	0.02	-	-
	Freeze-Thaw testing	+0.70	0.11	+0.53	0.09	-	-
Int. drying	Sawing-Preparation	-	-	-	-	-	-
	Prep.-Re-saturation	-0.80	0.03	-0.83	0.10	-	-
	Re-saturation	+0.77	0.04	+0.64	0.11	-	-
	Freeze-Thaw testing	+1.12	0.02	+1.06	0.01	-	-

Weight changes [%]	Re-saturation :	Water					
4 : 55-I	Testing medium :	3 % NaCl					
Curing :	Period of change :	Mean	Std.v.	Mean	Std.v.	Mean	Std.v.
Standard	Sawing-Preparation	-	-				
	Prep.-Re-saturation	-0.12	-0.02				
	Re-saturation	+0.36	+0.07				
	Freeze-Thaw testing	-	-				
Mod. stand.	Sawing-Preparation	-1.71	-0.14				
	Prep.-Re-saturation	-0.09	-0.02				
	Re-saturation	+0.65	+0.06				
	Freeze-Thaw testing	-	-				
Plastic cur.	Sawing-Preparation	-0.10	-0.07				
	Prep.-Re-saturation	-0.08	-0.00				
	Re-saturation	+0.07	+0.03				
	Freeze-Thaw testing	-	-				
Int. drying	Sawing-Preparation	-	-				
	Prep.-Re-saturation	-0.71	-0.06				
	Re-saturation	+0.58	+0.07				
	Freeze-Thaw testing	-	-				

Weight changes [%]	Re-saturation :			Water		3 % NaCl	
5 : 70-I	Testing medium :			Water		Water	
Curing :	Period of change :	Mean	Std.v.	Mean	Std.v.	Mean	Std.v.
Standard	Sawing-Preparation			-	-	-	-
	Prep.-Re-saturation			-0.11	0.01	-0.11	0.01
	Re-saturation			+0.56	0.02	+0.57	0.01
	Freeze-Thaw testing			+1.49	0.15	+1.93	0.29
Mod. stand.	Sawing-Preparation			-2.14	0.18	-2.06	0.10
	Prep.-Re-saturation			-0.06	0.01	-0.08	0.01
	Re-saturation			+1.02	0.12	+1.02	0.05
	Freeze-Thaw testing			+2.09	0.20	+1.89	0.08
Plastic cur.	Sawing-Preparation			-0.17	0.06	-0.06	0.01
	Prep.-Re-saturation			-0.04	0.01	-0.04	0.01
	Re-saturation			+0.58	0.21	+0.39	0.12
	Freeze-Thaw testing			+0.73	0.27	+0.82	0.13
Int. drying	Sawing-Preparation			-	-	-	-
	Prep.-Re-saturation			-0.97	0.02	-1.04	0.03
	Re-saturation			+1.00	0.02	+1.14	0.22
	Freeze-Thaw testing			+2.61	0.08	+2.33	0.09

Weight changes [%]	Re-saturation :	Water					
6 : 55-II-AE	Testing medium :	3 % NaCl					
Curing :	Period of change :	Mean	Std.v.	Mean	Std.v.	Mean	Std.v.
Standard	Sawing-Preparation	-	-				
	Prep.-Re-saturation	-0.20	0.01				
	Re-saturation	+0.28	0.04				
	Freeze-Thaw testing	+0.48	0.11				
Mod. stand.	Sawing-Preparation	-1.56	0.18				
	Prep.-Re-saturation	-0.08	0.01				
	Re-saturation	+0.53	0.02				
	Freeze-Thaw testing	+0.89	0.38				
Plastic cur.	Sawing-Preparation	-0.06	0.01				
	Prep.-Re-saturation	-0.08	0.01				
	Re-saturation	+0.10	0.02				
	Freeze-Thaw testing	+0.31	0.13				
Int. drying	Sawing-Preparation	-	-				
	Prep.-Re-saturation	-0.75	0.04				
	Re-saturation	+0.52	0.04				
	Freeze-Thaw testing	-	-				

Weight changes [%]	Re-saturation :			Water			
7 : 55-II	Testing medium :			Water			
Curing :	Period of change :	Mean	Std.v.	Mean	Std.v.	Mean	Std.v.
Standard	Sawing-Preparation			-	-		
	Prep.-Re-saturation			-0.15	0.03		
	Re-saturation			+0.41	0.07		
	Freeze-Thaw testing			-	-		
Mod. stand.	Sawing-Preparation			-1.89	0.21		
	Prep.-Re-saturation			-0.07	0.00		
	Re-saturation			+0.71	0.04		
	Freeze-Thaw testing			-	-		
Plastic cur.	Sawing-Preparation			-0.12	0.08		
	Prep.-Re-saturation			-0.08	0.00		
	Re-saturation			+0.06	0.00		
	Freeze-Thaw testing			-	-		
Int. drying	Sawing-Preparation			-	-		
	Prep.-Re-saturation			-0.72	0.11		
	Re-saturation			+0.59	0.05		
	Freeze-Thaw testing			-	-		

Weight changes [%]	Re-saturation :	Water					
8 : 45-IS-AE	Testing medium :	3 % NaCl					
Curing :	Period of change :	Mean	Std.v.	Mean	Std.v.	Mean	Std.v.
Standard	Sawing-Preparation	-	-				
	Prep.-Re-saturation	-0.15	0.02				
	Re-saturation	+0.22	0.04				
	Freeze-Thaw testing	+0.50	0.08				
Mod. stand.	Sawing-Preparation	-1.17	0.17				
	Prep.-Re-saturation	-0.19	0.00				
	Re-saturation	+0.41	0.04				
	Freeze-Thaw testing	+0.46	0.05				
Plastic cur.	Sawing-Preparation	-0.02	0.01				
	Prep.-Re-saturation	-0.06	0.01				
	Re-saturation	+0.06	0.01				
	Freeze-Thaw testing	+0.24	0.06				
Int. drying	Sawing-Preparation	-	-				
	Prep.-Re-saturation	-0.54	0.03				
	Re-saturation	+0.39	0.04				
	Freeze-Thaw testing	+0.60	0.11				

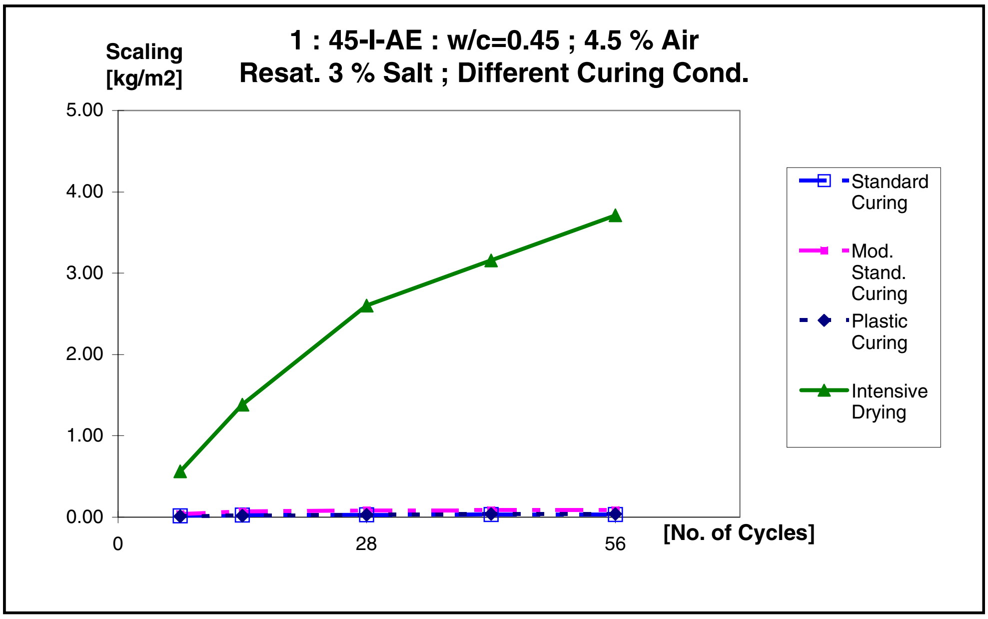
1 : 45-I-AE : w/c=0.45 ; 4.5 % Air
Resat. 3 % Salt ; Different Curing Cond.
Scaling [kg/m2]
5.00
4.00
3.00
2.00
1.00
0.00
0
28
56
[No. of Cycles]
Standard Curing
Mod. Stand. Curing
Plastic Curing
Intensive Drying

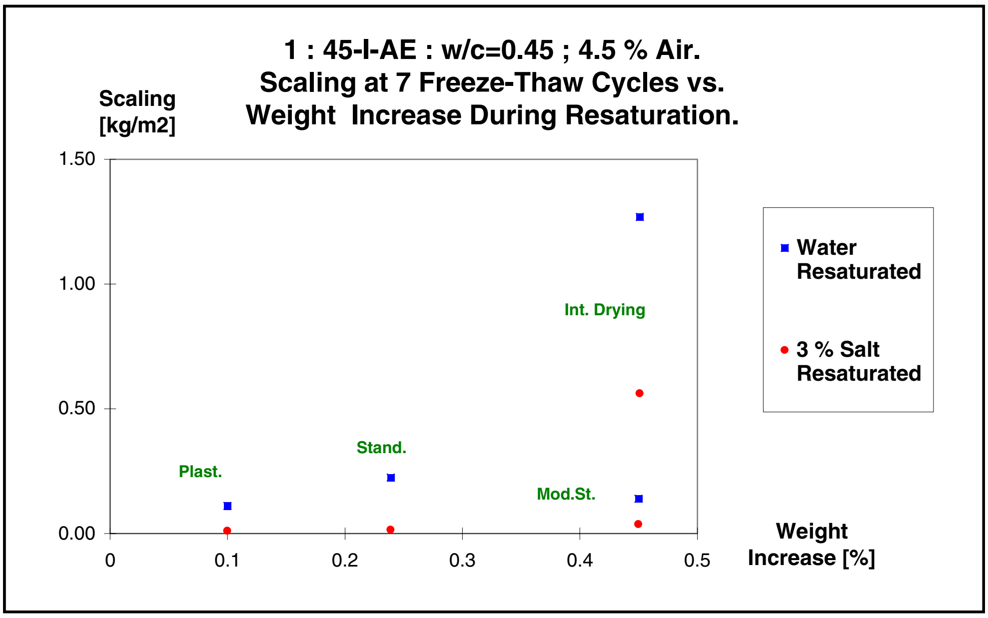
1 : 45-I-AE : w/c=0.45 ; 4.5 % Air.
Scaling at 7 Freeze-Thaw Cycles vs.
Weight Increase During Resaturation.
Scaling [kg/m2]
1.50
1.00
0.50
0.00
0
0.1
0.2
0.3
0.4
0.5
Weight Increase [%]
Int. Drying
Stand.
Plast.
Mod.St.
Water Resaturated
3 % Salt Resaturated

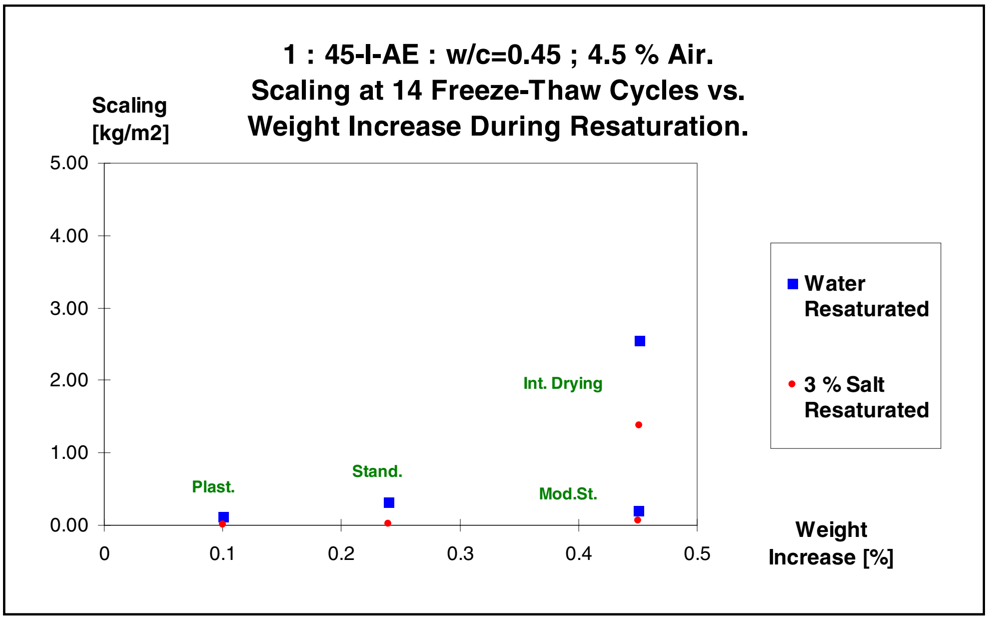
1 : 45-I-AE : w/c=0.45 ; 4.5 % Air.
Scaling at 14 Freeze-Thaw Cycles vs.
Weight Increase During Resaturation.
Scaling
[kg/m2]
5.00
4.00
3.00
2.00
1.00
0.00
0
0.1
0.2
0.3
0.4
0.5
Weight
Increase [%]
Int. Drying
Plast.
Stand.
Mod.St.
■ Water Resaturated
● 3 % Salt Resaturated

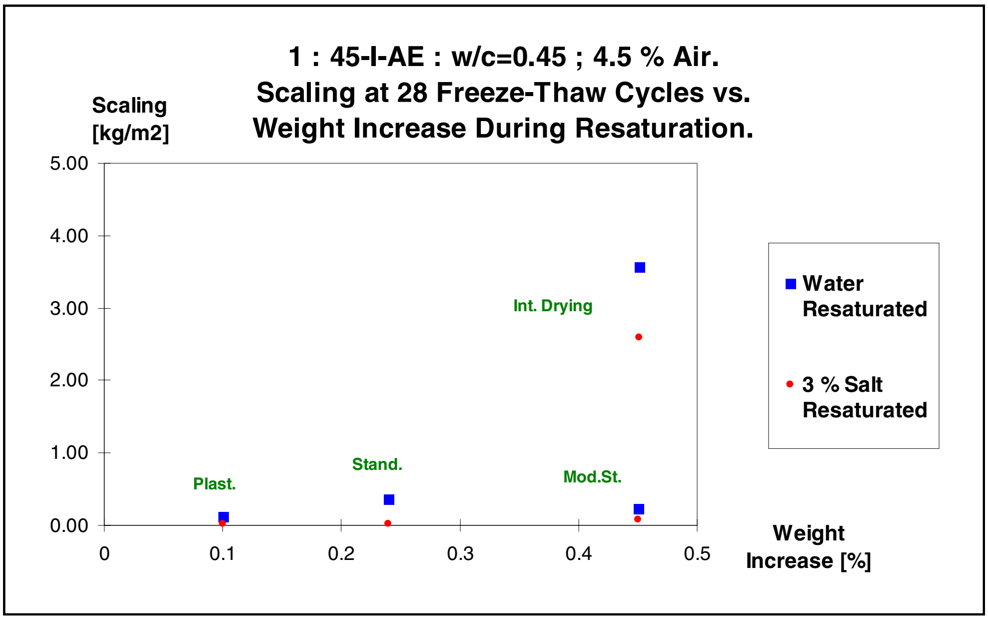
1 : 45-I-AE : w/c=0.45 ; 4.5 % Air.
Scaling at 28 Freeze-Thaw Cycles vs.
Weight Increase During Resaturation.
Scaling
[kg/m2]
5.00
4.00
3.00
2.00
1.00
0.00
0
0.1
0.2
0.3
0.4
0.5
Weight
Increase [%]
Int. Drying
Plast.
Stand.
Mod.St.
■ Water Resaturated
● 3 % Salt Resaturated

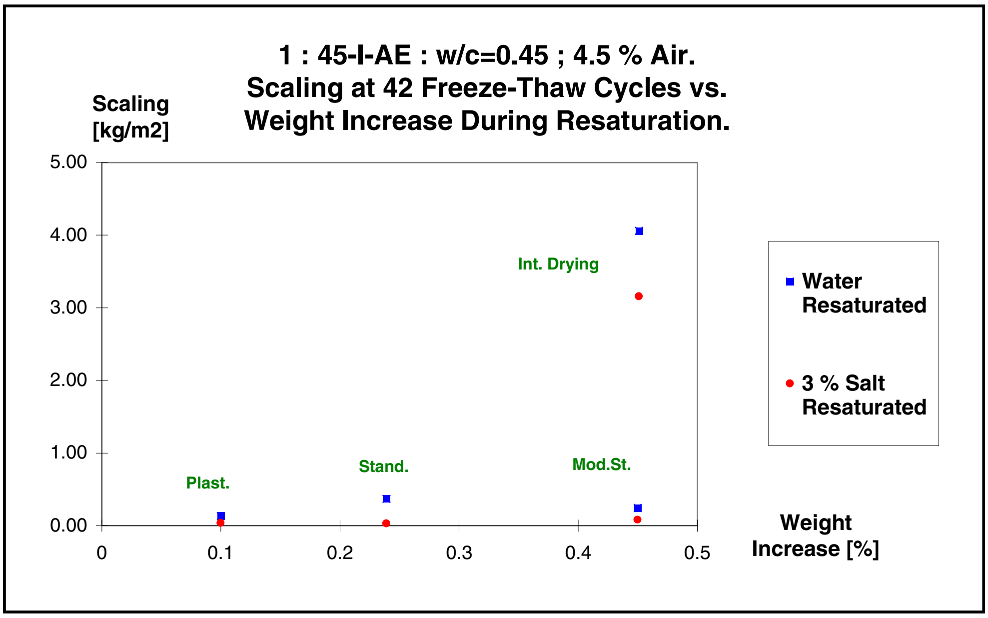
1 : 45-I-AE : w/c=0.45 ; 4.5 % Air.
Scaling at 42 Freeze-Thaw Cycles vs.
Weight Increase During Resaturation.
Scaling [kg/m2]
5.00
4.00
3.00
2.00
1.00
0.00
0
0.1
0.2
0.3
0.4
0.5
Weight Increase [%]
Int. Drying
Plast.
Stand.
Mod.St.
Water Resaturated
3 % Salt Resaturated

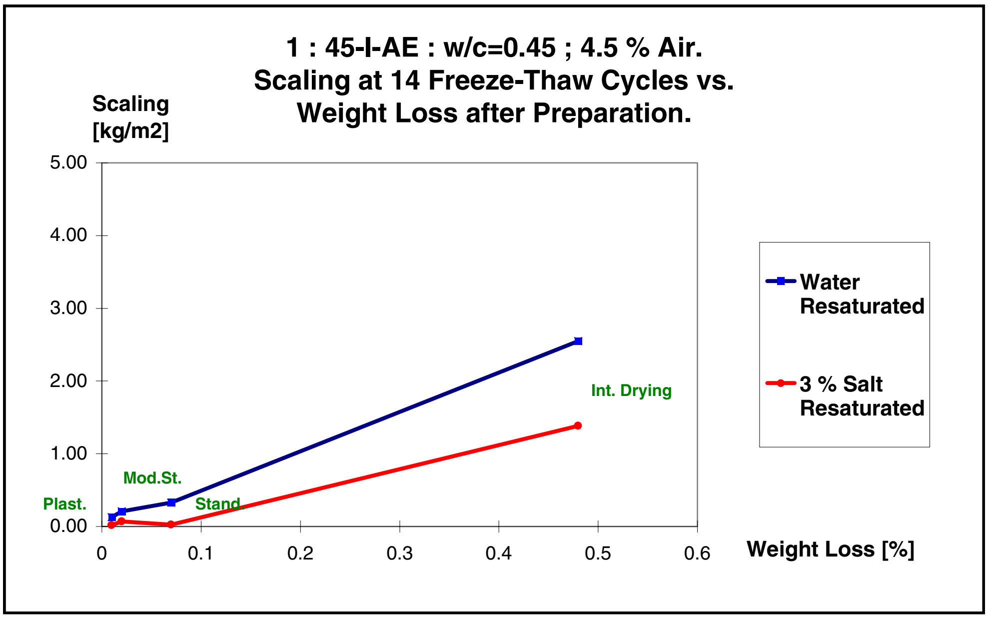
1 : 45-I-AE : w/c=0.45 ; 4.5 % Air.
Scaling at 14 Freeze-Thaw Cycles vs.
Weight Loss after Preparation.
Scaling [kg/m2]
5.00
4.00
3.00
2.00
1.00
0.00
0
0.1
0.2
0.3
0.4
0.5
0.6
Weight Loss [%]
Int. Drying
Mod.St.
Plast.
Stand.
Water Resaturated
3 % Salt Resaturated

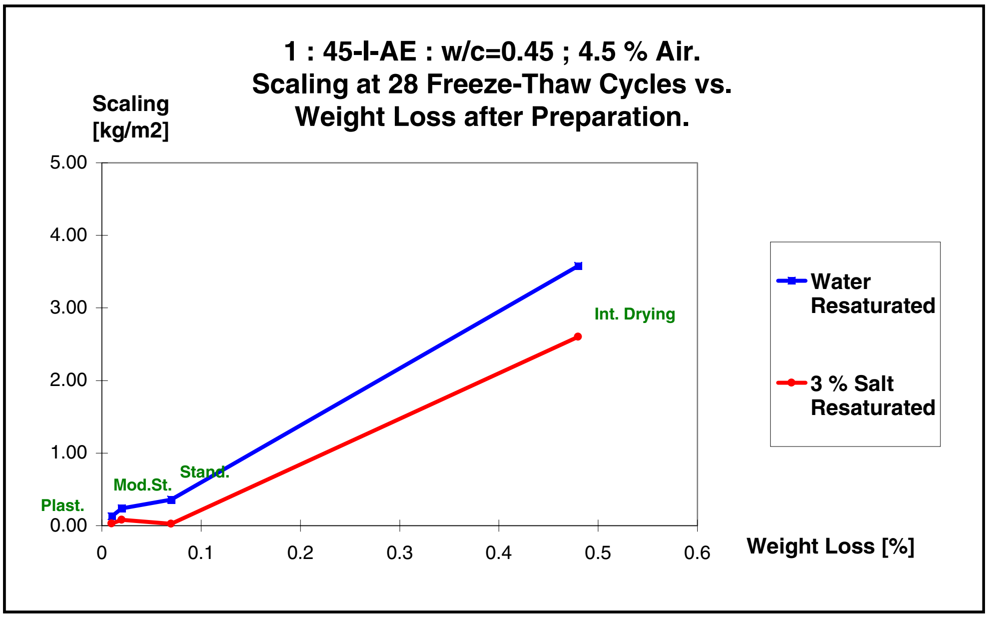
1 : 45-I-AE : w/c=0.45 ; 4.5 % Air.
Scaling at 28 Freeze-Thaw Cycles vs.
Weight Loss after Preparation.
Scaling [kg/m2]
5.00
4.00
3.00
2.00
1.00
0.00
0
0.1
0.2
0.3
0.4
0.5
0.6
Weight Loss [%]
Plast.
Mod.St.
Stand.
Int. Drying
Water Resaturated
3 % Salt Resaturated

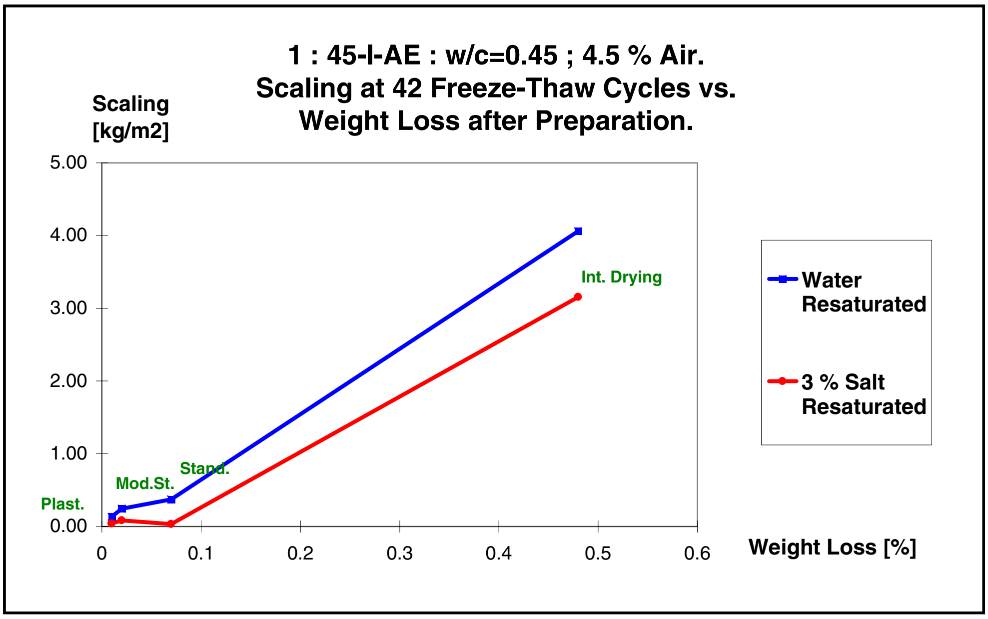
1 : 45-I-AE : w/c=0.45 ; 4.5 % Air.
Scaling at 42 Freeze-Thaw Cycles vs.
Weight Loss after Preparation.
Scaling [kg/m2]
5.00
4.00
3.00
2.00
1.00
0.00
0
0.1
0.2
0.3
0.4
0.5
0.6
Weight Loss [%]
Plast.
Mod.St.
Stand.
Int. Drying
Water Resaturated
3 % Salt Resaturated

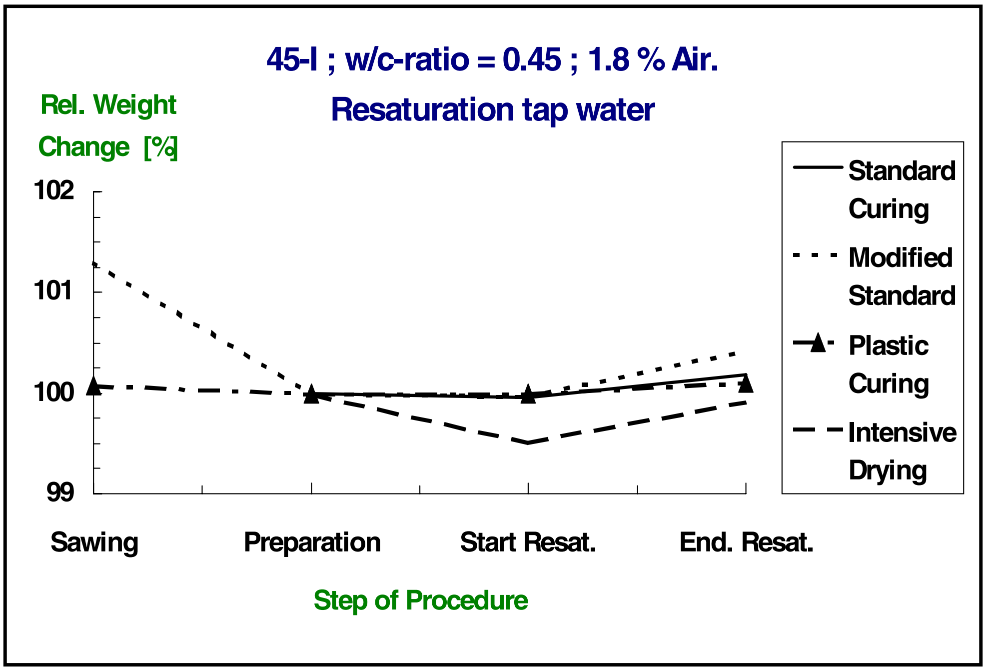
45-I ; w/c-ratio = 0.45 ; 1.8 % Air.
Resaturation tap water
Rel. Weight Change [%]
102
101
100
99
Sawing
Preparation
Start Resat.
End. Resat.
Step of Procedure
Standard Curing
Modified Standard
Plastic Curing
Intensive Drying

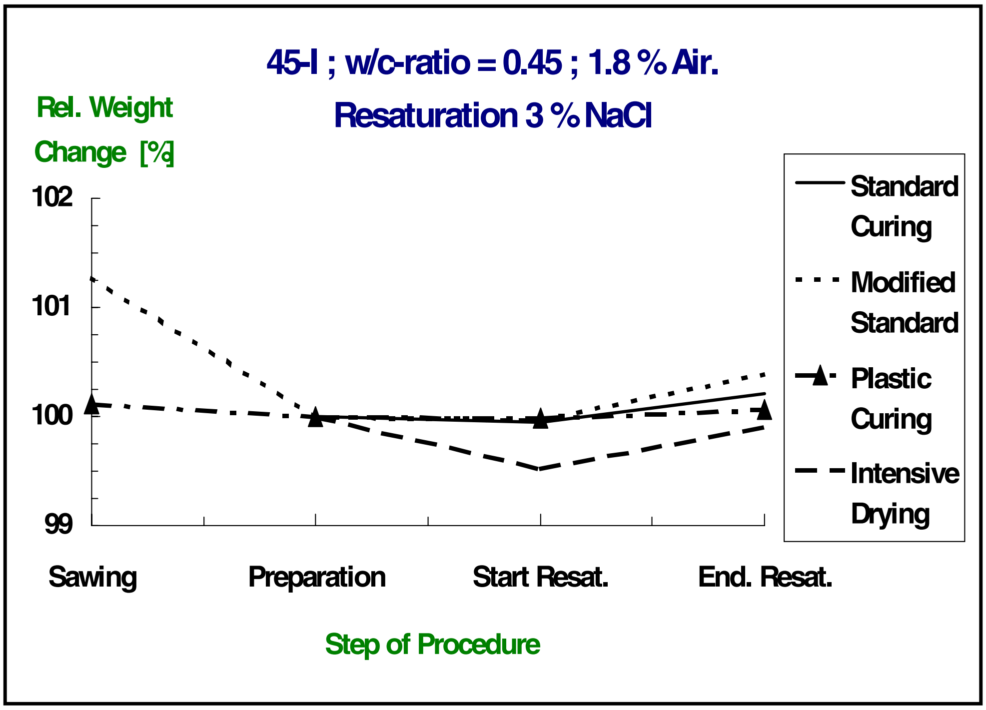
45-I ; w/c-ratio = 0.45 ; 1.8 % Air.
Resaturation 3 % NaCl
Rel. Weight Change [%]
102
101
100
99
Sawing
Preparation
Start Resat.
End. Resat.
Step of Procedure
Standard Curing
Modified Standard
Plastic Curing
Intensive Drying

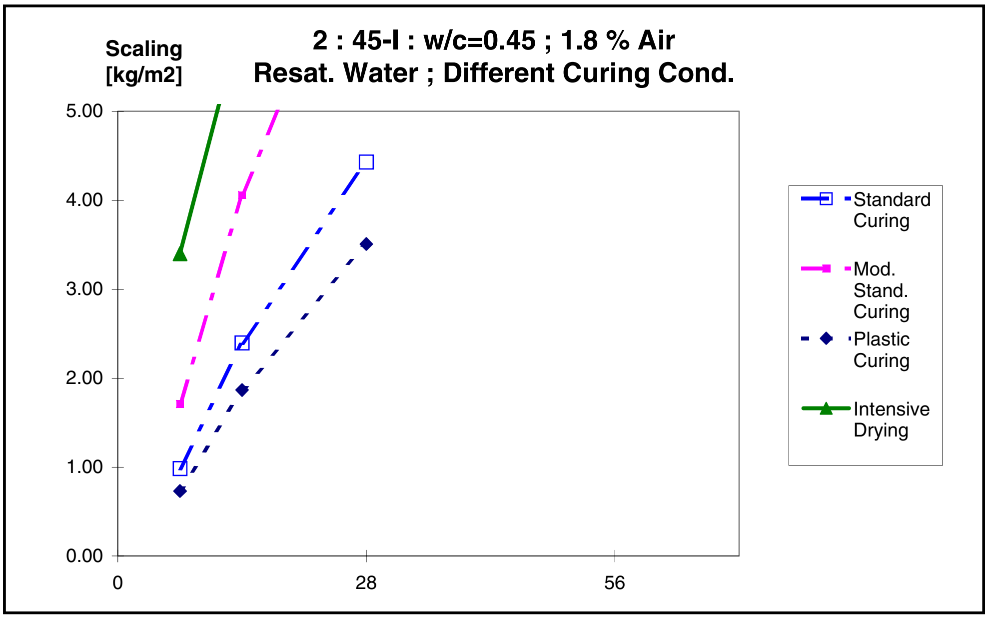
Scaling
[kg/m2]
2 : 45-I : w/c=0.45 ; 1.8 % Air
Resat. Water ; Different Curing Cond.
5.00
4.00
3.00
2.00
1.00
0.00
0
28
56
Standard Curing
Mod. Stand. Curing
Plastic Curing
Intensive Drying

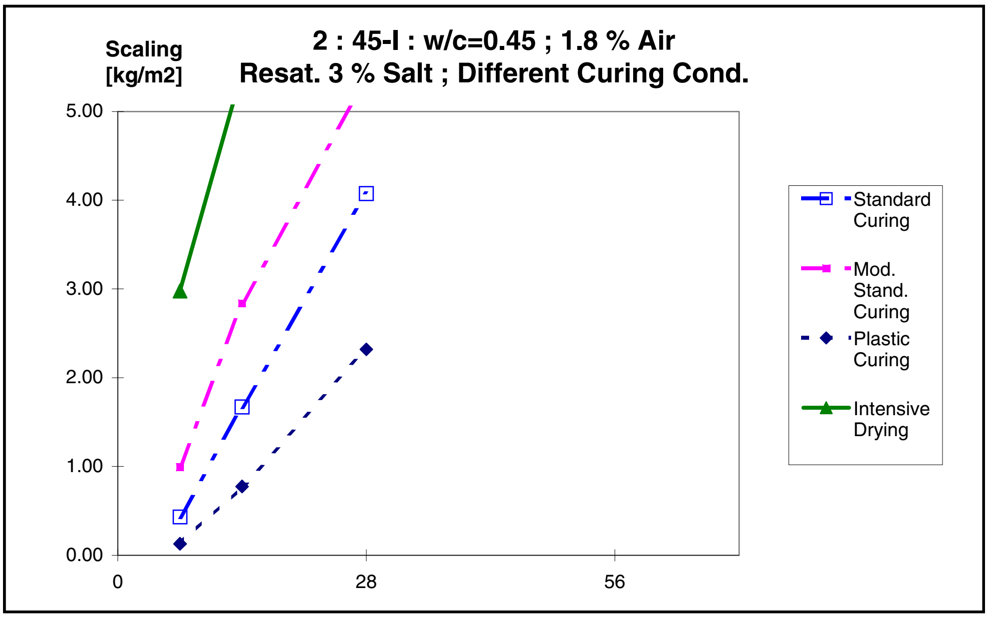
Scaling
[kg/m2]
2 : 45-I : w/c=0.45 ; 1.8 % Air
Resat. 3 % Salt ; Different Curing Cond.
5.00
4.00
3.00
2.00
1.00
0.00
0
28
56
Standard Curing
Mod. Stand. Curing
Plastic Curing
Intensive Drying

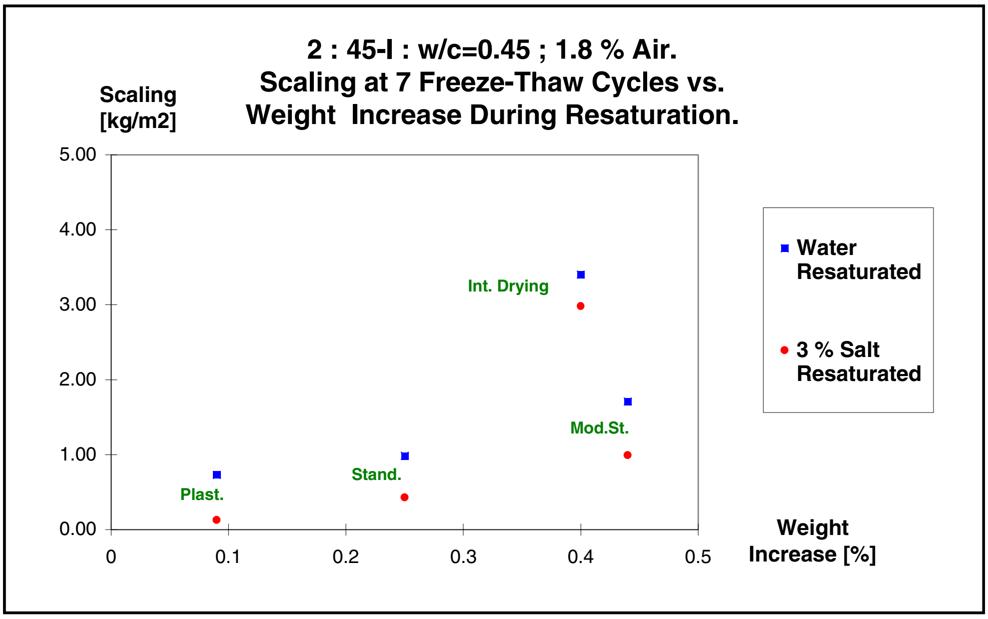
2 : 45-I : w/c=0.45 ; 1.8 % Air.
Scaling at 7 Freeze-Thaw Cycles vs.
Weight Increase During Resaturation.
Scaling [kg/m2]
5.00
4.00
3.00
2.00
1.00
0.00
0
0.1
0.2
0.3
0.4
0.5
Weight Increase [%]
Int. Drying
Mod.St.
Stand.
Plast.
■ Water Resaturated
● 3 % Salt Resaturated

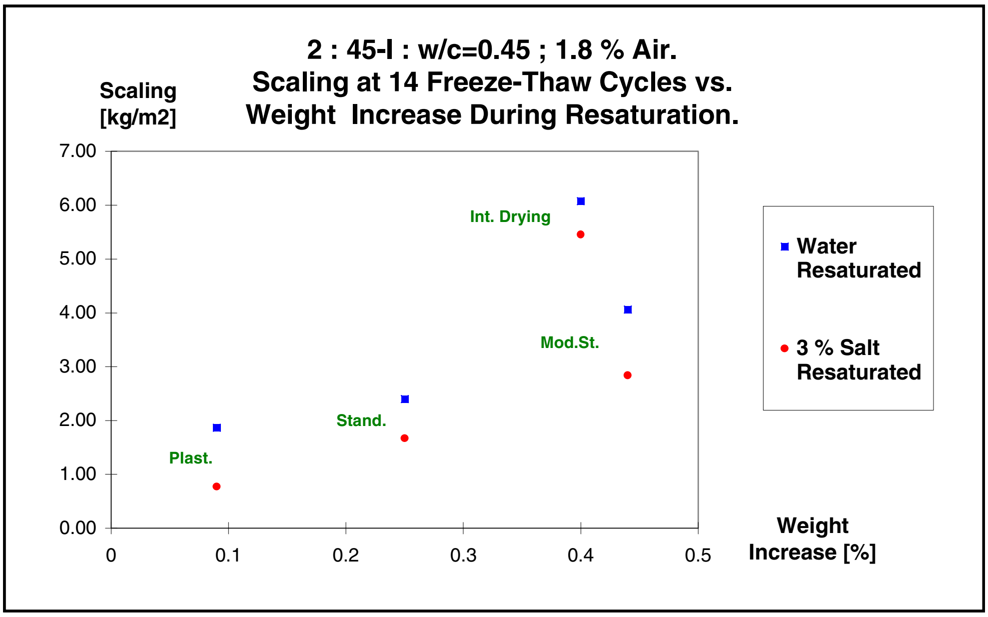
2 : 45-I : w/c=0.45 ; 1.8 % Air.
Scaling at 14 Freeze-Thaw Cycles vs.
Weight Increase During Resaturation.
Scaling [kg/m2]
7.00
6.00
5.00
4.00
3.00
2.00
1.00
0.00
0
0.1
0.2
0.3
0.4
0.5
Weight Increase [%]
Int. Drying
Mod.St.
Stand.
Plast.
■ Water Resaturated
● 3 % Salt Resaturated

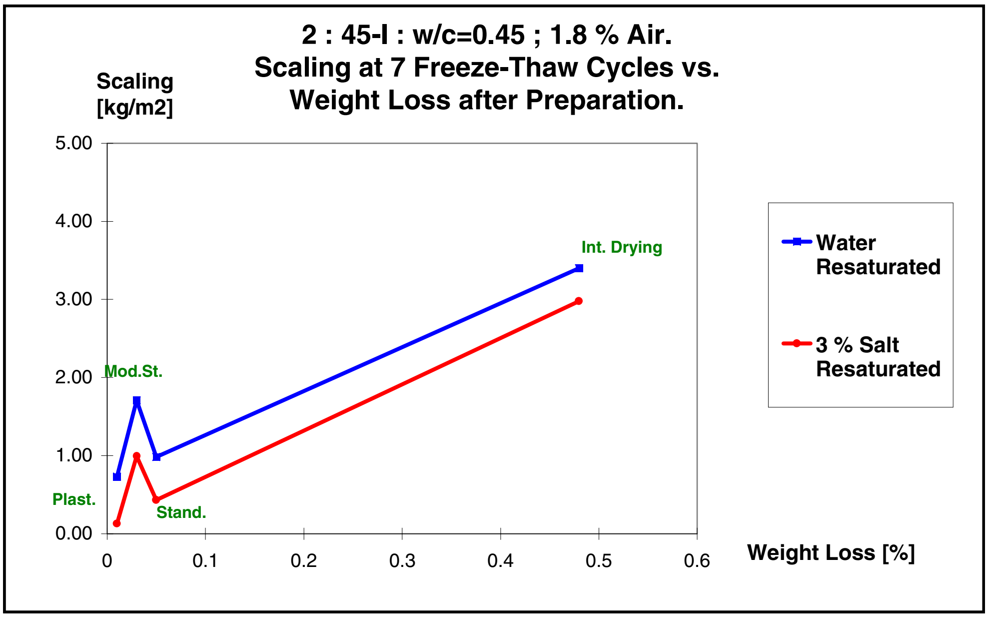
2 : 45-I : w/c=0.45 ; 1.8 % Air.
Scaling at 7 Freeze-Thaw Cycles vs.
Weight Loss after Preparation.
Scaling
[kg/m2]
5.00
4.00
3.00
2.00
1.00
0.00
0
0.1
0.2
0.3
0.4
0.5
0.6
Weight Loss [%]
Mod.St.
Plast.
Stand.
Int. Drying
Water Resaturated
3 % Salt Resaturated

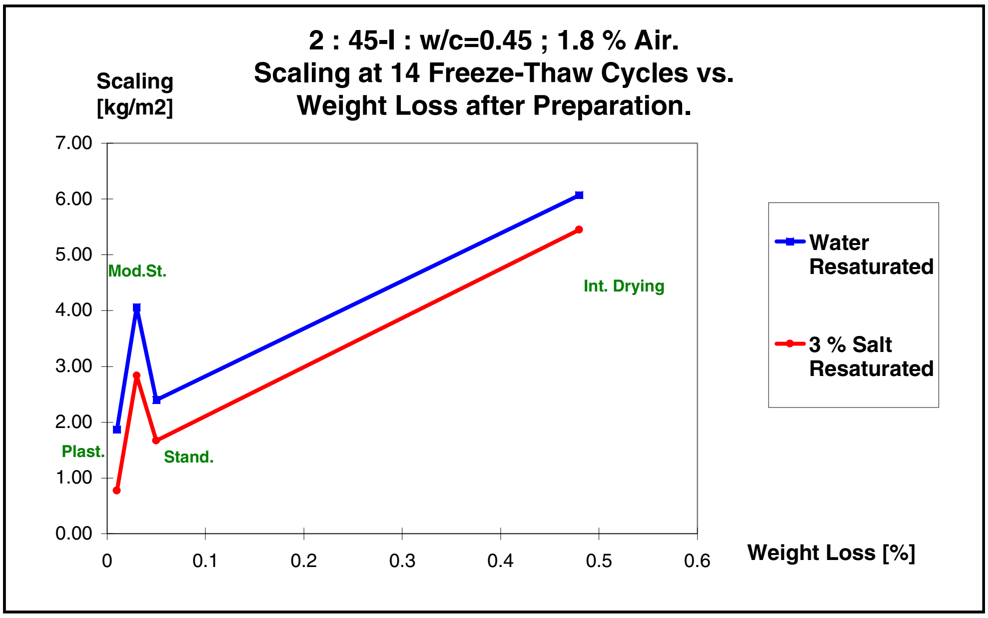
2 : 45-I : w/c=0.45 ; 1.8 % Air.
Scaling at 14 Freeze-Thaw Cycles vs.
Weight Loss after Preparation.
Scaling
[kg/m2]
7.00
6.00
5.00
4.00
3.00
2.00
1.00
0.00
0
0.1
0.2
0.3
0.4
0.5
0.6
Weight Loss [%]
Mod.St.
Plast.
Stand.
Int. Drying
Water Resaturated
3 % Salt Resaturated

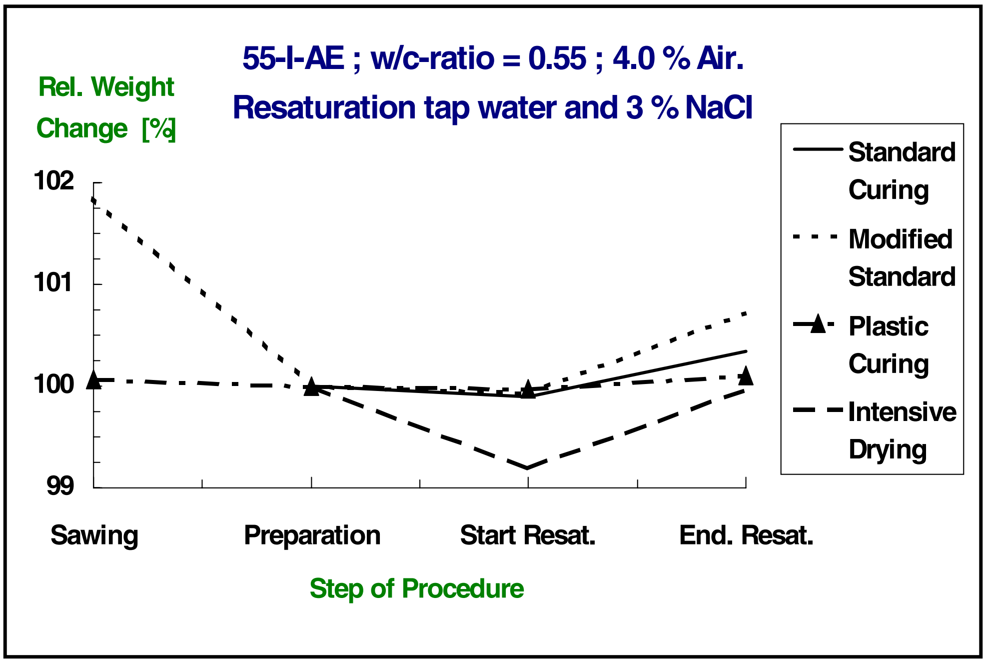
55-I-AE ; w/c-ratio = 0.55 ; 4.0 % Air.
Resaturation tap water and 3 % NaCl
Rel. Weight Change [%]
102
101
100
99
Sawing
Preparation
Start Resat.
End. Resat.
Step of Procedure
Standard Curing
Modified Standard
Plastic Curing
Intensive Drying

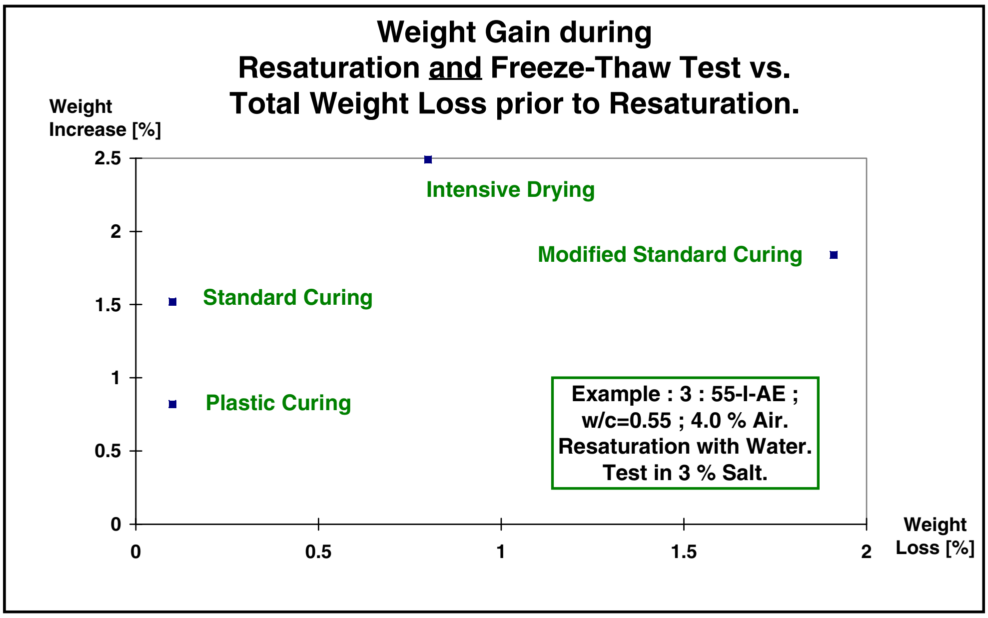
Weight Gain during Resaturation and Freeze-Thaw Test vs. Total Weight Loss prior to Resaturation.
Weight Increase [%]
2.5
2
1.5
1
0.5
0
0
0.5
1
1.5
2
Weight Loss [%]
Intensive Drying
Modified Standard Curing
Standard Curing
Plastic Curing
Example : 3 : 55-I-AE ; w/c=0.55 ; 4.0 % Air. Resaturation with Water. Test in 3 % Salt.

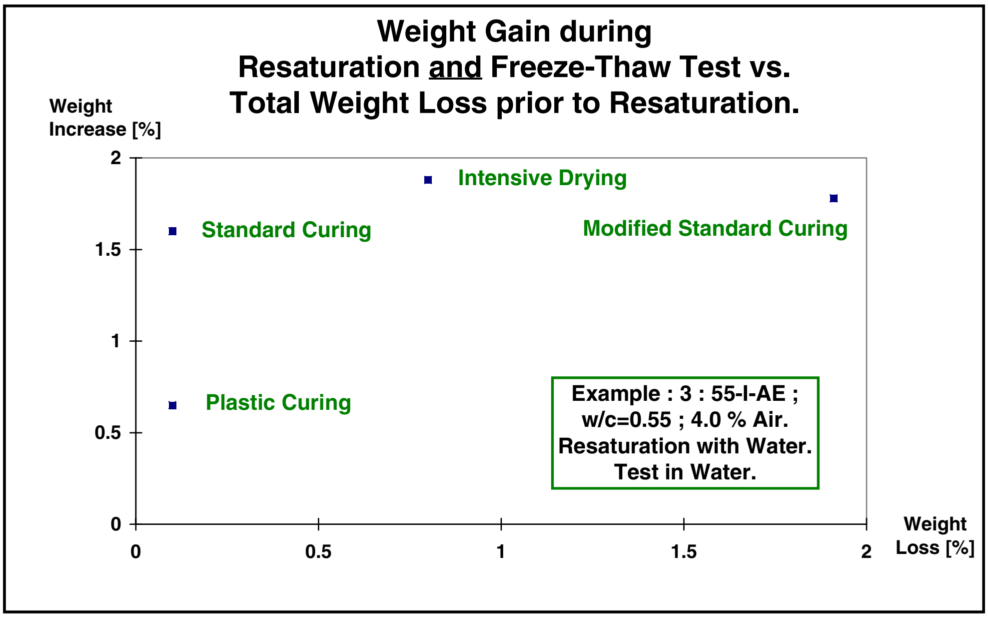
Weight Gain during
Resaturation and Freeze-Thaw Test vs.
Total Weight Loss prior to Resaturation.
Weight
Increase [%]
2
1.5
1
0.5
0
0
0.5
1
1.5
2
Weight
Loss [%]
Intensive Drying
Standard Curing
Modified Standard Curing
Plastic Curing
Example : 3 : 55-I-AE ;
w/c=0.55 ; 4.0 % Air.
Resaturation with Water.
Test in Water.

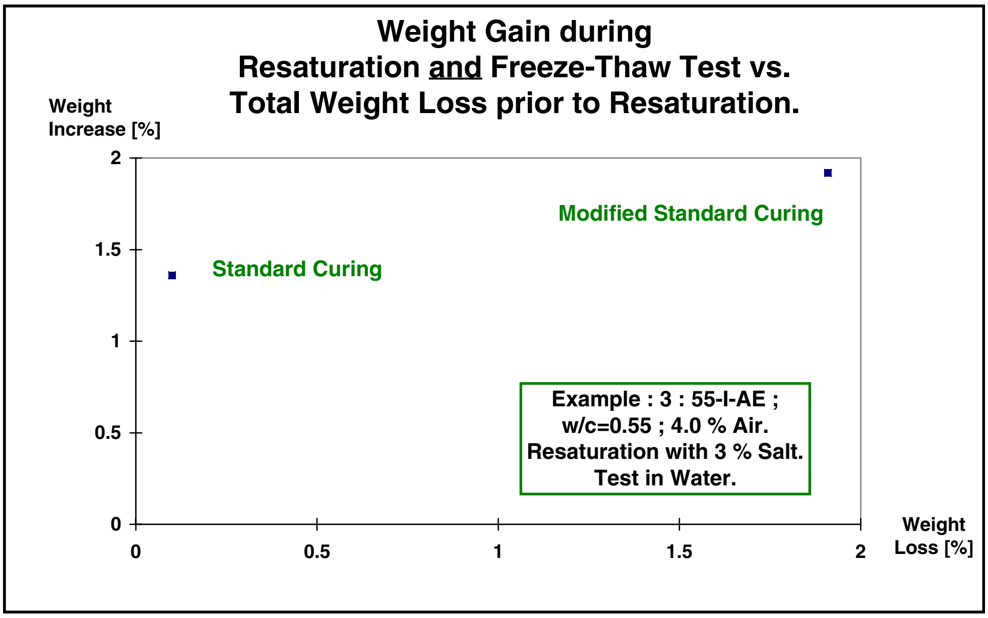
Weight Gain during
Resaturation and Freeze-Thaw Test vs.
Total Weight Loss prior to Resaturation.
Weight
Increase [%]
2
1.5
1
0.5
0
0
0.5
1
1.5
2
Weight
Loss [%]
Modified Standard Curing
Standard Curing
Example : 3 : 55-I-AE ;
w/c=0.55 ; 4.0 % Air.
Resaturation with 3 % Salt.
Test in Water.

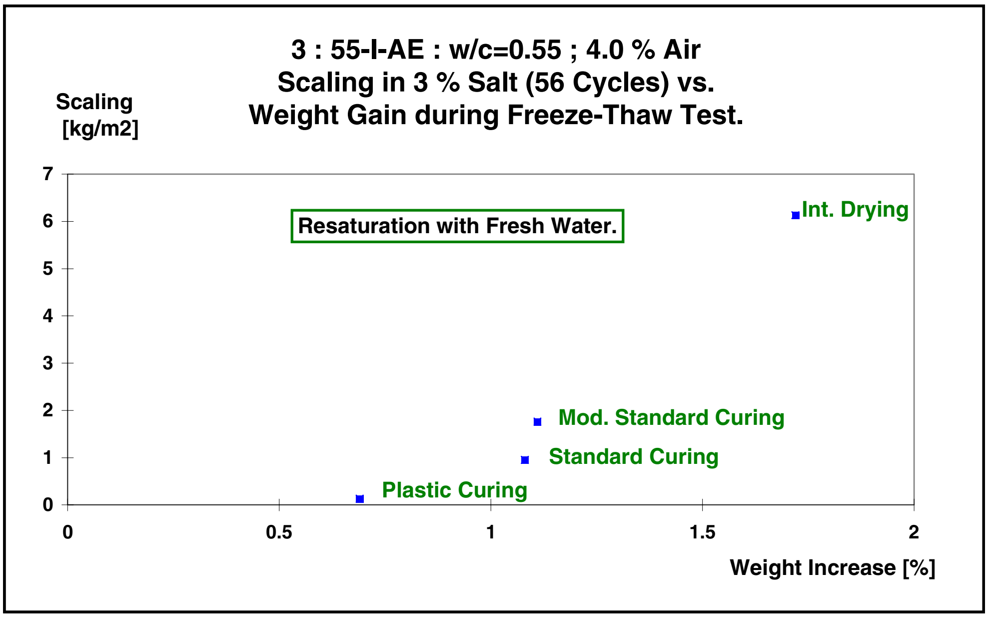
3 : 55-I-AE : w/c=0.55 ; 4.0 % Air
Scaling in 3 % Salt (56 Cycles) vs.
Weight Gain during Freeze-Thaw Test.
Scaling [kg/m2]
Resaturation with Fresh Water.
Int. Drying
Mod. Standard Curing
Standard Curing
Plastic Curing
0
1
2
3
4
5
6
7
0
0.5
1
1.5
2
Weight Increase [%]

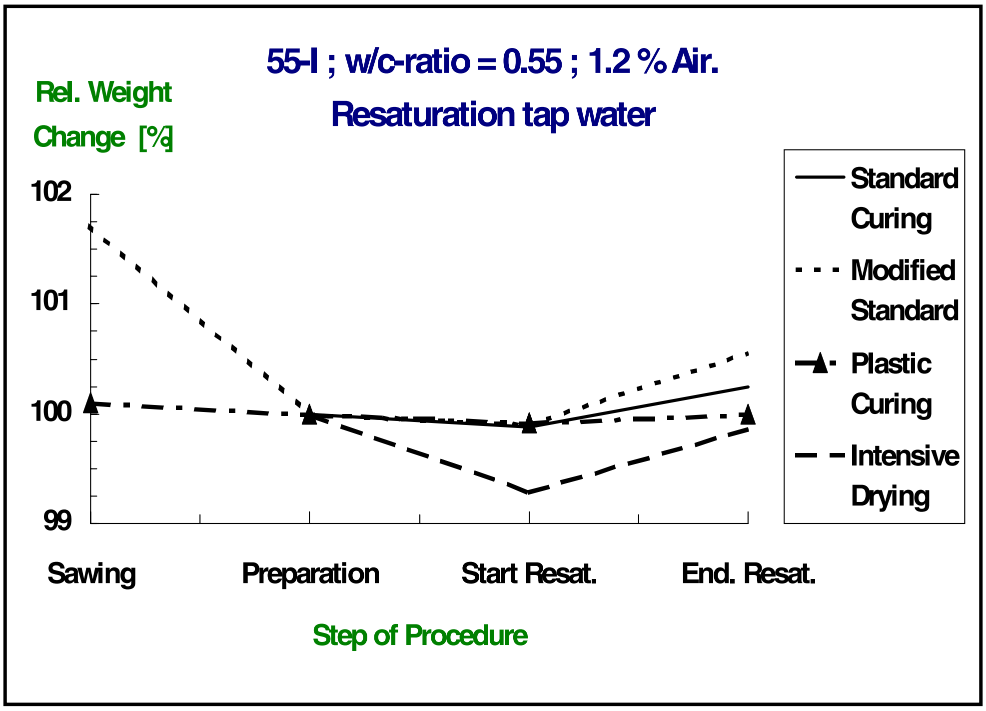
55-I ; w/c-ratio = 0.55 ; 1.2 % Air.
Resaturation tap water
Rel. Weight Change [%]
102
101
100
99
Standard Curing
Modified Standard
Plastic Curing
Intensive Drying
Sawing
Preparation
Start Resat.
End. Resat.
Step of Procedure

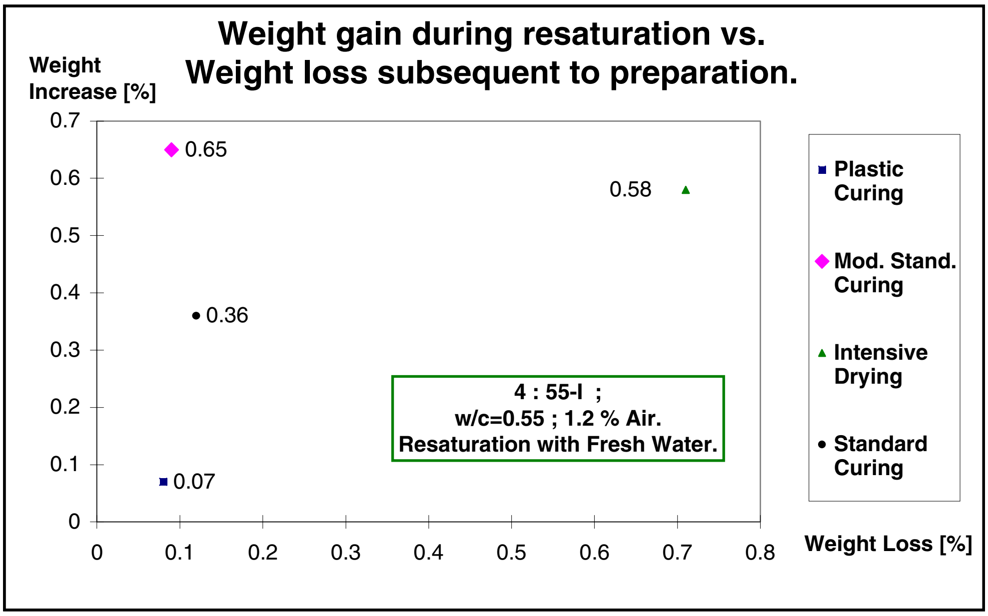
Weight gain during resaturation vs.
Weight loss subsequent to preparation.
Weight Increase [%]
0.7
0.6
0.5
0.4
0.3
0.2
0.1
0
0
0.1
0.2
0.3
0.4
0.5
0.6
0.7
0.8
Weight Loss [%]
0.65
0.58
0.36
0.07
4 : 55-I ;
w/c=0.55 ; 1.2 % Air.
Resaturation with Fresh Water.
Plastic Curing
Mod. Stand. Curing
Intensive Drying
Standard Curing

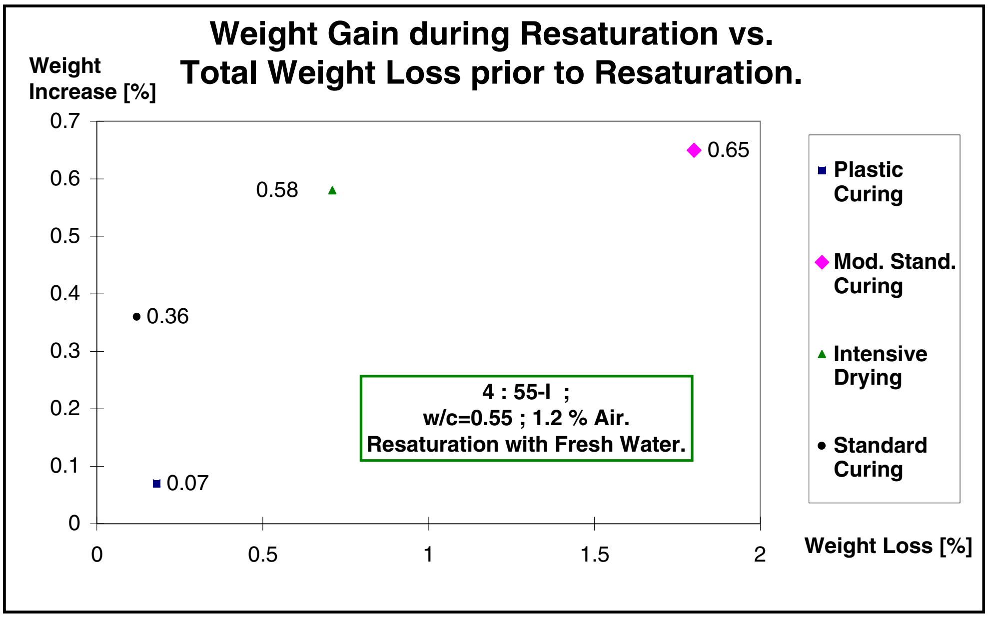
Weight Gain during Resaturation vs.
Total Weight Loss prior to Resaturation.
Weight Increase [%]
0.7
0.6
0.5
0.4
0.3
0.2
0.1
0
0
0.5
1
1.5
2
Weight Loss [%]
0.65
0.58
0.36
0.07
4 : 55-I ;
w/c=0.55 ; 1.2 % Air.
Resaturation with Fresh Water.
Plastic Curing
Mod. Stand. Curing
Intensive Drying
Standard Curing

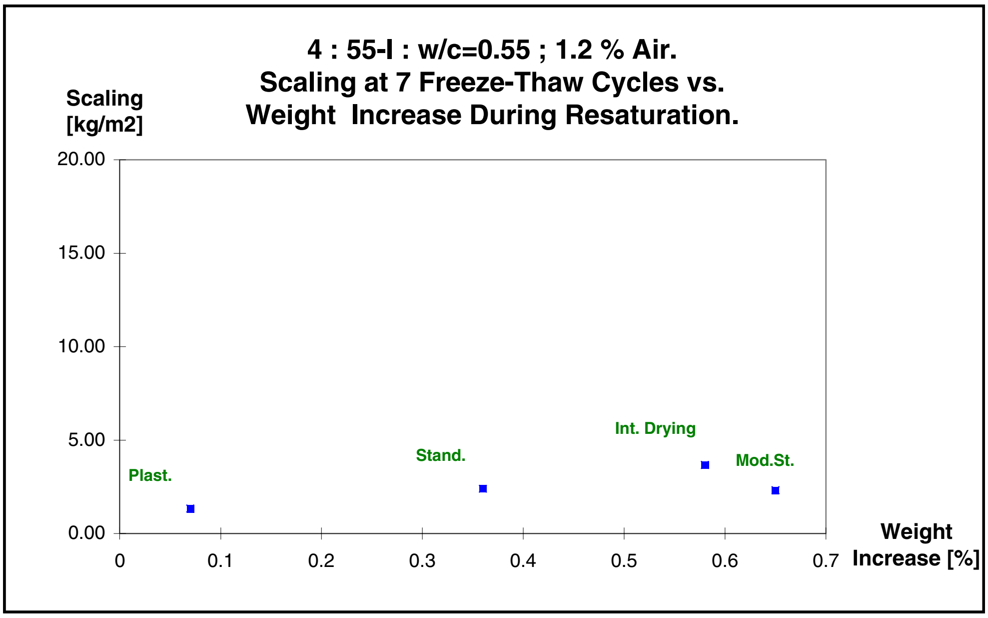
4 : 55-I : w/c=0.55 ; 1.2 % Air.
Scaling at 7 Freeze-Thaw Cycles vs.
Weight Increase During Resaturation.
Scaling [kg/m2]
20.00
15.00
10.00
5.00
0.00
0
0.1
0.2
0.3
0.4
0.5
0.6
0.7
Weight Increase [%]
Plast.
Stand.
Int. Drying
Mod.St.

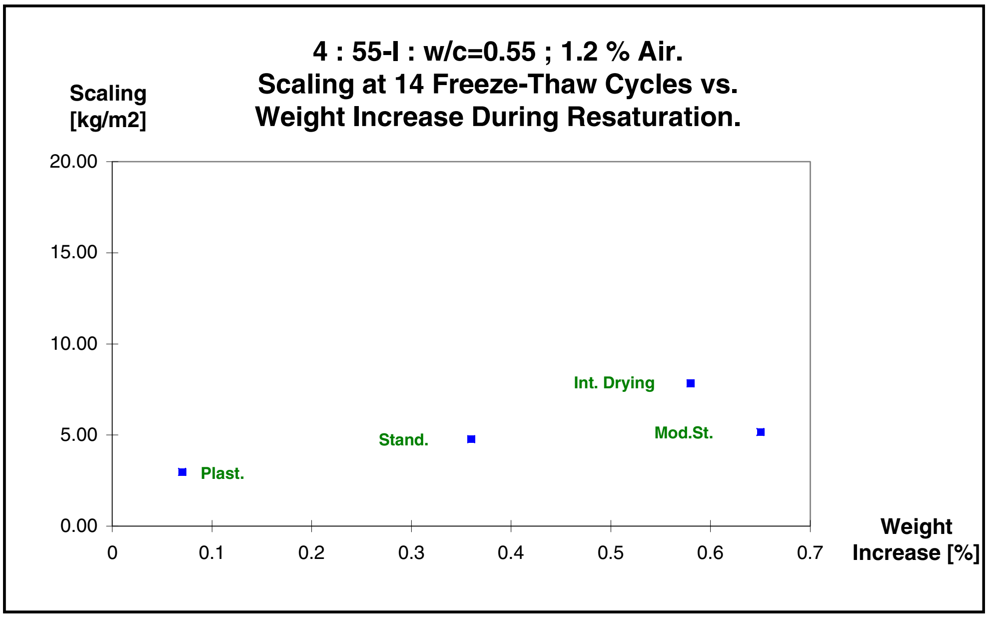
4 : 55-I : w/c=0.55 ; 1.2 % Air.
Scaling at 14 Freeze-Thaw Cycles vs.
Weight Increase During Resaturation.
Scaling [kg/m2]
20.00
15.00
10.00
5.00
0.00
0
0.1
0.2
0.3
0.4
0.5
0.6
0.7
Weight Increase [%]
Int. Drying
Stand.
Mod.St.
Plast.

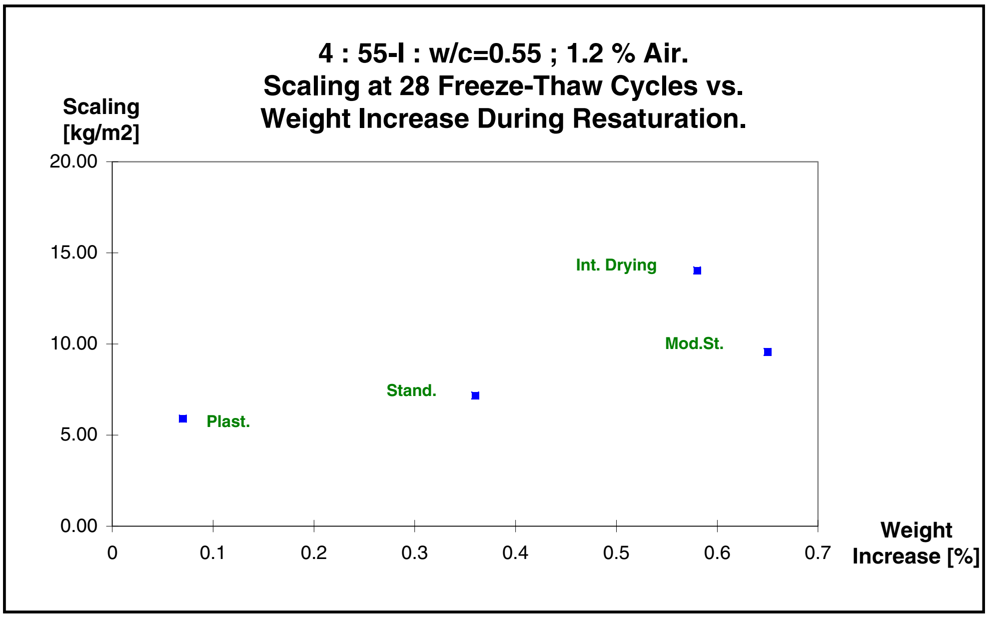
4 : 55-I : w/c=0.55 ; 1.2 % Air.
Scaling at 28 Freeze-Thaw Cycles vs.
Weight Increase During Resaturation.
Scaling
[kg/m2]
20.00
15.00
10.00
5.00
0.00
0
0.1
0.2
0.3
0.4
0.5
0.6
0.7
Weight
Increase [%]
Int. Drying
Mod.St.
Stand.
Plast.

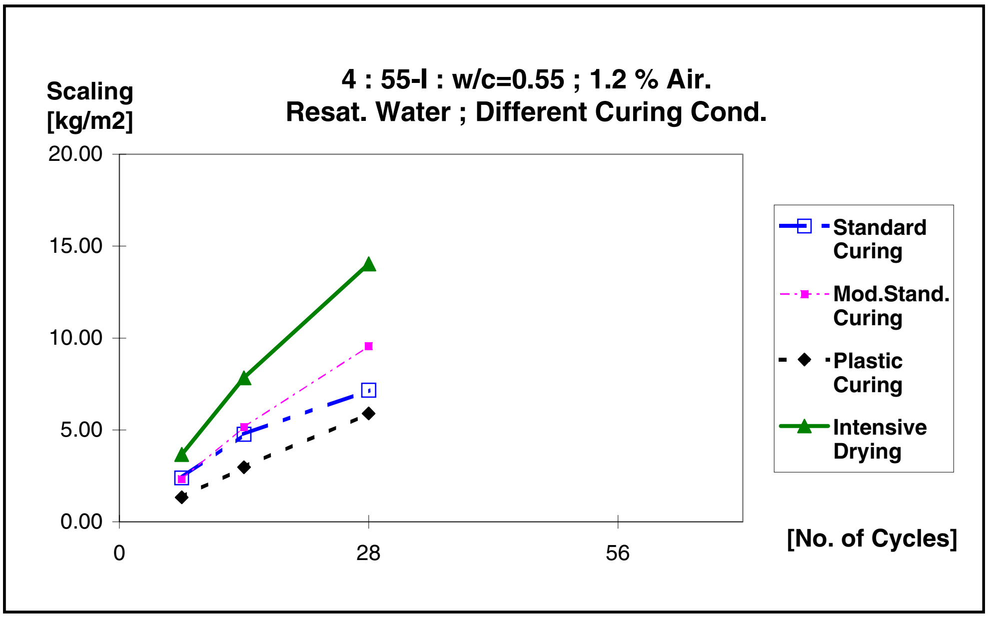
4 : 55-I : w/c=0.55 ; 1.2 % Air.
Resat. Water ; Different Curing Cond.
Scaling
[kg/m2]
20.00
15.00
10.00
5.00
0.00
0
28
56
[No. of Cycles]
Standard Curing
Mod.Stand. Curing
Plastic Curing
Intensive Drying

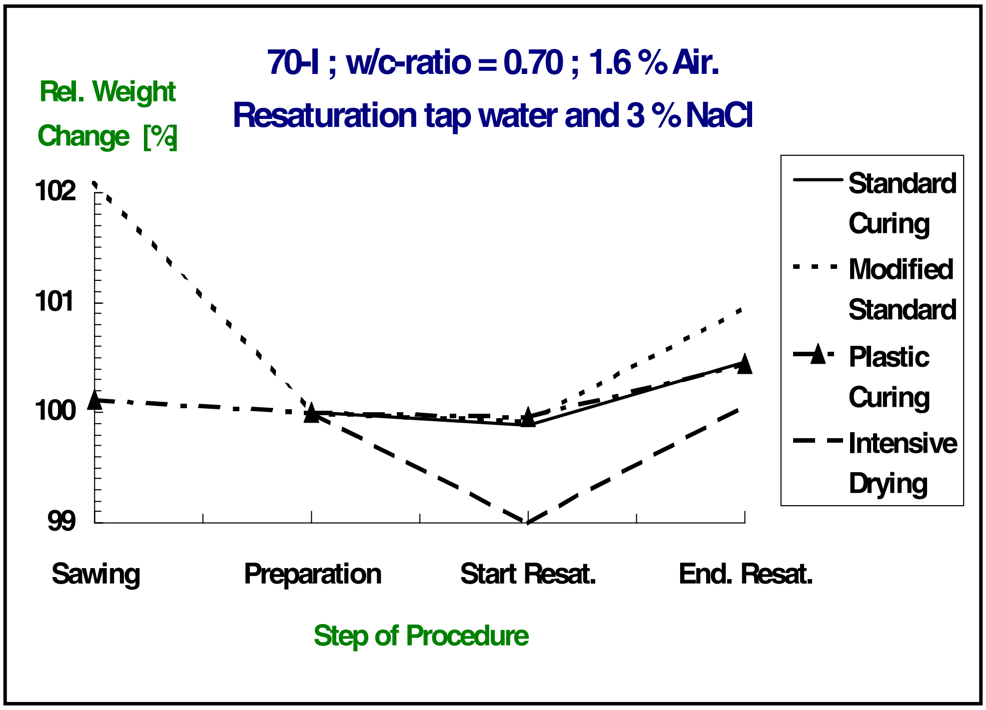
70-I ; w/c-ratio = 0.70 ; 1.6 % Air.
Resaturation tap water and 3 % NaCl
Rel. Weight Change [%]
102
101
100
99
Sawing
Preparation
Start Resat.
End. Resat.
Step of Procedure
Standard Curing
Modified Standard
Plastic Curing
Intensive Drying

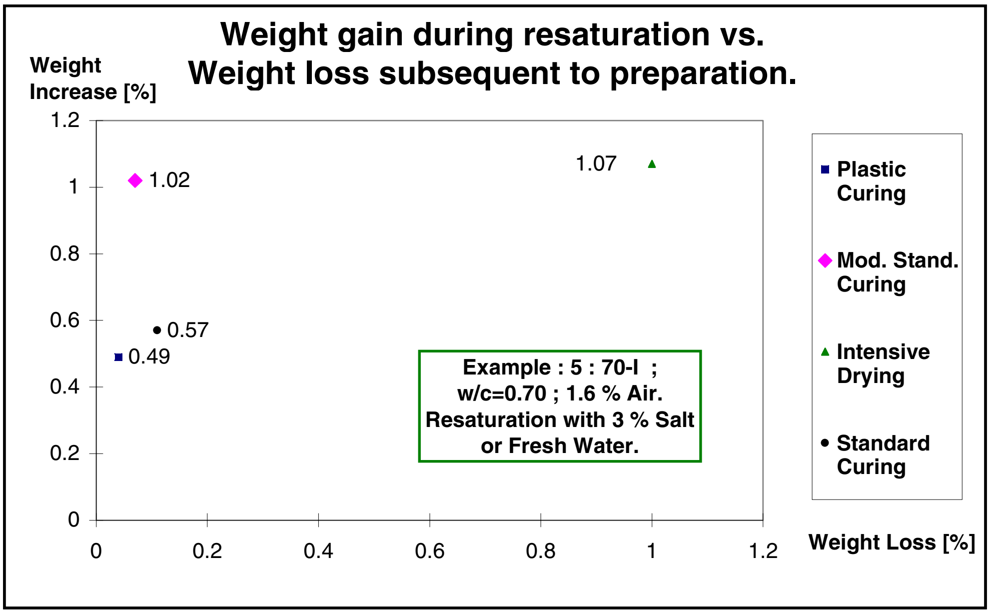
Weight gain during resaturation vs.
Weight loss subsequent to preparation.
Weight Increase [%]
1.2
1
0.8
0.6
0.4
0.2
0
0
0.2
0.4
0.6
0.8
1
1.2
Weight Loss [%]
1.02
1.07
0.57
0.49
Example : 5 : 70-I ; w/c=0.70 ; 1.6 % Air. Resaturation with 3 % Salt or Fresh Water.
Plastic Curing
Mod. Stand. Curing
Intensive Drying
Standard Curing

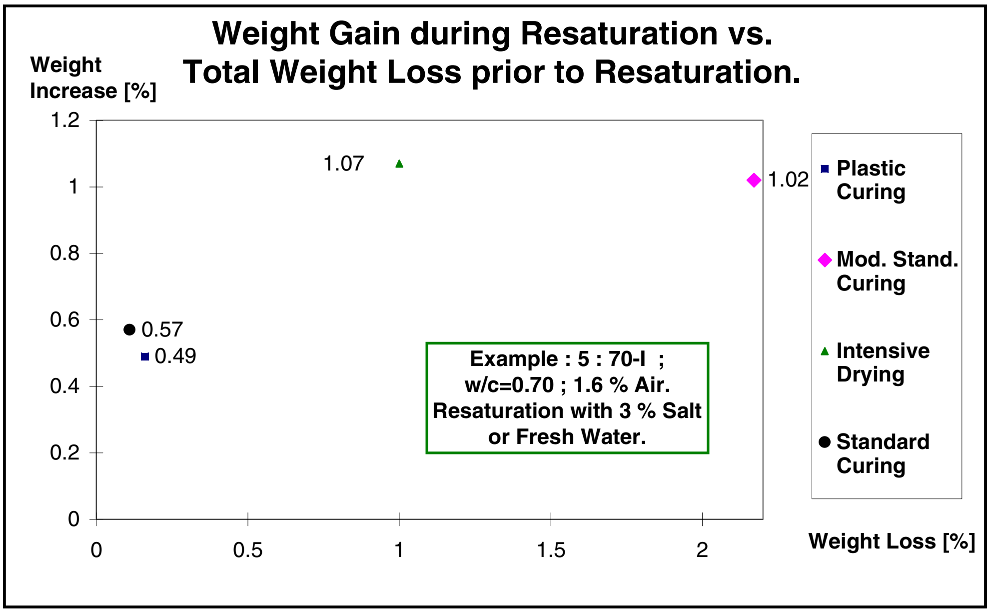
Weight Gain during Resaturation vs.
Total Weight Loss prior to Resaturation.
Weight Increase [%]
1.2
1
0.8
0.6
0.4
0.2
0
0
0.5
1
1.5
2
Weight Loss [%]
1.07
1.02
0.57
0.49
Example : 5 : 70-I ; w/c=0.70 ; 1.6 % Air. Resaturation with 3 % Salt or Fresh Water.
Plastic Curing
Mod. Stand. Curing
Intensive Drying
Standard Curing

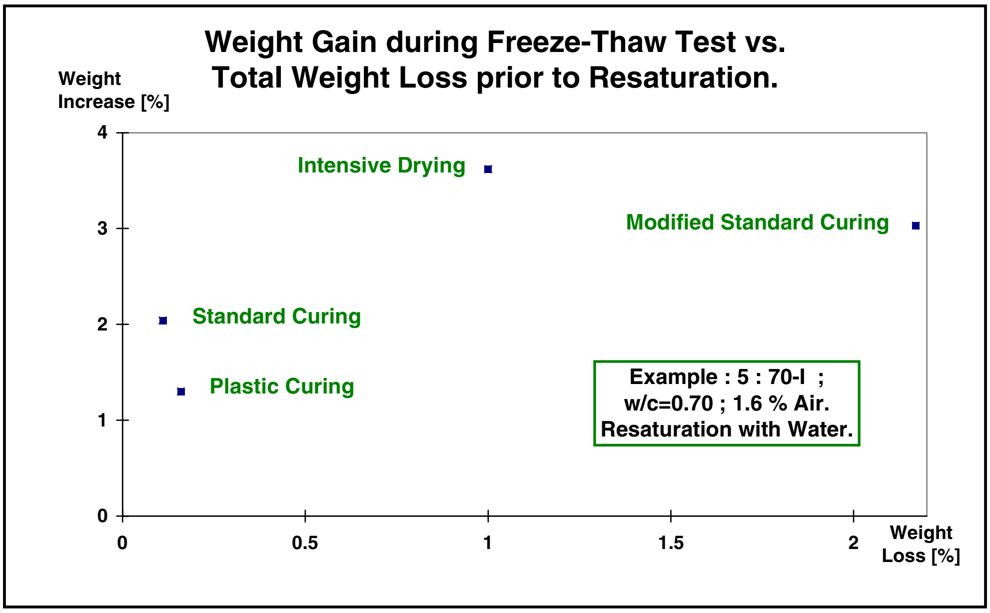
Weight Gain during Freeze-Thaw Test vs.
Total Weight Loss prior to Resaturation.
Weight Increase [%]
4
3
2
1
0
0
0.5
1
1.5
2
Weight Loss [%]
Intensive Drying
Modified Standard Curing
Standard Curing
Plastic Curing
Example : 5 : 70-I ; w/c=0.70 ; 1.6 % Air. Resaturation with Water.

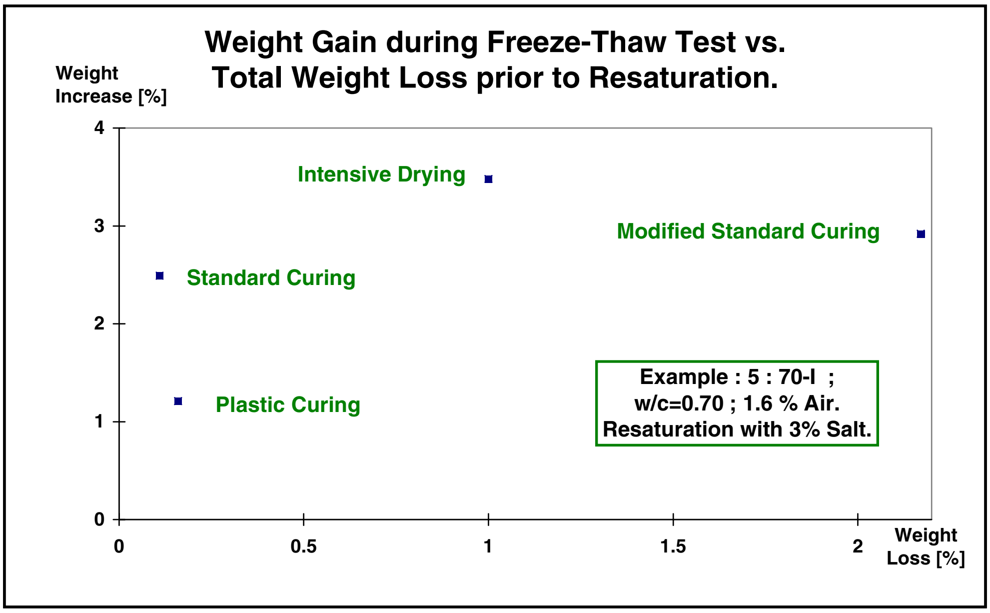
Weight Gain during Freeze-Thaw Test vs.
Total Weight Loss prior to Resaturation.
Weight Increase [%]
4
3
2
1
0
Intensive Drying
Modified Standard Curing
Standard Curing
Plastic Curing
Example : 5 : 70-I ; w/c=0.70 ; 1.6 % Air. Resaturation with 3% Salt.
0
0.5
1
1.5
2
Weight Loss [%]

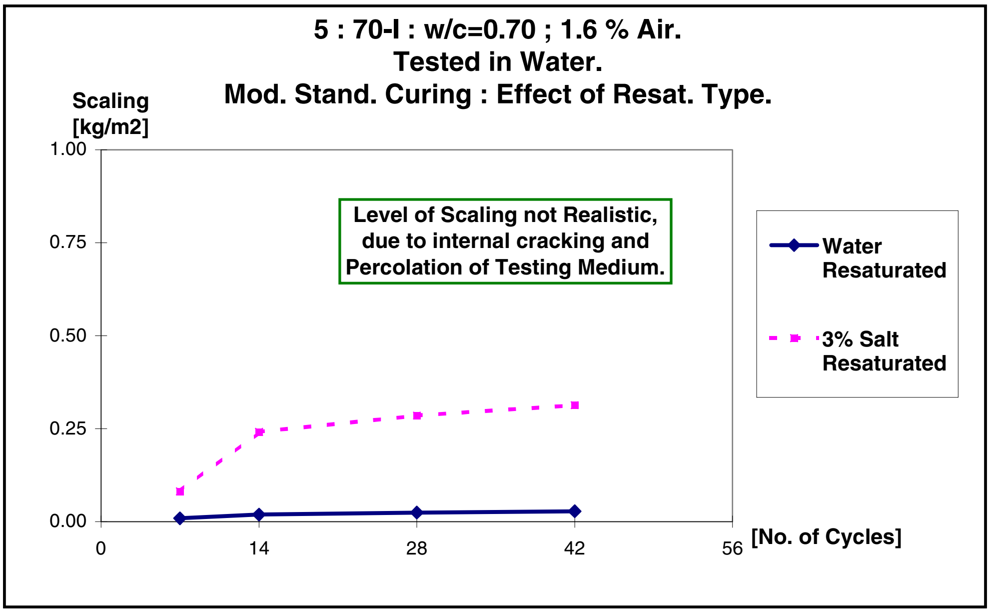
5 : 70-I : w/c=0.70 ; 1.6 % Air.
Tested in Water.
Mod. Stand. Curing : Effect of Resat. Type.
Scaling [kg/m2]
1.00
0.75
0.50
0.25
0.00
Level of Scaling not Realistic, due to internal cracking and Percolation of Testing Medium.
Water Resaturated
3% Salt Resaturated
0
14
28
42
56
[No. of Cycles]

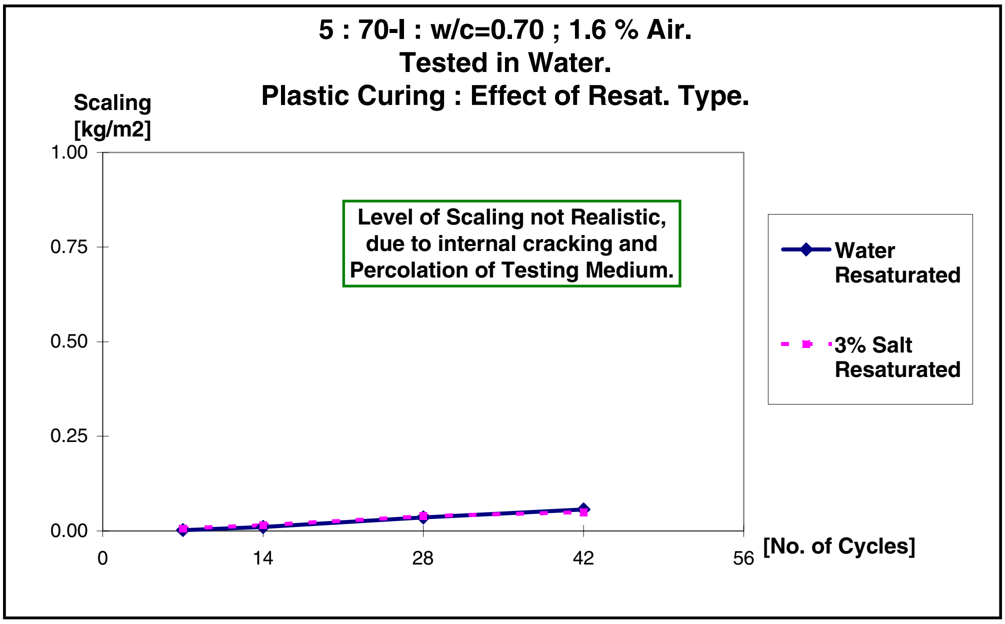
5 : 70-I : w/c=0.70 ; 1.6 % Air.
Tested in Water.
Plastic Curing : Effect of Resat. Type.
Scaling [kg/m2]
1.00
0.75
0.50
0.25
0.00
0
14
28
42
56
[No. of Cycles]
Level of Scaling not Realistic, due to internal cracking and Percolation of Testing Medium.
Water Resaturated
3% Salt Resaturated

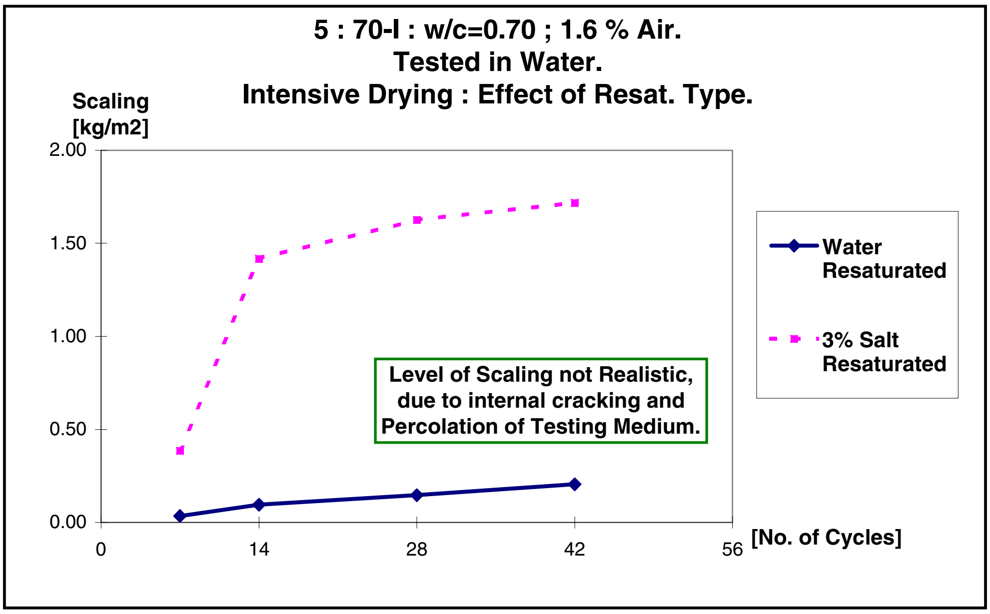
5 : 70-I : w/c=0.70 ; 1.6 % Air.
Tested in Water.
Intensive Drying : Effect of Resat. Type.
Scaling [kg/m2]
2.00
1.50
1.00
0.50
0.00
0
14
28
42
56
[No. of Cycles]
Level of Scaling not Realistic, due to internal cracking and Percolation of Testing Medium.
Water Resaturated
3% Salt Resaturated

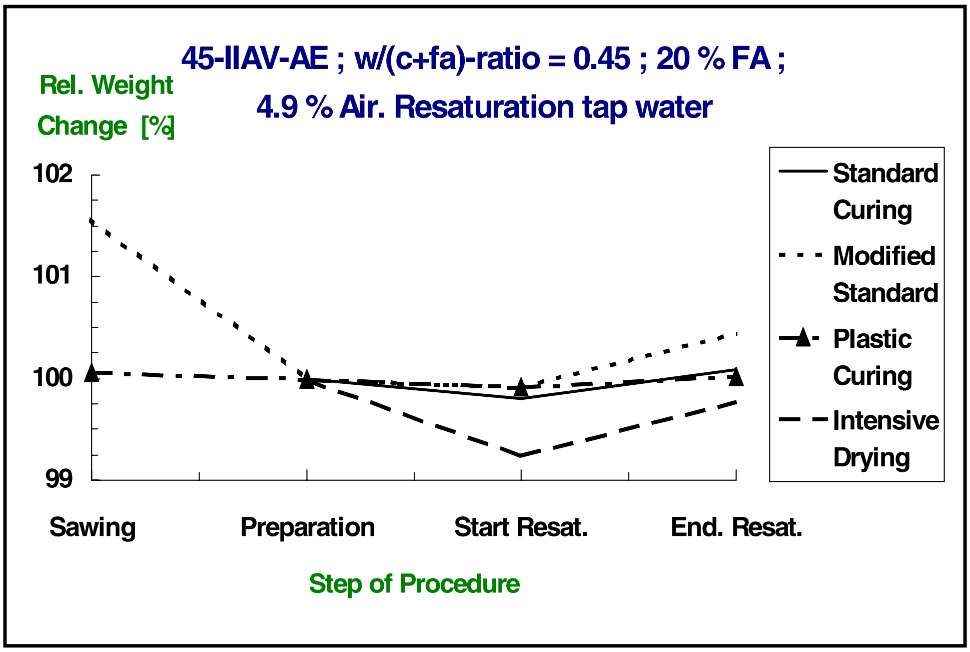
45-IIAV-AE ; w/(c+fa)-ratio = 0.45 ; 20 % FA ;
4.9 % Air. Resaturation tap water
Rel. Weight
Change [%]
102
101
100
99
Sawing
Preparation
Start Resat.
End. Resat.
Step of Procedure
Standard Curing
Modified Standard
Plastic Curing
Intensive Drying

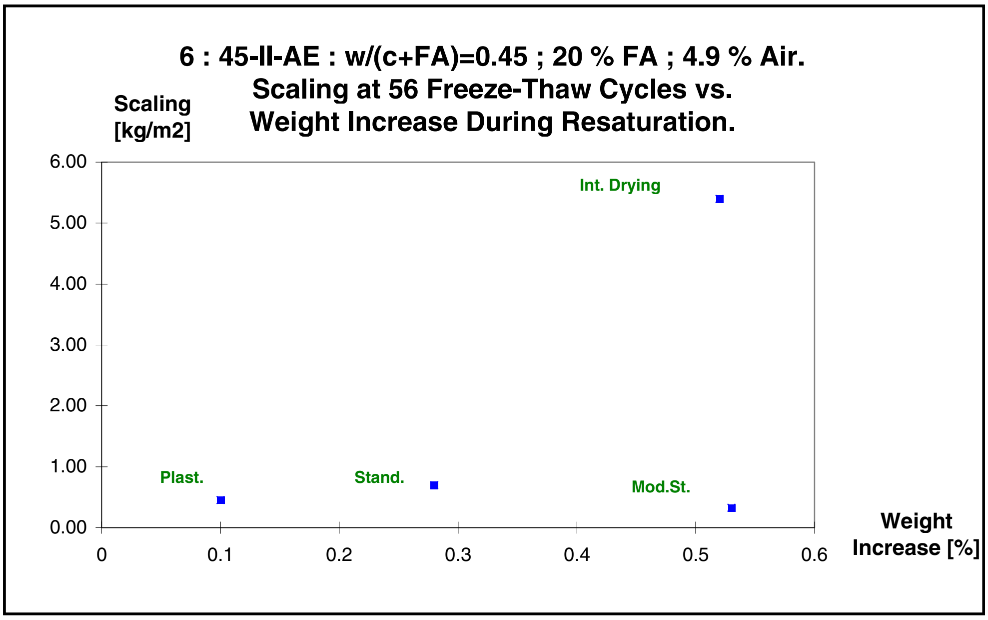
6 : 45-II-AE : w/(c+FA)=0.45 ; 20 % FA ; 4.9 % Air.
Scaling at 56 Freeze-Thaw Cycles vs.
Weight Increase During Resaturation.
Scaling
[kg/m2]
6.00
5.00
4.00
3.00
2.00
1.00
0.00
0
0.1
0.2
0.3
0.4
0.5
0.6
Weight
Increase [%]
Int. Drying
Plast.
Stand.
Mod.St.

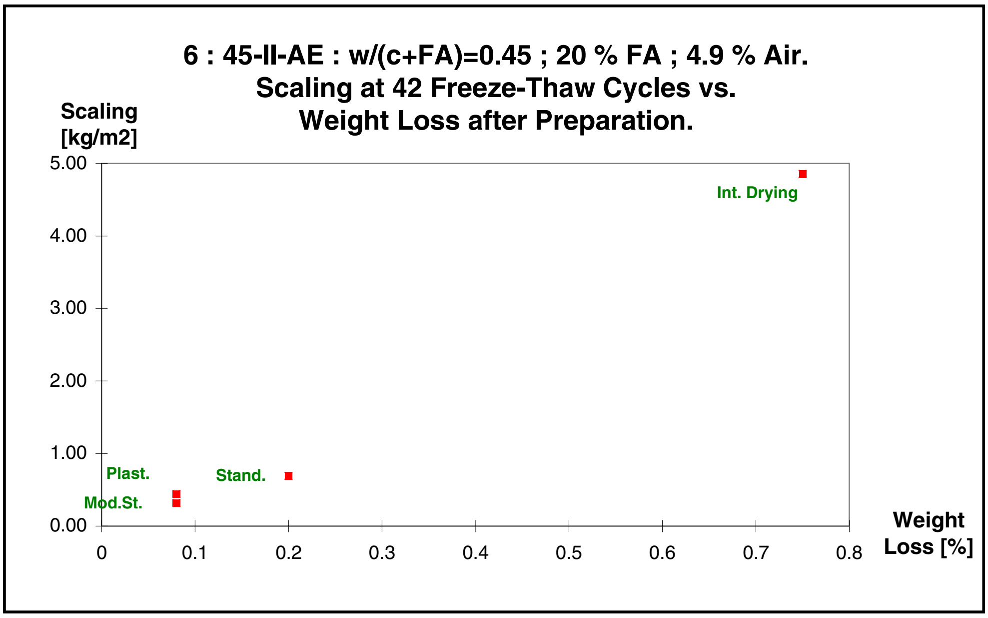
6 : 45-II-AE : w/(c+FA)=0.45 ; 20 % FA ; 4.9 % Air.
Scaling at 42 Freeze-Thaw Cycles vs.
Weight Loss after Preparation.
Scaling [kg/m2]
5.00
4.00
3.00
2.00
1.00
0.00
Int. Drying
Plast.
Stand.
Mod.St.
0
0.1
0.2
0.3
0.4
0.5
0.6
0.7
0.8
Weight Loss [%]

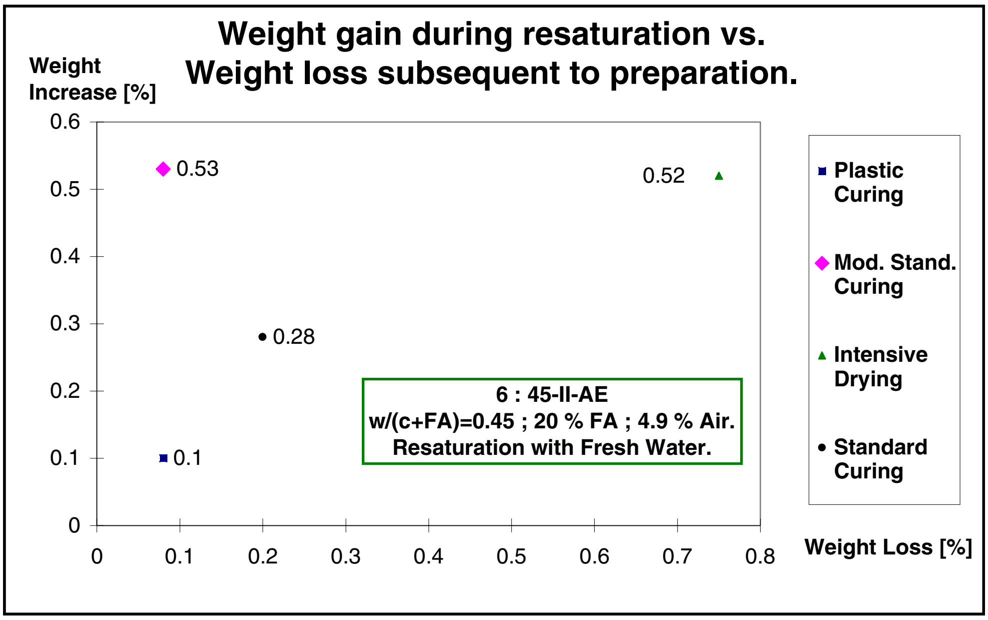
Weight gain during resaturation vs.
Weight loss subsequent to preparation.
Weight Increase [%]
0.6
0.5
0.4
0.3
0.2
0.1
0
0.53
0.52
0.28
0.1
6 : 45-II-AE
w/(c+FA)=0.45 ; 20 % FA ; 4.9 % Air.
Resaturation with Fresh Water.
Plastic Curing
Mod. Stand. Curing
Intensive Drying
Standard Curing
0
0.1
0.2
0.3
0.4
0.5
0.6
0.7
0.8
Weight Loss [%]

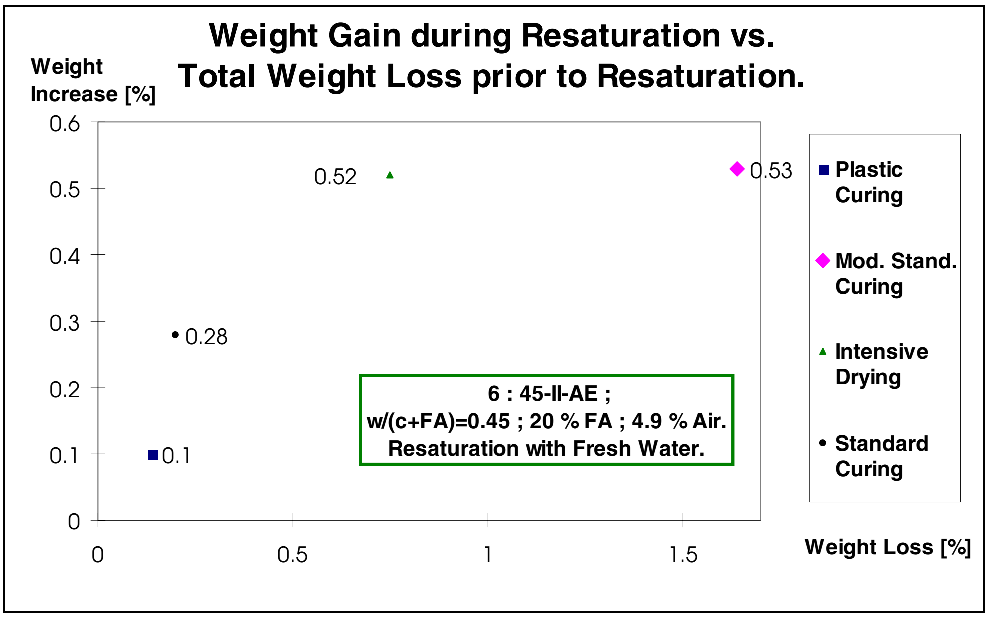
Weight Gain during Resaturation vs.
Total Weight Loss prior to Resaturation.
Weight Increase [%]
0.6
0.5
0.4
0.3
0.2
0.1
0
0
0.5
1
1.5
Weight Loss [%]
0.52
0.53
0.28
0.1
6 : 45-II-AE ;
w/(c+FA)=0.45 ; 20 % FA ; 4.9 % Air.
Resaturation with Fresh Water.
Plastic Curing
Mod. Stand. Curing
Intensive Drying
Standard Curing

APPENDIX C

Section 6.3.4 : Chemical shrinkage data

Ch. 6.3.4 : Chemical shrinkage

Accumulated water consumption per 100 g cement

Cement Paste

		Sample size [g] :					
		45.2	111.7	159.9	161.3	238.8	
Days		Sample 1	Sample 2	Sample 3	Sample 4	Sample 5	Mean
0.04		0.00	0.00	0.00	0.00	0.00	0.00
0.08		0.03	-0.09	-0.04	-0.04	0.00	-0.03
0.13		0.13	0.00	0.04	0.04	0.07	0.05
0.25		0.17	0.18	0.20	0.20	0.34	0.22
0.38		0.52	0.41	0.51	0.47	0.71	0.52
0.77		1.44	1.35	1.53	1.32	1.73	1.47
1.08		1.88	1.80	1.99	1.79	2.19	1.93
2.04		2.54	2.43	2.67	2.43	2.86	2.59
2.88		2.90	2.75	2.96	2.74	3.13	2.90
4.04		3.30	3.04	3.19	2.94	3.35	3.16
5.00		3.34	3.12	3.27	3.04	3.45	3.25
6.00		3.47	3.22	3.37	3.12	3.54	3.34
7.00		3.53	3.27	3.43	3.20	3.60	3.41
11.00		3.63			3.38	3.76	3.59
13.88		3.87				3.87	3.87
17.96		4.09				3.97	4.03
21.04		4.12				4.02	4.07
29.08		4.32				4.13	4.22
31.00		4.37				4.16	4.27

All values corrected for :

* Refilling of pipette.
* Weight loss due to evaporation.
* Temperature variation during storage / curing.

Ch. 6.3.4 : Chemical shrinkage

Accumulated water consumption per 100 g cement

3 % Mortar

	Sample size [g] :				
	201.4	200	198.5	199.9	
Days	Sample 1	Sample 2	Sample 3	Sample 4	Mean
0.04	0.00	0.00	0.00	0.00	0.00
0.08	0.13	0.09	0.09	0.04	0.09
0.13	0.30	0.26	0.28	0.21	0.26
0.17	0.51	0.49	0.54	0.38	0.48
0.21	0.67	0.65	0.66	0.54	0.63
0.38	1.36	1.37	1.38	1.21	1.33
0.93	2.71	2.71	2.77	2.66	2.71
1.01	2.82	2.82	2.88	2.75	2.82
1.96	3.52	3.54	3.59	3.46	3.53
3.21	3.92	3.92	4.02	3.88	3.93
4.02	4.06	4.11	4.18	4.04	4.10
5.08	4.21	4.24	4.32	4.17	4.23
6.10	4.34	4.37	4.44	4.32	4.37
7.08	4.40	4.46	4.51	4.39	4.44
16.63	4.95	4.98	5.11	4.94	5.00
19.58	5.07	5.10	5.25	5.10	5.13
23.63	5.19	5.24	5.31	5.18	5.23
31.00	5.34	5.38	5.42	5.33	5.37

All values corrected for :

* Refilling of pipette.
* Weight loss due to evaporation.
* Temperature variation during storage / curing.

Ch. 6.3.4 : Chemical shrinkage

Accumulated water consumption per 100 g cement

13 % Mortar

	Sample size [g] :				
	202.3	198.1	201.9	206.6	
Days	Sample 1	Sample 2	Sample 3	Sample 4	Mean
0.04	0.00	0.00	0.00	0.00	0.00
0.08	-0.27	-0.25	-0.25	-0.22	-0.25
0.13	-0.19	-0.19	-0.19	-0.14	-0.18
0.23	0.18	0.21	0.21	0.24	0.21
0.31	0.54	0.55	0.56	0.64	0.57
0.79	1.95	1.95	1.91	2.11	1.98
0.90	2.11	2.11	2.05	2.24	2.13
1.06	2.31	2.27	2.20	2.41	2.30
1.46	2.67	2.66	2.61	2.81	2.68
2.17	3.36	3.37	3.32	3.49	3.39
3.42	3.93	3.95	3.89	4.04	3.95
3.88	4.09	4.11	4.05	4.22	4.12
4.88	4.43	4.42	4.38	4.52	4.44
5.96	4.68	4.67	4.65	4.74	4.68
7.25	4.90	4.87	4.84	4.95	4.89
9.04	5.06	5.06	5.07	5.11	5.08
11.04	5.33	5.33	5.30	5.37	5.33
14.00	5.67	5.63	5.61	5.70	5.65
18.00	5.91	5.88	5.88	5.98	5.91
20.88	6.14	6.11	6.29	6.17	6.18
24.96	6.42	6.37	6.34	6.44	6.39
28.04	6.62	6.56	6.52	6.63	6.58
31.00	6.82	6.78	6.72	6.83	6.79

All values corrected for :

* Refilling of pipette.
* Weight loss due to evaporation.
* Temperature variation during storage / curing.

APPENDIX D

Section 6.3.5.2 : Moisture content and porosity

Detailed data and computation in tabular form, from spreadsheet.

URN:NBN:no-6354

Ch. 6.3.5.2 : Moisture content and porosity

Samples from chemical shrinkage measurements

All series / 7 d wet curing

	Cement Paste	3 % Mortar	13 % Mortar
Prior to saturation by pressure [g]	64.71	98.73	103.04
After 7 days 50 atm. pressure [g]	64.65	99.48	108.15
After 7 days drying at 105 °C [g]	50.22	90.56	94.44
Weight after suction 0.5 h [g]	63.14	96.74	101.02
Weight after suction 1.0 h [g]	63.29	97.64	102.26
Weight after suction 1.5 h [g]	63.35	97.78	102.56
Weight after suction 2.0 h [g]	63.40	97.81	102.59
Weight after suction 2.5 h [g]	63.42	97.82	102.59
Weight after suction 3.0 h [g]	63.44	97.82	102.59
Weight after suction 3.5 h [g]	63.45	97.82	102.59
Weight after suction 4.0 h [g]	63.45	97.82	102.59
After 7 days 50 atm. pressure [g]	64.26	99.14	107.80
Weight under water [g]	31.66	56.1	58.25
Calculations :			
Sample volume [ml]	32.60	43.04	49.55
Weight loss at drying [g]	14.43	8.92	13.71
Weight loss at drying [% of dry weight]	28.73	9.85	14.52
Weight loss of initial moisture [W-%]	28.85	9.02	9.11
Weight loss of initial moisture [Vol.-%]	44.45	18.98	17.36
Water cont. prior to pressure [g]	14.49	8.17	8.60
Total porosity [ml]	14.43	8.92	13.71
Initial degree of saturation [%]	100.42	91.59	62.73
Initially non-filled pores [ml]	-0.06	0.75	5.11
Initially non-filled pores [Vol.-%]	**-0.2**	**1.7**	**10.3**
Reduced "open porosity" on drying [ml]	0.39	0.34	0.35
Reduced "open porosity" [Vol.-%]	1.20	0.79	0.71
Suction part of porosity [ml]	13.23	7.26	8.15
Suction part of porosity [Vol.-%]	40.58	16.87	16.45
Protective pores [ml]	0.81	1.32	5.21
Protective pores [Vol.-%]	**2.5**	**3.1**	**10.5**
Prot. pores filled prior to first drying1) [Vol.-%]	**2.7**	**1.3**	**0.2**

1) Since suction part of the porosity in "virgin state" is unknown, the values attained after drying had to be applied. The corresponding total porosity is represented by the second saturation. To compensate for the deviation between first and second saturation, the change in total porosity has been subtracted when computing the "Protective pores filled prior to first drying". This assumption is based on the pore change taking place within the capillary pore size range.

Ch. 6.3.5.2 : Moisture content and porosity

Samples from chemical shrinkage measurements

All series / 7 d wet curing + plastic bag until 31 days

	Cement Paste	3 % Mortar	13 % Mortar
Prior to saturation by pressure [g]	84.99	112.25	118.65
After 7 days 50 atm. pressure [g]	84.89	113.05	123.86
After 7 days drying at 105 ^{o}C [g]	66.11	102.89	109.08
Weight after suction 0.5 h [g]	82.87	110.05	116.10
Weight after suction 1.0 h [g]	83.15	111.13	117.67
Weight after suction 1.5 h [g]	83.20	111.15	117.99
Weight after suction 2.0 h [g]	83.24	111.16	117.99
Weight after suction 2.5 h [g]	83.24	111.16	117.99
Weight after suction 3.0 h [g]	83.24	111.16	117.99
Weight after suction 3.5 h [g]	83.24	111.16	117.99
Weight after suction 4.0 h [g]	83.24	111.16	117.99
After 7 days 50 atm. pressure [g]	83.89	112.46	123.75
Weight under water [g]	41.11	63.73	67.11
Calculations :			
Sample volume [ml]	42.78	48.73	56.64
Weight loss at drying [g]	18.78	10.16	14.78
Weight loss at drying [% of dry weight]	28.41	9.87	13.55
Weight loss of initial moisture [W-%]	28.56	9.10	8.77
Weight loss of initial moisture [Vol.-%]	44.13	19.21	16.90
Water cont. prior to pressure [g]	18.88	9.36	9.57
Total porosity [ml]	18.78	10.16	14.78
Initial degree of saturation [%]	100.53	92.13	64.75
Initially non-filled pores [ml]	-0.10	0.80	5.21
Initially non-filled pores [Vol.-%]	**-0.2**	**1.6**	**9.2**
Reduced "open porosity" on drying [ml]	1.00	0.59	0.11
Reduced "open porosity" [Vol.-%]	2.34	1.21	0.19
Suction part of porosity [ml]	17.13	8.27	8.91
Suction part of porosity [Vol.-%]	40.04	16.97	15.73
Protective pores [ml]	0.65	1.30	5.76
Protective pores [Vol.-%]	**1.5**	**2.7**	**10.2**
Prot. pores filled prior to first drying[1)] [Vol.-%]	**1.8**	**1.0**	**1.0**

1) Since suction part of the porosity in "virgin state" is unknown, the values attained after drying had to be applied. The corresponding total porosity is represented by the second saturation. To compensate for the deviation between first and second saturation, the change in total porosity has been subtracted when computing the "Protective pores filled prior to first drying". This assumption is based on the pore change taking place within the capillary pore size range.

Ch. 6.3.5.2 : Moisture content and porosity

Samples from chemical shrinkage measurements

All series / 31 days wet curing

	Cement Paste	3 % Mortar	13 % Mortar
Prior to saturation by pressure [g]	78.37	110.20	111.76
After 7 days 50 atm. pressure [g]	78.22	110.93	116.28
After 7 days drying at 105 °C [g]	60.75	101.73	102.66
Weight after suction 0.5 h [g]	76.49	108.29	109.45
Weight after suction 1.0 h [g]	76.69	109.21	110.80
Weight after suction 1.5 h [g]	76.77	109.25	110.97
Weight after suction 2.0 h [g]	76.81	109.25	110.97
Weight after suction 2.5 h [g]	76.81	109.25	110.97
Weight after suction 3.0 h [g]	76.81	109.25	110.97
Weight after suction 3.5 h [g]	76.81	109.25	110.97
Weight after suction 4.0 h [g]	76.81	109.25	110.97
After 7 days 50 atm. pressure [g]	77.60	110.59	117.17
Weight under water [g]	37.94	63.11	63.07
Calculations :			
Sample volume [ml]	39.66	47.48	54.10
Weight loss at drying [g]	17.47	9.20	13.62
Weight loss at drying [% of dry weight]	28.76	9.04	13.27
Weight loss of initial moisture [W-%]	29.00	8.33	8.86
Weight loss of initial moisture [Vol.-%]	44.43	17.84	16.82
Water cont. prior to pressure [g]	17.62	8.47	9.10
Total porosity [ml]	17.47	9.20	13.62
Initial degree of saturation [%]	100.86	92.07	66.81
Initially non-filled pores [ml]	-0.15	0.73	4.52
Initially non-filled pores [Vol.-%]	**-0.4**	**1.5**	**8.4**
Reduced "open porosity" on drying [ml]	0.62	0.34	-0.89
Reduced "open porosity" [Vol.-%]	1.56	0.72	-1.65
Suction part of porosity [ml]	16.06	7.52	8.31
Suction part of porosity [Vol.-%]	40.49	15.84	15.36
Protective pores [ml]	0.79	1.34	6.20
Protective pores [Vol.-%]	**2.0**	**2.8**	**11.5**
Prot. pores filled prior to first drying1) [Vol.-%]	**2.4**	**1.3**	**3.1**

1) Since suction part of the porosity in "virgin state" is unknown, the values attained after drying had to be applied. The corresponding total porosity is represented by the second saturation. To compensate for the deviation between first and second saturation, the change in total porosity has been subtracted when computing the "Protective pores filled prior to first drying". This assumption is based on the pore change taking place within the capillary pore size range.

Ch. 6.3.5.2 : Moisture content and porosity

Samples from chemical shrinkage measurements

Cement Paste

31 days wet curing

To be continued :

	Sample 1	Sample 2
Prior to saturation by pressure [g]	105.41	154.04
After 50 atm. pressure [g]	105.30	153.90
Stable weight after pressure [g]	105.19	153.76
Weight under water, stable [g]	52.08	76.10
Weight prior to drying [g][1)]	105.19	153.76
After drying, const.weight [g][1)]	85.42	124.54
Calculations :		
Weight loss at drying [g]	19.77	29.22
Weight loss [% of dry weight]	23.14	23.46
Weight loss of initial moisture [W-%]	23.27	23.57
Weight loss of initial moisture [Vol.-%]	37.43	37.81
Sample volume [ml]	53.11	77.66
Expelled water at pressure relief [g]	0.11	0.14
Expelled water / Residual air [Vol.-%]	0.21	0.18
Water cont. prior to pressure [g]	19.99	29.50
Total porosity [ml]	19.88	29.36
Initial degree of saturation [%]	100.55	100.48
Initially non-filled pores [ml]	-0.11	-0.14
Initially non-filled pores [Vol.-%]	**-0.2**	**-0.2**

n.s.: i.e. not subjected to ~

[1)] A few g was lost in the crushing process.
The values were adjusted accordingly to
fit the correct, percentage loss on drying.

Ch. 6.3.5.2 : Moisture content and porosity

Samples from chemical shrinkage measurements

Cement Paste

31 days wet curing

Cont.:

	Sample 3	Sample 4	Sample 5
Prior to saturation by pressure [g]			
After 50 atm. pressure [g]	n.s.	n.s.	n.s.
Stable weight after pressure [g]			
Weight under water, stable [g]			
Weight prior to drying [g]¹⁾	41.00	150.25	218.56
After drying, const.weight [g]¹⁾	33.20	120.77	175.20
Calculations :			
Weight loss at drying [g]	7.80	29.48	43.36
Weight loss [% of dry weight]	23.49	24.41	24.75
Weight loss of initial moisture [W-%]	23.49	24.41	24.75
Weight loss of initial moisture [Vol.-%]			
Sample volume [ml]			
Expelled water at pressure relief [g]			
Expelled water / Residual air [Vol.-%]			
Water cont. prior to pressure [g]			
Total porosity [ml]			
Initial degree of saturation [%]			
Initially non-filled pores [ml]			
Initially non-filled pores [Vol.-%]			

n.s.: i.e. not subjected to ~

1) A few g was lost in the crushing process.
The values were adjusted accordingly to
fit the correct, percentage loss on drying.

Ch. 6.3.5.2 : Moisture content and porosity

Samples from chemical shrinkage measurements

Mortar 3 % Air

31 days wet curing

To be continued :

	Sample 1	Sample 2
Prior to saturation by pressure [g]	201.57	198.47
After 50 atm. pressure [g]	202.97	199.74
Stable weight after pressure [g]	202.64	199.47
Weight under water, stable [g]	115.79	113.73
Weight prior to drying [g][1)]	202.64	199.47
After drying, const.weight [g][1)]	187.18	184.38
Calculations :		
Weight loss at drying [g]	15.46	15.09
Weight loss [% of dry weight]	8.26	8.18
Weight loss of initial moisture [W-%]	7.51	7.50
Weight loss of initial moisture [Vol.-%]	16.19	16.12
Sample volume [ml]	86.85	85.74
Expelled water at pressure relief [g]	0.33	0.27
Expelled water / Residual air [Vol.-%]	0.38	0.31
Water cont. prior to pressure [g]	14.39	14.09
Total porosity [ml]	15.79	15.36
Initial degree of saturation [%]	91.13	91.73
Initially non-filled pores [ml]	1.40	1.27
Initially non-filled pores [Vol.-%]	**1.6**	**1.5**

n.s.: i.e. not subjected to ~

[1)] A few g was lost in the crushing process. The values were adjusted accordingly to fit the correct, percentage loss on drying.

Ch. 6.3.5.2 : Moisture content and porosity

Samples from chemical shrinkage measurements

Mortar 3 % Air

31 days wet curing

Cont.:

	Sample 3	Sample 4
Prior to saturation by pressure [g]		
After 50 atm. pressure [g]	n.s.	n.s.
Stable weight after pressure [g]		
Weight under water, stable [g]		
Weight prior to drying [g][1)]	199.50	196.30
After drying, const.weight [g][1)]	185.18	181.78
Calculations :		
Weight loss at drying [g]	14.32	14.52
Weight loss [% of dry weight]	7.73	7.99
Weight loss of initial moisture [W-%]	7.73	7.99
Weight loss of initial moisture [Vol.-%]		
Sample volume [ml]		
Expelled water at pressure relief [g]		
Expelled water / Residual air [Vol.-%]		
Water cont. prior to pressure [g]		
Total porosity [ml]		
Initial degree of saturation [%]		
Initially non-filled pores [ml]		
Initially non-filled pores [Vol.-%]		

n.s.: i.e. not subjected to ~

[1)] A few g was lost in the crushing process. The values were adjusted accordingly to fit the correct, percentage loss on drying.

Ch. 6.3.5.2 : Moisture content and porosity

Samples from chemical shrinkage measurements

Mortar 13 % Air

31 days wet curing

To be continued :

	Sample 1	Sample 2
Prior to saturation by pressure [g]	208.77	200.00
After 50 atm. pressure [g]	216.30	207.33
Stable weight after pressure [g]	215.50	206.58
Weight under water, stable [g]	113.75	109.11
Weight prior to drying [g][1)]	215.50	206.58
After drying, const.weight [g][1)]	193.04	185.38
Calculations :		
Weight loss at drying [g]	22.46	21.20
Weight loss [% of dry weight]	11.63	11.44
Weight loss of initial moisture [W-%]	7.73	7.48
Weight loss of initial moisture [Vol.-%]	14.67	14.23
Sample volume [ml]	101.75	97.47
Expelled water at pressure relief [g]	0.80	0.75
Expelled water / Residual air [Vol.-%]	0.79	0.77
Water cont. prior to pressure [g]	15.73	14.62
Total porosity [ml]	23.26	21.95
Initial degree of saturation [%]	67.63	66.61
Initially non-filled pores [ml]	7.53	7.33
Initially non-filled pores [Vol.-%]	**7.4**	**7.5**

n.s.: i.e. not subjected to ~

[1)] A few g was lost in the crushing process.
The values were adjusted accordingly to
fit the correct, percentage loss on drying.

Ch. 6.3.5.2 : Moisture content and porosity

Samples from chemical shrinkage measurements
Mortar 13 % Air
31 days wet curing

Cont.:

	Sample 3	Sample 4
Prior to saturation by pressure [g]		
After 50 atm. pressure [g]	n.s.	n.s.
Stable weight after pressure [g]		
Weight under water, stable [g]		
Weight prior to drying [g][1)]	200.24	201.69
After drying, const.weight [g][1)]	184.78	185.36
Calculations :		
Weight loss at drying [g]	15.46	16.33
Weight loss [% of dry weight]	8.37	8.81
Weight loss of initial moisture [W-%]	8.37	8.81
Weight loss of initial moisture [Vol.-%]		
Sample volume [ml]		
Expelled water at pressure relief [g]		
Expelled water / Residual air [Vol.-%]		
Water cont. prior to pressure [g]		
Total porosity [ml]		
Initial degree of saturation [%]		
Initially non-filled pores [ml]		
Initially non-filled pores [Vol.-%]		

n.s.: i.e. not subjected to ~

[1)] A few g was lost in the crushing process.
The values were adjusted accordingly to
fit the correct, percentage loss on drying.

APPENDIX E

Section 5 : Additional data

URN:NBN:no-6354

Mix No. / Parameter	**1**	**2**	**3**	**4**	**5**	**6**
w/c-ratio	0.35	0.35	0.40	0.45	0.35	0.35
w/(c+s)	0.35	0.35	0.40	0.45	0.35	0.35
Cement type[1]	SR-LA	SR-LA	FA	FA	LA	LA
Nominal air content [Vol.-%]	-	4.5	4.5	4.5	-	4.5
Cement [kg/m^3]	450	470	460	420	470	470
Silica fume [kg/m^3]	-	-	-	-	-	-
Water [kg/m^3]	157.5	164.5	184	189	164.5	164.5
Super plasticizer SP 40[2] [kg/m^3]	8.6	11.0	9.0	5.0	11.8	9.0
Super plasticizer Scanflyt 2[3] [kg/m^3]	-	-	-	-	-	-
Plasticizer P[4] [kg/m^3]	-	-	-	-	-	-
Air entrainer L(MF)[5] (1:9) [kg/m^3]	-	6.0	4.0	2.0	-	4.5
Aggregate I 0-8 mm [kg/m^3]	874	818	854	845	856	818
Aggregate I 8-16 mm [kg/m^3]	946	886	820	812	928	886
Aggregate NSBR 0-8 mm [kg/m^3]	-	-	-	-	-	-
Aggregate NSBR 8-11 mm [kg/m^3]	-	-	-	-	-	-
Aggregate NSBR 11-16 mm [kg/m^3]	-	-	-	-	-	-
Aggr. Nat.washed 0-2 mm [kg/m^3]	-	-	-	-	-	-
Aggr. Nat.washed 0-8 mm [kg/m^3]	-	-	-	-	-	-
Aggr. Nat.washed 8-11 mm [kg/m^3]	-	-	-	-	-	-
Aggr. Nat.washed 11-16 mm [kg/m^3]	-	-	-	-	-	-
Slump value [mm]	55	155	175	70	155	75
Fresh concrete air content [Vol.-%]	2.4	5.5	5.6	4.3	1.8	5.3
Fresh concr. spec.surface [mm^{-1}]	10	16	18	20	6	17
Fresh concr. spacing factor [mm]	1.0	0.30	0.29	0.33	1.4	0.36
Hardened concr. air cont. [Vol.-%]	1.9	3.0	4.8	3.0	2.5	5.5
Hard. concr. spec.surface [mm^{-1}]	31	19	23	20	21	20
Hard. concr. spacing factor [mm]	0.30	0.33	0.24	0.31	0.47	0.25
Strength F$_{c28}$ (100 mm, 28d wet) [MPa]	86	80	53	50	89	77
Strength F$_{c28}$ (150 mm, 7d wet) [MPa]	88	77	56	51	92	77

[1] SR-LA = CEM I 42.5 R-SR-LA ; FA = CEM II/A-V 42.5 R ; LA = CEM I 52.5 R LA ; I = CEM I 42.5 R ; I RR = CEM I 42.5 RR

[2] Sulph. melamine-formaldehyde resin, liquid of density 1250 kg/m^3, 40 % dry w.

[3] Mod. sulph. melamine condensate, liquid of density 1230 kg/m^3, 38 % dry weight

[4] Lignosulphonate, liquid of density 1200 kg/m^3, 40 % dry weight

[5] Air entrainer of the “micro-air” type, liquid of density 1002 kg/m^3, 1 % dry weight

Mix No. / Parameter	**7**	**8**	**9**	**10**	**11**	**12**
w/c-ratio	0.40	0.45	0.40	0.45	0.45	0.45
w/(c+s)	0.40	0.45	0.40	0.45	0.45	0.45
Cement type 1)	LA	LA	SR-LA	SR-LA	I	I RR
Nominal air content [Vol.-%]	4.5	4.5	4.5	4.5	4.5	4.5
Cement [kg/m^3]	430	400	430	400	420	430
Silica fume [kg/m^3]	-	-	-	-	-	-
Water [kg/m^3]	172	180	172	180	189	193.5
Super plasticizer SP 40 2) [kg/m^3]	6.5	2.0	6.5	2.5	6.5	6.5
Super plasticizer Scanflyt 2 3) [kg/m^3]	-	-	-	-	-	-
Plasticizer P 4) [kg/m^3]	-	-	-	-	-	-
Air entrainer L(MF) 5) (1:9) [kg/m^3]	2.0	1.5	2.5	1.0	1.1	2.4
Aggregate I 0-8 mm [kg/m^3]	876	878	886	899	858	847
Aggregate I 8-16 mm [kg/m^3]	842	844	851	864	824	814
Aggregate NSBR 0-8 mm [kg/m^3]	-	-	-	-	-	-
Aggregate NSBR 8-11 mm [kg/m^3]	-	-	-	-	-	-
Aggregate NSBR 11-16 mm [kg/m^3]	-	-	-	-	-	-
Aggr. Nat.washed 0-2 mm [kg/m^3]	-	-	-	-	-	-
Aggr. Nat.washed 0-8 mm [kg/m^3]	-	-	-	-	-	-
Aggr. Nat.washed 8-11 mm [kg/m^3]	-	-	-	-	-	-
Aggr. Nat.washed 11-16 mm [kg/m^3]	-	-	-	-	-	-
Slump value [mm]	55	30	65	25	60	50
Fresh concrete air content [Vol.-%]	4.8	5.2	5.0	4.9	4.4	5.0
Fresh concr. spec.surface [mm^{-1}]	16	27	16	27	15	25
Fresh concr. spacing factor [mm]	0.4	0.26	0.40	0.26	0.40	0.29
Hardened concr. air cont. [Vol.-%]	4.0	3.6	3.8	4.0	4.6	3.7
Hard. concr. spec.surface [mm^{-1}]	23	25	20	22	22	19
Hard. concr. spacing factor [mm]	0.27	0.27	0.31	0.29	0.30	0.32
Strength F_{c28} (100 mm, 28d wet) [MPa]	-	57	69	59	50	52
Strength F_{c28} (150 mm, 7d wet) [MPa]	70	59	71	58	55	54

1) SR-LA = CEM I 42.5 R-SR-LA ; FA = CEM II/A-V 42.5 R ; LA = CEM I 52.5 R LA ; I = CEM I 42.5 R ; I RR = CEM I 42.5 RR

2) Sulph. melamine-formaldehyde resin, liquid of density 1250 kg/m^3, 40 % dry w.

3) Mod. sulph. melamine condensate, liquid of density 1230 kg/m^3, 38 % dry weight

4) Lignosulphonate, liquid of density 1200 kg/m^3, 40 % dry weight

5) Air entrainer of the “micro-air” type, liquid of density 1002 kg/m^3, 1 % dry weight

Mix No. / Parameter	**13**	**14**	**15**	**16**	**17**	**18**
w/c-ratio	0.35	0.35	0.45	0.40	0.46	0.42
w/(c+2s)	0.35	0.35	0.45	0.40	0.39	0.39
Cement type[1]	SR-LA	LA	FA	LA	LA	FA
Nominal air content [Vol.-%]	-	-	4.5	4.5	4.5	4.5
Cement [kg/m^3]	470	470	400	410	375	400
Silica fume [kg/m^3]	-	-	-	-	33.8	16
Water [kg/m^3]	165.5	165.9	180	164	172	167.6
Super plasticizer SP 40[2] [kg/m^3]	1.67	2.33	-	-	-	-
Super plasticizer Scanflyt 2[3] [kg/m^3]	-	-	-	-	1.04	0.29
Plasticizer P[4] [kg/m^3]	2.35	2.35	2.0	2.05	3.5	3.5
Air entrainer L(MF)[5] (1:9) [kg/m^3]	-	-	2.0	1.8	0.70	1.3
Aggregate I 0-8 mm [kg/m^3]	-	-	-	-	-	-
Aggregate I 8-16 mm [kg/m^3]	-	-	-	-	-	-
Aggregate NSBR 0-8 mm [kg/m^3]	780	780	742	780	-	-
Aggregate NSBR 8-11 mm [kg/m^3]	663	663	632	652	-	-
Aggregate NSBR 11-16 mm [kg/m^3]	353	353	336	334	-	-
Aggr. Nat.washed 0-2 mm [kg/m^3]	-	-	-	-	100	92
Aggr. Nat.washed 0-8 mm [kg/m^3]	-	-	-	-	743	741
Aggr. Nat.washed 8-11 mm [kg/m^3]	-	-	-	-	290	290
Aggr. Nat.washed 11-16 mm [kg/m^3]	-	-	-	-	600	600
Slump value [mm]	65	32	125	65	165	150
Fresh concrete air content [Vol.-%]	2.3	2.3	4.5	4.8	4.5	4.4
Fresh concr. spec.surface [mm^{-1}]	-	-	24	43	15	14
Fresh concr. spacing factor [mm]	-	-	0.24	0.13	0.36	0.38
Hardened concr. air cont. [Vol.-%]	1.0	2.9	4.1	3.9	4.9	4.2
Hard. concr. spec.surface [mm^{-1}]	18	20	31	39	18	21
Hard. concr. spacing factor [mm]	0.57	0.43	0.20	0.17	0.35	0.31
Strength F_{c28} (100 mm, 28d wet) [MPa]	88	81	44	57	70	55
Strength F_{c28} (150 mm, 7d wet) [MPa]	-	-	-	-	-	-

[1] SR-LA = CEM I 42.5 R-SR-LA ; FA = CEM II/A-V 42.5 R ; LA = CEM I 52.5 R LA ; I = CEM I 42.5 R ; I RR = CEM I 42.5 RR

[2] Sulph. melamine-formaldehyde resin, liquid of density 1250 kg/m^3, 40 % dry w.

[3] Mod. sulph. melamine condensate, liquid of density 1230 kg/m^3, 38 % dry weight

[4] Lignosulphonate, liquid of density 1200 kg/m^3, 40 % dry weight

[5] Air entrainer of the “micro-air” type, liquid of density 1002 kg/m^3, 1 % dry weight

Accumulated scaling, mean values [kg/m2]

Mix No.	**1**	**2**	**3**	**4**	**5**	**6**
No. of cycles						
7	0.06	0.02	0.04	0.10	0.08	0.02
14	0.34	0.03	0.06	0.19	0.37	0.03
28	1.26	0.05	0.09	0.26	1.28	0.04
42	2.34	0.07	0.14	0.30	2.22	0.05
56	3.39	0.09	0.20	0.34	3.25	0.07
70	4.39	0.12	0.31	0.43	4.20	0.11
84	5.50	0.16	0.54	0.58	5.22	0.19
98	6.47	0.20	0.97	0.89	6.34	0.35
112	8.02	0.24	1.52	1.38	7.51	0.66
Coeff.of var.[%]	22	28	13	17	13	26

Ultrasonic pulse velocity

Before exposure [ms]	31.9	32.8	34.1	34.3	32.1	32.7
After 1rst winter [ms]	31.3	31.9	33.9	33.6	31.0	32.1
After 2nd winter [ms]	31.6	32.1	34.2	34.2	31.4	31.8

Relative change [m/s] :

Initial value [%]	100.0	100.0	100.0	100.0	100.0	100.0
After 1rst winter [%]	101.9	102.7	100.7	102.2	103.6	102.0
After 2nd winter [%]	100.9	101.9	99.7	100.3	102.4	102.8

Volume change

Initial value [cm3]	1624.0	1624.0	1628.6	1629.0	1621.9	1629.7
After 1rst winter [cm3]	1626.2	1627.5	1630.1	1631.8	1625.9	1631.9
After 2nd winter [cm3]	1626.3	1627.3	1629.3	1629.9	1624.7	1631.1

Relative change :

Initial value [%]	100.00	100.00	100.00	100.00	100.00	100.00
After 1rst winter [%]	100.13	100.22	100.10	100.18	100.24	100.13
After 2nd winter [%]	100.14	100.20	100.04	100.06	100.17	100.09

Weight change

Initial value [g]	3992.3	3871.2	3724.0	3783.7	3984.3	3879.7
After 1rst winter [g]	3989.6	3866.7	3720.8	3779.1	3983.5	3882.1
After 2nd winter [g]	3996.5	3877.7	3729.8	3787.6	3992.1	3888.7
Initial value [%]	100.00	100.00	100.00	100.00	100.00	100.00
After 1rst winter [%]	99.93	99.88	99.91	99.88	99.98	100.06
After 2nd winter [%]	100.11	100.17	100.15	100.10	100.19	100.23

Density change

Initial value [%]	100.00	100.00	100.00	100.00	100.00	100.00
After 1rst winter [%]	99.80	99.67	99.82	99.70	99.74	99.93
After 2nd winter [%]	99.97	99.97	100.11	100.04	100.03	100.15

Accumulated scaling, mean values [kg/m2]

Mix No.	**7**	**8**	**9**	**10**	**11**	**12**
No. of cycles						
7	0.02	0.01	0.01	0.01	0.15	0.08
14	0.03	0.02	0.02	0.02	0.32	0.10
28	0.04	0.02	0.02	0.02	0.47	0.13
42	0.05	0.03	0.03	0.03	0.54	0.15
56	0.07	0.04	0.04	0.03	0.59	0.18
70	0.11	0.04	0.06	0.03	0.65	0.22
84	0.20	0.05	0.11	0.04	0.74	0.28
98	0.38	0.07	0.25	0.04	0.93	0.40
112	0.71	0.10	0.60	0.05	1.22	0.62
Coeff.of var.[%]	22	46	35	12	36	12

Ultrasonic pulse velocity

Before exposure [ms]	33.2	33.9	33.0	33.7	33.9	34.8
After 1rst winter [ms]	32.3	33.1	32.3	33.0	33.0	33.8
After 2nd winter [ms]	32.1	33.0	32.1	32.8	32.5	33.8

Relative change [m/s] :

Initial value [%]	100.00	100.00	100.00	100.00	100.00	100.00
After 1rst winter [%]	102.55	102.57	102.17	101.97	102.81	103.11
After 2nd winter [%]	103.35	102.73	102.80	102.51	104.39	103.11

Volume change

Initial value [cm3]	1627.2	1624.9	1626.5	1626.8	1628.6	1634.9
After 1rst winter [cm3]	1628.9	1627.2	1629.9	1629.9	1630.0	1636.7
After 2nd winter [cm3]	1627.6	1625.6	1629.2	1628.8	1630.1	1636.0

Relative change :

Initial value [%]	100.00	100.00	100.00	100.00	100.00	100.00
After 1rst winter [%]	100.10	100.14	100.21	100.19	100.09	100.11
After 2nd winter [%]	100.02	100.04	100.16	100.12	100.10	100.07

Weight change

Initial value [g]	3846.1	3810.5	3855.9	3855.6	3831.7	3772.1
After 1rst winter [g]	3844.3	3806.7	3849.9	3847.2	3828.5	3772.1
After 2nd winter [g]	3851.4	3813.9	3855.1	3850.7	3836.0	3784.1
Initial value [%]	100.00	100.00	100.00	100.00	100.00	100.00
After 1rst winter [%]	99.95	99.90	99.85	99.78	99.91	100.00
After 2nd winter [%]	100.14	100.09	99.98	99.87	100.11	100.32

Density change

Initial value [%]	100.00	100.00	100.00	100.00	100.00	100.00
After 1rst winter [%]	99.85	99.76	99.64	99.59	99.83	99.89
After 2nd winter [%]	100.12	100.05	99.82	99.75	100.01	100.25

Accumulated scaling, mean values [kg/m2]

Mix No.		**13**	**14**	**15**	**16**	**17**	**18**
No. of cycles							
	7	0.05	0.07	0.10	0.01	0.05	0.13
	14	0.14	0.21	0.14	0.02	0.07	0.19
	28	0.40	0.69	0.15	0.02	0.09	0.23
	42	0.65	1.38	0.16	0.03	0.12	0.27
	56	0.90	2.51	0.17	0.03	0.14	0.31
	70						
	84						
	98						
	112						
Coeff.of var.[%]		74	10	13	32	12	13

Ultrasonic pulse velocity

Before exposure [ms]	34.1	33.9	36.4	35.9	35.3	36.0
After 1rst winter [ms]	33.0	32.5	35.5	34.8	34.7	35.0
After 2nd winter [ms]	32.9	32.7	35.4	34.8	34.8	35.3

Relative change [m/s] :

Initial value [%]	100.00	100.00	100.00	100.00	100.00	100.00
After 1rst winter [%]	103.34	104.15	102.68	103.17	101.59	102.86
After 2nd winter [%]	103.65	103.68	102.97	103.02	101.44	101.84

Volume change

Initial value [cm3]	1671.4	1674.8	1645.0	1673.6	1655.3	1657.0
After 1rst winter [cm3]	1668.9	1671.7	1642.9	1670.1	1652.4	1654.1
After 2nd winter [cm3]	1669.3	1671.7	1642.4	1670.5	1652.3	1653.7

Relative change :

Initial value [%]	100.00	100.00	100.00	100.00	100.00	100.00
After 1rst winter [%]	99.85	99.81	99.87	99.79	99.82	99.82
After 2nd winter [%]	99.88	99.81	99.84	99.81	99.82	99.80

Weight change

Initial value [g]	4157.3	4125.1	3833.0	3918.7	3899.8	3893.0
After 1rst winter [g]	4158.2	4126.1	3833.6	3920.7	3900.7	3892.1
After 2nd winter [g]	4162.6	4133.3	3844.9	3934.7	3908.2	3900.4

Initial value [%]	100.00	100.00	100.00	100.00	100.00	100.00
After 1rst winter [%]	100.02	100.03	100.01	100.05	100.02	99.98
After 2nd winter [%]	100.13	100.20	100.31	100.41	100.21	100.19

Density change

Initial value [%]	100.00	100.00	100.00	100.00	100.00	100.00
After 1rst winter [%]	100.17	100.21	100.14	100.26	100.20	100.15
After 2nd winter [%]	100.25	100.39	100.47	100.60	100.40	100.39

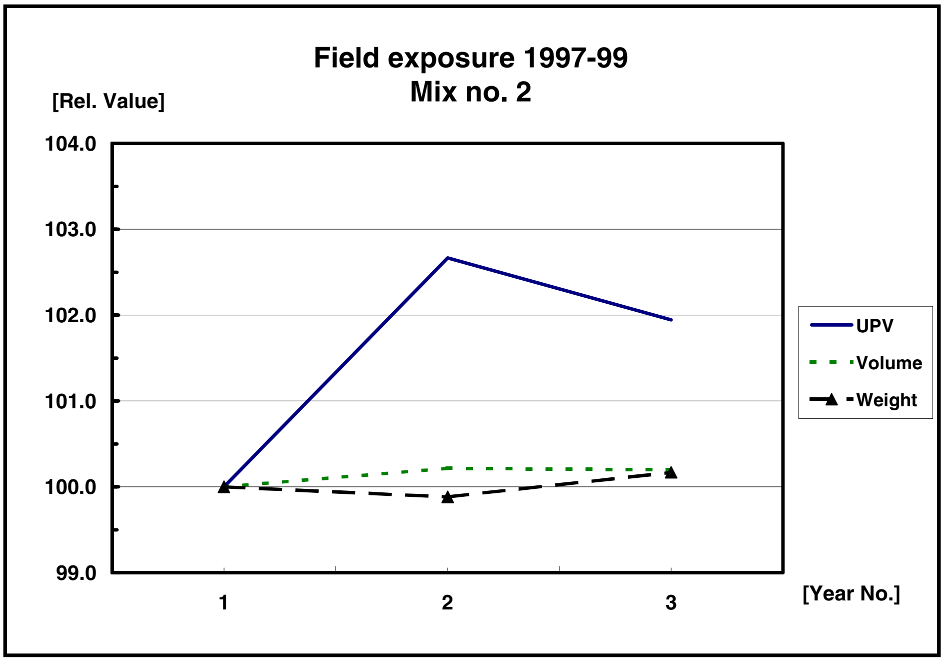
Field exposure 1997-99
Mix no. 2
[Rel. Value]
104.0
103.0
102.0
101.0
100.0
99.0
1
2
3
[Year No.]
UPV
Volume
Weight

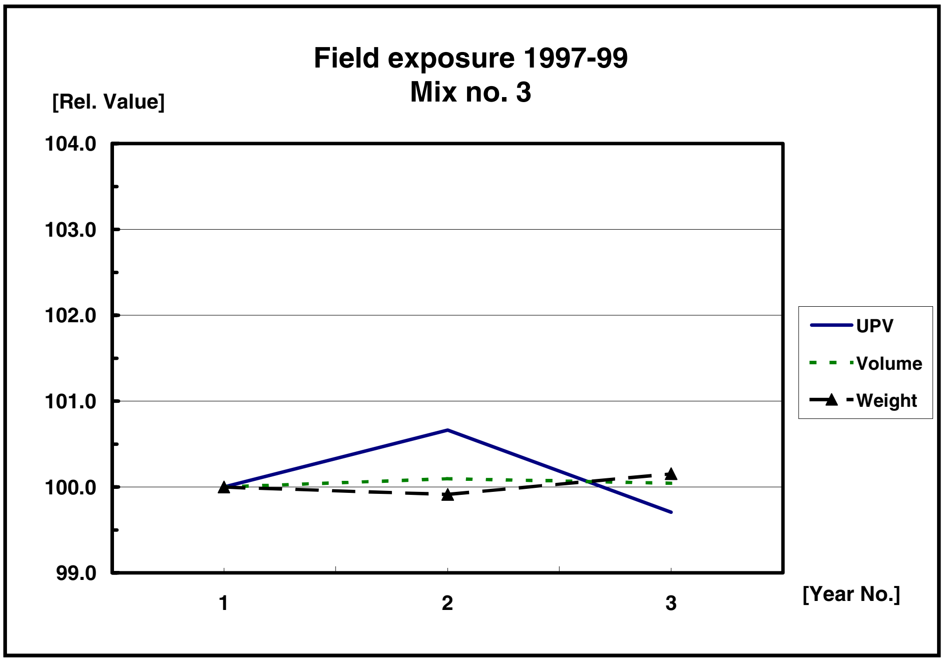
Field exposure 1997-99
Mix no. 3
[Rel. Value]
104.0
103.0
102.0
101.0
100.0
99.0
1
2
3
[Year No.]
UPV
Volume
Weight

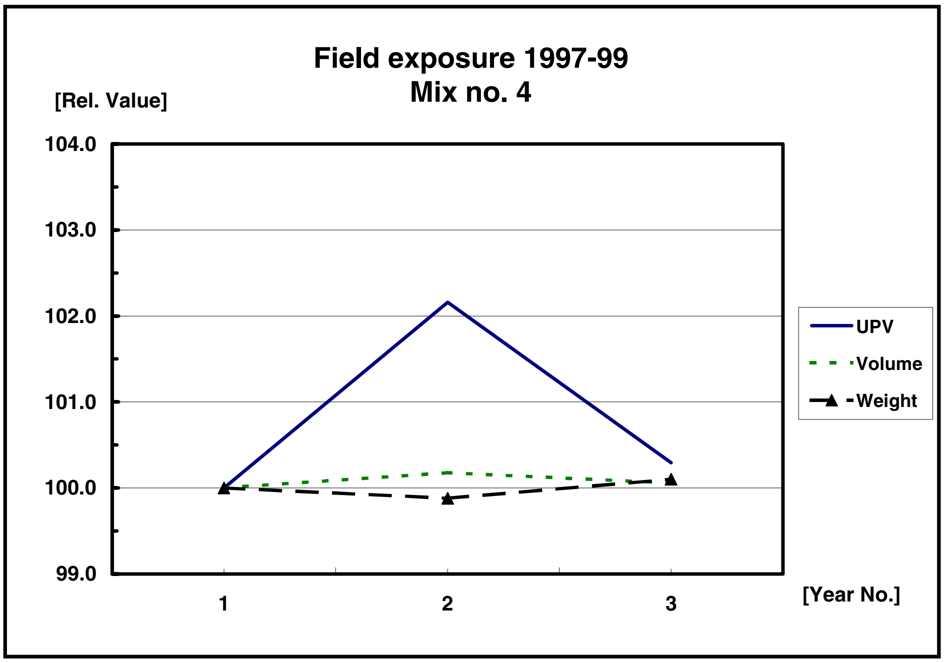
Field exposure 1997-99
Mix no. 4
[Rel. Value]
104.0
103.0
102.0
101.0
100.0
99.0
1
2
3
[Year No.]
UPV
Volume
Weight

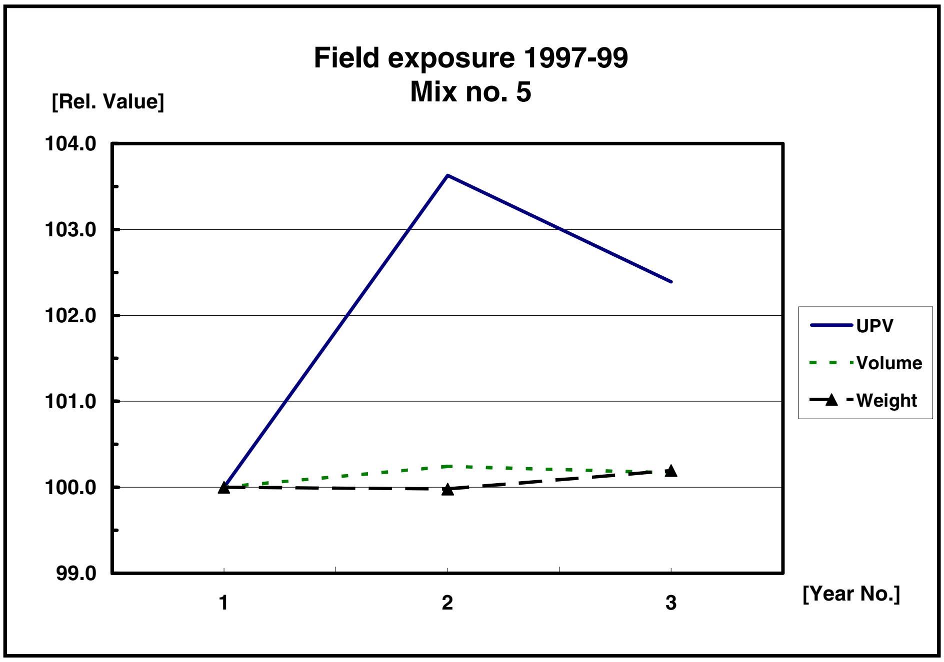
Field exposure 1997-99
Mix no. 5
[Rel. Value]
104.0
103.0
102.0
101.0
100.0
99.0
1
2
3
[Year No.]
UPV
Volume
Weight

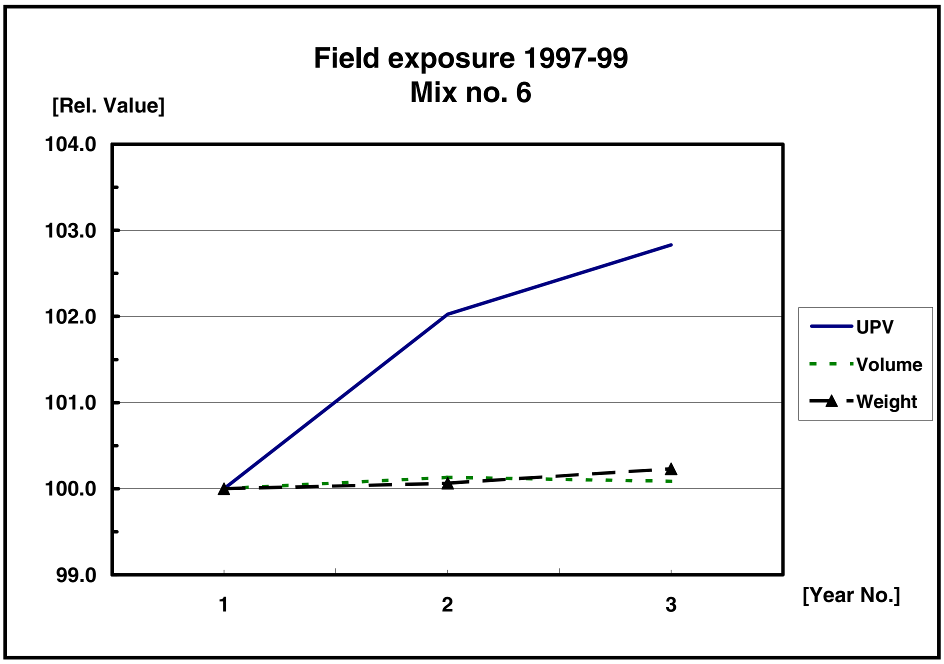
Field exposure 1997-99
Mix no. 6
[Rel. Value]
104.0
103.0
102.0
101.0
100.0
99.0
1
2
3
[Year No.]
UPV
Volume
Weight

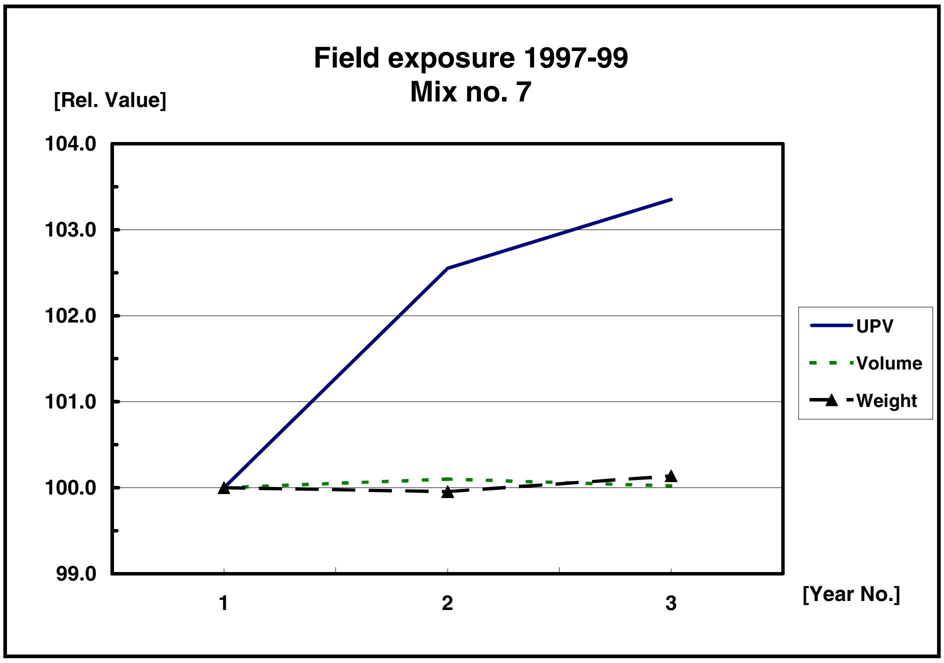
Field exposure 1997-99
Mix no. 7
[Rel. Value]
104.0
103.0
102.0
101.0
100.0
99.0
1
2
3
[Year No.]
UPV
Volume
Weight

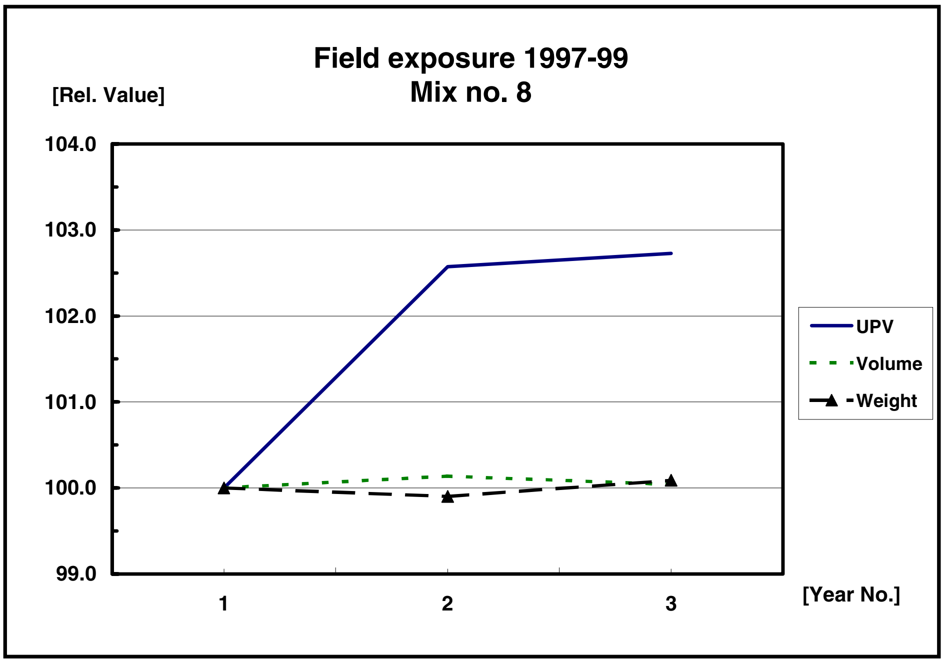
Field exposure 1997-99
Mix no. 8
[Rel. Value]
104.0
103.0
102.0
101.0
100.0
99.0
1
2
3
[Year No.]
UPV
Volume
Weight

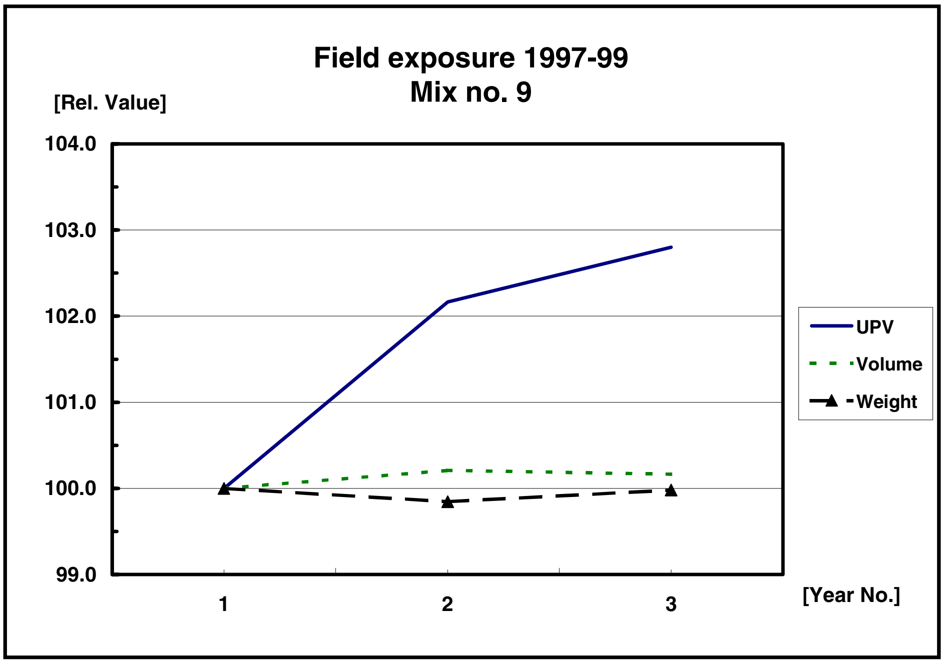
Field exposure 1997-99
Mix no. 9
[Rel. Value]
104.0
103.0
102.0
101.0
100.0
99.0
1
2
3
[Year No.]
UPV
Volume
Weight

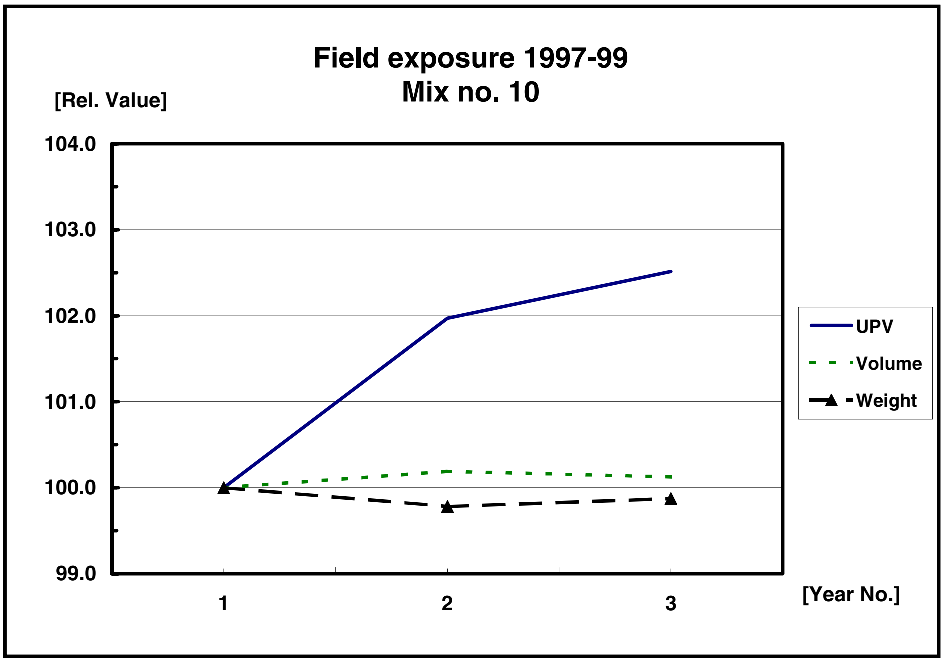
Field exposure 1997-99
Mix no. 10
[Rel. Value]
104.0
103.0
102.0
101.0
100.0
99.0
1
2
3
[Year No.]
UPV
Volume
Weight

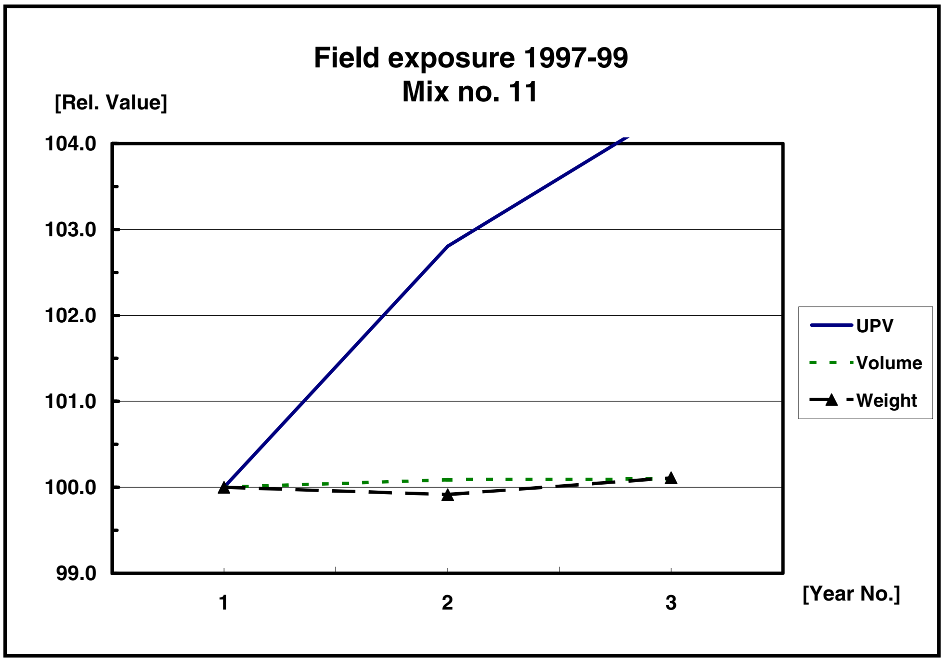
Field exposure 1997-99
Mix no. 11
[Rel. Value]
104.0
103.0
102.0
101.0
100.0
99.0
1
2
3
[Year No.]
UPV
Volume
Weight

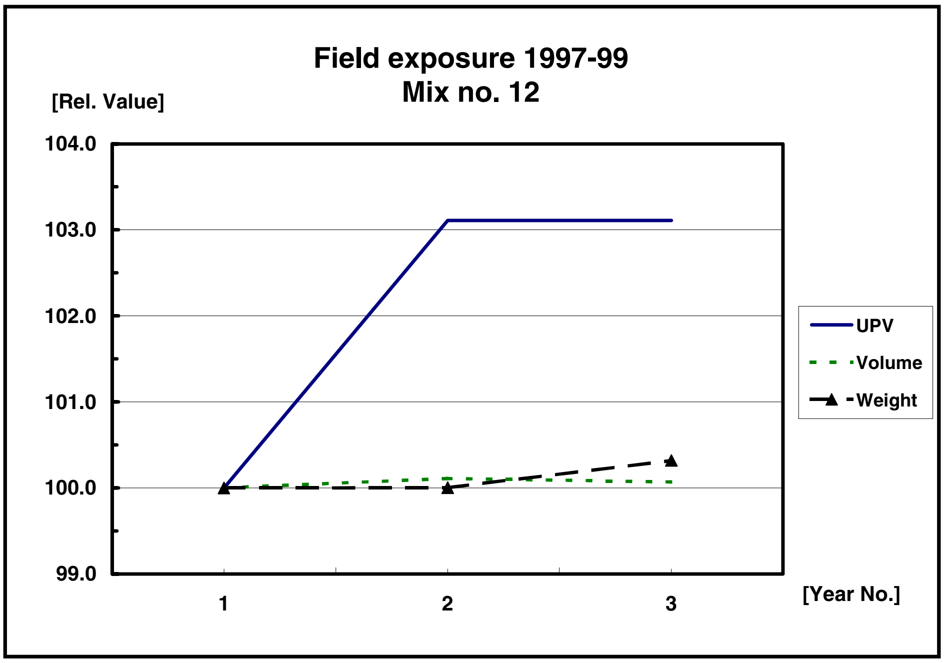
Field exposure 1997-99
Mix no. 12
[Rel. Value]
104.0
103.0
102.0
101.0
100.0
99.0
1
2
3
[Year No.]
UPV
Volume
Weight

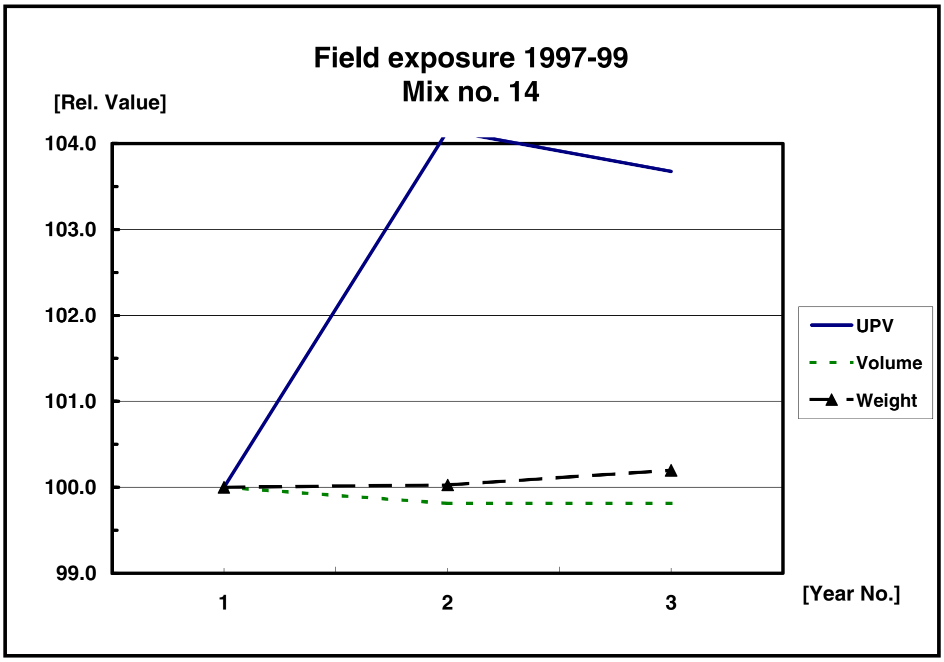
Field exposure 1997-99
Mix no. 14
[Rel. Value]
104.0
103.0
102.0
101.0
100.0
99.0
1
2
3
[Year No.]
UPV
Volume
Weight

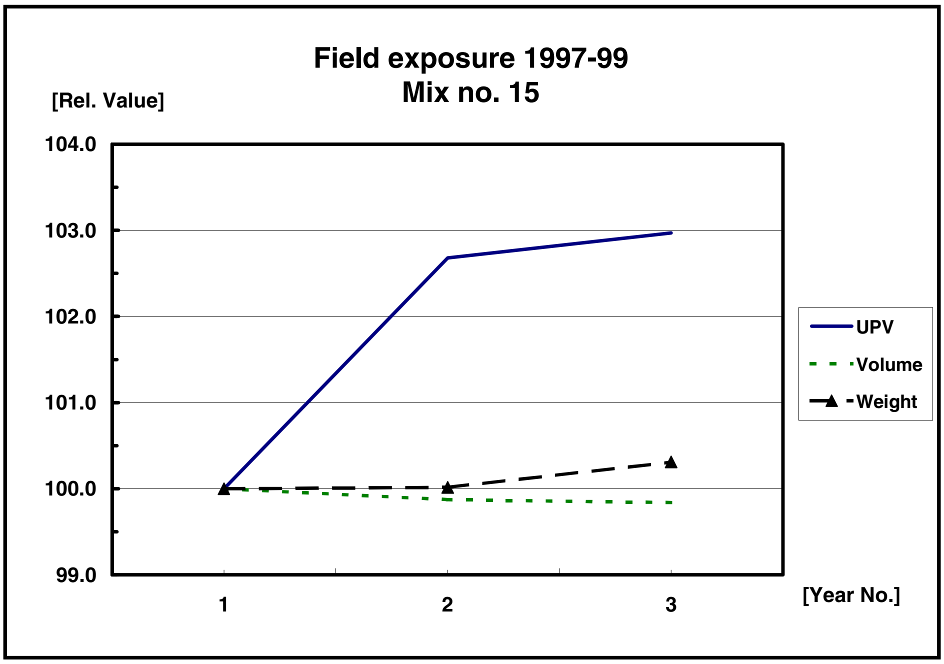
Field exposure 1997-99
Mix no. 15
[Rel. Value]
104.0
103.0
102.0
101.0
100.0
99.0
1
2
3
[Year No.]
UPV
Volume
Weight

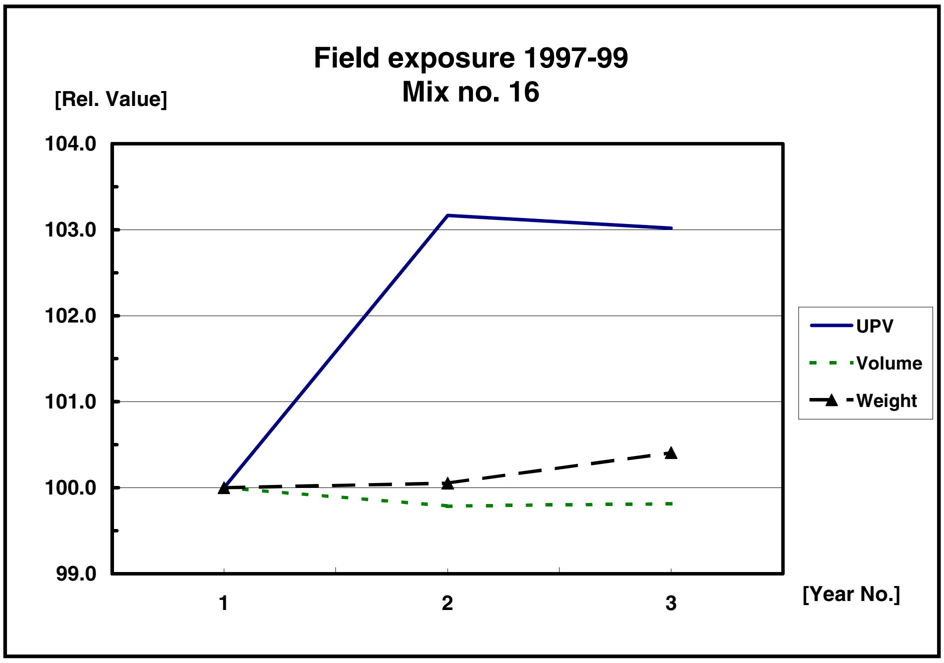
Field exposure 1997-99
Mix no. 16
[Rel. Value]
104.0
103.0
102.0
101.0
100.0
99.0
1
2
3
[Year No.]
UPV
Volume
Weight

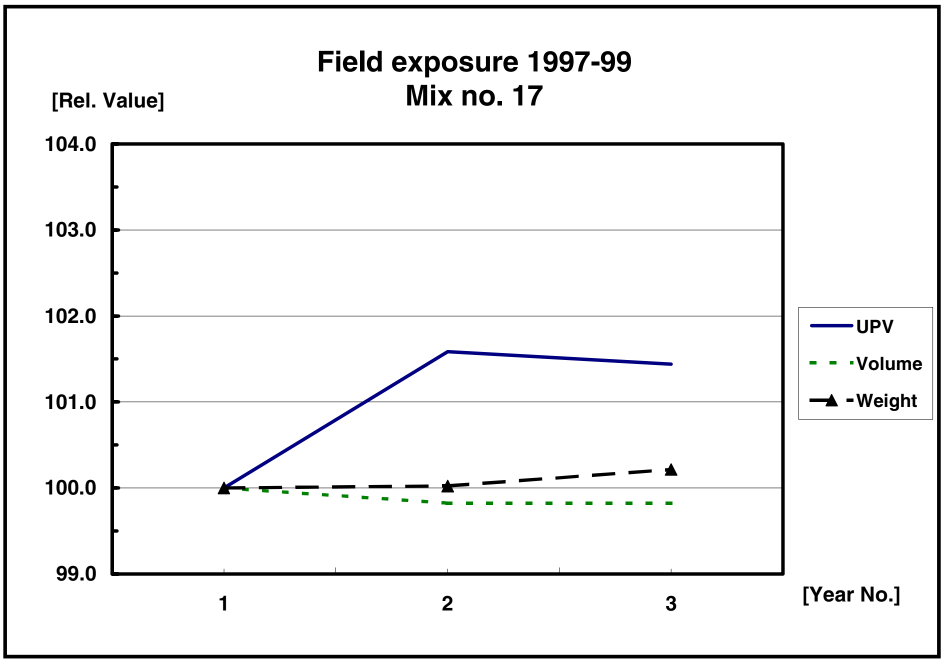
Field exposure 1997-99
Mix no. 17
[Rel. Value]
104.0
103.0
102.0
101.0
100.0
99.0
1
2
3
[Year No.]
UPV
Volume
Weight

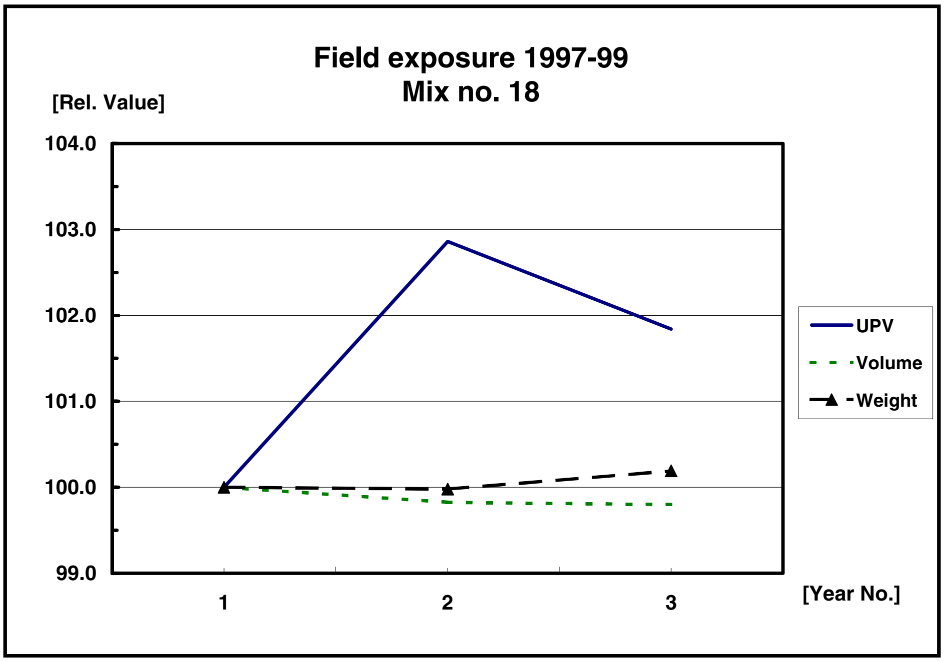
Field exposure 1997-99
Mix no. 18
[Rel. Value]
104.0
103.0
102.0
101.0
100.0
99.0
1
2
3
[Year No.]
UPV
Volume
Weight

URN:NBN:no-6354

APPENDIX F

Section 3 : Additional data and plots

URN:NBN:no-6354

	CEM I 42.5-R	CEM I 42.5-BV-SR-LA	Silica fume
CaO	63,05	63,9	-
SiO_2	20,45	22,5	90,6
Al_2O_3	5,09	3,50	0,88
Fe_2O_3	3,58	4,89	1,51
MgO	2,37	0,95	1,89
K_2O	1,23	0,68	2,00
Na_2O	0,50	0,08	0,47
SO_3	3,34	2,04	0,45
Loss on ignition	0,76	0,94	2,4
C	-	-	1,9
Clinker minerals according to Bogue :			
C_2S	19,1	27,3	-
C_3S	52,4	49,2	-
C_3A	7,4	1,0	-
C_4AF	10,9	14,9	-
Fineness:	326 m^2/kg	306 m^2/kg	1,9 %>44 micron

Table F1 : Chemical and physical properties of cement and silica fume.

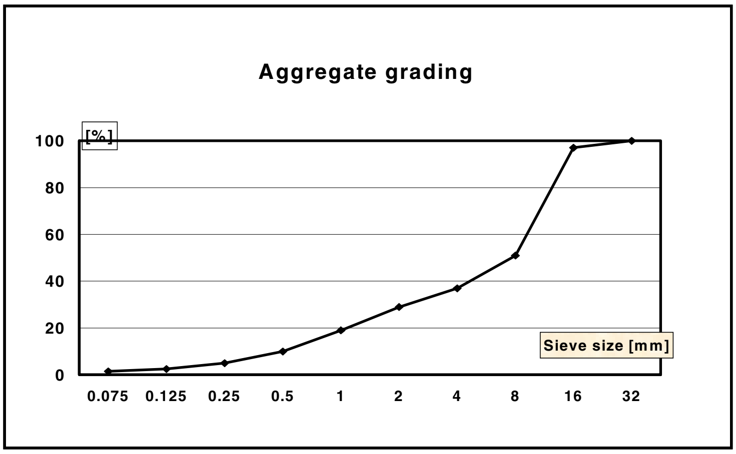

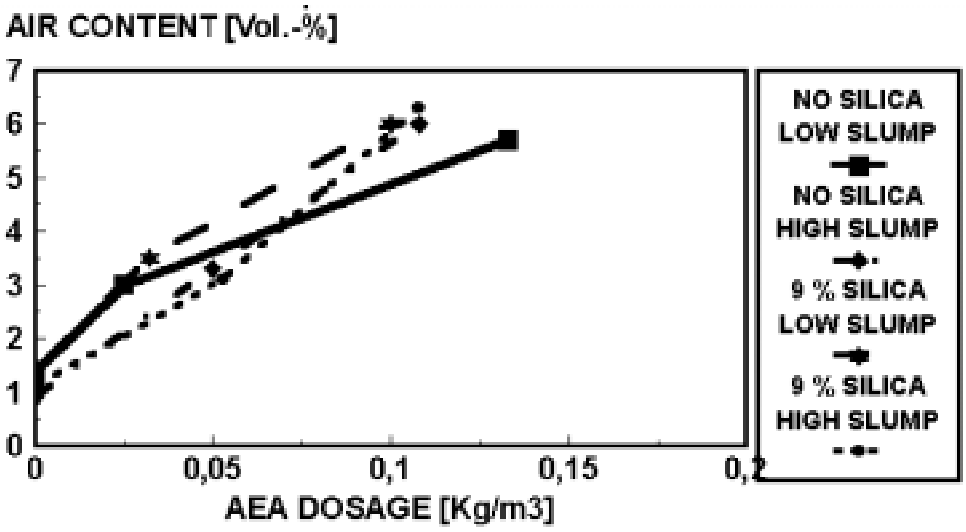

Fresh concrete air content versus air entraining dosage. Cement type CEM I 42.5-R.

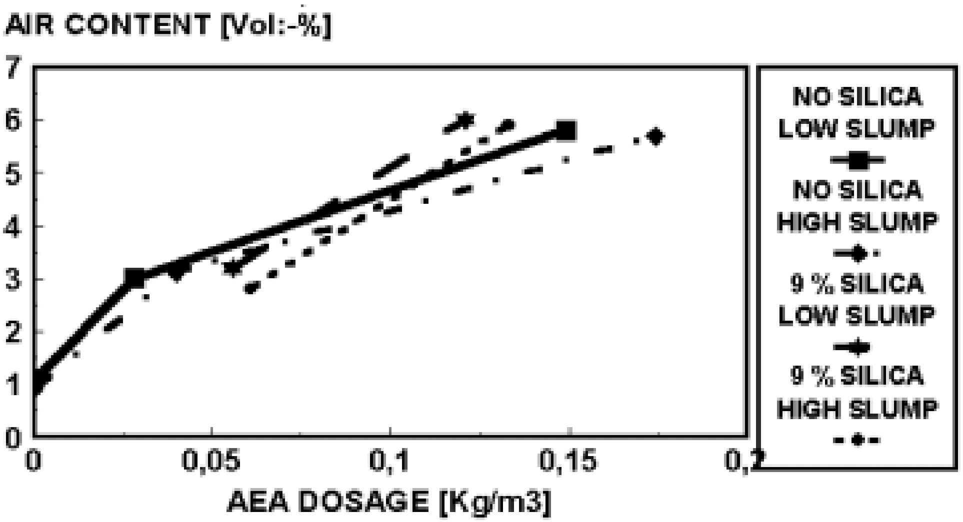

Fresh concrete air content versus air entraining dosage. Cement type CEM I 42.5-BV-SR-LA.

Mix No.	3 months Age			1 year Age		
	C1*)	C2*)	C3*)	C1*)	C2*)	C3*)
1	68	52	60	69	57	73
2	68	57	63	73	59	74
3	59	48	56	63	51	65
4	58	50	56	62	53	67
5	48	40	46	52	43	55
6	54	46	50	57	47	60
7	76	62	71	79	65	79
8	81	63	76	80	66	81
9	67	56	62	71	56	70
10	72	62	70	75	60	75
11	61	51	58	64	48	63
12	63	53	61	61	48	65
13	84	61	75	85	61	83
14	85	63	67	85	65	82
15	75	54	61	80	57	74
16	71	55	64	73	55	72
17	63	46	46	65	50	50
18	65	49	51	65	51	59
19	94	69	74	98	72	84
20	94	69	77	97	71	84
21	78	58	63	-	-	-
22	82	61	67	88	67	79
23	72	51	54	-	-	-
24	72	50	53	-	-	-

*Table F2 : Compressive strength at the age of 3 and 12 months, approximately corresponding to the age of freeze-thaw testing. *)C1, C2 & C3: Designates the curing conditions*

Freeze-thaw scaling [kg/m^2]

Details

Mix No.	Age 1 (2-3 months) Curing			Age 2 (1 year) Curing		
	C1	**C2**	**C3**	**C1+1Y**	**C2+1Y**	**C3+1Y**
1	13	8	6.4	22	18	11
2	15	11	11.2	27	26	31
3	2.1	0.21	0.15	0.32	0.53	0.64
4	1.8	0.24	0.04	0.41	0.19	0.65
5	0.25	0.05	0.17	0.08	0.08	0.12
6	0.24	0.06	0.02	0.07	0.08	0.78
7	3.9	3.6	4.8	7	4	5.5
8	3.9	5.0	5.4	5	4	8
9	0.18	0.10	0.18	0.10	0.11	0.21
10	0.43	1.1	1.05	0.40	0.25	1.3
11	0.04	0.02	0.03	0.02	0.02	0.14
12	0.08	0.05	0.10	0.08	0.09	0.05
13	1.8	0.06	0.14	4.9	0.15	0.81
14	2.2	0.32	1.5	8.5	0.9	0.65
15	0.02	0.03	0	0.02	0	0.01
16	0.05	0.02	0.01	0.03	0.04	0.04
17	0.03	0.04	0.01	0.01	0.01	0
18	0.05	0.02	0.01	0.01	0.01	0
19	1.1	0.21	3.3	1.7	0.43	0.82
20	1.8	0.27	4.5	1.2	0.42	1.8
21	1.0	0.03	0.02	0.09	0.02	0.02
22	0.82	0.15	0.94	0.71	0.06	1.4
23	0.02	0.02	0.02	0.02	0.01	0.01
24	0.03	0.01	0.02	0.05	0.02	0.04

**Values 18 kg and above are extrapolated (doubled) from 28 cycles.
Still, values are considered relevant for ranking**

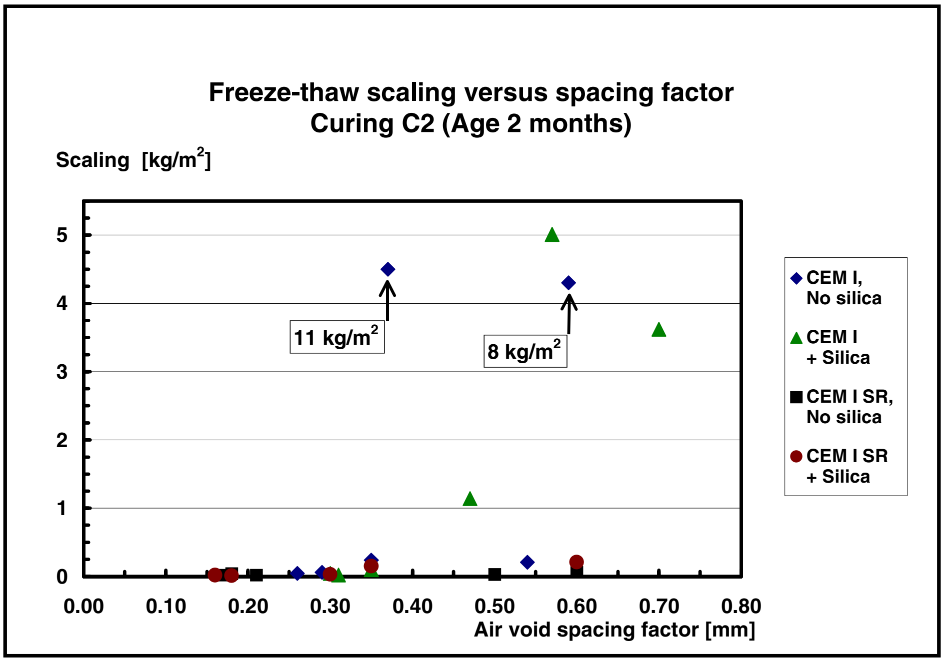
Freeze-thaw scaling versus spacing factor
Curing C2 (Age 2 months)
Scaling [kg/m²]
5
4
3
2
1
0
0.00
0.10
0.20
0.30
0.40
0.50
0.60
0.70
0.80
Air void spacing factor [mm]
11 kg/m²
8 kg/m²
CEM I, No silica
CEM I + Silica
CEM I SR, No silica
CEM I SR + Silica

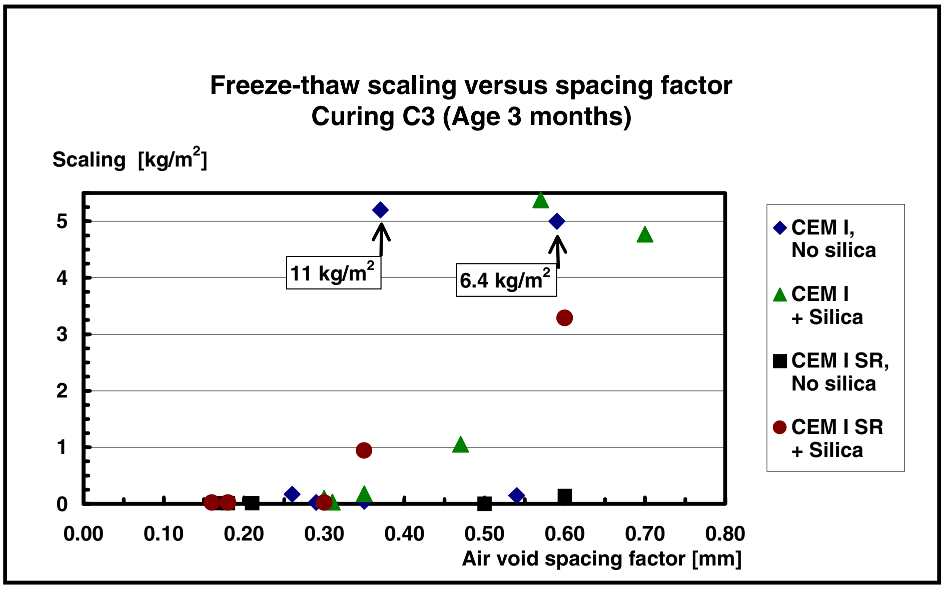
Freeze-thaw scaling versus spacing factor
Curing C3 (Age 3 months)
Scaling [kg/m²]
5
4
3
2
1
0
0.00
0.10
0.20
0.30
0.40
0.50
0.60
0.70
0.80
Air void spacing factor [mm]
11 kg/m²
6.4 kg/m²
CEM I, No silica
CEM I + Silica
CEM I SR, No silica
CEM I SR + Silica

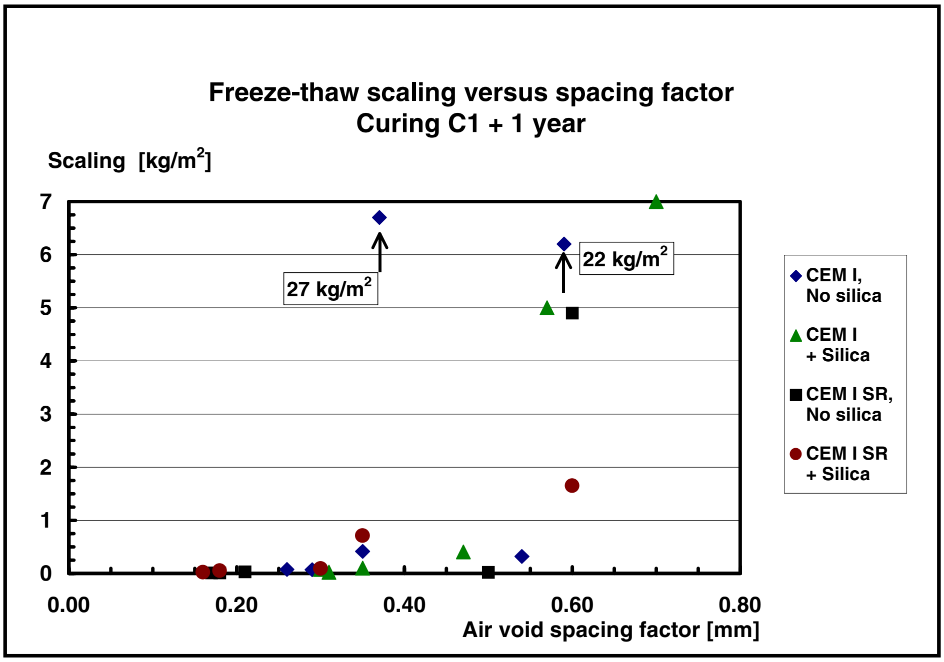
Freeze-thaw scaling versus spacing factor
Curing C1 + 1 year
Scaling [kg/m²]
7
6
5
4
3
2
1
0
0.00
0.20
0.40
0.60
0.80
Air void spacing factor [mm]
27 kg/m²
22 kg/m²
◆ CEM I, No silica
▲ CEM I + Silica
■ CEM I SR, No silica
● CEM I SR + Silica

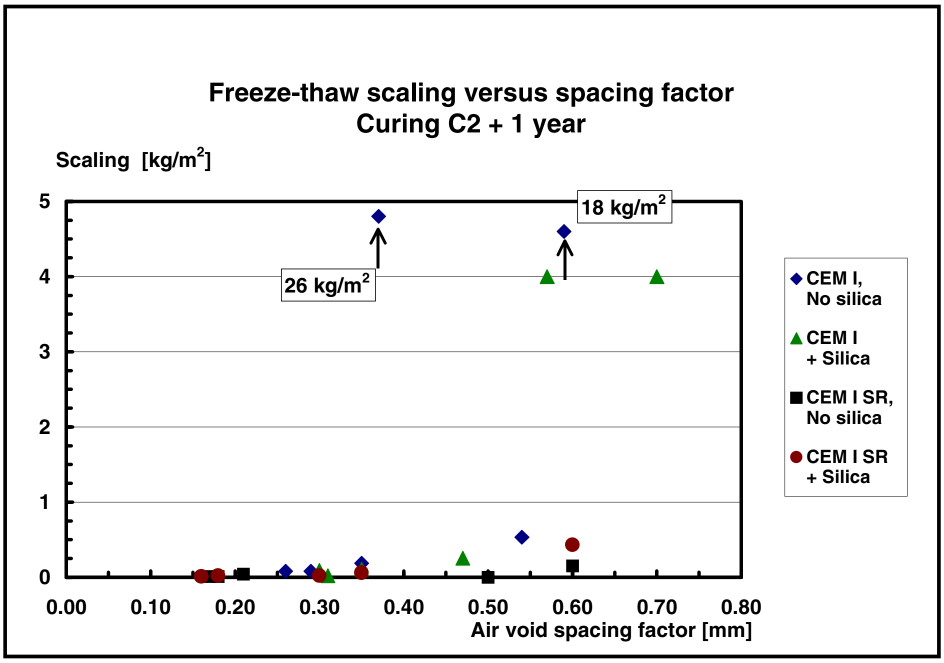
Freeze-thaw scaling versus spacing factor
Curing C2 + 1 year
Scaling [kg/m²]
5
4
3
2
1
0
0.00
0.10
0.20
0.30
0.40
0.50
0.60
0.70
0.80
Air void spacing factor [mm]
26 kg/m²
18 kg/m²
◆ CEM I, No silica
▲ CEM I + Silica
■ CEM I SR, No silica
● CEM I SR + Silica

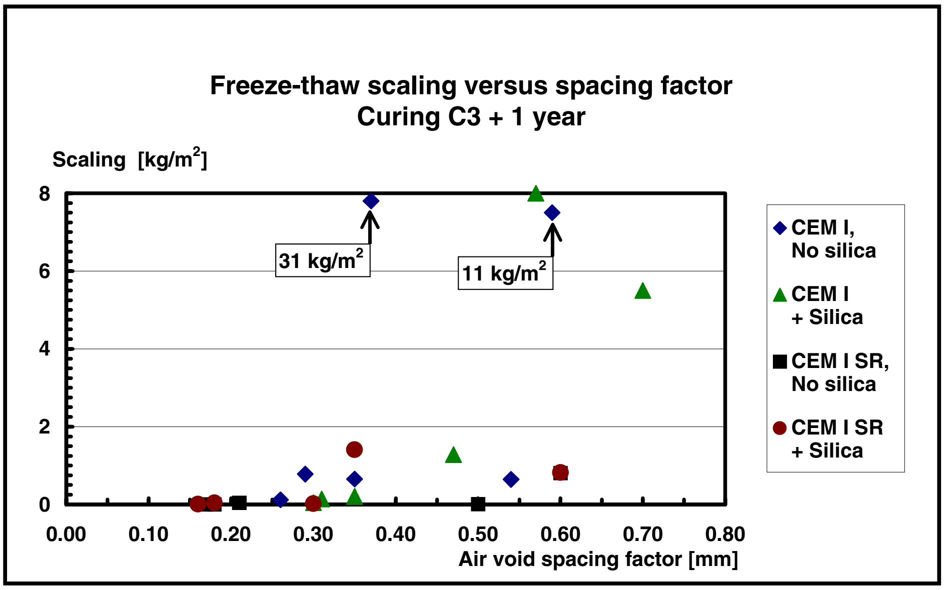
Freeze-thaw scaling versus spacing factor
Curing C3 + 1 year
Scaling [kg/m²]
8
6
4
2
0
31 kg/m²
11 kg/m²
0.00
0.10
0.20
0.30
0.40
0.50
0.60
0.70
0.80
Air void spacing factor [mm]
◆ CEM I, No silica
▲ CEM I + Silica
■ CEM I SR, No silica
● CEM I SR + Silica

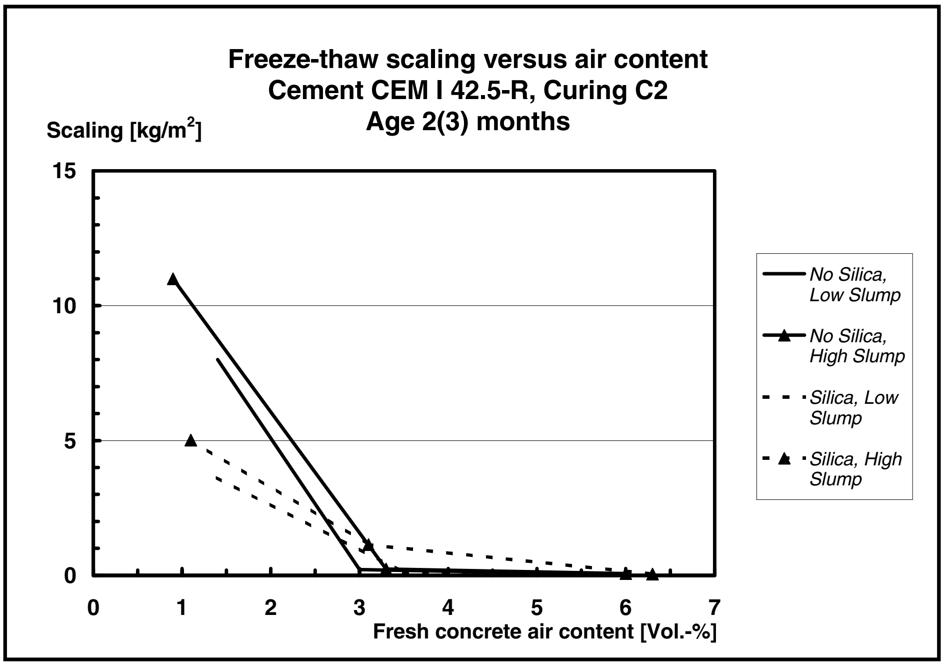
Freeze-thaw scaling versus air content
Cement CEM I 42.5-R, Curing C2
Age 2(3) months
Scaling [kg/m²]
15
10
5
0
0
1
2
3
4
5
6
7
Fresh concrete air content [Vol.-%]
No Silica, Low Slump
No Silica, High Slump
Silica, Low Slump
Silica, High Slump

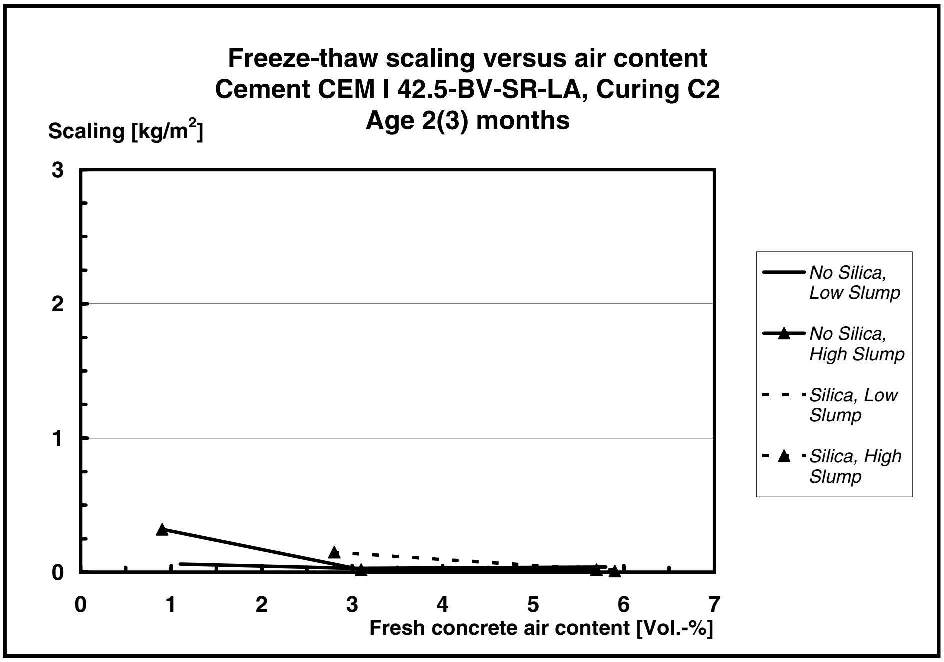
Freeze-thaw scaling versus air content
Cement CEM I 42.5-BV-SR-LA, Curing C2
Age 2(3) months
Scaling [kg/m²]
3
2
1
0
0
1
2
3
4
5
6
7
Fresh concrete air content [Vol.-%]
No Silica, Low Slump
No Silica, High Slump
Silica, Low Slump
Silica, High Slump

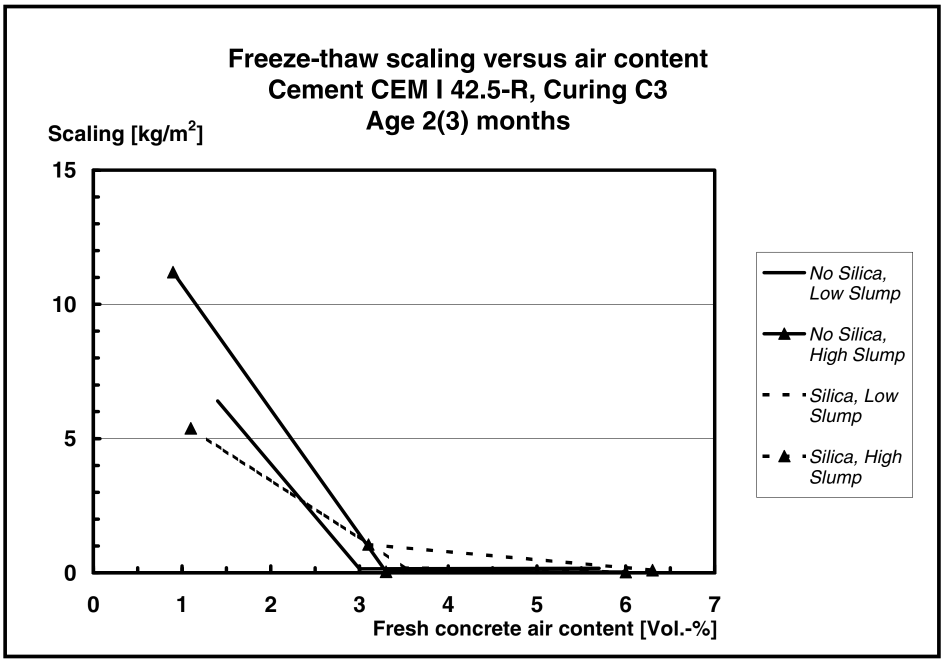
Freeze-thaw scaling versus air content
Cement CEM I 42.5-R, Curing C3
Age 2(3) months
Scaling [kg/m²]
15
10
5
0
0
1
2
3
4
5
6
7
Fresh concrete air content [Vol.-%]
No Silica, Low Slump
No Silica, High Slump
Silica, Low Slump
Silica, High Slump

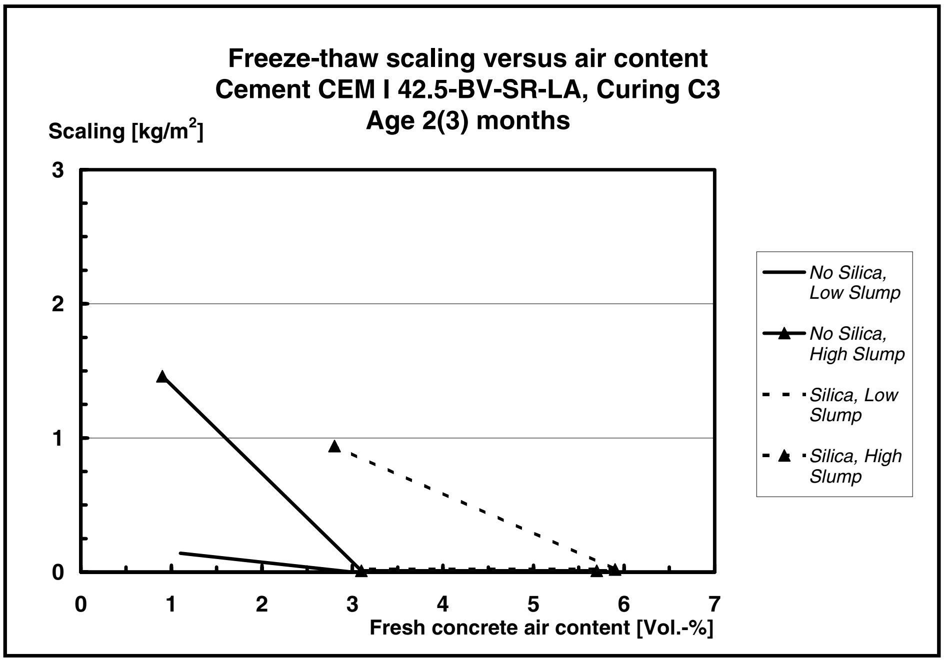
Freeze-thaw scaling versus air content
Cement CEM I 42.5-BV-SR-LA, Curing C3
Age 2(3) months
Scaling [kg/m²]
3
2
1
0
0
1
2
3
4
5
6
7
Fresh concrete air content [Vol.-%]
No Silica, Low Slump
No Silica, High Slump
Silica, Low Slump
Silica, High Slump

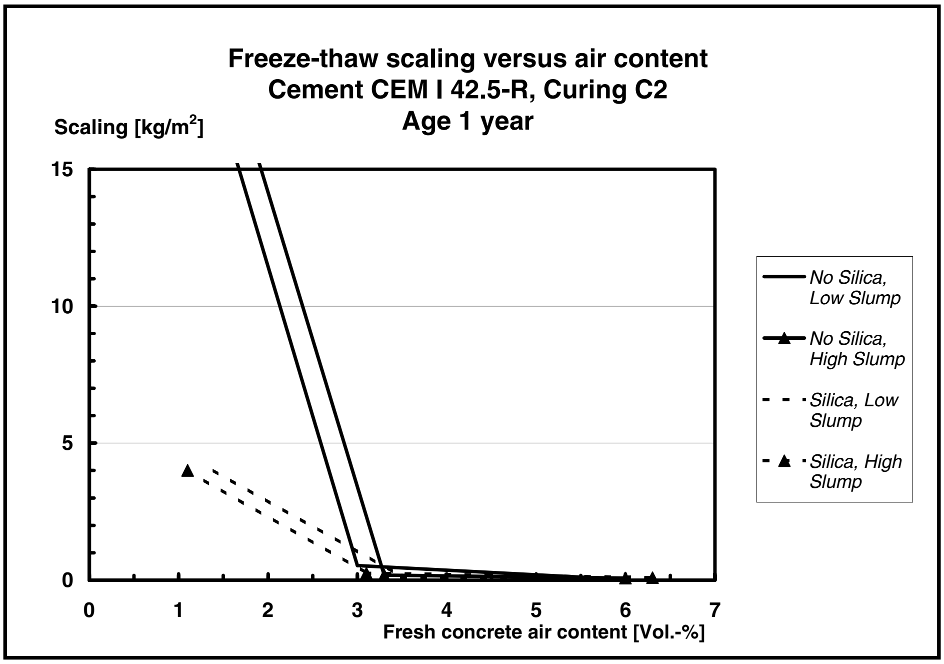
Freeze-thaw scaling versus air content
Cement CEM I 42.5-R, Curing C2
Age 1 year
Scaling [kg/m²]
15
10
5
0
0
1
2
3
4
5
6
7
Fresh concrete air content [Vol.-%]
No Silica, Low Slump
No Silica, High Slump
Silica, Low Slump
Silica, High Slump

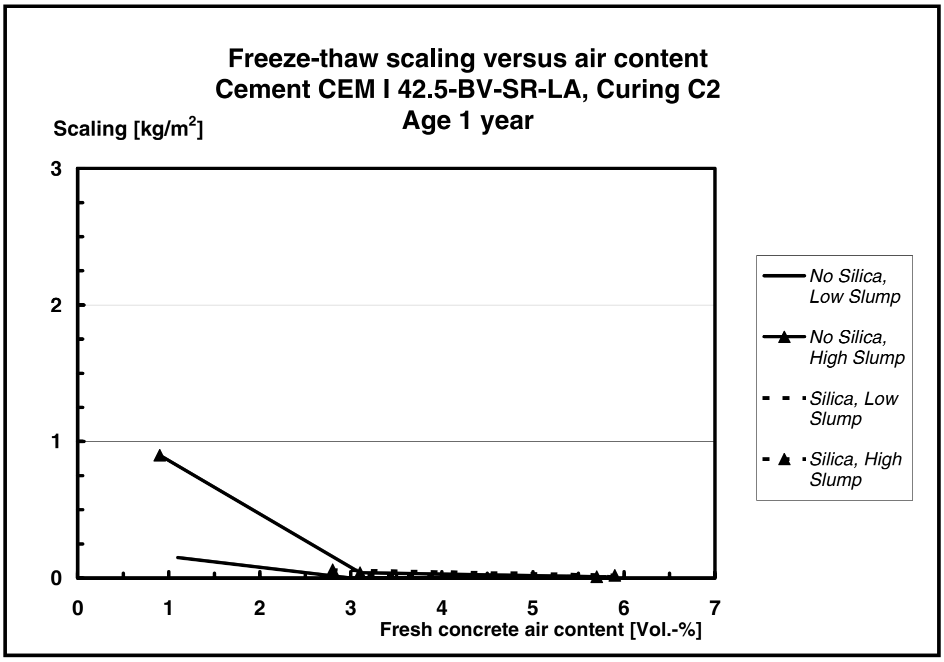
Freeze-thaw scaling versus air content
Cement CEM I 42.5-BV-SR-LA, Curing C2
Age 1 year
Scaling [kg/m²]
3
2
1
0
0
1
2
3
4
5
6
7
Fresh concrete air content [Vol.-%]
No Silica, Low Slump
No Silica, High Slump
Silica, Low Slump
Silica, High Slump

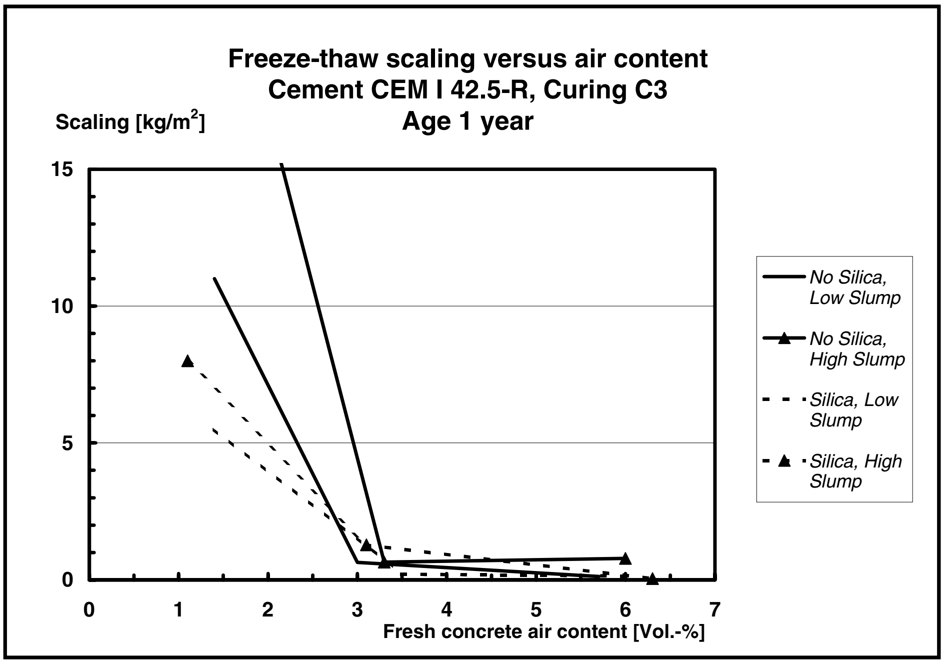
Freeze-thaw scaling versus air content
Cement CEM I 42.5-R, Curing C3
Age 1 year
Scaling [kg/m²]
15
10
5
0
0
1
2
3
4
5
6
7
Fresh concrete air content [Vol.-%]
No Silica, Low Slump
No Silica, High Slump
Silica, Low Slump
Silica, High Slump

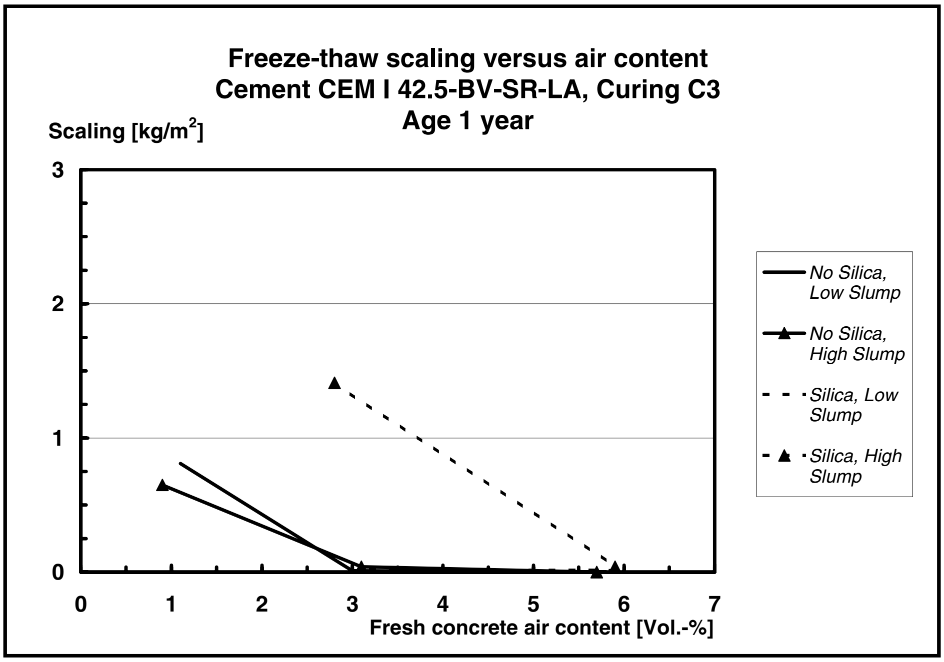
Freeze-thaw scaling versus air content
Cement CEM I 42.5-BV-SR-LA, Curing C3
Age 1 year
Scaling [kg/m²]
3
2
1
0
0
1
2
3
4
5
6
7
Fresh concrete air content [Vol.-%]
No Silica, Low Slump
No Silica, High Slump
Silica, Low Slump
Silica, High Slump

APPENDIX G

Section 7 : Additional data

Mortar Air Entrained Standard Curing / Isothermally Frozen	Sample	1c	2c	3c	4c	1d
	Time frozen [h] :					
		0	3	7	12	24
Stage :						
	Hours :					
After Preparation at 20C/65RH		1029.3	1055.0	1061.2	1037.2	1039.2
Loss before re-saturation		1.1	1.1	1.2	1.1	1.1
After preparation, before re-sat.		1028.2	1053.9	1060.0	1036.1	1038.1
After 3d re-saturation		1029.6	1055.1	1061.6	1037.4	1039.6
Suction during 3d re-saturation		1.4	1.2	1.6	1.3	1.5
End of frost, incl. scaled material		1029.6	1055.7	1062.7	1038.5	1040.7
End of frost, excl. scaled mat.	*0*	1029.6	1055.7	1062.7	1038.5	1040.7
1rst suction, one surface	*0.5*	1029.6	1055.7	1062.2	1037.9	1040.3
2nd suction, one surface	*1*	1029.6	1055.7	1062.1	1037.7	1040.0
3rd suction, one surface	*1.5*	1029.6	1055.7	1062.1	1037.7	1040.0
4th suction, one surface	*2*	1029.6	1055.7	1062.1	1037.7	1039.9
Suction during frost		0.0	0.6	1.1	1.1	1.1
Suction during frost [Vol.-%]		0.0	0.2	0.3	0.3	0.3
Change during thawing		0.0	0.0	-0.6	-0.8	-0.8
Change during thawing [Vol.%]		0.0	0.0	-0.2	-0.2	-0.2
Stripped sample, before subm.	*0*	766.3	793.2	794.6	745.9	776.0
1rst suction submerged	*0.5*	769.7	796.4	797.9	749.3	778.9
2nd suction submerged	*1*	770.3	797.1	798.5	749.9	779.2
3rd suction submerged	*1.5*	770.8	797.3	798.9	750.2	779.7
4th suction submerged	*2*	771.1	797.6	799.1		
etc.	*2.5*	771.2				
	3	771.3		799.7		
	4		798.7			780.1
	5			800.1		
	6					
	7					
	8		799.4		752.1	
	9					
	12		800.1	801.3		
Scaled material		0.0	0.0	0.0	0.0	0.0
Before saturation by pressure		771.3	800.1	801.3	752.1	780.1
After 7d pressure at 50 bar		813.2	837.9	841.8	789.8	813.7
Change during 7d pressure		41.9	37.8	40.5	37.7	33.6
After 7d at 105 C		719.6	744.6	745.9	701.0	728.4
Change during 7d of drying		93.6	93.3	95.9	88.8	85.3
Volume [cm^3]		371.8	386.9	390.1	364.7	374.3

All values in [g] unless otherwise stated.

Mortar Air Entrained	Sample	2d	3d	4d	8a	8b
Standard Curing / Isothermally Frozen					(Epoxy)	(Epoxy)
Continued	Time frozen [h] :					
		48	168	168	168	168
Stage :						
	Hours :					
After Preparation at 20C/65RH		1047.2	1051.5	1022.2		
Loss before re-saturation		1.0	1.1	1.0		
After preparation, before re-sat.		1046.2	1050.4	1021.2	966.0	985.7
After 3d re-saturation		1047.6	1053.1	1023.3	966.0	985.6
Suction during 3d re-saturation		1.4	2.7	2.1		
End of frost, incl. scaled material		1048.8	1053.6	1023.9	966.0	985.8
End of frost, excl. scaled mat.	*0*	1048.8	1053.6	1023.9	966.0	985.8
1rst suction, one surface	*0.5*	1048.2	1053.2	1023.5		
2nd suction, one surface	*1*	1048.1	1053.0	1023.4		
3rd suction, one surface	*1.5*	1048.1	1053.0	1023.4		
4th suction, one surface	*2*	1048.1	1053.0	1023.4		
Suction during frost		1.2	0.5	0.6		
Suction during frost [Vol.-%]		0.3	0.1	0.2		
Change during thawing		-0.7	-0.6	-0.5		
Change during thawing [Vol.%]		-0.2	-0.2	-0.1		
Stripped sample, before subm.	*0*	789.0	772.1	757.9	757.8	765.2
1rst suction submerged	*0.5*	790.9	773.8	760.1	758.2	765.5
2nd suction submerged	*1*	791.3	774.5	760.8	758.3	765.6
3rd suction submerged	*1.5*	791.5				
4th suction submerged	*2*		774.9	761.2	758.5	765.7
etc.	*2.5*					
	3		775.0	761.5	758.6	765.8
	4				758.7	765.9
	5		775.5	761.9		
	6				758.8	766.0
	7	792.6				
	8					
	9		775.9	762.3		
	12		776.2	762.5	759.1	766.3
Scaled material		0.0	0.0	0.0	0.0	0.0
Before saturation by pressure		792.6	776.2	762.5	759.1	766.3
After 7d pressure at 50 bar		822.3	807.7	794.9	795.9	800.8
Change during 7d pressure		29.7	31.5	32.4	36.8	34.5
After 7d at 105 C		741.2	724.4	711.5	703.4	711.4
Change during 7d of drying		81.1	83.3	83.4	92.5	89.4
Volume [cm^3]		378.6	373.9	366.8	375.7	378.0

All values in [g] unless otherwise stated.

Mortar Air Entrained Water stored / Isothermally frozen	Sample	1a	2a	3a	4a	1b
	Time frozen [h]	0	3	7	12	24
Stage :						
	Hours :					
After Prepar. at 20C/65RH		1035.6	1042.2	1037.7	1052.8	1037.6
Loss before re-saturation		1.3	1.7	1.6	1.5	1.3
After prep., before re-sat.		1034.3	1040.5	1036.1	1051.3	1036.3
After 3d re-saturation		1035.1	1041.5	1036.8	1052.4	1037.9
Suction during 3d re-sat.		0.8	1.0	0.7	1.1	1.6
End of frost, incl. scaled material		1035.1	1042.0	1037.9	1053.5	1038.2
End of frost, excl. scaled	*0*	1035.1	1042.0	1037.9	1053.5	1038.2
1rst suction, one surface	*0.5*	1035.1	1042.0	1037.4	1052.9	1037.8
2nd suction, one surface	*1*	1035.1	1042.0	1037.3	1052.9	1037.4
3rd suction, one surface	*1.5*	1035.1	1042.0	1037.3	1052.9	1037.5
4th suction, one surface	*2*	1035.1	1042.0	1037.3	1052.9	1037.5
Suction during frost		0.0	0.5	1.1	1.1	0.3
Suction during frost [Vol.-%]		0.0	0.1	0.3	0.3	0.1
Change during thawing		0.0	0.0	-0.6		
Change dur. thawing [Vol.%]		0.0	0.0	-0.2		
Stripped sample, bef. subm.	*0*	756.6	770.3	771.4	797.2	748.1
1rst suction submerged	*0.5*	758.8	772.9	773.7	799.3	749.9
2nd suction submerged	*1*	759.2	773.2	774.0	799.6	750.1
3rd suction submerged	*1.5*	759.5	773.5	774.2	799.9	
4th suction submerged	*2*	759.6	773.6	774.4		
etc.	*2.5*	759.7				
	3	759.7		774.7		
	4		774.2			750.7
	5			775.0		
	6					
	7					
	8		774.7		801.2	
	9					
	12		775.1	775.9		
Scaled material		0.0	0.0	0.0	0.0	0.0
Before sat. by pressure		759.7	775.1	775.9	801.2	750.7
After 7d pressure at 50 bar		792.5	803.1	807.8	835.2	788.4
Change during 7d pressure		32.8	28.0	31.9	34.0	37.7
After 7d at 105 C		703.2	715.5	716.7	739.6	695.0
Change during 7d of drying		89.3	87.6	91.1	95.6	93.4
Volume [cm^3]		370.5	375.0	379.1	389.7	366.3

All values in [g] unless otherwise stated.

Mortar Air Entrained **Water stored /** **Isothermally frozen**	Sample	2b	3b	4b	8a (Epoxy)	8b (Epoxy)
Continued	Time frozen [h]					
		48	168	168	168	168
Stage :						
	Hours :					
After Prep. at 20C/65RH		1002.2	962.9	1026.4		
Loss before re-saturation		1.4	1.2	1.2		
After prep., before re-sat.		1000.8	961.7	1025.2	966.0	985.7
After 3d re-saturation		1002.1	963.1	1027.2	966.0	985.6
Suction during 3d re-sat.		1.3	1.4	2.0		
End of frost, incl. scaled material		1002.4	963.8	1027.8	966.0	985.8
End of frost, excl. scaled	*0*	1002.4	963.8	1027.8	966.0	985.8
1rst suction, one surface	*0.5*	1002.0	963.4	1027.7		
2nd suction, one surface	*1*	1002.0	963.2	1027.4		
3rd suction, one surface	*1.5*	1001.9	963.2	1027.4		
4th suction, one surface	*2*	1001.9	963.2	1027.4		
Suction during frost		0.3	0.7	0.6		
Suction during frost [Vol.-%]		0.1	0.2	0.2		
Change during thawing		-0.5	-0.6	-0.4		
Change dur. thawing [Vol.%]		-0.1	-0.2	-0.1		
Stripped sample, bef. subm.	*0*	744.6	705.5	761.2	757.8	765.2
1rst suction submerged	*0.5*	746.2	706.8	762.6	758.2	765.5
2nd suction submerged	*1*	746.5	707.1	763.0	758.3	765.6
3rd suction submerged	*1.5*	746.7				
4th suction submerged	*2*		707.4	763.2	758.5	765.7
etc.	*2.5*					
	3		707.6	763.4	758.6	765.8
	4				758.7	765.9
	5		708.0	763.7		
	6				758.8	766.0
	7	747.7				
	8					
	9		708.1	763.9		
	12		708.3	764.2	759.1	766.3
Scaled material		0.0	0.0	0.0	0.0	0.0
Before sat. by pressure		747.7	708.3	764.2	759.1	766.3
After 7d pressure at 50 bar		783.1	743.2	798.5	795.9	800.8
Change during 7d pressure		35.4	34.9	34.3	36.8	34.5
After 7d at 105 C		692.0	655.2	705.4	703.4	711.4
Change during 7d of drying		91.1	88.0	93.1	92.5	89.4
Volume [cm^3]		361.6	345.7	368.3	375.7	378.0

All values in [g] unless otherwise stated.

Mortar Air Entrained Standard Curing / Cyclic Freeze-Thaw	Sample	1c	5c	6d	8c (Epoxy)	9a (Epoxy)
		No. of freeze-thaw cycles				
		0	7	7	7	7
Stage :						
After Preparation at 20C/65RH		1029.3	1025.9	1053.5		
Loss before re-saturation		1.1	1.2	1.1		
After preparation, before re-sat.		1028.2	1024.7	1052.4	985.6	1016.1
After 3d re-saturation		1029.6	1027.0	1054.7	985.5	1016.1
Suction during 3d re-saturation		1.4	2.3	2.3		
End of frost, incl. scaled mat.	*Hours*	1029.6	1028.5	1055.9	985.5	1016.3
End of frost, excl. scaled mat.	0	1029.6	1028.4	1055.9	985.5	1016.3
1rst suction, one surface	0.5	1029.6	1027.7	1055.5		
2nd suction, one surface	1	1029.6	1027.6	1055.2		
3rd suction, one surface	1.5	1029.6	1027.6	1055.2		
4th suction, one surface	2	1029.6	1027.6	1055.2		
Suction during frost		0.0	1.5	1.2		
Suction during frost [Vol.-%]		0.0	0.4	0.3		
Change during thawing		0.0	-0.8	-0.7		
Change during thawing [Vol.%]		0.0	-0.2	-0.2		
Stripped sample, before subm.	0	766.3	772.5	797.1	758.2	717.5
1rst suction submerged	0.5	769.7	775.9	799.1		
2nd suction submerged	1	770.3	776.6	799.7		
3rd suction submerged	1.5	770.8	776.9	799.9		
4th suction submerged	2	771.1				
etc.	2.5	771.2	777.4	800.4		
	3	771.3			758.7	718.9
	4				758.8	719.1
	5		778.0	800.6		
	6					
	7					
	8					
	9		778.7	801.0		
	12		778.9	801.2		
Scaled material		0.0	0.1	0.1	0.0	0.0
Before saturation by pressure		771.3	778.9	801.2	758.8	719.1
After 7d pressure at 50 bar		813.2	817.0	836.4	791.9	753.7
Change during 7d pressure		41.9	38.1	35.2	33.1	34.6
After 7d at 105 C		719.6	723.7	747.5	707.5	664.8
Change during 7d of drying		93.6	93.3	88.9	84.4	88.9
Volume [cm^3]		371.8	379.3	387.2	373.1	355.2

All values in [g] unless otherwise stated.

Mortar Air Entrained Standard Curing / Cyclic Freeze-Thaw	Sampl	5d	7c	6c	7d	8d (Epoxy)	9b (Epoxy)
Continued	Cycles						
		14	14	28	28	28	28
Stage :							
After Preparation at 20C/65RH		1001.8	978.9	1004.8	1054.6		
Loss before re-saturation		1.0	1.2	1.2	1.2		
After preparation, before re-sat.		1000.8	977.7	1003.6	1053.4	1063.2	979.1
After 3d re-saturation		1003.1	979.9	1005.6	1055.8	1063.1	979.1
Suction during 3d re-saturation		2.3	2.2	2.0	2.4		
End of frost, incl. scaled material	*Hours*	1004.9	982.5	1008.0	1059.2	1063.2	979.1
End of frost, excl. scaled mat.	0	1004.7	982.4	1007.9	1059.0	1063.2	979.1
1rst suction, one surface	0.5	1003.9	981.6	1007.3	1058.5		
2nd suction, one surface	1	1003.9	981.6	1007.2	1058.3		
3rd suction, one surface	1.5	1004.0	981.6	1007.2	1058.3		
4th suction, one surface	2	1004.0	981.6	1007.2	1058.3		
Suction during frost		1.8	2.6	2.4	3.4		
Suction during frost [Vol.-%]		0.5	0.7	0.7	0.9		
Change during thawing		-0.7	-0.8	-0.7	-0.7		
Change during thawing [Vol.%]		-0.2	-0.2	-0.2	-0.2		
Stripped sample, before subm.	0	745.2	712.6	751.0	791.3	834.8	768.3
1rst suction submerged	0.5	747.2	715.3	754.2	795.1	835.4	768.7
2nd suction submerged	1	747.7	715.8	754.5	795.5	835.5	768.7
3rd suction submerged	1.5	747.9	716.1				
4th suction submerged	2						
etc.	2.5						
	3			755.2	796.4	835.7	768.9
	4						
	5						
	6						
	7						
	8						
	9	749.5	718.0	756.5	797.7	836.2	769.2
	12	749.8	718.3	756.8	798.0	836.3	769.3
Scaled material		0.2	0.1	0.1	0.1	0.0	0.0
Before saturation by pressure		749.8	718.3	756.8	798.0	836.3	769.3
After 7d pressure at 50 bar		781.6	746.5	798.3	840.2	864.6	810.2
Change during 7d pressure		31.8	28.2	41.5	42.2	28.3	40.9
After 7d at 105 C		698.8	665.9	704.2	739.3	781.3	715.8
Change during 7d of drying		82.8	80.6	94.1	100.9	83.3	94.4
Volume [cm^3]		360.9	350.2	367.4	389.1	408.5	381.0

All values in [g] unless otherwise stated.

Mortar Air Entrained	Sample	1a	5a	6b	8c	9a
Water stored / Cyclic Freeze-Thaw		(Isoth.)			(Epoxy)	(Epoxy)
		No. of freeze-thaw cycles				
		0	7	7	7	7
Stage :						
After Preparation at 20C/65RH		1035.6	1054.6	982.1		
Loss before re-saturation		1.3	1.5	1.3		
After preparation, before re-sat.		1034.3	1053.1	980.8	985.6	1016.1
After 3d re-saturation		1035.1	1054.6	983.0	985.5	1016.1
Suction during 3d re-saturation		0.8	1.5	2.2		
End of frost, incl. scaled material	*Hours*	1035.1	1057.8	985.0	985.5	1016.3
End of frost, excl. scaled mat.	0	1035.1	1057.7	984.9	985.5	1016.3
1rst suction, one surface	0.5	1025.1	1057.0	983.9		
2nd suction, one surface	1	1035.1	1056.9	983.9		
3rd suction, one surface	1.5	1035.1	1056.9	983.9		
4th suction, one surface	2	1035.1	1056.9	983.9		
Suction during frost		0.0	3.2	2.0		
Suction during frost [Vol.-%]		0.0	0.8	0.6		
Change during thawing		0.0	-0.8	-1.0		
Change during thawing [Vol.%]		0.0	-0.2	-0.3		
Stripped sample, before subm.	0	756.6	789.0	713.9	758.2	717.5
1rst suction submerged	0.5	758.8	790.5	715.0		
2nd suction submerged	1	759.2	790.9	715.4		
3rd suction submerged	1.5	759.5	791.1	715.6		
4th suction submerged	2	759.6				
etc.	2.5	759.7	791.3	715.8		
	3	759.7			758.7	718.9
	4				758.8	719.1
	5		791.6	715.9		
	6					
	7					
	8					
	9		791.9	716.2		
	12		792.0	716.3		
Scaled material		0.0	0.1	0.1	0.0	0.0
Before saturation by pressure		759.7	792.0	716.3	758.8	719.1
After 7d pressure at 50 bar		792.5	828.6	749.2	791.9	753.7
Change during 7d pressure		32.8	36.6	32.9	33.1	34.6
After 7d at 105 C		703.2	729.8	662.1	707.5	664.8
Change during 7d of drying		89.3	98.8	87.1	84.4	88.9
Volume [cm^3]		370.5	385.9	347.8	373.1	355.2

All values in [g] unless otherwise stated.

Mortar Air Entrained **Water stored / Cyclic Freeze-Thaw**	Sampl	5b	7a	6a	7b	8d (Epoxy)	9b (Epoxy)
Continued		No. of cycles					
		14	14	28	28	28	28
Stage :							
After Preparation at 20C/65RH		1026.6	1093.2	1049.5	1012.6		
Loss before re-saturation		1.2	1.1	1.1	1.2		
After preparation, before re-sat.		1025.4	1092.1	1048.4	1011.4	1063.2	979.1
After 3d re-saturation		1026.9	1093.9	1049.9	1012.8	1063.1	979.1
Suction during 3d re-saturation		1.5	1.8	1.5	1.4		
End of frost, incl. scaled material	*Hours*	1028.9	1095.4	1053.0	1014.8	1063.2	979.1
End of frost, excl. scaled mat.	0	1028.8	1095.3	1052.9	1014.7	1063.2	979.1
1rst suction, one surface	0.5	1028.1	1094.7	1052.5	1014.3		
2nd suction, one surface	1	1028.1	1094.7	1052.3	1014.2		
3rd suction, one surface	1.5	1028.1	1094.7	1052.3	1014.2		
4th suction, one surface	2	1028.1	1094.7	1052.3	1014.2		
Suction during frost		2.0	1.5	3.1	2.0		
Suction during frost [Vol.-%]		0.6	0.4	0.8	0.6		
Change during thawing		-0.7	-0.6	-0.6	-0.5		
Change during thawing [Vol.%]		-0.2	-0.2	-0.2	-0.1		
Stripped sample, before subm.	0	744.8	818.1	787.3	750.0	834.8	768.3
1rst suction submerged	0.5	745.9	819.1	788.9	751.2	835.4	768.7
2nd suction submerged	1	746.3	819.3	789.1	751.3	835.5	768.7
3rd suction submerged	1.5	746.4	819.4				
4th suction submerged	2						
etc.	2.5						
	3			789.4	751.7	835.7	768.9
	4						
	5						
	6						
	7						
	8						
	9	747.4	820.3	790.1	752.4	836.2	769.2
	12	747.5	820.4	790.2	752.6	836.3	769.3
Scaled material		0.1	0.2	0.1	0.1	0.0	0.0
Before saturation by pressure		747.5	820.4	790.2	752.6	836.3	769.3
After 7d pressure at 50 bar		779.1	846.0	824.0	782.2	864.6	810.2
Change during 7d pressure		31.6	25.6	33.8	29.6	28.3	40.9
After 7d at 105 C		690.4	761.2	729.8	697.0	781.3	715.8
Change during 7d of drying		88.7	84.8	94.2	85.2	83.3	94.4
Volume [cm^3]		362.5	391.9	384.3	362.6	408.5	381.0

All values in [g] unless otherwise stated.

Mortar Non Air Entrained **Standard curing /** **Isothermally frozen**	Sample	1c	2c	3c	4c	1d
	Frozen time [h]	0	3	7	12	24
Stage :						
After Preparation at 20C/65RH		1009.1	1029.5	1072.4	1065.0	1091.7
Loss before re-saturation		1.2	1.1	0.9	1.0	1.1
After preparation, before re-sat.		1007.9	1028.4	1071.5	1064.0	1090.6
After 3d re-saturation		1008.5	1029.3	1072.1	1064.7	1091.2
Suction during 3d re-saturation		0.6	0.9	0.6	0.7	0.6
End of frost, incl. scaled mat.	*Hours :*	1008.5	1029.6	1073.0	1065.9	1092.2
End of frost, excl. scaled mat.	0	1008.5	1029.6	1073.0	1065.9	1092.2
1rst suction, one surface	0.5	1008.5	1029.6	1072.7	1065.4	1091.9
2nd suction, one surface	1	1008.5	1029.6	1072.5	1065.2	1091.7
3rd suction, one surface	1.5	1008.5	1029.6	1072.5	1065.2	1091.7
4th suction, one surface	2	1008.5	1029.6	1072.5	1065.2	1091.6
Suction during frost		0.0	0.3	0.9	1.2	1.0
Suction during frost [Vol.-%]		0.0	0.1	0.2	0.3	0.3
Change during thawing		0.0	0.0	-0.5	-0.7	-0.6
Change during thawing [Vol.%]		0.0	0.0	-0.1	-0.2	-0.2
Stripped sample, before subm.	0	741.5	773.7	811.8	784.1	828.5
1rst suction submerged	0.5	743.9	775.9	814.6	786.8	830.9
2nd suction submerged	1	744.3	776.3	815.0	787.0	831.1
3rd suction submerged	1.5	744.6	776.5	815.2	787.2	
4th suction submerged	2	744.8	776.7	815.3		
etc.	2.5	744.8				
	3	744.9		815.7		
	4		777.2			831.8
	5			815.9		
	6					
	7					
	8		777.6		788.5	
	9					
	12		778.0	816.7		
Scaled material		0.0	0.0	0.0	0.0	0.0
Before saturation by pressure		744.9	778.0	816.7	788.5	831.8
After 7d pressure at 50 bar		762.9	797.0	837.1	809.9	847.4
Change during 7d pressure		18.0	19.0	20.4	21.4	15.6
After 7d at 105 C		694.2	724.0	760.4	734.3	775.1
Change during 7d of drying		68.7	73.0	76.7	75.6	72.3
Volume [cm^3]		340.3	354.4	375.3	364.2	382.0

All values in [g] unless otherwise stated.

Mortar Non Air Entrained	Sample	2d	3d	4d
Standard curing /				
Isothermally frozen				
Continued		Frozen time [h]		
		48	168	168
Stage :				
After Preparation at 20C/65RH		1093.5	1107.7	1090.2
Loss before re-saturation		1.0	1.0	1.0
After preparation, before re-sat.		1092.5	1106.7	1089.2
After 3d re-saturation		1093.3	1108.4	1090.5
Suction during 3d re-saturation		0.8	1.7	1.3
End of frost, incl. scaled mat.	*Hours*	1094.1	1108.4	1090.8
End of frost, excl. scaled mat.	0	1094.1	1108.4	1090.8
1rst suction, one surface	0.5	1093.8	1108.2	1090.5
2nd suction, one surface	1	1093.6	1108.0	1090.4
3rd suction, one surface	1.5	1093.6	1108.0	1090.4
4th suction, one surface	2	1093.6	1108.0	1090.4
Suction during frost		0.8	0.0	0.3
Suction during frost [Vol.-%]		0.2	0.0	0.1
Change during thawing		-0.5	-0.4	-0.4
Change during thawing [Vol.%]		-0.1	-0.1	-0.1
Stripped sample, before subm.	0	826.6	841.6	828.6
1rst suction submerged	0.5	828.5	843.3	830.8
2nd suction submerged	1	828.7	843.7	831.4
3rd suction submerged	1.5	828.9		
4th suction submerged	2		844.0	831.7
etc.	2.5			
	3		844.3	832.0
	4			
	5		844.5	832.3
	6			
	7	829.8		
	8			
	9		844.7	832.6
	12		844.9	832.8
Scaled material		0.0	0.0	0.0
Before saturation by pressure		829.8	844.9	832.8
After 7d pressure at 50 bar		847.3	862.2	849.6
Change during 7d pressure		17.5	17.3	16.8
After 7d at 105 C		773.6	786.9	775.4
Change during 7d of drying		73.7	75.3	74.2
Volume [cm^3]		380.0	389.0	381.0

All values in [g] unless otherwise stated.

Mortar Non Air Entrained Water stored / Isothermally frozen	Sample	1a	2a	3a	4a	1b
		Frozen time [h]				
Stage :		0	3	7	12	24
After Preparation at 20C/65RH		1120.2	1114.4	1066.6	1111.0	1052.3
Loss before re-saturation		1.2	1.3	1.4	1.3	1.2
After preparation, before re-sat.		1119.0	1113.1	1065.2	1109.7	1051.1
After 3d re-saturation		1119.5	1113.6	1066.0	1110.9	1052.1
Suction during 3d re-saturation		0.5	0.5	0.8	1.2	1.0
End of frost, incl. scaled material	*Hours :*	1119.5	1114.2	1067.0	1112.1	1052.2
End of frost, excl. scaled mat.	0	1119.5	1114.2	1067.0	1112.1	1052.2
1rst suction, one surface	0.5	1119.5	1114.2	1066.6	1111.4	1051.9
2nd suction, one surface	1	1119.5	1114.2	1066.5	1111.2	1051.8
3rd suction, one surface	1.5	1119.5	1114.2	1066.5	1111.2	1051.7
4th suction, one surface	2	1119.5	1114.2	1066.5	1111.2	1051.7
Suction during frost		0.0	0.6	1.0	1.2	0.1
Suction during frost [Vol.-%]		0.0	0.2	0.3	0.3	0.0
Change during thawing		0.0	0.0	-0.5	-0.9	-0.5
Change during thawing [Vol.%]		0.0	0.0	-0.1	-0.2	-0.1
Stripped sample, before subm.	0	859.0	849.8	801.6	842.5	791.8
1rst suction submerged	0.5	861.4	851.9	803.3	844.4	793.7
2nd suction submerged	1	861.7	852.1	803.5	844.6	794.0
3rd suction submerged	1.5	862.0	852.4	803.7	844.9	
4th suction submerged	2	862.1	852.5	803.8		
etc.	2.5	862.1		803.9		
	3	862.1				
	4		852.9			794.4
	5			804.2		
	6					
	7					
	8		853.3		845.9	
	9					
	12		853.6	804.8		
Scaled material		0.0	0.0	0.0	0.0	0.0
Before saturation by pressure		862.1	853.6	804.8	845.9	794.4
After 7d pressure at 50 bar		879.6	872.4	822.4	862.5	810.0
Change during 7d pressure		17.5	18.8	17.6	16.6	15.6
After 7d at 105 C		796.2	787.9	742.7	780.9	734.7
Change during 7d of drying		83.4	84.5	79.7	81.6	75.3
After 2nd sat. for 7d at 50 bar		881.0	865.4	815.6	858.6	814.3
Volume [cm^3]		395.8	392.3	369.0	388.8	365.9

All values in [g] unless otherwise stated.

Mortar Non Air Entrained	Sample	2b	3b	4b	8a	8b
Water stored / Isothermally frozen					(Epoxy)	(Epoxy)
Continued	Frozen time [h]					
		48	168	168	168	168
Stage :						
After Preparation at 20C/65RH		1069.3	1040.4	1032.2		
Loss before re-saturation		1.0	1.1	1.1		
After preparation, before re-sat.		1068.3	1039.3	1031.1	1094.6	1039.4
After 3d re-saturation		1069.9	1040.4	1032.7	1094.6	1039.3
Suction during 3d re-saturation		1.6	1.1	1.6		
End of frost, incl. scaled material	*Hours :*	1070.1	1040.6	1033.2	1094.7	1039.4
End of frost, excl. scaled mat.	0	1070.1	1040.6	1033.2	1094.7	1039.4
1rst suction, one surface	0.5	1069.7	1040.2	1032.8		
2nd suction, one surface	1	1069.5	1040.1	1032.6		
3rd suction, one surface	1.5	1069.5	1040.1	1032.6		
4th suction, one surface	2	1069.5	1040.1	1032.6		
Suction during frost		0.2	0.2	0.5		
Suction during frost [Vol.-%]		0.1	0.1	0.1		
Change during thawing		-0.6	-0.5	-0.6		
Change during thawing [Vol.%]		-0.2	-0.1	-0.2		
Stripped sample, before subm.	0	811.6	779.5	775.1	815.7	816.8
1rst suction submerged	0.5	812.3	780.7	775.8	816.3	817.4
2nd suction submerged	1	812.5	781.1	776.1	816.4	817.5
3rd suction submerged	1.5	812.6				
4th suction submerged	2		781.3	776.2	816.5	817.7
etc.	2.5					
	3		781.4	776.4	816.6	817.8
	4				816.7	817.8
	5		781.7	776.6		
	6				816.9	818.0
	7	813.2				
	8					
	9		781.8	776.8		
	12		781.9	776.9	817.1	818.2
Scaled material		0.0	0.0	0.0	0.0	0.0
Before saturation by pressure		813.2	781.9	776.9	817.1	818.2
After 7d pressure at 50 bar		829.3	802.0	795.0	837.0	838.7
Change during 7d pressure		16.1	20.1	18.1	19.9	20.5
After 7d at 105 C		751.2	722.2	717.0	755.0	757.1
Change during 7d of drying		78.1	79.8	78.0	82.0	81.6
Volume [cm^3]		367.0	358.8	355.4	393.9	390.9

All values in [g] unless otherwise stated.

Mortar Non Air Entrained Standard Curing / Freeze-Thaw	Sample	1c	5c	6d	8c
		(Isoth.)			(Epoxy)
		No. of freeze-thaw cycles			
Stage :		0	7	7	7
After Preparation at 20C/65RH		1009.1	1098.8	1070.2	
Loss before re-saturation		1.2	1.0	1.0	
After preparation, before re-sat.		1007.9	1097.8	1069.2	1033.9
After 3d re-saturation		1008.5	1099.1	1070.8	1033.8
Suction during 3d re-saturation		0.6	1.3	1.6	
End of frost, incl. scaled material	*Hours*	1008.5	1099.9	1071.8	1033.9
End of frost, excl. scaled mat.	0	1008.5	1099.6	1071.4	1033.9
1rst suction, one surface	0.5	1008.5	1099.3	1070.7	
2nd suction, one surface	1	1008.5	1099.1	1070.6	
3rd suction, one surface	1.5	1008.5	1099.1	1070.6	
4th suction, one surface	2	1008.5	1099.1	1070.6	
Suction during frost		0.0	0.8	1.0	
Suction during frost [Vol.-%]		0.0	0.2	0.3	
Change during thawing		0.0	-0.5	-0.8	
Change during thawing [Vol.%]		0.0	-0.1	-0.2	
Stripped sample, before subm.	0	741.5	821.9	804.1	819.1
1rst suction submerged	0.5	743.9	825.0	806.0	
2nd suction submerged	1	744.3	825.5	806.4	
3rd suction submerged	1.5	744.6	825.8	806.5	
4th suction submerged	2	744.8			
etc.	2.5	744.8	826.1	806.7	
	3	744.9			820.0
	4				820.0
	5		826.4	807.0	
	6				
	7				
	8				
	9		826.8	807.3	
	12		827.0	807.4	
Scaled material		0.0	0.3	0.4	0.0
Before saturation by pressure		744.9	827.0	807.4	820.0
After 7d pressure at 50 bar		762.9	847.9	826.9	839.6
Change during 7d pressure		18.0	20.9	19.5	19.6
After 7d at 105 C		694.2	768.8	752.0	761.7
Change during 7d of drying		68.7	79.1	74.9	77.9
Volume [cm^3]		340.3	381.8	368.5	383.9

All values in [g] unless otherwise stated.

Mortar Non Air Entrained Standard Curing / Freeze-Thaw	Sample	5d	7c	6c	7d	8d (Epoxy)
Continued		No. of freeze-thaw cycles				
		14	14	28	28	28
Stage :						
After Preparation at 20C/65RH		1038.2	1074.9	1053.1	1061.5	
Loss before re-saturation		0.9	1.0	1.0	1.0	
After preparation, before re-sat.		1037.3	1073.9	1052.1	1060.5	1047.4
After 3d re-saturation		1038.7	1075.3	1053.6	1062.1	1047.3
Suction during 3d re-saturation		1.4	1.4	1.5	1.6	
End of frost, incl. scaled material	*Hours*	1040.2	1076.7	1060.1	1065.1	1047.3
End of frost, excl. scaled mat.	0	1039.8	1076.1	1059.6	1063.4	1047.3
1rst suction, one surface	0.5	1039.3	1075.3	1059.0	1062.0	
2nd suction, one surface	1	1039.4	1075.5	1058.8	1061.9	
3rd suction, one surface	1.5	1039.3	1075.4	1058.8	1061.8	
4th suction, one surface	2	1039.3	1075.4	1058.8	1061.8	
Suction during frost		1.5	1.4	6.5	3.0	
Suction during frost [Vol.-%]		0.4	0.4	1.8	0.8	
Change during thawing		-0.5	-0.7	-0.8	-1.6	
Change during thawing [Vol.%]		-0.1	-0.2	-0.2	-0.4	
Stripped sample, before subm.	0	770.3	822.3	801.5	802.7	824.2
1rst suction submerged	0.5	772.2	825.0	802.3	805.0	824.4
2nd suction submerged	1	772.4	825.3	802.3	805.1	824.5
3rd suction submerged	1.5	772.5	825.5			
4th suction submerged	2					
etc.	2.5					
	3			802.5	805.6	824.7
	4					
	5					
	6					
	7					
	8					
	9	773.6	826.8	802.9	806.3	824.9
	12	773.8	827.0	803.0	806.5	825.0
Scaled material		0.4	0.6	0.6	1.7	0.0
Before saturation by pressure		773.8	827.0	803.0	806.5	825.0
After 7d pressure at 50 bar		788.1	848.8	820.4	823.5	840.5
Change during 7d pressure		14.3	21.8	17.4	17.0	15.5
After 7d at 105 C		720.5	768.8	745.8	751.5	769.2
Change during 7d of drying		67.6	80.0	74.6	72.0	71.3
Volume [cm^3]		351.1	381.1	367.3	369.6	387.3

All values in [g] unless otherwise stated.

Mortar Non Air Entrained	Sample	1a	5a	6b	8c
Water stored / Freeze-Thaw		(Isoth.)			(Epoxy)
		No. of freeze-thaw cycles			
Stage :		0	7	7	7
After Preparation at 20C/65RH		1120.2	1102.4	1103.5	
Loss before re-saturation		1.2	1.1	1.0	
After preparation, before re-sat.		1119.0	1101.3	1102.5	1033.9
After 3d re-saturation		1119.5	1103.2	1104.1	1033.8
Suction during 3d re-saturation		0.5	1.9	1.6	
End of frost, incl. scaled material	*Hours*	1119.5	1105.1	1105.4	1033.9
End of frost, excl. scaled mat.	0	1119.5	1105.0	1105.0	1033.9
1rst suction, one surface	0.5	1119.5	1104.5	1104.3	
2nd suction, one surface	1	1119.5	1104.4	1104.3	
3rd suction, one surface	1.5	1119.5	1104.4	1104.3	
4th suction, one surface	2	1119.5	1104.4	1104.3	
Suction during frost		0.0	1.9	1.3	
Suction during frost [Vol.-%]		0.0	0.5	0.3	
Change during thawing		0.0	-0.6	-0.7	
Change during thawing [Vol.%]		0.0	-0.2	-0.2	
Stripped sample, before subm.	0	859.0	827.4	843.4	819.1
1rst suction submerged	0.5	861.4	828.4	844.0	
2nd suction submerged	1	861.7	828.7	844.3	
3rd suction submerged	1.5	862.0	829.1	844.5	
4th suction submerged	2	862.1			
etc.	2.5	862.1	829.0	844.6	
	3	862.1			820.0
	4				820.0
	5		829.1	844.8	
	6				
	7				
	8				
	9		829.3	844.9	
	12		829.4	845.0	
Scaled material		0.0	0.1	0.4	0.0
Before saturation by pressure		862.1	829.4	845.0	820.0
After 7d pressure at 50 bar		879.6	844.2	865.5	839.6
Change during 7d pressure		17.5	14.8	20.5	19.6
After 7d at 105 C		796.2	764.4	779.8	761.7
Change during 7d of drying		83.4	79.8	85.7	77.9
After 2nd sat. for 7d at 50 bar		881.0	846.5	863.4	840.0
Volume [cm^3]		395.8	379.2	385.1	383.9

All values in [g] unless otherwise stated.

Mortar Non Air Entrained	Sample	5b	7a	6a	7b	8d
Water stored / Freeze-Thaw						(Epoxy)
Continued		No. of freeze-thaw cycles				
		14	14	28	28	28
Stage :						
After Preparation at 20C/65RH		1069.0	1103.9	1076.4	1050.0	
Loss before re-saturation		1.0	1.1	1.2	1.2	
After preparation, before re-sat.		1068.0	1102.8	1075.2	1048.8	1047.4
After 3d re-saturation		1071.0	1103.9	1076.6	1050.2	1047.3
Suction during 3d re-saturation		3.0	1.1	1.4	1.4	
End of frost, incl. scaled material	*Hours*	1074.4	1105.5	1080.3	1051.8	1047.3
End of frost, excl. scaled mat.	0	1073.9	1105.2	1079.9	1051.1	1047.3
1rst suction, one surface	0.5	1073.0	1104.3	1079.3	1050.4	
2nd suction, one surface	1	1073.1	1104.4	1079.1	1050.3	
3rd suction, one surface	1.5	1073.1	1104.4	1079.0	1050.3	
4th suction, one surface	2	1073.1	1104.4	1079.0	1050.3	
Suction during frost		3.4	1.6	3.7	1.6	
Suction during frost [Vol.-%]		0.9	0.4	1.0	0.4	
Change during thawing		-0.8	-0.8	-0.9	-0.8	
Change during thawing [Vol.%]		-0.2	-0.2	-0.2	-0.2	
Stripped sample, before subm.	0	797.3	846.2	806.9	788.8	824.2
1rst suction submerged	0.5	797.3	847.9	807.7	789.9	824.4
2nd suction submerged	1	797.3	848.1	807.8	789.9	824.5
3rd suction submerged	1.5	797.2	848.3	808.1	790.2	
4th suction submerged	2					
etc.	2.5					
	3					824.7
	4					
	5					
	6					
	7					
	8					
	9	797.5	849.1	808.5	790.8	824.9
	12	797.6	849.2	808.6	790.9	825.0
Scaled material		0.5	0.5	0.4	0.7	0.0
Before saturation by pressure		797.6	849.2	808.6	790.9	825.0
After 7d pressure at 50 bar		814.9	866.4	823.7	806.6	840.5
Change during 7d pressure		17.3	17.2	15.1	15.7	15.5
After 7d at 105 C		735.2	783.7	746.2	731.4	769.2
Change during 7d of drying		79.7	82.7	77.5	75.2	71.3
Volume [cm^3]		360.5	387.1	371.4	362.1	387.3

All values in [g] unless otherwise stated.

URN:NBN:no-6354

APPENDIX H

Fresh concrete air void characteristics.
Brief description of the test method.

URN:NBN:no-6354

1. Introduction and references

The air void structure is a critical parameter for the durability of concrete subjected to saturation and freeze-thaw exposure. The determination of the parameters of the air void system is traditionally carried out on hardened concrete in accordance with ASTM C457 or similar guidelines.

The traditional procedures based on preparation of and measurements on hardened concrete may delay the quality assurance of produced concrete several days, i.e. until after it has been placed in the structure. When the test results are available, it is normally considered not appropriate to reject the concrete, since it would imply a complete renewal of the structural element.

A new testing procedure was developed about a decade ago, allowing the assessment of the air void structure on samples of the fresh concrete. The principles have been reported by Henrichsen [H 1995] and Lens [L 1995]. The testing method has been applied for larger quality assurance works [G 1995]. A limited survey of the method was reported in German research reports, referred to by Siebel [S 1995b], and was concluded to have acceptable correlation to ASTM C457. A comprehensive correlation study was carried out and reported by the developer of the test method [D 1996]. The following test description is based on these works, other material provided by the manufacturer and the experience of the present author.

2. Principle of testing method

It has been documented that air voids of a cement paste under certain conditions may be transferred to a liquid without affecting the quantity and sizes of the air voids. A successful transfer depends on the viscosity and hydrophilic character of the liquid. As soon as air bubbles are released from the cement paste, they will start to rise through the liquid. The larger bubbles rise faster than the small ones. A complete distribution of the air void structure may be calculated based on recordings of the volume of air that has risen to a given level related to the time elapsed, i.e. a buoyancy versus time recording, see figure H-1.

3. About the procedure

A mortar sample is extracted by a syringe from the (properly compacted) concrete through a wire basket, gently vibrated into the concrete. The basket allows a maximum aggregate size of 6 mm in the 20 cm^3 sample.

The sample is transferred to the column (figure H-2), containing a certain amount of liquid of specific viscosity and above that, water. A certain temperature range is prescribed, and a heating device is included in the base plate. The transfer of the air voids from the mortar/cement paste is promoted by automatic stirring. The air voids rise through the riser column and are collected under a submerged petri dish. A digital scale records the buoyancy of the submerged bowl, and the recordings are transferred to a computer. If properly prepared, the complete procedure takes about 30 minutes from the time of sample extraction.

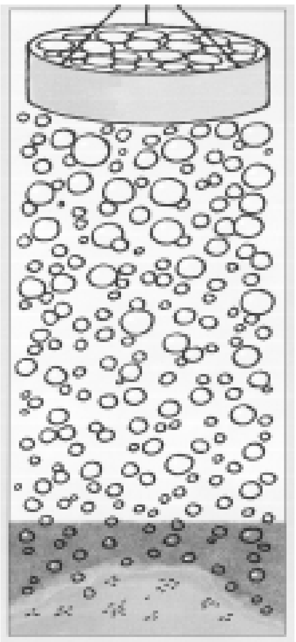

Figure H-1 : The buoyancy principle of the testing method. The lower part, the transfer zone (transfer of air voids from the cement paste into the liquid) also constitutes the zone where the sample is introduced into the column. The transfer zone contains a liquid of specific viscosity, allowing the transfer to take place properly within the temperature range prescribed. From leaflet provided by the manufacturer.

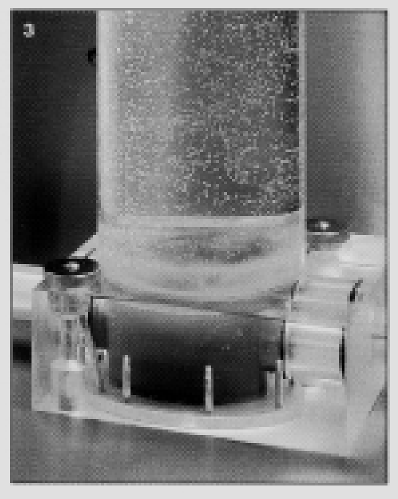

Figure H-2 : Lower part of riser column, containing sample with arising air bubbles, liquid of specific viscosity and de-aerated or distilled water. There is a heating device in the base plate. From leaflet provided by the manufacturer.

Figure H-3 : Complete equipment. From leaflet provided by the manufacturer.

4. Computation and output

According to the modelled correlation, the buoyancy versus time lapse is transferred to a pore size distribution curve by the computer programme. These data are used to compute the air void characteristics.

Prior to running the test, data on cement paste content and the (mortar) fraction below 6 mm of the total volume are necessary input values. Among the output values are :

- Air void spacing factor $\overline{L}$ [mm] (i.e. the half of the mean distance between the air voids).
- Specific air void surface area α [mm^{-1}] (i.e. air void surface per air void volume).

For information, the total air void content of the sample is also reported. However contrary to the parameters above, this value may easily be affected by the handling process, introducing coarse and false air into the system. It should be used for procedure documentation only, not material characterising. It is the experience of the present author that this precaution is often neglected.

5. Limitations and accuracy

Similarly to the ASTM C457 (often not considered), the test procedure has some limitation in the sense of parameter or measurement range. From 2 % air void level and below, the large air voids normally dominate, the number of small air voids collected decrease, and the accuracy of the values is poor. The poor accuracy in such cases is of no direct relevance, since the air void characteristics cases are so poor that the air void system should be considered inappropriate. A warning is automatically given in the report.

In the opposite end, the “sampling” of air voids will automatically terminate after approximately 20 minutes, even if (as always) small air bubbles still are arising. This will artificially increase the $\overline{L}$ and decrease the α. However, the non-assessed air voids are so small (< 20-30 μ) that they will easily become filled with deposits and not act according to the intention. If the lower pore size assessed on hardened concrete is lower (e.g. 7 μ), this may cause a “deviation” between the two procedures, the DBT method producing “poorer” values. However, the latter probably is more relevant.

When questioning or comparing the correlation between the DBT method and the ASTM C457 on hardened concrete, it should be kept in mind that the number of air voids assessed in the former is much higher than that of the latter. The "correlation" can never be better than the accuracy of the inferior method. Geiker et al [G 1995] refer to +/- 5-10 % on the absolute values of the spacing factor and the specific surface area as accuracy level of the DBT-method. The 95 % confidence limits between the two methods for the two parameters have been reported [D 1996].

APPENDIX I

Chemical Shrinkage Test Method : Pilot Study on the Effect of Sample Thickness and Some Potential Errors.

List of Contents

1. Objectives

The original objective of this study was to study the effect of sample size as a potential source of errors in the main study, the latter comparing cement paste and mortar.

However, as it turned out the pilot study provided no good information on the issue due to erroneous test results. For reasons given in section 4.1 below, it was still decided to include the study in the present publication as an appendix. The potential sources of errors revealed in this study are included in section 6.2 of the main part of the publication.

2 Programme and details

A cement paste of w/c-ratio 0.48 was mixed with the same mixing equipment as used in the main series (See Section 6.3 for details). Six samples with mass ranging from 45 g to 240 g were chosen. This would not provide a good statistical evaluation (linear correlation could not be assumed). However, with the reproducibility expected [J 1994], this alternative was believed to provide at least as much practical information – in term of finding the appropriate thickness for obtaining accurate results.

3 Casting and plugging

With the corresponding specimen thickness of approximately 4 mm to 22 mm, samples were deposited into Erlenmeyer flasks of 250 ml nominal capacity. The consistency of cement pastes with the w/c-ratio in question is very fluid (separation is a risk !), and the flasks were very carefully filled up with distilled water (section 6.2.1) to assure as little disturbance of the sample surface as possible.

Stoppers of silicon (in stead of rubber) were chosen to reduce the danger of slippage. Subsequent to plugging the flasks, they were placed in a water bath at 20 ^{o}C to maintain a stable and equal temperature for the combined sample and recipient. The water level of the surrounding water bath reached to the middle of the “neck” of the flasks. The relevance of this measure was to keep eventually emerging air bubbles within the temperature controlled level. Such air bubbles might result from escaping air from the samples if air voids in the samples become water filled. They might then accumulate underneath the stoppers (“missing” the opening of the pipette) and should not be subjected to the larger temperature variation of the ambient conditions (the surrounding air temperature is normally subject to larger fluctuations than the water bath).

The upper end of the pipettes was protected against water evaporation by a plastic bag. The plastic bag accommodated only a small amount of air - to prevent vacuum in the pipette - and was fixed by a rubber band. However, the pipette might require re-filling during the testing period, which is why a paraffin droplet was not chosen for evaporation protection. A needle or a steel wire may be convenient to assist the re-fill water to pass by the upper neck of the pipette. The adding of water into the pipette through a thin tube under light pressure will also facilitate the operation. Overfilling of the pipettes must be avoided : Attempts to empty an overfilled pipette will introduce air into the system.

4 Test results and discussion.

4.1 General

The results of the chemical shrinkage test are illustrated in figure AI-1.

However, before discussing the results, it would be appropriate at this stage to make a warning : Due to failure to take a number of precautions, the pilot study failed in the sense of producing reliable results. For this reason, it was considered to skip the results entirely in the present publication. However, it was decided to include the results in the appendix of this publication because :

- reporting failures of this methodology (Erlenmeyer flask) have not previously been reported, at least to the knowledge of the present author
- together with the list of the potential sources of errors in section 6.2, this may constitute a useful guide for performing such a test method
- illustrating the use of time-differentiated analyses in the context of a) searching for failures and b) analysing test results may provide a useful tip
- the working/examination process of the present study should be documented
- incorporating and illustrating the use of calculated degree of saturation (section 5.2 of this appendix) as a checkpoint for the measurements may still be useful

The first reading was made one hour after water addition to the mix. The time scale of all figures starts with the time of water addition.

In figure AI-2, the same results are given as non-evaporable water in [g per 100 g cement]. The reason for presenting the test results as non-evaporable water, is the subsequent comparison with loss on ignition values. The values were transformed, based on the following relations to be found in any cement and concrete technology book, e.g. as outlined by Neville [N 1995] :

$$\begin{aligned} \varepsilon_c &= 0.254 \times W_n \\ W_n &= \varepsilon_c / 0.254 \end{aligned} \qquad \text{(Eq. AI-1)}$$

where :

ε_c : contraction pore volume (the shrinkage measured, in the present work calculated as ml per 100 g cement)

W_n : non-evaporable, i.e. chemically bound water (also calculated as ml per 100 g cement)

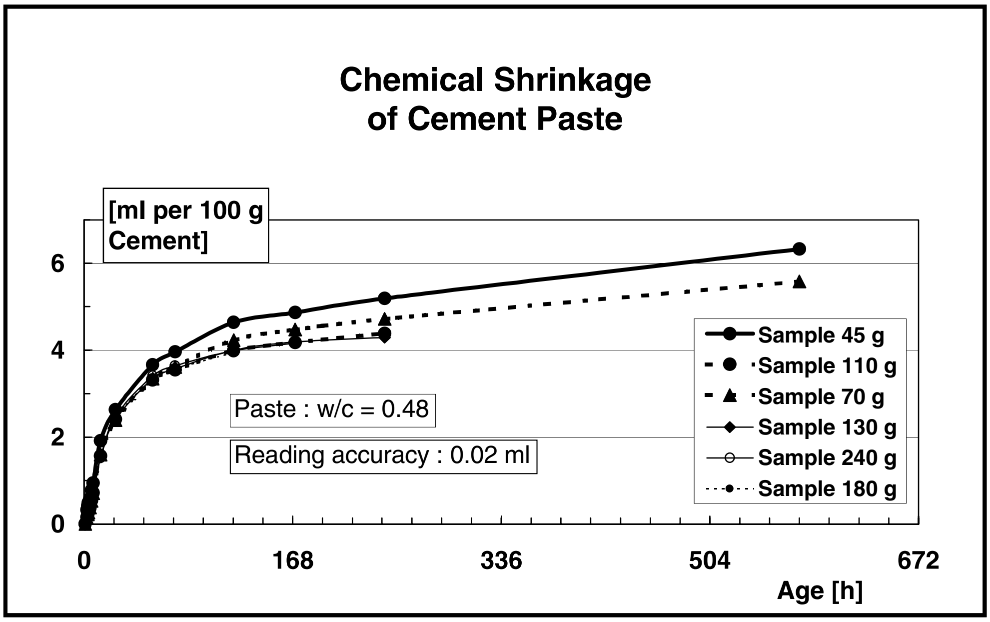

Figure AI-1: Chemical shrinkage, calculated per 100 g cement : Measured value is divided by the sample size, corrected for the initial cement content (67.6 %) and multiplied by 100. The test was terminated at 24 days, see text. Since the sample sizes in the legend box are not regularly increasing, it may be appropriate to confirm that the legends given are correct.

Accuracy relating to reading of the pipette (0.02 ml) and the time frame in question (for differentiated values) is indicated in the individual figures. Since the pilot study is mainly presented as a background, no data in tabular form are presented.

There are two striking features in figure AI-1 : Firstly, there appears to be a distinct effect of the sample size, even between the two smaller samples. Secondly, the smallest sample appears to continuously increase its amount of bound water beyond the value of 6 ml per 100 g cement. Calculated as chemically bound water, this would correspond to 25 g per 100 g of cement (Eq. AI-2 and figure AI-2), i.e. beyond or too close to the limit value of 23-26 % suggested by several authors [S 1992]. Additionally, the activity versus time tends to differ somewhat between the samples, and some samples “aborted”. The test was terminated at 24 days due to reasons mentioned later. These phenomena will be dealt with in consecutive order :

4.2 Apparent effect on the level of non-evaporable water

In the figures AI-3 - 4, the same results are differentiated with respect to time. Note the different scales of the vertical axes, facilitating between-sample comparison within the time frame of interest.

By comparing the early, numerical values (not included in the present report) of the chemical shrinkage, it became evident that the “activity” of the 45 g sample was not realistic. By comparing the level of all the samples after the first two hours, it was believed that the level of this sample is 0.8 g [non-evaporable water per 100 g cement] too high. All the remaining samples were very close to each other at this stage. This is also illustrated in figure AI-3 with an abnormal activity of this sample. The implication is that the total chemical shrinkage curve (figure AI-1) for the 45 g sample lies 0.2 ml too high.

The most immediate explanation is that the silicon stopper had been subjected to improper forces when plugging the flask – causing a sliding movement and trigging a “false” under-pressure in the flask in the initial phase of the experiment. The case illustrates the benefit of parallel samples.

As mentioned, the patterns of the remaining samples during the first hours are very close to each other. However, after a few hours there appears to be a significant and systematic influence of the sample size. This phenomenon is further discussed in subsequent sections.

4.3 Apparent effect on the absolute level of shrinkage

The initial deviation means that the absolute level measured for the 45 g sample should be corrected to about 24 g per 100 g cement. This is still too much. Also, the apparent linearly and continuously increasing level towards the end of the test indicates suction of water into some voids or cavities of the 45 g sample. Around the age of seven days, the apparent shrinkage vs. time drops to a level that is kept constant throughout the remaining testing period.

In contrast, the hydration activity at isothermal conditions is expected to continuously decline towards the age of four weeks. In [G 1983] this is illustrated by a linear development of the chemical shrinkage test, plotted on a *logarithmic* time scale. Consequently, there appears to be a deviation between water consumption in the test and actual degree of hydration.

Hence, the measurements should be supplemented with loss on ignition if the objective is to estimate the degree of hydration. See subsequent sections for further discussion on the issue.

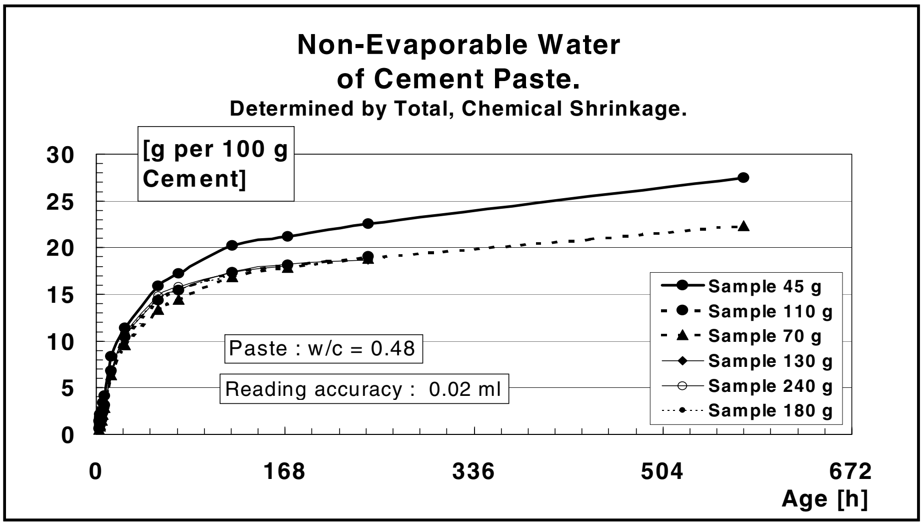

Figure AI-2 : Non-evaporable water, calculated as described in the text and expressed as ml per 100 g cement, independent of sample size. As in figure AI-1, the legends given are correct.

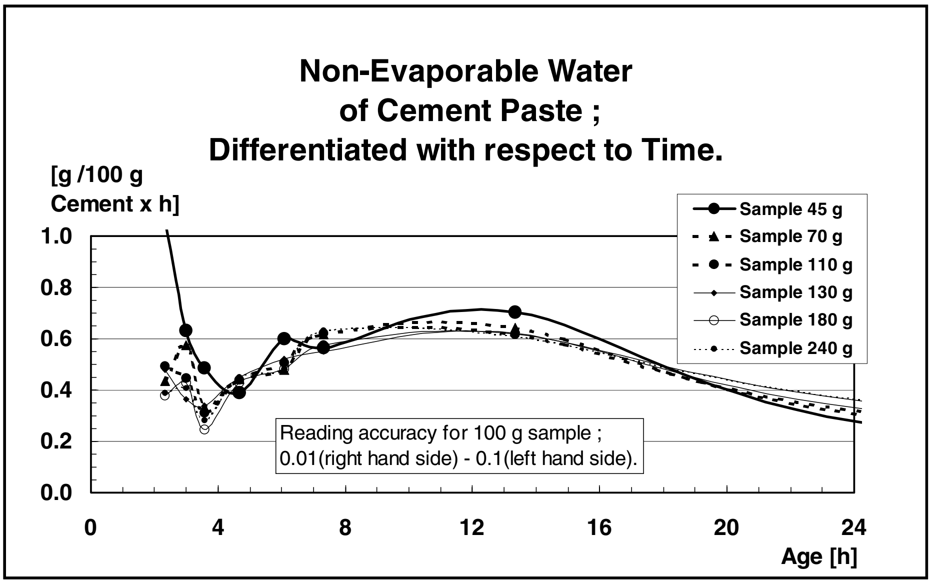

Figure AI-3 : Differentiation of figure AI-2 with respect to time – the initial 24 hours.

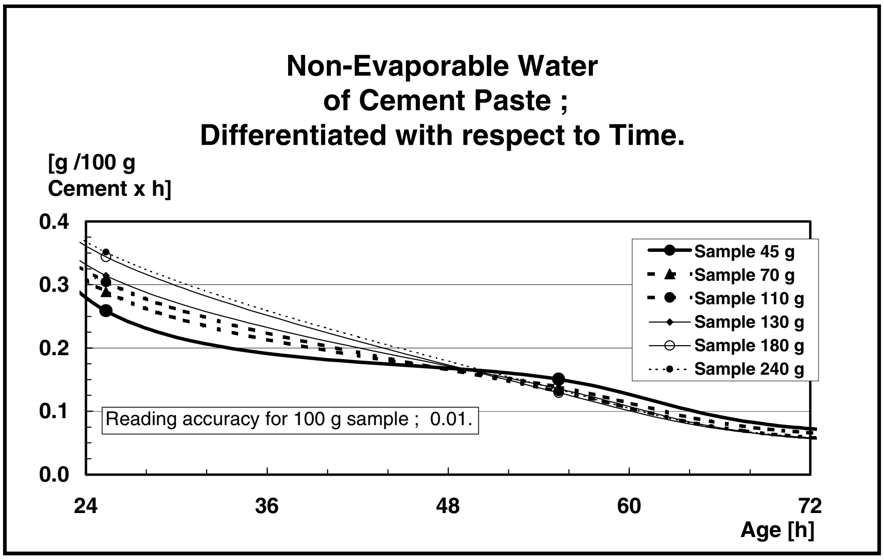

Figure AI-4 : Differentiation of figure AI-2 with respect to time – age 24 to 72 hours.

4.4 Aborted samples

After a while, some samples exhibited a sudden increase in apparent shrinkage activity, beyond the point of reading of the pipette. The samples were left - as normally - in the water storage container, and the reason remained unclear until after termination of all the series.

Separating the samples from the Erlenmeyer flasks, it became evident that the flasks of the samples that “broke down” actually had cracked. Upon doing so, the water column in the pipette disappeared. The hydraulic equilibrium with the surrounding water storage bath was established. When this happened, the defects of the flasks were on a very small scale ; only very small cracks in the bottom could be detected, which is why they initially were not noticed. Being left in the water storage until completion of the test, the cracks developed extensively.

The phenomenon happened in consecutive order for the samples of 17 mm thickness (at the age of 6-7 days), 22 mm (age 7-8 days), 13 mm (age 13 days) and 10 mm (age 23 days). It seems reasonable to assume that the cause of these incidents is the swelling forces of the cement paste, as the finally divided gel structure absorbs water. This is commonly seen as expansion in water stored concrete.

The most obvious lesson from the study at this point is to limit the thickness of the sample. A possible, different approach could be to use recipients of a material of somewhat lower stiffness. However, the swelling would cause a deformation of the recipient, again causing an erroneous reading of the pipette. At least theoretically, this error could be compensated for by weighing the system, comparing the weight change and change in reading.

Another alternative could be to cast parallel samples for water storage. Stepwise recording of the weight changes after de-moulding could provide data on chemical shrinkage after the initial stage (16 – 24 h) in an easy way.

4.5 Deviation in shrinkage versus time between the samples

Another striking feature becomes evident when analysing the change of intensity between the samples versus time. No statistical data are provided, but there seems to be a very systematic change in activity over the time range covered, depending on the sample size (figures AI-2 - 4). The sample thickness seems to affect the kinetics of the water absorption process, i.e. the apparent chemical shrinkage.

At the time of execution of this study, an extensive discussion was prepared to explain the observed phenomenon. However, at a later stage certain features became evident, leading to abandonment of these ideas. Hence, the discussion on this issue will be closed at this point and focus changed to the degree of hydration. Still before closing the issue, it should be mentioned that very recent publication [P 1999] made after the completion of the present study confirms an effect of the sample size on the rate of chemical shrinkage, due to incomplete water suction.

5 Degree of hydration

5.1 Investigation of the samples

In order to confirm or invalidate the former results concerning sample size effects on the reaction, it was decided to measure the loss on ignition. At this time, four out of six samples were in cracked flasks, which remained stored under water. Because of the water supply via the lateral and bottom cracks, these samples might partly have caught up with the intact ones. In order not to let this "catching-up" process go on longer than necessary – and not to "loose" the two last ones still intact, the latter were interrupted at 28 days to perform the ignition test. 24 days remained the last reading of chemical shrinkage.

Of course, the possible "catching-up" effect caused some restriction on the interpretation of the ignition test : If no effect was found, no conclusion could be drawn. In the opposite case, it would be an indication supporting a dimensional effect.

Four of the samples were stripped at the age of 28 days. They were quickly crushed and dried for seven days at 105 ^{o}C. Approximately 18 g of each sample was then ignited at 975 ^{o}C for approximately 20 hours. The results are given in table AI-1. The differences are just at the border of the accuracy level [K 2000] and may not be significant : The loss on ignition decreases very slightly with increasing sample thickness above 6 mm.

The most striking result, however, is the large deviation between the loss on ignition in table AI-1 (row number three) and figure AI-2. It becomes evident that the water consumption is much too high. As already mentioned, it may be appropriate to remind that the results of the chemical shrinkage test are not correct – prior to the continued and following discussion :

Sample size **[mm thickness] / [g]**	4 / 45	6 / 70	10 / 110	12 / 130
Loss on ignition (L.o.i.) **[% of ignited weight]**	17.77	17.79	17.67	17.42
L.o.i. corrected for L.o.i. of the cement (2,51%)[1) [% of ign.weight]	15.20	15.21	15.10	14.85
Apparent degree of hydration (L.o.i/0,23) (See Eq. 6.2.5) [%]	66.1	66.1	65.7	64.6

Table AI-1 : Loss on ignition of samples subjected to chemical shrinkage measurements / effects of specimen thickness. The relatively high L.o.i. of the cement is due to the CEM I 42.5-R containing 4 % lime stone. Some carbonation of the hydration products may also slightly have increased the average ignition loss. The values are not directly comparable to the determination of chemical shrinkage because the last reading of the latter was performed at least four days (depends on time of breakdown) prior to start of the drying procedure.1)L.o.i. of 2.51 % amounts to 2.51/(100-2.51) = 2.57 % of ignited weight.

5.2 Further considerations

A reduced degree of hydration caused by sample size must most likely be controlled by a shortage of water availability. It is well known that hydration will cease at some degree of relative humidity (RH) (70-80 % RH). Hence, the question arises whether the moisture conditions of the actual samples could be decisive in this respect.

Sellevold et al [S 1988] indicated “almost stable RH-levels”, i.e. implying very low hydration activity, above 90 % RH for samples with w/c-ratio of 0,60 and long term storage. Other researchers report lower levels for this apparent, stable RH level. The level is reduced when lowering the w/c-ratio. Persson [P 1999] indicate that RH of 95 % and 90 % may be achieved at a degree of saturation of 90 % and 85 %, respectively.

Substantiating a specimen thickness effect on degree of hydration, the measurements of the relative humidity within the samples would be useful. However, this parameter is difficult to obtain. If the degree of saturation could be estimated, the relation reported by Persson might provide an indirect tool of confirming or invalidating the effect.

The first step in this approach is to derive a formula for the degree of saturation, for which the actual water content (initial + externally supplied water) and the degree of hydration provide the input data :

a) Derivation of a formula :

At first, an expression for the degree of saturation may be derived, using the subsequent designation ;

W_0 : Initial water content, i.e. $W_e + W_n$. [kg]
W_n : Non-evaporable water [kg]
W_e : Evaporable water [kg]
W_{Ex} : Externally supplied water (after mixing and casting)
α : Degree of hydration [relative number]
C : Cement content [kg]
ρ_c : Density of cement [kg/dm^3] (= 3.12 in the actual case)
w/c : Water/cement-ratio [Dimensionless]
V_c : Volume of cement [dm^3]
V_w : Volume of (initially present) water [dm^3]
ε_T : Total porosity [Dimensionless]
ε_{H_2O} : Water filled part of the pore system [Dimensionless]
DS : Degree of saturation [%]

The standard assumption [N 1995] (factors of 0.23–0.25 may be applied) :

$$W_n = 0.23\alpha C \qquad \text{(Eq. AI-2)}$$

The water filled pore space, i.e. the amount of water in the system after hydration :

$$\varepsilon_{H_2O} = W_0 - 0.23\alpha C + W_{Ex} \qquad \text{[kg]} \quad \text{(Eq. AI-3)}$$

Relative amount (per C) :

$$\varepsilon_{H_2O} = w/c - 0.23\alpha + W_{Ex}/C \qquad \text{[Dimensionless]} \quad \text{(Eq. AI-4)}$$

Totally available pore space [N 1995] :

$$\varepsilon_T = W_0 - W_n + 0.254W_n$$
$$\varepsilon_T = W_0 - 0.23\alpha C + 0.254 \times 0.23\alpha C \quad \text{(Eq. AI-5)}$$
$$\varepsilon_T = (w/c - 0.172\alpha) \times C$$

If these segments of porosity are to be considered per unit volume of paste, the former must be related to the total volume (external shrinkage and air voids neglected) :

Volume initially available : $V_c + V_w = C[\text{kg}]/\rho_c\,[\text{kg/dm}^3] + V_w\,[\text{dm}^3]/1$

External volume per c (dividing with C both in the numerator and the

denominator) : $\frac{1}{\rho_c}\left[\frac{dm^3}{kg}\right] + \frac{V_w}{C}\left[\frac{dm^3}{kg}\right]$

$$(V_c+V_w)/C = 0.32 + w/c \qquad \text{(Eq. AI-6)}$$

Hence, water filled and total porosity, respectively, and derived degree of saturation :

$$\begin{aligned}
\varepsilon_{H_2O} &= \frac{w/c - 0.23\alpha + W_{Ex}/C}{0.32 + w/c} \\
\varepsilon_T &= \frac{w/c - 0.172\alpha}{0.32 + w/c} \qquad \text{(Eq. AI-7)} \\
DS &= \frac{\varepsilon_{H_2O}}{\varepsilon_T} = \frac{w/c - 0.23\alpha + W_{Ex}/C}{w/c - 0.172\alpha}
\end{aligned}$$

Thus, if externally supplied water is zero, the equation yields the degree of saturation for isolated curing conditions. The air voids are not included in the formula but are the last pores to become saturated (a possible exception is near the top surface) – and may be corrected for.

b) The actual case

Inserting the values 0.48 and 66 % for the w/c-ratio and the degree of hydration, respectively, yields a degree of saturation just below 90 % - if the samples had been cured under isolated conditions. According to [P 1999], this may typically lead to RH levels around 95 % but depends on the cement type and other factors.

If the externally provided water is identical to suction caused by the chemical reaction, it will equal the amount of contraction porosity, i.e. the determined chemical shrinkage. These values would at the age of 28 days probably (if they could have been acquired from the larger samples) range from approximately 5.5 to 6.5 g per 100 g cement. Inserted in the same formula, “DS” ends up between 104 % and 107 %, i.e. as “over-saturated”. The most obvious explanation – if the test results are correct –would be the accommodation of water in air voids.

The influence of saturated air voids may be estimated : Considering a unit volume of cement paste consisting of 100 g cement and 48 g water (w/c = 0.48) without air, the volume amounts to 100/3.12 + 48 = 80.05 cm^3. Thus, 1 vol-% air voids amounts to 0.80 cm^3 per 100 g cement. Again, inserting this value as externally supplied water and using the denominator in the formula above, we obtain :

$$\Delta DS = \frac{0.8/100}{0.48 - 0.172 \times 0.66} = 0.022 \qquad \text{(Eq. AI-8)}$$

i.e. 2.2 %. This implies that an air void volume of at least 3 % is required to achieve an “DS” of 107 % as calculated above. The value is in the absolute upper range of the expected level. Although the parameter was not determined on these specimens, they are supposedly identical to the pastes manufactured for the investigations in section 6.3. The latter exhibited an air content close to 0 %. The determination of the evaporable water content at the termination of the chemical shrinkage, if performed, would have provided useful information. Unfortunately, it was not.

However, the excessive water consumption could relate to some sort of water accommodation in cavities or cracks – or to swelling :

Cement paste or concrete continuously stored in water from the time of placing exhibit a net increase in volume and mass [N 1995]. This swelling is due to the absorption of water by the cement gel. This, again, is attributed to two effects : The water molecules a) act against the cohesive forces within the gel and b) due to the ingress, reduce the surface tension between the pore water and the pore walls.

If a swelling strain at 28 days age of 1000 x 10^{-6} is applied, based on data from [N 1995], the unit volume paste above (100 g cement, 80 cm^3) will amount to no more than 0.08 ml on the accumulated absorption values.

It is also hard to imagine that internal cracking would have an extent (volume) to be of significant importance. Thus, the only possible, remaining reason for the high shrinkage levels measured for some of the samples in this pilot study is measuring error. The water suction is too high for :

- The non-evaporable water content
- Available accommodation in the pores or other cavities

The measurements do not comply with those of numerous authors and have to be rejected.

6 Conclusions

The most important question arising from the pilot study is the lack of correlation between chemical shrinkage and the degree of hydration. Chemical shrinkage is actually by several authors reported to represent the true extent of chemical reaction, at least at the initial stage [J 1994]. Alone the stable activity level observed as linearly increasing shrinkage after the age of seven days indicates a lack of correlation to expected hydration development. Together with the considerations in the preceding section, this suggests that something went wrong in the performed study :

- From later work, it became evident that the evaporation protection by the plastic bags on the pipette was not sufficient. The samples must have been subjected to evaporation and weight loss.

- Accordingly, the study failed to reveal any effect of the sample size on the chemical shrinkage.

The contribution from the present study to the recommendations given in section 6.2.1-2 comprises the following measures :

- One measure to control the values of chemical shrinkage of the following work is to monitor the weight of the samples. NB : The relative changes to be recorded are small compared to the normal accuracy of a balance with sufficient capacity (weight range). This requires extra calibration procedures with reference weight in the same range as the sample weight.

- The sample size of cement paste should be limited in order to avoid flask breakage due to swelling of the paste, for testing periods exceeding one week.

- The silicon stoppers should be fixed to the Erlenmeyer flasks, or coated in such a way that sliding – and erroneous readings – can be revealed.

- Differentiation of the shrinkage versus time curve appears to give valuable information for critical evaluation of the test results.

- The degree of temperature control will determine to what extent corrections by coefficient of thermal expansion should be undertaken. Volume control of the recipient water and air voids is a potential factor of consideration at later stages, if differential values are to be calculated.

- One way of monitoring the long term, chemical shrinkage could possibly be to cast parallel samples for water storage. After de-moulding at 24 hours, stepwise recording of sample weight might be expected to represent an easier and more proof way to measure the chemical shrinkage.